

Issues 1-2

2023 | Volume 19

The Journal on Advanced Studies in Theoretical and Experimental Physics,
including Related Themes from Mathematics

PROGRESS IN PHYSICS



“All scientists shall have the right to present their scientific research results, in whole or in part, at relevant scientific conferences, and to publish the same in printed scientific journals, electronic archives, and any other media.” — Declaration of Academic Freedom, Article 8

ISSN 1555-5534

PROGRESS IN PHYSICS

A Scientific Journal on Advanced Studies in Theoretical and Experimental Physics, including Related Themes from Mathematics. This journal is registered with the Library of Congress (DC, USA).

Electronic version of this journal:
<http://www.ptep-online.com>

Editorial Board

Pierre Millette
millette@ptep-online.com
Andreas Ries
ries@ptep-online.com
Florentin Smarandache
fsmarandache@gmail.com
Ebenezer Chifu
chifu@ptep-online.com

Postal Address

Department of Mathematics and Science,
University of New Mexico,
705 Gurley Ave., Gallup, NM 87301, USA

Copyright © *Progress in Physics*, 2023

All rights reserved. The authors of the articles do hereby grant *Progress in Physics* non-exclusive, worldwide, royalty-free license to publish and distribute the articles in accordance with the Budapest Open Initiative: this means that electronic copying, distribution and printing of both full-size version of the journal and the individual papers published therein for non-commercial, academic or individual use can be made by any user without permission or charge. The authors of the articles published in *Progress in Physics* retain their rights to use this journal as a whole or any part of it in any other publications and in any way they see fit. Any part of *Progress in Physics* howsoever used in other publications must include an appropriate citation of this journal.

This journal is powered by L^AT_EX

A variety of books can be downloaded free from the Digital Library of Science:
<http://fs.gallup.unm.edu/ScienceLibrary.htm>

ISSN: 1555-5534 (print)

ISSN: 1555-5615 (online)

Standard Address Number: 297-5092

Printed in the United States of America

June 2023

Vol. 19, Issue 1

CONTENTS

Rabounski D., Borissova L. Physical Observables in General Relativity and the Zelmanov Chronometric Invariants	3
Burra G. S. Fission with a Difference	30
Nyambuya G. G. Avoiding Negative Energies in Quantum Mechanics	32
Porcelli E. B., Filho V. S. Novel Insights into Nonlocal Gravity	40
Belyakov A. V. Space and Gravity	50
Potter F. Fermion Mass Derivations: I. Neutrino Masses via the Linear Superposition of the 2T, 2O, and 2I Discrete Symmetry Binary Subgroups of SU(2)	55
Heymann Y. A Derivation of Planck's Constant from the Principles of Electrodynamics	62
Millette P. Zitterbewegung and the Non-Holonomy of Pseudo-Riemannian Spacetime	66
Santilli R. M. Reduction of Matter in the Universe to Protons and Electrons via the Lie-isotopic Branch of Hadronic Mechanics	73
Zhong Y. C. Calculation of Outgoing Longwave Radiation in the Absence of Surface Radiation of the Earth	100
Müller H. Natural Metrology in Physics of Numerical Relations	102

Information for Authors

Progress in Physics has been created for rapid publications on advanced studies in theoretical and experimental physics, including related themes from mathematics and astronomy. All submitted papers should be professional, in good English, containing a brief review of a problem and obtained results.

All submissions should be designed in L^AT_EX format using *Progress in Physics* template. This template can be downloaded from *Progress in Physics* home page <http://www.ptep-online.com>

Preliminary, authors may submit papers in PDF format. If the paper is accepted, authors can manage L^AT_EX typing. Do not send MS Word documents, please: we do not use this software, so unable to read this file format. Incorrectly formatted papers (i.e. not L^AT_EX with the template) will not be accepted for publication. Those authors who are unable to prepare their submissions in L^AT_EX format can apply to a third-party payable service for LaTeX typing. Our personnel work voluntarily. Authors must assist by conforming to this policy, to make the publication process as easy and fast as possible.

Abstract and the necessary information about author(s) should be included into the papers. To submit a paper, mail the file(s) to the Editor-in-Chief.

All submitted papers should be as brief as possible. Short articles are preferable. Large papers can also be considered. Letters related to the publications in the journal or to the events among the science community can be applied to the section *Letters to Progress in Physics*.

All that has been accepted for the online issue of *Progress in Physics* is printed in the paper version of the journal. To order printed issues, contact the Editors.

Authors retain their rights to use their papers published in *Progress in Physics* as a whole or any part of it in any other publications and in any way they see fit. This copyright agreement shall remain valid even if the authors transfer copyright of their published papers to another party.

Electronic copies of all papers published in *Progress in Physics* are available for free download, copying, and re-distribution, according to the copyright agreement printed on the titlepage of each issue of the journal. This copyright agreement follows the *Budapest Open Initiative* and the *Creative Commons Attribution-Noncommercial-No Derivative Works 2.5 License* declaring that electronic copies of such books and journals should always be accessed for reading, download, and copying for any person, and free of charge.

Consideration and review process does not require any payment from the side of the submitters. Nevertheless the authors of accepted papers are requested to pay the page charges. *Progress in Physics* is a non-profit/academic journal: money collected from the authors cover the cost of printing and distribution of the annual volumes of the journal along the major academic/university libraries of the world. (Look for the current author fee in the online version of *Progress in Physics*.)

Physical Observables in General Relativity and the Zelmanov Chronometric Invariants

Dmitri Rabounski and Larissa Borissova

Puschino, Moscow Region, Russia

E-mail: rabounski@yahoo.com, lborissova@yahoo.com

Chronometric invariants are mathematically determined as the projections of four-dimensional tensorial quantities onto the three-dimensional spatial section and the line of time belonging to a real particular observer. Such projections are physical observables to the observer; it is these quantities that are measurable in his real laboratory and depend on the physical and geometric properties of his local physical space. In other words, chronometric invariants are physical observable quantities in the space-time of General Relativity. Chronometric invariants and the mathematical apparatus for their calculation were introduced in 1944 by Abraham L. Zelmanov. In this article, we have collected everything (or almost everything) that we know about chronometric invariants to provide a convenient and most detailed reference to this mathematical apparatus originally scattered throughout many publications.

Physical observables were mathematically determined and introduced into General Relativity in 1941–1944 by Abraham L. Zelmanov (1913–1987), who called them chronometrically invariant quantities or, in brief, *chronometric invariants*. Zelmanov first presented his mathematical apparatus for calculating physical observables in 1944, in the form of his PhD thesis [1]. Later, in 1956–1957, he published a brief review of his theory in two journal articles [2, 3], of which his 1957 presentation is the most useful and complete. A more detailed account of Zelmanov’s mathematical apparatus can be found in the respective chapters of our three research monographs [4–6] and in one of our recent journal publications [7].

Chronometrically invariant quantities are determined as the projections of four-dimensional tensorial quantities onto the three-dimensional spatial section and the line of time in the real physical reference frame belonging to a particular observer. Such quantities depend on the physical and geometric properties of his local physical space (his physical reference space) and can be measured in his laboratory. In other words, chronometric invariants are physical observable quantities in the space-time of General Relativity.

For this reason and since we have always sought to obtain a theoretical result that can be registered in laboratory measurements, we used Zelmanov’s mathematical apparatus in our research studies. The chronological list of our publications in English and French, wherein we used chronometric invariants, is given in the end of this article.

Unfortunately, it just so happened that after Zelmanov’s death in 1987, we remain the only ones in the world who professionally master this mathematical apparatus and apply it in scientific research. In addition, Zelmanov’s mathematical apparatus was fragmentarily scattered throughout the aforementioned publications. Some of them pretended to be more or less complete, but were also limited due to the omission of some important parts (not relevant to the specific problem).

For this reason, and also because the problem of physical observables in General Relativity is of great importance for

experiment, Pierre A. Millette, Editor of *Progress in Physics*, prompted us to write a compendium containing “everything we know about chronometric invariants and would like to say”. Such an article, despite the obvious repetitions with the previous ones, would contain the entire mathematical apparatus of chronometric invariants, which is very convenient for ourselves and our future followers.

We are grateful to Pierre A. Millette for his proposal and will implement it here in this article.

Usually, when doing a research study on General Relativity, we present all equations and their terms in the general covariant (four-dimensional) form. This form has its own advantage as well as a substantial drawback. The advantage is the invariance of general covariant equations and their terms in all transitions from one reference frame to another. The drawback is that they do not show actual three-dimensional quantities, which can be measured in experiments by a real observer in his real physical laboratory. In other words, general covariant equations do not give us *physical observable quantities*, but only an intermediate theoretical result, which is not applicable in practice. Therefore, in order to obtain a theoretical result applicable in practice, we need to formulate our equations in terms of physical observables — the quantities that are experimentally measurable and depend on the physical and geometric properties of the physical local reference space belonging to a real particular observer.

Meanwhile, to determine physical observable quantities in the space-time of General Relativity is not a trivial problem. For instance, a four-dimensional vector, i.e., a contravariant tensor of the 1st rank, has just 4 components: 1 time component and 3 spatial components. In this case, we can heuristically assume that its three spatial components form a three-dimensional observable vector, while its time component is the observable potential of the vector field (which, generally speaking, does not prove that these quantities can actually be observed). A tensor of the 2nd rank, e.g., a rota-

tion or deformation tensor, has 16 components: 1 time component, 9 spatial components and 6 mixed (time-spatial) components. Are the mixed components physical observables? This is another question that seemingly has no definite answer. Tensors of higher ranks have even more components. For instance, the Riemann-Christoffel curvature tensor is a tensor of the 4th rank. It has 256 components. In such a case the problem of the heuristic recognition of physically observable components becomes far more complicated, or even impossible. Besides that, there is an obstacle related to the recognition of observable components of covariant tensors (in which indices occupy the lower position) and of mixed type tensors, which have both lower and upper indices.

Therefore, the most reasonable way out of the labyrinth of heuristic guesses is to create a strict mathematical theory that allows us to calculate observable components for any tensor quantity. As mentioned in the beginning of this article, such a complete mathematical theory was created in 1941–1944 by Zelmanov. His theory was called the mathematical apparatus of physical observable quantities in General Relativity, or, in brief, the *theory of chronometric invariants*.

It should be noted that in the 1930's and 1950's, independently from Zelmanov, some other researchers tried to give a mathematical definition to physical observable quantities in the space-time of General Relativity. In 1939, L. D. Landau and E. M. Lifshitz in their famous *The Classical Theory of Fields* [8] introduced observable time and observable three-dimensional interval similar to Zelmanov's definitions. But, Landau and Lifshitz limited themselves only to this particular case and they did not arrive at general mathematical methods to calculate physical observable quantities in the four-dimensional space-time. In the 1950's, the idea of presenting physical observables in the form of the projections of four-dimensional tensorial quantities onto the three-dimensional spatial section and the time line belonging to an observer was also voiced by the Italian mathematician Carlo Cattaneo [9–12]. Cattaneo highly appreciated Zelmanov's theory of chronometric invariants, and referred to it in his last publication [12]. Nevertheless, when evaluating the scientific contribution of Cattaneo, we must take two facts into account. Firstly, his research was done only in 1958, i.e. 14 years later than Zelmanov. And secondly, his result was very far from a complete theory: he limited himself to general considerations on this problem and did not take into account the physical and geometric observable properties of the local physical space belonging to an observer (as Zelmanov did). Therefore, the projections of four-dimensional tensor quantities considered by Cattaneo do not depend on the observable properties of the observer's reference space and cannot be considered physical observables.

We therefore call physical observable quantities in the space-time of General Relativity the *Zelmanov chronometric invariants* in order to fix this term and Zelmanov's priority in the history of science.

It is also necessary to understand that Zelmanov's mathematical apparatus of chronometric invariants is not just one of many other mathematical techniques used in the General Theory of Relativity, which require an experimental verification of their applicability in practice. The Zelmanov chronometric invariants are physical observables by definition, and there is no other mathematical technique to determine physical observables in General Relativity. In this sense, the mathematical apparatus of chronometric invariants does not require experimental verification, since all quantities that we register in experiments and astronomical observations are chronometric invariants by definition. This fact should always be taken into account, when a researcher seeks to obtain a theoretical result that can be verified in a laboratory experiment or astronomical observations.

Below we present the mathematical apparatus of Zelmanov's chronometric invariants in its entirety, based on his original publications, our personal conversations with him, as well as our own works. So, let us begin.

In order to recognize which of the components of a four-dimensional quantity are physical observables, we consider a physical frame of reference belonging to a real observer, which includes a three-dimensional *coordinate grid* spanned over his *reference body* (a real physical body near him, such as the planet Earth for an Earth-bound observer), at each point of which a *real physical clock* is installed. His reference body, like any other real physical body, has a gravitational field, can rotate and deform, thereby making the local reference space of the observer inhomogeneous and anisotropic. In fact, the reference body and its reference space can be considered as a set of the real physical standards to which the observer compares the results of his measurements. Mathematically, this means that the physical observable quantities registered by an observer are the projections of four-dimensional quantities onto the three-dimensional space (coordinate grid) and the time line of his reference body.

From a geometric point of view, the three-dimensional space of an observer is a *three-dimensional spatial section* drawn in space-time at the time coordinate $x^0 = ct = \text{const}$ determined by the moment of observation t . In fact, at any point in space-time, a local spatial section (local space) can be drawn orthogonally to the line of time. If there exists an enveloping curve to such local spatial sections (local three-dimensional spaces) in space-time, these local spatial sections create a global spatial section, everywhere orthogonal to the lines of time that "pierce" it. Such a space is known as a *holonomic space*. If there is not an enveloping curve for such local spaces, then there are only spatial sections locally orthogonal to the lines of time: such a space is *non-holonomic*.

Zelmanov applied these terms to the four-dimensional space-time of General Relativity, based on Schouten's theory of non-holonomic manifolds [13].

Assume that an observer is at rest with respect to his physical references (his reference body). The reference frame of

such an observer always accompanies his reference body in any of its displacements, so such a system is called an *accompanying reference frame*. Any coordinate grid that is at rest with respect to its reference body is connected to another coordinate grid through the transformation

$$\left. \begin{aligned} \tilde{x}^0 &= \tilde{x}^0(x^0, x^1, x^2, x^3) \\ \tilde{x}^i &= \tilde{x}^i(x^1, x^2, x^3), \quad \frac{\partial \tilde{x}^i}{\partial x^0} = 0 \end{aligned} \right\},$$

where the latter equation means that spatial coordinates in the tilde-marked grid are independent of time in the non-tilded coordinate grid, which is the same as setting a coordinate grid of fixed time lines $x^i = \text{const}$ at any point of the grid. Transformation of spatial coordinates is nothing but only transition from one coordinate grid to another within the same spatial section. Transformation of time means changing the whole set of clocks, so this is transition to another spatial section (another three-dimensional reference space). This means replacing one reference body and its physical references with another one that has its own physical references. But when using different physical references, the observer will obtain different measurement results (other observable quantities). Therefore, all physical observable quantities in the reference frame accompanying an observer must be invariant with respect to transformations of time throughout his entire three-dimensional spatial section $x^i = \text{const}$. In other words, such quantities must have the property of *chronometric invariance*. That is, all physical observable quantities in the reference frame accompanying an observer are “chronometrically” invariant quantities or, in brief, *chronometric invariants*.

Since the aforementioned transformations of time determine a set of fixed time lines “piercing” the observer’s three-dimensional spatial section, chronometric invariants (physical observable quantities) are all those quantities that are invariant with respect to these transformations.

In practice, in order to obtain physical observable quantities in the physical reference frame that accompanies a real observer, we need to calculate chronometrically invariant projections of four-dimensional quantities onto the spatial section and the time line of the observer’s physical reference body, and then formulate the projections with chronometrically invariant (physically observable) properties of his local physical reference space. Therefore, Zelmanov had introduced projection operators that completely characterize the reference space of a particular observer.

The operator of projection onto the time line of an observer is the unit vector of the observer’s four-dimensional velocity b^α with respect to his reference body

$$b^\alpha = \frac{dx^\alpha}{ds},$$

which is tangential to his four-dimensional (space-time) trajectory at each of its points. Because any individual reference

frame is characterized by its own tangential unit vector b^α , Zelmanov referred to the b^α as the *monad vector*. It is easy to see that since the vector b^α is tangential to the observer’s four-dimensional trajectory at each of its points, this vector has unit length

$$b_\alpha b^\alpha = g_{\alpha\beta} \frac{dx^\alpha}{ds} \frac{dx^\beta}{ds} = \frac{g_{\alpha\beta} dx^\alpha dx^\beta}{ds^2} = +1.$$

The operator of projection onto the three-dimensional reference space of the observer (which is an instant spatial section of space-time at the moment of observation) is a four-dimensional symmetric tensor $h_{\alpha\beta}$ having the form

$$h_{\alpha\beta} = -g_{\alpha\beta} + b_\alpha b_\beta,$$

$$h^{\alpha\beta} = -g^{\alpha\beta} + b^\alpha b^\beta,$$

$$h^\beta_\alpha = -g^\beta_\alpha + b_\alpha b^\beta.$$

It is easy to see that the vector b^α and the tensor $h_{\alpha\beta}$ have all the necessary properties characteristic of projection operators, namely — the properties

$$b_\alpha b^\alpha = +1, \quad h^\beta_\alpha b^\alpha = 0,$$

where the second property follows from the fact that the vector b^α and the tensor $h_{\alpha\beta}$ are orthogonal to each other in space-time: mathematically this means that their common contraction is zero

$$h_{\alpha\beta} b^\alpha = -g_{\alpha\beta} b^\alpha + b_\alpha b^\alpha b_\beta = 0,$$

$$h^{\alpha\beta} b_\alpha = -g^{\alpha\beta} b_\alpha + b^\beta b_\alpha b^\alpha = 0,$$

$$h^\alpha_\beta b_\alpha = -g^\alpha_\beta b_\alpha + b_\beta b^\alpha b_\alpha = 0,$$

$$h^\beta_\alpha b^\alpha = -g^\beta_\alpha b^\alpha + b^\beta b_\alpha b^\alpha = 0.$$

In the reference frame accompanying the observer, his three-dimensional velocity with respect to his reference body is zero, which means that $b^i = 0$. As a result, the components of the b^α in the accompanying reference frame are

$$b^0 = \frac{1}{\sqrt{g_{00}}}, \quad b_0 = g_{0\alpha} b^\alpha = \sqrt{g_{00}},$$

$$b^i = 0, \quad b_i = g_{i\alpha} b^\alpha = \frac{g_{i0}}{\sqrt{g_{00}}}.$$

Therefore, the components of the projection operator $h_{\alpha\beta}$ in the accompanying reference frame ($b^i = 0$) are

$$h_{00} = 0, \quad h^{00} = -g^{00} + \frac{1}{g_{00}}, \quad h^0_0 = 0,$$

$$h_{0i} = 0, \quad h^{0i} = -g^{0i}, \quad h^i_0 = \delta^i_0 = 0,$$

$$h_{i0} = 0, \quad h^{i0} = -g^{i0}, \quad h^0_i = \frac{g_{i0}}{g_{00}},$$

$$h_{ik} = -g_{ik} + \frac{g_{0i} g_{0k}}{g_{00}}, \quad h^{ik} = -g^{ik}, \quad h^i_k = -g^i_k = \delta^i_k.$$

The projection of a tensor onto the time line of an observer is the result of its contraction with the monad vector b^α of his reference frame.

The projection of a tensor onto the three-dimensional spatial section of the observer (his three-dimensional reference space) is the result of its contraction with the tensor $h_{\alpha\beta}$ of his reference frame.

Despite the fact that such projections of a tensor of the 1st rank (a vector) are chronometric invariants, i.e., physical observables, not all such projections (contractions) of higher rank tensors have the property of chronometric invariance. To solve this problem, Zelmanov developed a general mathematical method for calculating chronometrically invariant (physically observable) projections of any four-dimensional general covariant tensor and formulated it as a theorem. We refer to it as *Zelmanov's theorem*.

ZELMANOV'S THEOREM: Let there be a four-dimensional tensor $Q_{\alpha\beta\dots\sigma}^{\mu\nu\dots\rho}$ of the r -th rank, where $Q_{00\dots0}^{ik\dots p}$ is the three-dimensional part of $Q_{\alpha\beta\dots\sigma}^{\mu\nu\dots\rho}$, in which all upper indices are non-zero, and all m lower indices are zeroes. Then,

$$T^{ik\dots p} = (g_{00})^{-\frac{m}{2}} Q_{00\dots0}^{ik\dots p}$$

is a chronometrically invariant three-dimensional contravariant tensor of the $(r-m)$ -th rank. This means that the chr.inv.-tensor $T^{ik\dots p}$ is the result of m -fold projection of the initial tensor $Q_{\alpha\beta\dots\sigma}^{\mu\nu\dots\rho}$ onto the time line by the indices $\alpha, \beta, \dots, \sigma$ and onto the spatial section by $r-m$ indices μ, ν, \dots, ρ .

According to this theorem, the chronometrically invariant (physically observable) projections of a four-dimensional vector Q^α are the quantities

$$b^\alpha Q_\alpha = \frac{Q_0}{\sqrt{g_{00}}}, \quad h_\alpha^i Q^\alpha = q^i,$$

while the chr.inv.-projections of a symmetric tensor of the 2nd rank $Q^{\alpha\beta}$ are the quantities

$$b^\alpha b^\beta Q_{\alpha\beta} = \frac{Q_{00}}{g_{00}}, \quad h^{i\alpha} b^\beta Q_{\alpha\beta} = \frac{Q_0^i}{\sqrt{g_{00}}}, \quad h_\alpha^i h_\beta^k Q^{\alpha\beta} = Q^{ik},$$

where, in the case of an antisymmetric tensor of the 2nd rank, the first chr.inv.-projection is zero, because $Q_{00} = Q^{00} = 0$ for any antisymmetric 2nd rank tensor.

The chr.inv.-projections of a four-dimensional coordinate interval dx^α are the physically observable time interval

$$d\tau = \sqrt{g_{00}} dt + \frac{g_{0i}}{c\sqrt{g_{00}}} dx^i,$$

and the interval of the physically observable coordinates dx^i , which are the same as the regular spatial coordinates. Thus, the three-dimensional chr.inv.-vector

$$v^i = \frac{dx^i}{d\tau}, \quad v_i v^i = h_{ik} v^i v^k = v^2$$

is the physically observable velocity of a particle, which is different from the particle's coordinate velocity

$$u^i = \frac{dx^i}{dt}.$$

At isotropic trajectories (trajectories of light), the v^i transforms into the three-dimensional chr.inv.-vector of the physically observable velocity of light

$$c^i = v^i = \frac{dx^i}{d\tau}, \quad c_i c^i = h_{ik} c^i c^k = c^2.$$

When we project the fundamental metric tensor $g_{\alpha\beta}$ onto the three-dimensional spatial section of an observer (which is his three-dimensional reference space)

$$h_\alpha^i h_\beta^k g^{\alpha\beta} = g^{ik} = -h^{ik}, \quad h_\alpha^i h_k^\beta g_{\alpha\beta} = g_{ik} - b_i b_k = -h_{ik},$$

we see that the three-dimensional part of the projection operator $h_{\alpha\beta}$, i.e., the three-dimensional tensor h_{ik} , the components of which have the form

$$h_{ik} = -g_{ik} + b_i b_k, \quad h^{ik} = -g^{ik}, \quad h_k^i = -g_k^i = \delta_k^i,$$

is the *chr.inv.-metric tensor* or, in other words, the metric tensor physically observed in the reference frame accompanying the observer.

The chr.inv.-metric tensor h_{ik} has all properties of the fundamental metric tensor $g_{\alpha\beta}$ throughout the observer's three-dimensional spatial section (his three-dimensional reference space), i.e., it satisfies the condition

$$h_\alpha^i h_k^\alpha = \delta_k^i - b_k b^i = \delta_k^i, \quad \delta_k^i = \begin{pmatrix} 1 & 0 & 0 \\ 0 & 1 & 0 \\ 0 & 0 & 1 \end{pmatrix},$$

where δ_k^i is the unit three-dimensional tensor. The tensor δ_k^i is the three-dimensional part of the four-dimensional unit tensor δ_β^α , which can be used to lift and lower indices in four-dimensional quantities. For this reason, the chr.inv.-metric tensor h_{ik} can lift and lower indices in chronometrically invariant quantities.

Using $g_{\alpha\beta}$ from $h_{\alpha\beta} = -g_{\alpha\beta} + b_\alpha b_\beta$, we obtain the four-dimensional interval $ds^2 = g_{\alpha\beta} dx^\alpha dx^\beta$ in the form

$$ds^2 = b_\alpha b_\beta dx^\alpha dx^\beta - h_{\alpha\beta} dx^\alpha dx^\beta$$

expressed with the projection operators b^α and $h_{\alpha\beta}$. Because $b_\alpha dx^\alpha = c d\tau$, the first term of the above formula transforms into $b_\alpha b_\beta dx^\alpha dx^\beta = c^2 d\tau^2$. The second term of this formula, $h_{\alpha\beta} dx^\alpha dx^\beta = d\sigma^2$, in the reference frame accompanying the observer is the square of the three-dimensional physically observable interval

$$d\sigma^2 = h_{ik} dx^i dx^k,$$

since $h_{\alpha\beta}$ has all properties of the fundamental metric tensor $g_{\alpha\beta}$ in the accompanying reference frame.

As a result, the four-dimensional interval written in terms of physically observable chr.inv.-quantities has the form

$$ds^2 = c^2 d\tau^2 - d\sigma^2.$$

Obviously, the physical observables (chr.inv.-projections of four-dimensional quantities) registered by an observer depend on the physical and geometric observable properties of the observer's local space (his physical reference space), with which, therefore, all chr.inv.-quantities and equations must be expressed. Therefore, Zelmanov deduced the basic observable properties of the reference space accompanying an observer and introduced them into the theory.

Two main physical observable properties of the accompanying reference space can be obtained using the chr.inv.-derivation operators with respect to time and the spatial coordinates. The mentioned chr.inv.-derivation operators introduced by Zelmanov have the form

$$\frac{*\partial}{\partial t} = \frac{1}{\sqrt{g_{00}}} \frac{\partial}{\partial t}, \quad \frac{*\partial}{\partial x^i} = \frac{\partial}{\partial x^i} - \frac{g_{0i}}{g_{00}} \frac{\partial}{\partial x^0}$$

and are non-commutative, so the difference between the 2nd derivatives is not zero

$$\frac{*\partial^2}{\partial x^i \partial t} - \frac{*\partial^2}{\partial t \partial x^i} = \frac{1}{c^2} F_i \frac{*\partial}{\partial t},$$

$$\frac{*\partial^2}{\partial x^i \partial x^k} - \frac{*\partial^2}{\partial x^k \partial x^i} = \frac{2}{c^2} A_{ik} \frac{*\partial}{\partial t}.$$

Here, A_{ik} is the three-dimensional antisymmetric chr.inv.-tensor of the angular velocity with which the reference space of the observer rotates

$$A_{ik} = \frac{1}{2} \left(\frac{\partial v_k}{\partial x^i} - \frac{\partial v_i}{\partial x^k} \right) + \frac{1}{2c^2} (F_i v_k - F_k v_i),$$

where v_i is the linear velocity of this rotation

$$v_i = -c \frac{g_{0i}}{\sqrt{g_{00}}}, \quad v^i = -c g^{0i} \sqrt{g_{00}},$$

$$v_i = h_{ik} v^k, \quad v^2 = v_k v^k = h_{ik} v^i v^k.$$

In addition, the v_i gives detailed formulae for the physically observable time interval $d\tau$ and the chr.inv.-metric tensor h_{ik} , which are

$$d\tau = \sqrt{g_{00}} dt - \frac{1}{c^2} v_i dx^i, \quad h_{ik} = -g_{ik} + \frac{1}{c^2} v_i v_k.$$

The quantity F_i is the three-dimensional chr.inv.-vector of the gravitational inertial force

$$F_i = \frac{1}{\sqrt{g_{00}}} \left(\frac{\partial w}{\partial x^i} - \frac{\partial v_i}{\partial t} \right) = \frac{1}{1 - \frac{w}{c^2}} \left(\frac{\partial w}{\partial x^i} - \frac{\partial v_i}{\partial t} \right),$$

where

$$w = c^2 (1 - \sqrt{g_{00}})$$

is the gravitational potential, the origin of which is the gravitational field of the observer's reference body. In the framework of quasi-Newtonian approximation, i.e., in a weak gravitational field at velocities much lower than the velocity of light and in the absence of rotation of the space, the F_i transforms into the non-relativistic gravitational force

$$F_i = \frac{\partial w}{\partial x^i}.$$

It should be noted that the quantities w and v_i do not have the property of chronometric invariance, despite the fact that $v_i = h_{ik} v^k$ is obtained as for a chr.inv.-quantity, through lowering the upper index by the chr.inv.-metric tensor h_{ik} . On the other hand, the vector of the gravitational inertial force F_i and the tensor of the angular velocity of rotation of the observer's space, A_{ik} , built using them, are chr.inv.-quantities.

The chr.inv.-quantities F_i and A_{ik} are related to each other by two identities, which we call the *Zelmanov identities*

$$\frac{*\partial A_{ik}}{\partial t} + \frac{1}{2} \left(\frac{*\partial F_k}{\partial x^i} - \frac{*\partial F_i}{\partial x^k} \right) = 0,$$

$$\frac{*\partial A_{km}}{\partial x^i} + \frac{*\partial A_{mi}}{\partial x^k} + \frac{*\partial A_{ik}}{\partial x^m} + \frac{1}{2} (F_i A_{km} + F_k A_{mi} + F_m A_{ik}) = 0.$$

In addition to rotation and the presence of a gravitational field, the real reference body of an observer can deform. In this case, the observer's reference space with its coordinate grid deforms accordingly, which must be taken into account in experiments. Mathematically, this factor manifests itself in the non-stationarity of the physically observable chr.inv.-metric h_{ik} of the observer's space and must be taken into account in the physically observable chr.inv.-quantities registered by him. For this reason, Zelmanov had introduced the three-dimensional symmetric chr.inv.-tensor D_{ik} characterizing the rate of deformations of the observer's space

$$D_{ik} = \frac{1}{2} \frac{*\partial h_{ik}}{\partial t}, \quad D^{ik} = -\frac{1}{2} \frac{*\partial h^{ik}}{\partial t},$$

$$D = h^{ik} D_{ik} = D_n^n = \frac{*\partial \ln \sqrt{h}}{\partial t}, \quad h = \det \|h_{ik}\|.$$

Zelmanov had also introduced a theorem linking the holonomy of space-time to the tensor of the angular velocity of rotation of the observer's three-dimensional space.

ZELMANOV'S THEOREM ON THE HOLONOMY OF SPACE-TIME: The identical equality to zero of the tensor A_{ik} in a four-dimensional region of space-time is the necessary and sufficient condition for the orthogonality of the spatial sections to the time lines everywhere in this region.

In other words, $A_{ik} \neq 0$ in a non-holonomic space-time region, and $A_{ik} = 0$ in a holonomic one. Naturally, if the three-dimensional spatial sections are everywhere orthogonal to the time lines (in such a case the space-time region is holonomic), all the quantities g_{0i} are equal to zero. Since $g_{0i} = 0$, we have

$v_i = 0$ and $A_{ik} = 0$ too. Therefore, we also refer to the tensor A_{ik} as the *space non-holonomy tensor*.

The space-time of Special Relativity (Minkowski space) in the Galilean reference frame, as well as some cases of the space-time in General Relativity, do not rotate ($A_{ik} = 0$). These are examples of holonomic spaces: time lines are orthogonal to spatial sections in them. Rotating spaces ($A_{ik} \neq 0$) are non-holonomic; time lines are non-orthogonal to three-dimensional spatial sections in such spaces.

To understand why the rotation of a three-dimensional spatial section of space-time makes this spatial section non-orthogonal to the time lines “piercing” it, consider a *locally geodesic reference frame*. Within the infinitesimal vicinity of any point in such a reference frame, the fundamental metric tensor has the form

$$\tilde{g}_{\mu\nu} = g_{\mu\nu} + \frac{1}{2} \left(\frac{\partial^2 \tilde{g}_{\mu\nu}}{\partial \tilde{x}^\rho \partial \tilde{x}^\sigma} \right) (\tilde{x}^\rho - x^\rho) (\tilde{x}^\sigma - x^\sigma) + \dots,$$

which means that the numerical values of its components in the infinitesimal vicinity of any point differ from those at this point itself only in the 2nd order terms and the higher other terms, which can be neglected. Therefore, at any point in a locally geodesic reference frame, the fundamental metric tensor (within the 2nd order terms withheld) is constant, while the 1st derivatives of the metric tensor, i.e., the Christoffel symbols, are zeroes.

It is obvious that in any Riemannian space within the infinitesimal vicinity of any point of the space a locally geodesic reference frame can be set up. As a result, at any point belonging to the locally geodesic reference frame, a flat space can be set up tangential to the Riemannian space so that the locally geodesic reference frame in the Riemannian space is a globally geodesic frame in the tangential flat space. Since the fundamental metric tensor is constant in the flat space, there in the infinitesimal vicinity of any point in the Riemannian space the quantities $\tilde{g}_{\mu\nu}$ converge to those of the tensor $g_{\mu\nu}$ in the tangential flat space. This means that, in the tangential flat space, we can set up a system of the basis vectors $\vec{e}_{(a)}$ tangential to the curved coordinate lines of the Riemannian space. Because the coordinate lines of a Riemannian space are curved (in a general case), and, in the case where the space is non-holonomic, are not even orthogonal to each other, the lengths of the basis vectors are sometimes substantially different from unit length.

Consider the world-vector $d\vec{r}$ of an infinitesimal displacement from such a point, i.e., $d\vec{r} = \{dx^0, dx^1, dx^2, dx^3\}$. Then $d\vec{r} = \vec{e}_{(a)} dx^a$, where its components $e_{(a)}$ are

$$\begin{aligned} \vec{e}_{(0)} &= \{e_{(0)}^0, 0, 0, 0\}, & \vec{e}_{(1)} &= \{0, e_{(1)}^1, 0, 0\}, \\ \vec{e}_{(2)} &= \{0, 0, e_{(2)}^2, 0\}, & \vec{e}_{(3)} &= \{0, 0, 0, e_{(3)}^3\}. \end{aligned}$$

The scalar product of the vector $d\vec{r}$ with itself is equal to $d\vec{r}d\vec{r} = ds^2$. On the other hand, it is $ds^2 = g_{\alpha\beta} dx^\alpha dx^\beta$. Thus,

we obtain the general formula

$$g_{\alpha\beta} = \vec{e}_{(a)} \vec{e}_{(b)} = e_{(a)} e_{(b)} \cos(x^\alpha; x^\beta).$$

According to this formula we have

$$g_{00} = e_{(0)}^2,$$

while, on the other hand, $\sqrt{g_{00}} = 1 - \frac{w}{c^2}$. Hence, the length $e_{(0)}$ of the time basis vector $\vec{e}_{(0)}$ tangential to the time line $x^0 = ct$ is expressed with the gravitational potential w as

$$e_{(0)} = \sqrt{g_{00}} = 1 - \frac{w}{c^2}.$$

The stronger the gravitational potential w , the smaller $e_{(0)}$ is than 1. In the case of gravitational collapse ($w = c^2$), the length of the time basis vector $\vec{e}_{(0)}$ becomes zero: $e_{(0)} = 0$.

Thus, according to the above general formula, the component g_{0i} is expressed as

$$g_{0i} = e_{(0)} e_{(i)} \cos(x^0; x^i),$$

while, according to the definition of v_i , we have

$$g_{0i} = -\frac{1}{c} v_i \left(1 - \frac{w}{c^2} \right) = -\frac{1}{c} v_i e_{(0)},$$

whence we obtain the formula for v_i , which takes into account the angle of inclination of the time lines to the three-dimensional spatial section of space-time, i.e.

$$v_i = -c e_{(i)} \cos(x^0; x^i).$$

In addition, since the above general formula gives

$$g_{ik} = e_{(i)} e_{(k)} \cos(x^i; x^k),$$

and according to the definition of the chr.inv.-metric tensor h_{ik} (page 7), we obtain the formula for h_{ik} , which also takes into account the angle of inclination of the time lines to the three-dimensional spatial section

$$h_{ik} = e_{(i)} e_{(k)} \left[\cos(x^0; x^i) \cos(x^0; x^k) - \cos(x^i; x^k) \right].$$

From the above formula for v_i , we see that from a geometric point of view, the linear velocity v_i with which the three-dimensional reference space of an observer rotates is the projection (scalar product) of the time basis vector $\vec{e}_{(0)}$ of his reference space onto the spatial basis vectors $\vec{e}_{(i)}$, multiplied by the velocity of light. If the spatial sections of a space (space-time) are everywhere orthogonal to the time lines thereby giving the space holonomy, then $\cos(x^0; x^i) = 0$ and, hence, $v_i = 0$. In a non-holonomic space, the spatial sections are not orthogonal to the lines of time: $\cos(x^0; x^i) \neq 0$.

Generally $|\cos(x^0; x^i)| \leq 1$, hence the linear velocity v_i with which the three-dimensional reference space of an observer rotates cannot exceed the velocity of light.

If somewhere the conditions $F_i = 0$ and $A_{ik} = 0$ are met in common, there the conditions $g_{00} = 1$ and $g_{0i} = 0$ are present as well (the conditions $g_{00} = 1$ and $g_{0i} = 0$ can be satisfied through the transformation of time). In such a region, according to the definition of $d\tau$ (page 6), we have $d\tau = dt$: so, the difference between the coordinate time t and the physically observable time τ disappears in the absence of gravitational fields and rotation of space. In other words, according to the theory of chronometric invariants, the difference between the coordinate time t and the physically observable time τ comes from both gravitation and rotation attributed to the local reference space of the observer (in fact — from his reference body, which is a real physical body near him, for example, the planet Earth for an Earth-bound observer), or from each of the mentioned two factors separately.

On the other hand, it is doubtful to find such a region of the Universe where gravitational fields or rotation of the background space are clearly absent. Therefore, in practice the physically observable time τ differs from the coordinate time t . This means that the real space of our Universe is non-holonomic: it rotates and is filled with gravitational fields, while a holonomic space, free from rotation and gravity, can only be a local approximation to it.

The condition of holonomy of a space (space-time) is directly linked to the problem of integrability of time in it. In a non-holonomic space, the formula for the physically observable time interval $d\tau$ has no integrating multiplier, i.e., it cannot be transformed to the form

$$d\tau = A dt,$$

where the multiplier A depends on only t and x^i . In this case the formula for $d\tau$ (page 6) has a non-zero second term depending on the coordinate interval dx^i and g_{0i} . On the contrary, in a holonomic space, we have $A_{ik} = 0$, so $g_{0i} = 0$. In this case, the second term of the formula for $d\tau$ is zero, while the first term is the coordinate time interval dt with an integrating multiplier

$$A = \sqrt{g_{00}} = f(x^0, x^i),$$

so we can write the integral

$$d\tau = \int \sqrt{g_{00}} dt.$$

Hence time is integrable in a holonomic space ($A_{ik} = 0$), while it cannot be integrated if the space is non-holonomic ($A_{ik} \neq 0$). In the case where time is integrable, i.e., in a holonomic space, we can synchronize the clocks installed at two distantly located points by moving a control clock along the path between these two points. In the case where time cannot be integrated (in a non-holonomic space), synchronization of clocks in two distant points is impossible in principle: the larger is the distance between these two points, the more is the deviation of time on these clocks.

The space of our planet Earth, is non-holonomic due to the daily rotation of it around the Earth's axis. Hence, two clocks installed at different points on the surface of the Earth should manifest a deviation between the intervals of time registered on each of them. The larger is the distance between these clocks, the larger is the deviation of the physically observable time expected to be registered on them. This effect was surely verified by the well-known Hafele-Keating experiment performed in October 1971 by Joseph C. Hafele together with Richard E. Keating [14–16] and then successfully repeated by the UK's National Measurement Laboratory commonly with the BBC on its 25th anniversary in 2005 [17]. This experiment concerned with displacing standard atomic clocks by a jet airplane around the terrestrial globe, where rotation of the Earth's space sensibly changed the measured time. During the flight along the Earth's rotation, the local space of an observer on board of the airplane had more rotation than the space of another observer who stayed fixed on the airfield. During the flight against the Earth's rotation it was vice versa. The atomic clocks on board the airplane showed a significant deviation of the observed time depending on the velocity of rotation of the observer's space.

Since synchronization of clocks at various points on the Earth's surface is the highly important task of metrology, marine navigation, aviation, and orbital space flights, corrections for desynchronization were introduced in early times in the form of tables of empirically obtained corrections that take the Earth's rotation into account. Now, thanks to the theory of chronometric invariants, we know the origin of the corrections and therefore can calculate them on the basis of General Relativity.

With Zelmanov's definitions of chr.inv.-quantities above, we can not only calculate the physically observable chr.inv.-projections of any four-dimensional general covariant quantity or equation of theoretical physics, but also express them in terms of the physically observable chr.inv.-properties F^i , A_{ik} , and D_{ik} characteristic of the local reference space of a particular observer.

The Christoffel symbols (coherence coefficients of space) appear in the absolute derivatives, the equations of motion, and somewhere else in the equations of theoretical physics. The Christoffel symbols are not tensors [18]. Nevertheless, they can be expressed in terms of physical observable quantities. Following the analogy with the regular Christoffel symbols of the 2nd rank $\Gamma_{\mu\nu}^\alpha$ and the regular Christoffel symbols of the 1st rank $\Gamma_{\mu\nu,\sigma}$

$$\Gamma_{\mu\nu}^\alpha = g^{\alpha\sigma} \Gamma_{\mu\nu,\sigma} = \frac{1}{2} g^{\alpha\sigma} \left(\frac{\partial g_{\mu\sigma}}{\partial x^\nu} + \frac{\partial g_{\nu\sigma}}{\partial x^\mu} - \frac{\partial g_{\mu\nu}}{\partial x^\sigma} \right),$$

Zelmanov had introduced the chr.inv.-Christoffel symbols of the 2nd rank and 1st rank

$$\Delta_{jk}^i = h^{im} \Delta_{jk,m} = \frac{1}{2} h^{im} \left(\frac{\partial h_{jm}}{\partial x^k} + \frac{\partial h_{km}}{\partial x^j} - \frac{\partial h_{jk}}{\partial x^m} \right),$$

where the only difference is that the chr.inv.-Christoffel symbols use the chr.inv.-metric tensor h_{ik} instead of the fundamental metric tensor $g_{\alpha\beta}$.

It is not a problem to find out how the regular Christoffel symbols are expressed in terms of the physically observable chr.inv.-properties characteristic of the reference space of an observer. Expressing the components of $g^{\alpha\beta}$ and then the 1st derivatives of $g_{\alpha\beta}$ with F_i , A_{ik} , D_{ik} , w , and v_i , after some algebra we obtain

$$\begin{aligned}\Gamma_{00,0} &= -\frac{1}{c^3} \left(1 - \frac{w}{c^2}\right) \frac{\partial w}{\partial t}, \\ \Gamma_{00,i} &= \frac{1}{c^2} \left(1 - \frac{w}{c^2}\right)^2 F_i + \frac{1}{c^4} v_i \frac{\partial w}{\partial t}, \\ \Gamma_{0i,0} &= -\frac{1}{c^2} \left(1 - \frac{w}{c^2}\right) \frac{\partial w}{\partial x^i}, \\ \Gamma_{0i,j} &= -\frac{1}{c} \left(1 - \frac{w}{c^2}\right) \left(D_{ij} + A_{ij} + \frac{1}{c^2} F_j v_i\right) + \frac{1}{c^3} v_j \frac{\partial w}{\partial x^i}, \\ \Gamma_{ij,0} &= \frac{1}{c} \left(1 - \frac{w}{c^2}\right) \left[D_{ij} - \frac{1}{2} \left(\frac{\partial v_j}{\partial x^i} + \frac{\partial v_i}{\partial x^j}\right) + \frac{1}{2c^2} (F_i v_j + F_j v_i)\right], \\ \Gamma_{ij,k} &= -\Delta_{ij,k} + \frac{1}{c^2} \left[v_i A_{jk} + v_j A_{ik} + \frac{1}{2} v_k \left(\frac{\partial v_j}{\partial x^i} + \frac{\partial v_i}{\partial x^j}\right) - \right. \\ &\quad \left. - \frac{1}{2c^2} v_k (F_i v_j + F_j v_i)\right] + \frac{1}{c^4} F_k v_i v_j, \\ \Gamma_{00}^0 &= -\frac{1}{c^3} \left[\frac{1}{1 - \frac{w}{c^2}} \frac{\partial w}{\partial t} + \left(1 - \frac{w}{c^2}\right) v_k F^k\right], \\ \Gamma_{00}^k &= -\frac{1}{c^2} \left(1 - \frac{w}{c^2}\right)^2 F^k, \\ \Gamma_{0i}^0 &= \frac{1}{c^2} \left[-\frac{1}{1 - \frac{w}{c^2}} \frac{\partial w}{\partial x^i} + v_k \left(D_i^k + A_{i \cdot}^k + \frac{1}{c^2} v_i F^k\right)\right], \\ \Gamma_{0i}^k &= \frac{1}{c} \left(1 - \frac{w}{c^2}\right) \left(D_i^k + A_{i \cdot}^k + \frac{1}{c^2} v_i F^k\right), \\ \Gamma_{ij}^0 &= -\frac{1}{c \left(1 - \frac{w}{c^2}\right)} \left\{-D_{ij} + \frac{1}{c^2} v_n \times \right. \\ &\quad \times \left[v_j (D_i^n + A_{i \cdot}^n) + v_i (D_j^n + A_{j \cdot}^n) + \frac{1}{c^2} v_i v_j F^n\right] + \\ &\quad \left. + \frac{1}{2} \left(\frac{\partial v_i}{\partial x^j} + \frac{\partial v_j}{\partial x^i}\right) - \frac{1}{2c^2} (F_i v_j + F_j v_i) - \Delta_{ij}^n v_n\right\}, \\ \Gamma_{ij}^k &= \Delta_{ij}^k - \frac{1}{c^2} \left[v_i (D_j^k + A_{j \cdot}^k) + v_j (D_i^k + A_{i \cdot}^k) + \frac{1}{c^2} v_i v_j F^k\right].\end{aligned}$$

Respectively, some components of the regular Christoffel symbols are linked to the chr.inv.-properties of the observer's

space by the following relations

$$\begin{aligned}D_k^i + A_{k \cdot}^i &= \frac{c}{\sqrt{g_{00}}} \left(\Gamma_{0k}^i - \frac{g_{0k} \Gamma_{00}^i}{g_{00}}\right), \\ F^k &= -\frac{c^2 \Gamma_{00}^k}{g_{00}}, \\ g^{i\alpha} g^{k\beta} \Gamma_{\alpha\beta}^m &= h^{iq} h^{ks} \Delta_{qs}^m.\end{aligned}$$

By analogy with the respective absolute derivatives, Zelmanov had also introduced the chr.inv.-derivatives

$$\begin{aligned}{}^* \nabla_i Q_k &= \frac{{}^* \partial Q_k}{\partial x^i} - \Delta_{ik}^l Q_l, \\ {}^* \nabla_i Q^k &= \frac{{}^* \partial Q^k}{\partial x^i} + \Delta_{il}^k Q^l, \\ {}^* \nabla_i Q_{jk} &= \frac{{}^* \partial Q_{jk}}{\partial x^i} - \Delta_{ij}^l Q_{lk} - \Delta_{ik}^l Q_{jl}, \\ {}^* \nabla_i Q_j^k &= \frac{{}^* \partial Q_j^k}{\partial x^i} - \Delta_{ij}^l Q_l^k + \Delta_{il}^k Q_j^l, \\ {}^* \nabla_i Q^{jk} &= \frac{{}^* \partial Q^{jk}}{\partial x^i} + \Delta_{il}^j Q^{lk} + \Delta_{il}^k Q^{jl}, \\ {}^* \nabla_i Q^i &= \frac{{}^* \partial Q^i}{\partial x^i} + \Delta_{ji}^j Q^i, & \Delta_{ji}^j &= \frac{{}^* \partial \ln \sqrt{h}}{\partial x^i}, \\ {}^* \nabla_i Q^{ji} &= \frac{{}^* \partial Q^{ji}}{\partial x^i} + \Delta_{il}^j Q^{il} + \Delta_{il}^l Q^{ji}, & \Delta_{il}^l &= \frac{{}^* \partial \ln \sqrt{h}}{\partial x^i}.\end{aligned}$$

In particular, they show the following properties of the chr.inv.-metric tensor h_{ik}

$${}^* \nabla_i h_{jk} = 0, \quad {}^* \nabla_i h_j^k = 0, \quad {}^* \nabla_i h^{jk} = 0.$$

Next we give an account of tensor calculus in terms of physical observables (chronometric invariants).

Assume that there is a space (not necessarily metric) in which there is an arbitrary reference frame $\{x^\alpha\}$. Let this space contain an object G determined by n functions f_n of the x^α coordinates. Let us know the transformation rule to calculate these n functions in any other reference frame $\{\tilde{x}^\alpha\}$ in this space. If the n functions f_n and also the transformation rule have been given in the space, then G is a *geometric object*, which in the system $\{x^\alpha\}$ has axial components $f_n(x^\alpha)$, while in any other system $\{\tilde{x}^\alpha\}$ it has components $\tilde{f}_n(\tilde{x}^\alpha)$.

Assume that a tensor object (tensor) of zero rank is any geometric object φ , transformable according to the rule

$$\tilde{\varphi} = \varphi \frac{\partial x^\alpha}{\partial \tilde{x}^\alpha},$$

where the index takes numbers of all coordinate axes one-by-one (this notation is also known as *by-component notation* or *tensor notation*). Any tensor of zero rank has a single component and is called *scalar*.

From a geometric point of view, any scalar is a point to which a certain number is attributed. Therefore, a scalar field is a set of points of the space, which have a common property. For instance, a point mass is a scalar, while a distributed mass (a gas, for instance) makes up a scalar field.

It should be noted that the algebraic notations for a tensor and a tensor field are the same. The field of a tensor in a space is represented as the tensor in a given point of the space, but its presence in other points everywhere in this region of the space is assumed.

Contravariant tensors of the 1st rank A^α are geometric objects with components, transformable according to the rule

$$\tilde{A}^\alpha = A^\mu \frac{\partial \tilde{x}^\alpha}{\partial x^\mu}.$$

From a geometric point of view, such an object is an n -dimensional vector. For instance, the vector of an elementary displacement dx^α is a contravariant tensor of the 1st rank.

Contravariant tensors of the 2nd rank $A^{\alpha\beta}$ are geometric objects transformable according to the rule

$$\tilde{A}^{\alpha\beta} = A^{\mu\nu} \frac{\partial \tilde{x}^\alpha}{\partial x^\mu} \frac{\partial \tilde{x}^\beta}{\partial x^\nu}.$$

From a geometric point of view, such an object is the area (parallelogram) formed by two vectors. For this reason, contravariant tensors of the 2nd rank are also called *bivectors*.

So forth, contravariant tensors of higher ranks are formulated as the following geometric objects

$$\tilde{A}^{\alpha\dots\sigma} = A^{\mu\dots\tau} \frac{\partial \tilde{x}^\alpha}{\partial x^\mu} \dots \frac{\partial \tilde{x}^\sigma}{\partial x^\tau}.$$

A vector field or a higher rank tensor field are space distributions of the respective tensor quantities. For instance, because a mechanical strength characterizes both its own magnitude and direction, its distribution in a physical body can be presented by a vector field.

Covariant tensors of the 1st rank A_α are geometric objects, transformable according to the rule

$$\tilde{A}_\alpha = A_\mu \frac{\partial x^\mu}{\partial \tilde{x}^\alpha}.$$

Thus, the gradient of a scalar field φ , i.e., the quantity

$$A_\alpha = \frac{\partial \varphi}{\partial x^\alpha},$$

is a covariant tensor of the 1st rank. This is because for a regular invariant we have $\tilde{\varphi} = \varphi$, then

$$\frac{\partial \tilde{\varphi}}{\partial \tilde{x}^\alpha} = \frac{\partial \tilde{\varphi}}{\partial x^\mu} \frac{\partial x^\mu}{\partial \tilde{x}^\alpha} = \frac{\partial \varphi}{\partial x^\mu} \frac{\partial x^\mu}{\partial \tilde{x}^\alpha}.$$

Covariant tensors of the 2nd rank $A_{\alpha\beta}$ are geometric objects with the transformation rule

$$\tilde{A}_{\alpha\beta} = A_{\mu\nu} \frac{\partial x^\mu}{\partial \tilde{x}^\alpha} \frac{\partial x^\nu}{\partial \tilde{x}^\beta},$$

hence, covariant tensors of higher ranks are formulated as

$$\tilde{A}_{\alpha\dots\sigma} = A_{\mu\dots\tau} \frac{\partial x^\mu}{\partial \tilde{x}^\alpha} \dots \frac{\partial x^\tau}{\partial \tilde{x}^\sigma}.$$

Mixed tensors are tensors of the 2nd rank or of higher ranks with both upper and lower indices. For instance, any mixed symmetric tensor A^α_β is a geometric object, transformable according to the rule

$$\tilde{A}^\alpha_\beta = A^\mu_\nu \frac{\partial \tilde{x}^\alpha}{\partial x^\mu} \frac{\partial x^\nu}{\partial \tilde{x}^\beta}.$$

Tensor objects exist both in metric and non-metric spaces. In non-metric spaces, as it is known, the distance between any two points cannot be measured. This is in contrast to metric spaces. In the theories of space-time-matter, such as the General Theory of Relativity and its extensions, metric spaces are taken under consideration. This is because the core of such theories is the measurement of time intervals and spatial lengths, that is nonsense in a non-metric space.

Any tensor has a^n components, where a is its dimension and n is the rank. For instance, a four-dimensional tensor of zero rank has 1 component, a tensor of the 1st rank has 4 components, a tensor of the 2nd rank has 16 components, a tensor of the 4th rank (for example, the Riemann-Christoffel curvature tensor) has 256 components, and so on.

Indices in a geometric object, marking its axial components, are found not in tensors only, but in other geometric objects as well. For this reason, if we encounter a quantity in component notation, it is not necessarily a tensor quantity.

In practice, to know whether a given object is a tensor or not, we need to know a formula for this object in a reference frame and to transform it to any other reference frame. For instance, consider the classic question: are Christoffel's symbols (i.e., the coherence coefficients of space) tensors? To answer this question, we need to calculate the Christoffel symbols in a tilde-marked reference frame

$$\tilde{\Gamma}^\alpha_{\mu\nu} = \tilde{g}^{\alpha\sigma} \tilde{\Gamma}_{\mu\nu,\sigma}, \quad \tilde{\Gamma}_{\mu\nu,\sigma} = \frac{1}{2} \left(\frac{\partial \tilde{g}_{\mu\sigma}}{\partial \tilde{x}^\nu} + \frac{\partial \tilde{g}_{\nu\sigma}}{\partial \tilde{x}^\mu} - \frac{\partial \tilde{g}_{\mu\nu}}{\partial \tilde{x}^\sigma} \right)$$

proceeding from the general formula of them in a non-marked reference frame.

First, we calculate the terms in the brackets. The fundamental metric tensor like any other covariant tensor of the 2nd rank, is transformable to the tilde-marked reference frame according to the following rule

$$\tilde{g}_{\mu\sigma} = g_{\varepsilon\tau} \frac{\partial x^\varepsilon}{\partial \tilde{x}^\mu} \frac{\partial x^\tau}{\partial \tilde{x}^\sigma}.$$

Because the quantity $g_{\varepsilon\tau}$ depends on the non-tilde-marked coordinates, its derivative with respect to the tilde-marked coordinates (which are functions of the non-tilded ones) is calculated according to the rule

$$\frac{\partial g_{\varepsilon\tau}}{\partial \tilde{x}^\nu} = \frac{\partial g_{\varepsilon\tau}}{\partial x^\rho} \frac{\partial x^\rho}{\partial \tilde{x}^\nu},$$

and thus the first term in the brackets, taking the rule of transformation of the fundamental metric tensor into account, takes the form

$$\frac{\partial \tilde{g}_{\mu\sigma}}{\partial \tilde{x}^\nu} = \frac{\partial g_{\varepsilon\tau}}{\partial x^\rho} \frac{\partial x^\rho}{\partial \tilde{x}^\nu} \frac{\partial x^\varepsilon}{\partial \tilde{x}^\mu} \frac{\partial x^\tau}{\partial \tilde{x}^\sigma} + g_{\varepsilon\tau} \left(\frac{\partial x^\tau}{\partial \tilde{x}^\sigma} \frac{\partial^2 x^\varepsilon}{\partial \tilde{x}^\nu \partial \tilde{x}^\mu} + \frac{\partial x^\varepsilon}{\partial \tilde{x}^\mu} \frac{\partial^2 x^\tau}{\partial \tilde{x}^\nu \partial \tilde{x}^\sigma} \right).$$

Calculating the rest of the terms of the tilde-marked Christoffel symbols and transposing their free indices we obtain

$$\tilde{\Gamma}_{\mu\nu,\sigma} = \Gamma_{\varepsilon\rho,\tau} \frac{\partial x^\varepsilon}{\partial \tilde{x}^\mu} \frac{\partial x^\rho}{\partial \tilde{x}^\nu} \frac{\partial x^\tau}{\partial \tilde{x}^\sigma} + g_{\varepsilon\tau} \frac{\partial x^\tau}{\partial \tilde{x}^\sigma} \frac{\partial^2 x^\varepsilon}{\partial \tilde{x}^\mu \partial \tilde{x}^\nu},$$

$$\tilde{\Gamma}_{\mu\nu}^\alpha = \Gamma_{\varepsilon\rho}^\gamma \frac{\partial \tilde{x}^\alpha}{\partial x^\gamma} \frac{\partial x^\varepsilon}{\partial \tilde{x}^\mu} \frac{\partial x^\rho}{\partial \tilde{x}^\nu} + \frac{\partial \tilde{x}^\alpha}{\partial x^\gamma} \frac{\partial^2 x^\gamma}{\partial \tilde{x}^\mu \partial \tilde{x}^\nu}.$$

We see that the Christoffel symbols are not transformed in the same way as tensors, hence they are not tensors.

Tensors can be represented as matrices. But in practice, such a form can only be possible for tensors of the 1st or 2nd rank (one-row and flat matrices, respectively). For instance, the tensor of an elementary four-dimensional displacement can be represented in the form of a one-row matrix

$$dx^\alpha = (dx^0, dx^1, dx^2, dx^3),$$

the four-dimensional fundamental metric tensor can be represented in the form of a flat matrix

$$g_{\alpha\beta} = \begin{pmatrix} g_{00} & g_{01} & g_{02} & g_{03} \\ g_{10} & g_{11} & g_{12} & g_{13} \\ g_{20} & g_{21} & g_{22} & g_{23} \\ g_{30} & g_{31} & g_{32} & g_{33} \end{pmatrix},$$

and tensors of the 3rd rank are three-dimensional matrices. Representing tensors of higher ranks as matrices is problematic and not visual.

Now let us turn to tensor algebra, the branch of tensor calculus that focuses on algebraic operations with tensors.

Only same-type tensors of the same rank with indices in the same position can be added or subtracted. Adding up two n -rank tensors of the same type gives a new tensor of the same type and rank, the components of which are the sums of the corresponding components of the added tensors. For instance

$$A^\alpha + B^\alpha = D^\alpha, \quad A_\beta^\alpha + B_\beta^\alpha = D_\beta^\alpha.$$

Multiplication is allowed not only for tensors of the same type, but also for any tensors of any rank. External multiplication of a tensor of the n -rank by a tensor of the m -rank gives a new tensor of the $(n+m)$ -rank

$$A_{\alpha\beta} B_\gamma = D_{\alpha\beta\gamma}, \quad A_\alpha B^{\beta\gamma} = D_\alpha^{\beta\gamma}.$$

Contraction is the multiplication of tensors of the same rank when some of their indices are the same. Contraction of tensors across all indices yields a scalar

$$A_\alpha B^\alpha = C, \quad A_{\alpha\beta}^\gamma B_\gamma^{\alpha\beta} = D.$$

Often the multiplication of tensors entails the contraction of some of their indices. Such multiplication is known as inner multiplication, which means that some indices become contracted when the tensors are multiplied. Below is an example of internal multiplication

$$A_{\alpha\sigma} B^\sigma = D_\alpha, \quad A_{\alpha\sigma}^\gamma B_\gamma^{\beta\sigma} = D_\alpha^\beta.$$

Using internal multiplication of geometric objects we can determine whether they are tensors or not. This is the so-called *fraction theorem*.

FRACTION THEOREM: If $B^{\sigma\beta}$ is a tensor and its internal multiplication with a geometric object $A(\alpha, \sigma)$ is a tensor $D(\alpha, \beta)$, i.e., $A(\alpha, \sigma) B^{\sigma\beta} = D(\alpha, \beta)$, then this object $A(\alpha, \sigma)$ is also a tensor.

According to this theorem, if internal multiplication of an object $A_{\alpha\sigma}$ with a tensor $B^{\sigma\beta}$ gives another tensor D_α^β

$$A_{\alpha\sigma} B^{\sigma\beta} = D_\alpha^\beta,$$

then this object $A_{\alpha\sigma}$ is a tensor. Or, if internal multiplication of an object A_σ^α and a tensor $B^{\sigma\beta}$ gives a tensor $D^{\alpha\beta}$

$$A_\sigma^\alpha B^{\sigma\beta} = D^{\alpha\beta},$$

then the object A_σ^α is a tensor.

The geometric properties of any metric space are determined by its fundamental metric tensor, which can lift and lower the indices in the objects of this metric space. In Riemannian spaces, the space metric has a square form, which is $ds^2 = g_{\alpha\beta} dx^\alpha dx^\beta$ and is known also as the *Riemannian metric*, so the fundamental metric tensor of a Riemannian space is a tensor of the 2nd rank $g_{\alpha\beta}$. The mixed fundamental metric tensor g_α^β is equal to the unit tensor $g_\alpha^\beta = g_{\alpha\sigma} g^{\sigma\beta} = \delta_\alpha^\beta$. The diagonal components of the unit tensor are units, while its rest (non-diagonal) components are zeroes. Using the unit tensor we can replace the indices in four-dimensional quantities

$$\delta_\alpha^\beta A_\beta = A_\alpha, \quad \delta_\mu^\nu \delta_\rho^\sigma A^{\mu\rho} = A^{\nu\sigma}.$$

Contracting any tensor of the 2nd rank with the fundamental metric tensor $g_{\alpha\beta}$ yields a scalar known as the tensor spur or its trace

$$g^{\alpha\beta} A_{\alpha\beta} = A_\sigma^\sigma = A.$$

For example, the spur of the fundamental metric tensor in a four-dimensional pseudo-Riemannian space is 4

$$g_{\alpha\beta} g^{\alpha\beta} = g_\sigma^\sigma = g_0^0 + g_1^1 + g_2^2 + g_3^3 = \delta_0^0 + \delta_1^1 + \delta_2^2 + \delta_3^3 = 4.$$

As mentioned on page 6, the chr.inv.-metric tensor h_{ik} has all properties of the fundamental metric tensor $g_{\alpha\beta}$ throughout the observer's three-dimensional spatial section (his three-dimensional reference space). Therefore, h_{ik} can lower, lift and replace indices in chr.inv.-quantities. Accordingly, the spur (trace) of any three-dimensional chr.inv.-tensor is obtained by contracting it with h_{ik} . For instance, the spur (trace)

of the tensor of the rate of deformations of the observer's space, D_{ik} , is the chr.inv.-scalar

$$D = D_m^m = h^{ik} D_{ik},$$

the physical sense of which is the rate of relative expansion or contraction of the elementary volume of the observer's reference space.

The scalar product of two vectors A^α and B^α (tensors of the 1st rank) in a four-dimensional pseudo-Riemannian space is formulated as

$$g_{\alpha\beta} A^\alpha B^\beta = A_\alpha B^\alpha = A_0 B^0 + A_i B^i.$$

Scalar product is the result of contraction, because the multiplication of vectors contracts all their indices. Therefore, the scalar product of two vectors (tensors of the 1st rank) is always a scalar (tensor of zero rank). If both the vectors are the same, their scalar product

$$g_{\alpha\beta} A^\alpha A^\beta = A_\alpha A^\alpha = A_0 A^0 + A_i A^i$$

is the square of the given vector A^α , the length of which is expressed as

$$A = |A^\alpha| = \sqrt{g_{\alpha\beta} A^\alpha A^\beta}.$$

The four-dimensional pseudo-Riemannian space, which is the space-time of General Relativity, by its definition has the sign-alternating metric, i.e., the fundamental metric tensor has the sign-alternating signature (+---) or (-+++). In this case, the lengths of four-dimensional vectors can be real, imaginary or zero. Vectors with non-zero (real or imaginary) lengths are known as *non-isotropic vectors*; they are tangential to non-isotropic trajectories. Vectors with zero length are known as *isotropic vectors*; they are tangential to isotropic trajectories (trajectories of light-like particles).

In the three-dimensional Euclidean space, the scalar product of two vectors is a scalar quantity, the numerical value of which is equal to the product of their lengths and the cosine of the angle between them

$$A_i B^i = |A^i| |B^i| \cos(A^i; B^i).$$

From the above formula it follows that the scalar product of two vectors is zero, if the vectors are orthogonal to each other. In other words, from a geometric point of view, the scalar product of two vectors is the projection of one vector onto the other. If the vectors are the same, then the vector is projected onto itself, so the result of this projection is the square of its length.

Theoretically, at each point of any Riemannian space, a tangential flat space can be set, the basis vectors of which are tangential to the basis vectors of the Riemannian space at this point. Then, the metric of the tangential flat space is also the metric of the Riemannian space at this point. Therefore, the

above formula is also true, if we consider the angle between the three-dimensional coordinate lines and the time lines in the space thereby replacing the Roman (three-dimensional spatial) indices with the Greek (four-dimensional) ones.

Denote the chr.inv.-projections of arbitrary vectors A^α and B^α onto the time line and the three-dimensional spatial section of an observer as follows

$$a = \frac{A_0}{\sqrt{g_{00}}}, \quad a^i = A^i,$$

$$b = \frac{B_0}{\sqrt{g_{00}}}, \quad b^i = B^i,$$

then their remaining components have the form

$$A^0 = \frac{a + \frac{1}{c} v_i a^i}{1 - \frac{w}{c^2}}, \quad A_i = -a_i - \frac{a}{c} v_i,$$

$$B^0 = \frac{b + \frac{1}{c} v_i b^i}{1 - \frac{w}{c^2}}, \quad B_i = -b_i - \frac{b}{c} v_i.$$

Substituting the chr.inv.-projections of the vectors A^α and B^α into the formulae for $A_\alpha B^\alpha$ and $A_\alpha A^\alpha$, we obtain

$$A_\alpha B^\alpha = ab - a_i b^i = ab - h_{ik} a^i b^k,$$

$$A_\alpha A^\alpha = a^2 - a_i a^i = a^2 - h_{ik} a^i a^k.$$

From here, we see that the square of the length of any vector is the difference between the squares of the lengths of its time and spatial chr.inv.-projections. If both these projections are the same, then the vector's length is zero, so the vector is isotropic. Hence, any isotropic vector equally belongs to the time line and the spatial section. The equality of its time projection to its spatial projection also means that this vector is orthogonal to itself. If its time projection is "longer" than its spatial projection, then this vector is real. If the spatial projection is "longer", then this vector is imaginary.

The latter can be illustrated by the square of the length of the space-time interval

$$ds^2 = g_{\alpha\beta} dx^\alpha dx^\beta = dx_\alpha dx^\alpha = dx_0 dx^0 + dx_i dx^i,$$

which in terms of chr.inv.-quantities has the form

$$ds^2 = c^2 d\tau^2 - dx_i dx^i = c^2 d\tau^2 - h_{ik} dx^i dx^k = c^2 d\tau^2 - d\sigma^2.$$

Its length ds can be real, imaginary or zero, depending on whether ds is time-like $c^2 d\tau^2 > d\sigma^2$, which is the case along sublight-speed real trajectories, space-like $c^2 d\tau^2 < d\sigma^2$, which is the case of imaginary superluminal-speed trajectories, or isotropic $c^2 d\tau^2 = d\sigma^2$, which is the case of light-like (isotropic) trajectories, respectively.

The vector product of two vectors A^α and B^α is a tensor of the 2nd rank $V^{\alpha\beta}$, obtained from their external multiplication according to the rule

$$V^{\alpha\beta} = [A^\alpha; B^\beta] = \frac{1}{2} (A^\alpha B^\beta - A^\beta B^\alpha) = \frac{1}{2} \begin{vmatrix} A^\alpha & A^\beta \\ B^\alpha & B^\beta \end{vmatrix}.$$

As it is easy to see, in this case the order in which the vectors are multiplied matters, i.e., the order in which we write down the tensor indices is important. For this reason, the tensors obtained as vector products are called *antisymmetric tensors*. In an antisymmetric tensor we have $V^{\alpha\beta} = -V^{\beta\alpha}$, where its indices being moved “reserve” their places as dots, $g_{\alpha\sigma} V^{\sigma\beta} = V_{\alpha}^{\cdot\beta}$, thereby showing the place from where the specific index was moved. In symmetric tensors there is no need to “reserve” places for moved indices, because the order in which they appear does not matter. For example, the fundamental metric tensor is symmetric $g_{\alpha\beta} = g_{\beta\alpha}$, and the Riemann-Christoffel tensor of the curvature of space $R^{\alpha\cdots}_{\cdot\beta\gamma\delta}$ is symmetric with respect to transposition over a pair of its indices and antisymmetric within each pair of the indices. It is obvious that only tensors of the 2nd rank or higher ranks can be symmetric or antisymmetric.

All diagonal components of any antisymmetric tensor by its definition are zeroes. For instance, in an antisymmetric tensor of the 2nd rank we have

$$V^{\alpha\alpha} = [A^\alpha; B^\alpha] = \frac{1}{2}(A^\alpha B^\alpha - A^\alpha B^\alpha) = 0.$$

In the three-dimensional Euclidean space, the numerical value of the vector product of two vectors is defined as the area of the parallelogram formed by them and is equal to the product of their moduli multiplied by the sine of the angle between them

$$V^{ik} = |A^i||B^k| \sin(A^i; B^k).$$

This means that the vector product of two vectors, i.e., any antisymmetric tensor of the 2nd rank, is a pad oriented in space according to the directions of the vectors forming it.

The contraction of an antisymmetric tensor $V_{\alpha\beta}$ with any symmetric tensor $A^{\alpha\beta} = A^\alpha A^\beta$ is zero. Naturally, since $V_{\alpha\alpha} = 0$ and $V_{\alpha\beta} = -V_{\beta\alpha}$ we have

$$V_{\alpha\beta} A^\alpha A^\beta = V_{00} A^0 A^0 + V_{0i} A^0 A^i + V_{i0} A^i A^0 + V_{ik} A^i A^k = 0.$$

According to the theory of chronometric invariants, an antisymmetric tensor of the 2nd rank $V^{\alpha\beta}$ has the following chr.inv.-projections

$$\begin{aligned} \frac{V_{00}}{g_{00}} &= 0, \\ \frac{V_{0\cdot}^i}{\sqrt{g_{00}}} &= -\frac{V_{\cdot 0}^i}{\sqrt{g_{00}}} = \frac{1}{2}(ab^i - ba^i), \\ V^{ik} &= \frac{1}{2}(a^i b^k - a^k b^i), \end{aligned}$$

which are expressed here with the chr.inv.-projections of its forming (multiplied) vectors A^α and B^α : here a and b are the chr.inv.-projections of the multiplied vectors A^α and B^α onto the time line of the observer, and a^i and b^i are their chr.inv.-projections onto the observer’s spatial section (which is his three-dimensional reference space).

The first chr.inv.-projection of the antisymmetric tensor $V^{\alpha\beta}$ is zero, since in any antisymmetric tensor all its diagonal components are zeroes. The third physically observable chr.inv.-quantity V^{ik} is the projection of the tensor $V^{\alpha\beta}$ onto the observer’s spatial section. It is analogous to a vector product in the three-dimensional space. The second chr.inv.-quantity of the above is the space-time (mixed) projection of $V^{\alpha\beta}$. It has no equivalent among the components of a regular three-dimensional vector product.

The square of an antisymmetric tensor of the 2nd rank $V^{\alpha\beta}$, formulated with the chr.inv.-projections of its forming vectors A^α and B^α , is calculated as

$$\begin{aligned} V_{\alpha\beta} V^{\alpha\beta} &= \frac{1}{2}(a_i a^i b_k b^k - a_i b^i a_k b^k) + \\ &+ ab a_i b^i - \frac{1}{2}(a^2 b_i b^i - b^2 a_i a^i). \end{aligned}$$

The asymmetry of tensor fields is determined by reference antisymmetric tensors. Such references in the Galilean reference frame* are Levi-Civita’s tensors: for four-dimensional quantities this is the four-dimensional completely antisymmetric unit tensor $e^{\alpha\beta\mu\nu}$, while for three-dimensional quantities this is the three-dimensional completely antisymmetric unit tensor e^{ikm} . The components of the Levi-Civita tensors, which have all indices different, are either +1 or -1 depending on the number of transpositions of their indices. All the remaining components, i.e., those having at least two coinciding indices, are zeroes. Moreover, with the space signature (+---) we are using, all non-zero contravariant components of the Levi-Civita tensors have the opposite sign to their corresponding covariant components†. For instance, in the Minkowski space we have

$$\begin{aligned} g_{\alpha\sigma} g_{\beta\rho} g_{\mu\tau} g_{\nu\gamma} e^{\sigma\rho\tau\gamma} &= g_{00} g_{11} g_{22} g_{33} e^{0123} = -e^{0123}, \\ g_{i\alpha} g_{k\beta} g_{m\gamma} e^{\alpha\beta\gamma} &= g_{11} g_{22} g_{33} e^{123} = -e^{123}, \end{aligned}$$

since $g_{00} = 1$ and $g_{11} = g_{22} = g_{33} = -1$ with the space signature (+---) we are using. In this case, the components of the tensor $e^{\alpha\beta\mu\nu}$ are

$$\begin{aligned} e^{0123} &= +1, & e^{1023} &= -1, & e^{1203} &= +1, & e^{1230} &= -1, \\ e^{0123} &= -1, & e_{1023} &= +1, & e_{1203} &= -1, & e_{1230} &= +1, \end{aligned}$$

and the components of the tensor e^{ikm} are

$$\begin{aligned} e^{123} &= +1, & e^{213} &= -1, & e^{231} &= +1, \\ e_{123} &= -1, & e_{213} &= +1, & e_{231} &= -1. \end{aligned}$$

*A Galilean reference frame is one that does not rotate, is not subject to deformation, and falls freely in the space-time of Special Relativity (Minkowski space). The time lines in the Galilean reference frame are linear, as are the three-dimensional coordinate axes.

†If the space signature is (++++), then what has been said is true only for the four-dimensional Levi-Civita tensor $e^{\alpha\beta\mu\nu}$. The components of the three-dimensional Levi-Civita tensor e^{ikm} will have the same sign as well as the corresponding components of the e_{ikm} tensor.

In general, the tensor $e^{\alpha\beta\mu\nu}$ is related to the tensor e^{ikm} as follows $e^{0ikm} = e^{ikm}$. Because we have an arbitrary choice for the sign of the first component, we can choose $e^{0123} = -1$ and $e^{123} = -1$. Then the remaining components of e^{ikm} will change respectively.

Multiplying the four-dimensional antisymmetric unit tensor $e^{\alpha\beta\mu\nu}$ by itself we obtain a regular tensor of the 8th rank with the non-zero components determined by the matrix

$$e^{\alpha\beta\mu\nu} e_{\sigma\tau\rho\gamma} = - \begin{pmatrix} \delta_{\sigma}^{\alpha} & \delta_{\tau}^{\alpha} & \delta_{\rho}^{\alpha} & \delta_{\gamma}^{\alpha} \\ \delta_{\sigma}^{\beta} & \delta_{\tau}^{\beta} & \delta_{\rho}^{\beta} & \delta_{\gamma}^{\beta} \\ \delta_{\sigma}^{\mu} & \delta_{\tau}^{\mu} & \delta_{\rho}^{\mu} & \delta_{\gamma}^{\mu} \\ \delta_{\sigma}^{\nu} & \delta_{\tau}^{\nu} & \delta_{\rho}^{\nu} & \delta_{\gamma}^{\nu} \end{pmatrix}.$$

The remaining properties of the tensor $e^{\alpha\beta\mu\nu}$ are deduced from the previous by means of contraction of their indices

$$e^{\alpha\beta\mu\nu} e_{\sigma\tau\rho\nu} = - \begin{pmatrix} \delta_{\sigma}^{\alpha} & \delta_{\tau}^{\alpha} & \delta_{\rho}^{\alpha} \\ \delta_{\sigma}^{\beta} & \delta_{\tau}^{\beta} & \delta_{\rho}^{\beta} \\ \delta_{\sigma}^{\mu} & \delta_{\tau}^{\mu} & \delta_{\rho}^{\mu} \end{pmatrix},$$

$$e^{\alpha\beta\mu\nu} e_{\sigma\tau\mu\nu} = -2 \begin{pmatrix} \delta_{\sigma}^{\alpha} & \delta_{\tau}^{\alpha} \\ \delta_{\sigma}^{\beta} & \delta_{\tau}^{\beta} \end{pmatrix} = -2 (\delta_{\sigma}^{\alpha} \delta_{\tau}^{\beta} - \delta_{\sigma}^{\beta} \delta_{\tau}^{\alpha}),$$

$$e^{\alpha\beta\mu\nu} e_{\sigma\beta\mu\nu} = -6 \delta_{\sigma}^{\alpha}, \quad e^{\alpha\beta\mu\nu} e_{\alpha\beta\mu\nu} = -6 \delta_{\alpha}^{\alpha} = -24.$$

Multiplying the three-dimensional antisymmetric unit tensor e^{ikm} by itself we obtain a regular tensor of the 6th rank

$$e^{ikm} e_{rst} = \begin{pmatrix} \delta_r^i & \delta_s^i & \delta_t^i \\ \delta_r^k & \delta_s^k & \delta_t^k \\ \delta_r^m & \delta_s^m & \delta_t^m \end{pmatrix}.$$

The remaining properties of the tensor e^{ikm} are

$$e^{ikm} e_{rsm} = - \begin{pmatrix} \delta_r^i & \delta_s^i \\ \delta_r^k & \delta_s^k \end{pmatrix} = \delta_s^i \delta_r^k - \delta_r^i \delta_s^k,$$

$$e^{ikm} e_{rkm} = 2 \delta_r^i, \quad e^{ikm} e_{ikm} = 2 \delta_i^i = 6.$$

The completely antisymmetric unit tensor determines for a tensor object its corresponding *pseudotensor*, marked with asterisk. For instance, any four-dimensional scalar, vector and tensors of the 2nd, 3rd, and 4th ranks have corresponding four-dimensional pseudotensors of the following ranks

$$V^{*\alpha\beta\mu\nu} = e^{\alpha\beta\mu\nu} V, \quad V^{*\alpha\beta\mu} = e^{\alpha\beta\mu\nu} V_{\nu}, \quad V^{*\alpha\beta} = \frac{1}{2} e^{\alpha\beta\mu\nu} V_{\mu\nu},$$

$$V^{*\alpha} = \frac{1}{6} e^{\alpha\beta\mu\nu} V_{\beta\mu\nu}, \quad V^* = \frac{1}{24} e^{\alpha\beta\mu\nu} V_{\alpha\beta\mu\nu},$$

where pseudotensors of the 1st rank, such as $V^{*\alpha}$, are called *pseudovectors*, while pseudotensors of zero rank, such as V^* , are called *pseudoscalars*. Any tensor and its corresponding pseudotensor are known as *dual* to each other to emphasize

their common genesis. So, three-dimensional antisymmetric tensors have their corresponding three-dimensional pseudotensors

$$V^{*ikm} = e^{ikm} V, \quad V^{*ik} = e^{ikm} V_m,$$

$$V^{*i} = \frac{1}{2} e^{ikm} V_{km}, \quad V^* = \frac{1}{6} e^{ikm} V_{ikm}.$$

Pseudotensors are called such because, in contrast to regular tensors, they do not change when reflected with respect to one of the coordinate axes. For instance, when reflected with respect to the abscissa axis $x^1 = -\tilde{x}^1$, $x^2 = \tilde{x}^2$, $x^3 = \tilde{x}^3$, the reflected component of an antisymmetric tensor V_{ik} , orthogonal to x^1 , is $\tilde{V}_{23} = -V_{23}$, while the dual component of the pseudovector V^{*i} retains the original sign unchanged

$$V^{*1} = \frac{1}{2} e^{1km} V_{km} = \frac{1}{2} (e^{123} V_{23} + e^{132} V_{32}) = V_{23},$$

$$\tilde{V}^{*1} = \frac{1}{2} \tilde{e}^{1km} \tilde{V}_{km} = \frac{1}{2} e^{k1m} \tilde{V}_{km} = \frac{1}{2} (e^{213} \tilde{V}_{23} + e^{312} \tilde{V}_{32}) = V_{23}.$$

Since any four-dimensional antisymmetric tensor of the 2nd rank and its dual pseudotensor are of the same rank, their contraction yields a pseudoscalar, which is

$$V_{\alpha\beta} V^{*\alpha\beta} = V_{\alpha\beta} e^{\alpha\beta\mu\nu} V_{\mu\nu} = e^{\alpha\beta\mu\nu} B_{\alpha\beta\mu\nu} = B^*.$$

The square of a pseudotensor $V^{*\alpha\beta}$ and a pseudovector V^{*i} , expressed with their dual tensors, are

$$V_{\alpha\beta} V^{*\alpha\beta} = e_{\alpha\beta\mu\nu} V^{\mu\nu} e^{\alpha\beta\rho\sigma} V_{\rho\sigma} = -24 V_{\mu\nu} V^{\mu\nu},$$

$$V_{*i} V^{*i} = e_{ikm} V^{km} e^{ipq} V_{pq} = 6 V_{km} V^{km}.$$

We cannot set a Galilean reference frame in an inhomogeneous and anisotropic pseudo-Riemannian space. In such a general space, the antisymmetry references of tensor fields depend on the inhomogeneity and anisotropy of the space itself, which are determined by the fundamental metric tensor, and a reference antisymmetric tensor is the four-dimensional completely antisymmetric discriminant tensor

$$E^{\alpha\beta\mu\nu} = \frac{e^{\alpha\beta\mu\nu}}{\sqrt{-g}}, \quad E_{\alpha\beta\mu\nu} = e_{\alpha\beta\mu\nu} \sqrt{-g}.$$

The proof is the following. Transformation of the four-dimensional completely antisymmetric unit tensor $e_{\alpha\beta\mu\nu}$ from a Galilean (non-tilde-marked) reference frame into an arbitrary (tilde-marked) reference frame is

$$\tilde{e}_{\alpha\beta\mu\nu} = \frac{\partial x^{\sigma}}{\partial \tilde{x}^{\alpha}} \frac{\partial x^{\gamma}}{\partial \tilde{x}^{\beta}} \frac{\partial x^{\epsilon}}{\partial \tilde{x}^{\mu}} \frac{\partial x^{\tau}}{\partial \tilde{x}^{\nu}} e_{\sigma\gamma\epsilon\tau} = J e_{\alpha\beta\mu\nu},$$

where

$$J = \det \left\| \frac{\partial x^{\alpha}}{\partial \tilde{x}^{\sigma}} \right\| = \det \begin{pmatrix} \frac{\partial x^0}{\partial \tilde{x}^0} & \frac{\partial x^0}{\partial \tilde{x}^1} & \frac{\partial x^0}{\partial \tilde{x}^2} & \frac{\partial x^0}{\partial \tilde{x}^3} \\ \frac{\partial x^1}{\partial \tilde{x}^0} & \frac{\partial x^1}{\partial \tilde{x}^1} & \frac{\partial x^1}{\partial \tilde{x}^2} & \frac{\partial x^1}{\partial \tilde{x}^3} \\ \frac{\partial x^2}{\partial \tilde{x}^0} & \frac{\partial x^2}{\partial \tilde{x}^1} & \frac{\partial x^2}{\partial \tilde{x}^2} & \frac{\partial x^2}{\partial \tilde{x}^3} \\ \frac{\partial x^3}{\partial \tilde{x}^0} & \frac{\partial x^3}{\partial \tilde{x}^1} & \frac{\partial x^3}{\partial \tilde{x}^2} & \frac{\partial x^3}{\partial \tilde{x}^3} \end{pmatrix}$$

is the determinant of Jacobi's matrix known also as the Jacobian of the transformation. Because the fundamental metric tensor $g_{\alpha\beta}$ is transformable according to the rule

$$\tilde{g}_{\alpha\beta} = g_{\mu\nu} \frac{\partial x^\mu}{\partial \tilde{x}^\alpha} \frac{\partial x^\nu}{\partial \tilde{x}^\beta}$$

and since its determinant in the tilde-marked frame is

$$\tilde{g} = \det \left\| g_{\mu\nu} \frac{\partial x^\mu}{\partial \tilde{x}^\alpha} \frac{\partial x^\nu}{\partial \tilde{x}^\beta} \right\| = J^2 g,$$

then, in the Galilean (non-tilde-marked) reference frame,

$$g = \det \|g_{\alpha\beta}\| = \det \begin{vmatrix} 1 & 0 & 0 & 0 \\ 0 & -1 & 0 & 0 \\ 0 & 0 & -1 & 0 \\ 0 & 0 & 0 & -1 \end{vmatrix} = -1,$$

and, hence, $J^2 = -\tilde{g}^2$. Denoting $\tilde{\varepsilon}_{\alpha\beta\mu\nu}$ in an arbitrary reference frame as $E_{\alpha\beta\mu\nu}$ and writing down the metric tensor in a regular non-tilde-marked form, we obtain

$$E_{\alpha\beta\mu\nu} = e_{\alpha\beta\mu\nu} \sqrt{-g}$$

as expected at the very beginning, which was to be proved. In the same way, we obtain the transformation rule

$$E^{\alpha\beta\mu\nu} = \frac{e^{\alpha\beta\mu\nu}}{\sqrt{-g}}$$

for the components $E^{\alpha\beta\mu\nu}$, because for them

$$g = \tilde{g} \tilde{J}^2, \quad \tilde{J} = \det \left\| \frac{\partial \tilde{x}^\alpha}{\partial x^\sigma} \right\|.$$

The discriminant tensor $E^{\alpha\beta\mu\nu}$ is not a physical observable quantity. For this reason, Zelmanov had introduced the four-dimensional discriminant tensor $\varepsilon^{\alpha\beta\gamma}$

$$\varepsilon^{\alpha\beta\gamma} = h_\mu^\alpha h_\nu^\beta h_\rho^\gamma b_\sigma E^{\sigma\mu\nu\rho} = b_\sigma E^{\sigma\alpha\beta\gamma},$$

$$\varepsilon_{\alpha\beta\gamma} = h_\alpha^\mu h_\beta^\nu h_\gamma^\rho b^\sigma E_{\sigma\mu\nu\rho} = b^\sigma E_{\sigma\alpha\beta\gamma},$$

which in the accompanying reference frame of an observer ($b^i = 0$) and taking into account that $\sqrt{-g} = \sqrt{h} \sqrt{g_{00}}$ according to the theory of chronometric invariants transforms into the three-dimensional chr.inv.-discriminant tensor ε^{ikm}

$$\varepsilon^{ikm} = b_0 E^{0ikm} = \sqrt{g_{00}} E^{0ikm} = \frac{e^{ikm}}{\sqrt{h}},$$

$$\varepsilon_{ikm} = b^0 E_{0ikm} = \frac{E_{0ikm}}{\sqrt{g_{00}}} = e_{ikm} \sqrt{h},$$

for which, as is easy to obtain, we have

$${}^* \nabla_l \varepsilon_{ijk} = 0, \quad {}^* \nabla_l \varepsilon^{ijk} = 0,$$

$$\frac{{}^* \partial \varepsilon_{ijk}}{\partial t} = \varepsilon_{ijk} D, \quad \frac{{}^* \partial \varepsilon^{ijk}}{\partial t} = -\varepsilon^{ijk} D,$$

where D is the spur (trace) of the chr.inv.-tensor D_{ik} characterizing the rate of deformations of the observer's space

$$D = h^{ik} D_{ik} = D_n^n = \frac{{}^* \partial \ln \sqrt{h}}{\partial t}, \quad h = \det \|h_{ik}\|.$$

The three-dimensional chr.inv.-discriminant tensor ε^{ikm} is the physical observable reference of the asymmetry of tensor fields in the observer's reference space. Using the ε^{ikm} , we can transform antisymmetric chr.inv.-tensors into the corresponding chr.inv.-pseudotensors.

For example, for the chr.inv.-tensor A_{ik} of the angular velocity of rotation of the observer's space, we have the chr.inv.-pseudovector Ω^{*i} of this rotation

$$\Omega^{*i} = \frac{1}{2} \varepsilon^{ikm} A_{km}, \quad \Omega_{*i} = \frac{1}{2} \varepsilon_{imn} A^{mn}, \quad A^{ik} = \varepsilon^{mik} \Omega_{*m},$$

$$\varepsilon^{ipq} \Omega_{*i} = \frac{1}{2} \varepsilon^{ipq} \varepsilon_{imn} A^{mn} = \frac{1}{2} (\delta_m^p \delta_n^q - \delta_m^q \delta_n^p) A^{mn} = A^{pq}.$$

With the chr.inv.-pseudovector Ω^{*i} the Zelmanov identities (page 7) connecting the chr.inv.-quantities F_i and A_{ik} take the form, respectively,

$$\frac{2}{\sqrt{h}} \frac{{}^* \partial}{\partial t} (\sqrt{h} \Omega^{*i}) + \varepsilon^{ijk} {}^* \nabla_j F_k = 0,$$

$${}^* \nabla_k \Omega^{*k} + \frac{1}{c^2} F_k \Omega^{*k} = 0.$$

Next we consider the absolute differential and absolute directional derivative.

In geometry, a *differential* of a function is its variation between two infinitely close points with the coordinates x^α and $x^\alpha + dx^\alpha$. Respectively, the *absolute differential* in an n -dimensional space represents the change of an n -dimensional quantity between two infinitely close points in this space. For continuous functions, which we commonly deal with in practice, their variations between infinitely close points are infinitesimal. But in order to determine an infinitesimal variation of a tensor quantity, we cannot use a simple "difference" between its numerical values at the neighbouring points x^α and $x^\alpha + dx^\alpha$, because tensor algebra does not determine it. This ratio can only be determined using the rules for transforming tensors from one reference frame to another. As a consequence, differential operators and the results of their application to tensors must be tensors.

For instance, the absolute differential of a tensor quantity is a tensor of the same rank as the original tensor itself. The absolute differential of a scalar φ is the scalar

$$D\varphi = \frac{\partial \varphi}{\partial x^\alpha} dx^\alpha,$$

which in the accompanying reference frame of an observer ($b^i = 0$) takes the form

$$D\varphi = \frac{{}^* \partial \varphi}{\partial t} d\tau + \frac{{}^* \partial \varphi}{\partial x^i} dx^i,$$

where, apart from the three-dimensional observable differential (second term), there is an additional term that takes into account the dependence of the absolute differential $D\varphi$ on the physically observable time interval $d\tau$.

The absolute differential of a contravariant vector A^α is formulated with the absolute derivation operator ∇ (nabla) and has the following form

$$\begin{aligned} DA^\alpha &= \nabla_\sigma A^\alpha dx^\sigma = \frac{\partial A^\alpha}{\partial x^\sigma} dx^\sigma + \Gamma_{\mu\sigma}^\alpha A^\mu dx^\sigma = \\ &= dA^\alpha + \Gamma_{\mu\sigma}^\alpha A^\mu dx^\sigma, \end{aligned}$$

where $\nabla_\sigma A^\alpha$ is the absolute derivative of A^α with respect to x^σ , and d stands for regular differentials

$$\begin{aligned} \nabla_\sigma A^\alpha &= \frac{\partial A^\alpha}{\partial x^\sigma} + \Gamma_{\mu\sigma}^\alpha A^\mu, \\ d &= \frac{\partial}{\partial x^\alpha} dx^\alpha. \end{aligned}$$

Formulating the absolute differential with physical observable quantities is equivalent to projecting its general covariant form onto the time line and the spatial section in the accompanying reference frame of an observer. According to the theory of chronometric invariants, the physically observable chr.inv.-projections of the absolute differential of a vector A^α are the quantities

$$T = b_\alpha DA^\alpha = \frac{g_{0\alpha} DA^\alpha}{\sqrt{g_{00}}}, \quad B^i = h_\alpha^i DA^\alpha.$$

Denoting the chr.inv.-projections of the vector A^α as

$$\varphi = \frac{A_0}{\sqrt{g_{00}}}, \quad q^i = A^i,$$

we calculate its remaining components, which, when expressed in terms of the φ and q^i take the form

$$A_0 = \varphi \left(1 - \frac{w}{c^2}\right), \quad A^0 = \frac{\varphi + \frac{1}{c} v_i q^i}{1 - \frac{w}{c^2}}, \quad A_i = -q_i - \frac{\varphi}{c} v_i.$$

Taking the chr.inv.-formula for the regular differential

$$d = \frac{*}{\partial t} d\tau + \frac{*}{\partial x^i} dx^i$$

into account, we substitute them and also the regular Christoffel symbols expressed in terms of chr.inv.-quantities (see page 10) into the T and B^i . As a result we obtain the chr.inv.-projections of the absolute differential of the vector A^α in the final chr.inv.-form

$$\begin{aligned} T &= b_\alpha DA^\alpha = d\varphi + \frac{1}{c} (-F_i q^i d\tau + D_{ik} q^i dx^k), \\ B^i &= h_\sigma^i DA^\sigma = dq^i + \left(\frac{\varphi}{c} dx^k + q^k d\tau\right) (D_k^i + A_{k.}^i) - \\ &\quad - \frac{\varphi}{c} F^i d\tau + \Delta_{mk}^i q^m dx^k. \end{aligned}$$

The *directional derivative* of a function is its change with respect to the elementary displacement along the given direction. The *absolute directional derivative* in an n -dimensional space is the change of an n -dimensional quantity with respect to an elementary n -dimensional interval along the given direction in the space.

For instance, the absolute derivative of a scalar function φ to a direction along a curve $x^\alpha = x^\alpha(\rho)$, where ρ is a non-zero monotone parameter along this curve, expresses the rate at which this function φ changes

$$\frac{D\varphi}{d\rho} = \frac{d\varphi}{d\rho},$$

which in the accompanying reference frame of an observer is

$$\frac{D\varphi}{d\rho} = \frac{*}{\partial t} \frac{d\varphi}{d\rho} + \frac{*}{\partial x^i} \frac{d\varphi}{d\rho} dx^i.$$

The absolute derivative of a vector A^α to the given direction tangential to a curve $x^\alpha = x^\alpha(\rho)$ is

$$\frac{DA^\alpha}{d\rho} = \nabla_\sigma A^\alpha \frac{dx^\sigma}{d\rho} = \frac{dA^\alpha}{d\rho} + \Gamma_{\mu\sigma}^\alpha A^\mu \frac{dx^\sigma}{d\rho},$$

and its chr.inv.-projections are

$$\begin{aligned} b_\alpha \frac{DA^\alpha}{d\rho} &= \frac{d\varphi}{d\rho} + \frac{1}{c} \left(-F_i q^i \frac{d\tau}{d\rho} + D_{ik} q^i \frac{dx^k}{d\rho}\right), \\ h_\sigma^i \frac{DA^\sigma}{d\rho} &= \frac{dq^i}{d\rho} + \left(\frac{\varphi}{c} \frac{dx^k}{d\rho} + q^k \frac{d\tau}{d\rho}\right) (D_k^i + A_{k.}^i) - \\ &\quad - \frac{\varphi}{c} F^i \frac{d\tau}{d\rho} + \Delta_{mk}^i q^m \frac{dx^k}{d\rho}. \end{aligned}$$

The equations of motion of a particle are based on the absolute directional derivative of the particle's world vector. For this reason, the above chr.inv.-projections are the "generic" chr.inv.-equations of motion.

The *divergence* of a tensor field is its "change" along a coordinate axis. Respectively, the *absolute divergence* of an n -dimensional tensor field is its divergence in an n -dimensional space. The divergence of a tensor field is the result of contraction of the field tensor with the absolute derivation operator ∇ . The divergence of a vector field A^α is the scalar

$$\nabla_\sigma A^\sigma = \frac{\partial A^\sigma}{\partial x^\sigma} + \Gamma_{\sigma\mu}^\sigma A^\mu,$$

and the divergence of a field of a 2nd rank tensor, say the tensor $F^{\alpha\beta}$, is the vector

$$\nabla_\sigma F^{\sigma\alpha} = \frac{\partial F^{\sigma\alpha}}{\partial x^\sigma} + \Gamma_{\sigma\mu}^\sigma F^{\alpha\mu} + \Gamma_{\sigma\mu}^\alpha F^{\sigma\mu},$$

where, as it can be proved, $\Gamma_{\sigma\mu}^\sigma$ is

$$\Gamma_{\sigma\mu}^\sigma = \frac{\partial \ln \sqrt{-g}}{\partial x^\mu}.$$

To prove this, we use the definition of the regular Christoffel symbols (see page 9), which, when re-written with the above indices has the form

$$\Gamma_{\sigma\mu}^{\sigma} = g^{\sigma\rho} \Gamma_{\mu\sigma,\rho} = \frac{1}{2} g^{\sigma\rho} \left(\frac{\partial g_{\mu\rho}}{\partial x^{\sigma}} + \frac{\partial g_{\sigma\rho}}{\partial x^{\mu}} - \frac{\partial g_{\mu\sigma}}{\partial x^{\rho}} \right),$$

where, since σ and ρ are free indices here, they can change their sites. As a result, after contracting with the tensor $g^{\sigma\rho}$ the first and the last terms of the above formula for $\Gamma_{\sigma\mu}^{\sigma}$ cancel each other, so the formula for $\Gamma_{\sigma\mu}^{\sigma}$ simplifies as

$$\Gamma_{\sigma\mu}^{\sigma} = \frac{1}{2} g^{\sigma\rho} \frac{\partial g_{\sigma\rho}}{\partial x^{\mu}}.$$

The quantities $g^{\sigma\rho}$ are the components of a tensor reciprocal to the tensor $g_{\sigma\rho}$. For this reason, each component of the matrix $g^{\sigma\rho}$ is formulated as

$$g^{\sigma\rho} = \frac{a^{\sigma\rho}}{g}, \quad g = \det \|g_{\sigma\rho}\|,$$

where $a^{\sigma\rho}$ is the algebraic co-factor of the matrix element with indices $\sigma\rho$, equal to $(-1)^{\sigma+\rho}$, multiplied by the determinant of the matrix obtained by crossing the row and the column with numbers σ and ρ out of the matrix $g_{\sigma\rho}$. As a result, we obtain $a^{\sigma\rho} = g g^{\sigma\rho}$.

Because the determinant of the fundamental metric tensor by definition is formulated as

$$g = \det \|g_{\sigma\rho}\| = \sum_{\alpha_0 \dots \alpha_3} (-1)^{N(\alpha_0 \dots \alpha_3)} g_{0(\alpha_0)} g_{1(\alpha_1)} g_{2(\alpha_2)} g_{3(\alpha_3)},$$

then the quantity dg is $dg = a^{\sigma\rho} dg_{\sigma\rho} = g g^{\sigma\rho} dg_{\sigma\rho}$, or

$$\frac{dg}{g} = g^{\sigma\rho} dg_{\sigma\rho}.$$

Integrating the left hand side gives $\ln(-g)$, because the g is negative while logarithm is determined for only positive functions. Then, we have $d \ln(-g) = \frac{dg}{g}$. Taking into account that $\sqrt{-g} = \frac{1}{2} \ln(-g)$, we obtain

$$d \ln \sqrt{-g} = \frac{1}{2} g^{\sigma\rho} dg_{\sigma\rho},$$

so the above $\Gamma_{\sigma\mu}^{\sigma}$ takes the form

$$\Gamma_{\sigma\mu}^{\sigma} = \frac{1}{2} g^{\sigma\rho} \frac{\partial g_{\sigma\rho}}{\partial x^{\mu}} = \frac{\partial \ln \sqrt{-g}}{\partial x^{\mu}},$$

which was to be proved.

The divergence of a vector field A^{α} is a scalar quantity. Hence $\nabla_{\sigma} A^{\sigma}$ cannot be projected onto a time line and a spatial section. But this is enough to express $\nabla_{\sigma} A^{\sigma}$ with the chr.inv.-projections of the A^{α} and the physically observable properties of the observer's reference space. Besides that, the regular derivation operators must be replaced with the chr.inv.-derivation operators.

Assuming the above notation φ and q^i for the chr.inv.-projections of the vector A^{α} , we express the remaining components of the A^{α} with them. Then, substituting the regular derivation operators expressed with the chr.inv.-derivation operators (marked by asterisk, see their definition on page 7)

$$\frac{\partial}{\partial t} = \sqrt{g_{00}} \frac{* \partial}{\partial t}, \quad \sqrt{g_{00}} = 1 - \frac{w}{c^2},$$

$$\frac{\partial}{\partial x^i} = \frac{* \partial}{\partial x^i} - \frac{1}{c^2} v_i \frac{* \partial}{\partial t},$$

into the general formula for $\nabla_{\sigma} A^{\sigma}$ (page 17) and taking into account that $\sqrt{-g} = \sqrt{h} \sqrt{g_{00}}$, after some algebra we obtain the $\nabla_{\sigma} A^{\sigma}$ in the extended chr.inv.-form

$$\nabla_{\sigma} A^{\sigma} = \frac{1}{c} \left(\frac{* \partial \varphi}{\partial t} + \varphi D \right) + \frac{* \partial q^i}{\partial x^i} + q^i \frac{* \partial \ln \sqrt{h}}{\partial x^i} - \frac{1}{c^2} F_i q^i.$$

In the third term of this formula, the quantity

$$\frac{* \partial \ln \sqrt{h}}{\partial x^i} = \Delta_{ji}^j$$

stands for the chr.inv.-Christoffel symbols Δ_{ji}^k contracted by two indices. Therefore, by analogy with the definition of the absolute divergence of a four-dimensional vector field A^{α} (see page 17), Zelmanov called the quantity

$$* \nabla_i q^i = \frac{* \partial q^i}{\partial x^i} + q^i \frac{* \partial \ln \sqrt{h}}{\partial x^i} = \frac{* \partial q^i}{\partial x^i} + q^i \Delta_{ji}^j$$

the *chr.inv.-divergence* of a three-dimensional chr.inv.-vector field q^i . Thus the $\nabla_{\sigma} A^{\sigma}$ takes the final chr.inv.-form

$$\nabla_{\sigma} A^{\sigma} = \frac{1}{c} \left(\frac{* \partial \varphi}{\partial t} + \varphi D \right) + * \nabla_i q^i - \frac{1}{c^2} F_i q^i.$$

The first term of this formula has no equivalent. It is made up of two parts. The first part is the observable change in time of the time projection φ of the vector A^{α} . The second part φD , since the spur (trace) $D = h^{ik} D_{ik}$ of the chr.inv.-tensor D_{ik} is the observable rate of relative expansion or compression of an elementary volume of the observer's space, is the observable change of the elementary volume of the three-dimensional observable vector field q^i in time.

The difference between the last two terms of this formula, which make up the chr.inv.-quantity

$$* \tilde{\nabla}_i q^i = * \nabla_i q^i - \frac{1}{c^2} F_i q^i,$$

Zelmanov called the *physical chr.inv.-divergence*, because the chr.inv.-quantity $* \tilde{\nabla}_i q^i$ takes into account the fact that, in a real physical space, the flow of time is different on the opposite walls of an elementary volume.

Generally speaking, when calculating the divergence of a field we consider an elementary volume of the space, so we calculate the difference between the amounts of a "substance"

which flows in and out of the volume over an elementary time interval. The gravitational inertial force F^i results in a different flow of time at different points: the beginnings as well as the ends of the time intervals measured on the opposite walls of a volume will not coincide, which makes these time intervals inapplicable for comparison. Synchronization of clocks on the opposite walls of the volume will give the true result: the measured time intervals will be different. That is, the physical chr.inv.-divergence ${}^* \widetilde{\nabla}_i q^i$ is a physical observable in the observer's three-dimensional reference space, which is analogous to a regular divergence.

Next we deduce the chr.inv.-projections of the absolute divergence $\nabla_\sigma F^{\sigma\alpha}$ of an antisymmetric tensor $F^{\alpha\beta} = -F^{\beta\alpha}$

$$\begin{aligned} \nabla_\sigma F^{\sigma\alpha} &= \frac{\partial F^{\sigma\alpha}}{\partial x^\sigma} + \Gamma_{\sigma\mu}^\sigma F^{\alpha\mu} + \Gamma_{\sigma\mu}^\alpha F^{\sigma\mu} = \\ &= \frac{\partial F^{\sigma\alpha}}{\partial x^\sigma} + \frac{\partial \ln \sqrt{-g}}{\partial x^\mu} F^{\alpha\mu}, \end{aligned}$$

we need to obtain Maxwell's equations in chr.inv.-form. Here in this formula, the third term $\Gamma_{\sigma\mu}^\alpha F^{\sigma\mu}$ is zero, because contracting the Christoffel symbols $\Gamma_{\sigma\mu}^\alpha$ (they are symmetric by their lower indices) with the antisymmetric tensor $F^{\sigma\mu}$ gives zero as in the case of any symmetric and antisymmetric geometric objects.

The quantity $\nabla_\sigma F^{\sigma\alpha}$ is a four-dimensional vector, therefore its chr.inv.-projections are

$$T = b_\alpha \nabla_\sigma F^{\sigma\alpha}, \quad B^i = h_\alpha^i \nabla_\sigma F^{\sigma\alpha} = \nabla_\sigma F^{\sigma i}.$$

Denoting the chr.inv.-projections of the tensor $F^{\alpha\beta}$ as

$$E^i = \frac{F_{0\cdot}^i}{\sqrt{g_{00}}}, \quad H^{ik} = F^{ik},$$

we obtain the remaining non-zero components of the $F^{\alpha\beta}$ expressed with its chr.inv.-projections

$$\begin{aligned} F_{0\cdot}^0 &= \frac{1}{c} v_k E^k, \\ F_{k\cdot}^0 &= \frac{1}{\sqrt{g_{00}}} \left(E_i - \frac{1}{c} v_n H_{k\cdot}^n - \frac{1}{c^2} v_k v_n E^n \right), \\ F^{0i} &= \frac{E^i - \frac{1}{c} v_k H^{ik}}{\sqrt{g_{00}}}, \\ F_{0i} &= -\sqrt{g_{00}} E_i, \\ F_{i\cdot}^k &= -H_{i\cdot}^k - \frac{1}{c} v_i E^k, \\ F_{ik} &= H_{ik} + \frac{1}{c} (v_i E_k - v_k E_i), \end{aligned}$$

and also the square of the tensor $F^{\alpha\beta}$ in the form as well expressed with its chr.inv.-projections

$$F_{\alpha\beta} F^{\alpha\beta} = H_{ik} H^{ik} - 2 E_i E^i.$$

Substituting these formulae into the above general formulae for T and B^i and then replacing the regular derivation operators with the chr.inv.-derivation operators, after some algebra we obtain the formulae for the chr.inv.-projections T and B^i of the absolute divergence $\nabla_\sigma F^{\sigma\alpha}$ of the antisymmetric tensor $F^{\alpha\beta} = -F^{\beta\alpha}$ in detail

$$\begin{aligned} T &= \frac{\nabla_\sigma F_{0\cdot}^{\sigma\alpha}}{\sqrt{g_{00}}} = \frac{{}^* \partial E^i}{\partial x^i} + E^i \frac{{}^* \partial \ln \sqrt{h}}{\partial x^i} - \frac{1}{c} H^{ik} A_{ik}, \\ B^i &= \nabla_\sigma F^{\sigma i} = \frac{{}^* \partial H^{ik}}{\partial x^k} + H^{ik} \frac{{}^* \partial \ln \sqrt{h}}{\partial x^k} - \frac{1}{c^2} F_k H^{ik} - \\ &\quad - \frac{1}{c} \left(\frac{{}^* \partial E^i}{\partial t} + D E^i \right). \end{aligned}$$

Taking into account that

$$\frac{{}^* \partial E^i}{\partial x^i} + E^i \frac{{}^* \partial \ln \sqrt{h}}{\partial x^i} = {}^* \nabla_i E^i$$

is the chr.inv.-divergence of the vector E^i , and also that

$$\begin{aligned} \frac{{}^* \partial H^{ik}}{\partial x^k} + H^{ik} \frac{{}^* \partial \ln \sqrt{h}}{\partial x^k} - \frac{1}{c^2} F_k H^{ik} &= \\ = {}^* \nabla_k H^{ik} - \frac{1}{c^2} F_k H^{ik} &= {}^* \widetilde{\nabla}_k H^{ik} \end{aligned}$$

is the physical chr.inv.-divergence of the tensor H^{ik} , we arrive at the final formulae for chr.inv.-projections of the absolute divergence $\nabla_\sigma F^{\sigma\alpha}$ of the antisymmetric tensor $F^{\alpha\beta}$

$$\begin{aligned} T &= {}^* \nabla_i E^i - \frac{1}{c} H^{ik} A_{ik}, \\ B^i &= {}^* \widetilde{\nabla}_k H^{ik} - \frac{1}{c} \left(\frac{{}^* \partial E^i}{\partial t} + D E^i \right). \end{aligned}$$

Calculate the chr.inv.-projections of the absolute divergence $\nabla_\sigma F^{*\sigma\alpha}$ of the pseudotensor $F^{*\alpha\beta}$ dual to the antisymmetric tensor $F^{\alpha\beta}$. For such a dual pseudotensor we have

$$F^{*\alpha\beta} = \frac{1}{2} E^{\alpha\beta\mu\nu} F_{\mu\nu}, \quad F_{*\alpha\beta} = \frac{1}{2} E_{\alpha\beta\mu\nu} F^{\mu\nu}.$$

Denoting its chr.inv.-projections as

$$H^{*i} = \frac{F_{0\cdot}^{*i}}{\sqrt{g_{00}}}, \quad E^{*ik} = F^{*ik},$$

we see that the obvious relations $H^{*i} \sim H^{ik}$ and $E^{*ik} \sim E^i$ exist between the chr.inv.-projections of the antisymmetric tensor $F^{\alpha\beta}$ and the pseudotensor $F^{*\alpha\beta}$, which are due to the duality of these tensors to each other.

As a result of these relations, given that

$$\frac{F_{0\cdot}^{*i}}{\sqrt{g_{00}}} = \frac{1}{2} \varepsilon^{ipq} H_{pq}, \quad F^{*ik} = -\varepsilon^{ikp} E_p,$$

the remaining components of the pseudotensor $F^{*\alpha\beta}$, formulated with the chr.inv.-projections of its dual tensor $F^{\alpha\beta}$ have

the following form

$$\begin{aligned}
F_{0\cdot}^{*\cdot 0} &= \frac{1}{2c} v_k \varepsilon^{kpq} \left[H_{pq} + \frac{1}{c} (v_p E_q - v_q E_p) \right], \\
F_{i\cdot}^{*\cdot 0} &= \frac{1}{2\sqrt{g_{00}}} \left[\varepsilon_i^{\cdot pq} H_{pq} + \frac{1}{c} \varepsilon_i^{\cdot pq} (v_p E_q - v_q E_p) - \right. \\
&\quad \left. - \frac{1}{c^2} \varepsilon^{kpq} v_i v_k H_{pq} - \frac{1}{c^3} \varepsilon^{kpq} v_i v_k (v_p E_q - v_q E_p) \right], \\
F^{*0i} &= \frac{1}{2\sqrt{g_{00}}} \varepsilon^{ipq} \left[H_{pq} + \frac{1}{c} (v_p E_q - v_q E_p) \right], \\
F_{*0i} &= \frac{1}{2} \sqrt{g_{00}} \varepsilon_{ipq} H^{pq}, \\
F_{i\cdot}^{*k} &= \varepsilon_i^{\cdot kp} E_p - \frac{1}{2c} v_i \varepsilon^{kpq} H_{pq} - \frac{1}{c^2} v_i v_m \varepsilon^{mkp} E_p, \\
F_{*ik} &= \varepsilon_{ikp} \left(E^p - \frac{1}{c} v_q H^{pq} \right),
\end{aligned}$$

while the square of the pseudotensor $F^{*\alpha\beta}$ has the form

$$F_{*\alpha\beta} F^{*\alpha\beta} = \varepsilon^{ipq} (E_p H_{iq} - E_i H_{pq}).$$

With the above components, after some algebra we obtain the chr.inv.-projections of the absolute divergence $\nabla_\sigma F^{*\sigma\alpha}$ of the dual pseudotensor $F^{*\alpha\beta}$ in detail

$$\begin{aligned}
\frac{\nabla_\sigma F_{0\cdot}^{*\cdot\sigma}}{\sqrt{g_{00}}} &= \frac{*\partial H^{*i}}{\partial x^i} + H^{*i} \frac{*\partial \ln \sqrt{h}}{\partial x^i} - \frac{1}{c} E^{*ik} A_{ik}, \\
\nabla_\sigma F^{*\sigma i} &= \frac{*\partial E^{*ik}}{\partial x^i} + E^{*ik} \frac{*\partial \ln \sqrt{h}}{\partial x^k} - \frac{1}{c^2} F_k E^{*ik} - \\
&\quad - \frac{1}{c} \left(\frac{*\partial H^{*i}}{\partial t} + D H^{*i} \right),
\end{aligned}$$

then, using the formulae for the chr.inv.-divergence $*\nabla_i H^{*i}$ and the physical chr.inv.-divergence $*\tilde{\nabla}_k E^{*ik}$, we arrive at the final formulae for chr.inv.-projections of the absolute divergence $\nabla_\sigma F^{*\sigma\alpha}$ of the dual pseudotensor $F^{*\alpha\beta}$

$$\begin{aligned}
\frac{\nabla_\sigma F_{0\cdot}^{*\cdot\sigma}}{\sqrt{g_{00}}} &= *\nabla_i H^{*i} - \frac{1}{c} E^{*ik} A_{ik}, \\
\nabla_\sigma F^{*\sigma i} &= *\tilde{\nabla}_k E^{*ik} - \frac{1}{c} \left(\frac{*\partial H^{*i}}{\partial t} + D H^{*i} \right).
\end{aligned}$$

Apart from the absolute divergence of vectors, antisymmetric tensors and pseudotensors of the 2nd rank, we need to deduce the chr.inv.-projections of the absolute divergence of a symmetric tensor of the 2nd rank (we need them to obtain the conservation law in chr.inv.-form).

Just as Zelmanov did, we denote the chr.inv.-projections of a symmetric tensor $T^{\alpha\beta}$ as

$$\frac{T_{00}}{g_{00}} = \rho, \quad \frac{T_{0i}}{\sqrt{g_{00}}} = K^i, \quad T^{ik} = N^{ik},$$

whence, following the same algebra as above, we obtain the chr.inv.-projections of the absolute divergence $\nabla_\sigma T^{\sigma\alpha}$ of the symmetric tensor $T^{\alpha\beta}$ in detail

$$\begin{aligned}
\frac{\nabla_\sigma T_0^\sigma}{\sqrt{g_{00}}} &= \frac{*\partial \rho}{\partial t} + \rho D + D_{ik} N^{ik} + c *\nabla_i K^i - \frac{2}{c} F_i K^i, \\
\nabla_\sigma T^{\sigma i} &= c \frac{*\partial K^i}{\partial t} + c D K^i + 2c (D_k^i + A_k^i) K^k + \\
&\quad + c^2 *\nabla_k N^{ik} - F_k N^{ik} - \rho F^i.
\end{aligned}$$

In addition to the inner (scalar) product of a tensor with the absolute differentiation operator ∇ , which is the absolute divergence of this tensor field, there may also be a difference between the covariant derivatives of the field. This quantity is known as the *curl* of the field, because from a geometric point of view it is the vortex (rotation) of the field itself. The *absolute curl* is the curl of an n -dimensional tensor field in an n -dimensional space.

The curl of an arbitrary four-dimensional vector field A^α is a covariant antisymmetric tensor of the 2nd rank*

$$F_{\mu\nu} = \nabla_\mu A_\nu - \nabla_\nu A_\mu = \frac{\partial A_\nu}{\partial x^\mu} - \frac{\partial A_\mu}{\partial x^\nu},$$

where $\nabla_\mu A_\nu$ is the absolute derivative of the A_α with respect to the coordinate x^μ

$$\nabla_\mu A_\nu = \frac{\partial A_\nu}{\partial x^\mu} - \Gamma_{\nu\mu}^\sigma A_\sigma.$$

The curl contracted with the four-dimensional absolutely antisymmetric discriminant tensor $E^{\alpha\beta\mu\nu}$ is the pseudotensor

$$F^{*\alpha\beta} = E^{\alpha\beta\mu\nu} (\nabla_\mu A_\nu - \nabla_\nu A_\mu) = E^{\alpha\beta\mu\nu} \left(\frac{\partial A_\nu}{\partial x^\mu} - \frac{\partial A_\mu}{\partial x^\nu} \right).$$

In electrodynamics, the electromagnetic field tensor $F_{\mu\nu}$ (Maxwell's tensor) is the curl of the four-dimensional electromagnetic field potential A^α . Therefore, we need the formulae for the chr.inv.-projections of the four-dimensional curl $F_{\mu\nu}$ and its dual pseudotensor $F^{*\alpha\beta}$ expressed in terms of the chr.inv.-projections of the four-dimensional vector potential A^α that forms them.

After the same algebra as above, we obtain the chr.inv.-projections of the absolute curl $F_{\mu\nu} = \nabla_\mu A_\nu - \nabla_\nu A_\mu$ expressed in terms of the chr.inv.-projections φ and q^i of the vector A^α forming this curl

$$\begin{aligned}
\frac{F_{0\cdot}^i}{\sqrt{g_{00}}} &= \frac{g^{i\alpha} F_{0\alpha}}{\sqrt{g_{00}}} = h^{ik} \left(\frac{*\partial \varphi}{\partial x^k} + \frac{1}{c} \frac{*\partial q_k}{\partial t} \right) - \frac{\varphi}{c^2} F^i, \\
F^{ik} &= g^{i\alpha} g^{k\beta} F_{\alpha\beta} = h^{im} h^{kn} \left(\frac{*\partial q_m}{\partial x^n} - \frac{*\partial q_n}{\partial x^m} \right) - \frac{2\varphi}{c} A^{ik}.
\end{aligned}$$

*Strictly speaking, a real geometric curl is not a tensor, but its dual pseudotensor. This is because the invariance with respect to reflection is necessary for any rotation. See §98 in the very good textbook *Riemannsche Geometrie und Tensoranalysis* [18] written by Peter Raschewski (1907–1983), the well-known expert in Riemannian geometry.

The remaining components of the curl $F_{\mu\nu} = \nabla_\mu A_\nu - \nabla_\nu A_\mu$ with taking into account that $F_{00} = F^{00} = 0$ just like for any antisymmetric tensor have the form

$$\begin{aligned} F_{0i} &= \left(1 - \frac{w}{c^2}\right) \left(\frac{\varphi}{c^2} F_i - \frac{* \partial \varphi}{\partial x^i} - \frac{1}{c} \frac{* \partial q_i}{\partial t}\right), \\ F_{ik} &= \frac{* \partial q_i}{\partial x^k} - \frac{* \partial q_k}{\partial x^i} + \frac{\varphi}{c} \left(\frac{\partial v_i}{\partial x^k} - \frac{\partial v_k}{\partial x^i}\right) + \\ &+ \frac{1}{c} \left(v_i \frac{* \partial \varphi}{\partial x^k} - v_k \frac{* \partial \varphi}{\partial x^i}\right) + \frac{1}{c^2} \left(v_i \frac{* \partial q_k}{\partial t} - v_k \frac{* \partial q_i}{\partial t}\right), \\ F_{0\cdot}^{\cdot 0} &= -\frac{\varphi}{c^3} v_k F^k + \frac{1}{c} v^k \left(\frac{* \partial \varphi}{\partial x^k} + \frac{1}{c} \frac{* \partial q_k}{\partial t}\right), \\ F_{k\cdot}^{\cdot 0} &= -\frac{1}{\sqrt{g_{00}}} \left[\frac{\varphi}{c^2} F_k - \frac{* \partial \varphi}{\partial x^k} - \frac{1}{c} \frac{* \partial q_k}{\partial t} + \right. \\ &+ \frac{2\varphi}{c^2} v^m A_{mk} + \frac{1}{c^2} v_k v^m \left(\frac{* \partial \varphi}{\partial x^m} + \frac{1}{c} \frac{* \partial q_m}{\partial t}\right) - \\ &\left. - \frac{1}{c} v^m \left(\frac{* \partial q_m}{\partial x^k} - \frac{* \partial q_k}{\partial x^m}\right) - \frac{\varphi}{c^4} v_k v_m F^m\right], \\ F_{k\cdot}^{\cdot i} &= h^{im} \left(\frac{* \partial q_m}{\partial x^k} - \frac{* \partial q_k}{\partial x^m}\right) - \frac{1}{c} h^{im} v_k \frac{* \partial \varphi}{\partial x^m} - \\ &- \frac{1}{c^2} h^{im} v_k \frac{* \partial q_m}{\partial t} + \frac{\varphi}{c^3} v_k F^i + \frac{2\varphi}{c} A_{k\cdot}^{\cdot i}, \\ F^{0k} &= \frac{1}{\sqrt{g_{00}}} \left[h^{km} \left(\frac{* \partial \varphi}{\partial x^m} + \frac{1}{c} \frac{* \partial q_m}{\partial t}\right) - \frac{\varphi}{c^2} F^k + \right. \\ &\left. + \frac{1}{c} v^n h^{mk} \left(\frac{* \partial q_n}{\partial x^m} - \frac{* \partial q_m}{\partial x^n}\right) - \frac{2\varphi}{c^2} v_m A^{mk}\right]. \end{aligned}$$

Respectively, the chr.inv.-projections of the dual pseudo-tensor $F^{*\alpha\beta}$ of the curl $F_{\mu\nu} = \nabla_\mu A_\nu - \nabla_\nu A_\mu$ have the form

$$\begin{aligned} \frac{F_{0\cdot}^{\cdot i}}{\sqrt{g_{00}}} &= \frac{g_{0\alpha} F^{*\alpha i}}{\sqrt{g_{00}}} = \varepsilon^{ikm} \left[\frac{1}{2} \left(\frac{* \partial q_k}{\partial x^m} - \frac{* \partial q_m}{\partial x^k}\right) - \frac{\varphi}{c} A_{km}\right], \\ F^{*ik} &= \varepsilon^{ikm} \left(\frac{\varphi}{c^2} F_m - \frac{* \partial \varphi}{\partial x^m} - \frac{1}{c} \frac{* \partial q_m}{\partial t}\right), \end{aligned}$$

where $F_{0\cdot}^{\cdot i} = g_{0\alpha} F^{*\alpha i} = g_{0\alpha} E^{\alpha i \mu \nu} F_{\mu \nu}$ is calculated using the above components of the curl $F_{\mu\nu}$.

Laplace's operator known also as Laplacian is the three-dimensional derivation operator

$$\Delta = \nabla \nabla = \nabla^2 = -g^{ik} \nabla_i \nabla_k.$$

The four-dimensional generalization of Laplace's operator in a pseudo-Riemannian space is *d'Alembert's operator* known also as *d'Alembertian*

$$\square = g^{\alpha\beta} \nabla_\alpha \nabla_\beta.$$

Let us apply d'Alembert's operator to a scalar field and a vector field in the four-dimensional pseudo-Riemannian space (the space-time of General Relativity), and then express the calculation results in chr.inv.-form.

First we apply d'Alembert's operator to a scalar field φ

$$\square \varphi = g^{\alpha\beta} \nabla_\alpha \nabla_\beta \varphi = g^{\alpha\beta} \frac{\partial \varphi}{\partial x^\alpha} \left(\frac{\partial \varphi}{\partial x^\beta}\right) = g^{\alpha\beta} \frac{\partial^2 \varphi}{\partial x^\alpha \partial x^\beta},$$

because in this case the calculation is much simpler: the absolute derivative of a scalar, $\nabla_\alpha \varphi$, does not contain the Christoffel symbols, so it becomes the regular derivative.

We express the components of the fundamental metric tensor in terms of chronometric invariants. For g^{ik} we have $g^{ik} = -h^{ik}$ (see page 5). The components g^{0i} are obtained from the formula for the linear velocity of rotation of the observer's space $v^i = -c g^{0i} \sqrt{g_{00}}$ (see page 7)

$$g^{0i} = -\frac{1}{c \sqrt{g_{00}}} v^i.$$

The component g^{00} is obtained from the main property of the fundamental metric tensor $g_{\alpha\sigma} g^{\beta\sigma} = g_\alpha^\beta$. Setting up $\alpha = \beta = 0$ in the mentioned property, we obtain

$$g_{0\sigma} g^{0\sigma} = g_{00} g^{00} + g_{0i} g^{0i} = \delta_0^0 = 1,$$

whence, taking into account that

$$g_{00} = \left(1 - \frac{w}{c^2}\right)^2, \quad g_{0i} = -\frac{1}{c} v_i \left(1 - \frac{w}{c^2}\right),$$

we obtain the formula

$$g^{00} = \frac{1}{\left(1 - \frac{w}{c^2}\right)^2} \left(1 - \frac{1}{c^2} v_i v^i\right), \quad v_i v^i = h_{ik} v^i v^k = v^2.$$

Substituting the obtained formulae for g^{00} , g^{0i} and g^{ik} into the above general formula for $\square \varphi$ and then replacing the regular derivation operators with the chr.inv.-derivation operators, we obtain the d'Alembertian of the scalar field φ in chr.inv.-form

$$\square \varphi = \frac{1}{c^2} \frac{* \partial^2 \varphi}{\partial t^2} - h^{ik} \frac{* \partial^2 \varphi}{\partial x^i \partial x^k} = * \square \varphi,$$

where $* \square$ is the chr.inv.-d'Alembert operator, and $* \Delta$ is the chr.inv.-Laplace operator

$$* \square = \frac{1}{c^2} \frac{* \partial^2}{\partial t^2} - h^{ik} \frac{* \partial^2}{\partial x^i \partial x^k} = \frac{1}{c^2} \frac{* \partial^2}{\partial t^2} - * \Delta,$$

$$* \Delta = h^{ik} \frac{* \partial^2}{\partial x^i \partial x^k} = -g^{ik} * \nabla_i * \nabla_k.$$

Now, we apply d'Alembert's operator to an arbitrary four-dimensional vector field A^α

$$\square A^\alpha = g^{\mu\nu} \nabla_\mu \nabla_\nu A^\alpha.$$

Because $\square A^\alpha$ is a four-dimensional vector, the chr.inv.-projections of it are

$$T = b_\sigma \square A^\sigma = b_\sigma g^{\mu\nu} \nabla_\mu \nabla_\nu A^\sigma,$$

$$B^i = h^i_\sigma \square A^\sigma = h^i_\sigma g^{\mu\nu} \nabla_\mu \nabla_\nu A^\sigma.$$

It should be noted that the derivation of the d'Alembertian of a vector field in a Riemannian space is not a trivial task. This is because in this case, the Christoffel symbols are not zeroes and, therefore, the formulae for the chr.inv.-projections of the second derivatives take many pages*.

So, after some difficult algebra we had obtained formulae for the chr.inv.-projections of the d'Alembertian of the vector field A^α in the four-dimensional pseudo-Riemannian space. They have the following form†

$$T = {}^*\square\varphi - \frac{1}{c^3} \frac{\partial}{\partial t} (F_k q^k) - \frac{1}{c^3} F_i \frac{\partial q^i}{\partial t} + \frac{1}{c^2} F^i \frac{\partial \varphi}{\partial x^i} +$$

$$+ h^{ik} \Delta_{ik}^m \frac{\partial \varphi}{\partial x^m} - h^{ik} \frac{1}{c} \frac{\partial}{\partial x^i} [(D_{kn} + A_{kn}) q^n] + \frac{D}{c^2} \frac{\partial \varphi}{\partial t} -$$

$$- \frac{1}{c} D_m^k \frac{\partial q^m}{\partial x^k} + \frac{2}{c^3} A_{ik} F^i q^k + \frac{\varphi}{c^4} F_i F^i - \frac{\varphi}{c^2} D_{mk} D^{mk} -$$

$$- \frac{D}{c^3} F_m q^m - \frac{1}{c} \Delta_{kn}^m D_m^k q^n + \frac{1}{c} h^{ik} \Delta_{ik}^m (D_{mn} + A_{mn}) q^n,$$

$$B^i = {}^*\square A^i + \frac{1}{c^2} \frac{\partial}{\partial t} [(D_k^i + A_k^i) q^k] + \frac{D}{c^2} \frac{\partial q^i}{\partial t} +$$

$$+ \frac{1}{c^2} (D_k^i + A_k^i) \frac{\partial q^k}{\partial t} - \frac{1}{c^3} \frac{\partial}{\partial t} (\varphi F^i) - \frac{1}{c^3} F^i \frac{\partial \varphi}{\partial t} +$$

$$+ \frac{1}{c^2} F^k \frac{\partial q^i}{\partial x^k} - \frac{1}{c} (D^{mi} + A^{mi}) \frac{\partial \varphi}{\partial x^m} + \frac{1}{c^4} q^k F_k F^i +$$

$$+ \frac{1}{c^2} \Delta_{km}^i q^m F^k - \frac{\varphi}{c^3} D F^i + \frac{D}{c^2} (D_n^i + A_n^i) q^n -$$

$$- h^{km} \left\{ \frac{\partial}{\partial x^k} (\Delta_{mn}^i q^n) + \frac{1}{c} \frac{\partial}{\partial x^k} [\varphi (D_m^i + A_m^i)] + \right.$$

$$+ (\Delta_{kn}^i \Delta_{mp}^n - \Delta_{km}^n \Delta_{np}^i) q^p + \frac{\varphi}{c} [\Delta_{kn}^i (D_m^n + A_m^n) -$$

$$\left. - \Delta_{km}^n (D_n^i + A_n^i)] + \Delta_{kn}^i \frac{\partial q^n}{\partial x^m} - \Delta_{km}^n \frac{\partial q^i}{\partial x^n} \right\},$$

where ${}^*\square\varphi$ and ${}^*\square q^i$ are the result of applying the chr.inv.-d'Alembert operator to the quantities $\varphi = \frac{A_0}{\sqrt{g_{00}}}$ and $q^i = A^i$,

*This is one of the reasons why applications of the theory of electromagnetic fields are calculated in the Galilean reference frame in the Minkowski space (the space-time of Special Relativity), where the Christoffel symbols are zeroes. General covariant notation hardly allows unambiguous interpretation of calculation results, unless they are formulated with physical observable quantities (chronometric invariants) or demoted to a simple specific case like that in the Minkowski space, for instance.

†The above chr.inv.-projections of the d'Alembertian of a vector field in the four-dimensional pseudo-Riemannian space were deduced not by Zelmanov, but by one of us, L. Borisova, in the 1980s.

which are chr.inv.-projections (physically observable components) of the vector A^α

$${}^*\square\varphi = \frac{1}{c^2} \frac{\partial^2 \varphi}{\partial t^2} - h^{ik} \frac{\partial^2 \varphi}{\partial x^i \partial x^k},$$

$${}^*\square q^i = \frac{1}{c^2} \frac{\partial^2 q^i}{\partial t^2} - h^{km} \frac{\partial^2 q^i}{\partial x^k \partial x^m}.$$

The main criterion for correct calculations in such a complicated case as here is Zelmanov's rule of the chronometric invariance: "Correct calculations make all terms in the final equations chronometrically invariant quantities. That is to say, the final equations consist of the chr.inv.-quantities, their chr.inv.-derivatives, and also the chr.inv.-properties of the observer's reference space. If at least one error was made in the calculations, then some terms of the final equations will not be chronometric invariants."

In the Galilean reference frame in the Minkowski space (the space-time of Special Relativity), Laplace's and d'Alembert's operators take the simplified form

$$\Delta = \frac{\partial^2}{\partial x^1 \partial x^1} + \frac{\partial^2}{\partial x^2 \partial x^2} + \frac{\partial^2}{\partial x^3 \partial x^3},$$

$$\square = \frac{1}{c^2} \frac{\partial^2}{\partial t^2} - \frac{\partial^2}{\partial x^1 \partial x^1} - \frac{\partial^2}{\partial x^2 \partial x^2} - \frac{\partial^2}{\partial x^3 \partial x^3} = \frac{1}{c^2} \frac{\partial^2}{\partial t^2} - \Delta.$$

D'Alembert's operator applied to a tensor field and equated to zero or not zero, gives the *d'Alembert equations* for this field. From a physical point of view, these are the equations of propagation of waves of the field. If the d'Alembertian of a field is not zero, these are the equations of propagation of the waves enforced by the sources that induce this field; they are called the *d'Alembert equations with sources*. For instance, the sources of electromagnetic fields are electric charges and currents. If the d'Alembertian of a field is zero, then these are the equations of propagation of waves in the field not related to any sources. If the space-time region under consideration, in addition to the tensor field, is filled with another medium, then the d'Alembert equations gain an additional term characterizing this medium (this term can be found using the equations which determine the medium).

These are the basics of tensor calculus expressed in terms of chronometric invariants.

Next we present formulae for the most common equations used in General Relativity, in the form expressed in terms of physical observables (chronometric invariants).

First, consider the equations of motion of a particle. A particle under the influence of gravitation only falls freely and thus travels along the shortest (*geodesic*) line. Such motion is called *free* or *geodesic motion*. If an additional non-gravitational force also acts on the particle, then the force deviates this particle from its geodesic trajectory, and the motion becomes *non-geodesic*.

From a geometric point of view, motion of a particle in the four-dimensional pseudo-Riemannian space (space-time)

is parallel transport of the four-dimensional vector Q^α , which is tangential to the particle's trajectory at any of its points and completely characterizes this particle. Therefore, the equations of motion of a particle actually determine the parallel transport of the particle's vector Q^α along the particle's four-dimensional trajectory and they are the equations of the absolute derivative of this vector with respect to a parameter ρ , which is non-zero along the trajectory

$$\frac{DQ^\alpha}{d\rho} = \frac{dQ^\alpha}{d\rho} + \Gamma_{\mu\nu}^\alpha Q^\mu \frac{dx^\nu}{d\rho},$$

where $DQ^\alpha = dQ^\alpha + \Gamma_{\mu\nu}^\alpha Q^\mu dx^\nu$ is the absolute differential of the transported vector Q^α (i.e., its absolute increment) along the trajectory.

If a particle travels along a geodesic trajectory (free motion), then the particle's characteristic vector is transported in Levi-Civita's sense: the square of the transported vector remains unchanged $Q_\alpha Q^\alpha = const$ along the trajectory, while the absolute derivative of the transported vector is zero and such equations are called the *equations of free motion*.

A mass-bearing particle (such particles travel along non-isotropic space-time trajectories) is characterized by its own four-dimensional momentum vector

$$P^\alpha = m_0 \frac{dx^\alpha}{ds}, \quad P_\alpha P^\alpha = m_0^2 = const,$$

where m_0 is the particle's rest-mass. Respectively, the equations of motion of a free mass-bearing particle are

$$\frac{dP^\alpha}{ds} + \Gamma_{\mu\nu}^\alpha P^\mu \frac{dx^\nu}{ds} = 0.$$

A massless light-like particle (such particles travel along isotropic space-time trajectories) is characterized by its own four-dimensional wave vector

$$K^\alpha = \frac{\omega}{c} \frac{dx^\alpha}{d\sigma}, \quad K_\alpha K^\alpha = 0,$$

where ω is the characteristic frequency of the massless particle, and $d\sigma = h_{ik} dx^i dx^k$ is the three-dimensional chr.inv.-interval, which, since $ds^2 = c^2 d\tau^2 - d\sigma^2 = 0$ along isotropic trajectories, is invariant along them. Respectively, the equations of motion of a free massless (light-like) particle are

$$\frac{dK^\alpha}{d\sigma} + \Gamma_{\mu\nu}^\alpha K^\mu \frac{dx^\nu}{d\sigma} = 0.$$

The projections of the above four-dimensional equations of motion onto the time line and the three-dimensional spatial section of an observer are, respectively, the chr.inv.-equations of motion of a free mass-bearing particle

$$\frac{dm}{d\tau} - \frac{m}{c^2} F_i v^i + \frac{m}{c^2} D_{ik} v^i v^k = 0,$$

$$\frac{d(mv^i)}{d\tau} + 2m(D_k^i + A_k^i)v^k - mF^i + m\Delta_{nk}^i v^n v^k = 0,$$

and the chr.inv.-equations of motion of a free massless (light-like) particle

$$\frac{d\omega}{d\tau} - \frac{\omega}{c^2} F_i c^i + \frac{\omega}{c^2} D_{ik} c^i c^k = 0,$$

$$\frac{d(\omega c^i)}{d\tau} + 2\omega(D_k^i + A_k^i)c^k - \omega F^i + \omega\Delta_{nk}^i c^n c^k = 0,$$

where m is the relativistic mass of the travelling mass-bearing particle, ω is the characteristic frequency of the massless particle, $d\tau$ is the physically observable time interval, and v^i is the chr.inv.-vector of the physically observable velocity of the mass-bearing particle. Along isotropic trajectories (trajectories of light) the v^i transforms into the chr.inv.-vector of the physically observable velocity of light, the square of which is $c_i c^i = h_{ik} c^i c^k = c^2$ (see page 6).

If a particle travels along a non-geodesic trajectory, then $Q_\alpha Q^\alpha \neq const$, and the absolute derivative of the transported vector Q^α is equal to a force Φ^α that deviates the particle from a geodesic line. Such equations are called the *equations of non-geodesic motion* [5]. In this case, the right hand side of the above chr.inv.-equations of motion is different from zero and contains the respective chr.inv.-projections of the deviating force Φ^α .

The chr.inv.-equations of motion show how the observed motion of particles depends on the physically observable gravitational inertial force F^i , rotation A_{ik} , deformation D_{ik} and inhomogeneity (the coherence coefficients Δ_{kn}^i) of the observer's reference space.

Let us now turn to the basics of electrodynamics in the four-dimensional pseudo-Riemannian space.

The electromagnetic field tensor $F^{\mu\nu}$ is determined as the curl $F_{\mu\nu} = \nabla_\mu A_\nu - \nabla_\nu A_\mu$ of the four-dimensional electromagnetic field potential A^α . Following the terminology of electrodynamics, we call the chr.inv.-projections of the A^α (page 17) the chr.inv.-scalar potential φ and the chr.inv.-vector potential q^i of the electromagnetic field

$$\varphi = \frac{A_0}{\sqrt{g_{00}}}, \quad q^i = A^i,$$

and the chr.inv.-projections of the electromagnetic field tensor $F^{\mu\nu}$ (page 20) — the chr.inv.-electric strength E^i and the chr.inv.-magnetic strength H^{ik} of the field

$$E^i = \frac{F_0^i}{\sqrt{g_{00}}} = \frac{g^{i\alpha} F_{0\alpha}}{\sqrt{g_{00}}} = h^{ik} \left(\frac{* \partial \varphi}{\partial x^k} + \frac{1}{c} \frac{* \partial q_k}{\partial t} \right) - \frac{\varphi}{c^2} F^i,$$

$$H^{ik} = F^{ik} = g^{i\alpha} g^{k\beta} F_{\alpha\beta} = h^{im} h^{kn} \left(\frac{* \partial q_m}{\partial x^n} - \frac{* \partial q_n}{\partial x^m} \right) - \frac{2\varphi}{c} A^{ik},$$

where their covariant (lower-index) versions are

$$E_i = h_{ik} E^k = \frac{* \partial \varphi}{\partial x^i} + \frac{1}{c} \frac{* \partial q_i}{\partial t} - \frac{\varphi}{c^2} F_i,$$

$$H_{ik} = h_{im} h_{kn} H^{mn} = \frac{* \partial q_i}{\partial x^k} - \frac{* \partial q_k}{\partial x^i} - \frac{2\varphi}{c} A_{ik},$$

and the mixed components $H_k^m = -H_k^m$ are obtained from H^{ik} using the metric chr.inv.-tensor h_{ik} , i.e., $H_k^m = h_{ki} H^{im}$.

Respectively, the electromagnetic field pseudotensor $F^{*\alpha\beta}$ dual to the field tensor, i.e., $F^{*\alpha\beta} = \frac{1}{2} E^{\alpha\beta\mu\nu} F_{\mu\nu}$, has the following chr.inv.-projections

$$H^{*i} = \frac{F^{*i}}{\sqrt{g_{00}}} = \frac{1}{2} \varepsilon^{imn} \left(\frac{* \partial q_m}{\partial x^n} - \frac{* \partial q_n}{\partial x^m} - \frac{2\varphi}{c} A_{mn} \right) = \frac{1}{2} \varepsilon^{imn} H_{mn},$$

$$E^{*ik} = F^{*ik} = \varepsilon^{ikn} \left(\frac{\varphi}{c^2} F_n - \frac{* \partial \varphi}{\partial x^n} - \frac{1}{c} \frac{* \partial q_n}{\partial t} \right) = -\varepsilon^{ikn} E_n,$$

which we call the chr.inv.-magnetic strength pseudovector H^{*i} and the chr.inv.-electric strength pseudotensor E^{*ik} . It is obvious that the quantities H^{*i} and H_{mn} are dually conjugate, and the quantities E^{*ik} and E_m are also dually conjugate.

The above formulae show that the observed electric and magnetic strengths of the electromagnetic field depend on the physically observable gravitational inertial force F^i and rotation A_{ik} of the observer's reference space.

So forth, the electromagnetic field invariants

$$J_1 = F_{\mu\nu} F^{\mu\nu} = H_{ik} H^{ik} - 2 E_i E^i = -2(E_i E^i - H_{*i} H^{*i}),$$

$$J_2 = F_{\mu\nu} F^{*\mu\nu} = \varepsilon^{imn} (E_m H_{in} - E_i H_{nm}) = -4 E_i H^{*i},$$

the first of which is a scalar, and the second is a pseudoscalar, have the following detailed chr.inv.-formulation

$$J_1 = 2 \left[h^{im} h^{kn} \left(\frac{* \partial q_i}{\partial x^k} - \frac{* \partial q_k}{\partial x^i} \right) \frac{* \partial q_m}{\partial x^n} - h^{ik} \frac{* \partial \varphi}{\partial x^i} \frac{* \partial \varphi}{\partial x^k} - \frac{2}{c} h^{ik} \frac{* \partial \varphi}{\partial x^i} \frac{* \partial q_k}{\partial t} - \frac{1}{c^2} h^{ik} \frac{* \partial q_i}{\partial t} \frac{* \partial q_k}{\partial t} + \frac{8\varphi}{c^2} \Omega_{*i} \Omega^{*i} - \frac{2\varphi}{c} \varepsilon^{imn} \Omega_{*m} \frac{* \partial q_i}{\partial x^n} + \frac{2\varphi}{c^2} \frac{* \partial \varphi}{\partial x^i} F^i + \frac{2\varphi}{c^3} \frac{* \partial q_i}{\partial t} F^i - \frac{\varphi}{c^4} F_i F^i \right],$$

$$J_2 = \frac{1}{2} \left[\varepsilon^{imn} \left(\frac{* \partial q_m}{\partial x^n} - \frac{* \partial q_n}{\partial x^m} \right) - \frac{4\varphi}{c} \Omega^{*i} \right] \times \left(\frac{* \partial \varphi}{\partial x^i} + \frac{1}{c} \frac{* \partial q_i}{\partial t} - \frac{\varphi}{c^2} F_i \right).$$

Mathematically, any electromagnetic field in the four-dimensional pseudo-Riemannian space is completely characterized by a system of 10 equations in 10 unknowns. First, this system includes Maxwell's equations

$$\nabla_{\sigma} F^{\mu\sigma} = \frac{4\pi}{c} j^{\mu}, \quad \nabla_{\sigma} F^{*\mu\sigma} = 0,$$

the chr.inv.-projections of which give two groups of equations, which we call the chr.inv.-Maxwell equations* and which

*The chr.inv.-Maxwell equations were first deduced in the late 1960s independently by Nikolai Pavlov and José del Prado (unpublished). Zelmanov asked these students to do it as homework. These equations are deduced on the basis of the chr.inv.-projections of the absolute divergence of a 2nd rank antisymmetric tensor (page 19), as well as the chr.inv.-projections of the absolute divergence of its dual pseudotensor (page 20).

have the following form

$$\left. \begin{aligned} * \nabla_i E^i - \frac{1}{c} H^{ik} A_{ik} &= 4\pi\rho \\ * \nabla_k H^{ik} - \frac{1}{c^2} F_k H^{ik} - \frac{1}{c} \left(\frac{* \partial E^i}{\partial t} + D E^i \right) &= \frac{4\pi}{c} j^i \end{aligned} \right\} \text{I,}$$

$$\left. \begin{aligned} * \nabla_i H^{*i} - \frac{1}{c} E^{*ik} A_{ik} &= 0 \\ * \nabla_k E^{*ik} - \frac{1}{c^2} F_k E^{*ik} - \frac{1}{c} \left(\frac{* \partial H^{*i}}{\partial t} + D H^{*i} \right) &= 0 \end{aligned} \right\} \text{II,}$$

or, in another notation

$$\left. \begin{aligned} * \nabla_i E^i - \frac{2}{c} \Omega_{*m} H^{*m} &= 4\pi\rho \\ \varepsilon^{ikm} * \tilde{\nabla}_k (H_{*m} \sqrt{h}) - \frac{1}{c} \frac{* \partial}{\partial t} (E^i \sqrt{h}) &= \frac{4\pi}{c} j^i \sqrt{h} \end{aligned} \right\} \text{I,}$$

$$\left. \begin{aligned} * \nabla_i H^{*i} + \frac{2}{c} \Omega_{*m} E^m &= 0 \\ \varepsilon^{ikm} * \tilde{\nabla}_k (E_m \sqrt{h}) + \frac{1}{c} \frac{* \partial}{\partial t} (H^{*i} \sqrt{h}) &= 0 \end{aligned} \right\} \text{II.}$$

These are 8 equations in 10 unknowns, which are 3 components of the chr.inv.-electric strengths E^i , 3 components of the chr.inv.-magnetic strength H^{*i} , 1 component of the electric charge density ρ and 3 components of the chr.inv.-current density vector j^i . The latter two, known as the electromagnetic field sources, are the chr.inv.-projections

$$\rho = \frac{1}{c} b^{\alpha} j_{\alpha} = \frac{1}{c} \frac{j_0}{\sqrt{g_{00}}}, \quad j^i = h_{\alpha}^i j^{\alpha}$$

of the four-dimensional current vector j^{α} of the electromagnetic field (also known as the shift current).

The first equation of Group I is the Biot-Savart law, the second is Gauss' theorem, both in chr.inv.-notation. The first and second equations of Group II represent a chr.inv.-notation of Faraday's law of electromagnetic induction and the conditions for the absence of magnetic charges, respectively.

In particular, the 1st equation in Group II shows that, if the observer's reference space does not rotate, then $* \nabla_i H^{*i} = 0$ (the magnetic field is homogeneous), while the electric field is not, $* \nabla_i E^i = 4\pi\rho$ (the 1st equation in Group I). Therefore, a "magnetic charge", if it really exists, is directly connected with the rotation of space itself.

The 9th equation of the equation system mentioned above is Lorentz' condition

$$\nabla_{\sigma} A^{\sigma} = 0,$$

which is the conservation condition for the four-dimensional electromagnetic field potential A^{α} . The 10th equation that makes this system definite (the number of equations in this system must be the same as the number of unknowns), is the

law of conservation of electric charge (known also as the continuity equation)

$$\nabla_{\sigma} j^{\sigma} = 0,$$

which is the mathematical notation of the fact that electric charge cannot be destroyed, but merely redistributed between the charged bodies in contact.

Using the chr.inv.-formula for the divergence of an arbitrary vector field (see page 18), we obtain the Lorentz condition and the continuity condition in chr.inv.-form

$$\frac{1}{c} \frac{\partial \varphi}{\partial t} + \frac{\varphi}{c} D + {}^* \nabla_i q^i - \frac{1}{c^2} F_i q^i = 0,$$

$$\frac{\partial \rho}{\partial t} + \rho D + {}^* \nabla_i j^i - \frac{1}{c^2} F_i j^i = 0,$$

or, replacing the regular chr.inv.-divergence with the physical chr.inv.-divergence (see page 18), we finally have

$$\frac{1}{c} \frac{\partial \varphi}{\partial t} + \frac{\varphi}{c} D + {}^* \tilde{\nabla}_i q^i = 0,$$

$$\frac{\partial \rho}{\partial t} + \rho D + {}^* \tilde{\nabla}_i j^i = 0.$$

With the above chr.inv.-Lorentz condition and the chr.inv.-continuity equation, the mentioned system of 10 equations that completely characterizes any electromagnetic field in the four-dimensional pseudo-Riemannian space is complete.

Now consider the energy-momentum tensor of an electromagnetic field. It has the form

$$T^{\mu\nu} = \frac{1}{4\pi} \left(-F^{\mu\sigma} F_{\nu\sigma} + \frac{1}{4} g^{\mu\nu} F^{\alpha\beta} F_{\alpha\beta} \right).$$

This tensor is symmetric: $T^{\mu\nu} = T^{\nu\mu}$. For this reason, its chr.inv.-projections are calculated as for any symmetric tensor of the 2nd rank (see page 6)

$$q = \frac{T_{00}}{g_{00}}, \quad J^i = \frac{c T_0^i}{\sqrt{g_{00}}}, \quad U^{ik} = c^2 T^{ik}$$

and have the following form

$$q = \frac{E^2 + H^{*2}}{8\pi},$$

$$J^i = \frac{c}{4\pi} \varepsilon^{ikm} E_k H_{*m},$$

$$U^{ik} = q c^2 h^{ik} - \frac{c^2}{4\pi} (E^i E^k + H^{*i} H^{*k}),$$

where $E^2 = h_{ik} E^i E^k$ and $H^{*2} = h_{ik} H^{*i} H^{*k}$. These projections have the following physical sense: the scalar q is the physically observable energy density of the electromagnetic field, J^i is the physically observable density of the field momentum (the chr.inv.-Poynting vector), and U^{ik} is the physically

observable density of the field momentum flux (the chr.inv.-stress tensor).

Any electrically charged particle travelling in an electromagnetic field deviates from a geodesic trajectory due to the Lorentz force acting on its electric charge e from the electromagnetic field. The Lorentz force in the four-dimensional pseudo-Riemannian space has the form

$$\Phi^{\alpha} = \frac{e}{c} F_{\sigma}^{\alpha} U^{\sigma}, \quad U^{\alpha} = \frac{dx^{\alpha}}{ds},$$

where U^{α} is the four-dimensional velocity of the charged particle. Respectively, the four-dimensional equations of motion of a charged particle in an electromagnetic field (determined by the electromagnetic field tensor $F_{\alpha\beta}$) have the form

$$\frac{dP^{\alpha}}{ds} + \Gamma_{\mu\nu}^{\alpha} P^{\mu} U^{\nu} = \frac{e}{c^2} F_{\beta}^{\alpha} U^{\beta},$$

and their chr.inv.-projections

$$\frac{dE}{d\tau} - m F_i v^i + m D_{ik} v^i v^k = -e E_i v^i,$$

$$\begin{aligned} \frac{d(mv^i)}{d\tau} - m F^i + 2m(D_k^i + A_k^i) v^k + m \Delta_{nk}^i v^n v^k = \\ = -e \left(E^i + \frac{1}{c} \varepsilon^{ikm} v_k H_{*m} \right) \end{aligned}$$

are the chr.inv.-equations of motion of the charged particle. Here, $E = mc^2$ is the relativistic energy of the particle, so the first (scalar) equation is the theorem of live forces represented in chr.inv.-form.

The above chr.inv.-equations of motion show how the observed motion of charged particles is affected by the physically observable gravitational inertial force F^i , rotation A_{ik} , deformation D_{ik} and inhomogeneity Δ_{kn}^i of the observer's reference space.

Zelmanov had also introduced the chr.inv.-curvature tensor. It is deduced similarly to the Riemann-Christoffel tensor from the non-commutativity of the 2nd chr.inv.-derivatives of an arbitrary vector

$${}^* \nabla_i {}^* \nabla_k Q_l - {}^* \nabla_k {}^* \nabla_i Q_l = \frac{2A_{ik}}{c^2} \frac{\partial Q_l}{\partial t} + H_{lki}^{*j} Q_j,$$

where the 4th rank chr.inv.-tensor

$$H_{lki}^{*j} = \frac{\partial \Delta_{il}^j}{\partial x^k} - \frac{\partial \Delta_{kl}^j}{\partial x^i} + \Delta_{il}^m \Delta_{km}^j - \Delta_{kl}^m \Delta_{im}^j$$

is the basis for the chr.inv.-curvature tensor C_{lkij} , which has all properties of the Riemann-Christoffel tensor in the observer's three-dimensional spatial section, and its contraction gives the observable chr.inv.-scalar curvature C

$$C_{lkij} = \frac{1}{4} (H_{lkij} - H_{jkil} + H_{klji} - H_{iljk}),$$

$$C_{lk} = C_{lki}^{*i}, \quad C = h^{lk} C_{lk},$$

where

$$H_{lkij} = C_{lkij} + \frac{1}{2} (2A_{ki} D_{jl} + A_{ij} D_{kl} + A_{jk} D_{il} + A_{kl} D_{ij} + A_{li} D_{jk}),$$

$$H_{lk} = C_{lk} + \frac{1}{2} (A_{kj} D_l^j + A_{lj} D_k^j + A_{kl} D),$$

$$H = h^{lk} H_{lk} = C.$$

The above formulae show that the observed curvature of a space depends on not only the gravitational inertial force acting in the local reference space of the observer, but also the rotation and deformation of his reference space, and, therefore, does not vanish in the absence of the gravitational field. If the space does not rotate, then we have $H_{lkij} = C_{lkij}$. This is as well true for H_{lk} and C_{lk} . In this particular case, the tensor $C_{lk} = h^{ij} C_{ilkj}$ has the form

$$C_{lk} = \frac{* \partial}{\partial x^k} \left(\frac{* \partial \ln \sqrt{h}}{\partial x^l} \right) - \frac{* \partial \Delta_{kl}^i}{\partial x^i} + \Delta_{il}^m \Delta_{km}^i - \Delta_{kl}^m \frac{* \partial \ln \sqrt{h}}{\partial x^m}.$$

Zelmanov had also deduced chr.inv.-projections for the Riemann-Christoffel curvature tensor

$$R_{.jkl}^i = \frac{\partial \Gamma_{lj}^i}{\partial x^k} - \frac{\partial \Gamma_{kj}^i}{\partial x^l} + \Gamma_{kp}^i \Gamma_{lj}^p - \Gamma_{lp}^i \Gamma_{kj}^p.$$

The Riemann-Christoffel tensor $R_{\alpha\beta\gamma\delta}$ is symmetric with respect to transposition over a pair of its indices and antisymmetric within each pair of the indices. Therefore, it has three chr.inv.-projections as follows

$$X^{ik} = -c^2 \frac{R_{0..0}^{i..k}}{g_{00}}, \quad Y^{ijk} = -c \frac{R_{0...}^{ijk}}{\sqrt{g_{00}}}, \quad Z^{ijkl} = c^2 R^{ijkl}.$$

Substituting the necessary components of the Riemann-Christoffel tensor $R_{\alpha\beta\gamma\delta}$ into these formulae and then lowering the indices, Zelmanov had obtained the chr.inv.-projections of the Riemann-Christoffel tensor in the form

$$X_{ij} = \frac{* \partial D_{ij}}{\partial t} - (D_i^l + A_i^l)(D_{jl} + A_{jl}) + (* \nabla_i F_j + * \nabla_j F_i) - \frac{1}{c^2} F_i F_j,$$

$$Y_{ijk} = * \nabla_i (D_{jk} + A_{jk}) - * \nabla_j (D_{ik} + A_{ik}) + \frac{2}{c^2} A_{ij} F_k,$$

$$Z_{iklj} = D_{ik} D_{lj} - D_{il} D_{kj} + A_{ik} A_{lj} - A_{il} A_{kj} + 2A_{ij} A_{kl} - c^2 C_{iklj},$$

where we have $Y_{(ijk)} = Y_{ijk} + Y_{jki} + Y_{kij} = 0$, as in the Riemann-Christoffel tensor. Contraction of the observable spatial projection Z_{iklj} step-by-step as $Z_{il} = h^{kj} Z_{iklj}$ and $Z = h^{il} Z_{il}$ gives

$$Z_{il} = D_{ik} D_l^k - D_{il} D + A_{ik} A_{.l}^k + 2A_{ik} A_{.l}^k - c^2 C_{il},$$

$$Z = h^{il} Z_{il} = D_{ik} D^{ik} - D^2 - A_{ik} A^{ik} - c^2 C.$$

Using the above, Zelmanov was able to deduce chr.inv.-projections for Einstein's field equations

$$R_{\alpha\beta} - \frac{1}{2} g_{\alpha\beta} R = -\kappa T_{\alpha\beta} + \lambda g_{\alpha\beta},$$

where he used $\kappa = \frac{8\pi G}{c^2}$ instead of $\kappa = \frac{8\pi G}{c^4}$ as used by Landau and Lifshitz in their *The Classical Theory of Fields* [8]. To understand the reason, consider the chr.inv.-projections of the energy-momentum tensor $T_{\alpha\beta}$ of a distributed matter, which are calculated according to the rule

$$\varrho = \frac{T_{00}}{g_{00}}, \quad J^i = \frac{c T_0^i}{\sqrt{g_{00}}}, \quad U^{ik} = c^2 T^{ik}$$

as for any symmetric tensor of the 2nd rank (see page 6). The scalar ϱ is the physically observable mass density of the distributed matter, J^i is its physically observable momentum density, and U^{ik} is its physically observable momentum flux density (stress-tensor). Ricci's tensor $R_{\alpha\beta}$ has the dimension [cm⁻²]. This means that the scalar chr.inv.-projection of the field equations, $\frac{G_{00}}{g_{00}} = -\frac{\kappa T_{00}}{g_{00}} + \lambda$, as well as $\frac{\kappa T_{00}}{g_{00}} = \frac{8\pi G \varrho}{c^2}$ have the same dimension [cm⁻²]. Hence, the energy-momentum tensor has the dimension of mass density [gram/cm³]. Therefore, if we used $\kappa = \frac{8\pi G}{c^4}$ on the right hand side of the field equations, then we would not use the energy-momentum tensor $T_{\alpha\beta}$ itself, but $c^2 T_{\alpha\beta}$ as Landau and Lifshitz did.

Taking all the above into account, Zelmanov had obtained the chr.inv.-projections of Einstein's field equations. They are called the chr.inv.-Einstein equations and have the form

$$\frac{* \partial D}{\partial t} + D_{jl} D^{jl} + A_{jl} A^{lj} + * \nabla_j F^j - \frac{1}{c^2} F_j F^j = -\frac{\kappa}{2} (\varrho c^2 + U) + \lambda c^2,$$

$$* \nabla_j (h^{ij} D - D^{ij} - A^{ij}) + \frac{2}{c^2} F_j A^{ij} = \kappa J^i,$$

$$\frac{* \partial D_{ik}}{\partial t} - (D_{ij} + A_{ij})(D_k^j + A_k^j) + D D_{ik} + 3A_{ij} A_k^j - \frac{1}{c^2} F_i F_k + \frac{1}{2} (* \nabla_i F_k + * \nabla_k F_i) - c^2 C_{ik} = \frac{\kappa}{2} (\varrho c^2 h_{ik} + 2U_{ik} - U h_{ik}) + \lambda c^2 h_{ik}.$$

In addition, the energy-momentum tensor $T_{\alpha\beta}$ of the distributed matter must satisfy the conservation law

$$\nabla_\sigma T^{\sigma\alpha} = 0,$$

the chr.inv.-projections of which are calculated as for the absolute divergence of any symmetric tensor of the 2nd rank (see page 20), and are chr.inv.-conservation law equations

$$\frac{* \partial \varrho}{\partial t} + D \varrho + \frac{1}{c^2} D_{ij} U^{ij} + * \widetilde{\nabla}_i J^i - \frac{1}{c^2} F_i J^i = 0,$$

$$\frac{* \partial J^k}{\partial t} + D J^k + 2(D_i^k + A_i^k) J^i + * \widetilde{\nabla}_i U^{ik} - \varrho F^k = 0.$$

So, we have presented here Zelmanov's mathematical apparatus of chronometric invariants, which are physical observables in General Relativity. This mathematical apparatus is given here in its entirety and in the form it was introduced by Zelmanov in 1944 (except for the chr.inv.-Maxwell equations, the chr.inv.-d'Alembert and chr.inv.-Laplace operators, which were deduced later). The above description of this mathematical apparatus contains all its foundations and definitions, tensor calculus in terms of chronometric invariants, as well as the most common equations used in General Relativity, which are also expressed in terms of chronometric invariants. All this is collected here in one article, which is very convenient. Even if we have missed some details, these details are not essential for understanding and working with this mathematical apparatus.

Zelmanov's mathematical apparatus was applied to many problems of General Relativity. In general, Zelmanov always said that he liked creating "mathematical tools" more than applying them. Nevertheless, his contribution to relativistic cosmology, as well as his calculation of the main effects of General Relativity and the basics of electrodynamics in terms of chronometric invariants, are significant. We also made a contribution: the list of our works, published in English and French, can be found just after the References*.

We recommend the present article to all those readers who would like to work independently in the field of General Relativity using the mathematical apparatus of chronometric invariants. Good luck!

Submitted on January 3, 2023

References

1. Zelmanov A.L. Chronometric Invariants. Translated from the 1944 PhD thesis, American Research Press, Rehoboth (New Mexico), 2006.
2. Zelmanov A.L. Chronometric invariants and accompanying frames of reference in the General Theory of Relativity. *Soviet Physics Doklady*, 1956, v. 1, 227–230 (translated from *Doklady Akademii Nauk SSSR*, 1956, v. 107, no. 6, 815–818).

*It is necessary to say a word about the authorship of those articles in this list, which were published before 1991. It was the dark time of the communist dictatorship, when the personal contribution of a researcher, especially a woman, was neglected. Therefore, when L. Borisova submitted an article for publication through her superiors (because there was no other way to submit at that time), she could often find their names added to the submission. She was allowed to publish her articles only under her own name only after great troubles and a scandal. As one of the superiors publicly stated: "Science is a man's business. We will not allow this 'Einstein in a skirt' to be present in science." Even Zelmanov, who took custody of her from her student years, could not do anything against this suppression and lawlessness. As a result, those persons whose names can be found as "co-authors" in some of her publications before 1991 had nothing to do with her research: they, having an administrative power, simply added their names to her submissions. Their names must therefore be excluded from those published articles and forgotten (despite the fact that we mentioned them in the bibliography for this article). Fortunately, this dark era of our lives ended in 1991 after the collapse of the USSR and everything connected with it. All the mathematical problems that we considered in our works (from our student years to the present day) were posed and solved only by us, individually or together, but without any assistance or advice of a "supervisor" or another person.

3. Zelmanov A.L. On the relativistic theory of an anisotropic inhomogeneous universe. *The Abraham Zelmanov Journal*, 2008, v. 1, 33–63 (translated from the thesis of the 6th Soviet Conference on the Problems of Cosmogony, held in 1957 in Moscow, SSSR Acad. Science Publishers, Moscow, 1959, 144–174).
4. Rabounski D and Borissova L. Particles Here and Beyond the Mirror. The 3rd expanded edition, American Research Press, Rehoboth, New Mexico, 2012 (first published in 1999, in Russian; the 1st English edition — in 2001). Rabounski D. et Borissova L. Particules de l'univers et au delà du miroir. American Research Press, Rehoboth, New Mexico, 2012 (French translation).
5. Borissova L. and Rabounski D. Fields, Vacuum, and the Mirror Universe. The 2nd expanded edition, Svenska fysikarkivet, Stockholm, 2009 (first published in 1999, in Russian; the 1st English edition — in 2001). Borissova L. et Rabounski D. Champs, vide, et univers miroir. American Research Press, Rehoboth, New Mexico, 2010 (French translation).
6. Borissova L. and Rabounski D. Inside Stars: A Theory of the Internal Constitution of Stars, and the Sources of Stellar Energy According to General Relativity. 2nd expanded edition, American Research Press, Rehoboth, New Mexico, 2014.
7. Rabounski D. and Borissova L. Non-quantum teleportation in a rotating space with a strong electromagnetic field. *Progress in Physics*, 2022, no. 1, 31–49.
8. Landau L. D. and Lifshitz E. M. The Classical Theory of Fields. Pergamon Press, Oxford, 1951 (translated from the 1st Russian edition published in 1939).
9. Cattaneo C. General Relativity: relative standard mass, momentum, energy, and gravitational field in a general system of reference. *Nuovo Cimento*, 1958, v. 10, 318–337.
10. Cattaneo C. On the energy equation for a gravitating test particle. *Nuovo Cimento*, 1959, v. 11, 733–735.
11. Cattaneo C. Conservation laws in General Relativity. *Nuovo Cimento*, 1959, v. 13, 237–240. vol. 11, 733–735.
12. Cattaneo C. Problèmes d'interprétation en Relativité Générale. *Colloques Internationaux du Centre National de la Recherche Scientifique*, no. 170 "Fluides et champ gravitationnel en Relativité Générale", Éditions du Centre National de la Recherche Scientifique, Paris, 1969, 227–235.
13. Schouten J. A. und Struik D. J. Einführung in die neuen Methoden der Differentialgeometrie. Noordhoff, Groningen, 1938 (first published in *Zentralblatt für Mathematik*, 1935, Bd. 11 und Bd. 19).
14. Hafele J. Performance and results of portable clocks in aircraft. PTTI 3rd Annual Meeting, November 16–18, 1971, 261–288.
15. Hafele J. and Keating R. Around the world atomic clocks: predicted relativistic time gains. *Science*, July 14, 1972, v. 177, 166–168.
16. Hafele J. and Keating R. Around the world atomic clocks: observed relativistic time gains. *Science*, July 14, 1972, v. 177, 168–170.
17. Demonstrating relativity by flying atomic clocks. *Metromnia*, the UK's National Measurement Laboratory Newsletter, issue 18, Spring 2005.
18. Raschewski P.K. Riemannsche Geometrie und Tensoranalysis. Deutscher Verlag der Wissenschaften, Berlin, 1959; reprinted by Verlag Harri Deutsch, Frankfurt am Main, 1993.

Applying Chronometric Invariants

1. Borissova L. B. (née Grigor'eva) Chronometrically invariant representation of the classification of the Petrov gravitational fields. *Soviet Physics Doklady*, 1970, v. 15, 579–582 (translated from *Doklady Acad. Nauk SSSR*, 1970, v. 192, no. 6, 1251–1254).
2. Borissova L. B. (née Grigor'eva) and Zakharov V. D. Spaces of recurrent curvature in the General Theory of Relativity. *Soviet Physics Doklady*, 1973, v. 17, 1160–1163 (translated from *Doklady Acad. Nauk SSSR*, 1972, v. 207, no. 4, 814–816).

3. Borissova L. B. and Zakharov V. D. Gravitoinertial waves in vacuum. *Russian Physics Journal*, 1974, v. 17, no. 12, 1723–1728 (translated from *Izvestiia Vysshikh Uchebnykh Zavedenii, Fizika*, 1974, no. 12, 106–113).
4. Borissova L. B. Relative oscillations of test particles in comoving reference frames. *Soviet Physics Doklady*, 1976, v. 20, 816–819 (translated from *Doklady Acad. Nauk SSSR*, 1975, v. 225, no. 4, 786–789).
5. Borissova L. B. and Zakharov V. D. A system of probe particles in the field of planar gravitational waves. Part I. *Russian Physics Journal*, 1976, v. 19, no. 12, 1617–1619 (translated from *Izvestiia Vysshikh Uchebnykh Zavedenii, Fizika*, 1976, no. 12, 108–111).
6. Borissova L. B. and Zakharov V. D. A system of probe particles in the field of planar gravitational waves. Part II. *Russian Physics Journal*, 1976, v. 19, no. 12, 1620–1624 (translated from *Izvestiia Vysshikh Uchebnykh Zavedenii, Fizika*, 1976, no. 12, 111–117).
7. Borissova L. B. Quadrupole mass-detector in field of weak plane gravitational fields. *Russian Physics Journal*, 1978, v. 21, no. 10, 1341–1344 (translated from *Izvestiia Vysshikh Uchebnykh Zavedenii, Fizika*, 1978, no. 10, 109–114).
8. Borissova L. B. and Melnikov V. N. Laser interferometer in variable gravitational field. *Measurement Techniques*, 1985, v. 28, no. 4, 301–307 (translated from *Izmeritel'naya Tekhnika*, 1985, no. 4, 16–19).
9. Borissova L. B. and Melnikov V. N. Relativistic corrections to readings from a portable clock. *Measurement Techniques*, 1988, v. 31, no. 4, 323–327 (translated from *Izmeritel'naya Tekhnika*, 1988, no. 4, 13–15).
10. Borissova L. B., Bronnikov K. A., Melnikov V. N. Taking into account gravitational and relativistic effects in maintaining a unified time scale on the Earth and surrounding space. *Measurement Techniques*, 1988, v. 31, no. 5, 450–455 (translated from *Izmeritel'naya Tekhnika*, 1988, no. 5, 31–33).
11. Rabounski D. and Borissova L. *Particles Here and Beyond the Mirror*. Editorial URSS Publishers, Moscow, 2001.
12. Borissova L. and Rabounski D. *Fields, Vacuum, and the Mirror Universe*. Editorial URSS Publishers, Moscow, 2001.
13. Rabounski D. A new method to measure the speed of gravitation. *Progress in Physics*, 2005, no. 1, 3–6.
14. Borissova L. and Rabounski D. On the possibility of instant displacements in the space-time of General Relativity. *Progress in Physics*, 2005, no. 1, 17–19.
15. Rabounski D. A theory of gravity like electrodynamics. *Progress in Physics*, 2005, no. 2, 15–29.
16. Borissova L. Gravitational waves and gravitational inertial waves in the General Theory of Relativity: A theory and experiments. *Progress in Physics*, 2005, no. 2, 30–62.
17. Rabounski D., Borissova L., Smarandache F. Entangled states and quantum causality threshold in the General Theory of Relativity. *Progress in Physics*, 2005, no. 2, 101–107.
18. Rabounski D., Smarandache F., Borissova L. *Neutrosophic Methods in General Relativity*. Hexis, Phoenix, Arizona, 2005.
19. Rabounski D. Zelmanov's Anthropic Principle and the Infinite Relativity Principle. *Progress in Physics*, 2006, no. 1, 35–37.
20. Rabounski D. Correct linearization of Einstein's equations. *Progress in Physics*, 2006, no. 2, 3–5.
21. Rabounski D. and Borissova L. Exact theory of a gravitational wave detector. New experiments proposed. *Progress in Physics*, 2006, no. 2, 31–38.
22. Rabounski D., Smarandache F., Borissova L. S-denying of the signature conditions expands General Relativity's space. *Progress in Physics*, 2006, no. 3, 13–19.
23. Borissova L. and Smarandache F. Positive, neutral and negative mass-charges in General Relativity. *Progress in Physics*, 2006, no. 3, 51–54.
24. Rabounski D. New effect of General Relativity: Thomson dispersion of light in stars as a machine producing stellar energy. *Progress in Physics*, 2006, no. 4, 3–10.
25. Borissova L. Preferred spatial directions in the Universe: a General Relativity approach. *Progress in Physics*, 2006, no. 4, 51–58.
26. Borissova L. Preferred spatial directions in the Universe. Part II. Matter distributed along orbital trajectories, and energy produced from it. *Progress in Physics*, 2006, no. 4, 59–64.
27. Rabounski D. The theory of vortical gravitational fields. *Progress in Physics*, 2007, no. 2, 3–10.
28. Borissova L. Forces of space non-holonomy as the necessary condition for motion of space bodies. *Progress in Physics*, 2007, no. 2, 11–16.
29. Rabounski D. and Borissova L. A theory of the Podkletnov effect based on General Relativity: Anti-gravity force due to the perturbed non-holonomic background of space. *Progress in Physics*, 2007, no. 3, 57–80.
30. Borissova L. and Rabounski D. On the nature of the microwave background at the Lagrange 2 point. *Progress in Physics*, 2007, no. 4, 84–95.
31. Rabounski D. and Borissova L. *Particles Here and Beyond the Mirror*. The 2nd expanded edition, Svenska fysikarkivet, Stockholm, 2008.
32. Borissova L. and Rabounski D. PLANCK, the satellite: A new experimental test of General Relativity. *Progress in Physics*, 2008, no. 2, 3–14.
33. Rabounski D. An explanation of Hubble redshift due to the global non-holonomy of space. *Progress in Physics*, 2009, no. 1, L1–L2.
34. Rabounski D. Hubble redshift due to the global non-holonomy of space. *The Abraham Zelmanov Journal*, 2009, v. 2, 11–28.
35. Rabounski D. On the speed of rotation of the isotropic space: Insight into the redshift problem. *The Abraham Zelmanov Journal*, 2009, v. 2, 208–223.
36. Borissova L. The gravitational field of a condensed matter model of the Sun: The space breaking meets the Asteroid strip. *The Abraham Zelmanov Journal*, 2009, v. 2, 224–260.
37. Borissova L. and Rabounski D. *Fields, Vacuum, and the Mirror Universe*. The 2nd expanded edition, Svenska fysikarkivet, Stockholm, 2009.
38. Borissova L. et Rabounski D. *Champs, Vide, et Univers miroir*. American Research Press, Rehoboth, New Mexico, 2010 (French translation).
39. Rabounski D. et Borissova L. *Particules de l'Univers et au delà du Miroir*. American Research Press, Rehoboth, New Mexico, 2012 (French translation).
40. Borissova L. The Solar System according to General Relativity: The Sun's space breaking meets the Asteroid strip. *Progress in Physics*, 2010, no. 2, 43–47.
41. Borissova L. De Sitter bubble as a model of the observable Universe. *The Abraham Zelmanov Journal*, 2010, v. 3, 3–24.
42. Borissova L. Gravitational waves and gravitational inertial waves according to the General Theory of Relativity. *The Abraham Zelmanov Journal*, 2010, v. 3, 25–70.
43. Rabounski D. and Borissova L. A theory of frozen light according to General Relativity. *The Abraham Zelmanov Journal*, 2011, v. 4, 3–27.
44. Rabounski D. Cosmological mass-defect — a new effect of General Relativity. *The Abraham Zelmanov Journal*, 2011, v. 4, 137–161.
45. Rabounski D. Non-linear cosmological redshift: The exact theory according to General Relativity. *The Abraham Zelmanov Journal*, 2012, v. 5, 3–30.
46. Rabounski D. On the exact solution explaining the accelerate expanding Universe according to General Relativity. *Progress in Physics*, 2012, no. 2, L1–L6.

47. Rabounski D and Borissova L. *Particles Here and Beyond the Mirror*. The 3rd expanded edition, American Research Press, Rehoboth, New Mexico, 2012.
 48. Rabounski D. et Borissova L. *Particules de l'Univers et au delà du Miroir*. American Research Press, Rehoboth, New Mexico, 2012 (French translation).
 49. Borissova L. and Rabounski D. *Inside Stars: A Theory of the Internal Constitution of Stars, and the Sources of Stellar Energy According to General Relativity*. American Research Press, Rehoboth, New Mexico, 2013.
 50. Borissova L. and Rabounski D. *Inside Stars: A Theory of the Internal Constitution of Stars, and the Sources of Stellar Energy According to General Relativity*. 2nd expanded edition, American Research Press, Rehoboth, New Mexico, 2014.
 51. Borissova L. A telemetric multispace formulation of Riemannian geometry, General Relativity, and cosmology: Implications for relativistic cosmology and the true reality of time. *Progress in Physics*, 2017, no. 2, 57–75.
 52. Borissova L. and Rabounski D. Cosmological redshift in the de Sitter stationary Universe. *Progress in Physics*, 2018, no. 1, 27–29.
 53. Rabounski D. and Borissova L. Non-quantum teleportation in a rotating space with a strong electromagnetic field. *Progress in Physics*, 2022, no. 1, 31–49.
 54. Rabounski D. and Borissova L. Deflection of light rays and mass-bearing particles in the field of a rotating body. *Progress in Physics*, 2022, no. 1, 50–55.
 55. Rabounski D. and Borissova L. Length stretching and time dilation in the field of a rotating body. *Progress in Physics*, 2022, no. 1, 62–65.
-

Fission with a Difference

G. S. Burra

Adj. Professor, University of Udine, 201, Via delle Scienze 33100, Udine, Italy. E-mail: gsburra7748@gmail.com

Invoking a model of an elementary particle as a collection of ultrarelativistic transient particles, we show that it is possible to recover the energy of the particle by bombarding it with monochromatic high-energy radiation.

Introduction

We consider the possibility of using an alternative route to releasing fission energy. This is prompted by some recent developments by the team of scientists Cruz-Chu *et al* [1], which leads to the technological development of practically monochromatic radiation in the X-ray region.

Let us start from a relativistic point of view, and the Lorentz transformation,

$$x = \gamma(x' - vt), \quad \gamma = (1 - v^2/c^2)^{-1/2}. \quad (1)$$

Indeed it is known that for a collection of relativistic particles, the various mass centres form a two-dimensional disc perpendicular to the angular momentum vector \vec{L} and with radius [3]

$$r = \frac{L}{mc}. \quad (2)$$

Further if the system has positive energies, then it must have an extension greater than r , while at distances of the order of r , we begin to encounter negative energies.

If we consider the system to be a particle of spin or angular momentum $L = \hbar/2$, then (2) gives $r = \hbar/2mc$. That is, we are in the Compton wavelength region. Another interesting feature which is the two dimensionality of the disc of mass centres.

On the other hand it is known that (cf. [4]), if a Dirac particle is represented by a Gaussian packet, then we begin to encounter negative energies precisely at the same Compton wavelength as above. Thus a particle can indeed be treated as a spherical shell of relativistic transient sub-constituents or “particlets”. Indeed, this is an alternative description of Dirac’s zitterbewegung or rapid oscillation.

The above picture is also reminiscent of Dirac’s shell or membrane model of the electron [5–7].

Outside this Compton region we have the usual space (or space time) of physics. But as we approach the Compton wavelength region we encounter a region where the space axis becomes as it were a complex plane. This has been described at length by the author, in terms of the Feschbach formalism [8] which leads to the double Weiner process. Consider the following system [9]

$$\begin{aligned} i\hbar \frac{\partial \phi}{\partial t} &= \frac{1}{2m} \left(\frac{\hbar}{i\nabla} - \frac{e\mathbf{A}}{c} \right)^2 (\phi + \chi) + (e\phi + mc^2)\phi \\ i\hbar \frac{\partial \phi}{\partial t} &= -\frac{1}{2m} \left(\frac{\hbar}{i\nabla} - \frac{e\mathbf{A}}{c} \right)^2 (\phi + \chi) + (e\phi - mc^2)\phi. \end{aligned} \quad (3)$$

The merit of this formalism is that it enables us to give a particle interpretation to the usual wave-formalism (see [8] for further details.) However the advantage of the Feschbach Villars formalism is that we can now work with an ostensible particle interpretation.

In any case, we encounter the Compton scale again and again. Wigner [10] pointed out its remarkable universality.

From the above it is apparent that if an elementary particle in the above characterisation is bombarded with very high frequency radiation of the order of the Compton frequency such a particle would break up and yield its energy. What happens in this case is that the Bell curve becomes so compressed that it will be like a straight line or spike, almost (see [12, 13]). This sharp spike would break up the elementary particle releasing its mass as energy.

It is well known in Quantum Mechanics that what may be called monochromatic waves are an idealization. This is in the sense that we have in general a wave packet made up of several frequencies [2]. But suppose we can single out a pure or nearly pure frequency? This is a technological problem. Let us start with the Schrodinger equation [2]:

$$\frac{d^2\psi}{dx^2} + \frac{p^2}{\hbar^2}\psi = 0$$

where

$$p = \sqrt{2m[E - V(x)]}.$$

This leads to

$$\phi(x) \exp\left(\pm \frac{i}{\hbar} \int^x p(x) dx\right) \quad (4)$$

where $\phi(x)$ is the solution of the free equation, and we already have a wave packet over different values of p or effectively frequencies. However, if we have a wave function like $\psi' = e^{ikx-pt}$, such a wave would be an extreme idealization and at the same time would be monochromatic. Can we achieve this, is the question. There has been recently some progress in this direction thanks to the experiment of Cruz-Chu and co-workers [1] who have been able to conduct an experiment where single particle X-ray diffraction patterns could be analysed thanks to a machine learning algorithm.

Remarks

What happens in this case is, the Bell curve becomes so compressed that it will be like a straight line. This sharp spike

could break up the elementary particle releasing its mass as energy. Fortunately, in recent years there has been some progress in this direction [11–13]. Furthermore, it may be pointed out that a pure monochromatic signal would be useful in communications as well. This is because, effectively the bandwidth would increase [14]. Finally, we observe that, if we can break up quarkonium particles, we can extract even greater energy. There is one way of doing this: we know that with $g = 2$ factor, there is a sort of precession and, if we could radiate with resonant frequencies, the particle would break up. This could be a technological problem.

Received on January 18, 2023

References

1. Cruz-Chú E. R., Ahmad H., Ghoncheh M., *et al.* Selecting XFEL single-particle snapshots by geometric machine learning. *Structural Dynamics*, 2021, v. 8 (1), 014701.
2. Powell J. L. and Crasemann B. *Quantum Mechanics*. Addison-Wesley, Reading, Mass., 1961.
3. Moller C. *The Theory of Relativity*. Clarendon Press, Oxford, 1952, pp. 170 ff.
4. Bjorken J. D. and Drell S. D. *Relativistic Quantum Mechanics*. McGraw-Hill, New York, 1964, p. 39.
5. Dirac P. A. M. *Proc. Roy. Soc., London*, 1962, v. A268, 57.
6. Barut A. O. and Pavsic M. IC/92/399, ICTP Report, Miramare-Trieste, 1992.
7. Barut A. O. and Pavsic M. IC/88/2 ICTP Report, Miramare-Trieste, 1988.
8. Feshbach H. and Felix V. Elementary relativistic wave mechanics of spin 0 and spin 1/2 particles. *Reviews of Modern Physics*, 1958, v. 30 (1), 24.
9. Sidharth B. G. *Thermodynamic Universe*. World Scientific, Singapore, 2008.
10. Newton T. D. and Wigner E. P. *Rev. Mod. Phys.*, 1949, v. 21 (3), 400.
11. Rodriguez J. I. Parametric X-ray methods use 2D heterostructures to generate compact, tunable X-ray sources. <https://doi.org/10.1063/1.5005660>, 281103, 2021.
12. Berry M. V. and Dennis M. R. Natural superoscillations in monochromatic waves in D dimensions. *Journal of Physics A: Mathematical and Theoretical*, 2008, v. 42 (2), 022003.
13. Kostylev M., Gubbiotti G., Carlotti G., Socino G., Tacchi S., Wang C., Singh N., Adeyeye A. O. and Stamps R. L. Propagating volume and localized spin wave modes on a lattice of circular magnetic antidots. *Journal of Applied Physics*, 2008, v. 103 (7), 07C507.
14. Sidharth B. G. *Sciencescapes. New advances in physics*, 2021, v. 2.

Avoiding Negative Energies in Quantum Mechanics

G. G. Nyambuya

National University of Science and Technology, Faculty of Applied Sciences – Department of Applied Physics,
Fundamental Theoretical and Astrophysics Group, P. O. Box 939, Ascot, Bulawayo, Republic of Zimbabwe.
E-mail: physicist.ggn@gmail.com

Quantum mechanical observables are naturally assumed to be real. Herein, we depart from this traditional and seemingly natural assumption whereby we consider a Quantum Mechanics (QM) whose operators have corresponding complex eigenvalues. The motivation for this is that complex eigenvalues lead us directly to positive definite energy solutions, hence mass. The resulting QM is able to qualitatively explain in a coherent manner some physical phenomenon that are currently inexplicable from a QM whose operators have corresponding real eigenvalues – e.g. one is now able to explain the instability of particles, their localization, the observed matter-antimatter asymmetry and the supposed variation of fundamental natural constants amongst others. In addition to this, there is the difficulty in Dirac's interpretation of negative energy states appearing in his theory. While Dirac's negative energy problem is not considered a problem anymore, we provide an alternative way out of this problem. We propose that eigenvalues corresponding to quantum mechanical operators associated with physical observables ought to be complex. From this seemingly simple hypothesis, we demonstrate that negative energy states leading to negative mass can be avoided altogether.

I cannot imagine a reasonable Unified Theory containing an explicit number which the whim of the Creator could just as easily have chosen differently . . . Numbers arbitrarily chosen by God do not exist. Their alleged existence relies on our incomplete understanding [of the Laws of Nature and how God designed and fashioned the Universe].

Albert Einstein (1879-1955)

1 Introduction

Looking back – thus far, one can most confidently and safely say that the time period of the first thirty years of the twentieth century was perhaps a special time in the intellectual discourse of humanity with this period being a period of the greatest intellectual leaps in all the history of human thought and intellectual endeavour. For to date, these great intellectual leaps have found no equal. Perhaps, apart from CERN's famous 4th of July 2012 announcement that a strong signal mimicking a *Higgs-like* particle has been detected in the LHC data, it appears as though real progress in Physics has hit a serious brick wall. In all probability, it ought to be said that there has not been any real noteworthy and new exciting discoveries this century as those witnessed at the beginning of the twentieth century, especially on the *frontiers of fundamental theoretical Physics*.

Take for example: in 1905, Germany's youthful 26 years' old third class Swiss patent clerk Albert Einstein (1879-1955) [1] discovered the Special Theory of Relativity (STR), and shortly thereafter, in the period 1923-4, France's aristocrat and physicist Louis Victor Pierre Raymond de Broglie (1892-1987) [2–5] opened *Pandora's Box* with his wave-particle duality hypothesis, Germany's great physicist Werner Karl

Heisenberg (1901-1976) [6] theoretically argued his uncertainty principle into existence and Austria's own theoretical physicist Erwin Rudolf Josef Alexander Schrödinger (1887-1961) [7, 8] discovered the key wave equation of Quantum Mechanics (QM) which now bears his name, *etc.*

Once QM was inceptioned in the mid-1920s, no sooner was it realised that there was a need to unite these two theories which stand to this day as a major part of the twin pillars of modern physics – i.e. the STR and QM. At the time of these great discoveries and revolutionary paradigm shifts, nobody yet knew how to make the two theories consistent with each other. In 1928 while QM was still in its nascence, the then little-known British preeminent Paul Adrien Maurice Dirac (1902-1984), who ranks as one of the greatest fundamental theoretical physicists of his time, then only 26 years' old, succeeded where others found it difficult. Dirac [9, 10] successfully unified Einstein [1]'s STR and de Broglie [2–5], Heisenberg [6] and Schrödinger [7, 8]'s QM.

Dirac [9, 10]'s unified theory was an unprecedented success, except for one detail: a quantum system could have either positive or negative energy. How can something have negative energy? For example, according to Einstein [1]'s mass-energy equivalence, the mass (m) of a particle is related to its energy (E) by the relation $m = E/c_0^2$ (where: $c_0 = 2.99792458 \times 10^8 \text{ m s}^{-1}$ is the speed of light in *vacuo*), such that negative energy entails negative mass. For all we know, the measure of the resistance to any change of the state of motion of a given substance is a measure of its mass. Further, mass was and is understood as a measure of the quantity of matter in a substance. From this understanding, what does negative mass mean?

According to Newton's first law of motion, since a posi-

tive mass quantum system has the property that it has the tendency to preserve its current state of motion in such a manner that it resists all efforts to change this state of motion, does it then mean that a negative mass quantum system will have the exact opposite properties, that is, have the property that it has the tendency not to preserve the particle's current state of motion in such a manner that it does not resist any efforts to change the particle's current state of motion but only engenders it? Such are some of the plausible questions that have puzzled those that have attempted to comprehend what negative mass might actually be or mean. What will happen when positive energy-mass matter comes in contact with negative energy-mass matter? Will they nullify upon contact? These are just some of the pertinent questions out of many plausible ones that come to mind.

Be that as it may, Dirac was an extraordinary brilliant man who sought beauty in his work. He did not think of the negative energy quantum systems implied by his equation in ordinary terms, but thought of them mathematically and quantum mechanically. The negative energy solutions first appeared in the Klein [11] and Gordon [12] theory (KG-theory) on whose shoulders the Dirac's theory stands. In order to get rid of these negative energies, some notable figures of the time suggested that these negative energy solutions must be discarded with the simple remark that "these solutions have no correspondence with physical and natural reality". To that, Dirac [9] replied:

One gets over the difficulty on the classical theory by arbitrarily excluding those solutions that have a negative E . One cannot do this in the QM, since in general a perturbation will cause transitions from states with E -positive to states with E -negative.

So, it would strongly appear that negative energy states were here to stay – at least in theory. They needed a satisfying physical explanation.

While Dirac's theory was met with both enthusiasm and scepticism (e.g. by physicists Werner Heisenberg, Wolfgang Ernst Pauli (1900-1958), Ernst Pascual Jordan (1902-1980), George Gamow (1904-1968), amongst others), the enthusiasm was on the latent power wielded by the equation, e.g. the equation solved the difficult contemporary problem of spin; and scepticism was with respect to the negative energy solutions. Against this scepticism, Dirac [13] further proposed that the *vacuo* was an unobservable infinite sea of negative energy states, such that all negative energy states were filled! This invisible sea of negative energy states became known as the Dirac Sea.

According to Pauli [14]'s Exclusion Principle (PEP) that forbids more than two fermions to be in the same quantum state, a Universe in which there exists a Dirac Sea would forbid the transitions of positive energy quantum states to transit into negative energy states thereby resulting in a Universe that has stable positive energy states. Transitions from states with E -positive to states with E -negative are forbidden because the

E -positive state once in the E -negative state is going to be in the same quantum state as the E -negative state thus violating the PEP, hence, forbidden by Nature. In this way, the Dirac [9, 10] theory was safe.

To further clarify Dirac's theory, the preeminent American physicist Richard Phillips Feynman (1924-1987) proposed that the negative energy states be interpreted as antiparticles: they move backwards in time such that, in a Universe where time moves in a forward direction, these quantum states would appear as positive energy states. This is the current *de facto* interpretation of antiparticles. Other than the negative energy problem, Dirac [9, 10]'s equation exhibits a perfect symmetry and this property of the equation has no correspondence nor bearing with physical and natural reality as we know it. Often, the theory has had to be patched [15, for example] in order to measure up to physical and natural reality. These patches often propose that the combined Charge (C) and Space or Parity (P) reversal symmetry (CP violation) must explain the apparent matter-antimatter asymmetry [16]. While CP violation has been observed [17–22, for example], it is yet to be verified by experiment as the mechanism responsible for the observed matter-antimatter asymmetry.

We must hasten to say that, while this work will touch on other subjects that we had not intended to cover, the original and sole aim of this work is twofold:

1. To demonstrate that Dirac's negative energy solutions can be eliminated altogether by resorting to particles endowed with Complex Energy and Momentum (CEM) wherein under this new proposal, the energy and momentum of the quantum system of concern is measured as the magnitude of these complex quantities.
2. To show that the resultant energy from the resulting complex energy and momentum does solve without any need for exogenous ideas, the matter-antimatter asymmetry problem that the Dirac theory has so far failed to solve and possibly the recent issue to do with the plausible variation of *Fundamental Natural Constants* (FNCs).

To achieve our desired objective, we adopt the working hypothesis, that in general, all quantum mechanical observables such as the energy and momentum of quantum mechanical systems can take complex values ($z = x + iy$) such that the resultant observable that we measure in the laboratory is the magnitude of this complex quantity in question (i.e. $|z| = \sqrt{x^2 + y^2} \geq 0$). This assumption is all that we shall require in our exploration. As a result, we shall formulate a new basis for the further development of a QM that allows for observables to take complex values and from thereon, proceed to show that the theory resulting from the CEM hypothesis not only provides a plausible and perdurable solution to Dirac's problem of negative energies, but that, it also provides a plausible solution to the matter-antimatter asymmetry problem which the bare Dirac theory is unable to solve by its own.

In closing this introductory section, we give the synopsis of the reminder of this paper. That is: in §2, we dis-

cuss the idea of complex quantum mechanical observables: we discuss how this idea may provide a perdurable solution to Dirac's negative energy problem. In §3, we write down the usual Dirac equation and thereafter proceed to incorporate into its structure the CEM hypothesis. In §4, we apply the idea of complex quantum mechanical observables to the notion of the variation of FNCs. In §5, we work out the symmetries of the new CEM-Dirac equation, and lastly, in §6 and §7, we give a general discussion and the conclusion drawn thereof, respectively.

2 Complex energy and momentum

The negative probabilities manifesting in the KG-theory are a result of the fact that the emergent quantum probability (P_Q) expression in this theory is directly proportional to the energy (E) of the quantum system in question – i.e. $P_Q \propto E$, the consequential meaning of which is that, for negative energy quantum systems, the corresponding quantum probability will be negative. From this very fact $P_Q \propto E$, Dirac hatched the idea that these negative energies appearing in the quantum probability of the KG-theory could be removed if a theory linear in the temporal and spatial derivatives were possible because a linear system of equations will always have one solution, a quadratic two, a cubic three, a quad four, *etc.*

Further on his effort to eliminate these meaningless negative probabilities, Dirac hoped that with his linear solution, he might also eliminate the negative energy solutions as well. Because of the pivotal constraint that he imposed on his theory, namely that when his equation is *squared* it must yield the quantum mechanical wave equation of the KG-theory, this directly translates to the fact that the energy solutions of Dirac's quantum systems would exactly be as those obtained in the KG-theory, thus leading back to the same problem of negative energies faced by the KG-theory. The only way to eliminate these supposedly *nagging* negative energy solutions would be to build a theory from an energy-momentum equation that only admits positive definite energy solutions from the outset. This is the approach that we take here. We make use of a property of complex numbers – namely that the magnitude of a complex number is always a positive definite quantity.

To that end, we postulate that every physical observable ($O \in \mathbb{C}$) shall be considered to have two parts to it, namely: the real part ($O_R \in \mathbb{R}$), and the imaginary part ($O_I \in \mathbb{R}$), that is to say:

$$O = O_R + i O_I. \quad (1)$$

The subscripts R and I in (1) are used to label the real and imaginary parts of the complex physical quantity in question. For example, if the energy of a quantum system were complex, then $E = E_R + i E_I$, where E_R and E_I are the real and imaginary parts of the energy respectively. The imaginary part of the energy may lead to the possibility of naturally explaining the phenomenon of particle decay. In the case of

momentum, $\vec{p} = \vec{p}_R + i \vec{p}_I$, where \vec{p}_R and \vec{p}_I are the real and imaginary parts of the momentum respectively. Likewise, the imaginary part of the momentum may very well lead one to be able to naturally explain why particles are localised. These are interesting issues that can be tackled in a separate paper in the future.

Once the energy and momentum are complex physical variables, the rest-mass m_0 cannot be spared – i.e. $m_0 = m_R + i m_I$, where $(m_R, m_I) \in \mathbb{R}$. In summary:

$$E = E_R + i E_I, \quad (2a)$$

$$\vec{p} = \vec{p}_R + i \vec{p}_I, \quad (2b)$$

$$m_0 = m_R + i m_I. \quad (2c)$$

What (2) implies is that the four momentum p_μ , will have two parts to it – with one part that is associated with the real part and the other with the imaginary part, i.e.

$$\begin{aligned} p_\mu &= \left(\vec{p}, \frac{i E}{c_0^2} \right) \\ &= \left(\vec{p}_R, \frac{i E_R}{c_0^2} \right) + i \left(\vec{p}_I, \frac{i E_I}{c_0^2} \right) \\ &= p_\mu^R + i p_\mu^I, \end{aligned} \quad (3)$$

where:

$$\vec{p}_R = p_1^R \vec{i} + p_2^R \vec{j} + p_3^R \vec{k}, \quad (4a)$$

$$\vec{p}_I = p_1^I \vec{i} + p_2^I \vec{j} + p_3^I \vec{k}. \quad (4b)$$

For p^μ , we will have $p^\mu = (\vec{p}, i E/c_0^2)^* = (\vec{p}^*, -i E^*/c_0^2)$, so that the relativistic invariant quantity $p^\mu p_\mu$ is now such that $p^\mu p_\mu = m_0^* m_0 c_0^2$, i.e.

$$|E|^2 - |\vec{p}|^2 c_0^2 = |m_0|^2 c_0^4, \quad (5)$$

where:

$$|E| = \sqrt{E^* E} = \sqrt{E_R^2 + E_I^2} \geq 0, \quad (6a)$$

$$|\vec{p}| = \sqrt{\vec{p}^* \cdot \vec{p}} = \sqrt{|\vec{p}_R|^2 + |\vec{p}_I|^2} \geq 0, \quad (6b)$$

$$|m_0| = \sqrt{m_0^* m_0} = \sqrt{m_R^2 + m_I^2} \geq 0, \quad (6c)$$

hence, when written in full, (5) is given by:

$$(E_R^2 + E_I^2) - (|\vec{p}_R|^2 + |\vec{p}_I|^2) c_0^2 = (m_R^2 + m_I^2) c_0^4. \quad (7)$$

While the energy and momentum of the quantum system are complex, what we measure as the energy, momentum and the rest-mass of the quantum system are the magnitudes of these complex quantities. These magnitudes can only take positive values. So from (5), we will have:

$$|E| = m c_0^2 = \sqrt{|\vec{p}|^2 c_0^2 + |m_0|^2 c_0^4} \geq 0. \quad (8)$$

In this way, we find a clever and clear mathematical fix to Dirac [13]'s long-standing issue of negative mass and energies as these are now positive definite (i.e. $|E| \geq 0$; $m = |E|/c_0^2 \geq 0$) as we would naturally expect. As a disclaimer, we must say that we are not saying that this is the scheme which *Nature* has chosen in order to solve this problem, but that this is a plausible solution which can be taken seriously. In the next section, we will show how this idea of complex observables can be applied to the supposed problem of temporal and spatial variation of *Fundamental Constants of Nature* (FNCs).

3 CEM-Dirac equation

What kind of a Dirac equation does one get from the CEM hypothesis? Before we can answer this important question, we write down, for completeness purposes, the usual Dirac equation that assumes real-valued physical observables. Written in Dirac [23]'s *Bra-Ket notation*, the Dirac equation is given by:

$$\left[i \hbar \gamma^\mu \partial_\mu - m_0 c_0 \right] |\psi\rangle = 0, \quad (9)$$

where:

$$|\psi\rangle = \begin{pmatrix} \psi_0 \\ \psi_1 \\ \psi_2 \\ \psi_3 \end{pmatrix}, \quad (10)$$

is a four-component wavefunction which can further be written as a composition of two spinors, the left-hand $|\psi_L\rangle$ and the right-hand $|\psi_R\rangle$ spinors respectively, i.e.:

$$|\psi\rangle = \begin{pmatrix} \psi_L \\ \psi_R \end{pmatrix}, \quad (11a)$$

$$|\psi_L\rangle = \begin{pmatrix} \psi_0 \\ \psi_1 \end{pmatrix}, \quad (11b)$$

$$|\psi_R\rangle = \begin{pmatrix} \psi_2 \\ \psi_3 \end{pmatrix}, \quad (11c)$$

and

$$\gamma^0 = \begin{pmatrix} I_2 & 0 \\ 0 & -I_2 \end{pmatrix}, \text{ and } \gamma^i = \begin{pmatrix} 0 & \sigma^i \\ -\sigma^i & 0 \end{pmatrix}, \quad (12)$$

are the 4×4 Dirac gamma matrices with I_2 and 0, being the 2×2 identity and null matrices respectively. Throughout this paper, the Greek indices will be understood to mean $\mu, \nu, \dots = 0, 1, 2, 3$; and lower case English alphabet indices: $i, j, k, \dots = 1, 2, 3$. The matrices σ^j are the three 2×2 Pauli [24] matrices and are given by:

$$\sigma^1 = \begin{pmatrix} 0 & 1 \\ 1 & 0 \end{pmatrix}, \quad (13a)$$

$$\sigma^2 = i \begin{pmatrix} 1 & 0 \\ 0 & -1 \end{pmatrix}, \quad (13b)$$

$$\sigma^3 = \begin{pmatrix} 0 & -1 \\ 1 & 0 \end{pmatrix}. \quad (13c)$$

The Dirac equation admits free particle solutions of the form $\psi = u e^{-iS/\hbar}$, where $u = u(E, \vec{p})$, is a 4×1 component object and $S = p_\mu x^\mu = \vec{p} \cdot \vec{r} - Et \in \mathbb{R}$ is the phase of the quantum system in question. The Quantum Probability Amplitude (QPA) ρ of such a quantum system is such that $\rho = u^\dagger u$, and this QPA has no temporal nor spatial dependence. As we shall soon find out, for the CEM version of the Dirac equation, things are very different.

The phase of the CEM-Dirac quantum system is such that $S = S_R + i S_I$, where $S_R = p_\mu^R x^\mu \in \mathbb{R}$ and $S_I = p_\mu^I x^\mu \in \mathbb{R}$ are the real and imaginary parts of the phase of the quantum system in question. Another major difference is that the rest-mass will be a complex quantity as opposed to it being real as is the case with the original Dirac equation. As will be demonstrated in §5, this complex rest-mass leads to a Lorentz [25–27] invariant C , CP , CT , and CPT -violating equation. The QPA of a CEM-Dirac quantum system is such that $\rho = u^\dagger u e^{S_I/\hbar}$, and unlike the QPA of the normal Dirac particle, the QPA of a CEM-Dirac quantum system does have an explicit temporal and spatial dependence. It is this explicit temporal and spatial dependence that we strongly believe will lead to an explanation of why particles decay and why they appear to be localized. Like we said (in the text above), we are not in the present going to investigate this issue, but shall leave it for a future paper. This we have done so that we keep our focus on the paramount issue at hand.

In closing this section, we must say that what we have presented herein is what we have coined the *CEM-Dirac equation*. While the CEM-Dirac equation and the usual Dirac equation are identical in their symbols – i.e. the way we write these two equations down, the main difference between them is that the energy, momentum and rest-mass of the CEM-Dirac equation are complex physical variables while in the usual Dirac equation these are real physical variables. The real part of the energy and momentum (E_R, \vec{p}_R) can perhaps be understood as the four-momentum of the quantum system that we measure in the laboratory while the imaginary part (E_I, \vec{p}_I), can be understood as the energy responsible for the decay and localization of the particle in question. Once more, we shall reiterate that these are issues for a separate paper. In the next section, we shall apply the *CEM-hypothesis* to the contemporary issue of the supposed variation of FNCs.

4 Variation of fundamental physical constants

In this section, we show that the supposed variation of fundamental physical constants such as the dimensionless Fine Structure Constant (FSC) (or the Sommerfeld [28] constant) α_0 can be explained from the idea just laid down above – i.e. the idea of CEM eigenvalues. The FSC is given by:

$$\alpha_0 = \frac{e^2}{4\pi\epsilon_0\hbar c_0}. \quad (14)$$

Present measurements give $1/\alpha_0 = 137.035999084(21)$ (CODATA, 2018). If the FSC is varying, it could be any one,

or a combination, of the constituents making up this dimensionless quantity, namely e , ε_0 , \hbar , c_0 , or any one of the combination of these supposed constants.

The idea that fundamental constants may vary during the course of the Universe's evolution was first considered by the preeminent British physicists Edward Arthur Milne (1896-1950) and Dirac [29]. Independently, Milne [30] and Dirac [29] considered cosmological models which incorporated a time-variable gravitational constant G , thus setting the ball rolling for the serious theoretical consideration of FNCs. In the intervening years 1938 to about 1999, the idea that FNCs may vary over cosmological times had no backing from experimental philosophy, and because of this, the idea was considered as purely nothing more than an academic pursuit, speculation and curiosity with no bearing whatsoever to do with physical and natural reality. With Web *et al.* [31]'s ground breaking work, this position has since changed as further and strong evidence from observational experience suggesting a plausible variation of the supposedly sacrosanct constants of Nature has been put forward for serious consideration [32–36, for example]. The question is: *Is there a fundamental basis for this variation?* We think that the QM of complex eigenvalues might have something to say about this.

Without any doubt whatsoever, FNCs (e.g. e , ε_0 , \hbar , c_0 , etc) are observables since they cannot only be measured in the laboratory, but are intimately, intrinsically and inherently associated with quantum systems. With that having been said, it is clear that if a physical observable such as an FNC is a true constant of Nature, i.e. having no spatial nor temporal variation, then its total (and not partial) time derivative must vanish identically – i.e. $d\langle O \rangle / dt \equiv 0$. The total (and not partial) time derivative operator is given by:

$$\frac{d}{dt} = \frac{\partial}{\partial t} + \vec{v} \cdot \vec{\nabla}. \quad (15)$$

Applying this to the expectation value $\langle O \rangle = \langle \Psi | \widehat{\mathcal{T}} | \Psi \rangle$ of an arbitrary observable O , one gets:

$$i\hbar \frac{d\langle O \rangle}{dt} = \langle \Psi | [\widehat{\mathcal{T}}^\dagger, \widehat{\mathcal{H}}] | \Psi \rangle + \vec{v} \cdot \langle \Psi | [\widehat{\mathcal{T}}^\dagger, \vec{\hat{P}}] | \Psi \rangle, \quad (16)$$

where:

$$[\widehat{\mathcal{T}}^\dagger, \widehat{\mathcal{H}}] = \widehat{\mathcal{T}}^\dagger \widehat{\mathcal{H}} - \widehat{\mathcal{H}} \widehat{\mathcal{T}}^\dagger, \quad (17a)$$

$$[\widehat{\mathcal{T}}^\dagger, \vec{\hat{P}}] = \widehat{\mathcal{T}}^\dagger \vec{\hat{P}} - \vec{\hat{P}} \widehat{\mathcal{T}}^\dagger, \quad (17b)$$

and $\vec{\hat{P}} = -i\hbar\vec{\nabla}$ is the quantum mechanical momentum operator and \vec{v} is the velocity of the quantum system under consideration. We must say that it is more appropriate to think of this velocity:

$$\vec{v} = \frac{\hbar}{m} \text{Im} \left(\frac{\Psi^\dagger \vec{\nabla} \Psi}{\Psi^\dagger \Psi} \right), \quad (18)$$

as the Bohmian [37–39] velocity* field of the quantum system in question and the possible justification for this has been provided in [40].

What (16) is telling us, is that if an observable is a true constant, that is, it does not vary neither with time nor space, then the operator corresponding to this observable must commute with both the Hamiltonian and the momentum operator – i.e. $[\widehat{\mathcal{T}}^\dagger, \widehat{\mathcal{H}}] = 0$, and $[\widehat{\mathcal{T}}^\dagger, \vec{\hat{P}}] = 0$. Against the seemingly sacrosanct dictates of our current understanding of QM, the condition $[\widehat{\mathcal{T}}^\dagger, \widehat{\mathcal{H}}] = 0$ is here found not to be sufficient to guarantee that the observable O will be a truly conserved quantity and constant quantity throughout all of space and time. If for some reason we have that $[\widehat{\mathcal{T}}^\dagger, \widehat{\mathcal{H}}] \neq 0$, and $[\widehat{\mathcal{T}}^\dagger, \vec{\hat{P}}] \neq 0$, then for an observable to be a true constant, the spatial variation ought to be compensated by the temporal variation and *vice-versa*, and this will be in accordance with (16) under the setting $d\langle O \rangle / dt = 0$.

At this point, in order for us to proceed, we need to evaluate (16) in terms of *observable* quantities, i.e. we need to compute $\langle \Psi | [\widehat{\mathcal{T}}^\dagger, \widehat{\mathcal{H}}] | \Psi \rangle$ and $\vec{v} \cdot \langle \Psi | [\widehat{\mathcal{T}}^\dagger, \vec{\hat{P}}] | \Psi \rangle$. To that end, we know that:

$$\begin{aligned} \left\langle \widehat{\mathcal{T}} \frac{\partial \Psi}{\partial t} \right\rangle &= \frac{1}{i\hbar} \left\langle \widehat{\mathcal{T}} i\hbar \frac{\partial \Psi}{\partial t} \right\rangle, \\ &= \frac{1}{i\hbar} \left\langle \widehat{\mathcal{T}} \widehat{E} \Psi \right\rangle, \\ &= -\frac{1}{i\hbar} E \left\langle \widehat{\mathcal{T}} \Psi \right\rangle, \end{aligned} \quad (19)$$

and that:

$$\begin{aligned} \left\langle \widehat{\mathcal{T}} \frac{\partial \Psi}{\partial t} \right\rangle &= -\frac{1}{i\hbar} \left\langle \widehat{\mathcal{T}} i\hbar \frac{\partial \Psi}{\partial t} \right\rangle, \\ &= -\frac{1}{i\hbar} \left\langle \widehat{\mathcal{T}} \widehat{E} \Psi \right\rangle, \\ &= -\frac{1}{i\hbar} E^* \left\langle \widehat{\mathcal{T}} \Psi \right\rangle. \end{aligned} \quad (20)$$

Multiplying (19) from the left by $\langle \Psi |$ and (20) from the right by $|\Psi \rangle$ respectively, and thereafter adding the resulting equations, we will have:

$$\begin{aligned} \langle \Psi | [\widehat{\mathcal{T}}^\dagger, \widehat{\mathcal{H}}] | \Psi \rangle &= (E - E^*) \langle O \rangle, \\ &= 2i E_I \langle O \rangle, \\ &= i\hbar \frac{\partial \langle O \rangle}{\partial t}, \end{aligned} \quad (21)$$

hence:

$$\langle \Psi | [\widehat{\mathcal{T}}^\dagger, \widehat{\mathcal{H}}] | \Psi \rangle = -2i E_I \langle O \rangle. \quad (22)$$

* $\text{Im}()$ is an operator which extracts the imaginary part of a complex quantity – i.e. if $z = x + iy$, then $\text{Im}(z) = y$.

Further, we know that:

$$\begin{aligned} \left| \widehat{\mathcal{T}} \vec{\nabla} \Psi \right\rangle &= -\frac{1}{i\hbar} \left| \widehat{\mathcal{T}}(-i\hbar) \vec{\nabla} \Psi \right\rangle, \\ &= -\frac{1}{i\hbar} \left| \widehat{\mathcal{T}} \vec{P} \Psi \right\rangle, \\ &= -\frac{1}{i\hbar} \vec{p} \left| \widehat{\mathcal{T}} \Psi \right\rangle, \end{aligned} \quad (23)$$

and:

$$\begin{aligned} \left\langle \widehat{\mathcal{T}} \vec{\nabla} \Psi \right| &= \frac{1}{i\hbar} \left\langle \widehat{\mathcal{T}}(-i\hbar) \vec{\nabla} \Psi \right|, \\ &= \frac{1}{i\hbar} \left\langle \widehat{\mathcal{T}} \vec{P} \Psi \right|, \\ &= \frac{1}{i\hbar} \vec{p}^* \left\langle \widehat{\mathcal{T}} \Psi \right|. \end{aligned} \quad (24)$$

Likewise, multiplying (23) from the left by $\langle \Psi |$ and (24) from the right by $|\Psi\rangle$ respectively, and thereafter adding the resulting equations, we will have:

$$\begin{aligned} \left\langle \Psi \left| \left[\widehat{\mathcal{T}}, \vec{P}^\dagger \right] \right| \Psi \right\rangle &= -(\vec{p} - \vec{p}^*) \langle O \rangle \\ &= -2i \vec{p}_I \langle O \rangle \\ &= -i\hbar \vec{\nabla} \langle O \rangle, \end{aligned} \quad (25)$$

hence:

$$\vec{v} \cdot \left\langle \Psi \left| \left[\widehat{\mathcal{T}}, \vec{P}^\dagger \right] \right| \Psi \right\rangle = -2i \vec{v} \cdot \vec{p}_I \langle O \rangle. \quad (26)$$

Now, inserting (22) and (26) into (16), we obtain:

$$i\hbar \frac{d\langle O \rangle}{dt} = -2i\hbar (E_I - \vec{v} \cdot \vec{p}_I) \langle O \rangle. \quad (27)$$

From this, it follows that a system will have all of its observables being constants *if-and-only-if*:

$$E_I - \vec{v} \cdot \vec{p}_I = 0. \quad (28)$$

In passing – out of curiosity, we need to point out an indelible fact of experience namely that (28) has a seductive and irresistible semblance with Bartoli [41, 42] and Maxwell [43]’s energy-momentum dispersion relation for Light – i.e. $E - c_0 p = 0$. If any, what connection can one make of this (28) with the nature of the photon? At present, we can only exhibit our curiosity: that is, we shall leave it here and slate it for exploration in future papers.

Now, applying the above ideas to the case of the variation of the FSC and assuming the present Standard Big Bang Cosmology Model [44–46] which assumes co-moving coordinates [47–50], it would appear that this FSC variation ought to be temporal in nature, as logic dictates that it cannot be spatial since co-moving coordinates imply $\vec{v} \equiv 0$. This directly implies that those patches of the sky exhibiting different FSC-values ought to be of different ages! If the temporal homogeneity and isotropy of the Universe is to be preserved,

then the only way to explain the variation of the FSC across the night-sky is to drop the assumption of co-moving coordinates! We are not going to say anything further on this matter of the variation of the FSC and complex observables, as this is something that requires a dedicated piece of work of its own. All that we wanted, we have achieved, and this has been to demonstrate the latent power in the seemingly alien idea of complex quantum mechanical observables that we have here suggested. We shall now move to the next section, where we shall consider the symmetries of the CEM-Dirac equation.

5 Symmetries of the CEM-Dirac equation

Now, if the electromagnetic coupled CEM-Dirac equation $[i\hbar\gamma^\mu \mathcal{D}_\mu - m_0 c_0] |\psi\rangle = 0$, with $m_0 \in \mathbb{C}$, is to be symmetric,

$$\text{i.e. } q \mapsto -q \Rightarrow [i\hbar\gamma^\mu \mathcal{D}_\mu^* - m_0 c_0] |\psi\rangle = 0$$

under charge conjugation, then we need to show that there exists a set of mathematically legal operations that take this new charge conjugated equation $[i\hbar\gamma^\mu \mathcal{D}_\mu^* - m_0 c_0] |\psi\rangle = 0$, back to the original CEM-Dirac equation – i.e. an equation without the **-operation* on the covariant derivative \mathcal{D}_μ . If we can find these legal mathematical operations, it would mean that the CEM-Dirac equation applies equally to particles as to antiparticles – hence, it is symmetric with respect matter and antimatter. On the contrary, if we fail to find the said legal mathematical operations, it invariably means that the CEM-Dirac equation is not symmetric under charge conjugation.

To that end, let us start our attempt by removing the **-operator* on the covariant derivative \mathcal{D}_μ in the equation $[i\hbar\gamma^\mu \mathcal{D}_\mu^* - m_0 c_0] |\psi\rangle = 0$. We will do this by taking the complex conjugate throughout this equation. So doing, we obtain $[i\hbar\gamma^{\mu*} \mathcal{D}_\mu + m_0^* c_0] |\psi^*\rangle = 0$, and because $\gamma^5 \gamma^0 \gamma^{\mu*} = -\gamma^\mu \gamma^5 \gamma^0$, we can, in this resulting equation, remove the complex conjugate operator acting on $\gamma^{\mu*}$ and this we can achieve by multiplying throughout the resultant equation by $\gamma^5 \gamma^0$ and then making use of the fact that $\gamma^5 \gamma^0 \gamma^{\mu*} = -\gamma^\mu \gamma^5 \gamma^0$. So doing, we will have:

$$[i\hbar\gamma^\mu \mathcal{D}_\mu - m_0^* c_0] |\psi_c\rangle = 0, \quad (29)$$

where $|\psi_c\rangle = \gamma^5 \gamma^0 |\psi^*\rangle$ is the wavefunction of the corresponding antiparticle. Clearly, if we have that $m_I \propto q$, or $m_I \propto q^n$, where $(n \in \mathbb{O}) = 3, 5, 7, \text{ etc}$, this would mean that the transformation $q \mapsto -q$, would also lead to:

$$m_I \mapsto -m_I \Rightarrow m_0^* \mapsto m_0, \quad (30)$$

and in this way, (29) would simultaneously transform to:

$$[i\hbar\gamma^\mu \mathcal{D}_\mu - m_0 c_0] |\psi_c\rangle = 0, \quad (31)$$

thus making this CEM-Dirac equation (whose rest-mass $(m_0 \in \mathbb{C})$ is a complex quantity) symmetric under charge conjugation. Less for the fact that the wavefunction $|\psi\rangle$ has been replaced by the new wavefunction $|\psi_c\rangle$, (31) is the same

CEM-Dirac equation applicable to the particle counterpart. Since $|\psi_c\rangle$ represents the antiparticle, the original Dirac equation is said to be symmetric under charge conjugation. In Dirac [9, 10]'s original theory, m_0 is real, the meaning of which is that $m_I \equiv 0$, hence making this original Dirac [9, 10] equation symmetric under charge conjugation. In the new setting of the CEM-Dirac equation, if m_I is not related to the electrical charge of the particle as suggested in (29), then the CEM-Dirac equation (with $m_0 \in \mathbb{C}$) is going to be asymmetric with respect to charge conjugation. As the reader can verify for themselves, not only is the CEM-Dirac equation going to violate C symmetry, but also CP , CT , and CPT symmetries as well. The only preserved symmetries are the P , T and PT symmetries.

6 Discussion

We have shown herein that the issue to do with negative energies can be solved by way of making a proper choice of the energy and momentum eigenvalues of the energy and momentum operators, respectively. These eigenvalues need to be complex as opposed to them being real as is the case in the present formulation of QM. Once the energy and momentum eigenvalues are complex, the measurable values become the magnitude of the corresponding eigenvalues and these magnitudes are positive definite! In this way, the issues surrounding these negative energies vanish forthwith. What remains is whether or not this is the scheme which *Nature* has chosen in order to go round this problem. We are of the strong opinion that this may very well be the scheme *Nature* has chosen.

This issue of negative energies has similarities with negative probabilities. As already said in the main text, prior to the discovery of his equation, Dirac had hoped that the negative probabilities occurring in the KG-theory, if solved, would also solve, in his new anticipated theory, the issue of the negative energies as well. We now know that Dirac was wrong as his new anticipated theory, which has positive definite probabilities, also has these negative energies. We did show in [40] that the emergence of these negative probabilities in the KG-theory is a result of an improper choice of the quantum mechanical probability current density in the KG-theory. In the same vein, the emergence of negative energies in both the Dirac and the KG-theory is a result of an improper choice of the energy and momentum eigenvalues – they need to be complex as suggested therein.

While we have not explored the richness of the hypothesis of complex energy and momentum eigenvalues, we need to mention the latent power in this new way of thinking, namely that one may very well be able to explain the variation of FNCs using this idea. Apart from this, it should be possible, using the complex part of the energy and momentum, to explain why particles decay, as well as the localization of particles into a finite region of space. What we had wanted here is to show that Dirac's negative energies can be done away with,

once and for all!

7 Conclusion

The following conclusion is drawn on the *proviso* that the hypothesis of complex energy-momentum is acceptable:

1. The complex energy-momentum hypothesis when applied to both the Klein-Gordon and the Dirac theory, does solve the issue of negative energies. This problem ceases to exist as the energy of all particles now is positive definite.
2. Quantum mechanics as currently understood and constituted where *all* quantum mechanical operators are required to be hermitian so that the corresponding eigenvalues are real-valued, may have to be modified or reconsidered.
3. The long-standing issue of the asymmetry in the matter-anti-matter constitution of the Universe can be explained by the C , CP , CT and CPT violation that arises from the complex energy-momentum hypothesis when applied to the Dirac equation.

Received on January 27, 2023

References

1. Einstein A. On the Electrodynamics of Moving Bodies. *Ann. der Phys.*, 1905, v. 17, 981.
2. de Broglie L. XXXV. A Tentative Theory of Light Quanta. *The London, Edinburgh, and Dublin Philosophical Magazine and Journal of Science*, 1924, v. 47 (278), 446–458.
3. de Broglie L. Ondes et Quanta. (Waves and Quanta). *Nature*, 1923, v. 117 (2815), 507–510.
4. de Broglie L. Ondes et Quanta. (Waves and Quanta). *Nature*, 1923, v. 117 (2815), 548–550.
5. de Broglie L. Ondes et Quanta. (Waves and Quanta). *Nature*, 1923, v. 117 (2815), 630–632.
6. Heisenberg W. Ueber den anschaulichen Inhalt der quantentheoretischen Kinematik und Mechanik. *Zeitschrift für Physik*, 1927, v. 43, 172–198. English Translation: Wheeler J. A. and Zurek W. H., eds. *Quantum Theory and Measurement*. Princeton University Press, Princeton (NJ), 1983, pp. 62–84.
7. Schrödinger E. An Undulatory Theory of the Mechanics of Atoms and Molecules. *Physical Review*, 1926, v. 28 (6), 1049–1070.
8. Schrödinger E. Quantisierung als eigenwertproblem. *Annalen der Physik*, 1926, v. 84 (4), 361–376.
9. Dirac P. A. M. The Quantum Theory of the Electron. *Proceedings of the Royal Society of London A: Mathematical, Physical and Engineering Sciences*, 1928, v. 117 (778), 610–624.
10. Dirac P. A. M. The Quantum Theory of the Electron. Part II. *Proceedings of the Royal Society of London A: Mathematical, Physical and Engineering Sciences*, 1928, v. 118 (779), 351–361.
11. Klein O. Quantentheorie und fünfdimensionale Relativitätstheorie. *Zeitschrift für Physik*, 1926, v. 37 (12), 895–906.
12. Gordon W. Der Comptoneffekt nach der Schrödingerschen Theorie. *Zeitschrift für Physik*, 1926, v. 40 (1), 117–133.
13. Dirac P. A. M. A Theory of the Electrons and Protons. *Proc. Roy. Soc. (London)*, 1930, v. A126 (801), 360–365.
14. Pauli W. Über den Zusammenhang des Abschlusses der Elektronengruppen im Atom mit der Komplexstruktur der Spektren. *Zeitschrift für Physik*, 1926, v. 31 (1), 765–783.

15. Bars I., Deliduman C., and Andreev O. Gauged Duality, Conformal Symmetry, and Spacetime with Two Times. *Physical Review D*, 1998, v. 58 (6), 066004.
16. Sakhorov A. D. Violation of CP Symmetry, C-Asymmetry and Baryon Asymmetry of the Universe. *Pisma Zh. Eksp. Teor. Fiz.*, 1967, v. 5, 32–35. *JETP Lett.*, 1967, v. 5, 24–27; *Sov. Phys. Usp.*, 1991, v. 34, 392–393; *Usp. Fiz. Nauk.*, 1991, v. 161, 61–64.
17. Aaij R., Abellan Beteta C., Adeva B., and The LHCb-Collaboration. First Observation of CP Violation in the Decays of B_s^0 Mesons. *Phys. Rev. Lett.*, 2013, v. 110, 221601.
18. Aaij R., Abellan Beteta C., Adeva B., and The LHCb-Collaboration. Search for Baryon-Number Violating Ξ_b^0 Oscillations. *Phys. Rev. Lett.*, 2017, v. 119, 181807.
19. Abe K., Abe K., Abe R., and The Belle Collaboration. Observation of Large CP Violation in the Neutral B Meson System. *Physical Review Letters*, 2001, v. 87 (9), 091802.
20. Aubert B., Boutigny D., de Bonis I., and The BABAR Collaboration. Measurement of CP-Violating Asymmetries in B^0 Decays to CP Eigenstates. *Physical Review Letters*, 2001, v. 86 (12), 2515–2522.
21. Christenson J. H., Cronin J. W., Fitch V. V., and Turlay R. Evidence for the 2π Decay of the K_2^0 Meson. *Physical Review Letters*, 1964, v. 13 (4), 138–140.
22. Wu C. S., Ambler E., Hayward R. W., Hoppes D. D., and Hudson R. P. Experimental Test of Parity Conservation in Beta Decay. *Physical Review*, 1957, v. 105 (4), 1413–1415.
23. Dirac P. A. M. A New Notation for Quantum Mechanics. *Mathematical Proceedings of the Cambridge Philosophical Society*, 1939, v. 35 (3), 416–418.
24. Pauli W. Zur Quantenmechanik des Magnetischen Elektrons. *Zeitschrift für Physik*, 1927, v. 43 (9-10), 601–623.
25. Lorentz H. A. Electromagnetic Phenomena in a System Moving with any Velocity Smaller than that of Light. *Proceedings of the Royal Netherlands Academy of Arts and Sciences*, 1904, v. 6, 809–831.
26. Lorentz H. A. Versuch einer Theorie Electricischen und Optischen Erscheinungen in between Körpern. *Brill (Leyden)*, 1895. First published online: April 2014.
27. Lorentz H. A. La Théorie Electromagnétique de Maxwell et son Application aux Corps Mouvants. *Arch. Néerl. Sci.*, 1892, v. 25, 287–301.
28. Sommerfeld A. Optics lectures on theoretical physics, vol. iv. *Annalen der Physik*, 1916, v. 4 (51), 51–52.
29. Dirac P. A. M. The Cosmological Constants. *Nature*, 1937, v. 139 (3512), 323.
30. Milne E. A. Relativity, Gravitation and World Structure. Clarendon Press, Oxford, 1935.
31. Webb J. K., Flambaum V. V., Churchill C. W., Drinkwater M. J., and Barrow J. D. Search for Time Variation of the Fine Structure Constant. *Phys. Rev. Lett.*, 1999, v. 82 (5), 884–887, 1999.
32. Wilczynska M. R., Webb J. K., Bainbridge M., Barrow J. D., Bosman S. E. I., Carswell R. F., Dabrowski M. P., Dumont V., Lee C. C., Leite A. C., Leszczyńska K., Liske J., Marosek K., Martins C. J. A. P., Milaković D., Molaro P., and Pasquini L. Four Direct Measurements of the Fine-Structure Constant 13 Billion Years Ago. *Science Advances*, 2020, v. 6 (17).
33. Leefer N., Weber C. T. M., Cingöz A., Torgerson J. R., and Budker D. New Limits on Variation of the Fine-Structure Constant Using Atomic Dysprosium. *Phys. Rev. Lett.*, 2013, v. 111 (6), 060801.
34. Webb J. K., King J. A., Murphy M. T., Flambaum V. V., Carswell R. F., and Bainbridge M. B. Indications of a Spatial Variation of the Fine Structure Constant. *Phys. Rev. Lett.*, 2011, v. 107 (19), 191101.
35. Murphy M. T., J. K. Webb, and Flambaum V. V.. Keck Constraints on a Varying Fine-Structure Constant: Wavelength Calibration Errors. *MEMORIE della Società Astronomica Italiana*, 2009, v. 80 (H15), 833–841.
36. Webb J. K., Murphy M. T., Flambaum V. V., Dzuba V. A., Barrow J. D., Churchill C. W., Prochaska J. X., and Wolfe A. M. Further Evidence for Cosmological Evolution of the Fine Structure Constant. *Phys. Rev. Lett.*, 2001, v. 87 (9), 091301.
37. Bohm D. A Suggested Interpretation of the Quantum Theory in Terms of “Hidden” Variables. I. *Physical Review*, 1952, v. 85 (2), 166–179.
38. Bohm D. A suggested interpretation of the quantum theory in terms of “hidden” variables, i and ii. *Phys. Rev.*, 1952, v. 85 (2), 166–193.
39. Bohm D. Proof That Probability Density Approaches $|\Psi|^2$ in Causal Interpretation of the Quantum Theory. *Physical Review*, 1953, v. 89 (2), 458–466.
40. Nyambuya G. G. Avoiding Negative Probabilities in Quantum Mechanics. *J. Mod. Phys.*, 2013, v. 4 (8), 1066–1074.
41. Bartoli A. Sopra i Movimenti Prodotti Della Luce e Dal Calorie. *Il Nuovo Cimento Series 3*, 1876 v. 10 (1), 228–231. Also: Le Monnier F. *Nuovo Cimento*, 1884, v. XV, 193.
42. Bartoli A. Il Calorico Raggiante e il Secondo Principio di Termodinamica. *Il Nuovo Cimento Series 3*, 1884, v. 15 (1), 193–202.
43. Maxwell J. C. *A Treatise on Electricity and Magnetism, 1st edition*. Clarendon Press, Oxford, 1873. 3rd edition. Dover Publications, NY, 1892/1952.
44. Friedmann A. A. Über die Möglichkeit einer Welt mit Konstanter Negativer Krümmung des Raumes. *Zeitschrift für Physik*, 1924, v. 21 (1), 326–332.
45. Hubble E. P. A Relation Between Distance and Radial Velocity Among Extra-Galactic Nebulae. *Proceedings of the National Academy of Sciences*, 1929, v. 15 (3), 168–173.
46. Lemaître G. Über die Krümmung des Raumes. *Annales de la Société Scientifique de Bruxelles*, 1933, v. A53 (1), 51–85.
47. Robertson H. P. Kinematics and World-Structure II. *The Astrophysical Journal*, 1936, v. 83, 187–201.
48. Robertson H. P. Kinematics and World-Structure III. *The Astrophysical Journal*, 1936, v. 83, 257–271.
49. Robertson H. P. Kinematics and World-Structure. *The Astrophysical Journal*, 1935, v. 82, 284–301.
50. Walker A. G. On Milne’s Theory of World-Structure. *Proceedings of the London Mathematical Society*, 1937, v. s2-42 (1), 90–127.
51. Compton A. H. A General Quantum Theory of the Wave-Length of Scattered X-rays. *Physical Review*, 1924, v. 24 (2), 168–176.

Novel Insights into Nonlocal Gravity

Elio B. Porcelli, Victo S. Filho

H4D Scientific Research Laboratory, 1100 B15 Av. Sargento Geraldo Santana, CEP: 04674-225, São Paulo, SP, Brazil.

E-mail: elioporcelli@h4dscientific.com

Our various experiments, analyses and theoretical models to describe anomalous phenomena related to so many diverse physical systems like superconductors, capacitors and others led us to consolidate the idea that all existing particles are in a preexisting state of quantum entanglement. Such a generality involving weight reduction of the devices leads us to inevitably infer a direct relationship between such a state and gravity, considering it as a nonlocal force. In this work, we intend to explore this issue of generality and then propose, on the basis of such a theoretical framework of generalized quantum entanglement state, to investigate in this alternative way other issues such as the small order of magnitude of the gravitational force in relation to other known local forces, as the electromagnetic one, explain why the gravitational force is attractive in the Universe and why particles and bodies are limited to the speed of light in the vacuum even interacting through instantaneous interactions. We also explore the issue of quantum interference in neutron experiments as being induced by nonlocal gravity.

1 Introduction

One of most important topics of research in physics relates to the nature of the gravitational field, mainly considering that the quantum mechanics cannot describe the physics in the macroscopic and even astronomical scale, in which the gravity force is the prominent one. In Quantum Field Theory, it is well known that the fundamental interactions of Nature in the nuclear and atomic scale are possible through gauge bosons. In the nuclear medium, gluons are the gauge bosons of the weak and strong interactions. Further, in our macroscopic world, the electromagnetic forces are dominant and the interactions between bodies are mediated by photons. However, despite the proposal of the graviton as the gauge boson for gravity, till now, no evidence of its existence has been found, so that it becomes hard to obtain a theoretical framework that encloses all the interactions in Nature and as consequence a unified theory of fields, although a series of alternative theories [1–4], interpretations [3, 4] and unification theories have been proposed in literature [5, 6].

Although such investigations are very hard to be successful, many physicists have tried alternative theoretical explanations for understanding the nature of gravity and beyond. As examples, we can cite

- the Emergent Gravity theory [7];
- the possibility of a fractal physical space-time [8];
- the existence of the coupling between it and electromagnetism or the hypothesis that considers gravity as derived from the electromagnetic interaction [9];
- the idea from which relevant information on the emergence of space is hidden at the quark / hadron level, by following the line of thought from which space is an attribute of matter [10], so that quantum properties of matter or the discretization of mass induces us to

believe in some form of quantization of space, with intrinsic consequences to gravity.

In this context, it is natural to suppose that quantum mechanisms could really be responsible for generating the gravitational force. The possibility that the collapse of the wave function in quantum mechanics is not merely a mathematical formalism but a real physical effect and ultimately connected to classical gravity has been discussed a long time ago since the proposal of the Diósi-Penrose model (DP) [11–14]. The idea was first conceived by Diósi in the study of the influence of gravitational fluctuations on quantum systems. Next, Penrose reported an estimation for the collapse time of a superposition due to gravitational effects that was the same found by the precise dynamical equation given by Diósi, based on the idea of a noise-based dynamical reduction effect. Such a topic has been still explored up to recently [15].

Another relevant idea on the local action of gravity refers to the inclusion of quantum fluctuations effect, which is a nonlocal component in the description of cosmological physical systems. For instance, in [16] such a point is analyzed by assuming that a mass scale is dynamically generated in the infrared regime, giving rise to nonlocal terms in the quantum effective action of gravity. Hence, the associated nonlocal gravity models are analyzed in many conceptual aspects as causality, degrees of freedom and their cosmological consequences. In a recent work [17], we have an overview on many aspects of nonlocal gravity cosmology.

On the basis of such previous ideas, we think that the hypothesis of generalized quantum entanglements (GQE) that we have developed in some previous works [18–22] could be a candidate for understanding some aspects and properties related to gravity, mainly considering the recent report of the existence of a type of quantum force [23]. In addition, in another work [24], it was asserted that it would be

possible to infer entanglement gravitational generation by using an atom interferometer [24]. The basic idea consists in the hypothesis that if we suppose gravitational perturbations as being quantized into gravitons, then the resulting graviton interactions should lead to an entangling interaction between massive bodies. However, the authors proposal of an experimental test – introducing the concept of interactive quantum information sensing – was not robust as reported and an erratum was published [25] with basis on the calculations showed in [26]. Basically, in [26], the authors showed by means of an explicit example that an interaction between a harmonic oscillator and a two-level test mass mediated by a local operation and classical communication channel produces a signature that in [24] was claimed to be exclusively for transmitting quantum information. Although the result was not really highly robust, in [25] they suggest methods to overcome the weakness in the proposed experiment. So, with basis on [23] and [25], we see that the subject is really intriguing and motivating in the sense of investigating and deepening the possibility, consequences and implications of associating generalized states of quantum entanglement between microscopic particles and the gravitational force. Although preserving quantum entanglements effects over macroscopic scale [27] is very difficult due to physical interactions, in many specific situations, as for instance in cases of physical systems subjected to high magnetic fields (in which the spins of all the component particles point in the same direction), effects of such a quantum state can be experimentally verified [28–30]. In addition, it is also proposed in [27] a physically robust quantum entanglement process that indicates the persistence of such states to classical scales.

From the general lines that we here exposed, it is our proposal in this work to discuss a generality of ideas that corroborate for this line of thought and research, in order to motivate investigations on the area. In more specific terms, we intend to describe at least four relevant lines of work concerning such aspects. One of them refers to a work in which the expansion of the electromagnetic field in a power series indicates that relevant terms of the series are equal to a purely gravitational term. Further we discuss how such an approach can be improved so that quantum entanglements among all the particles in the system can induce the force of gravity. In another study, we discuss some relations between the gravity and quantum mechanisms, that is, that the speed of light in the vacuum is a limit to the matter as a consequence of its origin (quantum fluctuations of the vacuum) and the interferences on beams of neutrons by gravity. At last, we discuss the description of the nonlocal gravity proposal by adopting the GQE hypothesis.

2 Generality of gravity

In the early 1990s, one of the authors of this manuscript began studies in order to investigate possible effects of quantum

entanglements in the macroscopic environment, starting from the premise that all existing particles in the Universe are in a preexisting state of maximum quantum entanglement, considering that at their origin (Big Bang) they were all in causal contact in a very small volume and associating such a collective state with gravity and inertia [18]. At first, one could imagine that this would contradict the concept of quantum monogamy [31], in which is reported that the concept is related to the idea that an entangled state cannot be shared with many parties, that is, the more parties, the less entanglement occurs among them. However, in reality, such a property is valid considering that two particles are entangled with each other, but not with a third or others, so that when the entanglement spreads the state of maximum entanglement is no longer possible. In the model that we consider, all particles are already entangled with each other since the beginning of the Universe.

The generality of both the gravity and the preexisting collective quantum state that governs all particles is one of the main factors that they can be somehow related to each other. Here generality means that the interaction involves all existing particles. For instance, electromagnetism involves only the charged particles and does not present such a characteristic.

Using the quantum mechanics formalism [18], it was verified that the dynamics of particles can be governed by non-local potentials in addition to the local ones and that, therefore, there is a possibility that gravitational potentials are also nonlocal due to other existing evidences described in this paper. A recent work [19] showed in an experiment that there was a correlation between the polarization of electric dipoles and photons (without local interaction between them) via discrete observables and indicated the possible preexistence of generalized quantum entanglements (we will call it GQE or the GQE model from now on). Penrose [32] reported that the evolution of states indicated by the Schrödinger equation inevitably makes all particles entangled and other studies [33] have also indicated that quantum entanglements can exist even in particles that never coexisted, considering entanglement chains. A very interesting work that we will analyze further here by Buniy and Hsu [34] indicated that everything in the Universe is maximally entangled despite not associating this property with gravity. The main argument is that particles had causal contact at the beginning of the Universe and with its expansion, the vast majority of current entanglements occur between particles that are beyond the causal horizon and that must be uniformly distributed in thermodynamic equilibrium (as evidenced by cosmic radiation). Such entanglements cannot even be removed by local interactions. One of the consequences of degrees of freedom being beyond the causal horizon is that two particles or two groups composed of a few particles, called X and Y, chosen at random, are not likely directly entangled with each other. This is because in this condition, the vast majority of degrees of freedom are not

contained between the two subsystems X and Y, but outside them (causal horizon that involves both). Therefore, for this reason the two subsystems share a negligible entanglement with each other.

In order to formalize the analysis, one can describe the system by the equation

$$\rho_{XY} = \sum_i \omega_i \rho_X^i \otimes \rho_Y^i, \quad (1)$$

which shows the density matrix that describes the entanglement between the two subsystems, each of them described by its individual density matrix.

Both of the subsystems are casually connected and separated. Now if the subsystems X (small subsystem) and Y (rest of the Universe with large amount of particles) are separated by the causal horizon (space-like separated) so that the vast majority of degrees of freedom are contained between both, we have that the density matrix describes the entanglement between both subsystems as described in equation

$$\rho_{XY} = \sum_i \omega_i |\phi_{XY}^i\rangle\langle\phi_{XY}^i|, \quad (2)$$

in which the term ϕ_{XY}^i represents a pure state and ω_i are probabilities.

In the situation formalized by (2), unlike the previous situation formalized by (1), the two systems X and Y share a high degree of entanglement. Fig. 1 summarizes the two situations analyzed here about entanglement across causal horizons. On the left side we have the X and Y subsystems with few particles surrounded by the causal horizon (crosshatched background) where mutual entanglement is negligible. On the right side we have the subsystem X with few particles surrounded by the causal horizon (crosshatched background) smaller than the subsystem Y which contains the rest of the Universe (a myriad of particles) where mutual entanglement is immense.

It is notable that the degree of entanglement between such subsystems depends directly on their dimensionality in the correspondent Hilbert space with respect to the dimensionality of the causal horizon and that these grow exponentially according to the number of degrees of freedom they have, that is, with the amount of particles that constitute them and their possible states. This indicates that it is possible to make local manipulations of a myriad of particles so that the effects of entanglements between subsystems become detectable, that is, for local systems to pass from the condition indicated by (1) and diagram on the left side of Fig. 1 to the one indicated by (2) and the right side of Fig. 1.

That's what we actually performed in our previous experiments [20, 22, 35, 36]. In various experiments we polarized a myriad of electric dipoles inside a dielectric under intense electric fields, magnetized a myriad of magnetic dipoles inside solenoids under intense magnetic fields, placed a myriad of electric and magnetic dipoles in collective precession

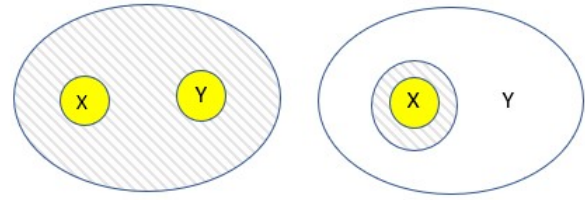


Fig. 1: Scheme of entanglement across horizons. At left, we see the systems X and Y with negligible amount of entanglement between them because their small areas (extremely small quantity of particles) compared to the area of the causal horizon (crosshatched background). At right, we see the opposite, the big amount of mutual entanglement between the systems X and Y, considering the big value of the sum of their areas (myriad of particles) compared to the small area of the causal horizon (crosshatched background).

and mobilized a myriad of charge carriers within conductors, superconductors and semiconductors. Considering only the nonlocal interaction between two separate simple dipoles and no local interaction via known forces as shown in Fig. 2, we have that the action of a local potential (magnetic or electric) in one of the dipoles affects the other dipole of the pair that is in the environment. The state of the pair of dipoles can be represented as being typically entangled [28] as represented by equations

$$|\Psi_1\rangle = \frac{|01\rangle - |10\rangle}{\sqrt{2}} \quad (3)$$

and

$$|\Psi_2\rangle = \frac{|01\rangle + |10\rangle}{\sqrt{2}}, \quad (4)$$

in which the state zero means orientation along the field and the state one means orientation against the field. These kets represent entangled states of a pair of dipoles in which one of them is oriented by a local field.

The nonlocal connection between the dipoles explains the supposedly anomalous forces in the form of weight variation that are measured in devices where high local potentials are applied and also in forces that such devices induce at a distance. Such inductions cannot be blocked as we have seen in our experiments [20, 22] because in fact there are no isolated systems and this is precisely one of the main properties of gravity.

We deal in our experiments with intense local potentials that have driven myriads of particles, but immense amounts of particles in the Universe are affected by local bound potentials of very weak magnitude so that nonlocal net effects are extremely weak, but we will show later in this work that these may explain the weakness of gravity through the other known forces.

A gravitational-like interaction was detected in our experiments in [20], where a shielded capacitor via Faraday cage

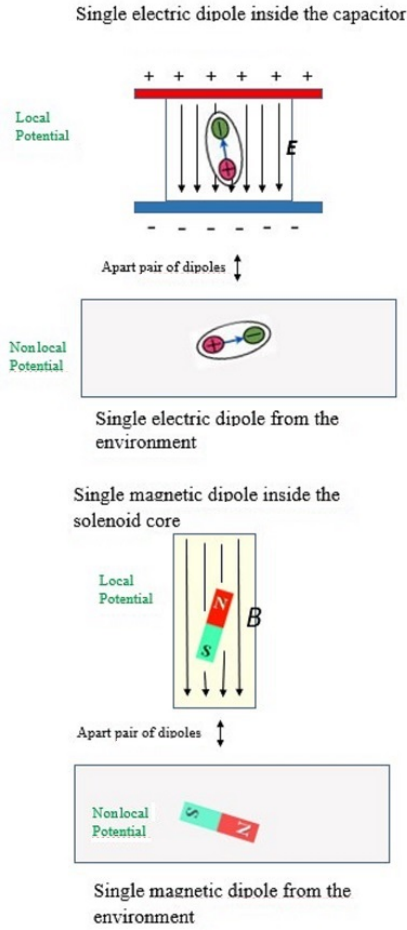


Fig. 2: Simplified analysis of the nonlocal interaction dipole-dipole.

enclosed inside a box was subject to a high voltage applied via shielded and insulated wires. Its weight variation cannot be explained via ionic winds and local interactions such as electrostatic, magnetic or acoustic ones.

The adoption of macroscopic observables as witnesses of entanglement of systems composed of many particles such as the electrical susceptibility χ_e and the magnetic susceptibility χ_m provides the necessary tools that can be applied in theoretical formalisms that explain the experimental results [21, 29, 30] considering the complexity involving quantum systems composed of myriads of particles. According to [29], the entanglement witness is shown as being more general (in the sense that it is not only valid for special materials), associating some macroscopic observables such as magnetic susceptibility χ_m with spin entanglement between individual constituents of a solid. It was proposed in [29] a macroscopic quantum complementary relation basically between magnetization M , representing local properties, and magnetic susceptibility χ_m , representing nonlocal properties. By defining for a system of N spins of an arbitrary spin length s in a lattice

the quantities:

$$G_l = 1 - \frac{kT\bar{\chi}}{N_s} \tag{5}$$

and

$$G_{nl} = \frac{\langle \vec{M} \rangle^2}{N^2 s^2}, \tag{6}$$

in which M is the modulus of the magnetization vector, k is the Boltzmann constant, T the temperature and the susceptibility of the system is defined as

$$\bar{\chi} = \chi_x + \chi_y + \chi_z, \tag{7}$$

hence, it was shown in [29] that one has:

$$G_l + G_{nl} \leq 1. \tag{8}$$

Such quantities have specific meanings, that is, G_{nl} represents the quantum correlations between the spins in the solid (nonlocal properties) and G_l represents the local properties of individual spins. The hypothesis of preexisting GQE indicates that there are no isolated systems as mentioned before, thus the magnetic core and the environment around it are both part of the same system where the inequality (8) can be considered accordingly. In other words, if one quantity increases then the corresponding counterpart quantity has to decrease. If G_l increases and G_{nl} decreases in the magnetic core, G_{nl} decreases and G_l increases in the environment and vice-versa. This is the same framework described before involving a simple system with two entangled magnetic dipoles. If we increase the intensity of a magnetic field (G_l) applied in one then the nonlocal forces (G_{nl}) must increase in the other.

Then, calculating the intensity of the nonlocal force F generated by a series of magnetic spins (dipoles) within the core of solenoid subjected to intense magnetic fields through classical quantities such as the magnetic susceptibility of the solenoid material (macroscopic observable) and the magnetization M can be defined by

$$F = \frac{1}{16\pi^2} \frac{SBI}{\theta}. \tag{9}$$

The product SBI represents the summation of the energy eigenstates of the internal spins (dipoles) of the solenoid, in which S is the area of the solenoid, B is the internal density of magnetic flux and I is the electric current that flows through the wires of the solenoid and which generates the magnetic field applied. The number in the denominator comes from the Planck constant \hbar squared existing in the Hamiltonian of the spin system and θ is the radius of the cylindrical solenoid. Such an equation corroborated the experimental results of experiments with magnetic solenoids.

Another experiment replicating Galileo's experiment in the Tower of Pisa and referring to spins or magnetic dipoles is related to locked magnets [37]. The experiments showed that in free fall two strong magnets in repulsion coupled fall more

slowly than equivalent ordinary (demagnetized) objects and two strong attractive magnets coupled to each other fall faster than demagnetized equivalent objects. In the GQE model, the phenomenon of difference of gravitational acceleration can be explained in a consistent way [37]. The theoretical predictions using such a formalism are corroborated by the results of the experiments and following the same criterion of using macroscopic quantum observables (considered as classical quantities) representing the entanglement of a myriad of particles with the environment, so that it was possible to build models that explain other systems such as dipole electrical charges in dielectrics and electrical charges flowing inside conductors, semiconductors and superconductors. It is known that light beams are deflected and distorted (gravitational lensing) by gravitational fields of massive bodies and considering such phenomena we performed experiments with isolated piezoelectric materials that also showed deformed laser beams effects [35]. This indicates another possible association of the GQE model with gravity.

Another experiment [38, 39] demonstrating force induction at a distance with gravitational characteristics was carried out involving the mechanical displacement of masses of different materials in a pendulum caused by collimated impulses produced by a superconductor subjected to high voltages. An explanation via the Theory of Relativity was proposed in [40]. Our GQE model [21] can also explain that effect in a consistent way with the experimental data, especially the relationship of applied energy and the mechanical energy of oscillation of the pendulum. All this argument possibly demonstrates the generality of both gravity and GQE and that both have a very close relationship with each other. Further we conclude that there is an intrinsic connection between these physical entities that affect all bodies and particles (fermions and bosons), regardless of their constitution.

3 The order of magnitude of gravity

According to GQE, all the particles transfer variations of moment indistinctly among them, considering as basic hypothesis that they are quantumly entangled and subjected to known nonlocal forces. Let us assume valid GQE hypothesis and investigate if quantum mechanisms like that can explain the gravity force. The question to be answered is: *But how to explain that the gravity force can be originated from such momenta exchange if it is extremely weak and the magnitudes of the local forces are much higher?* For instance, the gravitational force is 10^{-36} times smaller than the electrostatic force at the same distance [9].

In general, all the local forces such as the electromagnetic one, weak nuclear and strong nuclear forces are attractive and repulsive [41], but what explains the fact that only the gravitational force is attractive? In [9], a very interesting study was reported by Assis, indicating that two neutral electric dipoles where negative charges oscillate with small angular velocity

around an equilibrium position can attract each other through an average net electrostatic force that falls off as the inverse square of the distance between them and whose magnitude are compatible with that of the gravitational force. Besides he also showed that the same behavior is valid for groups of N dipoles; in other words, he showed that in that theoretical framework gravitation can be derived from electromagnetism. To reach this result, Assis used calculations based on Weber's generalized potential energy shown by equation

$$U = \frac{q_1 q_2}{4\pi\epsilon_0 r_{12}} \left[1 - \alpha \left(\frac{\dot{r}_{12}}{c} \right)^2 - \beta \left(\frac{\dot{r}_{12}}{c} \right)^4 - \gamma \left(\frac{\dot{r}_{12}}{c} \right)^6 - \dots \right], \quad (10)$$

considering dipole oscillations in the three x , y and z directions. Eq. (10) indicates the dependence of the potential energy between the dipoles in terms of the power series in parentheses, in which r_{12} is the average distance between the two particles of the dipole and α , β and γ are the parameters that indicate the magnitude of those power series terms. As known, q_1 and q_2 are the oscillating negative charges of the dipoles, ϵ_0 is the vacuum permittivity and c is the speed of light. The dot in the distance r_{12} is the notation used for the time variation of the distance between the two charges of the dipole.

The force between the dipoles is attractive and given by

$$\vec{F}_{12} = -\hat{r}_{12} \frac{dU}{dr_{12}}. \quad (11)$$

Eq. (11) indicates the force between two dipoles 1 and 2 apart by the distance r_{12} and its attractive feature.

Surprisingly, the calculations resulted in a cancellation of the most significant terms of the series so that the potential energy – and, therefore, also the force – started to decay according to c^{-4} reproducing Newtonian gravitation as being the fourth-order of the electromagnetic effect.

Considering the values of the charges equal to the electron charge, that is, $q_1 = q_2 = e$, and making $A_1 \sim 10^{-10}$ m, which is the typical size of the atom or molecule where the electrons are vibrating around the positive nucleus; and also considering equal the angular velocities of the oscillating charges of the dipoles $\omega_1 = \omega_2 = \omega$ and the coefficient $\beta = 1/8$, from (10) Assis interestingly simulated Newtonian gravitation with electromagnetism demonstrating an interesting relationship between electromagnetic parameters, as shown in the left term of equation:

$$\frac{7}{18} \frac{1}{8} \frac{e^2}{4\pi\epsilon_0} \frac{A_1^4 - \omega^4}{c^4} = GM^2, \quad (12)$$

as gravitational parameters shown in the term on the right, where G is the usual gravitational constant and M is the mass of the neutron or the mass of the hydrogen atom.

Assis also indicated other issues in his model, such as the relationship of inertia with gravity derived from electromagnetism that we will address in future works. In addition, he

also indicated possible limitations such as the fact that the calculations do not include relativistic corrections, as proposed by Phipps [42] for Weber's generalized potential energy. The model here investigated can explain the orders of magnitude of the gravitational interaction, its decay with the distance between the bodies and also its attractiveness characteristic through electromagnetic interactions between neutral dipoles, more specifically between the charged particles that compose them such as electrons. Despite the apparent success of this model, if we are supposed to isolate such dipoles through electromagnetic shields (Faraday cages) we could suppress them and it is known that in principle there is no gravitational shielding. In other words, there is an apparent paradox if we adopt such a model for gravity. Another issue is that electromagnetic interactions between electrically charged particles such as electrons and protons that make up neutral dipoles were considered to derive the gravitational interaction, but it is known that neutral particles such as photons and neutrinos (it is assumed that the latter can contribute most of the mass of the Universe) undergo the action of gravity. So, these arguments lead us to conclude that a very important feature must be added to the model studied here in order to derive gravity from local forces, which is to consider the GQE hypothesis. Thus, a potential energy such as Weber's generalized one given by (10) can be considered as a local potential energy V in the Hamiltonian \hat{H} of a multiparticle system represented by (18) that we discuss in more detail in section 5. Such a local potential can provide the interaction with particles external to the system through nonlocal forces that we can consider to be gravitational.

Our previous work [43–45] has corroborated that such nonlocal forces can indeed be induced and measured externally when, for example, strong electric fields are applied locally to a myriad of atomic and molecular dipoles contained in dielectrics even though they are shielded by a Faraday cage. In the model here discussed and represented by (10), we assume local potentials between dipoles. Assis indicated in [9] that terms lower than fourth-order are cancelled and are preponderant in the Universe groups of particles that interact with each other or particles that interact with themselves (for example, when a neutrino splits into two virtual particles and then the virtual particles become a neutrino again). This phenomenon occurs via electromagnetism but also via other known local forces.

To validate such a model, it is necessary to use a quantum approach as done with London dispersion forces [46] and also a relativistic approach.

4 The quantum origin of the speed of light

Quantum mechanics successfully demonstrates that particle dynamics have a dual nature where the mutual transfer of momentum is governed both by local interactions mediated by force-carrying particles such as the photon in the case of

electromagnetism and by nonlocal interactions arising from entangled quantum states between particles. In the first case, the interaction speed follows a finite upper limit and in the second case the interaction is instantaneous. Another fundamental feature of the theory of relativity is that the speed of light is independent of any source or reference, although a proposal to challenge such physical property has already been done in the literature [47]. Knowing the origin of the finite limiting velocity of local interactions, more specifically the speed of light, is critical because both special relativity and general relativity are built on this fundamental characteristic. A very interesting work by Urban and his collaborators [48] proposes to derive the speed of light from quantum mechanics. The model in question treats the velocity of the real photon as being instantaneous as well as with nonlocal interactions, but its propagation through the quantum vacuum occurs in leaps like those of a frog. It “jumps” instantaneously between the pairs of virtual particles of ephemeral duration being absorbed and re-emitted in a chain. The delay inherent in the absorption and re-emission process is what determines the finite propagation velocity c of the photon. Electromagnetic properties such as permeability μ_0 and permittivity ϵ_0 of the vacuum are determined by the creation and destruction of ephemeral particles such as electrons and positrons in addition to other fermions, and therefore both statistically determine on average the speed of light in the vacuum, given that

$$c = \frac{1}{\sqrt{\mu_0 \epsilon_0}}, \quad (13)$$

allowing some small variation to be confirmed experimentally. Einstein [49, 50] showed that the total mass m of a body is the measure of its energy content E (mass-energy equivalence) according to the relation $E = mc^2$, where c is the speed of light in vacuum. In order to reach this conclusion, he considered that the body yielded or absorbed energy in the form of electromagnetic radiation and that such an action caused its mass to change. So the exchange of force carriers like photons that are constrained in their propagation speed due to their interactions with the ubiquitous quantum vacuum that surrounds all bodies and particles appears to be a crucial factor for both special and general relativity, both experimentally validated.

A pioneering experiment among the various later experiments that validated such theories was the Hafele-Keating one [51] in the 1970s, which compared the measurements of time between precision atomic clocks inside an airplane that spent a certain time at high altitude and speed synchronized with others that were at rest on land. After the plane landed, the measurements of the clocks were compared and showed to be in notable disagreement with each other, obtaining an accuracy above 98% in relation to the theoretical predictions [52, 53] given that the clocks on board suffered an advance in the proper time due to the fact that they were at a higher altitude, that is, subject to a weaker gravitational

potential energy than at the surface, corroborating the relationship between proper time $d\tau_1$ (plane) and dt (surface) indicated in (14) derived from general relativity (Schwarzschild metric):

$$d\tau_1 = \sqrt{1 - \frac{2m}{R}} dt. \quad (14)$$

The clocks were also delayed due to the effect of special relativity with the plane's speed v , corroborating the relationship between the proper time $d\tau_2$ (plane) and dt (plane at rest on the ground) indicated in (15):

$$d\tau_2 = \sqrt{1 - \frac{v^2}{c^2}} dt. \quad (15)$$

In (14), R indicates the distance from the planet's center of mass (altitude) and m represents the relativistic mass of the planet according to the relationship $m = GM/c^2$, where G is the usual Newtonian gravitational constant and M is the planet's rest mass. The theory of relativity also predicts other effects [52, 53] such as the advanced perihelion of the planets, the deflection of light by the gravitational field and the spectral displacement of gravitational origin, all of which are experimentally proven. According to GQE theory, all particles are quantum entangled and, therefore, interact not locally instantaneously, but due to the fact that they also interact via local interactions mediated by force carriers limited to the velocity c taking into account their delayed propagation, through the ubiquitous quantum vacuum, the predictions of both general and special relativity support under certain conditions part of phenomena such as those mentioned above that Newtonian physics cannot explain.

The understanding of such "complementarity" in the co-existence of nonlocal and local interactions is analogous to what exists in the corpuscular and wave aspects because they seem contradictory, but are actually complementary according to quantum mechanics. Therefore, it is essential to study certain aspects of contradictory phenomena in relation to general relativity and special relativity, as indicated by van Flantern [54]. For example, according to him, the photons emitted by the Sun arrive at planet Earth 8.3 minutes after being emitted, time in which the Sun moves 20 arcs of a second in relation to the terrestrial reference. This causes the classic optical aberration studied by Bradley in 1728 to occur [54]. If such a phenomenon of aberration occurred with gravity, there would be a slight radial decrease in the intensity of the force so that the radial distance of the Earth's orbit would increase by 150 million kilometers every 1200 years, which in fact does not occur. Such an effect occurs with the radiation emitted by the Sun absorbed by dust particles where a transverse component affects their orbits (Poynting-Robertson effect). It is clear in this example the need to understand the complementary nature in which the gravitational interaction is instantaneous as proposed by the GQE theory and that the optical aberration in the radiation emitted by the Sun occurs

due to the photons having a finite propagation speed like the other force carriers. More examples are given by van Flantern such as the fact that gravity and light do not act in parallel directions, anomalies that occur during solar eclipses, *etc.* Other works such as [55] tried to answer why there is no aberration of gravity via General Relativity Theory without superluminal propagation of gravity assuming an approximation that the Sun and Earth have a mutual uniform motion. On the other hand, other works report possible superluminal different phenomena such as superluminal photonics tunneling [56] and superluminal X-rays [57]. Regarding the gravity waves with approximately the speed of light that were supposedly detected by the huge laser beam interferometers of LIGO-VIRGO collaboration, it must be necessary to investigate deeply as the authors [58] are proceeding in order to explain if the deviation of the beams was produced by other physical effects such as propagating vacuum fluctuations caused by huge cosmological events or by another local events. There is another experiment that supposedly evidences the nonlocal nature of gravity in [39], in which is reported the generation of a supposed gravitational-type interaction using superconductors under high-voltage discharges carried out, where impulses of up to 70 ns were induced at a distance at an apparently superluminal velocity (supposedly) 64 times the speed of light within the limitations of the equipment. The study of light interaction with gravity impulses and measurements of the speed of gravity impulses were also reported in [59].

Based on these promising analyses, the authors intend to continue the studies to deepen the understanding of the mentioned complementarity (local and nonlocal) of the interactions as well as to carry out new experiments involving the measurement of the velocity of the gravitational interaction. The authors also intend to publish another work containing important topics related to the association between inertia and gravity, the Mach principle and the principle of equivalence between gravitational mass and inertial mass.

5 Quantum interference via gravitation

The theory of Entropic Gravity or Emergent Gravity [7] proposes that gravity is not a fundamental interaction based on Quantum Field Theory, and therefore is not mediated by particles called force carriers such as gravitons. This characteristic is analogous to the GQE theory, which also proposes that gravity is not mediated by force carriers, but is the result of the transfer of momentum at a distance between particles that undergo the action of fundamental or canonical potential energies at their locations, considering that they are all in a pre-existing state of generalized quantum entanglement. The theory of Entropic Gravity has had a lot of opposition [60–62], but in this work we want to describe one of the oppositions [63, 64] that emphasizes that such a theory is not consistent with the result of the pioneering experiment of gravitational

induction of neutron phase shift [65]. In the aforementioned experiment that uses interferometry, a beam of neutrons with coherent quantum wave functions is split and separated into two beams that pass through different paths and are then recombined again to form an interference figure. The diagram in Fig. 3 shows one of the beams passing through positions A, B and D on a trajectory with higher altitude with respect to the Z axis (vertical) and another beam passing through positions A, C and D on a trajectory with lower altitude. Point D indicates the interference region where the two beams recombine.

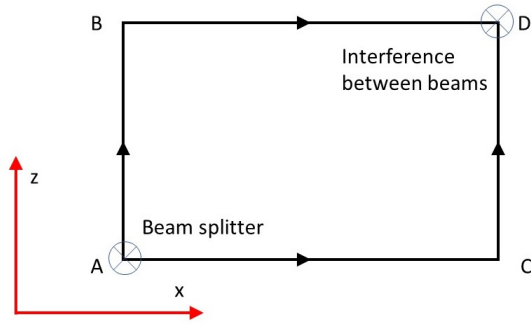


Fig. 3: Neutron interferometry experiment where a phase difference between the ABD and ACD beams was detected due to being subjected to different gravitational potentials [65].

The analysis of the interference figure clearly indicated that there was a phase difference depending on the neutron trajectory, related to the fact that the gravitational potential energy has a lower magnitude in the higher altitude trajectory (BD section) and higher magnitude in the lower altitude trajectory (CD section). The neutron momentum is therefore different on the trajectory ABD ($p_1 = \hbar k_{BD}$), with respect to the momentum of the trajectory ACD ($p_2 = \hbar k_{CD}$). The Schrödinger equation [66, 67]

$$-\frac{\hbar^2}{2m_n} \frac{\partial^2 \Psi}{\partial z^2} + m_n g z \Psi = i\hbar \frac{\partial \Psi}{\partial t} \quad \text{for } z > 0 \quad (16)$$

indicates dependence of the neutron dynamics on the gravitational potential energy represented by the term $m_n g z \Psi$ (the other term to the left of the equality represents the kinetic energy). The two terms to the left of the equality represent the standard Hamiltonian operator \hat{H} .

This Schrödinger equation (16) represents the dynamics of the neutron in the physical system described. The gravitational potential energy used in the formalism is that of classical physics, that is, it depends on the neutron mass m_n , the gravitational constant g and the altitude z (Z axis) according to the term $m_n g z \Psi$. The predicted phase difference theoretically calculated according to the standard Hamiltonian \hat{H} is consistent with the phase difference obtained experimentally.

But according to [63], in the case of entropic gravity, the interference pattern is destroyed because the gravitational interaction is not fundamental or canonical for this theory, that is, it behaves like a typical chaotic thermodynamic interaction so that the wave function of the neutron loses its coherence. In the theory of entropic gravity, the gradient of variation of the gravitational field with respect to altitude (Z axis) is a statistical average of the thermal fluctuations involving a myriad of microstates. The last two terms in the equation

$$\hat{H} = \frac{\hat{p}^2}{2m} + V_{grav}(r) = -\frac{\partial^2}{\partial r^2} - 4\pi m \frac{\partial}{\partial r} - 4\pi^2 m^2 + mgr. \quad (17)$$

indicate deviation from the standard Hamiltonian and demonstrate that entropic gravity does not explain the experimentally measured phase difference. Eq. (17) shows the Hamiltonian operator according to the entropic gravity theory, where m is the neutron mass and r is the altitude value (Z axis). In the experiment [65], according to the interpretation of the nonlocal gravitational interaction through the GQE theory, we can define the relevant Hamiltonian operator of the neutron-Earth system via equation

$$\hat{H} = -\frac{\hbar^2}{2} \left(\sum_{M=1}^N \frac{1}{M} \frac{\partial^2}{\partial z^2} + \frac{1}{m_n} \frac{\partial^2}{\partial z^2} \right) + \hat{V}_M. \quad (18)$$

which determines its dynamics in order to change the phase of its wave function coherently.

Eq. (18) shows the “standard” Hamiltonian operator of the nonlocal gravitational interaction of the neutron-Earth system according to GQE theory. The neutron moves on a trajectory with a certain kinetic energy (term on the right in parentheses in (18)) and in a state of quantum entanglement with the myriad of particles that make up the planet Earth whose total kinetic energy is represented in the sum of the term from the left in parentheses in (18). As the neutron is subject only to gravitational interaction with the planet Earth (its electromagnetic interaction is negligible because it has practically zero electric charge), the potential energy \hat{V}_M (fundamental or canonical) inherent to the particles of the planet Earth is represented in (18).

The analysis performed here allows us to suppose that the phase difference theoretically predicted via GQE theory and calculated according to the standard Hamiltonian \hat{H} shown in (18) is consistent with the phase difference obtained experimentally in the experiment in [65]. The potential energy inherent to the particles of the planet Earth of (18) can be equivalent to the classical gravitational potential energy of (16) with its main gravitational characteristics such as decay according to the inverse of the distance (height), attractiveness of the force and order of magnitude, for example, if it corresponds to potential energy like Weber’s generalized one, as shown earlier via (10). The fact that nonlocal gravity within the framework of GQE theory seems to be consistent with gravitational induction of quantum interference, considering

that the nonlocal potential \hat{V}_M is canonical or fundamental such as the local potential, is very interesting and encourages further studies for a more detailed understanding.

6 Conclusions

In this work, we outlined a discussion of the state of the art of the research on some gravitational phenomena and theories of gravity. Specifically, we discuss how the GQE hypothesis can be associated with gravity, explain all aspects of such an interaction as its very weak magnitude, the nonlocal effects of gravity, the limit of the light velocity as consequence of the quantum vacuum, the validity of the nonlocal gravity and its description by means of GQE and many other interesting theoretical issues concerning the gravitational interaction.

We assert that some previous experiments indicated that GQE is consistent with some gravitational effects reported in the literature, as the weight reduction of capacitors, the gravitational shield generated by superconductors or the change in the value of the gravity acceleration of two magnets locked with each other in free fall.

It is worth to mention that in a next work we also intend to analyze a lot of relevant topics that deserve a more profound study, as the earlier mentioned complementarity (local and nonlocal) of the interactions and the association between inertia and gravity, Mach's principle and the principle of equivalence between gravitational mass and inertial mass. In addition, we also intend to explore other themes not discussed here as the dark matter or MOND, in order to investigate more profoundly the consistency of GQE for explaining all such phenomena.

Received on February 17, 2023

References

- Rabounski D. A Theory of Gravity Like Electrodynamics. *Progress in Physics*, 2005, v. 2, 15–29.
- Tank H. K. Some Expressions for Gravity without the Big G and their Possible Wave-Theoretical-Explanation. *Progress in Physics*, 2013, v. 1, 3–6.
- Christianto V. and Smarandachey F. What Gravity Is. Some Recent Considerations. *Progress in Physics*, 2008, v. 3, 63–67.
- Marshall T. W. Repulsive Gravity in the Oppenheimer-Snyder Collapse. *Progress in Physics*, 2016, v. 12 (3), 219–221.
- Suhendro I. A Unified Field Theory of Gravity, Electromagnetism, and the Yang-Mills Gauge Field. *Progress in Physics*, 2008, v. 1, 31–37.
- Suhendro I. A New Semi-Symmetric Unified Field Theory of the Classical Fields of Gravity and Electromagnetism. *Progress in Physics*, 2007, v. 4, 47–62.
- Verlinde E. On the origin of gravity and the laws of Newton. *Journal of High Energy Physics*, 2011, N. 29, 1–26.
- Svozil K. Towards Fractal Gravity. *Foundations of Science*, 2020, v. 25, 275–280.
- Assis A. K. T. Deriving gravitation from electromagnetism. *Canadian Journal of Physics*, 1992, v. 70, 330–340.
- Żencykowski P. Quarks, Hadrons, and Emergent Space-time. *Foundations of Science*, 2019, v. 24, 287–305.
- Diósi L. A universal master equation for the gravitational violation of quantum mechanics. *Physics Letters A*, 1987, v. 120 (8), 377–381.
- Diósi L. Models for universal reduction of macroscopic quantum fluctuations. *Physics Letters A*, 1989, v. 40 (3), 1165–1174.
- Penrose R. On Gravity's role in Quantum State Reduction. *General Relativity and Gravitation*, 1996, v. 28 (5), 581–600.
- Penrose R. On the Gravitization of Quantum Mechanics 1: Quantum State Reduction. *Foundations of Physics*, 2014, v. 44 (5), 557–575.
- Vinante A. and Ulbricht H. Gravity-related collapse of the wave function and spontaneous heating: Revisiting the experimental bounds. *AVS Quantum Sci.*, 2021, v. 3, 045602–045603.
- Belgacem E., Dirian Y., Foffa S. and Maggiore M. Nonlocal gravity. Conceptual aspects and cosmological predictions. *Journal of Cosmology and Astroparticle Physics*, 2018, N. 3, 2.
- Capozziello S. and Bajardi F. Nonlocal gravity cosmology: An overview. arxiv: abs/2201.04512.
- Porcelli E. B. Theoretical Insight into the Connection between the Gravity and Generalized Quantum Entanglements. *Open Science Repository Physics*, 2015.
- Porcelli E. B. and Filho V. S. Detection of preexisting quantum entanglements between dipole-photon discrete observables. preprint, 2021.
- Porcelli E. B. and Filho V. S. Experimental Verification of Anomalous Forces on Shielded Symmetrical Capacitors. *Appl. Physics Research*, 2020, v. 12 (2), 33–41.
- Porcelli E. B. and Filho V. S. Theoretical Study of Anomalous Forces Externally Induced by Superconductors. *Natural Science*, 2017, v. 9 (9), 293–305.
- Porcelli E. B. and Filho V. S. Characterisation of Anomalous Asymmetric High-Voltage Capacitors. *IET Science, Measurement & Technology*, 2016, v. 10 (4), 383–388.
- Becker M., Guzzinati G., Béché A. and Verbeeck J. Asymmetry and non-dispersivity in the Aharonov-Bohm effect. *Nature Communications*, 2019, v. 10 (1700), 1–10.
- Carney D., Muller H. and Taylor J. M. Using an Atom Interferometer to Infer Gravitational Entanglement Generation. *PRX Quantum*, 2021, v. 2, 030330–030333.
- Carney D., Muller H. and Taylor J. M. Erratum: Using an atom interferometer to infer gravitational entanglement generation (*PRX Quantum*, 2021, v. 2, 030330). *PRX Quantum*, 2022, v. 3, 010902.
- Streltsov K., Pedernales J. S. and Plenio M. B. On the Significance of Interferometric Revivals for the Fundamental Description of Gravity. *Universe*, 2022, v. 8 (2), 58.
- Millette P. A. On the Classical Scaling of Quantum Entanglement. *Progress in Physics*, 2018, v. 14 (3), 121–130.
- Wei Q., Kais S. and Chen Y. P. Communications: Entanglement Switch for Dipole Arrays. *The Journal of Chemical Physics*, 2010, v. 132, 12110.
- Wieśniak M., Vedral V. and Brukner C. Magnetic Susceptibility as a Macroscopic Entanglement Witness. *New Journal of Physics*, 2005, v. 7, 2005, 258.
- Ghosh S., Rosenbaum T. F., Aeppli G. and Coppersmith S. N. Entangled Quantum State of Magnetic Dipoles. *Nature*, 2003, v. 425, 48–51.
- Yang D. A simple proof of monogamy of entanglement. *Phys. Lett. A*, 2006, v. 360, 249–250.
- Penrose R. *The Road to Reality: A Complete Guide to the Laws of the Universe*. Vintage Books, USA, 2007.
- Megidish E., Halevy A., Shacham T., Dvir T., Dovrat L. and Eisenberg H. Entanglement Swapping between Photons that have Never Coexisted. *Physical Review Letters*, 2013, v. 110, 210403–210406.
- Buniy R. V. and Hsu S. D. H. Everything is Entangled. *Physical Letters B*, 2013, v. 718 (2), 233–236.

35. Porcelli E. B. and Filho V. S. Analysis of Possible Nonlocal Effects in Laser Beams Generated by Piezoelectric Ceramic. *Journal of Power and Energy Engineering*, 2018, v. 6 (2), 20–32.
36. Porcelli E. B. and Filho V. S. Induction of Forces at Distance Performed by Piezoelectric Materials. *Journal of Power and Energy Engineering*, 2018, v. 6 (1), 33–50.
37. Porcelli E. B. and Filho V. S. New Experimental Evidences of Anomalous Forces in Free Fall Locked Magnets. *European Physics Journal Plus*, 2022, v. 137 (1), 128.
38. Podkletnov E. and Modanese G. Impulse Gravity Generator Based on Charged YBa₂Cu₃O_{7-y} Superconductor with Composite Crystal Structure. arXiv: physics/0108005.
39. Podkletnov E. and Modanese G. Investigation of High Voltage Discharges in Low Pressure Gases Through Large Ceramic Superconducting Electrodes. *Journal of Low Temperature Physics*, 2003, v. 132, 239–259.
40. Rabounski D. and Borissova L. A Theory of the Podkletnov Effect based on General Relativity: Anti-Gravity Force due to the Perturbed Non-Holonomic Background of Space. *Progress in Physics*, 2007, v. 3, 57–80.
41. OpenStax-College. Extended Topic: The Four Basic Forces — An Introduction. In: Introduction to Science and the Realm of Physics. Physical Quantities, and Units. 2022. <https://courses.lumenlearning.com/physics/chapter/4-8-extended-topic-the-four-basic-forces-an-introduction>
42. Phipps Jr. T. E. Toward modernization of Weber's force law. *Physics Essays*, 1990, v. 3, 414–420.
43. Porcelli E. B., Alves O. R. and Filho V. S. Experimental Verification of Anomalous Forces on Shielded Symmetrical Capacitors. *Applied Physics Research*, 2020, v. 12 (2), 33–41.
44. Porcelli E. B. and Filho V. S. Anomalous Effects from Dipole-Environment Quantum Entanglement. *Int. J. Adv. Eng. Res. Sci.*, 2017, v. 4 (1), 131–144.
45. Porcelli E. B. and Filho V. S. On the Anomalous Forces in High-Voltage Symmetrical Capacitors. *Physics Essays*, 2016, v. 29, 2–9.
46. Butt H. J. and Kappel M. Surface and the Interfacial Forces. Wiley VCH-Verlag Publishers, Weinheim, 2010.
47. Bilbao L. Does the Velocity of Light Depend on the Source Movement? *Progress in Physics*, 2016, v. 12 (4), 307–312.
48. Urban M., Couchot F., Sarazin X. and Djannati-Atai A. The quantum vacuum as the origin of the speed of light. *The European Physical Journal D*, 2013, v. 67, 58.
49. Pais A. *Subtle Is the Lord: The Science and the Life of Albert Einstein*. Oxford University Press, Oxford, 2005.
50. Einstein A. *The Meaning of Relativity: Including the Relativistic Theory of the Non-Symmetric Field*. Princeton University Press, Princeton, NJ, 2014.
51. Hafele J. C. and Keating R. E. Around-the-World Atomic Clocks: Predicted Relativistic Time Gains. *Science*, 1972, v. 177 (4044), 166–168.
52. Berman M. S. *Introduction to General Relativistic and Scalar-Tensor Cosmologies*. Nova Science Publisher, New York, 2007.
53. Berman M. S. and Gomide F. M. *Cálculo Tensorial e Relatividade Geral*. McGraw-Hill, 1987.
54. van Flandern T. The speed of gravity — What the experiments say. *Physics Letters A*, 1988, v. 250 (1-3), 1–11.
55. Ivison M. and Puthoff H. E. and Little S. R. The speed of gravity revisited. arXiv: physics/9910050.
56. Nimitz G. and Heitmann W. Superluminal Photonic Tunneling and Quantum Electronics. *Progress in Quantum Electronics*, 1997, v. 21, 81–108.
57. Gianfrate A., Dominici L., Voronych O., Matuszewski M., Stobińska M., Ballarini D., de Giorgi M., Gigli G. and Sanvitto D. The speed of gravity revisited. *Light: Science & Applications*, 2018, v. 7, 17119.
58. Porcelli E. B. Investigation if long range nonlocal inductions performed by laser diode resonant cavities can be detected by the interferometers of LIGO-VIRGO collaboration. preprint ResearchGate, 2020.
59. Podkletnov E. and Modanese G. Study of Light Interaction with Gravity Impulses and Measurements of the Speed of Gravity Impulses. In: Modanese G. and Robertson G. A., eds. *Gravity-Superconductors Interactions: Theory and Experiment*. Bentham Books, 2012, pp. 169–182.
60. Bhattacharya S., Charalambous P., Tomaras T. N. and Toumbas N. Comments on the entropic gravity proposal. *The European Physical Journal C*, 2018, v. 78, 627.
61. Pardo K. Testing Emergent Gravity with Isolated Dwarf Galaxies. *Journal of Cosmology and Astroparticle Physics*, 2020, 12.
62. Tortora C., Koopmans L. V. E., Napolitano N. R. and Valentijn E. A. Testing Verlinde's emergent gravity in early-type galaxies. *Monthly Notices of the Royal Astronomical Society*, 2018, v. 473 (2), 2324–2334.
63. Kobakhidze A. Once more: gravity is not an entropic force. arXiv: hep-th/1108.4161.
64. MIT Technology Review. Experiments Show Gravity Is Not an Emergent Phenomenon. <https://www.technologyreview.com/2011/08/24/258052/experiments-show-gravity-is-not-an-emergent-phenomenon>
65. Colella H., Overhauser A. W. and Werner S. A. Observation of Gravitationally Induced Quantum Interference. *Physical Review Letters*, 1975, v. 34 (23), 1472–1474.
66. Abele H. and Leeb H. Gravitation and quantum interference experiments with neutrons. *New Journal of Physics*, 2012, v. 14, 055010.
67. Sakurai J. J. *Modern Quantum Mechanics*. Addison Wesley, 1994.

Space and Gravity

Anatoly V. Belyakov

Tver, Russia. E-mail: belyakov.lih@gmail.com

Based on the mechanistic interpretation of J. Wheeler's geometrodynamics, where space has the properties of an ideal fluid surface, it was found that the ratio of the forces acting in the surface wave transverse component to the forces acting in its longitudinal component is equal to the ratio of the electric forces to the gravitational ones. The surface of a finite thickness is the original material entity, the fractalization of which leads to forming material bodies and the tension of the above surface, which is manifested as an attraction between the bodies. The speed of light has been determined and the gravitational constant calculation formula has been obtained. It is concluded that a radiating cell of the surface wave generates a radiation having the wavelength corresponding to the background radiation maximum.

1 Introduction and main provisions

Geometrodynamics, introduced by the famous scientist John A. Wheeler, who died in 2008, does not seem to be approved by modern physicists, since it requires the presence of some medium (ether). According to Wheeler's concept, charged microparticles are singular points on a non-unitary coherent connected two-dimensional surface of our world, connected by a "wormhole", a vortex tube or a current force line of the drain-source type in an additional dimension, forming a closed contour [1]. But "wormholes", if they are not considered purely mathematical constructions, in their physical embodiment can only be the vortex formations based on the surface (or phase boundary) of some substance that has the properties of an ideal fluid.

The presence of contours (vortex tubes) is also postulated, for example, in [2], where the vacuum structure is considered as a network of one-dimensional flow tubes (knotted/linked flux tubes), and it is claimed it is such a network that provides the spatial three-dimensionality of the Universe. At the same time this network, infinitely densely filled with such vortex formations, forms a continuous surface (the possibility of this was proved in the 19th century by J. Peano [3]). This surface, in turn, as it becomes more complex, can form three-dimensional material objects, which are, in fact, highly fractalized, up to the parameters of the microworld, *surfaces* with a fractional dimension. An undeformed (non-fractalized) surface is equivalent to the empty space, and bodies when driving in such a continuous medium does not feel any resistance up to the speed of light, i.e., until surface waves forms, and *for any observer the vacuum medium remains undetectable*. Recall that even when moving in a real liquid body, an observer does not feel a resistance up to the speed when a surface wave is formed (for water, the speed is 0.3...0.5 m/sec).

As for a completely entire three-dimensional body, it does not have an internal structure, does not carry any information about its structure (except for its own mass), and such bodies do not really exist. The fact that all objects are fractalized

surfaces is especially well manifested in the organic world: under the surface of outer shells there are the surfaces of organs, vessels, then – the surfaces of their fibers, then – the surfaces of cells, etc.

The Wheeler model's closest analogy on the scale of our world would be the ideal fluid surface, the vortex formations arising in it and corresponding interactions between them. In the mechanistic interpretation of Wheeler's idea, the charge reflects a measure of the medium nonequilibrium and is proportional to its momentum along the vortical current tube contour, spin, respectively, is proportional to its angular momentum relative to the contour longitudinal axis, and magnetic interaction between the conductors is similar to the forces acting between the current tubes. In this model, a point or a line is considered to be physical objects with certain dimensions, where the electron volume with mass m_e and radius r_e can be taken as a medium unit element. A free charged particle in such a scheme is represented as part of an open contour or a unipolar vortex resting on the surface of our world and directed along the "extra" dimension, where the particle charge and spin are determined by the "hidden mass" dynamics [4].

In such a model, the electric constant becomes the density per unit of the vortex tube length

$$\varepsilon_0 = \frac{m_e}{r_e} = 3.23 \times 10^{-16} \text{ kg/m}, \quad (1)$$

and the reciprocal of the magnetic constant is the centrifugal force

$$\frac{1}{\mu_0} = c^2 \varepsilon_0 = 29.06 \text{ N}, \quad (2)$$

arising from the rotation of the vortex tube element with mass m_e , at the speed of light c along the radius r_e ; it is also equivalent to the force acting between two elementary charges at this radius.

The paper [4] defines the vortex thread parameters: its mass M , circumferential velocity v , radius r , and length l for

an arbitrary p^+e^- -contour in dimensionless units of m_e , r_e and c :

$$M = l = (an)^2 \quad (3)$$

$$v = \frac{c_0^{1/3}}{(an)^2}, \quad (4)$$

$$r = \frac{c_0^{2/3}}{(an)^4}, \quad (5)$$

where n is the main quantum number, a is the reciprocal of the fine structure constant, c_0 is the dimensionless speed of light, c /[m/sec].

This approach has justified itself in determining the electron charge and radiation constants numerical value and other parameters both for the microworld [4, 5, 6, 7] and for cosmological objects [8]. The mechanistic interpretation of geometrodynamics does not introduce any additional entities, but, on the contrary, reduces them. So, the Coulomb is excluded from the set of dimensions and is replaced by the electron limiting momentum, which radically simplifies all the dimensions associated with electromagnetism [9].

2 On the surface wave parameters

The speed of light is one of the few fundamental quantities not derived in theory. However, as established in [10], it turns out the propagation of light to be similar to wave's moving on the liquid surface and *has the maximum equal to the speed of light*, which is determined from the well-known equation

$$v^2 = \frac{g\lambda}{2\pi} + \frac{2\pi\sigma}{\rho\lambda}, \quad (6)$$

where g is the acceleration, λ is the wavelength, σ is the surface tension (force relative to the perimeter), ρ is the specific density. The first term reflects the gravity effect on the wave speed, the second – the surface tension effect.

When this equation was solved, a radiating cell (toroid) was considered, in which the medium circulates along the contour with radius $R = a^2n^2r_e$ and rotates helically about the toroid longitudinal axis, creating z structurally ordered units (waves or photons) with centrifugal acceleration $g = zv^2/R$. The surface tension was defined as $(1/\mu_0)/R$, and the specific density as $m_p m_e / R^3$, where m_p is the relative proton mass in units of m_e .

The solution obtained, can be considered as a special case of the wave velocity maximum at $n = 4.23$ and does not depend on the parameters n and z . However, unlike a liquid where the surface wave velocity has a minimum, and, actually, their capillary and gravitational waves velocity depends on the surface tension and the basin depth, there is some natural mechanism for electromagnetic waves ensuring of their speed from the wavelength independence.

Let us express the wavelength from (6). Assuming $v = c$, after transformations we get (a plus radical formula is accepted)

$$\lambda = \frac{\pi r_e a^6 n^6}{c_0^{2/3}} \left[1 + \left(1 - \frac{4c_0^{2/3}}{a^2 n^2 m_p} \right)^{1/2} \right]. \quad (7)$$

The critical value $n = 0.227$ corresponds to the wavelength minimum value

$$\lambda_{min} = \frac{\pi r_e a^6 n^6}{c_0^{2/3}} = 1.81 \times 10^{-11} \text{ m}, \quad (8)$$

which is already gamma radiation. Thus, for $n < 0.227$, either a more accurate equation is required, or the radiation already completely loses its longitudinal component and becomes the capillary waves analogue; anyway, it is known gamma rays to behave like particles at $\lambda < 10^{-10}$ m.

It should be borne in mind that, as applied to (7), the parameter n determines the radiating cell physical size, i.e., the circular trajectory size, along which particles move under the surface in the liquid medium under the action of gravitational forces (in contrast to the proton-electron system main quantum number, which characterizes the atom excited state). Note that at $n = 4.23$, when $v = c$, from (7) follows $\lambda = 1.52 \times 10^{-3}$ m, which corresponds to the *background microwave radiation maximum*. Thus, it turns out the optimal radiative cell at which the wave speed is compared with the speed of light to be the cosmic background radiation natural source or, at least, be its longitudinal component.

As shown in [5], the proton-electron contour parameters are determined from the condition of the equality of the magnetic repulsive forces and gravitational attractive forces, which in the Coulombless form has the form

$$\frac{z_{g1} z_{g2} \gamma m_e^2}{r^2} = \frac{z_{e1} z_{e2} \mu_0 m_e^2 c^2 l}{2\pi r \times [\text{sec}^2]}, \quad (9)$$

where z_{g1} , z_{g2} , z_{e1} , z_{e2} are the gravitational masses and charges in the masses and charges of an electron, γ is the gravitational constant.

The largest contour size is possible when the entire proton mass, corrected for the Weinberg projection angle Θ , is involved in the circulation contour. Then at $z_{g2} = m_p / \cos \Theta$ for unit charges after transformations we obtain the geometric mean from (9) in units of r_e

$$l_k = (lr)^{1/2} = \left(\frac{m_p}{\cos \Theta} \right)^{1/2} (2\pi\gamma\rho_e)^{1/2} \times [\text{sec}], \quad (10)$$

where ρ_e is the specific electron density m_e/r_e^3 , $\Theta \approx 28.70^\circ$ is the Weinberg angle.

The l_k parameter is compound. Taking into account (3), (5) and (10), the values of l and r in units of r_e have the form:

$$l = \frac{c_0^{2/3}}{l_k^2}, \quad (11)$$

$$r = \frac{l_k^4}{c_0^{2/3}}. \tag{12}$$

Taking the parameter r as the major axis of the contour, bearing in mind (3) and (12), from (10) the limiting quantum number is determined

$$n_{max} = 2\pi \frac{m_p}{\cos \Theta} \frac{\gamma \rho_e \times [\text{sec}^2]}{ac_0^{1/3}}. \tag{13}$$

It follows from (13) that $n_{max} \approx 390$, then the largest circulation contour size (the surface wave depth) is $390^2 a^2 r_e$, and the recombination wavelength $\lambda_{max} = n^2 / R_\infty = 0.0139$ m, where R_∞ is the Rydberg constant. This result is consistent with the fact that there are no excited hydrogen radio lines at $n > 301$ even in open space [11]; recombination radio lines with more n were detected only in absorption and not from hydrogen, but from the hydrogen-like atoms [12].

As for the parameter n as applied to the radiating cell, even at λ_{max} , as it follows from formula (7), $n \approx 6$. That is, the hydrogen atom radiating cell size (this cell is, as it were, the analogue of an antenna) at any possible wavelength does not go beyond the VI-th period atoms size (the atoms containing electrons in the seventh shell are unstable). The location of an electron at a greater distance from the nucleus is his excited and short-term state.

The longitudinal waves length, apparently, will be determined by the same equation (6) and, if it is limited not by $n = 6$, but by $n_{max} = 390$, then their length can be very large. Perhaps, in some range, electromagnetic waves also have a longitudinal component, since there are studies indicating the existence of longitudinal electromagnetic waves [13].

3 Determination of the gravitational constant

Let us consider an extremely simplified scheme of a single radiating cell, when a medium with an arbitrary mass m circulates along the toroid contour with a radius R , and at the same time it also rotates in the spiral about the toroid longitudinal axis in a radius r . The surface wave is known to have longitudinal and transverse components. Let the circulation along R occur under the action of gravitational forces with acceleration v^2/R , and the spiral rotation along r occur under the action of surface tension forces (capillary forces) with acceleration v^2/r . Considering the surface wave components separately, it is logical to correlate these components with gravitational waves and electromagnetic waves. One can say the electromagnetic oscillations to form, as it were, a small ‘‘ripple’’ on the surface of gravitational waves. Such ripples – a real physical analogue – are easy to observe on the water surface over its ordinary disturbance.

So, it is possible to draw up the single ratio of electric forces to gravitational ones, or, bearing in mind the equality of masses, the ratio of accelerations, which will be the largest under extreme conditions, i.e., it should be equal to

the value $c^2 r_e / \gamma m_e$, where the gravitational constant should be considered unknown. For the transverse component, the highest velocity $v = c$, and the vortex thread smallest size r is the circumscribed circle size around three Planck dimensions r_h , which from geometric constructions is equal to

$$r = r_h \left(1 + \frac{2}{3^{1/2}} \right), \tag{14}$$

where

$$r_h = \left(\frac{\hbar \gamma}{c^3} \right)^{1/2}, \tag{15}$$

and

$$\hbar = am_e r_e c, \tag{16}$$

since it has been established the quantity r_h to have a physical meaning and be the neutrino vortex thread minimum size [14].

For the longitudinal component, bearing in mind (4), the lowest speed

$$v = \frac{c_0^{1/3} c}{(an_{max})^2} \tag{17}$$

and, bearing in mind (3), the largest radius (contour length)

$$R = (an_{max})^2 r_e. \tag{18}$$

Thus, for the largest ratio of accelerations, taking into account the above and bearing in mind (17) and (18), one should write

$$\frac{(an_{max})^6 r_e}{c_0^{2/3} r} = \frac{c^2 r_e}{\gamma m_e}. \tag{19}$$

As a result, bearing in mind (14), (15), (16) and separating the parameter γ , after transformations from (19) we obtain:

$$\gamma = \left(1 + \frac{2}{3^{1/2}} \right)^{2/13} a^{1/13} c_0^{16/39} \left(\frac{\cos \Theta}{2\pi m_p} \right)^{12/13} \times \\ \times w_e \left(\frac{c}{r_e} \right)^{2/13} \times [\text{sec}^{-24/13}], \tag{20}$$

where w_e is the electron specific volume, equal to r_e^3 / m_e , $m_p = 1836.2$.

This equation is exact, but the Weinberg angle Θ (parameter in the electroweak interaction theory) is determined experimentally and lies within $28.13^\circ \dots 28.75^\circ$, i.e., $\cos \Theta = 0.882 \dots 0.877$. However, it can be calculated as the projection angle [4], and in this case

$$\cos \Theta = \frac{c_0^{1/6}}{(2\pi a)^{1/2}} = 0.882, \tag{21}$$

and also as the radius to circumference reduced ratio [5]

$$\cos \Theta = \left(\frac{1}{2\pi} \right)^{1/14} = 0.877, \tag{22}$$

and in other ways, which gives the same results. It can be assumed that the currently observed experimental data inconsistency when determining the gravitational constant is associated not so much with the Weinberg angle's uncertainty, and how much with the projection uncertainty of "hidden" parameters on the selected direction of our world, i.e., with the position uncertainty of the medium velocity vector relative to this selected direction [4].

Interestingly, the product of geometry-related parameters $(1 + 2/3^{1/2})^{2/13}(\cos \Theta)^{12/13}$ is very close to 1, which is apparently not accidental. Indeed, the fundamental constants formulas, such as r_h , \hbar , r_e , also do not contain geometric coefficients. Formula (20) can be written, as a result, by making transformations and replacing c by $c_0 \times [\text{m/sec}]$ in a more compact form

$$\gamma = a^{1/13} c_0^{22/39} (2\pi m_p)^{-12/13} m_e^{-1} r_e^{37/13} \times [\text{m}^{2/13} \text{sec}^{-2}], \quad (23)$$

which gives the value γ with a negligible error (here $m_p = 1836.2$).

It should be noted that the parameter r_e can be excluded from the formula for γ , since by definition it is determined by the electron mass, speed of light, dielectric constant and charge values, the latter, in turn, being determined through the electron mass, speed of light and Weinberg' angle [4].

4 Conclusion

The connection of gravity with the proton-electron contour size confirms the existence of limiting sizes, both in the microcosm and in space. So the vortex thread smallest size (the neutrino size) turned out to be equal to the Planck value \hbar [14], and the hydrogen atom largest size, still capable of radiation, corresponds to $n = 390$; this is confirmed by the fact that even in space, no excited hydrogen radio lines with $n > 301$ have been found [11]. The ratio of these limiting values makes it possible to calculate the gravitational constant.

Determining the speed of light and the gravitational constant magnitude based on the proposed physical model proves space to have the ideal fluid surface properties, where the speed of light is the surface wave speed. It has been established the ratio of forces acting in the transverse component of this wave (capillary waves) to the forces in its longitudinal component (gravitational waves) to be equal to the electric forces to gravitational forces ratio.

Thus, the original material entity is the finite thickness surface, whose deformation (fractalization) leads to the formation of material objects. Since the surface wave longitudinal component is essentially an elastic medium, in which tension-compression forces are possible, the gravity forces are the forces of attraction between material bodies, arising due to tension of this surface during its fractalization (deformation, thickening, condensation) in these bodies formation process. This is consistent with the conclusions drawn by Pierre A. Millette in his elastodynamics based on the analysis

of space-time deformation in terms of continuum mechanics [15, 16]. That is, the very *existence of material bodies is the cause of their mutual attraction*, and electromagnetic waves contain the longitudinal component, which is the gravitational waves conductor.

It has also been established that the surface wave optimal radiating cell generates radiation with the length of 1.52×10^{-3} m, which corresponds to the background radiation maximum and, therefore, may be its natural cause.

And so, on the basis of the mechanistic interpretation of Wheeler's geometrodynamics, which, not being essentially physical and mathematical, but rather physical and logical, have determined the gravitational constant value (as well as the speed of light, electron charge, neutrino mass, etc., which was stated in the relevant articles). This model's possibility to obtain and predict results not achieved by mathematized methods proves the macroanalogies underlying its full compliance with the corresponding physical natural laws, which indicates the need for further development of this model at a higher level.

Received on March 27, 2023

References

1. Dewitt B.S. Quantum gravity. *Scientific American*, December 1983, v. 249, 112–129.
2. Berera A., Buniy R. V., Kephart T. W., Päs H., and Rosa J.G. Knotty inflation and the dimensionality of spacetime. arXiv: 1508.01458, August 6, 2015.
3. Peano G. Sur une courbe, qui remplit toute une aire plane. *Mathematische Annalen*, 1890, v. 36, issue 1, 157–160.
4. Belyakov A.V. Charge of the electron, and the constants of radiation according to J.A.Wheeler's geometrodynamics model. *Progress in Physics*, 2010, v. 6, issue 4, 90–94.
5. Belyakov A.V. Macro-analogies and gravitation in the micro-world: further elaboration of Wheeler's model of geometrodynamics. *Progress in Physics*, 2012, v. 8, issue 2, 47–57.
6. Belyakov A.V. The substantive model of the proton according to J. Wheeler's geometrodynamics concept. *Progress in Physics*, 2021, v. 17, issue 1, 15–19.
7. Belyakov A.V. Nuclear power and the structure of a nucleus according to J.Wheeler's geometrodynamics concept. *Progress in Physics*, 2015, v. 11, issue 1, 89–98.
8. Belyakov A.V. Evolution of stellar objects according to J. Wheeler's geometrodynamics concept. *Progress in Physics*, 2013, v. 9, issue 1, 25–40.
9. Belyakov A.V. On the uniform dimension system. Is there the necessity for Coulomb? *Progress in Physics*, 2013, v. 9, issue 3, 142–143.
10. Belyakov A.V. On the speed of light and the continuity of physical vacuum. *Progress in Physics*, 2018, v. 14, issue 4, 211–212.
11. Pedlar A., Davies R. D., Hart L., Shaver P. A. Studies of low-frequency recombination lines from the direction of the Galactic Centre and other galactic sources. *Monthly Notices of the Royal Astronomical Society*, 1978, v. 182, issue 3, 473–488.
12. Konovalenko A. A. Decametric astrospectroscopy. *Earth and Universe*, 1986, v. 5, 26–34.
13. Tomilin A. K., Lukin A. F., Gulkov A. N. Experiment to create a radio communication channel in the marine environment. *Technical Physics Letters*, 2021, v. 47, issue 11, 48–50.

14. Belyakov A. V. Determination of the neutrino mass. *Progress in Physics*, 2016, v. 12, issue 1, 34–38.
 15. Millette P. A. Elastodynamics of the spacetime continuum. *The Abraham Zelmanov Journal*, 2012, v. 5, 221–277.
 16. Millette P. A. Elastodynamics of the Spacetime Continuum. The 2nd expanded edition, American Research Press, Rehoboth, New Mexico, 2019, 415 pages.
-

Fermion Mass Derivations: I. Neutrino Masses via the Linear Superposition of the 2T, 2O, and 2I Discrete Symmetry Binary Subgroups of SU(2)

Franklin Potter

Sciencegems.com, 8642 Marvale Drive, Huntington Beach, CA 92646 USA. E-mail: frank11hb@yahoo.com

We derive neutrino masses from discrete symmetry binary subgroups of SU(2), 2T for the electron family, 2O for the muon family, and 2I for the tau family, acting collectively to generate the PMNS mixing angles. Using the modulus τ near $\omega = \exp(2\pi i/3)$ in the domain of SU(2) converts the PMNS matrix into the 24th root of unity and produces a factor of 3^{11} to predict neutrino masses: $m_1 = 0.3$ meV, $m_2 = 8.9$ meV, $m_3 = 50.7$ meV.

1 Introduction

One of the most challenging fundamental problems in particle physics is to calculate the mass values of the leptons and quarks. We tackle this problem within the framework of the Standard Model by considering the three specific discrete symmetry binary subgroups of SU(2) that we have established previously [1,2]. The three lepton families represent the binary tetrahedral group 2T for the electron family, the binary octahedral group 2O for the muon family, and the binary icosahedral group 2I for the tau family. The mass values for the quark families will be derived via an identical approach in a separate article.

After a brief review of some of the limitations of the Standard Model, we explain some of the consequences of the discrete symmetry binary subgroups of SU(2), including how we utilized their generators to derive the correct mixing angles for the lepton PMNS[‡] mixing matrix. These subgroups have a domain in the upper half of the complex plane and we use their modulus τ for fractional linear transformations near its symmetry point $\tau_0 = \omega = \exp(2\pi i/3)$ in our procedure to predict the lepton mass values. Note that the modular subgroups of SL(2,Z) used to calculate lepton masses via many parameters [3,4] are isomorphic to our subgroups of SU(2).

We find that by treating the three lepton families equivalently leads to the circulant matrix method used to derive [5,6] the 1982 Koide formula [7] that accurately predicted the mass value of the tau lepton. We move the value of τ slightly away from ω , thereby introducing CP symmetry breaking, to convert our PMNS mixing matrix into the 24th root of unity, from which we calculate neutrino mass values by using the factor of 3^{11} difference from the charged-lepton mass values.

Finally, we examine how the unique invariant N for each binary subgroup can be used to derive the lepton mass values from geometry. According to F. Klein [8] in 1884, each of the three binary subgroups has an invariant N inversely related to $j(\tau)$ of elliptic modular functions, the N being: 1 for 2T, 108 for 2O, and 1728 for 2I, integer values that have a similar hierarchy to the 0.511 MeV, 105.66 MeV, and 1776.82 MeV

mass values for the charged leptons!

2 SM limitations

The Standard Model (SM) of leptons and quarks has been an extremely successful effective field theory [9–12] for combining the unified electroweak interaction with the nuclear color interaction since its formulation in the 1970s. Its fundamental particles represent quantum fields, with the SM probably being an approximation to an underlying theory.

The physical world is artificially partitioned into a (3+1)-D spacetime and an internal symmetry space at each point in spacetime. The known fundamental particle quantum states are defined in the internal symmetry space, but the number of dimensions of the internal symmetry space has yet to be established.







The two particle quantum states for each lepton family and for each quark family represent the continuous symmetry group SU(2), i.e. the $\pm 1/2$ weak isospin states which are also called the up and down flavor states. Of the 3 known lepton families, the electron family (ν_e, e^-), the muon family (ν_μ, μ^-), and the tau family (ν_τ, τ^-), the more massive muon and tau charged leptons are known to not be excited higher mass states of the electron. Likewise, the two known quark families beyond the first quark family are not simply higher mass states of the first quark family.

The SM as presently understood cannot predict the number of lepton families nor the number of quark families. However, the weak interaction Z^0 boson decays suggest that there are exactly the 3 lepton families [13] if there are only neutrinos with mass values below about 90 GeV, which appears to be the case. In addition, there is a cosmological limit of 15 total fundamental leptons plus quarks. There being 12 known fundamental leptons plus quarks, at least one more family of two particles is possible. [14, 15]

Lepton mixing occurs [16–18] when one neutrino type or charged-lepton can change into another on the journey from source to detector. This behavior is in direct conflict with the SM expectation for massless neutrinos. However, most conserved quantities still hold true, such as electric charge conservation with the electromagnetic interaction being equiva-

[‡]Pontecorvo-Maki-Nakagawa-Sakata

Table 1: Lepton Family Group Assignments.

Family	Group	Order	3-D	Mass (MeV)
ν_e				< 0.001
e^-	2T	24		0.511
ν_μ				< 0.001
μ^-	2O	48		105.7
ν_τ				< 0.001
τ^-	2I	120		1776.8

lent for all electrically charged particles as well as the weak interaction being identical for each of the lepton and quark family particles, a property called weak universality. Further tests challenging this weak interaction lepton flavor universality (LFU) continue to be carried out at many different experiments worldwide.

3 Lepton mixing

In order to better understand the physical behavior of the SM particle states, in the 1990s we introduced [1] specific different discrete symmetry binary subgroups of SU(2) in R³ for each family of leptons and in R⁴ for each family of quarks. This approach has gained in importance in the past decade as other approaches have become less likely or eliminated. The discrete symmetry binary subgroups for the lepton families are the assignments listed in Table 1 along with their 3-D representations as the Platonic solids at the Planck scale. The justification for these specific binary subgroup assignments includes the correct mixing angles for the lepton PMNS matrix that relates the wave functions for the SM flavor states to their mass states.

One major consequence of having the fundamental particles represent specific discrete symmetry binary subgroups is that the lepton and quark SM weak isospin states are not the same as the mass states, in agreement with experimental results. Otherwise, in the traditional SM view with the lepton and quark families representing the continuous symmetry group SU(2), there is no known reason for the mass states to be different from the SM weak isospin states and this difference is simply attributed to a mismatch between the weak isospin states and the mass states!

We proposed [2] that the reason for the difference between the SM weak isospin flavor states and the mass states depends upon the continuous symmetry requirement of quantum field

Table 2: Quaternion Generators. $\phi = (1 + \sqrt{5})/2$

Fam.	Grp.	U3 Generator	Factor	Ang./2
ν_e, e^-	SU(2) 2T	k $-\frac{1}{2}i - \frac{1}{2}j + \frac{1}{2}k$	-0.2642	52.66°
ν_μ, μ^-	2O	$-\frac{1}{2}i - \frac{1}{\sqrt{2}}j + \frac{1}{2}k$	+0.8012	18.38°
ν_τ, τ^-	2I	$-\frac{1}{2}i - \frac{\phi}{2}j + \frac{1}{2\phi}k$	-0.5370	61.24°

Table 3: Comparison to NuFit 5.2 values for neutrino observables.

	bfp ±1σ	3σ range	predicted
$\sin^2 \theta_{12}$	0.303 ^{+0.012} _{-0.012}	0.270 → 0.341	0.3172
$\theta_{12}/^\circ$	33.41 ^{+0.75} _{-0.72}	31.31 → 35.74	34.29°
$\sin^2 \theta_{23}$	0.451 ^{+0.019} _{-0.016}	0.408 → 0.603	0.4627
$\theta_{23}/^\circ$	42.2 ^{+1.1} _{-0.9}	39.7 → 51.0	42.85°
$\sin^2 \theta_{13}$	0.0222 ^{+0.0006} _{-0.0006}	0.0205 → 0.0240	0.0223
$\theta_{13}/^\circ$	8.58 ^{+0.12} _{-0.12}	8.23 → 8.91	8.56°

theory (QFT) because the fields are required to be continuous. Having our specific discrete symmetry binary subgroups define their weak isospin states within the framework of the SM violates this QFT continuous symmetry requirement. Therefore, to eliminate this violation, we determined that a linear superposition of the binary subgroup generators was needed so that acting collectively the three discrete symmetry binary subgroups could mimic the continuous symmetry group SU(2).

This linear superposition is achieved separately for the lepton families and for the quark families. The quaternion generators for each of the three lepton binary subgroups are the same for the first two generators, i.e. the quaternions U1 = i and U2 = j of SU(2), but the third generators, the U3's, which should each be k, are different for each subgroup and are listed in Table 2. The normalized contributing factors to the linear superposition for each lepton family binary subgroup are listed in column four of Table 2 as well as their half-angle contributions whose differences determine the PMNS mixing angles.

The absolute values of our predicted mixing angles for the lepton PMNS mixing matrix are listed in Table 3, showing that they agree with the empirically determined ranges of values. Note that we predict the θ_{23} angle of 42.85° to be in the first quadrant, in agreement with some of the empirical values but in contrast to other results that suggest the second quadrant.

The PMNS matrix for the lepton families is the product

of the charged-lepton and the neutrino matrices

$$U_{PMNS} = U_e^\dagger U_\nu. \quad (1)$$

If the charged-lepton states do not mix, or their mixing is minimal, U_e is diagonal, an assumption that is discussed in a later section, then the PMNS mixing matrix represents neutrino mixing only. Therefore, the PMNS matrix relates the neutrino mass states (ν_1, ν_2, ν_3) to the SM weak isospin states $(\nu_e, \nu_\mu, \nu_\tau)$ as

$$\begin{pmatrix} \nu_e \\ \nu_\mu \\ \nu_\tau \end{pmatrix} = \begin{pmatrix} U_{e1} & U_{e2} & U_{e3} \\ U_{\mu1} & U_{\mu2} & U_{\mu3} \\ U_{\tau1} & U_{\tau2} & U_{\tau3} \end{pmatrix} \begin{pmatrix} \nu_1 \\ \nu_2 \\ \nu_3 \end{pmatrix}. \quad (2)$$

Keeping a phase factor δ for CP violation consideration, our PMNS matrix in the standard popular 3x3 formulation is

$$\begin{pmatrix} 0.817 & 0.557 & -0.1491e^{-i\delta} \\ -0.413 - 0.084e^{i\delta} & 0.606 - 0.057e^{i\delta} & -0.669 \\ -0.383 + 0.051e^{i\delta} & 0.558 + 0.062e^{i\delta} & 0.725 \end{pmatrix}. \quad (3)$$

Therefore, we have established the very important result that each lepton family represents its own specific discrete symmetry binary subgroup of SU(2) because our assigned groups lead directly to correct predictions of the mixing angles for the PMNS mixing matrix. And we know that the origin of this mixing is the QFT requirement for continuous symmetry behavior. So the discrete symmetries of the lepton families mix collectively via a linear superposition to mimic the continuous symmetry group SU(2).

Our binary subgroups of SU(2) have their fundamental domain \mathcal{D} in the upper half of the complex plane between $-1/2$ and $+1/2$ as shown in Fig. 1 with three symmetric points $\tau_{sym} = i\infty, i,$ and $\omega = \exp(2\pi i/3)$. Although no value of the modulus τ preserves the full symmetry of SU(2) (or its isomorphic modular group SL(2,Z)), at the three τ_{sym} values, specific \mathbb{Z}_N symmetries are preserved, with $N = 2, 3,$ or 4. When τ lies on the border of \mathcal{D} , CP symmetry is preserved [3, 4], but small deviations expressed by $|\tau - \tau_{sym}|$ lead to CP symmetry being broken and hierarchial mass patterns emerging according to the sequence $(1, \epsilon, \epsilon^2)$, where $\epsilon \ll 1$. See Appendix A for the details which were introduced in a modular group analysis.

4 Circulant matrix approach

We know from the collective action dictated by the continuous symmetry constraint of QFT that perhaps the three lepton families should be treated as equals, a symmetry that suggests they obey the group U(3). If we assume U(3) symmetry for this equal treatment, we can utilize its expression as a 3x3 circulant matrix [5,6], from which the famous Koide formula [7] has been derived.

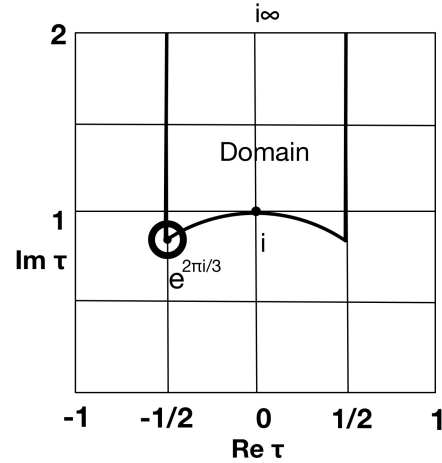


Fig. 1: The fundamental domain of our three SU(2) subgroups 2T, 2O, and 2I (and of the modular group $\Gamma = \text{SL}(2, \mathbb{Z})$) with its three symmetric points $\tau_{sym} = i\infty, i, \omega$, where $\omega = \exp(2\pi i/3) = -0.5 + 0.866i$, with a small ring of acceptable values around ω .

We now paraphrase a 2006 article by C. Brannen [5], which shows how to use this type of equality to derive the Koide formula for the charged-lepton mass values from a circulant matrix and then proceeds to derive the mathematical relations that lead to the prediction of reasonable neutrino mass values in the meV energy range.

The 3x3 1-circulant matrix

$$G(A, B, C) = \begin{pmatrix} A & B & C \\ C & A & B \\ B & C & A \end{pmatrix}, \quad (4)$$

where A, B and C are complex constants, has eigenvectors of the form

$$|n\rangle = \frac{1}{\sqrt{3}} \begin{pmatrix} 1 \\ \exp(+2n\pi/3) \\ \exp(-2n\pi/3) \end{pmatrix}, \quad (5)$$

with $n = 1, 2, 3$. By requiring the eigenvalues λ_n to be real, the circulant matrix can be rewritten in the form

$$G(\mu, \eta, \beta) = \mu \begin{pmatrix} 1 & \eta \exp(+i\beta) & \eta \exp(-i\beta) \\ \eta \exp(-i\beta) & 1 & \eta \exp(+i\beta) \\ \eta \exp(+i\beta) & \eta \exp(-i\beta) & 1 \end{pmatrix}, \quad (6)$$

with η assumed to be non-negative. The η and β are pure numbers, whereas μ will scale with the eigenvalues given by

$$G(\mu, \eta, \beta) |n\rangle = \lambda_n |n\rangle = \mu (1 + 2\eta \cos(\beta + 2n\pi/3)) |n\rangle. \quad (7)$$

From the traces of G and G^2 one derives the eigenvalue relationships

$$\lambda_1 + \lambda_2 + \lambda_3 = 3\mu \quad (8)$$

and

$$\lambda_1^2 + \lambda_2^2 + \lambda_3^2 = 3\mu^2(1 + 2\eta^2). \tag{9}$$

From here one obtains the Koide formula by setting $\eta^2 = 0.5$:

$$\frac{(\lambda_1 + \lambda_2 + \lambda_3)^2}{\lambda_1^2 + \lambda_2^2 + \lambda_3^2} = \frac{3}{2}. \tag{10}$$

By setting the eigenvalues $\lambda_i = \sqrt{m_i}$, the 1982 formula proposed by Koide for the masses of the charged leptons is:

$$\frac{(\sqrt{m_e} + \sqrt{m_\mu} + \sqrt{m_\tau})^2}{m_e + m_\mu + m_\tau} = \frac{3}{2}. \tag{11}$$

Using the known mass values of the electron and the muon, the mass value of the tau was predicted [7] to be in agreement with future experimental results to better than two decimal places!

Consequently, from knowing the masses of the charged leptons, one determines [5] that

$$\begin{aligned} \mu_1 &= 17716.13(109) \text{ eV}^{0.5} \\ \eta_1^2 &= 0.500003(23) \\ \beta_1 &= 0.2222220(19) \end{aligned} \tag{12}$$

where the subscript 1 has been added to distinguish these parameters from the future neutrino parameters. Notice that β_1 is essentially $2/9$ and perhaps could be related to the phase $\phi = -2\pi/9$ of the scalar potential in the modular group approach introduced in the Appendix.

5 Lepton mass hierarchy

Before there was any evidence of tau neutrino mixing with the electron neutrino, the tribimaximal matrix with its zero value in the (1,3) position was thought by researchers to be the PMNS matrix that best represented the neutrino data:

$$\begin{pmatrix} \frac{2}{\sqrt{6}} & \frac{1}{\sqrt{3}} & 0 \\ -\frac{1}{\sqrt{6}} & \frac{1}{\sqrt{3}} & -\frac{1}{\sqrt{2}} \\ -\frac{1}{\sqrt{6}} & \frac{1}{\sqrt{3}} & \frac{1}{\sqrt{2}} \end{pmatrix}. \tag{13}$$

Of course, we will substitute our PMNS matrix for this approximate matrix, but first we shall continue to follow the original article [5] in order to reveal its amazing result.

Left-multiplying this tribimaximal matrix by a matrix of the circulant eigenvectors achieves a simple product with the value of $\tau = \omega$, i.e. the lower left corner at $\tau_0 = \exp(2\pi i/3)$ in the domain region:

$$\alpha = \omega = e^{2\pi i/3} = -0.5 + 0.866i : \tag{14}$$

$$\frac{1}{\sqrt{3}} \begin{pmatrix} 1 & \alpha & \alpha^* \\ 1 & 1 & 1 \\ 1 & \alpha^* & \alpha \end{pmatrix} \begin{pmatrix} 0.8165 & 0.5773 & 0 \\ -0.4082 & 0.5773 & -0.7071 \\ -0.4082 & 0.5773 & 0.7071 \end{pmatrix} = \tag{15}$$

$$= \begin{pmatrix} 0.7071 & 0 & -0.7071i \\ 0 & 1 & 0 \\ 0.7071 & 0 & 0.7071i \end{pmatrix}.$$

This resulting matrix is the 24th root of unity! That is, its 24th power is the unit matrix.

Note there exists many mathematical relationships from here which we could list, such as relationships to the expansions of the j-invariant $j(\tau)$, the eta function, etc., which involve 24th powers or 24th roots, but we do not need these mathematical functions to derive the neutrino mass values. However, these functions would be needed for expressing the wave functions of the particles.

Continuing onward, we know that the true PMNS mixing matrix is not the tribimaximal matrix but our PMNS matrix determined by our binary subgroups. We can achieve the same result, i.e. the 24th root of unity matrix, by using a value of τ slightly different from ω . After trying several different values, using this value of τ :

$$\alpha = \tau = -0.496 + 0.877i, \tag{16}$$

to multiply the values in our PMNS matrix leads to

$$\begin{aligned} &\frac{1}{\sqrt{3}} \begin{pmatrix} 1 & \alpha & \alpha^* \\ 1 & 1 & 1 \\ 1 & \alpha^* & \alpha \end{pmatrix} \begin{pmatrix} 0.817 & 0.557 & -0.149 \\ -0.4213 & 0.6084 & -0.669 \\ -0.3936 & -0.5654 & 0.7248 \end{pmatrix} = \\ &= \begin{pmatrix} 0.7014 - 0.0731i & 0.021 & 0.021 - 0.7059i \\ 0.008 & 0.927 & 0.116 \\ 0.7014 - 0.0731i & 0.021 & 0.0707 + 0.7075i \end{pmatrix}. \end{aligned} \tag{17}$$

The result is within 1% of the 24th root of unity when using our PMNS mixing matrix and this value of α . A slight adjustment in the α value could make the fit closer.

As shown in the Appendix, the modular subgroup approach agrees that this value of α is a universal fit for the SU(2) subgroups or their equivalent modular subgroups.

Therefore, we will consider our α to be close enough and continue with this approach in order to establish the relationship between the charged-lepton states and the neutrino states as well as to determine the neutrino mass values.

Following the procedure, we define the mass operator M associated with the eigenvalue $\lambda_i = \sqrt{m_i}$ to take left-handed states to right-handed states and vice-versa:

$$\begin{aligned} M |R\rangle &= |L\rangle \\ M |L\rangle &= |R\rangle. \end{aligned} \tag{18}$$

In general, M^2 picks up a Berry-Panchartnam or topological phase to become complex upon returning to the original state, so we can express

$$M^2 |L\rangle = p^2 \exp(2i\kappa) |L\rangle. \tag{19}$$

Note that if $\kappa = 2\pi/24 = \pi/12$, then the state $|L\rangle$ is brought back to a multiple of $|L\rangle$ by

$$M^{24}|L\rangle = p^{24}|L\rangle. \quad (20)$$

Therefore, if M^2 operates on the left-handed electron as

$$M^2|e_L\rangle = p^2|e_L\rangle, \quad (21)$$

then we would have

$$M^{24}|\nu_L\rangle = p^{24}|\nu_L\rangle, \quad (22)$$

meaning that the masses of the two particle states in the lepton family differ by a factor of p^{22} .

The mass scale factors μ_1 for charged leptons and μ_0 for neutrinos are therefore related by

$$\mu_0^2 = \mu_1^2/3^{22} = 0.100^2, \quad (23)$$

where the factor of three comes from the square of the normalization factor $1/\sqrt{3}$ for the three eigenvectors in the matrix multiplying the PMNS matrix above. Likewise, there is a phase difference

$$\beta_1 - \beta_0 = -\frac{\pi}{12}. \quad (24)$$

Neutrino mass predictions using $\mu_1/\mu_0 = 3^{11}$ and the phase difference $\beta_1 - \beta_0 = -\pi/12$ in the eigenvalue $G(\mu, \eta, \beta)$ results in these reasonable predicted neutrino mass values:

$$\begin{aligned} m_1 &= 0.3 \text{ meV} \\ m_2 &= 8.9 \text{ meV} \\ m_3 &= 50.7 \text{ meV}, \end{aligned} \quad (25)$$

assuming still that $\eta^2 = 0.5$. Although these predicted mass values fit the neutrino values estimated from experimental results, we will need to wait for confirmation from ongoing and future experiments.

However, do these values produce the 3/2 value in the Koide formula? Not with the original version, but they do agree if we utilize the valid alternative version in which the square root of the lowest mass neutrino m_1 is preceded by a negative sign [5, 6].

Our results for the leptons being 3-D objects with the discrete symmetries of the binary subgroups 2T, 2O, 2I of SU(2) not only predict reasonable neutrino mass values but also predict the normal mass hierarchy NH of the neutrino mass states as $m_1 < m_2 < m_3$. However, the present experimental data also allows for an inverse hierarchy IH as $m_3 < m_1 < m_2$.

In addition, we have exactly 3 lepton families, in agreement with the Z^0 decay results, but there continues to be speculation about an additional lepton, such as a sterile neutrino. And, our approach treats the 3 lepton families as symmetrical contributors as eigenvectors of a 1-circulant matrix, whereas all other analyses place the charged leptons and the neutrinos into irreducible representations of a subgroup, usually in a 3 or 3' irreducible representation. Which method Nature has chosen will be determined by experiments in the near future.

6 Review of the derivation

Our sequence of steps to neutrino mass predictions were:

1. We first established that the three discrete symmetry 3-D binary subgroups 2T, 2O, 2I of SU(2) are represented by the three lepton families and are 3-D objects instead of point particles at the Planck scale. These are the correct groups because when they collectively mimic the continuous group SU(2) to satisfy the requirement of QFT they produce the correct mixing angles for the PMNS mixing matrix.
2. By treating the lepton families as equals in symmetry group U(3), the famous Koide formula is derived via a 3x3 1-circulant matrix, revealing that the important mass quantity is the square root of the mass values $\lambda = \sqrt{m}$ instead of the mass value itself. Three parameters μ_1, η_1 , and β_1 for calculating the mass eigenvalues of the charged leptons were determined.
3. With the value $\alpha = \tau = -0.496 + 0.877i$ in the domain of SU(2), we derived the 24th root of the unity matrix by multiplying our PMNS matrix by the appropriate 1-circulant eigenvector matrix. This specific value of α agreed with the findings of the modular group approach that uses subgroups of SL(2,Z), i.e. that the value applies equally to our three subgroups of SU(2).
4. By inserting the Berry-Panchartnam phase factor when returning a left-handed lepton state back to its original state for the mass-squared operator M^2 , there resulted a factor of p^{22} difference between the charged-lepton states and the neutrino states as well as a phase difference of $\pi/12$.
5. Finally, using the factor of 3^{11} that connected the neutrino mass values to the charged-lepton mass values for the parameter ratio μ_1/μ_0 , with the eigenvalue expression $G(\mu, \eta, \beta)$ we predicted reasonable neutrino mass values in the meV range in NH: $m_1 = 0.3 \text{ meV}, m_2 = 8.9 \text{ meV}, m_3 = 50.7 \text{ meV}$.

In the next section, our goal is to relate the above results to the invariants $N = 1, 108, 1728$ of the three lepton family binary subgroups 2T, 2O, 2I respectively. Therefore, we should be able to understand how the lepton family mass values originate from their 3-D geometric properties.

7 Invariant theory connection

Invariant theory connects the elliptic modular function $j(\tau)$ to invariants of our specific discrete symmetry binary subgroups. Each invariant N is related by

$$j(\tau) = \frac{W_1}{NW_2}, \quad (26)$$

where W_1 is expressed in two complex variables for the vertices and W_2 for the face centers of the polyhedrons [8] for

the binary groups 2T, 2O, and 2I, with $N = 1, 108, \text{ and } 1728$, respectively.

These invariants are similar to the charged-lepton mass values in MeV, i.e. 0.511, 105.66, and 1776.82, but they have no energy units, so we would naturally consider their ratios instead. However, the question remains, why is there a change from the original geometrical values N that are invariant under all fractional linear transformations to the experimentally determined universal values for the charged lepton masses?

One possible answer could be related to the change of the value of τ from $\omega = \exp(2\pi i/3) = -0.5 + 0.866i$ to the nearby value, $\alpha = \tau_0 = -0.496 + 0.877i$ in the domain. However, we realize that we have simply changed the question without providing the reason for the change.

However, recall that the lepton PMNS mixing matrix

$$U_{PMNS} = U_e^\dagger U_\nu, \tag{27}$$

relates the wave functions, so we can speculate that there could be a slight mixing among the charged-lepton states, particularly among the electron and the muon states. Experiments are being planned specifically to check for this mixing possibility.

If we want the tentative geometrical state mass values suggested by the SM binary group N values to become the measured mass state values, one would have a mass matrix very close to being the unitary matrix but containing some small off-diagonal terms. Such a mass matrix might look like

$$\begin{pmatrix} 1 & -0.0274 & 0 \\ 0.0274 & 1 & -0.0033 \\ 0 & 0.0558 & 1 \end{pmatrix} \begin{pmatrix} \sqrt{1} \\ \sqrt{108} \\ \sqrt{1728} \end{pmatrix} \tag{28} \\ = \begin{pmatrix} \sqrt{0.511} \\ \sqrt{105.66} \\ \sqrt{1776.82} \end{pmatrix},$$

in which we have used the square root of the mass values as determined by the Koide relationship. That is, the slight mixing among the charged-lepton wave functions could be carried over to a mass matrix relating our N values to the measured mass values. Of course, mass ratios would be preferred. But we are still left with determining an energy scale for these mass values.

8 Conclusions

We have been able to calculate the mass values of the neutrinos by following a series of steps beginning with the correct identification of the discrete symmetry binary subgroups of SU(2), which are equivalent to subgroups of the modular group SL(2,Z). The three lepton families represent 2T, 2O, and 2I, and we derived their PMNS mixing matrix for

their wave functions from their quaternion generators in order to agree with a continuous symmetry constraint dictated by quantum field theory (QFT).

Assuming that these binary subgroups together act as a U(3) symmetry, the famous Koide formula follows directly via a 1-circulant matrix approach that also relates the PMNS matrix to the 24th root of unity matrix by using a modulus τ value slightly different from the symmetry point value $\omega = \exp(2\pi i/3) = -0.5 + 0.866i$ in the fundamental domain of SU(2) and its isomorphic modular group SL(2,Z). That is, we set $\tau = -0.496 + 0.877i$. This method then produced a factor of 3^{11} difference in the mass values of the charged leptons and the neutrinos, which led directly to the predicted neutrino mass values being $m_1 = 0.3 \text{ meV}, m_2 = 8.9 \text{ meV}, m_3 = 50.7 \text{ meV}$.

Although we assumed that the charged-lepton mixing matrix was diagonal, the invariants $N = 1, 108, \text{ and } 1728$ from geometry and invariant theory for the electron family, muon family, and tau family binary subgroups, respectively, indicated that there is a slight mixing of the charged leptons also. We suggested a matrix that has unit values on the diagonal but also has a few very small off-diagonal terms to relate the N values to the actual charged lepton universal mass values 0.511 MeV, 105.66 MeV, and 1776.82 MeV. Of course, the mass scale would still remain to be determined.

In a future article, i.e. part II, we determine the origin of the quark mass values. We will establish that a similar approach succeeds for modulus τ values near to the other symmetric point $\tau = i$ within the fundamental domain. In the quark case, we predict 4 quark families, (u,d), (c,s), (t,b), and (t',b'), which represent [1, 2] the discrete symmetry binary subgroups [333], [433], [343], and [533], respectively, in R^4 . QFT dictates a continuous symmetry group behavior, so the linear superposition of their generators to mimic SU(2) produces the CKM4 mixing matrix with CKM[‡] submatrix values.

The quark mass values fit a four term Koide formula separately for the up and the down states, and a 4x4 circulant matrix defines eigenvectors. The predicted t' quark should have a mass value of about 3 TeV, a mass value large enough to gain a factor of about 10^{13} multiplying the present Jarlskog constant, thereby providing a value large enough to help explain the baryon asymmetry of the Universe [BAU] in terms of CP violation [19].

Appendix: Modular group

A brief look into what researchers in the past decade have achieved using subgroups of the modular group SL(2,Z) in order to calculate neutrino mass values will demonstrate some agreement with our results. We therefore provide a summary of their research by paraphrasing a recent article [3, 4] to illustrate how our bottoms-up approach from the binary sub-

[‡]Cabibbo-Kobayashi-Maskawa

groups of SU(2) can relate to the top-down calculations using modular groups related to superstring theory. The modulus τ of $SL(2, \mathbb{Z})$ is the single field quantity associated with the fermion particle states.

Our three discrete symmetry binary subgroups 2T, 2O, and 2I of SU(2) for the lepton families are isomorphic to these modular double cover subgroups:

$$2T = \Gamma'_3, \quad 2O = \Gamma'_4, \quad 2I = \Gamma'_5. \quad (29)$$

Therefore, their modular mathematical properties apply to our discrete symmetry binary subgroups of SU(2) as well.

Lepton flavor models based upon the modular symmetry group $\Gamma = SL(2, \mathbb{Z})$ utilize its subgroups $\Gamma'_N = SL(2, \mathbb{Z}_N)$, such as the double covers $\Gamma'_2 = S'_3$, $\Gamma'_3 = A'_4$, $\Gamma'_4 = S'_4$, $\Gamma'_5 = A'_5$ of the permutation groups S_3, A_4, S_4, A_5 . With significant fine-tuning and a number of coupling constants, the mass hierarchies of the leptons can be reproduced in terms of a small parameter when the three lepton families are assigned to an irreducible representation of a modular subgroup, such as $\Gamma'_3 = A'_4$.

The modular group's fundamental domain \mathcal{D} shown in Fig. 1 has the three symmetric points $\tau_{sym} = i\infty, i$, and $\omega = \exp(2\pi i/3)$ with its three τ_{sym} values preserving specific \mathbb{Z}_N symmetries, i.e. those with $N = 2, 3$, or 4. When τ lies on the border, CP symmetry is preserved, but small deviations lead to CP symmetry being broken and hierarchal mass patterns emerging according to the sequence $(1, \epsilon, \epsilon^2)$.

This recent research has revealed that the lepton data suggests a value of τ near the cusp $\tau_0 = \omega = -0.5 + 0.866i$, with the best fit being

$$\tau = -0.496 + 0.877i \quad (30)$$

with a viable region being a small ring of values around the cusp ω , as shown in Fig. 1. The result is universal, meaning that its value is independent of which modular subgroup is being considered.

The research defined a scalar potential V_m near $\tau_0 = \omega$ that depends upon an integer parameter m and a phase angle ϕ , with a minimum in the scalar potential at

$$\frac{0.0145}{m + 0.0025}. \quad (31)$$

If the phase angle is included, the minimum occurs at

$$\phi_{min} = \frac{-2\pi}{9} \quad (32)$$

independent of m , producing for $m = 2$ the result

$$\frac{0.0145}{2 + 0.0025} \exp\left(\frac{-2\pi i}{9}\right) \leftrightarrow \tau_{min} = -0.492 + 0.875i. \quad (33)$$

The scalar potential V_m has a deep trench from ω upward from ω in the first quadrant direction that depends upon the quantity

$$[j(\tau) - 1728]^{m/2} \quad (34)$$

where $j(\tau)$ is the j -invariant of elliptic modular functions.

Therefore the modular group approach has revealed some very important results, particularly telling us that there seems to be no dependence upon which modular subgroup Γ'_N is being used as the modular subgroup for lepton flavor symmetry! Whence, the above results apply to all the modular subgroups equally or, equivalently, to our specific binary subgroups of SU(2) for the lepton families.

Acknowledgements

We thank Sciencegems.com for financial support and physicist Joe Marasco for suggestions and encouragement. The author is solely responsible for errors and omissions.

Received on April 12, 2023

References

- Potter F. Geometrical Basis for the Standard Model. *Int. J. of Theor. Phys.*, 1994, v. 33, 279–305.
- Potter F. CKM and PMNS mixing matrices from discrete subgroups of SU(2). *J. Phys.: Conf. Ser.*, 2015, v. 631, 012024.
- Novichkov P.P., Penedo J. T., Petcov S. T. Fermion Mass Hierarchies, Large Lepton Mixing and Residual Modular Symmetries. arXiv: hep-ph/2102.07488v1.
- Novichkov P.P., Penedo J. T., Petcov S. T. Modular Flavour Symmetries and Modulus Stabilisation. arXiv: hep-ph/2201.02020.
- Brannen C. The Lepton Masses. 2006, www.brannenworks.com/MASSES2.pdf.
- Brannen C. Koide mass equations for hadrons. 2008, www.brannenworks.com/koidehadrons.pdf.
- Koide Y. What Physics Does The Charged Lepton Mass Relation Tell Us? arXiv: hep-ph/1809.00425.
- Klein F. Lectures on the Icosahedron and the Solution (of Equations) of the Fifth Degree. Cosimo Classics, New York, 2007.
- Particle Data Group. Review of Particle Physics. cds.cern.ch/record/1481544/files/PhysRevD.86.010001.pdf.
- Workman R. L. *et al* (Particle Data Group). The Review of Particle Physics. *Prog. Theor. Exp. Phys.*, 2022, 083C01.
- Cohen T. D., Poniatowski N. R. A Somewhat Random Walk Through Nuclear and Particle Physics. arXiv: hep-ph/2006.12564v3.
- Charley S. Six fabulous facts about the Standard Model. *Symmetry Magazine*, 2021, //www.symmetrymagazine.org/article/six-fabulous-facts-about-the-standard-model.
- Blondel A. The Number of Neutrinos and the Z Line Shape. 2016. cds.cern.ch/record/2217139/files/9789814733519_0008.pdf.
- Wysozka S. R. J., Kielanowski P. Test of the 4-th quark generation from the Cabibbo-Kobayashi-Maskawa matrix. arXiv: 2101.05386v3.
- Brobrowski M., Lenz A., Riedl J., Rohrwild J. How much space is left for a new family? arXiv: hep-ph/0902.4883.
- Kang S. K. Lectures on Neutrino Physics. Asian European Pacific School of High Energy Physics, indico.cern.ch/event/884244.
- Huber P., Scholberg K., Worcester E. *et al*. Snowmass Neutrino Frontier Report. arXiv: hep-ex/2211.086417v1.
- Gonzalez-Garcia M. C., Maltoni M., Schwetz T. NuFIT: Three-Flavor Global Analyses of Neutrino Oscillation Experiments. arXiv: hep-ph/2111.03086v1.
- Hou W. S. Source of CP Violation for the Baryon Asymmetry of the Universe. *Int. J. of Mod. Phys.*, 2011, v. D20, 1521–1532. arXiv: hep-ph/1101.2161v1.

A Derivation of Planck's Constant from the Principles of Electrodynamics

Yuri Heymann

3 rue Chandieu, 1202 Geneva, Switzerland. E-mail: y.heyman@yahoo.com

A formula for Planck's constant is derived from the Bohr model and Larmor formula, leading to its expression as a function of the proton-to-electron mass ratio, the elementary charge of an electron, and variables as the speed of light and vacuum permittivity. While Planck's constant obtained from its theoretical formula deviates from the Committee on Data of the International Science Council (CODATA) value by a tiny epsilon due to modelling assumptions or geometrical aspects, 98.6% of this deviation is explained by the relativistic effect of electron mass and the mass gap due to the binding energy of electron. As such the relative error of Planck's constant adjusted for the aforementioned factors remains about 22.2 parts per million.

1 Introduction

The Planck's constant known as quantity h , is a fundamental constant in physics of importance in quantum mechanics, statistical mechanics, electronics and metrology. The constant h appears in Max Planck's work on black-body radiation and its spectrum [11–13], a collaborative effort on Kirchhoff's law. In 1905, Einstein publishes the photoelectric effect for the measurement of quantized energies of photons $E = h\nu$, where ν is the frequency of electromagnetic waves [3]. The photoelectric experiment is conducted inside a vacuum chamber exposed to light at different frequencies, causing electrons to be ejected from a metal plate. Einstein's photoelectric relation expresses the kinetic energy of ejected electrons by the relation $eV = h\nu - w$, where w is the work function of the metal, representing the energy level that electromagnetic waves must exceed to eject electrons from the plate. Early photoelectric experiments by Hughes [14] and Richardson and Compton [4], yield estimates of h/e with uncertainties of about 10%. As Millikan refined the experiment, he obtained a value of $h = 6.57 \times 10^{-34}$ J s [9].

The Kibble balance, formerly called a watt balance, is a metrological instrument to measure the weight of a tiny object very precisely by the electric current and voltage powering the balance. This instrument, developed in 1975 by Bryan Kibble, is used to measure Planck's constant on the basis of the Josephson and quantum Hall effect. The Josephson effect, is described by the set of equations $I(t) = I_c \sin(\varphi(t))$ and

$$\frac{\partial \varphi}{\partial t} = \frac{2e}{\hbar} V(t),$$

where $V(t)$ and $I(t)$ are the voltage and current flowing through the Josephson junction, I_c the critical current, \hbar the reduced Planck's constant, and e the elementary charge. A Josephson junction is a superconducting tunnel junction made of a thin film of a few micrometers separating superconducting wires [5, 6], whereas the Hall effect is produced by a current flowing through a conductor exposed to a magnetic field perpendicular to the current. The method exploits discretised

jumps in the resistivity computed as

$$R = \frac{V_{Hall}}{I_{ch}} = \frac{h}{e^2 \nu},$$

where V_{Hall} is the Hall voltage and I_{ch} the channel current, e the elementary charge, and h Planck's constant. The divisor ν can be an integer $\nu = 1, 2, 3, \dots$ or a fractional number $\nu = 1/3, 2/5, 3/7, \dots$ producing jumps as the density of electrons varies. An example of such quantization are Landau levels representing discretised energies as a proposed solution to the Schrödinger's equation [7].

A Planck's constant of $h = 6.62607034(12) \times 10^{-34}$ J s was obtained in recent work by a team of researchers using a watt balance to demonstrate its capability [15]. The joule balance is an enhanced watt balance where dynamic measurements are replaced by a static measurement for convenience purpose. The performance of the joule balance was demonstrated by measuring Planck's constant, $h = 6.626104(59) \times 10^{-34}$ J s with an 8.9 ppm uncertainty [18]. A detailed view of the historical development of Planck's constant measurements is provided in Reiner [16].

In the present work, a formula for Planck's constant was obtained from the Bohr model and Larmor formula, see Section 2. The coupling between both models into a single expression for quantity h involves a membrane representation of the electron as a surface covering the Bohr sphere, where the flux of energies radiating across the membrane is determined by the mass of the proton.

Table 1: Fundamental constants from Committee on Data for Science and Technology (CODATA), 2014 [10].

Constant	Symbol	Value	Unc. u *
Planck constant	h	$6.626070040(81) \times 10^{-34}$ J s	8.7×10^{-8}
Electron mass	m_e	$9.10938356(11) \times 10^{-31}$ kg	8.8×10^{-8}
Proton mass	m_p	$1.672621898(21) \times 10^{-27}$ kg	8.9×10^{-8}
Elementary charge	q, e	$1.602176620(89) \times 10^{-19}$ C	4.4×10^{-8}
Vacuum permittivity	ϵ_0	$8.8541878128(13) \times 10^{-12}$ F/m	–
Speed of light	c	299 792 458 m/s	–

SI units, Intern. Committee for Weights and Measures.
* u, means relative standard uncertainty, source [17].

Planck's constant predicted by the present model and its deviation from CODATA (see Table 1) are provided in Section 3. The attribution of errors by modeling assumptions is described at the end. Of the deviation, 98.6% is explained by the relativistic effect of electron mass and mass gap due to the binding energy of an electron in its orbital, which is a fairly promising result.

2 Method

2.1 Larmor formula

The Larmor formula expresses the power radiated by a non-relativistic charged particle as a result of acceleration [8]. The Larmor formula in its current form appears in more recent works, see the Bremsstrahlung effect and the study of electromagnetic radiation emitted in cyclotrons. The electromagnetic wave as a bimodal function is often represented as a tuple of two undulatory waves moving in the same direction, where functions in Hilbert space \mathcal{L}^2 are orthogonal by the inner product. The magnetic cardioid or lemniscate are geometric representations, involving the interaction between an electron and an electric field. These basics of currents and electromagnetism are useful wave representation of the electron. The magnetic field, commonly denoted by the letter B , is represented by an E-field in the current context. Such an E-field is denoted as E_θ , where θ is the angle between the radial electric field E_r and the orientation of E_θ itself.

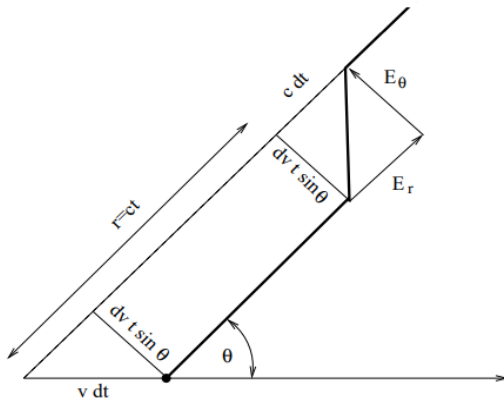


Fig. 1: E-field in the region of an electromagnetic pulse in polar coordinates.

As we suppose the E-field is proportional to the inverse of the wave frequency, where the ratio of wave frequencies is equal to the ratio of velocities, we have $\frac{E_\theta}{E_r} = \frac{v_r}{v_\theta}$. By the Pythagorean theorem, we get:

$$\frac{E_\theta}{E_r} = \frac{\Delta v t \sin(\theta)}{c \Delta t}, \quad (1)$$

where E_θ and E_r are the tangential and radial components of the E-field respectively, c the speed of light, and t the time of

a pulse Δt . From equality $v/t = dv/dt$, we get $v\Delta t = t\Delta v$. By definition, t is the time to accelerate a charged particle q from rest to velocity v .

The radial component of an E-field as in Coulomb's law, is expressed as follows:

$$E_r = \frac{q}{4\pi\epsilon_0} \frac{1}{r^2}, \quad (2)$$

where r is the radius, q the charge of the particle and ϵ_0 the vacuum permittivity.

Given the acceleration term $a = \frac{\Delta v}{\Delta t}$ and joint relation $r = ct$, (1) and (2) lead to:

$$E_\theta = \frac{qa}{4\pi\epsilon_0 c^2 r} \sin(\theta). \quad (3)$$

By Poynting's theorem, i.e. $S = c\epsilon_0 E^2$, the flux is expressed as:

$$S = \frac{1}{16\pi^2 c^3 \epsilon_0 r^2} q^2 a^2 \sin^2 \theta. \quad (4)$$

The angular element in spherical coordinates is

$$d\Omega = r^2 \sin \theta d\theta d\varphi,$$

leading to the below expression for the power radiated by an electron:

$$P = \int_{\theta=0}^{\pi} \int_{\varphi=0}^{2\pi} S r^2 \sin \theta d\theta d\varphi. \quad (5)$$

As

$$\int_{\theta=0}^{\pi} \int_{\varphi=0}^{2\pi} \sin^3 \theta d\theta d\varphi = \frac{8\pi}{3},$$

we obtain:

$$P = \frac{8\pi}{3} \frac{q^2 a^2}{16\pi^2 c^3 \epsilon_0}, \quad (6)$$

which is the Larmor formula for the power radiated by a particle of charge q under acceleration a , in say Watt per squared steradians where the variables in the argument are expressed in the International System of Units (SI).

2.2 Thomson cross section to Planck formula

Considering an E-field where the field lines are collinear and pulsed in the direction orthogonal to the electron orbital, the energy flux over a cross section σ_e transverse to the power inflow, is given by:

$$P_{in} = c\epsilon_0 E_r^2 \sigma_e, \quad (7)$$

where the energy flux is the speed of light times the energy density as given by Poynting's theorem.

The power radiated by a ground state electron revolving around a nucleus is given by the Larmor formula, which can be expressed as follows:

$$P_{out} = \frac{8\pi}{3} \frac{q^2 (q E_r / m_e)^2}{16\pi^2 c^3 \epsilon_0}. \quad (8)$$

As $P_{in} = P_{out}$, (7) and (8) lead to the well-known Thomson cross section for a free electron in its orbital:

$$\sigma_e = \frac{8\pi}{3} \left(\frac{q^2}{4\pi\epsilon_0 m_e c^2} \right)^2. \quad (9)$$

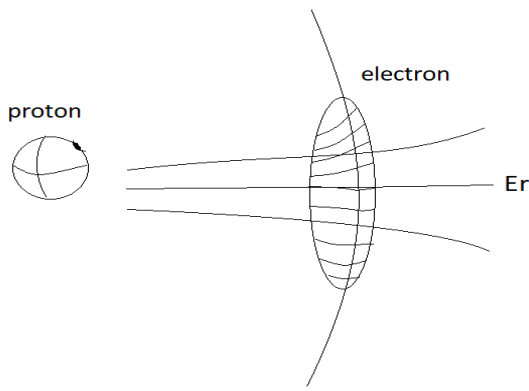


Fig. 2: Membrane representation of the electron where the electron is represented as a surface covering the Bohr sphere. A more natural shape for the atom of hydrogen would be a Horn Torus, or “apple shape” having field lines connecting its poles. The flux of energy crossing the membrane is determined by the mass of the proton as used in the scaling of the Thomson cross section.

By the squared-mass scaling rule, we multiply (9) by $(m_p/m_e)^2$, a scaling of the Thomson cross section to the Bohr sphere, yielding:

$$\sigma_0 = \frac{8\pi}{3} \left(\frac{q^2 m_p}{4\pi\epsilon_0 m_e^2 c^2} \right)^2. \quad (10)$$

The scaled Bohr radius, expressed as

$$r_1 = \frac{\epsilon_0 h^2}{4\pi^2 m_e q^2},$$

is a non-standard Bohr radius of electron orbital obtained by rescaling in a way that E in Poynting’s theorem $S = c\epsilon_0 E^2$ is the standard wave of an electric field, for consistency with the Thomson cross section. By the scaled Bohr radius, the surface of the Bohr sphere $4\pi r_1^2$ is expressed as follows:

$$\sigma_s = \frac{\epsilon_0^2 h^4}{4\pi^3 m_e^2 e^4}. \quad (11)$$

The standard Bohr radius

$$r_0 = \frac{\epsilon_0 h^2}{\pi m_e e^2}$$

representing the radius of an electron orbital in the Bohr model [1, 2], is based on the electron identity $n\frac{h}{2\pi r} = m_e v$, where h is a quantity defined as the product of electron momentum

by one circumference of the ring, n the number of electrons, m_e the mass of an electron, and v its velocity.

As the electron from the Thomson cross section rescaled by the squared-mass scaling rule covers the whole surface of the Bohr sphere, we can match σ_0 with σ_s , i.e. (10) and (11). As such the Bohr sphere stands as a membrane of the electron, as seen in Fig. 2. As a result, the one circumference momentum of the electron, also known as the Planck’s constant, is expressed as follows:

$$h = \frac{e^2}{c \epsilon_0} \sqrt{\pi \sqrt{\frac{2}{3}} \frac{m_p}{m_e}}, \quad (12)$$

where e is the elementary charge of an electron, m_e the mass of an electron, m_p the mass of a proton, ϵ_0 the vacuum permittivity, and c the speed of light.

3 Results

The Planck’s constant computed from (12) with values in Table 1, yields $h = 6.6368 \times 10^{-34}$ J s, deviating from its CODATA value by 1.62 parts per thousand. Of this deviation, 87.4% is explained by the non-relativistic approximation of electron mass, 11.2% by the binding energy of the electron orbital, and 1.37% remains unexplained (see Fig. 3).

By introducing the relativistic mass of the electron $m_{el} = \frac{1}{\sqrt{1-(v_e/c)^2}} m_e$ into (12), with the electron velocity

$$v_e = \frac{e}{\sqrt{4\pi\epsilon_0 r_0 m_e}}$$

resulting from the equilibrium between centripetal and Coulomb’s force, where e is the elementary charge of the electron, r_0 the standard Bohr radius, m_e the mass of an electron, and ϵ_0 the vacuum permittivity, leads to the new value $h = 6.6247 \times 10^{-34}$ J s.

The binding energy of the electron in its orbital, as given by the potential energy using the rescaled Bohr radius r_e ,

Planck’s constant deviation from CODATA

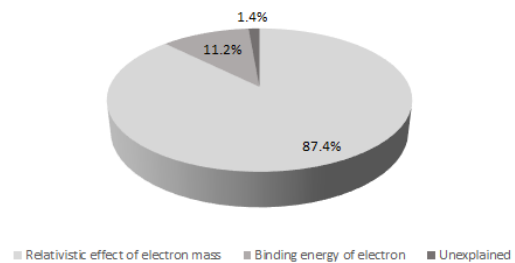


Fig. 3: Attribution of Planck’s constant deviation from its CODATA value. Of a relative error of 1.62 parts per thousand, 87.4% is explained by the non-relativistic approximation of electron mass, 11.2% by the binding energy of the electron orbital, and 1.37% remains unexplained.

gives $K = \frac{1}{2} \frac{e^2}{4\pi\epsilon_0 r_e}$. By subtracting the mass gap $\Delta m_e = K/c^2 \approx 3.059 \times 10^{-34}$ kg from the mass of the electron and applying relativistic adjustment (multiplying electron mass by the inverse of the Lorentz-FitzGerald contraction), yields a new Planck's value $h = 6.62592 \times 10^{-34}$ J s, of an accuracy of about 22.2 parts per million with respect to actual measurements (as explained by modelling assumptions or geometrical aspects, e.g. shape of atom departing from a perfect sphere).

Received on April 9, 2023

References

1. Bohr N. I. On the constitution of atoms and molecules. *Phil. Mag., Series 6*, 1913, v. 26, S1–S25.
2. Bohr N. XLII. On the quantum theory of radiation and the structure of the atom. *Phil. Mag., Series 6*, 1915, v. 30, S394–S415.
3. Einstein A. Über einen die Erzeugung und Verwandlung des Lichtes betreffenden heuristischen Gesichtspunkt. *Ann. Phys.*, 1905, v. 17, 132–148.
4. Hughes A. L. VII. On the emission velocities of photo-electrons. *Phil. Trans. R. Soc.*, 1913, v. 212, 205–226.
5. Josephson B. D. Possible new effects in superconductive tunnelling. *Phys. Lett.*, 1962, v. 1, 251–253.
6. Josephson B. D. The discovery of tunnelling supercurrents. *Rev. Mod. Phys.*, 1974, v. 46, 251–254.
7. Landau L. D., Lifshitz E. M. Quantum Mechanics, Non-Relativistic Theory, Vol 3, 3rd ed. *Pergamon Press*, Oxford, 1977.
8. Larmor J. LXIII. On the theory of the magnetic influence on spectra; and on radiation from a moving ion. *Phil. Mag., Series 5*, 1897, v. 44, 503–512.
9. Millikan R. A. A direct photoelectric determination of Planck's "h". *Phys. Rev.*, 1916, v. 7, 355–388.
10. Mohr P. J., Newell D. B., Taylor B. N. CODATA Recommended Values of the Fundamental Physical Constants: 2014. 2015.
11. Planck, M. Über eine verbesserung der wienschen spectralgleichung. *Verh. Dtsch. Phys. Ges.*, 1900, v. 2, 202–204.
12. Planck M. Zur theorie des gesetzes der energieverteilung im normal-spectrum. *Verh. Dtsch. Phys. Ges.*, 1900, v. 2, 237–245.
13. Planck M. Über das gesetz der energieverteilung im normalspektrum. *Ann. Phys.*, 1901, v. 4, 553–563.
14. Richardson O. W., Compton K. T. LIII. The Photoelectric Effect. *Phil. Mag.*, 1912, v. 24, 575–594.
15. Sanchez C. A., Wood B. M., Green R. G., Liard J. O., Inglis D. A determination of Planck's constant using the NCR watt balance. *Metrologia*, 2014, v. 51 (2), S5–S14.
16. Steiner R. History and progress on accurate measurements of the Planck constant. *Rep. Prog. Phys.*, 2013, v. 76, 1–46.
17. Williams E. R., Steiner, R. L., Newell, D. B., Olsen, P. T. Accurate measurement of the Planck constant. *Phys. Rev. Lett.*, 1998. v. 81 (12), 2404–2407.
18. Zhonghua Z., Qing, H., Zhengkun, L. et al. The joule balance in NIM of China. *Metrologia*, 2014, v. 51 (2), S25–S31.

Zitterbewegung and the Non-Holonomy of Pseudo-Riemannian Spacetime

Pierre A. Millette

E-mail: pierre.millette@uottawa.ca, Ottawa, Canada

In this paper, we explore the connection between *zitterbewegung* for free particles, and the work of Rabounski and Borissova on Zelmanov's chronometric invariant formulation of General Relativity to calculate space and time physical observables [2, 6]. In the chr.inv.-analysis, the spin of a particle interacts with the space non-holonomy field of pseudo-Riemannian spacetime. From this, the particle gains an additional momentum which imparts a non-geodesic component to the particle's motion. The solution of the particle with spin chr.inv.-equation of motion is a spiral that can be visualized as being wound on a pulsating cylinder. Free electron oscillations occur at a frequency equal to the double angular velocity of the space rotation Ω , with fluctuations of the particle position on the order of its reduced Compton wavelength. We thus show that *zitterbewegung* is a direct manifestation of general relativistic space and time physical observables at the elementary particle level.

1 Introduction

In this paper, we explore the connection between *zitterbewegung*, German for “jittery” or “trembling motion”, as calculated for Dirac free particles [1], and the work of Rabounski and Borissova on Zelmanov's chronometric invariant formulation of General Relativity to calculate space and time physical observables [2, 6]. We will show that *zitterbewegung* is a direct manifestation of general relativistic space and time physical observables at the elementary particle level.

2 Zitterbewegung

Zitterbewegung was first recognized by Breit [7] and further analyzed and the name coined by Schrödinger [8, 9]. This solution is obtained in the Heisenberg representation equation of motion for the velocity operator α of the Dirac equation for a free particle

$$H_0 = \alpha \cdot \mathbf{p} + \beta m, \quad (1)$$

where m and \mathbf{p} are the mass and momentum of the free particle respectively, and the α and β matrices are used instead of the γ^μ ($\beta = \gamma_0$ and $\alpha_i = \gamma_0 \gamma_i$) [1, 10].

The space operator solution in the Heisenberg representation $\mathbf{x}(t)$ (i.e. $\alpha = \dot{\mathbf{x}}$) is then given by

$$\mathbf{x}(t) = \mathbf{x}(0) + \frac{\mathbf{p}c^2}{H_0} t + \left(\alpha(0) - \frac{\mathbf{p}c}{H_0} \right) \frac{i\hbar c}{2H_0} \exp(-2iH_0 t/\hbar), \quad (2)$$

where the first two terms on the right hand side of (2) correspond to the classical equation of motion trajectory of the particle, with the third term corresponding to a rapid oscillatory motion (*zitterbewegung*) about the classical trajectory.

The angular frequency of these oscillations is of order $2mc^2/\hbar \sim 2 \times 10^{21} \text{ s}^{-1}$ and their amplitude of order $\hbar/mc \equiv \lambda_C$, corresponding to fluctuations of the particle position on the order of its reduced Compton wavelength. Schrödinger found that the *zitterbewegung* results from the interference

between positive and negative-energy state amplitudes. Consequently, there has been a tendency to dismiss *zitterbewegung*, as its expectation value vanishes for wave-packets consisting entirely of positive-energy or negative-energy waves. In addition, it has not been observed experimentally due to its high-frequency, low amplitude motion, although indirect evidence of its presence has been suggested in numerous areas by some investigators [11–14]. One is reminded of the situation with Brownian motion, where it has not been observed directly, but evidence of its presence is now unquestionably accepted.

However, *zitterbewegung* has been investigated by many researchers, and identified in many areas. Indeed, there is other evidence that points to the reality of *zitterbewegung*. For example, the Darwin term which provides a small correction in the fine-structure of the energy level of s -orbitals of the hydrogen atom can be shown to result from *zitterbewegung* [15]. In the 1990s, David Hestenes revived *zitterbewegung* as a physical process when he recast it in terms of his Geometric Algebra [16–19]. Since then, much work has been done on modelling and detecting *zitterbewegung* — see for example [20–25] among many others.

3 Physical observables in General Relativity

Many practitioners of General Relativity do not realize that the theory is based on a 4-dimensional pseudo-Riemannian representation of spacetime and that the calculations they perform give results in that particular spacetime description. The pseudo-Riemannian characterization refers to the three space and one time dimensions, described by a metric with signature $(+---)$ or $(-+++)$, which uniquely results in space-like and time-like intervals. To properly understand the results obtained, the 4-dimensional calculations in general covariant form must be projected onto the observer's 3+1 space and time dimensions separately as space and time physical

observables.

This requires developing a mathematical theory to enable the calculation of observable components for any tensor. This work started in the 1930s — Landau and Lifshitz introduced the observable time interval and the observable three-dimensional interval in their classic *The Classical Theory of Fields* [26, §84]. Zelmanov, starting in 1941, developed such a comprehensive theory over many decades — it is known as the *theory of chronometric invariants* [2, 3]. The most complete description of the mathematical apparatus of physically observable quantities in General Relativity is given in the recent review article by Rabounski and Borissova [4]. It provides an up-to-date compendium of the results obtained by Zelmanov and the authors over the past decades, and allows for the calculation of the physical observable components of any tensor.

The basic approach consists in projecting a general covariant 4-dimensional tensor onto an observer's physical object frame of reference (e.g. the Earth's surface), consisting of a three-dimensional coordinate grid with “real” physical clocks (a spatial section $x_0 = ct = \text{constant}$, orthogonal to the observer's physical time line at time of observation t), known as the observer's *accompanying reference frame*.

The projection operator onto an observer's time line is the unit vector of the observer's four-dimensional velocity b^α with respect to his physical object frame of reference, which is tangential at each point of the observer's four-dimensional trajectory

$$b^\alpha = \frac{dx^\alpha}{ds}. \quad (3)$$

The projection of a tensor onto an observer's time line is given by its contraction with the vector b^α of his reference frame. In an observer's accompanying reference frame, his three-dimensional velocity with respect to his reference object is zero, $b^i = 0$, and its components are given by

$$b^0 = \frac{1}{\sqrt{g_{00}}}, \quad b_0 = g_{0\alpha}b^\alpha = \sqrt{g_{00}}, \quad b_i = g_{i\alpha}b^\alpha = \frac{g_{i0}}{\sqrt{g_{00}}}.$$

The projection operator onto an observer's three-dimensional spatial section is the four-dimensional symmetric tensor

$$h_{\alpha\beta} = -g_{\alpha\beta} + b_\alpha b_\beta, \quad h^{\alpha\beta} = -g^{\alpha\beta} + b^\alpha b^\beta. \quad (4)$$

The projection of a tensor onto an observer's three-dimensional spatial section is given by its contraction with the tensor $h_{\alpha\beta}$ of his reference frame.

The observer's physical object reference frame has a gravitational field that can be rotated and deformed, and hence, the observer's local reference space can be inhomogeneous and anisotropic. If there is a spatial section everywhere orthogonal to the time lines, then the space is an *holonomic space*. If only spatial sections locally orthogonal to the time lines exist, then the space is a *non-holonomic space*.

Any coordinate grid that is at rest with respect to its reference physical object can be transformed to another coordinate grid through standard coordinate transformations, within the same spatial section. However, time transformations imply a change of spatial section (i.e. new clocks), and hence a change in the measurements of observable quantities. This requires that physical observable quantities in an observer's reference frame must be invariant with respect to time transformations throughout his three-dimensional spatial section $x^i = \text{constant}$, so these must be *chronometric invariant quantities*, and are named *chr.inv.-quantities* for short. Thus Zelmanov developed a general mathematical method to calculate physically observable chr.inv.-projections of any four-dimensional general covariant tensor (see [4] for details).

Accordingly, Zelmanov introduced chr.inv.-derivative operators with respect to time and the spatial coordinates given by

$$\frac{* \partial}{\partial t} = \frac{1}{\sqrt{g_{00}}} \frac{\partial}{\partial t}, \quad \frac{* \partial}{\partial x^i} = \frac{\partial}{\partial x^i} - \frac{g_{0i}}{g_{00}} \frac{\partial}{\partial x^0}, \quad (5)$$

where g_{00} and g_{0i} are components of the metric tensor $g_{\mu\nu}$, and the superscripted symbol $* \partial$ indicates a chr.inv.-partial derivative. These are non-commutative: the order in which their second derivatives are taken gives different results, and their difference is not zero.

From these, three tensors can be defined:

1. A_{ik} : three-dimensional antisymmetric chr.inv.-tensor of the angular velocity with which the reference space of the observer rotates.
2. F_i : three-dimensional chr.inv.-vector of the gravitational inertial force.
3. D_{ik} : three-dimensional symmetric chr.inv.-tensor characterizing the rate of deformation of the observer's space.

Specifically, these tensors are explicitly given by:

$$A_{ik} = \frac{1}{2} \left(\frac{\partial v_k}{\partial x^i} - \frac{\partial v_i}{\partial x^k} \right) + \frac{1}{2c^2} (F_i v_k - F_k v_i), \quad (6)$$

where v_i is the tangential (linear) velocity of the rotation and c is the speed of light *in vacuo*,

$$F_i = \frac{1}{\sqrt{g_{00}}} \left(\frac{\partial w}{\partial x^i} - \frac{\partial v_i}{\partial t} \right) = \frac{1}{1 - \frac{w}{c^2}} \left(\frac{\partial w}{\partial x^i} - \frac{\partial v_i}{\partial t} \right), \quad (7)$$

where $w = c^2(1 - \sqrt{g_{00}})$ is the gravitational potential, originating from the gravitational field of the observer's reference object,

$$D_{ik} = \frac{1}{2} \frac{* \partial h_{ik}}{\partial t}, \quad D = \frac{* \partial \ln \sqrt{h}}{\partial t}, \quad h = \det \|h_{ik}\|, \quad (8)$$

where h_{ik} is the physically observable chr.inv.-metric of the observer's space, $D = h^{ik} D_{ik} = D_m^m$, the trace of the tensor of

the space deformation rate, is the relative dilatation rate of an elementary volume of the observer's space.

In addition, the tensor A_{ik} is further identified as the *space non-holonomy tensor*, which Zelmanov defined in the following theorem:

Zelmanov's theorem on the holonomy of space-time:

The identical equality to zero of the tensor A_{ik} in a four-dimensional region of space-time is the necessary and sufficient condition for the orthogonality of the spatial sections to the time lines everywhere in this region.

In other words, $A_{ik} \neq 0$ in a non-holonomic space-time region, and $A_{ik} = 0$ in a holonomic one. [4, p. 7]

Rotating spaces ($A_{ik} \neq 0$) are non-holonomic, as three-dimensional spatial sections are non-orthogonal to time lines in rotating spaces.

This section has covered the basics of Zelmanov's chronometric invariants theory to generate physically observable quantities in General Relativity by projecting general covariant 4-dimensional tensors onto an observer's physical object frame of reference to obtain physically observable chr.inv.-projections. The reader is encouraged to consult the recent compendium article of Rabounski and Borissova [4] for a deeper complete coverage of the chr.inv.-theory.

4 Geodesic motion of particles in pseudo-Riemannian spacetime

We first apply this formalism to the equations of motion of a particle. The motion of a particle under the influence of gravitation is characterized as freely falling along a geodesic (shortest-distance) line, known as free or geodesic motion. Under the action of additional non-gravitational forces, the particle deviates from its geodesic trajectory, and its motion is known as non-geodesic.

In a four-dimensional pseudo-Riemannian spacetime, the motion of a particle is geometrically determined by the parallel transport of the four-dimensional vector Q^α tangential to the points along the particle's four-dimensional trajectory, given by [6, see p. 9]

$$\frac{DQ^\alpha}{ds} = \frac{dQ^\alpha}{ds} + \Gamma_{\mu\nu}^\alpha Q^\mu \frac{dx^\nu}{ds}, \quad Q_\alpha Q^\alpha = \text{constant}, \quad (9)$$

where DQ^α is the absolute differential of the transported vector Q^α along the trajectory, dQ^α is the differential of the vector and $\Gamma_{\mu\nu}^\alpha$ is the Christoffel symbol of the second kind.

For a particle of rest mass m_0 and four-dimensional momentum vector P^α given by [6, see p. 12]

$$P^\alpha = m_0 \frac{dx^\alpha}{ds}, \quad P_\alpha P^\alpha = m_0^2 = \text{constant}, \quad (10)$$

the equation of motion of the free particle is given by

$$\frac{dP^\alpha}{ds} + \Gamma_{\mu\nu}^\alpha P^\mu \frac{dx^\nu}{ds} = 0. \quad (11)$$

For a massless particle of four-dimensional wave vector K^α given by

$$K^\alpha = \frac{\omega}{c} \frac{dx^\alpha}{d\sigma}, \quad K_\alpha K^\alpha = 0, \quad (12)$$

where ω is the characteristic frequency of the massless particle and $d\sigma = h_{ik} dx^i dx^k$ is the three-dimensional chr.inv.-interval, the equation of motion of the free massless particle is given by

$$\frac{dK^\alpha}{d\sigma} + \Gamma_{\mu\nu}^\alpha K^\mu \frac{dx^\nu}{d\sigma} = 0. \quad (13)$$

The projection of the four-dimensional equation of motion (11) onto the time line and the spatial section of an observer for a free particle is then given respectively by [4, see p.23]

$$\frac{dm}{d\tau} - \frac{m}{c^2} F_i v^i + \frac{m}{c^2} D_{ik} v^i v^k = 0, \quad (14)$$

$$\frac{d(mv^i)}{d\tau} + 2m(D_k^i + A_k^i)v^k - mF^i + m\Delta_{nk}^i v^n v^k = 0,$$

where m is the relativistic mass of the particle, $d\tau$ is the physically observable time interval, v^i is the chr.inv.-vector of the physically observable velocity of the particle and Δ_{nk}^i is the chr.inv.-Christoffel symbol of the second kind, while the equivalent chr.inv.-equations of motion for a free massless particle are given by

$$\frac{d\omega}{d\tau} - \frac{\omega}{c^2} F_i c^i + \frac{\omega}{c^2} D_{ik} c^i c^k = 0, \quad (15)$$

$$\frac{d(\omega c^i)}{d\tau} + 2\omega(D_k^i + A_k^i)c^k - \omega F^i + \omega\Delta_{nk}^i c^n c^k = 0,$$

where c^i is the chr.inv.-vector of the physically observable velocity of light, with $c^i c_i = c^2$.

In the case where $Q_\alpha Q^\alpha \neq \text{constant}$, the trajectory of the particle is non-geodesic and the absolute derivative of the transported vector $\frac{DQ^\alpha}{ds} = \Phi^\alpha$, which is a force that deviates the particle from a geodesic trajectory. The right hand side of (14) and (15) are set equal to the chr.inv.-projections of the deviating force Φ^α instead of 0. These are called the equations of non-geodesic motion.

5 Fields and charged spin particles in pseudo-Riemannian spaces

The previous section §4 has covered the necessary background on the calculation of equations of motion in the theory of chronometric invariants to permit their generalization to charged particles with spin. In their book *Fields, Vacuum and the Mirror Universe: Fields and particles in the space-time of General Relativity*, Rabounski and Borissova apply the chronometric invariants formalism to the analysis of fields and charged particles with spin [6, see Chapters 3 & 4].

Chapter 3 provides the chronometrically invariant theory of electrodynamics in a pseudo-Riemannian space. It takes

into account the impact on the electromagnetic field of the physically observable chr.inv.-properties of the reference space, specifically the gravitational inertial force (i.e. acceleration) F_i , the space non-holonomy tensor of space rotation A_{ik} , and the rate of deformation of space tensor D_{ik} . This theory will not be covered here as it is beyond the scope of this paper.

Chapter 4 covers the chronometrically invariant theory of particles with spin in a pseudo-Riemannian space. It is based on the premise that spin is a fundamental property of matter, such as mass and charge. The analysis will show that the field of the space non-holonomy from the spatial rotation of the space A_{ik} interacts with the particle's spin and imparts it an additional momentum. From this will be derived the equations of motion of a particle with an internal rotation momentum (i.e. spin).

5.1 Spin particle equation of motion

Based on these considerations, the four-dimensional dynamic vector Q^α for the parallel transport equations is assumed to be given by [6, see pp. 155]

$$Q^\alpha = P^\alpha + S^\alpha, \quad (16)$$

where P^α is given by (10) and S^α is the spin momentum which the particle gains from its internal momentum resulting from the spin, thus making the motion of the particle non-geodesic.

To deduce the spin momentum vector S^α , we start from the known properties of the spin of elementary particles. Their numerical value is given by $\pm n\hbar$, where \hbar is the reduced Planck constant which has units of angular momentum, and $n = 0, \frac{1}{2}, 1, \frac{3}{2}, 2$, with the \pm sign indicating right-wise or left-wise internal rotation of the spin particle respectively. This suggests that the spin vector would be an antisymmetric tensor of the 2nd rank, similar to a tensor of angular momentum.

From Bohr's second postulate on the length of an electron orbit in an atom and the experimental finding that an electron has an internal magnetic moment proportional to its internal rotation spin momentum, Rabounski and Borissova make an argument to define a four-dimensional antisymmetric 2nd rank angular momentum-like tensor, which they call the Planck tensor and write as $\hbar^{\alpha\beta}$, given by [6, see pp. 155–156]

$$[r^i, p^k] = \frac{1}{2} (r^i p^k - r^k p^i) = k\hbar^{ik} \quad (17)$$

for some constant k , to characterize the spin of a particle in four-dimensional pseudo-Riemannian space.

The diagonal and space-time components of the Planck tensor are zero, while the non-diagonal spatial components are $\pm\hbar$, based on the spatial direction of the spin and the right- or left-handedness of the reference frame. Note that the antisymmetric Planck tensor \hbar^{ik} is not to be confused with

the symmetric physically observable chr.inv.-metric of the observer's space tensor h^{ik} .

This represents a general mathematical approach that requires no assumption on the internal structure of a particle's spin. Instead, it is based on a fundamental quantum space rotation. We have already encountered an antisymmetric rotation of space chr.inv.-tensor A_{ik} in §3, given by (6). In the absence of gravitational fields, the tensor of angular velocity A_{ik} is given by

$$A_{ik} = \frac{1}{2} \left(\frac{\partial v_k}{\partial x^i} - \frac{\partial v_i}{\partial x^k} \right), \quad (18)$$

which can be more specifically denoted as $A_{\alpha\beta} = \Omega_{\alpha\beta}$, with components

$$\Omega_{00} = 0 \quad \Omega_{0i} = -\Omega_{i0} = 0 \quad \Omega_{ik} = \frac{1}{2} \left(\frac{\partial v_k}{\partial x^i} - \frac{\partial v_i}{\partial x^k} \right). \quad (19)$$

The quantum principle of wave-particle duality results in a particle's energy being given by $E = mc^2 = \hbar\omega$ where ω is the characteristic frequency of the particle with relativistic mass m . Rabounski and Borissova suggest a generalization of that equation into the geometric tensor relation $mc^2 = \hbar^{\alpha\beta}\omega_{\alpha\beta}$.

The additional momentum S^α in (16) gained by a particle from its spin can be determined from the *action* S of a particle with spin. The action to displace a spin particle generated by the interaction of its spin with the space non-holonomy field $A_{\alpha\beta}$ is given by [6, see pp. 162]

$$S = \alpha(S) \int_a^b \hbar^{\alpha\beta} A_{\alpha\beta} ds = \frac{n}{c} \int_a^b \hbar^{\alpha\beta} A_{\alpha\beta} ds, \quad (20)$$

where $\alpha(S)$ is a scalar constant characteristic of the particle in the spin interaction. One then obtains [6, see pp. 164]

$$S^\alpha = \frac{1}{c^2} n \hbar^{\mu\nu} A_{\mu\nu} \frac{dx^\alpha}{ds}, \quad (21)$$

such that the dynamic vector Q^α that characterizes the motion of the spin particle is given by

$$Q^\alpha = P^\alpha + S^\alpha = m_0 \frac{dx^\alpha}{ds} + \frac{1}{c^2} n \hbar^{\mu\nu} A_{\mu\nu} \frac{dx^\alpha}{ds}, \quad (22)$$

where P^α is given by (10).

The equations of motion of a spin particle are obtained from the parallel transport equations of Q^α given by (22) along the trajectory of the particle

$$\frac{d}{ds} (P^\alpha + S^\alpha) + \Gamma_{\mu\nu}^\alpha (P^\mu + S^\mu) \frac{dx^\nu}{ds} = 0, \quad (23)$$

where $Q_\alpha Q^\alpha = \text{constant}$. The chr.inv.-equations of a particle

with mass and spin is given by [6, see pp. 170]

$$\begin{aligned} \frac{dm}{d\tau} - \frac{m}{c^2} F_i v^i + \frac{m}{c^2} D_{ik} v^i v^k &= \\ &= -\frac{1}{c^2} \frac{d\eta}{d\tau} + \frac{\eta}{c^4} F_i v^i - \frac{\eta}{c^4} D_{ik} v^i v^k, \\ \frac{d(mv^i)}{d\tau} + 2m(D_k^i + A_k^i)v^k - mF^i + m\Delta_{nk}^i v^n v^k &= \\ &= -\frac{1}{c^2} \frac{d(\eta v^i)}{d\tau} - \frac{2\eta}{c^2} (D_k^i + A_k^i)v^k + \frac{\eta}{c^2} F^i - \frac{\eta}{c^2} \Delta_{nk}^i v^n v^k, \end{aligned} \tag{24}$$

where η is given by

$$\eta = \frac{n \hbar^{\mu\nu} A_{\mu\nu}}{\sqrt{1 - \frac{v^2}{c^2}}}. \tag{25}$$

The left hand side of equations (24) is the same as that of equations (14), and represents the geodesic part of a spinless particle's motion. However, while the right hand side of equations (14) are equal to zero, in the case of a particle with spin, the right hand side of equations (24) are non-zero, and thus represent the non-geodesic component of the motion of a particle with spin. That, is the component that gives rise to zitterbewegung, while the left hand side represents the classical geodesic trajectory of the particle.

Allowing for the weak gravitational interaction, compared to others, by setting $w \rightarrow 0$ in (7) and $D = 0$ in (8) [6, p. 176], results in the elimination of the F_i and D_{ik} terms, and a simplification of (24). The kinematic equations of motion (24) become

$$\frac{dv^i}{d\tau} + 2A_k^i v^k + \Delta_{nk}^i v^n v^k = 0. \tag{26}$$

Assuming that the space rotates with a constant angular velocity Ω around the x^3 -axis (z -axis), from (18) and (19) and the linear velocity of rotation of the space given by $v_i = \Omega_{ik} x^k$, then the space non-holonomy tensor A_{ik} has only two non-zero components,

$$A_{12} = -A_{21} = -\Omega, \tag{27}$$

and the chr.inv.-vector equations of motion become

$$\frac{dv^1}{d\tau} + 2\Omega v^2 = 0, \quad \frac{dv^2}{d\tau} - 2\Omega v^1 = 0, \quad \frac{dv^3}{d\tau} = 0, \tag{28}$$

where the superscripts are numerical vector indices.

Solving the equations of motion, we obtain the solutions [6, p. 179–183]

$$v^1 = v_{(0)}^1 \cos(2\Omega\tau), \quad v^2 = v_{(0)}^2 \sin(2\Omega\tau), \quad v^3 = v_{(0)}^3, \tag{29}$$

where the $v_{(0)}^i$ represent the initial values of v^i . Integrating (29) with respect to $d\tau$, we obtain the particle's trajectory dis-

placements

$$\begin{aligned} x^1 &= x_{(0)}^1 + \frac{v_{(0)}^1}{2\Omega} \sin(2\Omega\tau) \\ x^2 &= x_{(0)}^2 + \frac{v_{(0)}^1}{2\Omega} - \frac{v_{(0)}^1}{2\Omega} \cos(2\Omega\tau) \\ x^3 &= x_{(0)}^3 + v_{(0)}^3 \tau, \end{aligned} \tag{30}$$

where the $x_{(0)}^i$ represent the initial values of x^i .

Setting the initial displacement of the particle to be zero, $x_{(0)}^1 = x_{(0)}^2 = x_{(0)}^3 = 0$, (30) can be simplified as

$$\begin{aligned} x^1 &= x = a \sin(2\Omega\tau) \\ x^2 &= y = a [1 - \cos(2\Omega\tau)] \\ x^3 &= z = b\tau, \end{aligned} \tag{31}$$

where $a = \frac{v_{(0)}^1}{2\Omega}$ and $b = v_{(0)}^3$. From this, we can move from the τ parametric representation to the coordinate representation of the solution to determine the shape of the three-dimensional trajectory covered by the particle. We obtain [6, p. 184]

$$x^2 + y^2 = 2a^2 [1 - \cos(2\Omega\tau)] = 4a^2 \sin^2(\Omega\tau), \tag{32}$$

where $\tau = z/b$, which is similar to a spiral line equation $x^2 + y^2 = a^2$, $z = b\tau$. The particle has a constant velocity $b = v_{(0)}^3$ along the axis of the spiral, with the radius of the particle's trajectory oscillating with a frequency Ω in the range 0 to $2a = v_{(0)}^1/\Omega$ at distances $z = \frac{\pi kb}{2\Omega}$, for $k = 0, 1, 2, 3, \dots$. The spiral can be visualized as being wound on a pulsating cylinder.

5.2 Charged spin particle in an electromagnetic field

For a charged spin particle in an electromagnetic field, the four-dimensional dynamic vector Q^α for the parallel transport equations takes the form [6, p. 186]

$$Q^\alpha = P^\alpha + \frac{e}{c^2} A^\alpha + S^\alpha, \tag{33}$$

where e is the electric charge and A^α is the electromagnetic field potential. There is thus an additional momentum gained by the particle from the interaction of its charge with the electromagnetic field. The chr.inv.-scalar equation of motion of a charged spin particle in an electromagnetic field is then given by [6, p. 204]

$$\frac{d}{d\tau} \left(m + \frac{\eta}{c^2} \right) = -\frac{e}{c^2} E_i v^i, \tag{34}$$

where E_i is the i^{th} component of the electric field. Then for particles with mass,

$$m_0 c^2 = -n \hbar^{mn} A_{mn} \tag{35}$$

where again \hbar^{mn} is the Planck tensor and A_{mn} is the rotation of space chr.inv.-tensor. The right hand side of this equation (without the negative sign) characterizes the interaction energy of the particle's spin with the space non-holonomy field, i.e. the "spin energy". Rabounski and Borissova refer to (35) as the *law of quantization of the masses of elementary particles*:

The rest-energy of any mass-bearing spin particle is equal to the energy of its spin interaction with the space non-holonomy field, taken with the opposite sign. [6, p. 205]

From (35), it can be shown that for any elementary particle with mass, the following relationship exists between its rest-mass m_0 and the angular velocity of the space rotation Ω [6, p. 207]:

$$\Omega = \frac{m_0 c^2}{2n\hbar}. \quad (36)$$

5.3 The Compton wavelength and zitterbewegung

The wavelength corresponding to the frequency of the space rotation Ω given by (36) can be calculated by assuming that the wave of the space non-holonomy propagates at the speed of light c [6, p. 209]:

$$\lambda_\Omega = \frac{c}{\Omega} = 2n \frac{\hbar}{m_0 c}. \quad (37)$$

For an electron, with $n = \frac{1}{2}$, (37) becomes

$$\lambda_C = \frac{\hbar}{m_0 c}, \quad (38)$$

i.e. the wavelength of the space non-holonomy rotation Ω is equal to the reduced Compton wavelength of the electron.

This confirms that (31) and (32) are the candidate equations to describe zitterbewegung: free electron oscillations occur at a frequency equal to the double angular velocity of the space rotation Ω given by (31), with fluctuations of the particle position on the order of its reduced Compton wavelength given by (38) while following a trajectory described by a pulsating spiral equation of motion.

6 Discussion and conclusion

In this paper, we have explored the connection between *zitterbewegung* for free particles, and the work of Rabounski and Borissova on Zelmanov's chronometric invariant formulation of General Relativity to calculate space and time physical observables [2, 6]. They introduced a four-dimensional antisymmetric tensor of the 2nd rank they called the Planck tensor to characterize the spin of an elementary particle. In the chr.inv.-analysis, the spin of a particle interacts with the space non-holonomy field of pseudo-Riemannian spacetime.

From this, the particle gains an additional momentum which imparts a non-geodesic component to the particle's

motion. The solution of the particle with spin chr.inv.-equation of motion is a spiral that can be visualized as being wound on a pulsating cylinder. It has a constant velocity $b = v_{(0)}^3$ along the x^3 -axis of the spiral, with the radius of the particle's trajectory oscillating with a frequency Ω in the range 0 to $2a = v_{(0)}^1/\Omega$ at distances $z = \frac{\pi kb}{2\Omega}$, for $k = 0, 1, 2, 3, \dots$. The wavelength of the space non-holonomy rotation Ω is equal to the reduced Compton wavelength of the electron.

Free electron oscillations occur at a frequency equal to the double angular velocity of the space rotation Ω , with fluctuations of the particle position on the order of its reduced Compton wavelength. Thus, we have shown that within the chr.inv.-equation of motion of particles with spin derived in Rabounski and Borissova's work [6], zitterbewegung is a direct manifestation of general relativistic space and time physical observables at the elementary particle level.

Received on May 10, 2023

References

1. Milonni P.W. The Quantum Vacuum: An Introduction to Quantum Electrodynamics. Academic Press, San Diego, 1994, pp. 322–323.
2. Zelmanov A.L. Chronometric Invariants. Translated from the 1944 PhD Thesis, American Research Press, Rehoboth, NM, 2006.
3. Zelmanov A.L. Chronometric invariants and accompanying frames of reference in the General Theory of Relativity. *Soviet Physics Doklady*, 1956, vol. 1, 227–230.
4. Rabounski D. and Borissova L. Physical Observables in General Relativity and the Zelmanov Chronometric Invariants. *Progress in Physics*, 2023, vol. 19(1), 3–29.
5. Rabounski D. and Borissova L. Particles Here and Beyond the Mirror: Three kinds of particles inherent in the space-time of General Relativity, 4th revised edition. New Scientific Frontiers, London, UK, 2023.
6. Rabounski D. and Borissova L. Fields, Vacuum and the Mirror Universe: Fields and particles in the space-time of General Relativity, 3rd revised edition. New Scientific Frontiers, London, UK, 2023.
7. Breit G. An interpretation of Dirac's theory of the electron. *Proc. of the National Acad. of Sciences*, 1928, vol. 14(7), 553–559.
8. Schrödinger E. Über die kräftefreie Bewegung in der relativistischen Quantenmechanik. Transl: On the free movement in relativistic quantum mechanics, 1930, pp. 418–428.
9. Schrödinger E. Zur Quantendynamik des Electrons. Transl: Quantum Dynamics of the Electron, 1931, pp. 63–72.
10. Greiner W. Relativistic Quantum Mechanics; Wave Equations. Springer-Verlag, Berlin Heidelberg, 1994, pp. 91–93.
11. Catillon P., Cue N., Gaillard M.J. et al. A Search for the de Broglie Particle Internal Clock by Means of Electron Channeling. *Foundations of Physics*, 2008, v. 38(7), 659–664.
12. Wunderlich C. Quantum physics: Trapped ion set to quiver. *Nature News and Views*, 2010, v. 463, 37–39.
13. Gerritsma R., Kirchmair G., Zähringer F., Solano E., Blatt R., Roos F. Quantum simulation of the Dirac equation. *Nature*, 2010, v. 463, 68–71. arXiv: quant-ph/0909.0674.
14. Leblanc L.J., Beeler M.C., Jimenez-Garcia K., Perry A.R., Sugawa S., Williams R.A., Spielman B. Direct observation of zitterbewegung in a Bose-Einstein condensate. *New Journal of Physics*, 2013, v. 15(7), 073011. arXiv: cond-mat/1303.0914.

15. Gross F. *Relativistic Quantum Mechanics and Field Theory*. John Wiley & Sons, New York, 1993, pp. 138–139.
16. Hestenes D. Zitterbewegung in quantum mechanics.
17. Hestenes D. The zitterbewegung interpretation of quantum mechanics. *Foundations of Physics*, 1990, v. 20 (10), 1213–1232.
18. Hestenes D. Zitterbewegung Modeling. *Foundations of Physics*, 1993, v. 23 (3), 365–387.
19. Hestenes D. Zitterbewegung in Quantum Mechanics – a research program. arXiv: quant-ph/0802.2728.
20. Dávid G., Cserti J. General Theory of the Zitterbewegung. arXiv: cond-mat.mes-hall/0909.2004v3.
21. Deriglazov A. A. Spinning-particle model for the Dirac equation and the relativistic Zitterbewegung. arXiv: hep-ph/1106.5228v3.
22. Leary Z.-Y. and Smith K. H. Unified Dynamics of Electrons and Photons via Zitterbewegung and Spin-Orbit Interaction. arXiv: quant-ph/1310.1995v1.
23. Wang C. C., Xiong C.-D. Zitterbewegung by Quantum Field Theory Considerations. arXiv: quant-ph/0712.0491.
24. Zawadski W. and Rusin T. M. Zitterbewegung (trembling motion) of electrons in semiconductors: a Review. arXiv: cond-mat.mes-hall/1101.0623v1.
25. Sidharth B. G.. ZPF, Zitterbewegung and Inertial Mass. arXiv: gen-ph/0804.1984v1.
26. Landau L. D. and Lifshitz E. M. *The Classical Theory of Fields*, Fourth Revised English Edition. Butterworth Heinemann, Amsterdam, 1975.

Reduction of Matter in the Universe to Protons and Electrons via the Lie-isotopic Branch of Hadronic Mechanics

Ruggero Maria Santilli

The Institute for Basic Research, 35246 U. S. 19N, Suite 215, Palm Harbor, FL 34684, USA.
E-mail: research@i-b-r.org

Matter was originally conceived as bound states of the permanently stable protons and electrons because stars initiate their lives as sole aggregates of Hydrogen atoms, and must synthesize neutrons from protons and electrons as a necessary condition to produce light via nuclear fusions. In oblivion to the Einstein-Podolsky-Rosen argument that *quantum mechanics is not a complete theory*, said conception was abandoned despite its plausibility because of the unverified assumption that the exact validity of Heisenberg's uncertainty principle for point-like particles in vacuum was equally valid for extended protons and neutrons under strong nuclear forces, resulting in the assumption that electrons cannot remain within a nuclear structure. In this paper, we review and update: the insufficiencies of quantum mechanics in nuclear physics; the completion of quantum mechanics into the axiom-preserving, Lie-isotopic branch of *hadronic mechanics* for the invariant representation of *extended* protons and neutrons under potential and contact/non-potential interactions; the exact hadronic representation of *all* characteristics of the neutron in its synthesis from the proton and the electron at the non-relativistic and relativistic levels; the completions of Bell's inequalities with ensuing *iso-deterministic principle* for strong interactions. We then present the apparent resolution of the historical objections against the reduction of all stable matter in the universe to protons and electrons and point out a number of open problems whose treatment is beyond the capabilities of quantum mechanics, such as: the cosmological implications of the missing energy in the neutron synthesis, the prediction of negatively charged pseudo-protons, and the possible recycling of radioactive nuclear waste by nuclear power plants via their stimulated decay.

Content

1. Introduction

- 1.1. Historical notes
- 1.2. Insufficiencies of quantum mechanics in nuclear physics.
- 1.3. Rudiments of isotopic theories

2. Non-relativistic representation of the neutron synthesis from the Hydrogen atom

- 2.1. Historical notes
- 2.2. Santilli's studies on the neutron synthesis
- 2.3. Non-relativistic representation of the neutron synthesis
 - 2.3.1. Representation of the neutron mass, mean life and charge radius
 - 2.3.2. Representation of the neutron spin
 - 2.3.3. Representation of the neutron magnetic moment

3. Relativistic representation of the neutron synthesis from the Hydrogen atom

- 3.1. The main open problem for particle fusions
- 3.2. Iso-Minkowskian iso-spaces
- 3.3. The Fundamental theorem on iso-symmetries
- 3.4. Lorentz iso-symmetries
- 3.5. Poincaré iso-symmetries
- 3.6. Dirac iso-equations
- 3.7. Iso-spinorial Poincaré iso-symmetries

- 3.8. Special iso-relativities

- 3.9. Relativistic representation of the neutron synthesis

4. Applications of the neutron synthesis

- 4.1. Detection of smuggled fissile material
- 4.2. Representation of nuclear stability
- 4.3. Representation of the gravitational stability of the Sun
- 4.4. Stimulated decay of the neutron
- 4.5. The pseudo-proton hypothesis
- 4.6. Recycling of nuclear waste
- 4.7. Resolution of the Coulomb barrier for nuclear fusion

5. Reduction of matter to protons and electrons

Acknowledgments

References

1 Introduction

1.1 Historical notes

As it is well known to historians (see, e.g. [1] [2]), nuclei were originally conceived to be bound states of protons and electrons because stars initiate their lives as aggregates of Hydrogen atoms and they must synthesize neutrons from protons

and electrons as a necessary condition to initiate the production of light via nuclear fusions.

The above original conception of the nuclear structure was abandoned in oblivion of the Einstein-Podolsky-Rosen (EPR) argument that *Quantum mechanics is not a complete theory* [3] (see also the recent verifications [4]–[8]), under the experimentally unverified *assumption* that the validity of Heisenberg's uncertainty principle for *point-like* particles in vacuum was also valid for the *extended* protons and neutrons under strong nuclear forces, resulting in the *assumption* that electrons cannot remain within the dense nuclear structure on various grounds, such as:

1.1) The inability for the electron to remain within a nucleus [1]. By recalling the value of the electron mass $m_e = 0.511 \text{ MeV} = 9.1 \times 10^{-31} \text{ kg}$ and the nuclear radius $R = 10^{-14} \text{ m}$, *Heisenberg's uncertainty principle* [9]

$$\begin{aligned} \Delta r \Delta p &= \frac{1}{2} \langle \psi | [r, p] | \psi \rangle \geq \frac{1}{2} \hbar = \\ &= 5.26548578 \times 10^{-34} \text{ J Hz}^{-1}, \end{aligned} \quad (1)$$

would imply the electron to have the superluminal velocity

$$v \geq \frac{\hbar}{\Delta r \times m_e} = 5.79 \times 10^{10} \text{ m/s}. \quad (2)$$

1.2) Under the validity of principle (1), an electron would have the linear momentum uncertainty [10]

$$\Delta p = 1.05 \times 10^{20} \text{ kg m/s}, \quad (3)$$

with corresponding energy

$$E = 19.5 \text{ MeV}, \quad (4)$$

contrary to the evidence that electrons emitted in Beta decays have a maximum energy of 3 MeV.

1.3) The excessive value for nuclear standards of the magnetic moment of the electron [7]. In fact, expressed in nuclear magnetron μ_N , the magnetic moment of the electron has the value

$$\begin{aligned} \mu_e^{spin} &= -9.284764 \times 10^{-24} \text{ J/T} \\ &= -9.284764 \times 10^{-24} \times 1.9798907610^{26} \mu_N \\ &= -928.4784 \times 1.979890 \mu_N = 1838.2851 \mu_N, \end{aligned} \quad (5)$$

which is 961 times the magnetic moment of the neutron $\mu_n = -1.91304 \mu_N$.

In this paper we show that, thanks to the availability of new mathematics for the time-invariant representation of extended protons and neutrons under strong nuclear forces, and the related completion of quantum into hadronic mechanics, Heisenberg's uncertainty principle for point-like particles in vacuum is replaced by a progressive validity of Einstein's determinism for extended protons and neutron under strong nuclear forces [3]–[8], with ensuing resolution of the historical objections against the reduction of matter to protons and electrons.

1.2 Insufficiencies of quantum mechanics in nuclear physics

By using well known nuclear experimental data [11]–[18], we recall the following, century-old, generally ignored insufficiencies of quantum mechanics in nuclear physics:

Quantum mechanical insufficiency I: Inability to represent the synthesis of the neutron from a proton and an electron in the core of stars [19]. Notwithstanding the extremely big (for particle standards) *attractive* Coulomb force of about 230 Newtons between the (negatively charged) electron and the (positively charged) proton,

$$\begin{aligned} F &= -\frac{e^2}{r^2} = \\ &= -(8.99 \times 10^9) \frac{(1.60 \times 10^{-19})^2}{(10^{-15})^2} = -230 \text{ N}, \end{aligned} \quad (6)$$

quantum mechanics allows no quantitative representation of the fundamental synthesis of the neutron in the core of stars. This insufficiency was first identified by R. M. Santilli in the 1978 Harvard's Lyman Laboratory of Physics [20] (see also the subsequent 1979 paper from Harvard's Department of Mathematics [22] on grounds that the mass/rest energy of the neutron is 0.782 MeV *bigger* than the sum of the masses/ rest energies of the proton and of the electron

$$\begin{aligned} E_p &= 938.272 \text{ MeV}, \quad E_e = 0.511 \text{ MeV}, \\ E_n &= 939.565 \text{ MeV}, \\ \Delta E &= E_n - (E_p + E_e) = 0.782 \text{ MeV} > 0, \end{aligned} \quad (7)$$

by therefore requiring a *positive binding energy* and resulting in a *rest energy excess* for which the Schrödinger equation admits no physically meaningful solutions (for a two-body bound state). A similar case occurs for the Dirac equation, which after achieving an exact relativistic representation of the bound state of a proton and the electron at large mutual distances in the Hydrogen atom, the Dirac equation fails to provide any quantitative representation of the bound state of the same particles at nuclear mutual distances.

By no means the neutron synthesis is an isolated case because as we shall see in Sect. 4.1, the representation of *unstable* leptons, mesons and baryons as generalized bound states of particles and antiparticles generally produced free in their spontaneous decays, permits the numerically exact representation of *all* their characteristics, including the mechanism of their spontaneous decays, which has been impossible to date via quantum mechanics.

Quantum mechanical insufficiency II: Inability to achieve a numerically exact representation of nuclear magnetic moments. In fact, under the use of the tabulated values of the magnetic moments of the proton and of the neutron in vacuum [12]

$$\mu_p = +2.79285 \mu_N, \quad \mu_n = -1.91304 \mu_N, \quad (8)$$

quantum mechanics (qm) predicts that the magnetic moment of the Deuteron is given by

$$\mu_D^{qm} = (2.79285 - 1.91304)\mu_N = 0.87981\mu_N, \quad (9)$$

while the experimentally measured value is given by

$$\mu_D^{ex} = 0.85647\mu_N, \quad (10)$$

resulting in the *deviation* of the quantum mechanical prediction from the experimental value of about 3%, with embarrassing deviations for heavier nuclei such as the zirconium.

Quantum mechanical insufficiency III: Inability to achieve a consistent representation of nuclear spins. According to quantum mechanics, the only stable bound state of two particles with spin $1/2$, such as the proton and the neutron, is the *singlet coupling*. Consequently, quantum mechanics predicts that the Deuteron D has the structure

$$D = (p_{\uparrow}, n_{\downarrow})_{qm}, \quad (11)$$

for which the total angular momentum is null, $J_D = 0$, contrary to the experimental value of the spin of the Deuteron $J_D = 1$. As a result of this insufficiency, quantum mechanics represents the spin of the Deuteron via such a *collection of orbital contributions to have the value $L_D = 1$* (see, e.g. [21]) in clear disagreement with experimental evidence for which *the spin $S_D = 1$ has been measured for the Deuteron in its true ground state*, i.e. the state for which $L_D \equiv 0$.

Quantum mechanical insufficiency IV: Inability to represent the nuclear stability despite the natural instability of the neutron. As it is well known, the neutron is naturally unstable with spontaneous decay following 887.7 s [17], at which point nuclei should disintegrate evidently due to the excessive number of positive charges. In view of the inability to represent the neutron synthesis from the proton and the electron, quantum mechanics does not allow a meaningful treatment of the mechanism according to which neutrons become stable when members of a nuclear structure.

Quantum mechanical insufficiency V: Inability to represent the nuclear stability despite strongly repulsive protonic Coulomb forces. As it is well known [11], nuclei contain a number of positively charged protons indicated with the atomic number Z , thus experiencing a *repulsive* Coulomb force of type (6) which is so big to overcome known nuclear forces.

Needless to say, the above insufficiencies also apply to relativistic quantum mechanics, as well as to related space time symmetries and relativities.

1.3 Rudiments of isotopic theories

The indicated insufficiencies of quantum mechanical methods, space time symmetries and relativities for the representation of the synthesis of the neutron from the Hydrogen are primarily due to the *local* character of quantum mechanical

methods [3], here referred to the sole dependence of the wave function $\psi(r)$, the potential $V(r)$, and the differential calculus, on a finite number of isolated points r in empty space, as it is the case, e.g. for the linear momentum

$$p\psi(r) = -i\partial_r\psi(r), \quad (12)$$

of the Schrödinger equation

$$\left[\sum_{k=1,2,\dots,A} \frac{1}{2m_k} p_k p_k + V(r) \right] \psi(r) = E\psi(r). \quad (13)$$

Such an approximation of nature has been effective for *atomic structures* due to the large mutual distances between the constituents which allow particles to be approximated as the Newtonian *massive points*. However, the indicated local character of quantum mechanics is excessively approximated for nuclear structures since, according to clear experimental measurements [16]–[18], protons and neutron are *extended charge distributions*, and nuclear volumes are generally *smaller* than the sum of the volumes of their protons and neutrons.

Consequently, *nuclei are generally composed by extended protons and neutrons in condition of partial mutual penetration*, resulting in the expectation that nuclear forces comprise conventional, action-at-a-distance, linear, local and potential interactions (herein called *Hamiltonian interactions*), plus contact, thus zero-range, non-linear, non-local and non-potential interactions (herein called *non-Hamiltonian interactions*).

By noting that a point-like electron cannot possibly be bonded to a point-like proton, we expect that the neutron synthesis requires the representation of the charge distribution of the proton and of the electron wave packet as being extended, with ensuing Hamiltonian and non-Hamiltonian interactions at mutual distances smaller than their size.

Since at the time of the initiation of the studies herein reported (late 1970's), mathematical and physical theories for the time invariant representation of extended particles did not exist, they had to be constructed. In this paper, we adopt *isotopic methods* comprising:

- 1) The *Lie-isotopic mathematics*, or *iso-mathematics* for short.
- 2) The *Lie-isotopic branch of hadronic mechanics*, or *iso-mechanics* for short.
- 3) The non-relativistic and relativistic *iso-symmetries and iso-relativities*.

The above isotopic methods were proposed by R. M. Santilli (when at Harvard University under DOE support) in the 1978 Springer-Verlag monographs [23, 24] and they do achieve the needed time invariant representation of extended particles and/or their wave packets, with consequential Hamiltonian and non-Hamiltonian interactions.

As it is well known, the mathematics of quantum mechanics is based on the universal, enveloping, associative algebra $\xi\{A, B, \dots; A \times B, I\}$ of operators A, B, \dots on a linear space \mathcal{H}

with conventional associative product and related (multiplicative) unit

$$AB = A \times B, \tag{14}$$

$$I : IA = AI \equiv A \forall A \in \xi,$$

which envelope allows a rigorous treatment of Lie's theory via algebra L isomorphic to the antisymmetric sub-algebra $L \approx \xi^-$ with the familiar Lie product $[A, B] = AB - BA$, and ensuing mechanics, symmetries and relativities.

Santilli's iso-mathematics is based on the *axiom-preserving*, thus isotopic lifting of the enveloping algebra $\xi\{A, B, \dots; A \times B, I\}$ into the universal enveloping *iso-associative algebra* $\hat{\xi}\{\hat{A}, \hat{B}, \dots; A \hat{\times} B, \hat{I}\}$ of iso-operators \hat{A}, \hat{B}, \dots on an iso-linear iso-space $\hat{\mathcal{H}}$ with *iso-product* introduced in the 1978 Harvard's paper [20], extended in the 1979 paper [22] and systematically studied in Sect. 5.2, p. 154 on of [24])

$$\hat{A} \hat{\times} \hat{B} = \hat{A} \times \hat{T} \times \hat{B}, \tag{15}$$

and related *iso-unit*

$$\hat{I} = 1/\hat{T} : \hat{I} \hat{\times} \hat{A} = \hat{A} \hat{\times} \hat{I} \equiv \hat{A} \forall \hat{A} \in \hat{\mathcal{H}}. \tag{16}$$

Under the condition that, for consistency, iso-product (15) is applied to the *totality* of the products of the new mathematics, including numbers, functions, operators, etc., the associativity-preserving lifting $\xi \rightarrow \hat{\xi}$ allowed in 1978:

1) The foundations of iso-mathematics, including the Lie-Isotopic theory (nowadays called the *Lie-Santilli iso-theory*) consisting of the step by step isotopic lifting of Lie's theory, including Lie algebras, Lie groups and the transformation theory, with generic N -dimensional iso-algebra \hat{L} of Hermitean operators $X_k, k = 1, \dots, N$ and *iso-commutation rules* (Eq. (38c), p 170 of [42])

$$[X_i \hat{\times} X_j] == X_i \hat{\times} X_j - X_j \hat{\times} X_i = \tag{17}$$

$$= X_i \times \hat{T} \times X_j - X_j \times \hat{T} \times X_i = C_{ij}^k X_k.$$

After leaving Harvard University, Santilli completed the above studies with the 1994 construction of the new *iso-number theory* [89] with iso-unit (16), the 1996 construction of the new *iso-differential calculus* [50] defined for *volumes*, rather than points, and other advances.

2) The foundations of iso-mechanics comprising the *Schrödinger-Santilli iso-equation* (Eq. (14), p. 259 of [24])

$$\hat{H} \hat{\times} |\hat{\psi}\rangle = \left[\sum_{k=1,2,\dots,A} \frac{1}{2m_k} \hat{p}_k \hat{\times} \hat{p}_k + V(r) \right] \hat{\times} |\hat{\psi}\rangle = \tag{18}$$

$$= \hat{E} \hat{\times} |\hat{\psi}\rangle = (E \times \hat{I}) \times \hat{T} \times |\hat{\psi}\rangle = E \times |\hat{\psi}\rangle,$$

and the *Heisenberg-Santilli iso-equation* (Eq. (16), p. 153 of [24]) in its infinitesimal and finite form

$$i \frac{dA}{dt} = [\hat{A}, \hat{\times} \hat{H}] = \hat{A} \hat{\times} \hat{H} - \hat{H} \hat{\times} \hat{A}, \tag{19}$$

$$A(t) = e^{\hat{H} \hat{T} t} \times A(0) \times e^{-i \hat{T} \hat{H} t},$$

thus requiring *two* quantities for the characterization of nuclear structures, the conventional Hamiltonian $H > 0$ for the representation of linear, local and potential interactions, and the isotopic element $\hat{T} > 0$ for the representation of the extended character of particles and their non-linear, non-local and non-potential interactions.

3) The iso-Galilean symmetry and relativity (Chapter 6, p. 199 on of [24]).

Following the above foundations, hadronic mechanics has been studied by various scholars (see monographs [25]–[34] and papers quoted therein) at about thirty workshops and various international conferences (see representative proceedings [35]–[40], comprehensive presentations [41]–[43]) (see also the summary of the various branches of hadronic mechanics [49], the overviews [45]–[49], and the recent summaries [46]–[48]).

Nowadays, hadronic mechanics has various branches of increasing complexity for the description of particles with increasingly complex physical conditions [49].

The above mathematical and theoretical studies, combined with experimental verifications [43], allowed the identification of the following explicit form of *the isotopic element (15) and iso-unit (16) for a two-body hadronic system* [44]

$$\hat{T} = \Pi_{\alpha=1,2} \text{Diag.} \left(\frac{1}{n_{1,\alpha}^2}, \frac{1}{n_{2,\alpha}^2}, \frac{1}{n_{3,\alpha}^2 z}, \frac{1}{n_{4,\alpha}^2} \right) \times e^{-\Gamma} \ll 1, \tag{20}$$

$$\hat{I} = 1/\hat{T}$$

$$= \Pi_{\alpha=1,2} \text{Diag.} (n_{1,\alpha}^2, n_{2,\alpha}^2, n_{3,\alpha}^2, n_{4,\alpha}^2) \times e^{+\Gamma} \gg 1,$$

$$\Gamma(r, p, a, E, d, \pi, \tau, \psi, \dots) > 0, \quad n_{\mu,\alpha} > 0,$$

$$\mu = 1, 2, 3, 4, \quad \alpha = 1, 2,$$

where \hat{T} is solely restricted by the condition of being positive-definite, but otherwise possess an unrestricted functional dependence (hereon tacitly assumed) on coordinates r , momenta p , accelerations a , energy E , density d , pressure π , temperature τ , wave functions ψ , and any other needed local variable:

1) The representation of the dimension and shape of the individual nucleons is done via semi-axes $n_{k,\alpha}^2, k = 1, 2, 3$ (with n_3 parallel to the spin) and normalization for the vacuum $n_{k,\alpha}^2 = 1$.

2) The representation of the density is done via the characteristic quantity $n_{4,\alpha}^2$ per individual nucleons with normalization for the vacuum $n_{4,\alpha}^2 = 1$.

3) The representation of the non-Hamiltonian interactions between extended nucleons which is achieved by the exponential term $e^{-\Gamma}$.

On pedagogical grounds, it should be indicated that any given quantum mechanical model with point-like nucleons and sole Hamiltonian interactions can be uniquely and unambiguously completed into the covering hadronic model for

extended nucleons with Hamiltonian and non-Hamiltonian interactions via the simple *non-unitary transformation* (first proposed in Eq. (11), p. 249 of [24])

$$U \times U^\dagger = \hat{I} = 1/\hat{T} > 0, \quad (21)$$

provided that, to avoid insidious inconsistencies, it is applied to the totality of the quantum formalism with no exception known to this author. In fact, under transformation (8), the conventional associative product of quantum operators A, B is mapped into the *iso-product* of *iso-operators*

$$U \times (A \times B) \times U^\dagger = \hat{A} \hat{\times} \hat{B} = \hat{A} \times \hat{T} \times \hat{B}, \quad (22)$$

$$\hat{T} = (UU^\dagger)^{-1}, \quad \hat{A} = U \times A \times U^\dagger, \quad \hat{B} = U \times B \times U^\dagger,$$

and the same holds for all aspects of iso-mechanics as we shall see in detail in Section 3.

Finally, it is important to indicate from these initial notes that *the representation of the dimensions of particles and their non-Hamiltonian interactions via hadronic mechanics is invariant over time*, of course, not under the *unitary* time evolution of Heisenberg's equations, but under the *iso-unitary* time evolution of the Heisenberg-Santilli iso-equation,

$$U = \hat{U} \hat{T}^{1/2}, \quad (23)$$

$$\hat{U} \hat{\times} \hat{U}^\dagger = \hat{U}^\dagger \hat{\times} \hat{U} = \hat{I},$$

under which the iso-unit and the isotopic element of hadronic mechanics are *numerically invariant* [51]

$$\hat{U} \hat{\times} \hat{I} \hat{\times} \hat{U}^\dagger \equiv \hat{I}, \quad (24)$$

$$\hat{U} \hat{\times} (\hat{A} \hat{\times} \hat{B}) \hat{\times} \hat{U}^\dagger = \hat{A}' \times \hat{T}' \times \hat{B}', \quad \hat{T}' \equiv \hat{T}.$$

By using a language accessible to the general physics audience, in Section 2 we review half a century of mathematical, theoretical, experimental and industrial studies in the *non-relativistic* synthesis of the neutron from the proton and the electron.

In Section 3, we report the relativistic studies in the synthesis of the neutron with particular reference to the space time iso-symmetries and iso-relativities necessary for their derivation.

In Section 4, we show that all objections against electrons being part of the nuclear structure are resolved by the recent EPR verifications [4]–[8] and more particularly, by the progressive validity of the *iso-deterministic principle under strong interactions* which occurs in the structure of hadrons, nuclei and stars and the full achievement of Einstein's determinism at the limit of the Schwarzschild horizon.

An initial understanding of this paper can be reached via a knowledge of reviews [46]–[48], with the understanding that a technical knowledge of this paper can solely be reached via a technical knowledge of hadronic mechanics according to the general presentations [41]–[43].

2 Non-relativistic representation of the neutron synthesis from the Hydrogen atom

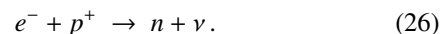
In this section, we shall outline and update one century of studies on the synthesis of the neutron from the Hydrogen atom in the core of stars as well as in laboratory. Needless to say, we can only outline the main aspects of such a vast topic and provide the references for detailed studies.

2.1 Historical notes

As recalled in Sect. 1.1, stars initiate their lives as an aggregate of Hydrogen that grows by accretion during travel in interstellar spaces. At the moment when the temperature in the core of the aggregate reaches a value of the order of 10 MK, E. Rutherford [19] suggested in 1920 that the Hydrogen atom is “compressed” into a new neutral particle which he called the *neutron*,



The existence of the neutron was experimentally established in 1932 by J. Chadwick [52]. In 1933, W. Pauli [53] pointed out that synthesis (11) violates the conservation of angular momentum. Therefore, E. Fermi [54] submitted in 1935 the hypothesis that the synthesis of the neutron occurs with the joint *emission* of a neutral and massless particle ν with spin 1/2 which he called the *neutrino* (meaning “little neutron” in Italian)



Subsequent tests (see the recent review [17]) established that *the neutron is naturally unstable* with a mean life of $\tau = 877$ s and spontaneous decay



where $\bar{\nu}$ is the *antineutrino*.

Predictably, the synthesis of the neutron from the Hydrogen attracted attention soon following the Chadwick confirmation. According to the historical account [55], Ernest J. Sternglass conducted in 1951 the first test for the laboratory synthesis of the neutron from Hydrogen, followed by tests in 1952 by E. Trounson and others, although none of these initial tests were reported in published papers in view of the incompatibility of the neutron synthesis with quantum mechanics (Insufficiency I) and for other reasons.

To the author's best knowledge, the first published tests on the laboratory synthesis of the neutron from Hydrogen were done in the 1960's by the Italian priest-physicist, Don Carlo Borghi and his associates [56]. In essence the experimentalists constructed a cylindrical metal chamber (called *klystron*) filled up with the Hydrogen gas (at a fraction of 1 bar pressure) kept the gas mostly ionized via an electric arc with about 500 V and 10 mA. Additionally, the gas was traversed by microwaves with the frequency of 10^{-10} s^{-1} . The experimentalists then placed in the exterior of the Klystron

various materials suitable to be activated when exposed to a neutron flux (such as gold or silver). Following exposures over several weeks, the experimentalists reported clear and reproducible nuclear transmutations that can only be due to a neutral hadron emitted from the Klystron. Due to insufficient evidence on neutron emission, the experimentalists conjectured that the detected nuclear transmutations were due to a new neutral particle with the mass of the neutron but spin different than $1/2$ that they called the *neutroid*.

2.2 Santilli's studies on the neutron synthesis

In view of its fundamental character for all quantitative sciences, R. M. Santilli has conducted over the past five decades mathematical, theoretical, experimental and industrial research on the synthesis of the neutron from the Hydrogen atom in the core of stars, as well as in laboratory (see the mathematical studies [20,23,24,41,50] [57]–[67], the physical studies [42] [68]–[73], the experimental studies [43, 74, 80], and the independent studies [25]–[34] [81]–[85]).

These studies were initiated in the late 1970's at Harvard University under DOE support with the inapplicability of quantum mechanics for the neutron synthesis [20] (Quantum insufficiency I) followed by the proposal to construct *hadronic mechanics* in monographs [23, 24].

By far the biggest difficulty of the above studies has been the representation of the spin of the neutron $S_n = 1/2$ from two particles each having spin $1/2$, as originally conceived by Rutherford [19]. This problem stimulated the construction of the Lie-Santilli iso-theory (see Sect. 4.4, p. 173 on of [24] and independent work [26]), followed by systematic studies on the isotopies of spacetime symmetry [57]–[67], with particular reference to the isotopies $\widehat{SO}(3)$ and $\widehat{SU}(2)$ of the angular momentum and spin symmetries at the classical and operator levels [57]–[60] and then passing to the isotopies of spacetime symmetries [61]–[67].

As a result of these preparatory studies, Santilli was able to achieve a numerically exact and time invariant representation of *all* characteristics of the neutron at the non-relativistic level in the 1990 paper [68], and at the relativistic level in the 1995 paper [72], with additional studies available in monograph [73].

Following, and only following, the achievement of a consistent representation of the neutron synthesis via the Lie-isotopic branch of hadronic mechanics, Santilli initiated in 2007 experimental tests on the laboratory synthesis of the neutron from Hydrogen [74]–[80]. According to these experiments, the neutron synthesis from Hydrogen can be generated by *hadronic reactors* consisting of a metal vessel containing in their interior a commercially available Hydrogen gas at pressure and a pair of submerged carbon electrodes powered by a specially designed (patent pending) DC source with a gap controllable from the outside. During operations (Fig. 1), the DC arc is continuously connected and disconnected be-

cause of the consumption of the carbon electrodes. During its activation (left of Fig. 2), the special form of the DC arc ionizes the Hydrogen gas by creating a plasma mostly composed by protons and electrons in its cylindrical surroundings, while during its deactivation (right of Fig. 2), the specially designed DC electric arc compresses the ionized gas from all radial directions toward its symmetry axis.

Interested readers should be aware that commercially available DC electric arcs between carbon electrodes submerged within a Hydrogen gas may synthesize neutroids (Fig. 2) and other unstable hadronic bound states under their big Coulomb attraction, but they are not designed to *compress electrons inside the proton* according to Rutherford's original conception [19].

Experiments [74]–[80] have confirmed: 1) The production of Don Borghi's neutroids (Fig. 2) for DC power of the order of 5 kw, gas pressure of 5 psi and electrode gap of 2 mm. 2) The production of neutrons (Fig. 3) for DC power with at least 50 kw, gas pressure from 10 psi on and electrode gas of at least 5 mm. In particular, the synthesis of neutroids (Fig. 2) resulted to be an unavoidable step prior to the synthesis of the neutron (Fig. 3).

Following, and only following sufficient experimental evidence on the laboratory synthesis of the neutron from a Hydrogen gas, Santilli founded in 2012 the U.S. publicly traded company *Thunder Energies Corporation* (now the privately held Hadronic Technologies Corporation www.hadronictechnologies.com) for the production and sale of a thermal neutron source (see Sect. 4.1).

2.3 Non-relativistic representation of the neutron synthesis

This study was initiated by Santilli with his 1978 Harvard University memoir [20], continued in various works [68]–[73] thanks to the collaboration by various scholars, and reviewed in the 2021 paper [48].

These studies have been conducted under the assumption [20] that the angular momentum of the electron compressed inside the proton is *constrained* to be equal to the spin of the proton as a necessary condition to prevent *extreme resistive forces* caused by the motion of its *extended* wave packet against the *dense* medium in the interior of the proton.

More particularly, when compressed inside the dense proton, the electron e is mutated into a new particle called the *eleton* in Sect. 5.1 of [20] and indicated with the symbol ϵ^- to distinguish it from the electron and the elementary charge e , but recently called the *iso-electron*

$$\hat{\epsilon}^- = U\epsilon^-U^\dagger, \quad (28)$$

because characterized by the complex lifting of the elementary charge (identified in Sect. 3 as an open problem) generated by the isotopic completion $\hat{G}(3.1)$ of the Galilean symmetry [87, 88] (see monograph [25] for an extensive inde-

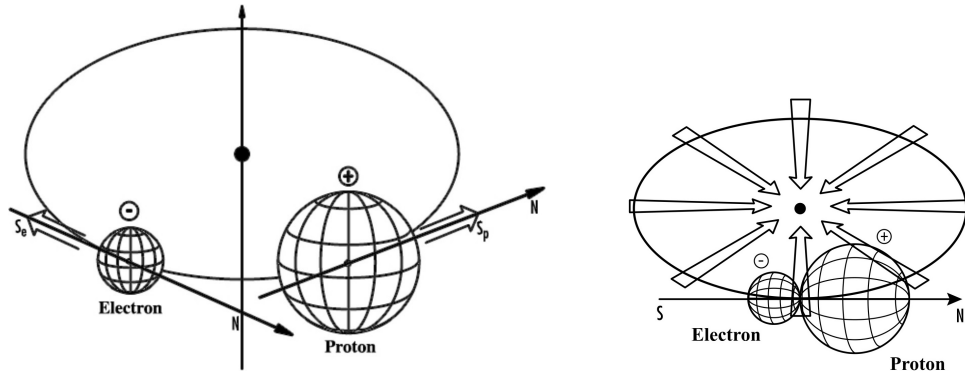


Fig. 1: In this figure, we illustrate the mechanism used by hadronic reactors for the synthesis of neutroids and neutrons via a specially designed (patent pending) DC electric arc between Carbon electrodes submerged within a Hydrogen gas. The mechanism comprises the ionization of Hydrogen atoms into electrons and protons by the activation of the arc (left view) and the compression of the electron within the proton by the de-activation of the arc (right view).

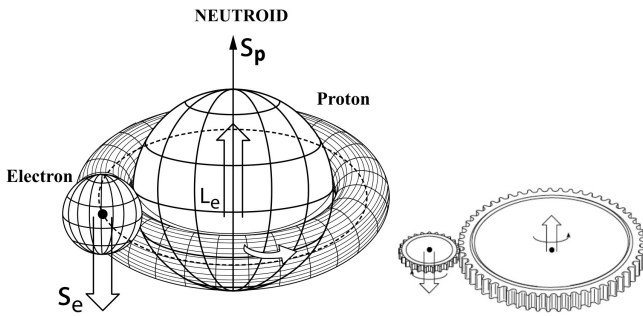


Fig. 2: In the left of this figure, we illustrate the predicted structure of the neutroid in its ground state as a hadronic bond of electrons and protons under their very big Coulomb attraction, Eq. (6), in singlet couplings with null eigenvalues of the angular momentum and of the spin. In the right view, we present a conceptual gear equivalent of the left view to illustrate the reason for the half life of neutroids as being about 10% that of neutrons, i.e. of about 8 s.

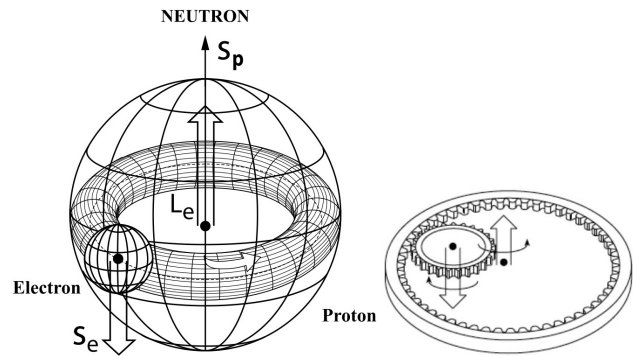


Fig. 3: In the left view, we illustrate the compression of the neutroid of Fig.2 via the mechanism of Fig.1, resulting in a constrained hadronic angular momentum of the electron within the dense medium inside the proton that, to avoid extreme resistive forces, has to be equal to the proton spin with ensuing total angular momentum 1/2. In the right of this figure, we provide a conceptual rendering of the left view via coupled gears to illustrate the rather large half life of the neutron of 887 s.

pendent study), with corresponding relativistic extension characterized by the isotopy $\widehat{SO}(3.1)$ of the Lorentz symmetry $SO(3.1)$ [61] and the isotopy $\widehat{\mathcal{P}}(3.1)$ of the spinorial covering of the Poincaré symmetry $\mathcal{P}(3.1)$ characterizing the 20th century notion of *particle*.

By comparison, the proton is assumed in first approximation to be un-mutated, $\widehat{p}^+ = p^+$ since the iso-electron is about 1800-times lighter than the proton.

The above assumptions imply the following *structure model of the neutron* as a bound state of a proton p^+ and an iso-electron \widehat{e}^- according to hadronic mechanics (hm)

$$n = \left(\widehat{\epsilon}_\downarrow^{spin}, \widehat{\epsilon}_\uparrow^{orb}, p_\uparrow^{spin} \right)_{hm}, \tag{29}$$

under the Coulomb attraction in the macroscopic value of 230 Newton, Eq. (6).

It should be stressed that, in view of the extremely big value of Coulomb attraction (6), *the numeric value of the*

mean life of the neutron according to model (29) can be subject to scientific debates, but not its existence.

2.3.1 Representation of the neutron mass, mean life and charge radius

Let us recall the well known essential elements of the non-relativistic, quantum mechanical representation of the Hydrogen atom as a bound state of a proton p and an electron e , which are given by:

1) The geometric representation on the *Euclidean space* $E(r, \delta, I)$ with relative coordinate $r = r_p - r_e$, metric $\delta = \text{Diag.}(1, 1, 1)$, unit $I = \text{Diag.}(1, 1, 1)$, and invariant

$$r^2 = r^i \times \delta_{ij} \times r^j = r_1^2 + r_2^2 + r_3^2. \tag{30}$$

2) The operator representation on the *Hilbert space* \mathcal{H} over the field of complex numbers C with states $|\psi(r)\rangle$, normalization

$$\langle\psi(r)|\times|\psi(r)\rangle = I, \quad (31)$$

and expectation value of a Hermitean operator A

$$\langle A \rangle = \langle\psi(r)|\times A \times|\psi(r)\rangle. \quad (32)$$

3) The *Schrödinger representation*, comprising the linear momentum

$$p \times |\psi(r)\rangle = -i \times \hbar \times \partial_r |\psi(r)\rangle, \quad (33)$$

the eigenvalue equation

$$\begin{aligned} H(r, p) \times |\psi(r)\rangle &= E_H \times |\psi(r)\rangle \\ &= \left[\sum_{k=1,2,3} \frac{1}{2m} \times p_k \times p_k - \frac{e^2}{r} \right] \times |\psi(r)\rangle, \end{aligned} \quad (34)$$

where m is the reduced mass

$$m = \frac{m_e \times m_p}{m_e + m_p}, \quad (35)$$

and the canonical commutation rules

$$\begin{aligned} [r^i, p_j] \times |\psi(r)\rangle &= (r^i \times p_j - p_j \times r^i) \times |\psi(r)\rangle = \\ &= -i \times \hbar \times \delta_j^i \times |\psi(r)\rangle, \end{aligned} \quad (36)$$

$$[r^i, r^j] \times |\psi(r)\rangle = [p_i, p_j] \times |\psi(r)\rangle = -0.$$

As it is well known, the above formulation characterizes the Hydrogen atom binding energy

$$E_H = 13.6 \text{ eV}, \quad (37)$$

stability, Bohr's radius and all other features.

According to studies first done in the 1990 paper [68], completed in the 1995 monograph [73] and updated in Sect. 2 of the 2021 memoir [47], the non-relativistic hadronic treatment of structure model (29) is given by the following, step-by-step, *non-unitary* transformation of the quantum treatment of the Hydrogen atom

$$U \times U^\dagger = \hat{I} = 1/\hat{T} > 0, \quad (38)$$

where, for the non-relativistic treatment, we assume iso-unity (20) with value for the density $n_{4,k} = 1$, $k = 1, 2$ whose treatment is done at the relativistic level (Sect. 3.4).

In fact, the geometric treatment of model (29) is done in the *iso-Euclidean iso-space* $\hat{E}(\hat{r}, \hat{\delta}, \hat{I})$ [41,61] over the iso-real iso-field $\hat{R}(\hat{n}, \hat{\times}, \hat{I})$ [41, 89] (see also monograph [29]) with iso-unit (20), iso-coordinates $\hat{r} = UrU^\dagger = r\hat{I}$, iso-metric $\hat{\delta} = \hat{T} \times \delta$ and *iso-invariant*

$$\begin{aligned} \hat{r}^2 &= Ur^2U^\dagger = U(r^i \times \delta_{ij}r^j)U^\dagger = \\ &= (Ur^iU^\dagger)(UU^\dagger)^{-1}[(U\delta_{ij}U^\dagger)(UU^\dagger)^{-1}](Ur^jU^\dagger) = \\ &= \hat{r}^i \hat{\times} \hat{\delta}_{ij} \hat{\times} \hat{r}^j = \left(\frac{r_1^2}{n_1^2} + \frac{r_2^2}{n_1^2} + \frac{r_3^2}{n_1^2} \right) \hat{I}, \end{aligned} \quad (39)$$

where the exponential term of iso-unit (20) has been embedded in the characteristic n -quantities, and one should note the final multiplication by \hat{I} which is necessary for the iso-invariant to be an *iso-scalar*, that is an element of $\hat{R}(\hat{n}, \hat{I})$.

The operator treatment of structure model (29) is done in the *Hilbert-Myung-Santilli isospace* [90] over the iso-field of iso-complex iso-numbers \hat{C} [89] with *iso-states*

$$|\hat{\psi}(\hat{r})\rangle = U(|\psi(r)\rangle)U^\dagger, \quad (40)$$

iso-normalization

$$\langle\hat{\psi}(\hat{r})|\hat{\times}|\hat{\psi}(\hat{r})\rangle = \langle\hat{\psi}(\hat{r})|\times\hat{T}\times|\hat{\psi}(\hat{r})\rangle = \hat{T}, \quad (41)$$

and *iso-expectation values* of an iso-operator

$$\begin{aligned} \hat{\lambda}\hat{A} &= \langle\hat{\psi}(\hat{r})|\hat{\times}\hat{A}\hat{\times}|\hat{\psi}(\hat{r})\rangle = \\ &= \langle\hat{\psi}(\hat{r})|\times\hat{T}\times\hat{A}\times\hat{T}\times|\hat{\psi}(\hat{r})\rangle. \end{aligned} \quad (42)$$

The reader should note that iso-normalization (41) is characterized by the isotopic element \hat{T} (rather than the iso-unit \hat{I}) for consistency because \hat{T} can be a constant as a particular case, but also because from normalization (31), we expect

$$[[\hat{\psi}(\hat{r})]^\dagger]|\hat{\psi}(\hat{r})\rangle = \langle\hat{\psi}(\hat{r})|\times|\hat{\psi}(\hat{r})\rangle = I. \quad (43)$$

Iso-Schrödinger iso-representation (see Chapter 5, p. 182 of [42] for a detailed treatment). It should be indicated that despite considerable efforts reviewed earlier, by the early 1990's the hadronic form of the Schrödinger equation was still unknown due to the inapplicability of the Newton-Leibnitz differential calculus in general and in particular, the inapplicability for hadronic mechanics of the conventional form (33) of the quantum mechanical linear momentum, with ensuing inability to compute the iso-Hamiltonian.

The axiomatic origin of this impasse was the incompatibility between the sole applicability of the differential calculus to *isolated points* r compared to isotopic methods which are entirely devoted to the representation of *volumes* via iso-unit $\hat{I} = \hat{I}(r, \dots)$, Eq. (20), iso-coordinates $\hat{r} = r\hat{I}(r, \dots)$ and iso-functions $\hat{f}(\hat{r}) = [f(r\hat{I})]\hat{I}$.

This impasse left R. M. Santilli with no other option than that of generalizing the Newton-Leibnitz differential calculus from its sole applicability to isolated points r to volumes \hat{r} . This generalization was first achieved in the 1994 paper submitted for the 1996 memoir [50] (see the 1995 general study [41,42] and systematic independent works from 2014 on [33,34]) via the introduction of the infinite class of *iso-differentials of an iso-coordinate* $\{\hat{d}\hat{r}\}$ on $\hat{E}(\hat{r}, \hat{\delta}, \hat{I})$ on \hat{R} solely restricted to admit the conventional differential dr for the particular case $\hat{I} = 1$

$$\{\hat{d}\hat{r}\}_{\hat{I}=1} = dr, \quad (44)$$

with selected solution (Eq. (1.27), p. 20 of [50])

$$\hat{d}\hat{r} = \hat{T}d[r\hat{I}(r, \dots)] = dr + r\hat{T}d\hat{I}(r, \dots), \quad (45)$$

consequential *iso-derivative*

$$\frac{\hat{\partial} \hat{f}(\hat{r})}{\hat{\partial} \hat{r}} = \hat{I} \times \frac{\partial \hat{f}(\hat{r})}{\partial \hat{r}}, \quad (46)$$

and finally, the needed expression for the *iso-linear iso-momentum* of hadronic mechanics, first achieved in Sect. 2.5, p. 52 of [50] and Eq. (3.1.10), p. 82 of [42]

$$\hat{p} \hat{\times} |\hat{\psi}(\hat{r})\rangle = -\hat{i} \hat{\times} \hat{h} \hat{\times} \hat{\partial}_r |\hat{\psi}(\hat{r})\rangle = -\hat{i} \hat{I} \hat{\partial}_r |\hat{\psi}(\hat{r})\rangle. \quad (47)$$

By using non-unitary transformations of the type

$$\begin{aligned} U \left[\sum_{k=1,2,3} \frac{1}{2m} p_k p_k - \frac{e^2}{r} \right] |\psi(r)\rangle U^\dagger &= \\ = \left[\sum_{k=1,2,3} \frac{1}{2m} (U p_k U^\dagger) (U U^\dagger)^{-1} (U p_k U^\dagger) - \right. \\ \left. - (U \frac{e^2}{r} U^\dagger) \right] (U U^\dagger)^{-1} (U |\psi(r)\rangle) U^\dagger &= \\ = U [E |\psi(r)\rangle] U^\dagger = E [U |\psi(r)\rangle] U^\dagger &= E |\hat{\psi}(\hat{r})\rangle, \\ U \left(\frac{e^2}{r} \right) U^\dagger = \frac{e^2}{r} \hat{I} = \frac{\hat{I}^2 e^2}{\hat{I} r} = \frac{\hat{e}^2}{\hat{r}}. \end{aligned} \quad (48)$$

Schrödinger's equation (34) for the Hydrogen atom on \mathcal{H} over C is mapped into the *iso-Schrödinger equation for the neutron on iso-space $\hat{\mathcal{H}}$ over the iso-field \hat{C}*

$$\begin{aligned} \hat{H}(\hat{r}, \hat{p}) \hat{\times} |\hat{\psi}(\hat{r})\rangle &= \\ = \left[\sum_{k=1,2,3} \frac{\hbar^2}{2m} \hat{p}_k \hat{\times} \hat{p}_k - \frac{\hat{e}^2}{\hat{r}} \right] \hat{\times} |\hat{\psi}(\hat{r})\rangle &= E_n |\hat{\psi}(\hat{r})\rangle, \end{aligned} \quad (49)$$

and the canonical commutation rules (36) are mapped into the *iso-canonical iso-commutation rules*

$$\begin{aligned} [\hat{r}^i, \hat{p}_j] \hat{\times} |\hat{\psi}(\hat{r})\rangle &= (\hat{r}^i \hat{T} \hat{p}_j - \hat{p}_j \hat{T} \hat{r}^i) \hat{T} |\hat{\psi}(\hat{r})\rangle = \\ = -\hat{i} \hat{\times} \hat{h} \hat{\times} \delta_j^i \hat{\times} |\hat{\psi}(\hat{r})\rangle &= -i \hbar \delta_j^i |\hat{\psi}(\hat{r})\rangle, \\ [\hat{r}^i, \hat{r}^j] \hat{\times} |\hat{\psi}(\hat{r})\rangle &= [\hat{p}_i, \hat{p}_j] \hat{\times} |\hat{\psi}(\hat{r})\rangle = 0. \end{aligned} \quad (50)$$

As one can see, (49) is formally equivalent to (34) and therefore, it can be solved on the iso-space over the iso-field, yielding the following value of the *neutron binding energy* similar to that for the positronium [14]

$$E_n \approx 7 \text{ eV}, \quad (51)$$

by therefore confirming the expectation, from the high centripetal force of the iso-electrons compressed inside the proton, that *the neutron is a quasi-free hadronic bound state of an (iso-)proton and an iso-electron*.

To identify the impact of the non-Hamiltonian interactions in the neutron structure model (29), it is necessary to assume an explicit realization of the isotopic element and

iso-unit of (20). We here assume the original realization of Sect. 5.1, p. 827 on of the 1978 memoir [20], merely reformulated according to iso-mathematics and iso-mechanics with the simplifying assumptions $n_{\mu,\alpha} = 1$, $\mu = 1, 2, 3, 4$, $k = 1, 2$,

$$\begin{aligned} \hat{I} = 1/\hat{T} = U U^\dagger &= e^{+\frac{V_h(r)}{v_c(r)}} \approx 1 + \frac{V_h(r)}{v_c(r)} \gg 1, \\ \hat{T} = (U U^\dagger)^{-1} &= e^{-\frac{V_h(r)}{v_c(r)}} \approx 1 - \frac{V_h(r)}{v_c(r)} \ll 1, \end{aligned} \quad (52)$$

where $V_h(r)$ is the *Hulten potential* first adopted in Eq. (5.1.6) p. 833 of [20]

$$V_h(r) = K \frac{e^{-br}}{1 - e^{-br}}, \quad (53)$$

with

$$b = R^{-1} \approx 10^{-13} \text{ cm}, \quad (54)$$

and $V_c(r)$ is the conventional Coulomb potential

$$V_c(r) = \frac{e^2}{r}. \quad (55)$$

We consider now the *projection* of iso-equation (49) into the conventional Euclidean and Hilbert spaces. By using isotopic element (52), the needed projection can be written

$$\begin{aligned} \left[\sum_{1,2,3} \frac{\hbar}{2m} (-i \hat{I} \hat{\partial}_r) (-i \hat{I} \hat{\partial}_r) - (U V_c(r) U^\dagger) \right] |\psi(r)\rangle &= \\ = E_n |\psi(r)\rangle, \end{aligned} \quad (56)$$

where, in first approximation,

$$U V_c(r) U^\dagger = V_c(r) \hat{I} \approx V_c(r) + V_h(r). \quad (57)$$

But the Hulten potential behaves at very short distances like the Coulomb potential (Eq. (5.1.5) p. 936 of [20]) by therefore absorbing the latter with a mere re-definition K' of the constant K . Consequently, (56) can be reduced in one space dimension to

$$\left[\frac{1}{2m} (-i \hat{I} \hat{\partial}_r) (-i \hat{I} \hat{\partial}_r) + K' \frac{e^{-br}}{1 - e^{-br}} \right] |\psi(r)\rangle = E |\psi(r)\rangle, \quad (58)$$

whose radial form

$$\left[\frac{1}{r^2} \left(\frac{d}{dr} r^2 \frac{d}{dr} \right) + \bar{m} K' \frac{e^{-br}}{1 - e^{-br}} \right] = 0, \quad (59)$$

has been studied in great details in Sect. 5.1, p. 827 on of the 1978 memoir [20], including its full analytic solution with boundary conditions.

By adding the isotopy of the non-relativistic quantum mechanical mean life, yielding the expression (Eq. (5.1.13), p. 835 of [20])

$$\tau^{-1} = 2\pi \lambda^2 |\hat{\psi}(0)|^2 \frac{\alpha^2 E \hat{e}}{\hbar}, \quad (60)$$

we reach the *hadronic equations for the mass mean life and charge radius of the neutron according to model (29)* (Eq. (5.1.14), p. 836 of [20])

$$\left[\frac{1}{r^2} \left(\frac{d}{dr} r^2 \frac{d}{dr} \right) + \bar{m} \left(E + K' \frac{e^{-br}}{1 - e^{-br}} \right) \right] \psi(r) = 0,$$

$$E_n^{tot} = E_p + E_{\tilde{e}} - E_n - E = 939.565 \text{ MeV},$$

$$\tau^{-1} = 2\pi\lambda^2 |\hat{\psi}(0)|^2 \frac{\alpha^2 E_{\tilde{e}}}{\hbar} = 877 \text{ s},$$

$$R = b^{-1} - 10^{-13} \text{ cm},$$

where \bar{m} is the *iso-renormalized reduced mass* (Eq. (5.1.7), p. 833 of [20]), and the last three equations are subsidiary constraints on the first equation.

The analytic solution of the above equations was reduced to the solution of the following two algebraic equations on the parameters k_1 and k_2 (Eq. (5.1.32), p. 840 of [20])

$$E_n^{tot} = \frac{2\hbar ck_1}{b} [k_1 - (k_2 - 1)^2] = 939.37 \text{ MeV},$$

$$\tau = \frac{48 \times (137)^2}{4\pi bc} \frac{k_1}{(k_2 - 1)^3} = 877 \text{ s},$$

with numeric solutions (Eq. (2.20), p. 521 of [68])

$$k_1 = 0.34, \quad k_2 = 1 + 0.81 \times 10^{-8}. \quad (63)$$

The energy spectrum results to be the typical *finite* spectrum of the Hulthen potential (for $k_2 = 1$)

$$E = \frac{1}{4R^2\bar{m}} \left(\frac{1}{n} - n \right)^2, \quad n = 1, 2, 3, \dots \quad (64)$$

whose sole consistent solution occurs for $n = 1$, as a result of which *the sole possible value for the binding energy E caused by the Hulthen potential is null*

$$E = \frac{1}{4R^2\bar{m}} \left(\frac{1}{n} - n \right)^2 = 0, \quad n = 1, \quad (65)$$

because, as expected, *all the excited states of neutron structure (29) are the various states of the Hydrogen atom*. Alternatively, the null value of the binding energy E is expected from the fact that *contact, zero-range interactions have no potential energy by central assumption*.

2.3.2 Representation of the neutron spin

The central assumption of hadronic model (29) requires that, to avoid extreme resistive forces, the hadronic angular momentum of the iso-electron \tilde{e}^- be equal to the spin of the proton, thus having value $\hat{L}_{3,\tilde{e}} = 1/2$. The study of this assumption was initiated in the 1984 papers on the isotopies of the rotational symmetry [57, 58] and continued in the 1990 paper [68] via the iso-trigonometric iso-functions (see p. 304 on



Fig. 4: In this figure, we illustrate some of the hadronic reactors used for the synthesis of the neutron from Hydrogen (see [80] for a complete presentation).

of [41]), under the use of the Lie-Santilli iso-algebra $\widehat{SO}(3)$. Regrettably, we cannot review these studies to avoid an excessive length.

We here present, apparently for the first time, the non-relativistic representation of the hadronic angular momentum $\hat{L}_3 = 1/2$ under the assumptions that *the orbit of the extended iso-electron within the dense proton is a perfect circle perpendicular to the proton symmetry axis with radius $R = 10^{-13}$ cm*. In fact, deviations from the above assumptions imply instabilities generally preventing a representation of the significant (for particle standards) neutron mean life of 887 s, under which assumptions the acting iso-symmetry is the two-dimensional Lie-Santilli iso-group $\widehat{SO}(2)$ [57, 58] (see also Sect. 6.4, p. 233 on of [42]).

Consider the conventional $O(2)$ symmetry which is classically formulated on the two-dimensional Euclidean space $E(z, \delta, D)$, and quantum mechanically treated on a Hilbert space \mathcal{H} over \mathbb{C} . By continuing the construction of hadronic models via a non-unitary transformation of quantum models of the preceding section, we map the entire classical and quantum mechanical formulation of $O(2)$ under the nonunitary transformation

$$UU^\dagger = \hat{I} = 1/\hat{T} = \text{Diag.}(n_1^2, n_2^2) =$$

$$= \text{Diag.}(b_1^{-2}, b_2^{-2}), \quad b_k = 1/n_k > 0, \quad k = 1, 2, \quad (66)$$

and represent the orthogonality condition via Bohm's hidden variable [91]

$$\frac{1}{n_1} = \frac{1}{n_2} = b_1 = b_2 = \lambda > 0. \quad (67)$$

Therefore, the iso-representation occurs in the two-dimensional iso-Euclidean iso-space $\hat{E}(\hat{r}, \hat{\delta}, \hat{I})$ over the isofield \hat{C} with iso-coordinates

$$\hat{r} = r\hat{I} = \{x, y\}\lambda^2 I_{2 \times 2}, \quad (68)$$

iso-metric

$$\hat{\delta} = \hat{I}\delta = \lambda^2\delta, \quad (69)$$

iso-invariant

$$\hat{r}^2 = \lambda^2 r^2, \quad (70)$$

and iso-trigonometric representation (Appendix 5C, p. 300 on of [41])

$$\begin{aligned} x &= r\lambda^{-1} \cos \hat{\phi}, \quad y = r\lambda^{-1} \sin \hat{\phi}, \\ \hat{\phi} &= T_{\phi}\phi = n_1 n_2 \phi = \lambda^{-2} \phi, \quad \hat{T}_{\phi} = b_1 - 1b_2^{-2} = \lambda^{-2}. \end{aligned} \quad (71)$$

The iso-unitary and iso-irreducible iso-representations of $\widehat{SO}(2)$ is defined on the iso-space \mathcal{H} [90] C with iso-states $|\hat{\psi}(\hat{r})\rangle$, iso-normalization (41), iso-generator $\hat{R}(\hat{\phi})$ and related iso-eigenvalues

$$\begin{aligned} \hat{R}(\hat{\phi})\hat{\times}|\hat{\psi}\rangle &= \hat{e}^{iM\hat{\phi}}\hat{\times}|\hat{\psi}\rangle = (e^{i\hat{M}\hat{\phi}})\hat{I}_{\psi}\hat{\times}|\hat{\psi}\rangle = (e^{i\lambda^2 M\hat{\phi}})|\hat{\psi}\rangle, \\ \hat{M} &= b_1 b_2 M = \frac{1}{n_1 n_2} M, \\ \lambda^2 &= b_1 b_2 = \frac{1}{n_1} \frac{1}{n_2}, \end{aligned} \quad (72)$$

(where \hat{e} is, this time, the iso-exponentiation in the ϕ -plane) with Lie-Santilli iso-group laws

$$\begin{aligned} \hat{R}(\hat{\phi})\hat{\times}\hat{R}(\hat{\phi}')\hat{\times}|\hat{\psi}\rangle &= \hat{R}(\hat{\phi}')\hat{\times}\hat{R}(\hat{\phi})\hat{\times}|\hat{\psi}\rangle = \hat{R}(\hat{\phi} + \hat{\phi}')\hat{\times}|\hat{\psi}\rangle, \\ \hat{R}(\hat{\phi})\hat{\times}\hat{R}(-\hat{\phi})\hat{\times}|\hat{\psi}\rangle &= \hat{R}(0)\hat{\times}|\hat{\psi}\rangle = |\hat{\psi}\rangle. \end{aligned} \quad (73)$$

The iso-eigenvalue of the hadronic angular momentum \hat{L} is given by

$$\hat{L}\hat{\times}|\hat{\psi}\rangle = \hat{M}|\hat{\psi}\rangle = \lambda^2 M|\hat{\psi}\rangle. \quad (74)$$

But isotopies preserve original numeric values. Therefore,

$$\hat{M} = \lambda^2 M = 0, 1, 2, 3, \dots \quad (75)$$

Consequently, the angular momentum measured by the experimentalist in our space is given by

$$M = \frac{\hat{M}}{\lambda^2}, \quad (76)$$

and can represent the *constrained* angular momentum of the electron inside the proton for the value

$$M = \frac{\hat{M}}{\lambda^2} = \frac{1}{2}, \quad (77)$$

resulting in the *numeric value of Bohm's hidden variable*, here presented for the first time,

$$\lambda = \sqrt{b_1 b_2} = \sqrt{\frac{1}{n_1 n_2}} = \sqrt{2} = 1.4142, \quad (78)$$

which should be compared with essentially the double value of Bohm's hidden variable for the representation of the Deuteron spin [7, 8].

The total spin of the neutron is then given by

$$S_n = s_p + s_{\hat{e}} + L_{\hat{e}} = \frac{1}{2} - \frac{1}{2} + \frac{1}{2}. \quad (79)$$

Hence, according to hadronic structure model (29), *the spin of the neutron coincides with the spin of the proton* as expected. Alternatively, we can say that *the total angular momentum of the iso-electron compressed inside the proton is identically null*, with intriguing applications, e.g. for the exact representation of nuclear spins to be studied in a separate work.

For brevity, we leave to the interested reader the representation of the spin $S = 1/2$ of the iso-electron via the iso-symmetry $\widehat{SO}(2)$, which can be derived from the above treatment with the $\widehat{SO}(2)$ symmetry.

The spin of the neutroid according to Fig. 2 is characterized by the following value for the hadronic angular momentum of the iso-electron

$$M = \frac{\hat{M}}{\lambda} = 0, \quad \hat{M} = 0, \quad \lambda > 0. \quad (80)$$

Consequently, *the spin of the neutroid according to Fig. 2 is predicted to be zero*, by therefore explaining the reason for their lack of detection via commercially available neutron detectors.

2.3.3 Representation of the neutron magnetic moment

The anomalous magnetic moment of the neutron according to model (29) has been first represented in the 1990 original paper [68] via the following *three* contributions

$$\mu_n = \mu_p + \mu_{\hat{e}}^{spin} + \mu_{\hat{e}}^{orb}. \quad (81)$$

The biggest difficulty for the above representation is that the magnetic moment of the electron $\nu_{\hat{e}}^{spin}$, Eq. (5), is so big for nuclear standard to prevent a quantum mechanical model of the neutron synthesis as well as to prevent that electrons can be members of nuclear structures (Section 1). These insufficiencies are here resolved, apparently for the first time via the magnetic moment of the *orbital* motion of the iso-electron $\mu_{\hat{e}}^{orb}$ which is *opposite* that of the iso-electron (Fig. 3) and its value is predicted to be [68]

$$\mu_{\hat{e}}^{orb} = 1833.580 \mu_N. \quad (82)$$

By recalling the known values of the magnetic moments of the proton and the neutron [12] $\mu_p = 2.792\mu_N$, $\mu_n = -1.913\mu_N$, we reach in this way the *numerically exact and time invariant representation of the anomalous magnetic moment of the neutron* [68]

$$\mu_n = \mu_p + \mu_e^{spin} + \mu_e^{orb} = 2.792\mu_N - 1838.285\mu_N + 1833.5801\mu_N = -1.913\mu_N \quad (83)$$

It should be noted that the assumption of the above orbital contribution of the iso-electron not only allows a representation of the *numeric value* of the anomalous magnetic moment of the neutron, but also of its *negative value*.

3 Relativistic representation of the neutron synthesis from the Hydrogen atom

Recall that the relativistic treatment of the Hydrogen atom is based on the rotational symmetry $SO(3)$, the spin symmetry $SU(2)$, the Lorentz symmetry $SO(3,1)$, the Poincaré symmetry $P(3,1) = SO(3,1) \times \mathcal{T}(3,1)$, the spinorial covering of the Poincaré symmetry $\mathcal{P}(3,1) = SL(2, C) \times \mathcal{T}(3,1)$ and related special relativity.

Immediately following the construction in 1983 of the isotopies of the various branches of Lie's theory (Sect. 5.2 on p. 154 of [24]), Santilli constructed the isotopies of the above symmetries and relativities on iso-spaces over iso-fields as a condition to achieve a relativistic representation of the neutron synthesis from the proton and electron, and prove its compatibility with the non-relativistic treatment [57]–[67], including:

- 1) The rotational iso-symmetry $\widehat{SO}(3)$ [57]–[59].
- 2) The spin iso-symmetry $\widehat{SU}(2)$ [60].
- 3) The Lorentz iso-symmetry $\widehat{SO}(3,1)$ [61, 62].
- 4) The Poincaré iso-symmetry $\widehat{P}(3,1) = \widehat{SO}(3,1) \times \widehat{\mathcal{T}}(3,1)$ [63, 64].
- 5) The spinorial covering of the Poincaré iso-symmetry $\widehat{\mathcal{P}}(3,1) = \widehat{SL}(\widehat{2}, \widehat{C}) \times \widehat{\mathcal{T}}(3,1)$ [66, 67].

The use of the above iso-symmetries then allowed Santilli to construct the unique and unambiguous isotopies of special relativity for the description of extended particles and electromagnetic waves propagating within a physical medium, known under the name of *special iso-relativity*, or *iso-relativity* for short, which was first presented in the 1983 Nuovo Cimento paper [61] for the classical part and in the adjoining paper [62] for the operator counterpart, and subsequently treated in the 1991 monographs [92, 93] with 1996 update [41]–[43] and in 2021 overview [44] (see also the review in monograph [25] from Santilli's lecture notes at the ICTP, Trieste, Italy, monographs [28, 32], and papers quoted therein).

Note that the above extended scientific journey was necessary for the *time invariant representation of the size and density of extended particles* without which experimental verifications cannot be consistently formulated.

Note also that *iso-symmetries and iso-relativities coincide at the abstract level with conventional symmetries and relativities*. Therefore, the representation of the dynamics within physical media solely occur in their *projection* on conventional spaces over conventional fields.

Therefore, *the same symmetries and relativities represent, at the abstract level, both the Hydrogen atom and the neutron*. All differences between the two bound states of a proton and an electron solely occur in their *realizations*.

3.1 The main open problem for particle fusions

As indicated in Sect. 5, p. 819 on of the 1978 Harvard University memoir [20], hadronic mechanics was proposed and constructed not only for a more accurate representation of *nuclear fusions*, but also for the representation of *particle fusions* (also called synthesis), beginning with the fusion of the proton and the electron into the neutron. Additionally, the 1978 memoir [20] proposed isotopic methods for the representation of the structure of *unstable* particles as hadronic bound states of lighter particles and antiparticles generally produced free in their spontaneous decays.

While the quantum mechanical point-like abstraction of particles and nuclei has provided a first approximation of nuclear fusions, quantum mechanics is inapplicable for the representation of particle fusions (Sect. 1.2) due to the *mass excess/rest energy excess*, namely, the mass of the synthesized particle is bigger than the sum of the masses of the constituents as it is clearly the case for the neutron synthesis, (7) while by comparison, nuclear fusions cause the well known *mass defect/energy defect*.

Following the identification of the open problem of the neutron synthesis, in Sect. 5.1, p. 827 on of [20], Santilli achieved the first known representation of *all* characteristics of the π^0 meson as the hadronic bound state (i.e. the fusion) of a mutated electron, then called *eletron* ϵ^- (more recently called *iso-electron*) and a mutated positron ϵ^+ ,

$$\pi^0 = (\epsilon^-, \epsilon^+)_{hm} \quad (84)$$

This proposal was based in the following experimental evidence: 1) The extremely big Coulomb attraction (6) between the $\epsilon^- - \epsilon^+$ constituents. 2) The spontaneous decay of the π^0 into an electron and a positron

$$\pi^0 \rightarrow e^- + e^+, \quad 7.5 \times 10^{-8}, \quad (85)$$

via a process interpreted as a *hadronic tunnel effect of the constituents*. 3) The π^0 primary decay which is evidently due to electron-positron annihilation

$$\pi^0 \rightarrow \gamma + \gamma, \quad 98.5\%, \quad (86)$$

which decay allowed the first known identification of the *mechanism* triggering the spontaneous decay of the π^0 and the *exact* representation of its mean life $\tau = 0.828 \times 10^{-16}$ s. The

extension of the model to all remaining mesons was also proposed in the same section 5.1 of [20].

Another important aim of Sect. 5.1 of [20] was to show that quantum mechanics is completely inapplicable for any structure model of the π^0 as a bound state of lighter constituents due to the *rest energy excess* similar to that for the neutron (7) which, for the case of model (84) is given by

$$\pi^0 = (\hat{e}_\uparrow^-, \hat{e}_\downarrow^+)_{hm}, \quad \Delta E = -133.954 \text{ MeV}. \quad (87)$$

In the author's view, the indicated inapplicability of quantum mechanics for the *structure* of particles, jointly with the unavailability at the time of a suitable covering method, explains (and justifies) the sole studies of particles in the 20th century via *classification* methods, such as *mass spectra* that as such, has never produced a structure equation for any particle.

In the subsequent Sect 5.2, p. 849 on of [20] (see also the recent confirmations [48, 98, 99]), Santilli confirmed the results of Sect. 5.1 by reaching the first known representation of *all* characteristics of the μ^\pm leptons via the hadronic structure model (i.e. particle fusion)

$$\mu_\uparrow^\pm = (\epsilon_\uparrow^-, \epsilon_\uparrow^\pm, \epsilon_\downarrow^\pm)_{hm}, \quad (88)$$

on the experimental ground that the μ^\pm leptons decay spontaneously into the indicated constituents via a hadronic tunnel effect

$$\mu^\pm \rightarrow e^- + e^\pm + e^+, \quad 1.0 \times 10^{-12}, \quad (89)$$

while the electron-positron pair annihilation explains the spontaneous character of the decay and its mean life, which annihilation is experimentally confirmed by the muon decay

$$\mu^\pm \rightarrow e^\pm + 2\gamma, \quad 7.2 \times 10^{-11}. \quad (90)$$

Santilli concluded Sect. 5.2, p. 849 on of [20] by indicating the complete inapplicability of quantum mechanics for any structure model of the leptons with lighter constituents due to the rest energy excess

$$\mu_\uparrow^\pm = (\epsilon_\uparrow^-, \epsilon_\uparrow^\pm, \epsilon_\downarrow^\pm)_{hm} \rightarrow \Delta E = -104.636 \text{ MeV}. \quad (91)$$

The extension of the model to the remaining (unstable) leptons was also proposed in the same section 5.2 of [20].

The use of hadronic mechanics under the same principles (the physical constituents of unstable particles are produced free in the spontaneous decays) allowed similar structure models of unstable baryons, such as the model for the Λ^0 [48, 100]

$$\Lambda_\uparrow^0 = (\hat{p}_\uparrow^+, \hat{\pi}^-)_{hm}, \quad (92)$$

(where the "hat" indicates isotopic mutation due to total mutual immersion) based on the primary spontaneous decay

$$\Lambda_\uparrow^0 \rightarrow p_\uparrow^+ + \pi^-, \quad 20 - 30\%, \quad (93)$$

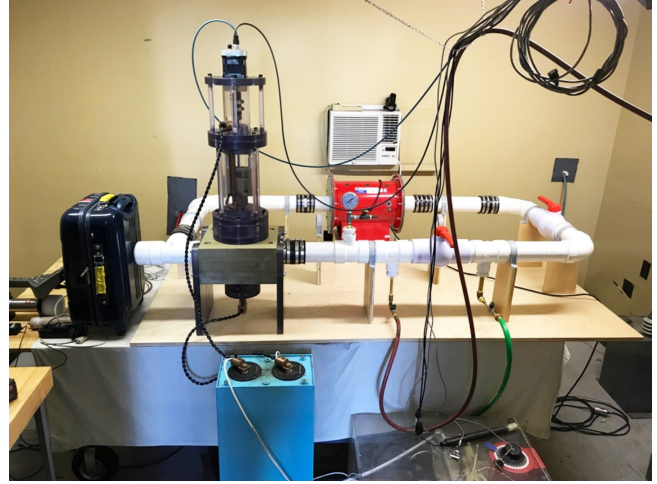


Fig. 5: In this picture, we illustrate the Directional Neutron Source (DNS) produced and sold by Thunder Energies Corporation (now Hadronic Technologies Corporation) generating a flux of thermal neutrons in the desired direction and intensity. The DNS is suggested for the detection of fissile material that may be hidden in baggages, and other applications.

with rest energy excess

$$\Lambda_\uparrow^0 = (\hat{p}_\uparrow^+, \hat{\pi}^-)_{hm} \quad \Delta E = -37.812 \text{ MeV}. \quad (94)$$

The extension of the above hadronic structure model to the remaining (unstable) baryons is left to the interested reader.

The compatibility of the above *structure* models of unstable particles with their known *classification* was shown to be possible via the *iso-units* of the representations that turned out to be different for different particles (see Fig. 4 for mesons and Fig. 12 for baryons of [48]).

Evidently, the indicated excess energies are *physically* acquired by the constituents. The open problem to be addressed in this section is that we are currently unable to calculate the kinetic energy of an extended particle moving within a dense hadronic medium. Consequently, in this section we shall review and upgrade the isotopic methods used for the *geometric* representation of the excess energy for the neutron, in a form extendable to all other particle fusions.

3.2 Iso-Minkowskian iso-spaces

As it is well known, the Minkowski space in 3+1-dimensions provides a geometric representation of the *homogeneity and isotropy of empty space*. By contrast, the primary function of the *Minkowski iso-space* in 3+1-dimensions (first proposed in the 1983 paper [61] and called *Minkowski-Santilli iso-space*) is to provide a geometric representation of the *inhomogeneity and anisotropy of physical media*.

Let $M(x, \eta, I)$ be the conventional Minkowski space over the reals \mathcal{R} with space time coordinates, metric, unit and in-

variant

$$x = \{x^\mu\} = \{x^1, x^2, x^3, x^4 = ct\},$$

$$\eta = \text{Diag.}(1, 1, 1, -1), \quad I = \text{Diag.}(1, 1, 1, 1), \quad (95)$$

$$\mu, \nu = 1, 2, 3, 4,$$

and invariant

$$x^2 = x^\mu \eta_{\mu,\nu} x^\nu = x_1^2 + x_2^2 + x_3^2 - t^2 c^2. \quad (96)$$

Relativistic isotopic methods, including most importantly the Lie-Santilli iso-theory [24] (see also independent studies [25, 26] and review [47]), are uniquely and unambiguously characterized by the conventional Minkowski space $M(x, \eta, I)$ and the infinite family of positive-definite isotopic elements which, for the case of iso-relativities, are assumed to have the simplified form of the general expression (20)

$$T = 1/\hat{I} = \text{Diag.} \left(\frac{1}{n_1^2}, \frac{1}{n_2^2}, \frac{1}{n_3^2}, \frac{1}{n_4^2} \right) =$$

$$= \text{Diag.} (b_1^2, b_2^2, b_3^2, b_4^2), \quad n_\mu > 0, \quad b_\mu > 0, \quad (97)$$

where we have indicated the characteristic quantities $b_\mu = 1/n_\mu$ mostly used in the early literature in the field, and the exponent of isotopic element (20) is embedded in the characteristic quantities to be factored out whenever needed.

Relativistic methods are then formulated on the infinite family of *iso-Minkowski iso-spaces* $\hat{M}(\hat{x}, \hat{\Omega}, \hat{I})$ over the iso-real iso-field $\hat{\mathcal{R}}$ with iso-unit $\hat{I} = 1/\hat{T}$ [89], *iso-coordinates*

$$\hat{x} = x\hat{I} = \left(\frac{x_1}{n_1}, \frac{x_2}{n_2}, \frac{x_3}{n_3}, \frac{x_4}{n_4} = t^2 \frac{c}{n_4} \right), \quad (98)$$

iso-metric

$$\hat{\Omega} = \hat{\eta}\hat{I} = (\hat{T}\eta)\hat{I}, \quad (99)$$

where one should note the final multiplication by \hat{I} as a necessary consistency condition for the *iso-metric to be an iso-matrix* (namely, a matrix whose elements are iso-numbers) [41]), and *iso-invariant*

$$\hat{x}^2 = \hat{x}^\mu \hat{\Omega}_{\mu,\nu} \hat{x}^\nu = \hat{x}_1^2 + \hat{x}_2^2 + \hat{x}_3^2 - t^2 \hat{c}^2 =$$

$$\hat{x}^\mu \hat{T} \hat{\Omega}_{\mu,\nu} \hat{T} \hat{x}^\nu = x^\mu \hat{\eta}_{\mu,\nu} x^\nu =$$

$$\frac{x_1^2}{n_1^2} + \frac{x_2^2}{n_2^2} + \frac{x_3^2}{n_3^2} - t^2 \frac{c^2}{n_4^2}, \quad (100)$$

illustrating the *identity* at the abstract level between the Minkowski invariant (85) and its iso-Minkowskian image in the first line of invariant (88), all differences occurring in the projection of the latter in the conventional Minkowski space.

It should be noted that, as it was the case for isotopic element (20), the iso-metric has the Minkowskian topological structure (+, +, +, -) but an unrestricted functional dependence on local (space time) coordinates x , momenta p , acceleration a , energy E , density d , pressure π , temperature τ ,

wave function ψ , and any other needed local variable,

$$\hat{\eta}_{\mu\nu} = \hat{\eta}_{\mu\nu}(x, p, a, E, d, \pi, \tau, \psi, \dots). \quad (101)$$

Consequently, the *iso-Minkowskian geometry* with iso-invariant (89) (first introduced in the 1996 paper [50] on the iso-differential calculus and treated in more details in the 1998 paper [67]) is the most general possible geometry with a symmetric invariant in (3 + 1)-dimensions, thus including in particular the Minkowskian, Riemannian, Fynslerian and other geometries (see Sect. 3.8 for details).

3.3 The Fundamental theorem on iso-symmetries

The following theorem was first presented in the 1983 paper [61] and upgraded in Section 4.6, page 169 on of [41] as well as in other publications.

3.3.1. FUNDAMENTAL THEOREM ON ISO-SYMMETRIES: *Let G be an N -dimensional Lie symmetry of a K -dimensional space $S(x, m, F)$ with coordinates x and metric m over a numeric field F ,*

$$G : x' = a(w)x, \quad y' = a(w)y, \quad x, y \in S, \quad w \in F, \quad (102)$$

leaving invariant the interval

$$(x' - y')^\dagger m(x' - y') \equiv (x - y)^\dagger m(x - y) \quad (103)$$

with main property

$$(x' - y')^\dagger a^\dagger(w)ma(w)(x - y) \equiv (x - y)^\dagger m(x - y), \quad (104)$$

$$a^\dagger(w)ma(w) \equiv m, \quad \forall x, y \in S.$$

Then, all infinitely possible iso-symmetries \hat{G} on iso-spaces $\hat{S}(\hat{x}, \hat{M}, \hat{F})$, where $\hat{M} = \hat{m}\hat{I} = (\hat{T}_i^k m_{kj})\hat{I}$ over iso-fields \hat{F} with iso-unit $\hat{I} = 1/\hat{T}$

$$\hat{G} : x' = \hat{A}(\hat{w})\hat{x} = (\hat{a}\hat{I})\hat{T}\hat{x} = \hat{a}\hat{x}, \quad (105)$$

$$\hat{y}' = \hat{A}(\hat{w})\hat{y} = (\hat{a}\hat{I})\hat{T}\hat{y} = \hat{a}\hat{y}, \quad \forall \hat{x}, \hat{y} \in \hat{S}, \quad \hat{w} \in \hat{F},$$

leave invariant the iso-interval

$$(\hat{x}' - \hat{y}')^\dagger \hat{\Omega}^\dagger(\hat{w})\hat{\Omega}(\hat{w})\hat{M}(\hat{w})\hat{\Omega}(\hat{w})\hat{\Omega}(\hat{x} - \hat{y}) \equiv$$

$$\equiv (\hat{x} - \hat{y})^\dagger \hat{\Omega}^\dagger(\hat{w})\hat{\Omega}(\hat{w})\hat{M}(\hat{w})\hat{\Omega}(\hat{w})\hat{\Omega}(\hat{x} - \hat{y}), \quad (106)$$

with main property

$$\hat{A}^\dagger(\hat{w})\hat{\Omega}^\dagger(\hat{w})\hat{\Omega}(\hat{w})\hat{M}(\hat{w})\hat{\Omega}(\hat{w})\hat{A}(\hat{w}) \equiv \hat{M}, \quad \forall \hat{x}, \hat{y} \in \hat{S}, \quad \hat{w} \in \hat{F}, \quad (107)$$

and all so-constructed iso-symmetries \hat{G} are isomorphic to the original symmetry G .

The verification of the above theorem by all space time iso-symmetries [57]–[67] is an instructive exercise by the interested reader. Note that all iso-symmetries are uniquely and unambiguously characterized by the original symmetry and the infinite class of possible isotopic elements $\hat{T} > 0$.

We finally note that the *iso-exponentiation* [41]

$$\hat{e}^{X_k w_k} = (e^{X_k \hat{T} w_k})\hat{I} = \hat{I}(e^{w_k \hat{T} X_k}), \quad (108)$$

allows the explicit construction of iso-transformations (105).

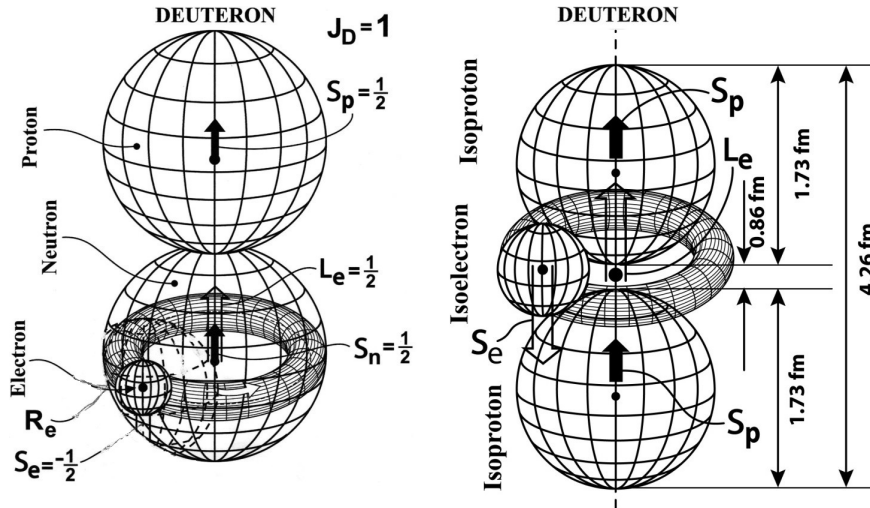


Fig. 6: In the left view, we illustrate the new axial triplet coupling of a proton and a neutron that has achieved the first known representation of the spin $S_D = 1$ of the Deuteron in its true ground state, that with null orbital contributions (Insufficiency II of Sect. 1.2) [44, 102]. In the right view, we illustrate the decoupling of the iso-electron from the neutron to achieve the first known representation of the stability of the Deuteron despite the natural instability of the neutron (Insufficiency IV of Sect. 1.2). Note that said stability is possible if and only if the proton and the electron are the actual physical constituents of the neutron.

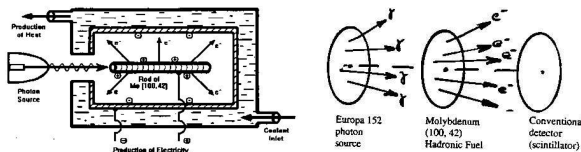


Fig. 7: In this figure, we illustrate the stimulated nuclear transmutations (174) which are predicted to be triggered by irradiation with resonating photons γ_r with energy $E_r = E_{\hat{r}} = 1,293 \text{ MeV}$ [115] which has been tentatively verified in [117]. In this figure, we reproduce the original drawing of paper [115] showing (from the left) a beam of resonating photons irradiating a cylinder of $\text{Mo}(100, 42, 0)$ which emits electrons easily trapped by a metal casing with the production of a clean DC electric current of nuclear origin, plus clean heat triggered by said metal screen absorbing electrons with 0.782 MeV kinetic energy. In the right of this figure, we reproduce the original figure of paper [115] illustrating the simplicity as well as the low cost of experimental verifications consisting of the purchase of a small sample of the commercially available radioisotope Europium-152 (emitting photons with E_r) and of the pure isotope $\text{Mo}(100, 42, 0)$, which samples are placed next to each other. In the event of confirmation of the emission of electrons from the $\text{Mo}(100, 42, 0)$ sample, or of traces of $\text{Ru}(100, 44, 0)$ in the originally pure sample of $\text{Mo}(100, 42, 0)$, the production of clean nuclear energies via stimulated neutron decays would be confirmed.

3.4 Lorentz iso-symmetries

As it is well known, the Lorentz symmetry characterizes the propagation of point-like particles and electromagnetic waves in the homogeneous and isotropic vacuum represented by the Minkowskian space. The six generators of the connected component of the Lorentz algebra $so(3,1)$ are given by the (Hermitian) generators of rotations J_k , $k = 1, 2, 3$ and the Lorentz boosts M_k on the Hilbert space \mathcal{H} over the field of complex numbers $calC$ with commutation rules

$$[J_i, J_j] = -\epsilon_{ij}^k J_k, \tag{109}$$

$$[M_i, M_j] = c^2 \epsilon_{ij}^k J_k, \quad [J_i, M_j] = -\epsilon_{ij}^k M_k.$$

The exponentiation of the above commutation rules according to Lie's theorems yields the celebrated *Lorentz transformations* on the (3, 4)-Minkowski space $M(x, \eta, I)$ according to Theorem 3.2.1

$$x'^3 = \gamma(x^3 - vt), \quad x'^4 = \gamma\left(t - \frac{vx^3}{c^2}\right), \tag{110}$$

where

$$\beta = \frac{v^2}{c^2}, \quad \gamma = \frac{1}{\sqrt{1 - \beta^2}}, \tag{111}$$

whose historical role has been *the invariance of the speed of light c in vacuum expressed in line element (84)*.

The infinite family of *Lorentz iso-symmetries* $\widehat{SO}(3,1)$, first introduced in the 1983 *Nuovo Cimento* paper [61] following the preparatory papers on the *rotational and spin iso-symmetries* [57]–[60] (whose knowledge is here assumed to

prevent a prohibitive length), are defined on the Iso-Minkowski iso-spaces $\hat{M}(\hat{x}, \hat{\Omega}, \hat{I})$.

The Lie-Santilli iso-algebra $\widehat{SO}(3.1)$ is characterized by six iso-generators defined on the Hilbert-Myung-Santilli iso-space $\hat{\mathcal{H}}$ [90] over the iso-complex iso-field \hat{C} [89] (Eq. (54), p. 44 of [58])

$$\hat{J}_k = J_k \hat{I}, \quad \hat{M}_k = M_k \hat{I}, \quad (112)$$

(where J_k, M_k are the conventional 4-dimensional matrix generators of $SO(3.1)$) with explicit expressions (Eq. (10), p. 550 of [61])

$$\hat{J}_1 = n_2 n_3 J_1, \quad \hat{J}_2 = n_1 n_3 J_2, \quad \hat{J}_3 = n_1 n_2 J_3, \quad (113)$$

$$\hat{M}_k = n_k M_k,$$

with iso-commutation rules

$$[\hat{J}_i, \hat{J}_j] = \hat{J}_i \hat{\times} \hat{J}_j - \hat{J}_j \hat{\times} \hat{J}_i = -\epsilon_{ij}^k \hat{J}_k, \quad (114)$$

$$[\hat{M}_i, \hat{M}_j] = c^2 \epsilon_{ij}^k \hat{J}_k, \quad [\hat{J}_i, \hat{M}_j] = -\epsilon_{ij}^k \hat{M}_k,$$

with related Casimir iso-invariant (Eq. (13), p.551 of [61])

$$\hat{C}_1 = \hat{J}^2 - \frac{1}{c} \hat{M}^2 = -3\hat{I}, \quad (115)$$

$$\hat{C}_2 = \hat{J} \hat{\times} \hat{M} = \hat{J}_k \hat{I}^{kk} \hat{M}_k = 0.$$

The realization of the Lorentz-Santilli iso-group via iso-exponents (108) (Eq. (11), p. 550 of [61]) yields the *Lorentz-Santilli iso-transformations* in the (3, 4) plane (see [42] for the general case) for motion of an extended particle with speed v along the x^3 -axis *under the initial assumption that its density has unit value*, $n_4 = 1$ (Eq. (15), p. 551 of [61])

$$x'^3 = \hat{\gamma}(x^3 - vt), \quad (116)$$

$$t' = \hat{\gamma} \left(t - \frac{vb_3^2 x^3}{c^2} \right) = \hat{\gamma} \left(t - \frac{vx^3}{n_3^2 c^2} \right),$$

where

$$\hat{\beta} = \frac{v^2 b_3^2}{c^2}, \quad \hat{\gamma} = \frac{1}{\sqrt{(1 - \hat{\beta}^2)}}. \quad (117)$$

By reinstating generic values of the density $n_4 \neq 1$, and by noting that

$$\hat{\beta} \frac{n_3}{n_4} = \frac{v_3/n_3}{c/n_4} \frac{n_3}{n_4} = \frac{v_3}{c}, \quad (118)$$

$$\hat{\beta} \frac{n_4}{n_3} = \frac{v_3/n_3}{c/n_4} \frac{n_4}{n_3} = \frac{v_3}{c} \frac{n_4^2}{n_3^2},$$

iso-transforms (116) acquire the symmetrized form [42, 44, 93]

$$x'^1 = x^1, \quad x'^2 = x^2,$$

$$x'^3 = \hat{\gamma} \left(x^3 - \hat{\beta} \frac{n_3}{n_4} x^4 \right) = \hat{\gamma} \left(x^3 - \hat{\beta} \frac{b_4}{b_3} x^4 \right), \quad (119)$$

$$x'^4 = \hat{\gamma} \left(x^4 - \hat{\beta} \frac{n_4}{n_3} x^3 \right) = \hat{\gamma} \left(x^4 - \hat{\beta} \frac{b_3}{b_4} x^3 \right),$$

where

$$\hat{\beta} = \frac{v_3}{c} \frac{n_4}{n_3}, \quad \hat{\gamma} = \frac{1}{\sqrt{1 - \hat{\beta}^2}}, \quad (120)$$

which achieved in 1983: 1) The invariance of the iso-Minkowskian line element (100). 2) The first known invariant description of extended, thus deformable particles or extended wave packets with semi-axes n_1^2, n_2^2, n_3^2 propagating within a physical medium with density n_4 . 3) The first known *invariance of the local speed of light propagating within transparent physical media*, called *iso-light*

$$C = \frac{c}{n_4} \leq c, \quad (121)$$

which, as we shall see, is generally *smaller* than c ($n_4 > 1$) for media of low density (such as Earth's atmosphere) and *bigger* than c ($n_4 < 1$) for media of high density (such as hadrons).

The following comments are in order:

3.4.1. On historical grounds, let us recall that Lorentz first attempted the invariance of the local speed of light of his times, $C = c/n_4$, but had to restrict his study to the invariance of the constant speed c , due to unsolvable technical difficulties caused by the fact that Lie's theory is notoriously a *linear* problem, while the invariance of local speeds (121) is a highly *non-linear* problem. Hence, the Lie-Santilli iso-theory was constructed with a non-linear structure precisely for the solution of the historical Lorentz problem.

3.4.2. As it is well known, Albert Einstein justly received the 1921 Nobel Prize in Physics for the *quantized absorption*, and not for the *quantized propagation* of light. For the evident intent of preserving special relativity, light propagating within physical media is generally reduced to photons scattering among the molecules of the medium, thus traveling in vacuum with speed c rather than the Lorentz speed $C = c/n_4$. While the quantized *absorption* of light is a historical reality, the quantized *propagation* of light reduced to photons is disproved by experimental evidence, e.g. because it has to occur for all visible frequencies, thus including the reduction to photons of infrared light (see Inconsistencies 1 to 7 in Sect. 8.4.4, p. 134 of [44]). As one can see, the only way known to this author to resolve these inconsistencies is that *visible light propagating within transparent physical media is a "wave" with local speed (121)*, as well known since Lorentz's time.

3.4.3. It was generally believed in the 20th century that the Lorentz symmetry is broken for locally varying speed of light within physical media. In reality, *the axioms of the Lorentz symmetry are fully preserved under isotopies* in view of the evident isomorphism $SO(3.1) \approx \widehat{SO}(3.1)$.

3.4.4. It was also believed in the 20th century that *the axioms of the Lorentz symmetry do not allow speeds bigger than c* , with ensuing academic opposition for the initiation studies on interstellar travel, and other problems implying speeds

$C > c$. In 1982, Santilli [95] pointed out that *strong interactions may accelerate particles faster than the speed of light in vacuum* under the admission that strong interactions have a contact non-potential component between the extended protons and neutrons. In fact, the acceleration of point-particles via potential energy up to c notoriously requires infinite energy. By contrast, non-potential interactions can accelerate particles without any use of potential energy and, in any case, special relativity is inapplicable under non-potential interactions.

3.4.5. In 1997, Santilli [96] (see the 2016 update [97]) showed that the following simple transformation of the Minkowski coordinates

$$x^\mu \rightarrow \tilde{x}^\mu = \frac{x^\mu}{n_\mu}, \quad (122)$$

maps the conventional Minkowski invariant (96) with maximal speed c into iso-invariant (100) for which the local speed of light (121) is arbitrary.

To conclude, in view of the isomorphism $\widehat{\text{SO}}(3.1) \approx \text{SO}(3.1)$, we can state that *the abstract axioms of the Lorentz symmetry do indeed predict arbitrary speeds of light*.

3.5 Poincaré iso-symmetries

Consider the conventional Poincaré symmetry on the Minkowskian space $M(x, \eta, I)$ over a field F , as the semi-direct product of the Lorentz symmetry $\text{SO}(3.1)$ and the translations in space time $\mathcal{T}(3.1)$,

$$\text{P}(3.1) = \text{SO}(3.1) \times \mathcal{T}(3.1), \quad (123)$$

with generators

$$J_{\mu\nu} = \{J_k, M_k\}, \quad P_\mu \quad \mu, \nu = 1, 2, 3, 4, \quad k = 1, 2, 3, \quad (124)$$

commutation rules

$$[J_{\mu\nu}, J_{\alpha\beta}] = i(\eta_{\nu\alpha} J_{\beta\mu} - \eta_{\mu\alpha} J_{\beta\nu} - \eta_{\nu\beta} J_{\alpha\mu} + \eta_{\mu\beta} J_{\alpha\nu}), \quad (125)$$

$$[J_{\mu\nu}, P_\alpha] = i(\eta_{\mu\alpha} P_\nu - \eta_{\nu\alpha} P_\mu), \quad [P_\mu, P_\nu] = 0,$$

and Casimir invariants

$$C_1 = I, \quad (126)$$

$$C_2 = P^2 = P_\mu P^\mu, \quad (\eta_{\mu\nu} P^\mu P^\nu),$$

$$C_3 = W^2 = W_\mu W^\mu, \quad W_\mu = \epsilon_{\mu\alpha\beta\rho} J^{\alpha\beta} P^\rho.$$

The infinite family of *Poincaré iso-symmetries*, first presented by Santilli in 1993 at the Department of Physics of Moscow State University [63, 64], also called the *Poincaré-Santilli iso-symmetries*

$$\hat{\text{P}}(3.1) = \widehat{\text{SO}}(3.1) \hat{\times} \hat{\mathcal{T}}(3.1), \quad (127)$$

is defined on iso-Minkowski iso-spaces $\hat{M}(\hat{x}, \hat{\Omega}, \hat{I})$ (where $\hat{\Omega} = \hat{\eta}\hat{I}$) over iso-real iso-field $\hat{\mathcal{R}}$ with iso-generators from definition (110)

$$\{\hat{J}_{\mu\nu}\} = \{\hat{J}_k, \hat{M}_k\}, \quad \hat{P}_\mu, \quad (128)$$

and iso-commutation rules [63, 64]

$$[\hat{J}_{\mu\nu}, \hat{J}_{\alpha\beta}] = i(\hat{\eta}_{\nu\alpha} \hat{J}_{\beta\mu} - \hat{\eta}_{\mu\alpha} \hat{J}_{\beta\nu} - \hat{\eta}_{\nu\beta} \hat{J}_{\alpha\mu} + \hat{\eta}_{\mu\beta} \hat{J}_{\alpha\nu}),$$

$$[\hat{J}_{\mu\nu}, \hat{P}_\alpha] = i(\hat{\eta}_{\mu\alpha} \hat{P}_\nu - \hat{\eta}_{\nu\alpha} \hat{P}_\mu), \quad (129)$$

$$[\hat{P}_\mu, \hat{P}_\nu] = 0,$$

where one should note the appearance of the *structure functions* with the functional dependence (98), i.e. $\hat{\eta}(x, p, a, E, d, \pi, \tau, \psi, \dots)$, rather than the traditional structure constants. Consequently, the Poincaré-Santilli iso-symmetry is *irregular*, namely, it cannot be obtained from the original symmetry via non-unitary transforms, as it is the case for regular Lie-Santilli iso-algebra [101].

The use of iso-commutation rules (128) yields the *Casimir-iso-invariants* [63, 64]

$$\hat{C}_1 = \hat{I} > 0,$$

$$\hat{C}_2 = \hat{P}^2 = \hat{P}_\mu \hat{\times} \hat{P}^\mu = (\hat{\eta}^{\mu\nu} P_\mu P_\nu) \hat{I} =$$

$$= \left(\sum_{k=1,2,3} \frac{1}{n_k^2} \hat{P}_k^2 - \frac{c^2}{n_4^2} \hat{P}_4^2 \right) \hat{I}, \quad (130)$$

$$\hat{C}_3 = \hat{W}^2 = \hat{W}_\mu \hat{\times} \hat{W}^\mu, \quad \hat{W} = W \hat{I},$$

$$\hat{W}_\mu = \hat{\epsilon}_{\mu\alpha\beta\rho} \hat{\times} J^{\alpha\beta} \hat{\times} \hat{P}^\rho,$$

and they are at the foundation of classical and operator *relativistic iso-mechanics* with deep implications for structure models of particles, nuclei and stars.

Note that *all possible Poincaré-Santilli iso-symmetries are isomorphic to the conventional Poincaré symmetry*. However, the conventional Poincaré symmetry is *linear* in view of the commutativity of the linear momenta $[P_\mu, P_\nu] = 0$, while the *Poincaré-Santilli iso-symmetry is iso-linear* because the property $[\hat{P}_\mu, \hat{P}_\nu] = 0$ holds on iso-spaces over iso-fields, but its projection into conventional spaces over conventional fields is not, in null, $[\hat{P}_\mu, \hat{P}_\nu] \neq 0$, with ensuing non-linearity of the theory. Consequently, the iso-translations $\hat{\mathcal{T}}(3.1)$ are generally nonlinear.

3.6 Dirac iso-equations

As it is well known, the Dirac equation achieved a justly historical role for the relativistic representation of the electron of the Hydrogen atom under the external field of the proton. The infinite family of *Dirac iso-equations*, first introduced in the 1995 papers [65, 66] and called the *Dirac-Santilli iso-equations* have been constructed for the relativistic representation of the iso-electron of the neutron while considering the proton as external.

The Dirac equation is generally obtained via the linearization of the second order Casimir invariant of the Poincaré symmetry (125). The Dirac-Santilli iso-equations are then best obtained via the linearization of the second order iso-Casimir invariant (130).

The carrier iso-spaces of the Dirac-Santilli iso-equations are given by the iso-product of the real-valued, *orbital* (or) iso-Minkowskian iso-spaces and of the complex-valued, *spin* (sp) iso-Euclidean iso-space

$$\hat{M}^{tot} = \hat{M}(\hat{x}, \hat{\Omega}^{or}, \hat{I}^{or}) \hat{\times} \hat{E}(\hat{z}, \hat{\Delta}^{sp}, \hat{I}^{sp}), \tag{131}$$

with orbital specifications

$$\begin{aligned} \hat{x} &= x \hat{I}^{or}, \quad \hat{\Omega}^{or} = \hat{\eta}^{or} \hat{I}^{or} = (\hat{T}^{or} \hat{\eta}) \hat{I}^{or}, \\ \hat{I}^{or} &= \text{Diag.}(n_1^2, n_2^2, n_3^2, n_4^2) = 1/\hat{T}^{or} > 0, \\ \hat{x}^{\hat{\lambda}} &= \hat{x}^{\mu} \hat{\times}^{or} \hat{\Omega}_{\mu\nu}^{or} \hat{\times}^{or} \hat{x}^{\nu} = \left(\frac{x_1^2}{n_1^2} + \frac{x_2^2}{n_2^2} + \frac{x_3^2}{n_3^2} - \frac{x_4^2}{n_4^2} \right)^{or}, \end{aligned} \tag{132}$$

and spin specifications

$$\begin{aligned} \hat{z} &= (z_1, z_2) \hat{I}^{sp}, \quad \hat{\Delta}^{sp} = \hat{\delta}^{sp} \hat{I}^{sp} = (\hat{T}^{sp} \hat{\delta}) \hat{I}^{sp}, \\ \hat{I}^{sp} &= \text{Diag.}(\lambda^{-1}, \lambda) = 1/\hat{T}^{sp} > 0, \quad \text{Det.} \hat{I}^{sp} = 1, \\ \hat{z}^{\hat{\lambda}} &= \hat{z}^i \hat{\times}^{sp} \hat{\Delta}_{ij}^{sp} \hat{\times}^{sp} \hat{z}^j = (\lambda z_1^2 + \lambda^{-1} z_2^2)^{sp}, \end{aligned} \tag{133}$$

where λ is Bohm's "hidden variable" [91].

Let us recall the explicit form of the iso-linear four-momentum on a Hilbert-Myung-Santilli isospace $\hat{\mathcal{H}}$ over an iso-complex iso-field \hat{C}

$$\hat{p}_{\mu} \hat{\times}^{or} |\hat{b}\rangle = -\hat{i}^{or} \hat{\times}^{or} \hat{\partial}_{\mu}^{or} |\hat{b}\rangle = -i \hat{I}^{or} \partial_{\mu} |\hat{b}\rangle. \tag{134}$$

By using the iso-mass of iso-particles and the iso-speed of iso-light

$$\hat{m} = m \hat{I}^{tot}, \quad \hat{C} = C \hat{I}^{tot} = \frac{C}{n_4} \hat{I}^{tot}, \tag{135}$$

we have the iso-linearization of the second order iso-Casimir invariant (130) acting on an iso-basis $|\hat{b}\rangle$ (see Eq. (6.1), page 189, [66])

$$\begin{aligned} &(\hat{\Omega}^{\mu\nu} \hat{\times}^{tot} \hat{P}_{\mu} \hat{\times}^{tot} \hat{P}_{\nu} - \hat{m}^{\hat{\lambda}} \hat{\times}^{tot} \hat{C}^{\hat{\lambda}}) \hat{\times}^{tot} |\hat{b}\rangle = \\ &= (\hat{\Omega}^{\mu\nu} \hat{\times}^{tot} \hat{I}_{\mu} \hat{\times}^{tot} \hat{P}_{\nu} + i^{tot} \hat{\times}^{tot} \hat{m} \hat{\times} \hat{C}) \hat{\times}^{tot} \\ &\hat{\times}^{tot} (\hat{\Omega}^{\mu\nu} \hat{\times}^{tot} \hat{I}_{\mu} \hat{\times}^{tot} \hat{P}_{\nu} - i^{tot} \hat{\times}^{tot} \hat{m} \hat{\times} \hat{C}) \hat{\times}^{tot} |\hat{b}\rangle, \end{aligned} \tag{136}$$

which holds if and only if the following conditions are verified

$$\begin{aligned} \hat{I}_{\mu} &= \hat{\gamma}_{\mu} \hat{I}^{or}, \\ \{\hat{\gamma}_{\mu}, \hat{\gamma}_{\nu}\}^{or} &= \hat{\gamma}_{\mu} \hat{\times}^{or} \hat{\gamma}_{\nu} + \hat{\gamma}_{\nu} \hat{\times}^{or} \hat{\gamma}_{\mu} = 2\hat{\eta}_{\mu\nu}, \end{aligned} \tag{137}$$

with realization given by the *Dirac-Santilli iso-gamma matrices*

$$\begin{aligned} \hat{\gamma}_k &= \frac{1}{n_k} \begin{pmatrix} 0 & \hat{\sigma}_k \\ -\hat{\sigma}_k & 0 \end{pmatrix}, \\ \hat{\gamma}_4 &= \frac{i}{n_4} \begin{pmatrix} I_{2 \times 2} & 0 \\ 0 & -I_{2 \times 2} \end{pmatrix}, \end{aligned} \tag{138}$$

where $\hat{\sigma}_k$ are the *Pauli-Santilli iso-matrices* first proposed in Eq. (6.8.20), p. 248, [42]

$$\begin{aligned} \hat{\sigma}_1 &= \begin{pmatrix} 0 & \lambda \\ \lambda^{-1} & 0 \end{pmatrix}, \quad \hat{\sigma}_2 = \begin{pmatrix} 0 & -i\lambda \\ i\lambda^{-1} & 0 \end{pmatrix}, \\ \hat{\sigma}_3 &= \begin{pmatrix} \lambda^{-1} & 0 \\ 0 & -\lambda \end{pmatrix}, \end{aligned} \tag{139}$$

with Lie-Santilli iso-commutation rules

$$\begin{aligned} [\hat{\sigma}_i, \hat{\sigma}_j] &= \hat{\sigma}_i \hat{\times} \hat{\sigma}_j - \hat{\sigma}_j \hat{\times} \hat{\sigma}_i = \\ &= \hat{\sigma}_i \hat{T} \hat{\sigma}_j - \hat{\sigma}_j \hat{T} \hat{\sigma}_i = i2\epsilon_{ijk} \hat{\sigma}_k, \end{aligned} \tag{140}$$

with iso-eigenvalues on $\hat{\mathcal{H}}$ over \hat{C}

$$\begin{aligned} \hat{S}_k &= \frac{\hat{1}}{2} \hat{\times} \hat{\sigma}_k = \frac{1}{2} \hat{\sigma}_k, \\ \hat{\sigma}_3 \hat{\times} |\hat{b}\rangle &= \hat{\sigma}_3 \hat{T} |\hat{b}\rangle = \pm |\hat{b}\rangle, \\ \hat{\sigma}^{\hat{\lambda}} \hat{\times} |\hat{b}\rangle &= (\hat{\sigma}_1 \hat{T} \hat{\sigma}_1 + \hat{\sigma}_2 \hat{T} \hat{\sigma}_2 + \hat{\sigma}_3 \hat{T} \hat{\sigma}_3) \hat{T} |\hat{b}\rangle = 3|\hat{b}\rangle, \end{aligned} \tag{141}$$

clearly showing the representation of the spin 1/2 of the considered iso-particle.

The Dirac-Santilli iso-equations can then be written

$$\begin{aligned} &(\hat{\Omega}^{\mu\nu} \hat{\times}^{or} \hat{I}_{\mu} \hat{\times}^{or} \hat{P}_{\nu} + \hat{i} \hat{\times}^{or} \hat{m} \hat{\times} \hat{C}) \hat{\times}^{or} |\hat{b}\rangle = \\ &= (\hat{\eta}^{\mu\nu} \hat{\gamma}_{\mu} \hat{\times}^{or} \hat{P}_{\nu} + \hat{i} \hat{m} \hat{\times} \hat{C}) \hat{\times}^{or} |\hat{b}\rangle = 0, \end{aligned} \tag{142}$$

which will be used in Sect. 3.9 for the relativistic representation of the neutron structure.

To avoid insidious, because unfounded inconsistencies in applications, the reader should keep in mind that the iso-metric $\Omega^{\mu\nu}$ for iso-momenta is the *contra-variant version* of the iso-metric $\Omega^{\mu\nu}$ for iso-coordinates.

3.7 Iso-spinorial Poincaré iso-symmetries

In view of the spin 1/2 of the electron, the space time symmetry for the relativistic treatment of the Hydrogen atom is given by the spinorial covering of the Poincaré symmetry

$$\mathcal{P}(3.1) = \mathcal{SL}(\epsilon.C) \times \mathcal{T}(\exists.\infty), \tag{143}$$

with realization of the generators in terms of the Dirac gamma matrices

$$\begin{aligned} \mathcal{SL}(2.C) : \quad S_k &= \frac{1}{2} \gamma_k \times \Gamma_4, \quad R_k = \frac{1}{2} \epsilon_i^k \gamma_i \times \gamma_j, \\ \mathcal{T}(3.1) : \quad P_{\mu}, \end{aligned} \tag{144}$$

which verify commutation rules (136).

Similarly, the *iso-spinorial coverings of the Poincaré iso-symmetries*, first presented in the 1995 paper [66] is given by

$$\hat{\mathcal{P}}(3.1) = \hat{\mathcal{S}}\hat{\mathcal{L}}(\hat{2},\hat{C})\hat{\times}\hat{\mathcal{T}}(3.1), \quad (145)$$

and admits the realization of the iso-generators in terms of the Dirac-Santilli iso-gamma iso-matrices $\hat{\Gamma}_\mu = \hat{\gamma}\hat{\Gamma}^{or}$

$$\begin{aligned} \hat{\mathcal{S}}\hat{\mathcal{L}}(\hat{2},\hat{C}) : \hat{S}_k &= \frac{1}{2}\hat{\Gamma}_k\hat{\times}\hat{\Gamma}_4, \quad \hat{R}_k = \frac{1}{2}\epsilon_{ijk}\hat{\Gamma}_i\hat{\times}\hat{\Gamma}_j, \\ \hat{\mathcal{T}}(3.1) : \hat{P}_\mu, \end{aligned} \quad (146)$$

which verify iso-commutation rules (128).

We also have the *rotational iso-sub-symmetries*

$$\hat{O}(3) : L_k = \epsilon_{kij}r_jp_i, \quad [L_i,L_j] = \epsilon_{ijk}n_k^2L_k, \quad (147)$$

with iso-eigenvalues

$$\begin{aligned} \hat{L}^2\hat{\times}|\hat{b}\rangle &= (\hat{L}_1\hat{\times}\hat{L}_1 + \hat{L}_2\hat{\times}\hat{L}_2 + \hat{L}_3\hat{\times}\hat{L}_3)\hat{\times}|\hat{b}\rangle = \\ &= (n_1^2n_2^2 + n_2^2n_3^2 + n_3^2n_1^2)|\hat{b}\rangle, \\ \hat{L}_3\hat{\times}|\hat{b}\rangle &= n_1n_2|\hat{b}\rangle, \end{aligned} \quad (148)$$

and the *spinorial iso-sub-symmetries*

$$\begin{aligned} \hat{S}\hat{U}(2) : \hat{S}_k &= \frac{1}{2}\epsilon_k^{ij}\hat{\gamma}_i\hat{\times}\hat{\gamma}_j, \\ [\hat{S}_i,\hat{S}_j] &= \frac{1}{n_k}\hat{S}_k \text{ (no sum)}, \end{aligned} \quad (149)$$

with iso-eigenvalues

$$\begin{aligned} \hat{S}^2 &= (\hat{S}_1\hat{\times}\hat{S}_1 + \hat{S}_2\hat{\times}\hat{S}_2 + \hat{S}_3\hat{\times}\hat{S}_3)\hat{\times}|\hat{b}\rangle = \\ &= \frac{1}{4}\left(\frac{1}{n_1^2n_2^2} + \frac{1}{n_2^2n_3^2} + \frac{1}{n_3^2n_1^2}\right)|\hat{b}\rangle \\ \hat{S}_3\hat{\times}|\hat{b}\rangle &= \frac{1}{2}\frac{1}{n_1n_2}|\hat{b}\rangle, \end{aligned} \quad (150)$$

that will be used in Sect. 3.9 for the identification of the main characteristics of the iso-electron in the neutron structure.

3.8 Special iso-relativities

Special Relativity (SR) has achieved a justly historical role for the characterization of *time reversal invariant, thus stable systems of point-like particles and electromagnetic waves propagating in the homogeneous and isotropic vacuum*, where the restriction to time reversal invariance follows from the dependence of Minkowski's invariant (96) on t^2 .

SR is only approximately valid for the characterization of time reversal invariant, thus stable systems of *extended particles* (such as the proton in a nucleus) because extended

particles imply features outside the representational capabilities of the *mathematics* underlying SR, such as the existence of contact, thus zero-range interactions without potential, the *mass/energy excess* of particle fusions (Sect. 3.1), the generally inhomogeneous and anisotropic character of the medium, and other problems.

In the author's view, SR is inapplicable (rather than violated) for an axiomatically consistent representation of *irreversible processes, such as nuclear fusions* for various axiomatic and physical reasons, including the possible violation of causality (e.g. the admission of solutions in which the effect precedes the cause) [102].

Special isotopic (i.e. axiom-preserving) relativity, or *Special Iso-Relativity* (SIR) for short, has been introduced by R. M. Santilli in the 1983 Nuovo Cimento papers [61, 62] for their classical and operator formulations, respectively, and then studied in various works [92]–[97] (see also reviews [25, 28, 32]) for the characterization of *time reversal invariant systems of extended, thus deformable and dense particles under conditions of mutual penetration, as occurring in stable nuclei, under the most general known, linear, local and potential interactions represented by a Hamiltonian H and the most general possible non-linear, non-local and non-potential interactions represented by the isotopic element \hat{T} of (20)*. In this paper, we use SIR with *constant n-characteristic quantities* for the representation of the neutron synthesis even though the neutron is *unstable* (when isolated), yet it decays into the original constituents (27), as a result of which the neutron synthesis can be assumed to be *reversible over time*.

The formulation of SIR used in this paper *is not* recommended for the treatment of nuclear fusions (because of the possible violation of causality indicated earlier) in favor of the *Lie-admissible relativity* studied in [24, 42] with an *irreversible axiomatic structure* [103, 104].

The correct classical formulation of SIR should be done on iso-Minkowskian iso-spaces $\hat{M}(\hat{x},\hat{\Omega},\hat{I})$ over iso-fields $\hat{\mathcal{R}}$, while the operator formulation should be done on Hilbert-Myung-Santilli iso-spaces $\hat{\mathcal{H}}$ over iso-complex iso-fields $\hat{\mathcal{C}}$. At the abstract level, SR and SIR coincide by conception and construction. Therefore, by continuing to follow [66] we present below the *projection* of SIR iso-axioms in the conventional Minkowski space $M(x,\eta,I)$ over the field \mathcal{R} . Said iso-axioms are then uniquely and unambiguously characterized by the iso-symmetries reviewed in preceding sections, and are expressed below for the *k-direction*, e.g. that of the third space component,

ISO-AXIOM I: The speed of light within (transparent) physical media is given by the locally varying speed:

$$C = \frac{c}{n_4} \cong c. \quad (151)$$

ISO-AXIOM II: The maximal causal speed within physical

media is given by:

$$V_{max,K} = c \frac{n_k}{n_4}. \tag{152}$$

ISO-AXIOM III: The addition of speeds within physical media follows the isotopic law:

$$V_{tot} = \frac{\frac{v_{1,k}}{n_k} + \frac{v_{2,k}}{n_k}}{1 + \frac{v_1 v_2}{c^2} \frac{n_4^2}{n_k^2}}. \tag{153}$$

ISO-AXIOM IV: The iso-dilation of time, the iso-contraction of lengths, the iso-variation of mass with speed and the mass-energy iso-equivalence (iso-renormalization) within physical media follow the isotopic laws:

$$t'_k = \hat{\gamma}_k t, \tag{154}$$

$$\ell'_k = \hat{\gamma}_k^{-1} \ell, \tag{155}$$

$$m'_k = \hat{\gamma}_k m, \tag{156}$$

$$\hat{E}_k = m V_{max,k}^2 = m_k c^2 \frac{n_k^2}{n_4^2}. \tag{157}$$

ISO-AXIOM V: The frequency shift within physical media follows the isotopic law (for null aberration)

$$\omega_{exp} = \frac{\omega_{sou}}{\hat{\gamma} [1 - \hat{\beta} \text{iso} \cos(\hat{\alpha})]}. \tag{158}$$

To avoid a prohibitive length, in regard to the experimental verifications of Iso-Axioms I–V in classical physics, particle physics, nuclear physics, astrophysics and other fields, we suggest the interested reader to inspect the 1995 [43] and the 2021 upgrade [44].

The following comments are now in order:

3.8.1. Note that the maximal causal speed in SIR is no longer given by the speed of light, and it is given instead by value (152), because *physical media are generally opaque to light*, thus requiring the broader geometric notion $v_{max,k}$ derivable from the expression in (3, 4)-space coordinates

$$\frac{dx_k^2}{n_k^2} - dt^2 \frac{c^2}{n_4^2} = 0. \tag{159}$$

3.8.2. By recalling that we are dealing with inhomogeneous and anisotropic physical media, the reader should be aware that the numeric values of Iso-Axioms (151)–(158) generally vary with the variation of the k -direction.

3.8.3. The sole known geometric representation of the excess mass/excess rest energy of the neutron synthesis, as well as of particle fusions at large (Sect. 3.1), will be done in the next section with Iso-Axiom (157).

3.8.4. When the isotopic element \hat{T} , and therefore, the n -characteristic quantities, solely depend on space time coordinates $\hat{T} = \hat{T}(x)$, $n_\mu = n_\mu(x)$, iso-Minkowskian intervals (00)

coincide with Riemannian intervals [67], and characterize the *Exterior General Iso-Relativity* (EGIR) for the formulation of Einstein’s field equations under the universal Poincaré-Santilli *iso-symmetry* $\hat{\mathcal{P}}(3.1)$ [64] (rather than the known covariance), including the representation of the Schwartzschild metric with the isotopic element (for brevity, see Sect. 8.5, p. 155 on of [44])

$$\hat{T}_{kk} = \frac{\delta_{kk}}{\left(1 - \frac{2M}{r}\right)}, \quad \hat{T}_{44} = 1 - \frac{2M}{r}, \tag{160}$$

with the apparent resolution of the century-old problematic aspects of general relativity [105].

3.8.5. When the isotopic element \hat{T} has the general functional dependence (101), Iso-Axioms I–V characterize the *Interior General Iso-Relativity* (IGIR) which is intended to study the *origin* (rather than the sole description) of the gravitational field, that expectedly occurs in the nuclear structure (see Santilli’s paper [106] from his stay at MIT in 1974–1977), thus including the structure of the neutron (see Sect. 8.6, p. 161 of [44]).

3.9 Relativistic representation of the neutron synthesis

Recall that, under the invariance of the spinorial covering of the Poincaré symmetry $\mathcal{P}(3.1) = \text{SL}(2, \mathbb{C}) \times \mathcal{T}(3.1)$ (which is needed for the spin $S = 1/2$ of the electron), the Dirac equation has provided an exact and time invariant relativistic representation of the *point-like* electron under the *external* field of the proton in the structure of the Hydrogen atom.

The Dirac-Santilli iso-equation (142) has been constructed to attempt the exact and time invariant representation of the *extended* wave packet of the iso-electron within the *extended* proton in the structure of the neutron according to Fig. 3, thus requiring its characterization via the isotopies of the spinorial covering of the Poincaré symmetry $\hat{\mathcal{P}}(3.1) = \widehat{\text{SL}}(2, \hat{\mathbb{C}}) \hat{\times} \hat{\mathcal{T}}(3.1)$, first introduced in the 1995 paper [66] jointly with the Dirac-Santilli iso-equation and the first relativistic representation of the neutron synthesis.

For consistency, the neutron structure model (29) requires that the hadronic angular momentum of the iso-electron \hat{L}_3 be equal to the proton spin \hat{S}_3 , thus requiring that

$$\hat{L}_3 = \hat{S}_3, \quad \hat{L}^2 = \hat{S}^2. \tag{161}$$

From (148) and (150) of the iso-spinorial iso-symmetry $\hat{\mathcal{P}}(3.1)$, we therefore obtain the following two conditions on the characteristic quantities for the basic isotopic element (97) expressed in the symbols $b_\mu = 1/n_\mu$ of [66]

$$\begin{aligned} b_1^{-1} b_2^{-1} &= \frac{1}{2} b_1 b_2, \\ b_1^{-2} b_2^{-2} + b_2^{-2} b_3^{-2} + b_3^{-2} b_1^{-2} &= \\ \frac{1}{4} (b_1^2 b_2^{-2} + b_2^2 b_3^{-2} + b_3^2 b_1^{-2}), \end{aligned} \tag{162}$$

with numeric value confirming the expected spheroidal shape of the neutron (Eqs. (7.2), (7.3), p. 192 of [66])

$$\begin{aligned} b_1^2 = b_2^2 &= \frac{1}{n_1^2} = \frac{1}{n_2^2} = \sqrt{2} = 1.415, \\ b_1 = b_2 &= \frac{1}{n_1} = \frac{1}{n_2} = 1.189. \end{aligned} \quad (163)$$

Consequently, the above relativistic representation is in remarkable axiomatic and numerical agreement with the corresponding non-relativistic value (Sect. 2.3.2) via Bohm's hidden variable (78),

$$\lambda = \sqrt{b_1 b_2} = b = \sqrt{\frac{1}{n_1} \frac{1}{n_2}} = \frac{1}{n} \sqrt{2} = 1.189, \quad (164)$$

by therefore establishing the *compatibility between the non-relativistic and the relativistic structure models (29) of the neutron*.

The value of the third semi-axis $1/b_3^2 = n_3^2$ of the iso-electron can be found by assuming the preservation of the volume V of the original sphere with semi-axes $n_k^2 = 1$, $k = 1, 2, 3$ plus values (162) for the first two semi-axes

$$\begin{aligned} V &= \frac{4}{3} \pi (n_1^2)^2 n_3^2 = 4.192 \left(\frac{1}{1.415} \right)^2 n_3^2 = 4.19, \\ n_3^2 &= \frac{4.19}{2.087} = 2.007, \end{aligned} \quad (165)$$

resulting in the values

$$n_1^2 = n_2^2 = 0.707, \quad n_3^2 = 2.007, \quad (166)$$

suggesting that the spheroidal shape of the iso-electron is *prolate* (because $n_3^2 > n_1^2 = n_2^2$).

The representation of the excess energy $\Delta E = 0.782$ MeV in the neutron synthesis from the proton and the electron (7), is done via Iso-Axiom (157), requiring a numeric value of $n_4^2 = 1/b_4^2$ which in this case, represents the density of the *proton*, since the charge of the iso-electron has no dimension.

From Iso-Axiom (157) we obtain the iso-renormalized rest energy of the neutron

$$\begin{aligned} \tilde{E}_n &= m_e c^2 = \\ &= m_e c^2 \frac{b_3^2}{b_4^2} = m_e c^2 \frac{n_3^2}{n_4^2} = 939.565 \text{ MeV}, \end{aligned} \quad (167)$$

from which

$$\frac{b_4^2}{b_3^2} = \frac{n_3^2}{n_4^2} = \frac{1.293}{0.511} = 2.530. \quad (168)$$

From values (166) we then obtain the numeric value of the density n_4^2 which is needed for the iso-renormalization of the mass/rest energy of the iso-electron here presented apparently for the first time

$$n_4^2 = \frac{1}{b_4^2} = \frac{n_3^2}{2.530} = 0.793, \quad n_4 = \frac{1}{b_4} = 0.891, \quad (169)$$

which is compatible with the density $n_4^2 = \frac{1}{b_4^2} = 0.429$ of the fireball of the proton-antiproton annihilation of the Bose-Einstein correlation [107, 108], see Eq. (10.27), p. 127 of [107] (see also [108]).

Intriguingly, taken in *prima facie*, the above data suggest that *the proton is about 50% denser than the proton-antiproton fireball of the Bose-Einstein correlation*.

4 Applications of the neutron synthesis

In this section, we briefly indicate some of the applications of the synthesis/fusion of the proton and the electron into the neutron with related references.

4.1 Detection of smuggled fissile material

Recall that fissile material, such as Uranium-233, Uranium-235 and Plutonium-239, are *metals* that, as such, cannot be distinguished from ordinary metals via all scanning equipment currently available at airports and ports. Thanks to the studies reported in this paper, the U.S. publicly traded company *Thunder Energies Corporation*, (now the private *Hadronic Technologies Co*) did develop, produce and sell a scanner permitting a clear detection of fissile material via the irradiation of baggages with the *Directional Neutron Source* (DNS) of Fig. 5 which produces on demand from a commercially available Hydrogen gas *a beam of thermal neutrons* ($E < 100$ eV) *in the desired direction and intensity*, resulting in a shower of easily detectable radiation from the disintegration of a few fissile nuclei [68]–[80].

It should be noted that various neutron sources are commercially available but they all produce *high energy neutrons* that, as such, are not recommendable for use in public places because of the risk of triggering a chain reaction which is absent for irradiation of fissile material with a controlled small beam of thermal neutrons.

4.2 Representation of nuclear stability

It appears that hadronic mechanics has permitted a quantitative solution of the problem of nuclear instability despite the neutron natural instability (Insufficiency IV of Sect. 1.2) via the *decoupling of the permanently stable electron from the neutron when members of a nuclear structure* (Fig. 6), which was first presented in Appendix C.1 and Fig. 13, p. 152 of [102]. Note that the indicated decoupling introduces a new, very strong, Coulomb *attraction* in the Deuteron structure between the iso-electron and the proton pair. Note also that *the indicated nuclear stability is possible if and only if the proton and the electron are the actual physical constituents of the neutron*.

The resolution of Insufficiency V of Sect. 1.2 (on the nuclear stability despite the very big, repulsive, protonic, Coulomb force) requires separate future studies on the *structure* of the elementary iso-charge.

4.3 Representation of the gravitational stability of the Sun

The Sun releases into light the energy of [109]

$$\Delta E_{out}^{Sun} = 2.3 \times 10^{38} \text{ MeV/s}, \quad (170)$$

which corresponds to about 4.3×10^6 t/s. Since, in a Gregorian year, there are 10^7 seconds, the loss of mass by the Sun per year ΔM_{year}^{Sun} due to light emission is given by

$$\Delta M_{year}^{Sun} = 10^{23} \text{ metric tons per year}. \quad (171)$$

The above loss of mass by the Sun is of such a magnitude to cause a change of planetary orbits that should be detectable by contemporary, sufficiently sensitive instruments in astrophysical laboratories contrary to centuries of measurements on the stability of planetary orbits, i.e. the stability of the Sun's gravitational field.

For these and other reasons, Santilli [110] proposed in 2007 the hypothesis that *the missing energy in the neutron synthesis is provided by the ether conceived as a universal substratum with extremely big energy density*, and that the energy of 0.782 MeV is transferred from the ether to the neutron by a massless, chargeless and spinless *longitudinal impulse* called *etherino* (denoted with the letter *a* from the Latin *aether*) in the *left hand side* of the neutron synthesis

$$\hat{e}^- + a + \hat{p}^+ \rightarrow n. \quad (172)$$

In fact, a medium size star such as our Sun synthesizes about 10^{40} neutrinos per second [13], that requires the total energy of about

$$\Delta E_n^{star} = 7.8 \times 10^{39} \text{ MeV per second}. \quad (173)$$

The etherino hypothesis [110] was formulated on grounds that the energy needed for the neutron synthesis by the Sun (173), is essentially equal to the Sun's loss of energy into light (170). Consequently, the assumption that the missing energy for the neutron synthesis is provided by the ether as a universal substratum permits a quantitative representation of the stability of the Sun's gravitational field.

In any case, the missing energy of 0.782 MeV cannot be provided by the relative kinetic energy between the proton and the electron, because at that value, the $e - p$ cross section is essentially null, thus prohibiting any synthesis. Similarly, said missing energy cannot be provided by the Sun because the total missing energy (173) is so big that the Sun would cool down and never produce light.

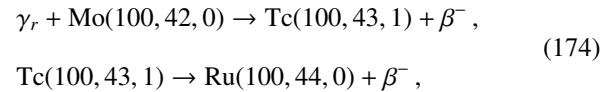
Note that the indicated representation of the gravitational stability of the Sun implies a *return to the continuous creation of matter in the universe* [112], with intriguing implications, e.g. for a realistic representation of the energy released in supernova explosions. Note finally that experiments on the

predictions of the neutrino hypothesis [113] may be numerically representable via the corresponding *predictions* of the etherino hypothesis.

Note also that the indicated gravitational stability of the Sun requires the acceptance of the ether as a universal substratum for the structure and propagation of truly “elementary” particles and electromagnetic waves without any real conflict with special relativity due to our evident inability to reach a reference frame at rest with the ether (for the absence of the “etherial wind” under the indicated conditions, see the 1956 paper [114] and Chapter 3 of [32]).

4.4 Stimulated decay of the neutron

The hypothesis that the neutron is a hadronic bound state of a proton and an electron implies the *possible stimulated decay of one or more neutrons when members of selected nuclear structures* via irradiation with resonating photons γ_r with energy equal to the total energy of the iso-electron $E_r = E_{\hat{e}} = 1,293$ MeV. Intriguing, said stimulated decay implies the production of nuclear energy without the emission of harmful radiation and without the release of radioactive waste, e.g. as occurring in the stimulated decay [115]



which has been tentatively verified by the experimental team [117] (see also [83]). Regrettably, no physics laboratory contacted by the author has shown interest to date in dismissing or confirming Tsagas' results via the repetition of the very simple and inexpensive measurements of transmutation (174) (see Fig. 7 for details).

4.5 The pseudo-proton hypothesis

The synthesis of the neutron via Rutherford's “compression” of an electron within the dense proton, implies the synthesis, in statistical smaller amounts of *negatively charged, strongly interacting particles* preliminarily confirmed by tests [118], such as: the *protoid* \tilde{p}_1^- with spin 0, mass essentially that of the neutron and mean-life predicted to be of about 7 s, and the *pseudo-proton* \tilde{p}_2^- with spin 1/2, mass equal to that of the neutron and mean-life of the order of 5 s, both representable with the synthesis/fusion $\tilde{p}^- = (\hat{e}^-, n)_{hm}$.

Note that, being negatively charged and strongly interacting, *protoids and pseudo-protons are attracted by nuclei* with new nuclear transmutations here expressed for N protoids

$$N \tilde{p}_1^- + N(Z, A, J) \rightarrow \tilde{N}(Z - N, A + N, J), \quad (175)$$

having an evident significance for possible new forms of nuclear energies and recycling of nuclear waste.

4.6 Recycling of nuclear waste

Due to known public opposition, it appears that the sole possible recycling of radioactive nuclear waste should be done by the nuclear power plants themselves via their stimulated decay. Unfortunately, the latter recycling is prohibited by quantum mechanics with ensuing mainstream academic opposition against its study. Interested readers may be interested to know that hadronic mechanics predicts a number of mechanisms for the recycling of radioactive nuclear waste via their stimulated decay triggered by irradiation with thermal neutrons (Sect. 4.1 and Fig. 5), pseudo-protons (Sect. 4.5) as well as other means, and ensuing production of new nuclear energy (see, for brevity, Sect. 8.2.10-II, p. 111 of [44] and [115, 116]).

4.7 Resolution of the Coulomb barrier for nuclear fusion

In the author's view, the most important environmental implication of the synthesis/fusion of the proton and the electron into the neutron is the consequential synthesis/fusion, under the extremely strong Coulomb attraction (6), of at least a pair negatively charged electrons generally coupled in singlet and a positively charged Deuteron into a new negatively charged nucleus $\tilde{D}(-1, 2, 1)$, called *pseudo-Deuteron* with sufficiently long mean life (of the order of $\tau = 1$ s) to be attracted by a natural, positively charged Deuteron, resulting in a new nuclear fusion, called *HyperFusion*, without the historical Coulomb barrier that has prevented the achievement to date of new clean nuclear energies (see [102] for brevity).

5 Reduction of matter to protons and electrons

During his graduate studies at the University of Torino, Italy, in the mid 1960's, after learning that stars initiate their lives as aggregates of Hydrogen atoms, R. M. Santilli accepted the historical hypothesis [1, 2] that matter is composed of the permanently stable protons and electrons, and could not accept the various opposing arguments [10] on grounds that Heisenberg's uncertainty principle has been experimentally verified solely for *point-like particles* (i.e. as the electron) in vacuum under electromagnetic/Hamiltonian interactions. In line with the 1935 legacy by A. Einstein, B. Podolsky and N. Rosen that *quantum mechanics is not a complete theory* [3], Santilli argued that the same principle should not be applied to the *extended protons and neutrons under strong nuclear interactions* without due scrutiny.

Subsequently, Santilli learned from experimental measurements [16, 18] that nuclear volumes are generally *smaller* than the sum of the volumes of the constituents, thus implying that the hyper-dense protons and neutrons are in conditions of partial mutual penetration in a nuclear structure. In turn, this implies the expectation that strong nuclear forces have a contact-zero range, non-linear, non-local and non-potential, thus non-Hamiltonian component under which *Heisenberg's*

uncertainty principle cannot be consistently formulated, let alone tested.

In the late 1970's, when he was at Harvard University under DOE support, Santilli proposed the foundation of the EPR completion of quantum into *hadronic mechanics* for the invariant representation of extended nucleons under Hamiltonian and non-Hamiltonian interactions [23, 24]. He then initiated in 1981 studies [4] on the *completion of Heisenberg's uncertainties for strong interactions* via generalized uncertainties of the type (Eq. (2.18), p. 654 of [4])

$$\Delta r \times \Delta p \approx \frac{1}{2} \hbar F(r, p, \psi, \dots), \quad F > 0, \quad (176)$$

and conducted systematic mathematical, theoretical, experimental and industrial studies (reported in the preceding sections) on the synthesis/fusion of a proton and an electron into the neutron.

Santilli became aware in the early 1990's that mathematical and physical theories can be completed into a form representing the astrophysical evidence that the neutron, and therefore all matter in the universe, is a collection of suitable bound states of the permanently stable protons and electrons. Final studies in the field are reported in this section on the explicit form of the uncertainty principle which is applicable under the most general possible, Hamiltonian and non-Hamiltonian strong nuclear forces.

In 1964, J. S. Bell published the theorem below under the assumption of quantum mechanics according to its Copenhagen interpretation, thus including Heisenberg's uncertainty principle, the representation of the spin 1/2 of particles via the SU(2)-invariant Pauli matrices, and other assumptions:

THEOREM 5.1 [119]: *A system of two point-like particles verifying the SU(2) Lie symmetry does not admit a classical counterpart.*

The theorem was proved by showing that a certain expression D^{Bell} (whose numeric value depends on the relative conditions of the two particles) is always *smaller* than the corresponding classical value D^{Clas} ,

$$D^{Bell} < D^{Clas}, \quad (177)$$

for all possible values of D^{Bell} .

The importance of the Theorem 5.1 for the identification of the ultimate constituents of matter is that of *strengthening* the general acceptance of Heisenberg's uncertainty principle for all possible conditions existing in the universe, thus leading to the unverified *assumption* that electrons cannot be members of a nuclear structure (Sect. 1.2).

Following the achievement of maturity of the iso-mathematical and iso-mechanical branches of hadronic mechanics [50, 89], and following the formulation of the $\widehat{SU}(2)$ -iso-invariant Pauli-Santilli iso-matrices reviewed in Sect. 3.6, Santilli proved in 1998 the following:

THEOREM 5.2 [5]: *A system of two extended particles verifying the $\widehat{SU}(2)$ Lie-Santilli iso-symmetry does admit a classical counterpart.*

The theorem was first proved on grounds that contact, zero-range, non-potential interactions are outside the class of unitary equivalence of quantum mechanics, while being fully representable via a non-unitary transformation of quantum mechanical models (21). Consequently, there always exists a non-unitary transformation $UU^\dagger = \hat{I}$ of Bell's quantity D^{Bell} such to verify the equality

$$D^{hm} = U(D^{Bell})U^\dagger \equiv D^{Clas}. \quad (178)$$

Additionally, Santilli conducted a step-by-step isotopic lifting of Bell's proof of Theorem 5.1 via the Pauli-Santilli iso-matrices (139) resulting in the equality (Eq. (5.8), p. 189 of [5])

$$D^{hm} = \frac{1}{2} (\lambda_1 \lambda_2^{-1} + \lambda_1^{-1} \lambda_2) D^{Bell} \equiv D^{class}, \quad (179)$$

which is always verified by particular values of Bohm's hidden variables [91] λ_1 and λ_2 . [5] also provided specific examples of identity (178) in terms of the iso-Minkowski iso-spaces over iso-fields.

Finally, by combining the results of [4] and [5], in 2019 Santilli proved the following:

THEOREM 5.3 [6]: *The iso-standard iso-deviations for iso-coordinates Δr and iso-momenta Δp , as well as their product, progressively approach Einstein's determinism for extended particles in the interior of hadrons, nuclei and stars, and achieve the full determinism at the limit of Schwarzschild's singularity (ss).*

The theorem was proved by showing that the invariance under the Lie-Santilli iso-symmetry $\widehat{SU}(2)$ implies the following property known as *iso-deterministic principle* derived via iso-commutation rules (50) and iso-normalization (41) (see for details Lemma 3.7, p. 34 of review [47] and its Corollary 3.7.1 on the ensuing removal of divergencies here ignored for brevity)

$$\begin{aligned} \Delta r \Delta p &\approx \frac{1}{2} \langle \hat{\psi}(\hat{r}) | \hat{\times} [\hat{r}, \hat{p}] \hat{\times} | \hat{\psi}(\hat{r}) \rangle = \\ &= \frac{1}{2} \langle \hat{\psi}(\hat{r}) | \hat{T} [\hat{r}, \hat{p}] \hat{T} | \hat{\psi}(\hat{r}) \rangle = \frac{1}{2} \hbar \hat{T} \ll 1, \quad (180) \\ \{\Delta r \Delta p\}_{ss} &= 0. \end{aligned}$$

Theorem 5.3 then holds in view of the fact that the isotopic element has always values smaller than $\hat{T} \ll 1$, from the fitting of all experimental data dealing with hadronic media [43], and the value of the isotopic element is null for gravitational collapse (160) $\hat{T}_{ss} = 0$.

It is easy to see that Theorems 5.2 and 5.3 resolve Objection 1.1 and 1.2 against electrons being members of a nuclear

structure. In fact, under iso-principle (180), electrons would have the *sub-luminal speed*

$$v \geq \frac{\hbar}{\Delta r \times m_e} = 5.79 \hat{T} 10^{10} \text{ m/s}, \quad \hat{T} \ll 1. \quad (181)$$

Similarly, the linear momentum uncertainty would have the value

$$\Delta p = 1.05 \hat{T} 10^{20} \text{ kg m/s}, \quad \hat{T} \ll 1, \quad (182)$$

as a result of which the energy of the electrons can be the expected value $E_{\hat{e}} = 1.293 \text{ MeV}$, thus being much less than the 18.5 MeV predicted via Heisenberg's uncertainty principle (4). The understanding is that the final numerical values of the isotopic element for the neutron require additional studies as well as experimental measurements. Objection 1.3 has been resolved in Section 2.3.3 by showing that excessive value (5) of the magnetic moment of the electron for nuclear standards is counterbalanced by the magnetic moment of the constrained angular momentum within the proton structure.

In conclusion, rather than adapting experimental evidence to a preferred theory, it appears that mathematical and physical methods can indeed be completed to verify the evidence that the permanently stable proton and electron are the constituents of the neutron, with ensuing reduction of all matter in the universe to protons and electron in conditions of increasing complexity.

Acknowledgements

The author would like to express sincere thanks for penetrating critical comments received from the participants of the 2020 *International Teleconference on the EPR argument*, the 2021 *International Conference on Applied Category Theory and Graph-Operad-Logic dedicated to the memory of Prof. Zbigniew Oziewicz* and the *Seminars on Fundamental Problems in Physics*. Additional thanks are due to various colleagues for technical controls and to Mrs. Sherri Stone for linguistic control of the manuscript. However, the author is solely responsible for the content of this paper due to several revisions in its final form.

Received on June 5, 2023

References

1. Kmane A. S. *Introductory Nuclear Physics*. Wiley, 2008.
2. Encyclopedia Britannica. Structure of the nucleus. www.britannica.com/science/atom/Structure-of-the-nucleus
3. Einstein A., Podolsky B. and Rosen N. Can quantum-mechanical description of physical reality be considered complete? *Phys. Rev.* 1935, v. 47, 777–780. www.eprdebates.org/docs/epr-argument.pdf
4. Santilli R. M. Generalization of Heisenberg's uncertainty principle for strong interactions. *Hadronic J.*, 1981, v. 4, 642–663. www.santilli-foundation.org/docs/generalized-uncertainties-1981.pdf
5. Santilli R. M. Isorepresentation of the Lie-isotopic $SU(2)$ Algebra with Application to Nuclear Physics and Local Realism. *Acta Applicandae Mathematicae*, 1998, v. 50, 177–190. www.santilli-foundation.org/docs/Santilli-27.pdf

6. Santilli R. M. Studies on the classical determinism predicted by A. Einstein, B. Podolsky and N. Rosen. *Ratio Mathematica*, 2019, v. 37, 5–23. www.eprdebates.org/docs/epr-paper-ii.pdf
7. Santilli R. M. A quantitative representation of particle entanglements via Bohm's hidden variables according to hadronic mechanics. *Progress in Physics*, 2022, v. 18, 131–137. www.santilli-foundation.org/docs/pip-entanglement-2022.pdf
8. Santilli R. M. and Sobczyk G. Representation of nuclear magnetic moments via a Clifford algebra formulation of Bohm's hidden variables. *Scientific Reports*, 2022, v. 12, 1–10. www.santilli-foundation.org/Santilli-Sobczyk.pdf
9. Heisenberg W. Über den anschaulichen Inhalt der quantentheoretischen Kinematik und Mechanik. *Zeitschrift für Physik*, 1927, v. 43, 172–198., springer.com/article/10.1007/BF01397280
10. Amsh B. Non-existence of electrons in the nucleus. winnerscience.com/applications-of-heisenbergs-uncertainty-principle-non-existence-of-electrons-in-the-nucleus
11. KAERI Table of Nuclide. [//pripyat.mit.edu/KAERI/](http://pripyat.mit.edu/KAERI/)
12. Vonsovsk S. Magnetism of Elementary Particles. Mir Publishers, 1975.
13. Oberauer L., Ianni A. and Serenelli A. Solar Neutrino Physics. Wiley, 2020.
14. Egil A. and Ore A. Binding Energy of the Positronium Molecule. *Phys. Rev.*, 1947, v. 71, 493–521.
15. Rau S., *et al.* Penning trap measurements of the deuteron and the HD^+ molecular ion. *Nature*, 2020, v. 585, 43–47.
16. Science Direct. Helium nucleus. www.sciencedirect.com/topics/mathematics/helium-nucleus
17. Wietfeldt F. E. Measurements of the Neutron Lifetime. *Atoms*, 2018, v. 6, 1–19. www.mdpi.com/2218-2004/6/4/70
18. Pohl R., Antognini A. and Kottmann F. The size of the proton. *Nature*, 2010, v. 466, 213–216.
19. Rutherford E. The Existence of a Neutron, Bakerian Lecture: Nuclear Constitution of Atoms. *Proc. Roy. Soc. A*, 1920, v. 97, 374–382.
20. Santilli R. M. Need of subjecting to an experimental verification the validity within a hadron of Einstein special relativity and Pauli exclusion principle. *Hadronic Journal*, 1978, v. 1, 574–901. www.santilli-foundation.org/docs/santilli-73.pdf
21. Blatt J. M. and Weisskopf V. F. Theoretical Nuclear Physics. Wiley and Sons, 1952.
22. Santilli R. M. Initiation of the representation theory of Lie-admissible algebras of operators on bimodular Hilbert spaces. *Hadronic J.*, 1979, v. 3, 440–467. www.santilli-foundation.org/docs/santilli-1978-paper.pdf
23. Santilli R. M. Foundation of Theoretical Mechanics, Vol. I The Inverse Problem in Newtonian Mechanics. Springer-Verlag, Heidelberg, Germany, 1978. www.santilli-foundation.org/docs/Santilli-209.pdf
24. Santilli R. M. Foundation of Theoretical Mechanics, Vol. II Birkhoffian Generalization of Hamiltonian Mechanics. Springer-Verlag, Heidelberg, Germany, 1983. www.santilli-foundation.org/docs/santilli-69.pdf
25. Aringazin A. K., Jannussis A., Lopez F., Nishioka M. and Veljanosky B. Santilli's Lie-Isotopic Generalization of Galilei and Einstein Relativities. Kostakaris Publishers, Athens, Greece, 1991. www.santilli-foundation.org/docs/Santilli-108.pdf
26. Sourlas D. S. and Tsagas Gr. T. Mathematical Foundation of the Lie-Santilli Theory. Ukraine Academy of Sciences, 1993. www.santilli-foundation.org/docs/santilli-70.pdf
27. Lohmus J., Paal E. and Sorgsepp L. Non-associative Algebras in Physics. Hadronic Press, 1994. www.santilli-foundation.org/docs/Lohmus.pdf
28. Kadeisvili J. V. Santilli's Isotopies of Contemporary Algebras, Geometries and Relativities, 2nd ed. Ukraine Academy of Sciences, 1997. www.santilli-foundation.org/docs/Santilli-60.pdf
29. Jiang C.-X. Foundations of Santilli Isonumber Theory. International Academic Press, 2001, www.i-b-r.org/docs/jiang.pdf
30. Ganfornina R. M. F. and Valdes J. N. Fundamentos de la Isotopia de Santilli. International Academic Press, 2001. www.i-b-r.org/docs/spanish.pdf. English translation: *Algebras, Groups and Geometries*, 2015, v. 32, 135–308. www.i-b-r.org/docs/Aversa-translation.pdf
31. Davvaz B and Vougiouklis Th. A Walk Through Weak Hyperstructures and H_0 -Structures. World Scientific, 2018.
32. Gandzha I. and Kadeisvili J. V. New Sciences for a New Era: Mathematical, Physical and Chemical Discoveries of Ruggero Maria Santilli. Sankata Printing Press, Nepal. 2011. www.santilli-foundation.org/docs/RMS.pdf
33. Georgiev S. Foundations of IsoDifferential Calculus Vols. I to VI. Nova Publishers, New York, 2014 on.
34. Georgiev S. Iso-Mathematics. Lambert Academic Publishing, 2022.
35. Proceedings of the First International Conference on Nonpotential Interactions and their Lie-Admissible Treatment, Part D: Contributed Papers. *Hadronic J.*, 1982, v. 5 (5). www.santilli-foundation.org/docs/hj-5-5-1982.pdf
36. Proceedings of the First Workshop on Hadronic Mechanics. *Hadronic J.*, 1983, v. 6 (6). www.santilli-foundation.org/docs/hj-6-6-1983.pdf
37. Proceedings of the Second Workshop on Hadronic Mechanics, Vol. I. *Hadronic J.*, 1984, v. 7 (5). www.santilli-foundation.org/docs/hj-7-5-1984.pdf
38. Proceedings of the Second Workshop on Hadronic Mechanics, Vol. II. *Hadronic Journal*, 1984, v. 7 (6). www.santilli-foundation.org/docs/hj-7-6-1984.pdf
39. Proceedings of the third international conference on the Lie-admissible treatment of non-potential interactions. Kathmandu University, Nepal, 2011. Vol. I: www.santilli-foundation.org/docs/2011-nepal-conference-vol-1.pdf. Vol. II: www.santilli-foundation.org/docs/2011-nepal-conference-vol-2.pdf
40. Beghella-Bartoli S. and Santilli R. M., Editors. Proceedings of the 2020 Teleconference on the Einstein-Podolsky-Rosen argument that 'Quantum mechanics is not a complete theory'. Curran Associates, New York, NY. 2021.
41. Santilli R. M. Elements of Hadronic Mechanics, Vol. I Mathematical Foundations. Ukraine Academy of Sciences, Kiev, 1995. www.santilli-foundation.org/docs/Santilli-300.pdf
42. Santilli R. M. Elements of Hadronic Mechanics, Vol. II Theoretical Foundations. Ukraine Academy of Sciences, Kiev, 1995. www.santilli-foundation.org/docs/Santilli-301.pdf
43. Santilli R. M. Elements of Hadronic Mechanics, Vol. III Experimental verifications. Ukraine Academy of Sciences, Kiev, 2016. www.santilli-foundation.org/docs/elements-hadronic-mechanics-iii.compressed.pdf
44. Santilli R. M. Overview of historical and recent verifications of the Einstein-Podolsky-Rosen argument and their applications to physics, chemistry and biology. APAV - Accademia Piceno Aprutina dei Velati, Pescara, Italy, 2021. www.santilli-foundation.org/epr-overview-2021.pdf
45. Dunning-Davies J. A Present Day Perspective on Einstein-Podolsky-Rosen and its Consequences. *Journal of Modern Physics*, 2021, v. 12, 887–936.
46. Santilli R. M. Studies on A. Einstein, B. Podolsky and N. Rosen prediction that quantum mechanics is not a complete theory, I: Basic methods. *Ratio Mathematica*, 2020, v. 38, 5–69. eprdebates.org/docs/epr-review-i.pdf

47. Santilli R. M. Studies on A. Einstein, B. Podolsky and N. Rosen prediction that quantum mechanics is not a complete theory, II: Apparent proof of the EPR argument. *Ratio Mathematica*, 2020, v. 38, 71–138. eprdebates.org/docs/epr-review-ii.pdf
48. Santilli R. M. Studies on A. Einstein, B. Podolsky and N. Rosen prediction that quantum mechanics is not a complete theory, III: Illustrative examples and applications. *Ratio Mathematica*, 2020, v. 38, 139–222. eprdebates.org/docs/epr-review-iii.pdf
49. Anderson R. Outline of Hadronic Mathematics, Mechanics and Chemistry as Conceived by R. M. Santilli. *Journal of Modern Physics*, 2016, v. 6, 1–106. www.santilli-foundation.org/docs/HMMC-2017.pdf
50. Santilli R. M. Nonlocal-Integral Isotopies of Differential Calculus, Mechanics and Geometries. *Rendiconti Circolo Matematico Palermo*, 1996, Suppl. v. 42, 7–82. www.santilli-foundation.org/docs/Santilli-37.pdf
51. Santilli R. M. Invariant Lie-isotopic and Lie-admissible formulation of quantum deformations. *Found. Phys.*, 1997, v. 27, 1159–1177. www.santilli-foundation.org/docs/Santilli-06.pdf
52. Chadwick J. *Proc. Roy. Soc. A*, 1932, v. 136, 692–723.
53. Rapports du Septième Conseil de Physique Solvay. Gauthier Villars, Paris, 324, 1933. www.worldcat.org/title/23422639?oclcNum=23422639
54. Fermi E. Nuclear Physics. University of Chicago Press, 1949.
55. Norman R. and Dunning-Davies J. Hadronic paradigm assessed: neutroid and neutron synthesis from an arc of current in hydrogen gas. *Hadronic Journal*, 2017, v. 40, 119–132. santilli-foundation.org/docs/norman-dunning-davies-hj.pdf
56. Borghi C., Giori C. and Dall’Olio A. *Communications of CENUFPE*, Numbers 8 (1969) and 25 (1971), reprinted in *Phys. Atomic Nuclei*, 1993, v. 56, 205–221.
57. Santilli R. M. Isotopies of Lie Symmetries, I: Basic theory. *Hadronic J.*, 1985, v. 8, 8–35. www.santilli-foundation.org/docs/santilli-65.pdf
58. Santilli R. M. Isotopies of Lie Symmetries, II: Isotopies of the rotational symmetry. *Hadronic J.*, 1985, v. 8, 36–52. www.santilli-foundation.org/docs/santilli-65.pdf
59. Santilli R. M. Rotational isotopic symmetries. ICTP communication No. IC-91-261, 1991. www.santilli-foundation.org/docs/Santilli-148.pdf
60. Santilli R. M. Isotopic Lifting of the $SU(2)$ Symmetry with Applications to Nuclear Physics. *JINR rapid Comm.*, 1993, v. 6, 24–38. <http://www.santilli-foundation.org/docs/Santilli-19.pdf>
61. Santilli R. M. Lie-isotopic Lifting of Special Relativity for Extended Deformable Particles. *Lettere Nuovo Cimento*, 1983, v. 37, 545–555. www.santilli-foundation.org/docs/Santilli-50.pdf
62. Santilli R. M. Lie-isotopic Lifting of Unitary Symmetries and of Wigner’s Theorem for Extended and Deformable Particles. *Lettere Nuovo Cimento*, 1983, v. 38, 509–521. www.santilli-foundation.org/docs/Santilli-51.pdf
63. Santilli R. M. Lie-isotopic generalization of the Poincaré symmetry. classical formulation, ICTP communication No. IC/91/45, 1991. www.santilli-foundation.org/docs/Santilli-140.pdf
64. Santilli R. M. Nonlinear, Nonlocal and Noncanonical Isotopies of the Poincaré Symmetry. *Moscow Phys. Soc.*, 1993, v. 3, 255–269. www.santilli-foundation.org/docs/Santilli-40.pdf
65. Santilli R. M. Isotopies of the spinorial covering of the Poincaré symmetry. Comm. of the JINR, Dubna, Russia, No. E4-93-352, 1993. www.santilli-foundation.org/docs/JINR-E4-93-352.pdf
66. Santilli R. M. Recent theoretical and experimental evidence on the cold fusion of elementary particles. *Chinese J. System Eng. and Electr.*, 1995, v. 6, 177–199. www.santilli-foundation.org/docs/Santilli-18.pdf
67. Santilli R. M. Isominkowskian Geometry for the Gravitational Treatment of Matter and its Isodual for Antimatter. *Intern. J. Modern Phys.*, 1998, v. D7, 351–407. www.santilli-foundation.org/docs/Santilli-35.pdf
68. Santilli R. M. Apparent consistency of Rutherford’s hypothesis on the neutron as a compressed hydrogen atom. *Hadronic J.*, 1990, v. 13, 513–533. <http://www.santilli-foundation.org/docs/Santilli-21.pdf>
69. Santilli R. M. Apparent consistency of Rutherford’s hypothesis on the neutron structure via the hadronic generalization of quantum mechanics, nonrelativistic treatment. ICTP communication IC/91/47, 1992. www.santilli-foundation.org/docs/Santilli-150.pdf
70. Santilli R. M. The synthesis of the neutron according to hadronic mechanics and chemistry. *Journal Applied Sciences*, 2006, v. 5, 32–47.
71. Santilli R. M. Recent theoretical and experimental evidence on the synthesis of the neutron. Communication of the JINR, Dubna, Russia, No. E4-93-252, 1993.
72. Santilli R. M. Recent theoretical and experimental evidence on the synthesis of the neutron. *Chinese J. System Eng. and Electr.*, 1995, v. 6, 177–195. www.santilli-foundation.org/docs/Santilli-18.pdf
73. Santilli R. M. The Physics of New Clean Energies and Fuels According to Hadronic Mechanics, Special issue. *Journal of New Energy*, 1998. www.santilli-foundation.org/docs/Santilli-114.pdf
74. Santilli R. M. Apparent confirmation of Don Borghi’s experiment on the laboratory synthesis of neutrons from protons and electrons. *Hadronic J.*, 2007, v. 30, 29–41. www.i-b-r.org/NeutronSynthesis.pdf
75. Santilli R. M. Confirmation of Don Borghi’s experiment on the synthesis of neutrons. arXiv: physics/0608229v1.
76. Burande C. S. On the experimental verification of Rutherford-Santilli neutron model. *AIP Conf. Proc.*, 2013, v. 158, 693–721. www.santilli-foundation.org/docs/Burande-2.pdf
77. Santilli R. M. and Nas A. Confirmation of the Laboratory Synthesis of Neutrons from a Hydrogen Gas. *Journal of Computational Methods in Sciences and Eng.*, 2014, v. 14, 405–414. www.hadronictechnologies.com/docs/neutron-synthesis-2014.pdf
78. Santilli R. M. Apparent Nuclear Transmutations without Neutron Emission Triggered by Pseudoprotons. *American Journal of Modern Physics*, 2015, v. 4, 15–18.
79. Haan V. de. Possibilities for the Detection of Santilli Neutroids and Pseudo-protons. *American Journal of Modern Physics*, 2015, v. 5, 131–136.
80. Norman R., Beghella Bartoli S., Buckley B., Dunning-Davies J., Rak J. and Santilli R. M. Experimental Confirmation of the Synthesis of Neutrons and Neutroids from a Hydrogen Gas. *American Journal of Modern Physics*, 2017, v. 6, 85–104. www.santilli-foundation.org/docs/confirmation-neutron-synthesis-2017.pdf
81. Driscoll Bohrs R. B. Atom Completed: the Rutherford-Santilli Neutron. *APS Conf. Proc.*, 2003, April 5-8, APR03. ui.adsabs.harvard.edu/abs/2003APS.APR.D1009D/abstract
82. Chandrakant S. and Burande C. S. On the Rutherford-Santilli Neutron Model. *AIP Conf. Proc.*, 2015, v. 1648, 51000-1–51000-6. [www.santilli-foundation.org/docs/1.4912711\(CS-Burande\(1\)\).pdf](http://www.santilli-foundation.org/docs/1.4912711(CS-Burande(1)).pdf)
83. Kadeisvili J. V. The Rutherford-Santilli Neutron. *Hadronic J.*, 2005, v. 31, 1–125. www.i-b-r.org/Rutherford-Santilli-II.pdf
84. Burande C. S. Santilli Synthesis of the Neutron According to Hadronic Mechanics. *American Journal of Modern Physics*, 2016, v. 5, 17–36. www.santilli-foundation.org/docs/pdf3.pdf
85. Beghella-Bartoli S. Significance for the EPR Argument of the Neutron Synthesis from Hydrogen and of a New Controlled Nuclear Fusion without Coulomb Barrier. Proceedings of the 2020 Teleconference on the EPR argument, Curran Associates Conference Proceedings, New York, 459–466, 2021.
86. Santilli R. M. The notion of non-relativistic isoparticle. ICTP release IC/91/265, 1991. www.santilli-foundation.org/docs/Santilli-145.pdf

87. Santilli R. M. Isotopic Generalizations of Galilei and Einstein Relativities, Vol. I Mathematical Foundations. International Academic Press, 1991. www.santilli-foundation.org/docs/Santilli-01.pdf
88. Santilli R. M. Isotopic Generalizations of Galilei and Einstein Relativities, Vol. II Classical Formulations. International Academic Press, 1991. www.santilli-foundation.org/docs/Santilli-61.pdf
89. Santilli R. M. Isonumbers and Genonumbers of Dimensions 1, 2, 4, 8, their Isoduals and Pseudoduals, and 'Hidden Numbers' of Dimension 3, 5, 6, 7. *Algebras, Groups and Geometries*, 1993, v. 10, 273–295. www.santilli-foundation.org/docs/Santilli-34.pdf
90. Myung H. C. and Santilli R. M. Modular-isotopic Hilbert space formulation of the exterior strong problem. *Hadronic Journal*, 1982, v. 5, 1277–1366. www.santilli-foundation.org/docs/Santilli-201.pdf
91. Bohm D. A Suggested Interpretation of the Quantum Theory in Terms of 'Hidden Variables'. *Phys. Rev.*, 1952, v. 85, 166–182. journals.aps.org/pr/abstract/10.1103/PhysRev.85.166
92. Santilli R. M. Isotopic Generalizations of Galilei and Einstein Relativities, Vol. I Mathematical Foundations. International Academic Press, 1991. www.santilli-foundation.org/docs/Santilli-01.pdf
93. Santilli R. M. Isotopic Generalizations of Galilei and Einstein Relativities, Vol. II Classical Formulations. International Academic Press, 1991. www.santilli-foundation.org/docs/Santilli-61.pdf
94. Santilli R. M. Isodual Theory of Antimatter with Application to Antigravity, Grand Unification and the Spacetime Machine. Springer Nature, 2001. www.santilli-foundation.org/docs/santilli-79.pdf
95. Santilli R. M. Can strong interactions accelerate particles faster than the speed of light? *Lettere Nuovo Cimento*, 1982, v. 33, 145. www.santilli-foundation.org/docs/Santilli-102.pdf
96. Santilli R. M. Universality of special isorelativity for the invariant description of arbitrary speeds of light. arXiv: physics/9812052.
97. Santilli R. M. Compatibility of Arbitrary Speeds with Special Relativity Axioms for Interior Dynamical Problems. *American Journal of Modern Physics*, 2016, v. 5, 143. www.santilli-foundation.org/docs/ArbitrarySpeeds.pdf
98. Santilli R. M. Representation of the anomalous magnetic moment of the muons via the Einstein-Podolsky-Rosen completion of quantum into hadronic mechanics. *Progress in Physics*, 2021, v. 17, 210–215. www.santilli-foundation.org/muon-anomaly-pp.pdf
99. Santilli R. M. Representation of the anomalous magnetic moment of the muons via the novel Einstein-Podolsky-Rosen entanglement Guzman J. C., Ed. Scientific Legacy of Professor Zbigniew Oziewicz: Selected Papers from the International Conference Applied Category Theory Graph-Operad-Logic. Word Scientific, in press. www.santilli-foundation.org/ws-rv961x669.pdf
100. Santilli R. M. Relativistic hadronic mechanics: nonunitary, axiom-preserving completion of relativistic quantum mechanics. *Found. Phys.*, 1997, v. 27, 625–655. www.santilli-foundation.org/docs/Santilli-15.pdf
101. Muktibodh A. S. and Santilli R. M. Studies of the Regular and Irregular Isorepresentations of the Lie-Santilli Isotheory. *Journal of Generalized Lie Theories*, 2007, v. 11, 1–7. www.santilli-foundation.org/docs/isorep-Lie-Santilli-2017.pdf
102. Santilli R. M., Apparent Resolution of the Coulomb Barrier for Nuclear Fusions Via the Irreversible Lie-admissible Branch of Hadronic Mechanics. *Progress in Physics*, 2022, v. 18, 138–163. www.ptep-online.com/2022/PP-64-09.pdf
103. Santilli R. M. Initiation of the representation theory of Lie-admissible algebras of operators on bimodular Hilbert spaces. *Hadronic J.*, 1979, v. 3, 440–467. www.santilli-foundation.org/docs/santilli-1978-paper.pdf
104. Santilli R. M. Lie-admissible invariant representation of irreversibility for matter and antimatter at the classical and operator levels. *Nuovo Cimento*, 2006, v. B121, 443–485. www.santilli-foundation.org/docs/Lie-admiss-NCB-I.pdf
105. Flapf P. Einstein's General Relativity or Santilli's Iso-Relativity? eprdebates.org/general-relativity.php
106. Santilli R. M. Partons and Gravitation: some Puzzling Questions. *Annals of Physics*, 1974, v. 83, 108–132. <http://www.santilli-foundation.org/docs/Santilli-14.pdf>
107. Santilli R. M. Nonlocal formulation of the Bose-Einstein correlation within the context of hadronic mechanics. *Hadronic J.*, 1992, v. 15, 1–50 and v. 15, 81–133. www.santilli-foundation.org/docs/Santilli-116.pdf
108. Cardone F. and Mignani R. Nonlocal approach to the Bose-Einstein correlation. *JETP*, 1996, v. 83, 435. www.santilli-foundation.org/docs/Santilli-130.pdf
109. American Chemical Society. Energy from the Sun. www.acs.org/content/acs/en/climate-science/energybalance/energyfromsun.html
110. Santilli R. M. The etherino and/or the neutrino Hypothesis? *Found. Phys.*, 2007, v. 37, 670–695. www.santilli-foundation.org/docs/EtherinoFoundPhys.pdf
111. Santilli R. M. Perché lo spazio é rigido. (Why space is rigid). Il Pungolo Verde, Campobasso, Italy, 1956. www.santilli-foundation.org/docs/rms-56-english.pdf
112. Rigamonti A. and Carretta P. Structure of Matter. Springer Nature, 2015.
113. Kikawa T. Measurement of Neutrino Interactions and Three Flavor Neutrino Oscillations in the T2K Experiment. Springer Nature, 2016.
114. Santilli R. M. Perché lo spazio é rigido. (Why space is rigid). Il Pungolo Verde, Campobasso, Italy, 1956. English translation: www.santilli-foundation.org/docs/rms-56-english.pdf
115. Santilli R. M. Hadronic energy. *Hadronic J.*, 1994, v. 17, 311–325. www.santilli-foundation.org/docs/hadronic-energy.pdf
116. Santilli R. M. Apparent Nuclear Transmutations without Neutron Emission Triggered by Pseudoprotons. *American Journal of Modern Physics*, 2015, v. 4, 15–18.
117. Tsagas N. F., Mystakidis A., Bakos G., Sfetelis L., Koukoulis D. and Trassanidis S. Experimental verification of Santilli's clean subnuclear hadronic energy. *Hadronic Journal*, 1996, v. 19, 87–90. www.santilli-foundation.org/docs/N-Tsagas-1996.pdf
118. Santilli R. M. Apparent Experimental Confirmation of Pseudoprotons and their Application to New Clean Nuclear Energies. *International Journal of Applied Physics and Mathematics*, 2019, v. 9, 72–100. www.santilli-foundation.org/docs/pseudoproton-verification-2018.pdf
119. Bell J. S. On the Einstein Podolsky Rosen paradox. *Physics*, 1964, v. 1, 195 (1964).

LETTERS TO PROGRESS IN PHYSICS**Calculation of Outgoing Longwave Radiation
in the Absence of Surface Radiation of the Earth**

Y. C. Zhong

ERICHEN Consulting, Queensland, Australia. E-mail: drzhong88@yahoo.com

Based on the observed equilibrium at the surface of the earth, it is argued that almost no infrared radiation would be emitted by the surface of the earth that is in physical contact with the nearest isothermic air layer. By assuming the outgoing longwave radiation is the cumulative upward thermal radiation by the air, an analytic formula with four dependent observables is proposed which is used for the first time to calculate the effective air emissivities at different lapse rates in the troposphere. Given the observed global mean outgoing longwave radiation 239 W m^{-2} and the stable tropospheric lapse rate 6.5 K km^{-1} , the calculated effective air emissivity near the surface is 0.135, in agreement with early experimental observations.

1 Introduction

It has been recently shown that the earth is capable of self-regulating outgoing infrared radiation without changing the long-term global mean surface temperature [1]. In line with this study, it becomes clear that the radiation cooling at the surface seems unrealistically overestimated. Since 1896, it has been assumed that the surface of the earth emits infrared at radiation flux close to 390 W m^{-2} , similar to a blackbody at its thermal equilibrium temperature 288 K in vacuum, based on a model atmosphere that is physically separated from the surface [2,3]. Nevertheless, it could be argued that the widely used assumption cannot be justified in the presence of the isothermic gaseous atmosphere that is physically attached to the surface. At such a thermodynamic equilibrium, the net energy transfer between the condensed-matter surface and the nearest layer of air should be negligible if not zero. This implies that the surface infrared radiation should be absent as far as the long-term global climate stability is concerned, which is supported by recent experimental measurements that the proportion of the non-radiative heat and mass transfer at the sea level is close to 99.6% [4]. In light of this argument, an analytical formula is introduced to directly calculate the outgoing longwave radiation (OLR) in the absence of the surface infrared radiation as reported in this Letter.

2 Formulation

In the absence of the atmosphere, the thermal temperature of vacuum space is close to 4 K. Under this condition, the terrestrial infrared radiation intensity can be described by the Stefan-Boltzmann law,

$$I = \sigma T_S^4. \quad (1)$$

where σ is the Stefan-Boltzmann constant, T_S is the thermal equilibrium temperature of the condensed-matter surface that is approximated as a blackbody. However, (1) becomes in-

valid as the temperature gradient should be zero at the surface in the presence of the gaseous atmosphere. Thus, it is reasonable to assume that the OLR is merely the cumulative thermal radiation by the atmosphere from different isothermic layers. Further, it is assumed that the effective air emissivity ϵ is scaled by the air density, viz.

$$\epsilon = \epsilon_0 \frac{\rho}{\rho_0}. \quad (2)$$

where ρ is the air density with its value at the surface $\rho_0 = 1.225 \text{ kg m}^{-3}$, respectively; ϵ_0 is the atmospheric emissivity measured near the surface. To be specific, the vertical air density distribution in this study is written as

$$\rho = \rho_0 \exp(-0.135z). \quad (3)$$

where z is the altitude in km. The assumption (2) is consistent with the fact that the air thermal radiation must vanish in the absence of air molecules in the atmosphere. By approximating each thin atmospheric layer as isothermic with its local thermal equilibrium temperature, the OLR in W m^{-2} observable at the top of the atmosphere can be formulated in terms of the Stefan-Boltzmann law by the following integral

$$\text{OLR} = \int_0^\infty \epsilon \sigma T_a^4 dz. \quad (4)$$

where T_a denotes the atmospheric temperature at different altitudes.

3 Calculation

To proceed further, the troposphere and the stratosphere from the ground to altitude 85 km are divided into four parts whose vertical temperature distributions can be approximated as a step-wise linear function based on the International Standard Atmosphere [5]. Substituting (2) and (3) into (4) and integrating in each of the four parts yields

$$\text{OLR} = \epsilon_0 \sigma (A + B + C + D), \quad (5)$$

where

$$A = \int_0^a (T_s - Lz)^4 \exp(-0.135z) dz \quad (6)$$

$$B = \int_a^{20} (210)^4 \exp(-0.135z) dz \quad (7)$$

$$C = \int_{20}^{50} (164 + 2.3z)^4 \exp(-0.135z) dz \quad (8)$$

$$D = \int_{50}^{85} (389 - 2.2z)^4 \exp(-0.135z) dz, \quad (9)$$

where L denotes the lapse rate in the troposphere, the altitude a is dependent of L . Notice that $T_a = T_s$ at the surface in (6). It is apparent that the OLR is determined by two variables, the lapse rate and the effective air emissivity close to the surface when the surface temperature is fixed. It is found that the integration is nearly a constant above 85 km, as the air density exponentially decreases with the altitude. For the lapse rate 6.5 K km^{-1} , the calculated effective air emissivity near the surface is 0.135. The range of the calculated effective air emissivity, 0.12 to 0.16, for the lapse rates between 4 K km^{-1} and 10.5 K km^{-1} is consistent with some early observed atmospheric emissivities [6].

Using the observed long-term global mean OLR value, 239 W m^{-2} , the explicit dependence of the effective emissivity on the lapse rate can be fitted with a linear function with $R^2 = 0.996$,

$$\epsilon_0 = 0.0065L + 0.091. \quad (10)$$

By way of extrapolation, it is predicted that the effective emissivity of the atmosphere near the surface is 0.091 as the troposphere becomes isothermic. Besides, when the effective air emissivity and the lapse rate are fixed at 0.135 and 6.5 K km^{-1} , respectively, it is found that the calculated OLR also linearly depends on the surface temperature with $R^2 = 0.999$, viz.

$$\text{OLR} = 3.24 T_s - 695.49, \quad (11)$$

which gives the gradient

$$\frac{d(\text{OLR})}{dT_s} = 3.24 \text{ W m}^{-2} \text{K}^{-1}. \quad (12)$$

4 Discussion and conclusion

To explore the implications of the zero surface radiation hypothesis, the outgoing thermal radiation by the air is formulated and quantitatively calculated in the absence of the surface infrared radiation. Based on the calculation, it appears that long-term global climate stability might be simply explained in relation to the tropospheric lapse rate, adjustable by changing the water vapor in the troposphere, that provides a natural mechanism to control the OLR for the earth to re-emit the absorbed solar radiation back to outer space while

keeping the global mean surface temperature constant. Further, it is revealed that the four coupled variables, namely OLR, effective air emissivity, the tropospheric lapse rate, and the surface temperature, are *linearly* dependent on each other, as shown in (10) and (11). So far, the linear dependence of the monthly mean OLR on the sea surface temperature (SST) has been observed on several locations [7], but the theoretical interpretations in terms of water vapor feedback and speculated emergent properties seem complicated and confined to the cloud-free observations [8]. By way of contrast, (11) is simply deduced from the hypothesis that the surface radiation is zero.

Without invoking the greenhouse effect, it seems the current global energy balance can be quantitatively explained, i.e. the solar shortwave radiation at the surface, 161 W m^{-2} , is completely transferred into the atmosphere by means of convection and conduction and then is thermally radiated by the atmosphere into outer space, together with the shortwave absorption by the atmosphere at 78 W m^{-2} , which makes the OLR at the top of the atmosphere equal to

$$161 + 78 = 239 \text{ W m}^{-2}$$

as observed [3]. Further experimental observations both in lab and in space are necessary for further evaluating this proposed description with fundamental implications for understanding the long-term global climate stability.

Acknowledgements

This work was inspired by the paper by Svante Arrhenius published in 1896.

Received on June 19, 2023

References

1. Zhong Y.C. A quantitative description of atmospheric absorption and radiation at equilibrium surface temperature. *Progress in Physics*, 2021, v. 17 (2), 151–157.
2. Arrhenius S. On the influence of carbonic acid in the air upon the temperature of the ground. *Phil. Mag.*, 1896, v. 41, 251.
3. Wild M. Progress and challenges in the estimation of the global energy balance. *Conference Proceedings*, 2017, v.1810, 020004.
4. Shula T. unpublished results.
5. Standard Atmosphere. ISO 2533:1975, 1975.
6. Brooks F. A. Observation of atmospheric radiation. *Pap. Phys. Ocean. Meteor. Mass. Inst. Tech. and Woods Hole Ocean. Instn*, 1941, v. 8 (2), 23 pp.
7. Raval A., Oort A. H. Ramaswamy V., Observed Dependence of outgoing longwave radiation on sea surface temperature and moisture. *Journal of Climate*, 1994, v. 4 (2), 807–821.
8. Koll D. D. B. and Cronin T. W. Earth's outgoing longwave radiation linear due to H_2O greenhouse effect. *PNAS*, 2018, v. 115 (41), 10293–10298.

Natural Metrology in Physics of Numerical Relations

Hartmut Müller

Rome, Italy

E-mail: hm@interscalar.com

The paper introduces the natural electron metrology that is based on the electron mass, the speed of light in a vacuum, and the Planck constant. Since the units of the electron metrology are natural, their application gives physical meaning to the numerical properties of the readings and allows to identify and predict physical effects caused by numerical relations. In this paper, the electron metrology is applied to real systems of coupled periodic processes, in particular to the solar system and exoplanetary systems. It is shown that the application of the electron metrology allows to define numerical conditions for lasting stability and to identify evolutionary trends.

Introduction

In physics, measurement is the source of data that allows to develop and verify theoretical models of reality. The result of a measurement is the ratio of physical quantities where one of them is the reference quantity called unit of measurement. Obviously, the value of this ratio depends on the chosen unit of measurement. Moreover, any change of the unit of measurement changes also the numerical properties of the value. For example, a 20 cm microwave and a 7.874... inch microwave both have the same wavelength. However, 20 is integer, but 7.874... is not. Thus, an arbitrarily chosen unit of measurement results in random values of the measured ratios. In this case, also the numerical properties of the measured values are random, and their physical interpretation has no sense. This is why in theoretical physics numerical ratios usually remain outside the realm of interest.

The situation changes fundamentally, if we choose natural units of measurement, for instance, a natural frequency of a real periodical process. In this case, all the harmonics have rational values. Thus, the use of natural units gives physical meaning to the numerical properties of the readings. Now the numerical properties of the measured frequencies provide information about whether they are harmonics or not.

Indeed, the history of metrology shows a clear trend to natural units of measurement. For instance, the current SI definition [1] of a second is based on the radiation corresponding to the transition between the two hyperfine levels of the ground state of the caesium-133 atom. One second takes 9,192,631,770 periods of this radiation. However, the number of periods is arbitrarily chosen. Therefore, in the current definition, one second is not a natural unit of measurement, although it is based on the frequency of a natural subatomic process. Also the current SI unit meter is not a natural unit as it is based on the current definition of a second.

The current SI definition of the kilogram is based on the fixed numerical value of the Planck constant, expressed in units of meter and second. Therefore, one kilogram is not a natural unit of measurement. Consequently, all secondary units of measurement based on kilogram, meter and second

cannot be considered natural. Therefore, the current SI is not a system of natural units.

The concept of natural units was first introduced in 1874, when George Stoney [2], noting that electric charge is quantized, derived units of length, time, and mass, now named Stoney units in his honor. Stoney chose his units so that the Newtonian gravitational constant, the speed of light in a vacuum, and the electron charge would be numerically equal to 1. In 1899, Max Planck proposed a system of units that is based on the quantum of action. Planck underlined the universality of the new system, writing [3]: ... it is possible to set up units for length, mass, time and temperature, which are independent of special bodies or substances, necessarily retaining their meaning for all times and for all civilizations, including extraterrestrial and non-human ones, which can be called natural units of measure. Planck derived units for length, time, mass, and temperature from the Newtonian gravitational constant, the speed of light, the quantum of action, and the Boltzmann constant.

Regrettably, using Newton's gravitational constant G increases not only the uncertainty of the Planck system, but also its dependence on theoretical assumptions. The constancy of G is only postulated, its value is measured in laboratory scale only, and there is no guaranty of its universality in astronomical scales, because the mass of a planet, planetoid or moon cannot be measured without using G .

In [4] we proposed a system of natural units that is based on the electron mass, the speed of light in a vacuum, the Planck constant, and the Boltzmann constant. The only difference to the Planck system is that we use the electron mass instead of G . However, this difference seems to be significant enough to give physical meaning to the numerical properties of the readings.

In [5] we have shown that in electron units, the masses of elementary particles including the proton have numerical values that approximate integer and reciprocal integer powers of Euler's transcendental number $e = 2.71828...$

As we have shown in [6], the orbital and rotational periods of the planets, planetoids and large moons of the solar

system have numerical values that approximate integer powers of Euler’s number, if expressed in electron units (table 1). This we have shown also for 1430 exoplanets. Furthermore, the gravitational parameters of the Sun and the planets of the solar system, if expressed in electron units, approximate integer powers of Euler’s number [7].

The electron mass is actually the key component in the natural metrology that we propose in this paper. The electron mass defines an absolute reference value, and the Planck constant in combination with the speed of light are interdimensional converters that allow to derive absolute spatial and temporal reference values, which are the Compton wavelength of the electron, and its natural frequency. The Boltzmann constant allows to derive the electron black body temperature as additional natural unit.

The electron is not a rare substance since it is ubiquitous in the universe. The uniqueness of the electron stems from its elementarity and exceptional stability, with an estimated lifetime of over 10^{28} years. In fact, stability and high precision are fundamental requirements for units of measurement. The electron mass is given with an accuracy of 10^{-10} , as shown in table 1. Since the speed of light and the Planck constant are fixed, the accuracy of the electron metrology depends only on the accuracy of the electron mass.

In the following we will show that the application of the electron metrology gives physical meaning to the numerical properties of the readings and allows to identify and predict physical effects caused by numerical relations. For reasons of clarity, in this paper we deal with periodical processes.

Theoretical Approach

The starting point of our approach is frequency as obligatory characteristic of a periodical process. As the result of a measurement is always a *ratio* of physical quantities, one can measure only *ratios* of frequencies. This ratio is always a real number. Being a real value, this ratio can approximate an integer, rational, irrational algebraic or transcendental number. In [8] we have shown that the difference between rational, irrational algebraic and transcendental numbers is not only a mathematical task, but it is also an essential aspect of stability in systems of coupled periodical processes. For instance, integer frequency ratios, in particular fractions of small integers, make possible parametric resonance that can destabilize such a system [9, 10]. This is why asteroids cannot maintain orbits that are unstable because of their resonance with Jupiter [11]. These orbits form the Kirkwood gaps that are areas in the asteroid belt where asteroids are absent.

According to this idea, irrational frequency ratios should not cause destabilizing parametric resonance, because irrational numbers cannot be represented as a ratio of integers. However, algebraic irrational numbers, being real roots of algebraic equations, can be converted to rational numbers by multiplication. For example, $\sqrt{2} = 1.41421\dots$ cannot be

ELECTRON UNITS	DEFINITION	VALUE
Electron rest energy	$E = m/c^2$	0.51099895000(15) MeV
Angular frequency	$\omega = E/\hbar$	$7.76344 \cdot 10^{20}$ Hz
Oscillation period	$\tau = 1/\omega$	$1.28809 \cdot 10^{-21}$ s
Compton wavelength	$\lambda = c/\omega$	$3.86159 \cdot 10^{-13}$ m

Table 1: Basic units of the electron metrology. The units are calculated from the measured electron rest energy. The speed of light c in a vacuum, and the Planck constant \hbar are fixed. Data from Particle Data Group [12].

come a frequency scaling factor in real systems of coupled periodical processes, because $\sqrt{2} \cdot \sqrt{2} = 2$ creates the conditions for the occurrence of parametric resonance. Thus, only transcendental ratios can prevent parametric resonance, because they cannot be converted to rational or integer numbers by multiplication. Actually, it is transcendental numbers that define the preferred frequency ratios which allow to avoid destabilizing parametric resonance [13]. In this way, transcendental frequency ratios sustain the lasting stability of coupled periodical processes.

Among all transcendental numbers, Euler’s number $e = 2.71828\dots$ is unique, because its real power function e^x coincides with its own derivatives. In the consequence, Euler’s number allows avoiding parametric resonance between any coupled periodical processes including their derivatives.

Because of this unique property of Euler’s number, we expect that periodical processes in real systems prefer frequency ratios close to Euler’s number and its roots. For rational exponents, the natural exponential function is always transcendental [14]. The natural logarithms of those frequency ratios are therefore close to integer or reciprocal integer values, which are attractors of transcendental numbers of the type e^x , as we have shown in [13]. With reference to the evolution of a planetary system and its stability, we may therefore expect that the ratio of any two orbital periods should finally approximate an integer or reciprocal integer power of Euler’s number [15].

The electron shares its exceptional stability with the proton with an estimated lifetime of over 10^{29} years [12]. Within our approach, the stability of the proton results from the numerical properties of the proton-to-electron ratio that approximates the 7th power of Euler’s number and its square root [7]. In this way, the metric properties of the proton can be derived from the metric properties of the electron theoretically.

The eigenfrequencies and harmonics of the proton and the electron are natural frequencies of any type of matter, also of the accreted matter of a planet. Conventional models of the solar system do not take into account this aspect, which lies at the core of our numeric physical approach to the electron metrology. Given the enormous number of protons and electrons that form a planet, eigenresonance must be avoided in

the long term. This affects any periodical process including orbital and rotational motion. This is why the planets in the solar system and in hundreds of exoplanetary systems have orbital periods that approximate integer and rational powers of Euler's number relative to the natural oscillation periods of the proton and the electron, as shown in my paper [6].

In the following, we discuss exemplary applications of the electron metrology to the analysis of orbital and rotational periods in the solar system.

Exemplary Applications

Kepler's laws of planetary motion do not explain why the planets of the solar system have the orbital periods 87.969, 224.701, 365.256, 686.971 days, and 11.862, 29.457, 84.02, 164.8, 247.94 years, because there are infinitely many pairs of orbital periods and distances that fulfill Kepler's laws. Einstein's field equations do not reduce the theoretical variety of possible orbits, but increases it even more.

However, if we express the orbital periods in electron units, we can realize that they approximate integer powers and roots of Euler's number, and in this way, they avoid destabilizing parametric resonance. This requirement reduces dramatically the number of possible orbits.

For instance, if we express Jupiter's orbital period in years (11.862), in days (4332.59) or in seconds ($3.74343 \cdot 10^8$), there is no way to verify whether this value is special or not. If we express Jupiter's orbital period in oscillation periods of the electron, we can realize that it is indeed very special, because it approximates the 66^{th} power of Euler's number:

$$\ln\left(\frac{T_O(\text{Jupiter})}{2\pi \cdot \tau_e}\right) = \ln\left(\frac{3.74343 \cdot 10^8 \text{ s}}{2\pi \cdot 1.28809 \cdot 10^{-21} \text{ s}}\right) = 66.00$$

The same is valid for the orbital period 686.98 days ($5.93551 \cdot 10^7$ seconds) of the planet Mars that equals the 66^{th} power of Euler's number multiplied by the *angular* oscillation period of the electron:

$$\ln\left(\frac{T_O(\text{Mars})}{\tau_e}\right) = \ln\left(\frac{5.93551 \cdot 10^7 \text{ s}}{1.28809 \cdot 10^{-21} \text{ s}}\right) = 66.00$$

Consequently, the Jupiter-to-Mars orbital period ratio is 2π :

$$T_O(\text{Jupiter}) = 2\pi \cdot T_O(\text{Mars})$$

This transcendental ratio allows Mars to avoid parametric orbital resonance with Jupiter. Approaching an integer power of Euler's number relative to the electron's natural period of oscillation prevents both Jupiter's and Mars' periodic orbital motion from provoking electron based eigenresonance. Since the proton-to-electron ratio approximates an integer power of Euler's number and its square root, both planets avoid also proton based eigenresonance.

In [16] we have shown that integer and rational powers of $e = 2.71828 \dots$ and $\pi = 3.14159 \dots$ form two complementary fractal scalar fields of transcendental attractors – the *Euler field* and the *Archimedes field*.

The rotational periods of planets and planetoids of the solar system approximate integer powers of Euler's number and its square root relative to the angular oscillation period of the electron. Since the proton-to-electron ratio approximates the 7^{th} power of Euler's number and its square root, the rotational periods approximate integer powers of Euler's number relative to the angular oscillation period of the proton, as we have shown in [16].

For instance, the current sidereal rotational period of the Earth equals 23 h, 56 min and 4.1 s, or 86164.1 s. In general, the duration of the sidereal day should increase, because it is believed that the rotation of the Earth is slowing down. Indeed, if we express the sidereal rotational period of the Earth in electron units, we can realize that it must increase in order to reach the 59^{th} power of Euler's number and its square root:

$$\ln\left(\frac{T_R(\text{Earth})}{\tau_e}\right) = \ln\left(\frac{86164.1 \text{ s}}{1.28809 \cdot 10^{-21} \text{ s}}\right) = 59.47$$

However, our numeric physical approach suggests that the rotation of the Earth will slow down only until the sidereal day reaches a duration of 24 hours, 47 minutes and 1 second, or 89221 s that corresponds with the Euler-attractor:

$$\tau_e \cdot e^{59} \cdot \sqrt{e} = 89221 \text{ s}$$

When the sidereal period of rotation has reached that Euler-attractor, the rotation of the Earth should be stabilized, and should not slow down more. By the way, the sidereal rotational period of the planet Mars 24 hours, 37 minutes and 22.7 seconds, or 88642.7 s is much closer to that attractor:

$$\ln\left(\frac{T_R(\text{Mars})}{\tau_e}\right) = \ln\left(\frac{88642.7 \text{ s}}{1.28809 \cdot 10^{-21} \text{ s}}\right) = 59.49$$

Probably, smaller bodies with faster rotation can reach numerical attractors faster than larger bodies. The sidereal rotational period 9.07417 h = 32667 s of the planetoid Ceres, for example, has already reached an Euler-attractor:

$$\ln\left(\frac{T_R(\text{Ceres})}{\tau_e}\right) = \ln\left(\frac{32667 \text{ s}}{1.28809 \cdot 10^{-21} \text{ s}}\right) = 58.50$$

In general, every prime, irrational or transcendental number generates a unique fundamental fractal field of its own integer and rational powers that causes physical effects which are typical for that number.

For instance, integer and rational powers of 2 and 3 generate two different fractal scalar fields – the fundamental binary and the fundamental ternary fields, which are the strongest providers of parametric resonance.

On the contrary, the golden ratio $\phi = (\sqrt{5} + 1)/2 = 1.618 \dots$ makes difficult its rational approximation, since its continued fraction does not contain large denominators. So, the fundamental field of its integer and rational powers should be a perfect inhibitor of resonance amplification. This is why

the Venus-to-Earth orbital period ratio approximates $1/\phi$, as already shown by Butusov [17] in 1978.

In [16] we have proposed to name this field after Hippasus of Metapontum who was an ancient Greek philosopher and early follower of Pythagoras, and is widely credited with the discovery of the existence of irrational numbers, and the first proof of the irrationality of the golden ratio.

Although the golden ratio is irrational, it is a Pisot number, so its powers are getting closer and closer to whole numbers, for example, $\phi^{10} = 122.99\dots$. This is why the Hippasus field can inhibit resonance within small frequency ranges only. Hence, in systems with many coupled periodic processes, the Hippasus field can produce two opposing effects: over small frequency ranges, the Hippasus field can inhibit parametric resonance, but over large frequency ranges, it provides the long-period appearance of resonance amplification. Euler's number is not a Pisot number, so that the Euler field permits coupled periodic processes to avoid parametric resonance also over very large frequency ranges. As we have shown in [6, 7], typical examples are the orbital and rotational periods of planets and planetoids.

Conclusion

The use of natural units of measure gives physical meaning to the numerical properties of the readings and allows the study of physical effects caused by their numerical relations.

In the case of frequency ratios, the readings are real numbers that can approximate integer, rational, irrational algebraic or transcendental values.

In application to real systems of coupled periodic processes, transcendental numerical relations can avoid destabilizing parametric resonance and provide lasting stability.

In units of the electron metrology (table 1), the orbital and rotational periods of large bodies of the solar system approximate integer powers of Euler's number and its roots multiplied by the natural oscillation period of the electron. This we have verified [6] also for 1430 exoplanets.

The perihelion and aphelion of a planetary orbit, if expressed in units of the electron metrology, give the lower and upper approximations of integer powers of Euler's number, as we have shown in [7]. As a consequence, the gravitational parameters of the Sun and its planets, if expressed in electron units, approximate integer powers of Euler's number.

The maxima in the frequency distribution of the number of stars as function of the distance between them, expressed in electron units, correspond with integer powers of Euler's number and its roots. In [18] we have shown this for 18336 interstellar distances in the solar neighborhood.

All these findings allow us to interpret the approximation of integer powers of Euler's number and its roots as general evolutionary trend.

In this context, also the current temperature 2.726 K of the cosmic microwave background radiation (CMBR) does

not appear as to be accidental. In [8] we have shown that this temperature, if expressed in electron units, approximates an integer power of Euler's number. Consequently, it is very unlikely that the temperature of the CMBR will still decrease. This conclusion contradicts the big bang model of a cooling down universe. However, a resonating with protons and electrons fulfilling the entire cosmic space microwave radiation could probably impede the formation of molecules essential for life. By obeying the Euler field, the CMBR allows life to arise. From this point of view, the Euler field can be seen as a promoter of life on a cosmic scale.

Acknowledgements

The author is grateful to Oleg Kalinin, Viktor Bart, Alexandr Beliaev, Michael Kauderer, Ulrike Granögger, Clemens Kuby and Leili Khosravi for valuable discussions.

Submitted on July 1, 2023

References

1. The International System of Units. International Bureau of Weights and Measures, 2019, ISBN 978-92-822-2272-0
2. Barrow J. D. Natural Units Before Planck. *Quarterly Journal of the Royal Astronomical Society*, vol. 24, pp. 24–26.
3. Planck M. Über Irreversible Strahlungsvorgänge. *Sitzungsbericht der Königlich Preußischen Akademie der Wissenschaften*, 1899, v.1, 479–480.
4. Müller H. Scale-Invariant Models of Natural Oscillations in Chain Systems and their Cosmological Significance. *Progress in Physics*, 2017, v. 13, 187–197.
5. Müller H. Fractal Scaling Models of Natural Oscillations in Chain Systems and the Mass Distribution of Particles. *Progress in Physics*, 2010, v. 6, 61–66.
6. Müller H. Physics of Transcendental Numbers meets Gravitation. *Progress in Physics*, 2021, vol. 17, 83–92.
7. Müller H. Physics of Transcendental Numbers as Forming Factor of the Solar System. *Progress in Physics*, 2022, v. 18, 56–61.
8. Müller H. On the Cosmological Significance of Euler's Number. *Progress in Physics*, 2019, v. 15, 17–21.
9. Dombrowski K. Rational Numbers Distribution and Resonance. *Progress in Physics*, 2005, v. 1, no. 1, 65–67.
10. Panchelyuga V.A., Panchelyuga M. S. Resonance and Fractals on the Real Numbers Set. *Progress in Physics*, 2012, v. 8, no. 4, 48–53.
11. Minton D. A., Malhotra R. A record of planet migration in the main asteroid belt. *Nature*, Vol. 457, 1109–1111, (2009).
12. Workman R. L. et al. (Particle Data Group), *Prog. Theor. Exp. Phys.*, 083C01 (2022), www.pdg.lbl.gov
13. Müller H. The Physics of Transcendental Numbers. *Progress in Physics*, 2019, vol. 15, 148–155.
14. Hilbert D. Über die Transcendenz der Zahlen e und π . *Mathematische Annalen*, 43, 216–219, (1893).
15. Müller H. Global Scaling of Planetary Systems. *Progress in Physics*, 2018, v. 14, 99–105.
16. Müller H. Physics of Irrational Numbers. *Progress in Physics*, 2022, vol. 18, 103–109.
17. Butusov K. P. The Golden Ratio in the Solar system. *Problems of Cosmological Research*, vol. 7, Moscow–Leningrad, 1978.
18. Müller H. Physics of Transcendental Numbers Determines Star Distribution. *Progress in Physics*, 2021, vol. 17, 164–167.

PROGRESS IN PHYSICS

A Scientific Journal on Advanced Studies in Theoretical and Experimental Physics, including Related Themes from Mathematics. This journal is registered with the Library of Congress (DC, USA).

Electronic version of this journal:
<http://www.ptep-online.com>

Editorial Board

Pierre Millette
millette@ptep-online.com
Andreas Ries
ries@ptep-online.com
Florentin Smarandache
fsmarandache@gmail.com
Ebenezer Chifu
ebenechifu@yahoo.com

Postal Address

Department of Mathematics and Science,
University of New Mexico,
705 Gurley Ave., Gallup, NM 87301, USA

Copyright © *Progress in Physics*, 2023

All rights reserved. The authors of the articles do hereby grant *Progress in Physics* non-exclusive, worldwide, royalty-free license to publish and distribute the articles in accordance with the Budapest Open Initiative: this means that electronic copying, distribution and printing of both full-size version of the journal and the individual papers published therein for non-commercial, academic or individual use can be made by any user without permission or charge. The authors of the articles published in *Progress in Physics* retain their rights to use this journal as a whole or any part of it in any other publications and in any way they see fit. Any part of *Progress in Physics* howsoever used in other publications must include an appropriate citation of this journal.

This journal is powered by L^AT_EX

A variety of books can be downloaded free from the Digital Library of Science:
<http://fs.gallup.unm.edu/ScienceLibrary.htm>

ISSN: 1555-5534 (print)

ISSN: 1555-5615 (online)

Standard Address Number: 297-5092

Printed in the United States of America

December 2023

Vol. 19, Issue 2

CONTENTS

Noh Y. J. Interpretation of Quantum Mechanics in Terms of Discrete Time I	109
Thomas G. F. The Arrow of Time and Its Irreversibility	115
Müller H. Fractal Quantization of Speed in Physics of Numerical Relations	153
Consiglio J. From Particle Physics to Cosmology, on the Gravitational Sub-structure of Everything	156
Zhang T. X., Salonis C. Gamow Theory for Diproton Decays of Proton-Rich Heavy Nuclei ⁴⁵ Fe and ⁶⁷ Kr	178
Meng X. Surprising Results from Experiments of a Longitudinally Separated Slit	183
Raief H. Scalar Field Effects on the Space-Time Continuum and the Appearance of the Rest-Mass	188

Information for Authors

Progress in Physics has been created for rapid publications on advanced studies in theoretical and experimental physics, including related themes from mathematics and astronomy. All submitted papers should be professional, in good English, containing a brief review of a problem and obtained results.

All submissions should be designed in L^AT_EX format using *Progress in Physics* template. This template can be downloaded from *Progress in Physics* home page <http://www.ptep-online.com>

Preliminary, authors may submit papers in PDF format. If the paper is accepted, authors can manage L^AT_EX typing. Do not send MS Word documents, please: we do not use this software, so unable to read this file format. Incorrectly formatted papers (i.e. not L^AT_EX with the template) will not be accepted for publication. Those authors who are unable to prepare their submissions in L^AT_EX format can apply to a third-party payable service for LaTeX typing. Our personnel work voluntarily. Authors must assist by conforming to this policy, to make the publication process as easy and fast as possible.

Abstract and the necessary information about author(s) should be included into the papers. To submit a paper, mail the file(s) to the Editor-in-Chief.

All submitted papers should be as brief as possible. Short articles are preferable. Large papers can also be considered. Letters related to the publications in the journal or to the events among the science community can be applied to the section *Letters to Progress in Physics*.

All that has been accepted for the online issue of *Progress in Physics* is printed in the paper version of the journal. To order printed issues, contact the Editors.

Authors retain their rights to use their papers published in *Progress in Physics* as a whole or any part of it in any other publications and in any way they see fit. This copyright agreement shall remain valid even if the authors transfer copyright of their published papers to another party.

Electronic copies of all papers published in *Progress in Physics* are available for free download, copying, and re-distribution, according to the copyright agreement printed on the titlepage of each issue of the journal. This copyright agreement follows the *Budapest Open Initiative* and the *Creative Commons Attribution-Noncommercial-No Derivative Works 2.5 License* declaring that electronic copies of such books and journals should always be accessed for reading, download, and copying for any person, and free of charge.

Consideration and review process does not require any payment from the side of the submitters. Nevertheless the authors of accepted papers are requested to pay the page charges. *Progress in Physics* is a non-profit/academic journal: money collected from the authors cover the cost of printing and distribution of the annual volumes of the journal along the major academic/university libraries of the world. (Look for the current author fee in the online version of *Progress in Physics*.)

Interpretation of Quantum Mechanics in Terms of Discrete Time I

Young Joo Noh

E-mail: yjnoh777@gmail.com, Seongnam, Korea.

From the discretization of time, the nonlocality of matter and electromagnetic waves can be inferred. These nonlocal waves provide a new perspective on the nonlocality of quantum phenomena, such as wave collapse and entanglement, and the wave-particle duality. Interactions can be divided into bound states and scattering, which are all described by the modified Dirac equation. From the modified Dirac equation, the quantum condition of the bound state can be obtained. Regarding scattering, elastic scattering is related to wave nature, and inelastic scattering is related to particle nature. The wave nature is expressed in all bound states and elastic scattering, and the particle nature corresponds to the case of inelastic scattering. And, in the case of inelastic scattering, a model for wave collapse is presented.

1 Introduction

The significance of this paper is to newly understand quantum mechanics from the point of view of discrete time. Quantum mechanics is a system established by experiment, but its interpretation is diverse. However, it is rare to have a perspective that integrates and coherently interprets the various phenomena of quantum mechanics. The perspective of discrete time is very different from existing interpretations, but it provides an interesting perspective. Since the new perspective is very unfamiliar, I will briefly summarize the contents presented in the previous papers [1–3].

The analysis of the dynamical system from the perspective of discrete time has opened a new way to see things that have not been understood in the existing quantum mechanics or existing results from a completely different perspective. In the first paper [1], from the point of view of discrete time, matter is divided into two types with completely different dynamic principles. Type 1 is an ordinary matter that satisfies the Dirac equation, and type 2 is completely new. Type 2 does not interact with the gauge fields and is only affected by gravity. And considering its energy density, it can be interpreted as dark matter.

Since existing relativistic quantum mechanics cannot explain anomalies during interactions, it has no choice but to lead to quantum field theory that assumes second quantization and vacuum energy. This theory is based on the ontological basis of the statistical mechanical analogy that a field is a collection of independent infinite harmonic oscillators. On the other hand, the type 1 field does not make such an ontological assumption. If type 1 is a free particle, it can be interpreted as an ordinary matter that satisfies the Dirac equation, but the concept of the field is quite different from the existing one. In the type 1 field, the current harmonic oscillation is determined by contributions from the past and future of discrete time Δt . From this point of view, it was shown that the mass and charge of elementary particles during interactions must be corrected by causal delay, and this correction

showed that it can explain anomalies such as anomalous magnetic moment and Lamb shift [2,3].

2 The meaning of discrete time

Discrete time means that there is a minimum value of time change, which is a unit of time that cannot be further divided. In other words, it can be said that “time does not pass” from one click of time to the next, and if we consider the hypothetical events on this unit of time, we can infer that they all occurred at the same time. Thus, a discrete unit of time is a collection of simultaneous events.

By the way, this collection of simultaneous events has a special character. Before discussing that, consider the following thought experiment. Observer A is in a car moving at speed v . There is a light source in the middle of the car and light detectors on the front and rear walls of the car. The events in which light reaches both detectors are simultaneous for observer A. However, for B, a stationary observer outside the car, the two events are not simultaneous. Because the car is moving, the light reaching the rear becomes an event that occurs earlier than the light reaching the front. This relativity of simultaneity is a natural result of the special theory of relativity based on the concept of continuous space-time.

However, in discrete time, the relativity of simultaneity is limited. Under the same circumstances, if a car moves by Δl in discrete time Δt , what happens to observer B during which simultaneous events to observer A occur? For observer B, Δt is a situation in which time does not pass from one click to the next click, so the events until the movement by Δl are simultaneous. Thus, within the range of time Δt , simultaneous events for observer A are also simultaneous events for observer B. In other words, in discrete time, local absolute simultaneity is established. Such a discussion holds within Δt . Of course, the relativity of simultaneity is established as time passes beyond the click of Δt . Hypothetical events in Δt do not hold the Lorentz transformation and cannot be expressed in Minkowski space-time, which is based on the concept of continuous space-time. However, since the theory of relativ-

ity is established beyond the Δt click, for example, the time Δt for observer B is $\Delta t' = \Delta t/\gamma$ for observer A. In summary, discrete time can be said to be a collection of events in which local absolute simultaneity is established.

In the previous paper [2], Δt was defined as the time for light to pass through the Compton wavelength of a matter, $\Delta t \stackrel{\text{def}}{=} \frac{\hbar}{mc^2}$. If the Compton wavelength is regarded as the “spatial domain” of a matter, Δt can be regarded as the “temporal domain” of the matter. Therefore, what the above discussion means is that the relativity of simultaneity is established outside matter, and the absoluteness of simultaneity dominates inside matter. Discrete time is not a concept of objective reality that clicks regardless of matter, like Newton’s concept of absolute time, but a unique click inherent in matter.

Let’s find out the characteristics of the field defined in discrete time. Since the field defined in continuous space-time holds the local principle, the local parts of the field can change independently. However, if the field defined in discrete time can change locally and independently, the basic premise of discrete time is violated because time must also change as a variable in response to the change of field. Therefore, a field defined in discrete time cannot be changed locally, and all parts of the field must act simultaneously. That is, a field defined in discrete time cannot be divided.

3 Formation of nonlocal waves

In discrete time, the spinor $\Psi(x^\mu)$ at any point x^μ of type 1 is given by the sum of Δt future and past contributions to x^μ , so that $\Psi(x^\mu)$ evolves into $e^{-i\Delta x^\alpha p_\alpha} \Psi(x^\mu)$ [1]. Eq. (1) and Fig. 1 show this as a formula and figure, respectively.

$$\begin{aligned} (x^\mu + \Delta x^\mu) \Psi(x^\mu) - x^\mu \Psi(x^\mu + \Delta x^\mu) \\ = \Delta x^\mu e^{-i\Delta x^\alpha p_\alpha} \Psi(x^\mu) . \end{aligned} \tag{1}$$

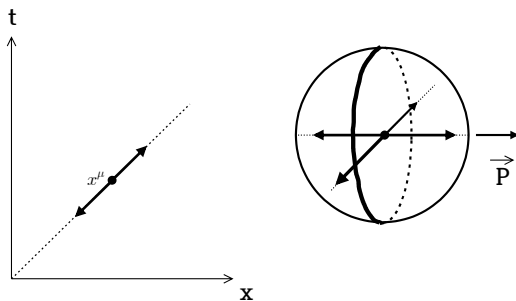


Fig. 1: Contributions of spinors at x^μ .

The left side of Fig. 1 shows spinors contributing from Δt future and past at x^μ , in the 1+1 dimension, and the right side shows them in 3-dimensional real space. All points on the right hemisphere are Δt future and all points on the left hemisphere are past. At the center point, all spinors contributing

from the future appear to the left, and all spinors contributing from the past appear to the right. As discussed in the previous section, all events in the right hemisphere are simultaneous events, and all events in the left hemisphere are also simultaneous events.

Furthermore, spinors at every point on the right hemisphere can also be represented as contributions from future and past spinors. Then, the same sphere can be drawn at every point on the right hemisphere, and this process can be repeated over and over again. As a result, a wavefront with the same phase can be represented as the left side of Fig. 2.

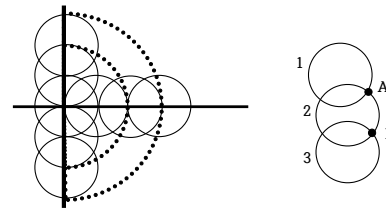


Fig. 2: Formation of simultaneous wavefronts.

By the way, the wavefront formed in this way has special properties. On the right side of Fig. 2, A is the common point of 1 and 2. Point A is simultaneous with all points on hemisphere 1 and also with all points on hemisphere 2. Therefore, all points on hemispheres 1 and 2 are simultaneous with each other. This is established only when hemispheres 1 and 2 overlap. Since this process can continue to expand, all the points on the wavefront shown on the left in Fig. 2 are simultaneous.

This simultaneous wavefront is not local. If we consider the field defined on this wavefront, as discussed in the previous section, it cannot change locally. Interactions occurring at one point on the wavefront occur simultaneously at all points on the wavefront. A wavefront is nonlocal, but the local principle still applies between one wavefront and another. This non-locality of type 1 waves is fundamentally different from the wave concept explained only by the existing local principle.

So far, we have discussed the nonlocality of a type 1 wave, that is, a matter field wave. We will now discuss the nonlocality of electromagnetic waves. The electric and magnetic fields individually obviously apply the local principle. But what about electromagnetic waves? In judging the nonlocality of electromagnetic waves, I will refer again to the proposition discussed earlier. In discrete time, the collection of simultaneous events establishes local absolute simultaneity. Therefore, if a wavefront composed of certain simultaneous events has local absolute simultaneity, it can be judged that the wavefront is a nonlocal wave.

Electromagnetic waves are produced by accelerating electric charge. Around the accelerating charge, there are kinks of the field, and these kinks are what form the wave. The kinks depend on the motion of the charge, and the motion of the charge is performed in units of discrete time Δt . Then, the kinks formed between Δt can also be said to be simultaneous events to the observer fixed on the charge, which, according to the above discussion, can also be said to be simultaneous events to the stationary observer. Therefore, electromagnetic waves can be said to have local absolute simultaneity, so they can be said to be nonlocal waves like matter field waves.

Until now, we have had a somewhat unfamiliar discussion that matter field waves and electromagnetic waves are nonlocal waves. However, in my opinion, the fact that these are nonlocal waves is already included in the existing quantum mechanics. In quantum mechanics, the energy of light is $E = h\nu$. What does this equation mean? If we try to understand it as a wave, there is no local nature of a wave at all. So, it should be understood as a particle, but what does the frequency of a particle mean? The fact that the energy of light does not depend on the local properties of the wave means that the wave is nonlocal. Light is created by kinks, the magnitude of which determines the frequency, and the total kinks form a nonlocal wavefront. An interaction at one point of the wavefront acts simultaneously on all parts of the wavefront. Therefore, the energy of light does not depend on the local properties of the wave, but is proportional only to its frequency.

4 Wave collapse and wave-particle duality

Quantum mechanics has various interpretations depending on the meaning of the wave function and measurement. In this paper, these meanings are as follows. The wavefunction is not a probability concept, but an objective real field, and the measurement is merely the interaction between elementary particles.

Based on the discussion in the previous section, let's infer the wave collapse, which is an intrinsic property of nonlocal waves, and the particle nature of matter and light.

When an electron interacts with an electromagnetic wave, the wavefront of the electron and the wavefront of the electromagnetic wave meet. If one part of the wavefront of an electron is affected by an electromagnetic wave, all parts of the wavefront of an electron are simultaneously affected because of the intrinsic property of nonlocal waves. It is as if all the information of the electron wavefront is concentrated at the point of contact and interacts with the electromagnetic wave. This can be seen as a kind of wave collapse, and it can be said to be the definition of the particle nature of electrons. This discussion can be equally applied to electromagnetic waves interacting with electrons. Electromagnetic waves are also nonlocal waves, and when interacting with electrons, the entire wave is concentrated in a local area, which is the particle

nature of light, that is, the definition of a photon. The electrons and photons concentrated in this local area exchange energy and momentum as particles. In other words, the interaction—which we will discuss in the next section, corresponds to inelastic scattering—occurs on a “quantum” unit. After the interaction, they move as new free waves, each with new energy and momentum. In the next section I will present a mathematical model for the collapse of matter waves.

The wave-particle duality is one of the most important phenomena that reveals the essence of quantum mechanics, and contains a deep mystery about the existence of matter. However, current understanding of this remains superficial. It is difficult to understand that matter or photons choose one state among particle or wave depending on the situation*. If there is a correct theory, there must be a clear reason for having a particular state in a particular situation. The reality of quantum mechanical existence presented in this paper is as follows. A nonlocal wave causes a wave collapse at a specific interaction to acquire particle properties, and when the interaction disappears, the wave properties are restored. This process is repeated.

Speaking of electromagnetism, fields with local properties are real, and their waves (as nonlocal waves) are real, and photons formed by the collapse of waves are real. We discussed earlier that the quantum of a photon energy should depend only on its frequency, but there is one more thing to consider here. When an electromagnetic wave is generated by kinks caused by the acceleration of an electric charge, the amount of the charge becomes a variable of the photon energy. The quantum concept of photon energy is established only when the charge amount of all free elementary particles is the same. In reality it is. That is, quantization of photon energy is established by quantization of charge.

5 Bound state and scattering

In terms of discrete time, interacting particles satisfy the modified Dirac equation [2].

$$D_m \Psi = \left(i\gamma^\mu \partial_\mu - f_{1r} \gamma^\mu p_\mu - f_{2r} \gamma^\mu \Delta p_\mu \right) \Psi = 0. \quad (2)$$

where

$$\begin{aligned} f_{1r} = \text{Re}(f_1) &= \frac{1}{3} \text{Re} \left(\frac{e^{-ix^\alpha} p_\alpha}{e^{-ix^\alpha} p_\alpha + 2(e^{-ix^\alpha} \Delta p_\alpha - 1)} \right) \\ f_{2r} = \text{Re}(f_2) &= \frac{1}{3} \text{Re} \left(\frac{2e^{-ix^\alpha} \Delta p_\alpha}{e^{-ix^\alpha} p_\alpha + 2(e^{-ix^\alpha} \Delta p_\alpha - 1)} \right). \end{aligned} \quad (3)$$

Eq. (2) is a first-order linear differential equation, and the way it is applied differs depending on the type of interaction

*Wheeler's delayed choice experiment clearly shows the contradiction of the existing quantum mechanical view of duality. And the Elitzur-Vaidman bomb tester claims that interaction-free measurements are possible based on the existing viewpoint. In my next paper, I will present a new interpretation of these experiments from the new perspective presented above.

– scattering and bound state. In the case of the scattering process, for example, the scattering of electron and photon interacts in an extremely limited space-time region, so the modified Dirac equation is also applied only in such a limited space-time region. On the other hand, in the case of ceaseless interaction, such as in the bound state, the modified Dirac equation holds without limitation because the interaction occurs in a relatively wide space-time region.

5.1 Bound state

5.1.1 $\Delta p_\mu \ll p_\mu$

In this case, that is, when the interaction is very small, f_{1r} , f_{2r} , and the modified Dirac equation is as follows

$$f_{1r} \cong \frac{1}{3}, \quad f_{2r} \cong \frac{2}{3} \cos(x^\alpha p_\alpha)$$

$$\left(i\gamma^\mu \partial_\mu - \frac{1}{3} \gamma^\mu p_\mu - \frac{2}{3} \cos(x^\alpha p_\alpha) \gamma^\mu \Delta p_\mu \right) \Psi = 0. \tag{4}$$

The solution of (4) satisfies the following equation

$$\partial_\mu \Psi = -\frac{i}{3} (p_\mu + 2 \cos(x^\alpha p_\alpha) \Delta p_\mu) \Psi. \tag{5}$$

And the solution of (5) is as follows

$$\Psi = c \exp \left[-\frac{i}{3} \int^{x^\mu} (p_\mu + 2 \cos(x'^\alpha p_\alpha) \Delta p_\mu) dx'^\mu \right]$$

$$= c \exp \left[-\frac{i}{3} p_\mu x^\mu - \frac{2i}{3} \int^{x^\mu} \cos(x'^\alpha p_\alpha) \Delta p_\mu dx'^\mu \right]. \tag{6}$$

Δp_μ means interaction, so it is determined according to the specific situation. If it is an electrostatic potential like the potential in a hydrogen atom, Δp_μ is independent of the integral variable in (6) because there is only a scalar potential energy component that is independent of time. Thus

$$\Psi = c \exp \left[-\frac{i}{3} (p_\mu x^\mu + 2\epsilon (\Delta p_\mu) \sin(x^\mu p_\mu)) \right]. \tag{7}$$

$\epsilon (\Delta p_\mu)$ is a small quantity linear to Δp_μ . In (7), for Ψ to be a free wave, i.e. harmonic oscillation, $\sin(x^\mu p_\mu) = 0$, so the following quantum condition is derived

$$x^\mu p_\mu = n\pi \quad (n = 0, \pm 1, \pm 2, \dots). \tag{8}$$

For any given p_μ , x^μ that satisfies (8) has as its solution a certain region in space-time. Harmonic oscillations that exist in this region can be referred to as standing waves. As a simple example, consider the case where the electron in a hydrogen atom is in uniform circular motion. In this case, the phase value is as follows

$$\oint (E dt - \vec{P} \cdot d\vec{x}) = E \oint dt - \vec{P} \cdot \oint d\vec{x}$$

$$= -mvr\pi = n\pi \tag{9}$$

$$\therefore L = mvr = n.$$

Eq. (9) agrees with the well-known Bohr’s quantum condition for the hydrogen atom.

In (7), when $\epsilon \rightarrow 0$, the 4-momentum appearing in the phase part is not p_μ but $p_\mu/3$. This result is questionable because the system we are dealing with is a system in which a free particle with 4-momentum p_μ becomes $p_\mu + \Delta p_\mu$ by interaction. However, as we will see later, this does not violate the law of conservation of energy at all.

In the case of $\Delta p_\mu \rightarrow 0$, if $\gamma^\mu p_\mu = m$ is used, (4) can be expressed as follows

$$i \frac{\partial \Psi}{\partial t} = \left(\vec{\alpha} \cdot \hat{P} + \frac{1}{3} \beta m \right) \Psi. \tag{10}$$

In (7), the free wave solution is as follows for $\epsilon \rightarrow 0$

$$\Psi = \begin{pmatrix} \varphi \\ \chi \end{pmatrix} \exp \left(-\frac{i}{3} x^\mu p_\mu \right). \tag{11}$$

In (11), φ and χ are two-component spinors. Using (12), (10) becomes (13)

$$\frac{\partial \Psi}{\partial t} = \frac{1}{3} E \Psi, \quad \hat{P} \Psi = \frac{1}{3} \vec{P} \Psi. \tag{12}$$

$$E \Psi = \left(\vec{\alpha} \cdot \vec{P} + \beta m \right) \Psi. \tag{13}$$

In (13), the energy of Ψ is $\pm \sqrt{\vec{P}^2 + m^2}$, which is equal to the energy of the free particle before interaction. So, as expected, energy is conserved.

5.1.2 $\Delta p_\mu = p_\mu$

In this case, the modified Dirac equation is:

$$\{ i\gamma^\mu \partial_\mu - (f_{1r} + f_{2r}) m \} \Psi = 0. \tag{14}$$

$$G(x^\mu) \stackrel{\text{def}}{=} f_{1r} + f_{2r} = \text{Re} \left(\frac{1}{3 - 2e^{ix^\mu p_\mu}} \right)$$

$$= \frac{3 \cos(x^\mu p_\mu) - 2}{13 - 12 \cos(x^\mu p_\mu)}. \tag{15}$$

In (14), the condition for Ψ to become a plane wave in a specific space-time region is that G must be constant, which means that G has an extreme value in that region. Therefore, the following condition must be satisfied

$$\partial_\lambda G(x^\mu) = -\frac{15 p_\lambda \sin(x^\mu p_\mu)}{(13 - 12 \cos(x^\mu p_\mu))^2} = 0. \tag{16}$$

Eq. (16) is the same quantum condition as in $\Delta p_\mu \ll p_\mu$.

Eq. (14) is related to pair production. If Δp_μ is the 4-momentum of the incident photon and $p_\mu = p_\mu^{\text{electron}} + p_\mu^{\text{positron}}$, that is, the sum of the 4-momentum of the electron and the positron, Ψ in (14) becomes the wave function for the entire

electron and positron. This plane wave will persist until a new interaction occurs. If an interaction occurs on one side (electron) of this free wave, the whole system will be affected at the same time due to the characteristics of nonlocal waves, so the other side (positron) will also “experience the same interaction at the same time”. This can be said to be the mechanism of entanglement.

5.2 Scattering

In the case of elastic scattering, there is no change in the energy of the incident particle. That is, since $\Delta p_0 = 0$ and $|\vec{P}'| = |\vec{P}|$ hold, the incident wave and the reflected wave have the same wavelength, so it is predicted that wave collapse will not occur when they interact. Assuming that the interaction occurs within the range of Δt during elastic scattering, $\Delta p_\mu = 0$ and $f_{1r} = 1/3$ just before and after the interaction, so the following free wave equation is established

$$\left(i\gamma^\mu \partial_\mu - \frac{1}{3}m\right)\Psi = 0. \tag{17}$$

On the other hand, in inelastic scattering, there is a change in the energy of the incident particle and the target particle. This means that the properties of the wave before and after the interaction are different. The mechanism that enables this process is the concept of wave collapse discussed in section 4. During inelastic scattering, a nonlocal wave instantly collapses and becomes a particle state. In this particle state, energy and momentum are exchanged, and as a result, a new wave corresponding to new energy and momentum is formed. We will now present a model for this wave collapse.

When an interaction occurs in a local region in space-time, the modified Dirac equation is also applied only in a local region. In this case, f_{1r} and f_{2r} must, of course, be quantities defined in a local region. Therefore, f_{1r} and f_{2r} must be corrected to converge to 0 at large x^μ . In this case, the collapse of the wave inevitably occurs.

In order to model the wave collapse during inelastic scattering, we introduce a damping factor ϵ_μ that satisfies the following condition

$$x^\mu = (t, |\vec{x}| \hat{n}_{\vec{x}}), \quad \epsilon_\mu = (\epsilon_0, |\vec{\epsilon}| \hat{n}_{\vec{\epsilon}}) \tag{18}$$

$$e^{-\epsilon_\mu x^\mu} \rightarrow 0, \text{ as } x^\mu \rightarrow \infty, \text{ for } \hat{n}_{\vec{x}} \cdot \hat{n}_{\vec{\epsilon}} = -1.$$

And if the new 4-momentum p'_μ is defined as follows, the modified Dirac equation and f'_{1r} , f'_{2r} are as follows. For simplicity, we will discuss wave collapse for the special case $\Delta p_\mu = ap_\mu$ (a is a real number)

$$p'_\mu = p_\mu - i\epsilon_\mu \tag{19}$$

$$\left\{i\gamma^\mu \partial_\mu - (f'_{1r} + af'_{2r})\gamma^\mu p'_\mu\right\}\Psi = 0.$$

where

$$f'_{1r} = \frac{1}{3} \operatorname{Re} \left(\frac{e^{-ix \cdot p'}}{e^{-ix \cdot p'} + 2(e^{-iax \cdot p'} - 1)} \right)$$

$$= \frac{1}{3} \operatorname{Re} \left(\frac{e^{-\epsilon \cdot x} e^{-ix \cdot p}}{e^{-\epsilon \cdot x} e^{-ix \cdot p} + 2(e^{-\epsilon \cdot x} e^{-iax \cdot p} - 1)} \right)$$

$$f'_{2r} = \frac{2}{3} \operatorname{Re} \left(\frac{e^{-iax \cdot p'}}{e^{-ix \cdot p'} e^{-ix \cdot p} + 2(e^{-iax \cdot p'} - 1)} \right)$$

$$= \frac{2}{3} \operatorname{Re} \left(\frac{e^{-\epsilon \cdot x} e^{-iax \cdot p}}{e^{-\epsilon \cdot x} e^{-ix \cdot p} + 2(e^{-\epsilon \cdot x} e^{-iax \cdot p} - 1)} \right).$$
(20)

In (20), both f'_{1r} and f'_{2r} converge to 0 at large x^μ by $e^{-\epsilon_\mu x^\mu}$ factor. Now let's find the solution of (19)

$$\partial_\mu \Psi = -\frac{i}{3} p'_\mu (1 + S') \Psi$$

where $S'(x) = \operatorname{Re} \left(\frac{2(a-1)e^{-\epsilon \cdot x} e^{-iax \cdot p} + 2}{e^{-\epsilon \cdot x} e^{-ix \cdot p} + 2(e^{-\epsilon \cdot x} e^{-iax \cdot p} - 1)} \right).$

(21)

$$\Psi = c \exp \left\{ -\frac{i}{3} p'_\mu \int^{x^\mu} (1 + S') dx'^\mu \right\}$$

$$= c \exp \left\{ -\frac{i}{3} \left(x^\mu p_\mu + p_\mu \int^{x^\mu} S' dx'^\mu \right) \right\} \times$$

$$\times \exp \left(-\frac{1}{3} \epsilon_\mu x^\mu - \frac{1}{3} \epsilon_\mu \int^{x^\mu} S' dx'^\mu \right).$$
(22)

As expected, since the factor $e^{-\frac{1}{3}\epsilon_\mu x^\mu}$ exists in Ψ , it converges to 0 at large t . This means the collapse of the wave.

Of course, these results are different from the concept of simultaneous wave collapse of nonlocal waves discussed above. The reason is the fundamental limitation of the modified Dirac equation. Since the modified Dirac equation does not accurately represent the behavior of non-local waves, but approximates it to the behavior of local waves in continuous space-time, it cannot describe concepts such as simultaneous collapse of waves. But, it can be said that it has value as a model of wave collapse. On the other hand, in the interaction such as the bound state, there is no phenomenon such as wave collapse, but a standing wave is formed, so the modified Dirac equation representing the behavior of a local wave represents the exact behavior of the wave.

6 Conclusions

One of the most important concepts inferred from the discretization of time is the nonlocality of matter and electromagnetic waves. The nonlocality of waves can naturally cause wave collapse when interacting. This state of wave collapse means particle nature and also corresponds to the quantum state. What this paper concludes about the wave-particle duality is that particle and wave properties are not selected by matter according to circumstances, but are determined only

by the way of interaction. It is done by analysis of the modified Dirac equation.

Interactions can be divided into bound states and scattering, which are all described by the modified Dirac equation. Quantum conditions can be obtained in a bound state, which is expected to be the same as in conventional quantum mechanics. Scattering can be divided into elastic scattering and inelastic scattering, both of which are forms of interaction. Elastic scattering is related to wave nature and inelastic scattering is related to particle nature. According to the analysis of the modified Dirac equation, the wave nature is expressed in all bound states and elastic scattering. An example is the Davisson–Germer experiment which demonstrates the wave nature of electrons. The particle nature correspond to the case of inelastic scattering. Examples include the photoelectric effect and Compton scattering.

The particle nature resulting from the collapse of nonlocal waves encompasses the quantum concept of the existing quantum mechanics, and the nonlocal wave concept encompasses the existing classical field. For matter (nonlocal waves, and particle nature due to wave collapse), and for electromag-

netics (classical fields, nonlocal waves, and particle nature due to wave collapse), each stage of existence participates in interaction as a physical reality.

Received on August 1, 2023

References

1. Noh Y.J. Propagation of a Particle in Discrete Time. *Progress in Physics*, 2020, v. 16, 116–122.
2. Noh Y.J. Anomalous Magnetic Moment in Discrete Time. *Progress in Physics*, 2021, v. 17, 207–209.
3. Noh Y.J. Lamb Shift in Discrete Time. *Progress in Physics*, 2022, v. 18, 126–130.
4. Elitzur A. and Vaidman L. Quantum Mechanical Interaction-Free Measurements. *Foundations of Physics*, 1993, v. 23, 987–997.
5. Wheeler J. A. The “Past” and the “Delayed-Choice” Double-Slit Experiment. In: Marlow A. R. *Mathematical Foundations of Quantum Theory*. Academic Press, New York, 1978, pp. 9–48.
6. Penrose R. *The Road to Reality*. Jonathan Cape, 2004.
7. Cohen-Tannoudji C., Diu B., Laloe F. *Quantum Mechanics*. Hermann, Paris, France, 1977.

The Arrow of Time and Its Irreversibility

Gerald F. Thomas

MINOS Technologies Inc., 176-6A The Donway West, Toronto, ON, M3C 2E8, Canada.

E-mail: gthomas@minostechinc.com

Quantum thermodynamics strives to extend classical thermodynamics and nonequilibrium statistical physics to ensembles of sizes below the thermodynamic limit with the full inclusion of quantum effects. This paper uses the nonrelativistic quantum mechanics of a lone system in a thermal bath to relate its wave function's local phase to Lorentz-Faraday forces acting thereon. In the intake of heat from its surroundings, such a system's entropy increases with the gain connected to the gradient field of its local phase whose subharmonicity within the boundary of its volume is a necessary and sufficient condition for it to comply with the second law of thermodynamics (SLT). The thermodynamic arrow of time necessitates irreversible over reversible processes as determined by the gradient field of the phase. Conservative Lorentz-Faraday forces identified herein impress on the system to engender irreversible (reversible) change and entropy gain (stasis) in its exchange of heat with its environment under the discernment of the thermodynamic arrow of time and regardless of the time-reversal symmetry of such venerable frameworks as electrodynamics and quantum mechanics. Entropy production is greatest when the local phase is subharmonic within the system's nominal volume. A means of time-averaging entropy and free energy changes under nonstandard-state conditions with the accommodation of phenomenological relaxation is provided. Both the SLT and Faraday's law of induction are of similar vintage and status. Surprisingly, they share a hitherto unrecognized connection at the microscopic level. Faraday's law of induction is shown to hold for a lone system provided the gradient of its local phase is finite, a necessary and sufficient condition for it not to present with its alleged paradoxes and contradictions despite its technological successes rivalling those of the SLT. There is no evidence to deny the successes of both the SLT and Faraday's law for science and technology. In compliance with Earnshaw's theorem, the potential of the Lorentz-Faraday force is shown to stabilize a lone system just like the Coulomb (or Newtonian) potential while continuing to fulfill the virial theorem. A consequence of the time asymmetry of entropy is the impossibility of travel to the past as to cause entropy changes to decrease contrary to the SLT. Further consequences of entropy's time asymmetry include at least the nonexistence of magnetic monopoles, the observed matter-antimatter asymmetry in leptonic and baryonic matter, and the role of axion-like particles in accounting for the absence of charge-parity violations in strong interactions without necessarily answering for dark matter. Within the range of validity of gravito(electro)magnetism, dark energy is identified as the work done by the Heaviside analog of the Lorentz-Faraday force in causing the accelerated expansion of the Universe without reference to either a finite cosmological constant or an unstable vacuum state transition. In the practice of reductionism, macroscopic physics supervenes upon the microscopic, the SLT being the most conspicuous exception to that superfluous tenet. The supersedence of classical thermodynamics over quantum mechanics and electrodynamics across spatio-temporal scales ranging from an individual quantized system to its known Universe has been shown herein. Additionally, in showing that reversible (irreversible) processes are affiliated with the particle (wave) behavior of matter, attention has been drawn to a heretofore overlooked connection between the different roles of classical thermodynamics and quantum mechanics and electrodynamics in respect to arrow-of-time asymmetry and wave-particle duality.

1 Introduction

1.1 Background and purpose

Charge conjugation (C), parity (P), and time (T) are the three most important discrete symmetries and hold for all physical phenomena in Nature: C symmetry conjugates all charges, P symmetry flips spatial orientations, and T-symmetry reverses

the direction of time. The CPT theorem [1] asserts that any local field theory that is invariant under Lorentz transformations must also be invariant under the combined operation of the three discrete transformations for all fundamental interactions with causality and energy positivity as obligatory, if stealth, constraints [2,3, for e.g.]. The CPT triad is an exact symmetry

with any combination short of the three being a violation of the remainder so that, for example, a violation of CP symmetry is equivalent to a violation of T-symmetry [4]. Essentially, the CPT theorem links the charges C (matter and antimatter) of states with their spacetime PT symmetries. These symmetries are broken in the known Universe as first acknowledged in the early 1950's with the revelation of P asymmetry in weak interactions by Lee and Yang [5] and quickly confirmed by Chien-Shiung Wu and her team [6].

T-asymmetry is what gives rise to our experience of the passage of time. Its basis is the second law of thermodynamics (SLT), the only T-asymmetric law in physics, one which stipulates that the entropy of a system can never decrease. Time symmetry ensures that physical laws follow their time-reversed paths when we imagine reversing time. The SLT says differently. Max Planck, thermodynamicist and one of the founders of quantum physics, remarks [7, loc. cit., pp. 103–104] in respect to the SLT that:

The limitations to the law, if any, must lie in the same province as its essential idea, in the observed Nature, and not in the Observer. That man's experience is called upon in the deduction of the law is of no consequence; for that is, in fact, our only way of arriving at a knowledge of natural law. But the law once discovered must receive recognition of its independence at least in so far as Natural Law can be said to exist independent of Mind. Should any one deny this, he would have to deny the possibility of natural science.

Planck foresaw that a myriad versions of the SLT would be proposed [8–10, for e.g.], not by Nature but by Mind.

T-symmetry is the symmetry of most physical laws under a time-reversal transformation. Physical processes – whether classical or quantum mechanical – are time-symmetric and following Newton's lead, Maxwell, Einstein, and Schrödinger expressed their respective theories in terms of deterministic equations necessitating initial and occasionally boundary conditions on the collegial assumption that there was a beginning and an ambient space from where such evolutions would occur.

It has been known [11] for some time that electroweak interactions in neutral K mesons exhibit a small violation of CP symmetry. Direct CP violation was observed in the KTeV Collaboration [12] so that, by the CPT theorem, T violation must occur. Independently of the CPT theorem (i.e. no assumptions about CP or CPT violation or invariance were made), direct detection of T reversal violation was achieved by the BaBar Collaboration [13] proving that the laws of physics are not identical whether time runs forwards or backwards. So far, CP violations have not been observed [14, 15, et passim] in strong interactions and since there is no known reason for this absence it is referred to as the strong CP problem.

An extensive body of work exists on attempts to measure permanent electric dipole moments (EDMs) of subatomic particles which, with their spin angular momenta, would directly violate both CP and T symmetries [16, et passim]. Current searches for T reversal violations through precision laboratory measurements of the EDMs of atoms and molecules [17–23] are now sufficiently sensitive to detect signatures of some particles with masses of more than 10 TeV. There are many experiments [24, for e.g.] attesting to the inviolability of CPT in Nature. Among the phenomena that the Standard Model of Particle Physics (SM) – and extensions beyond the SM – do not explain include the absence of magnetic monopoles, matter-antimatter asymmetry, neutrino masses, supersymmetry, and gravity. While the possibility of CP violations in the baryon sector was anticipated in 1958 by Okubo [25], it is only lately that such effects beyond the SM have been observed [26, 27].

Nor does the SM provide the connection between microscopic T violations and irreversibility in thermodynamics. Discrete symmetries have just recently been investigated with entangled neutral kaons [28] and in ortho-positronium decays [29]: neither investigation drew any connection between their null results with the T-asymmetry of the SLT as established herein. That T-symmetry is counterintuitive is generally excused by the claim that the SM handles only local properties, not global ones like entropy. One outcome of this paper is to provide that connection in which the two rub shoulders to the advantage of entropy and its governing SLT.

The Standard Model of Cosmology (SMC) is based on the SM and the General Theory of Relativity (GTR) [30, for e.g.]. It also depends on several additional assumptions: that the Universe was created in the Big Bang from pure energy; that the known mass-energy content of the Universe is given by luminous matter whose gravitational interaction is described by the GTR; and the cosmological principle by which the idea that the Universe is homogeneous and isotropic on cosmic scales was popularized. The Λ Cold Dark Matter (Λ CDM) variant of the SMC, with six free parameters and several ansatzes, posits that only $\sim 5\%$ of the content of the Universe is in the form of baryonic matter with the balance comprised of cold, slow-moving dark matter – invisible matter that interacts with baryons via gravity alone and thought to make up $\sim 25\%$ of the total mass content in addition to dark energy – a repulsive force inferred from observational data of type Ia supernovae and thought to promote the accelerating expansion [31, 32] of the Universe against gravity and accounting for $\sim 70\%$ of its matter-energy inventory. Cold dark matter is thought to have clumped into large masses which gravitationally attracted baryonic matter, forming the large-scale structures of the Universe. Remnants of dark matter clumps are observed as halos surrounding galaxies. Currently the primary candidates for dark matter are primordial black holes [33], axions [34], sterile neutrinos [35], weakly interacting massive particles (WIMP) [36, et passim], and the lat-

est, erebons [37]. Despite a wealth of evidence favoring their existence [38, 39, for e.g.], neither dark matter [40] nor dark energy [41] have been conclusively detected to date.

With improvements in the accuracy of cosmological observations, so too do challenges [42] to Λ CDM appear. Alternatives [43, 44, et passim] to Λ CDM that dispense with dark matter, dark energy, or both do so [45] by altering the known long-range nature of gravity, an approach not without its own perils and pitfalls [46, 47]. As with the SM and its shortcomings, the Λ CDM, for all its successes, cannot explain such key concepts in our understanding of the known Universe as dark matter, cosmic inflation [48], dark energy, and with the advent of the JWST data, the surprising appearance of massive candidate galaxies [49–51] within ~ 600 Myr of the Big Bang.

First introduced by Sadi Carnot [52] and Rudolf Clausius [53], the concept of entropy in classical thermodynamics related to systems away from equilibrium. What is meant here by entropy is that which the early adopter of Bayesian probability [54], the physical chemist Linhart [55–57] considered in deriving an expression for the heat capacity as a function of temperature from classical thermodynamic principles that he then successfully applied to the experimental standard entropy data of many substances over a broad range in temperature. As Bekenstein remarked (*Scientific American*, April 1, 2007), “This law is central to physical chemistry and engineering; it is arguably the physical law with the greatest impact outside physics.” Without regard to the microscopic details of a system, thermodynamics is tasked with identifying which operations are technically feasible and which resources can be exploited to effect economically sustainable state transformations. Generally, macroscopic phenomena are not time-reversal invariant, prompting Eddington [58] to term this dichotomy in the nature of time as the thermodynamic “arrow of time”.

Statistical mechanics was developed later and applied to many-bodied systems at or near equilibrium by such luminaries as Gibbs, Boltzmann, Planck [7] et *inter alia*. Discounting any perceived disrespect, that framework and its principles, in the absence of evidence to the contrary, does not regulate a single molecule or its known Universe. Just so, a horde of molecules in their Universe(s) are subject to the SLT without exception. This is the primary premise of this paper.

Many papers and books [59–70, for e.g.] intended to provide an explanation of the arrow of time focus on the initial (and to a lesser extent, boundary conditions) of the Universe whose initial conditions unknown [71, 72, et passim]. Feynman [73, loc. cit., p. 116]’s “past hypothesis” posits that the early Universe had low entropy in compliance with the SLT. Subsequently, Roger Penrose argued [74, 75, et passim] that the curvature of the Weyl tensor vanishes at any initial singularity (including the Big Bang) so that the evolution of the Universe be close to a Friedman-Robertson-Walker model of matter in near perfect thermal equilibrium at $\sim 10^{15}$ K \approx

1 GeV whose gravitational degrees of freedom remain unexcited until triggered at the $\sim 375,000$ yr cosmic microwave background (CMB) milestone in the aftermath of a low-entropy proxy constraint as had been hypothesized by Feynman.

Penrose [76] proposed a conformal cyclic cosmology (CCC). This is an eternal recurrence process, whereby universes are spawned, grow, and die in a sequence of aeons, with post-evaporating black holes and the arguable loss of information [77] at their singularity leaving traces of Hawking points (large temperature gradients between ring-like anomalies) of their primordial existences in the CMB of progeny universes based on evidence [78, for e.g.] that has so far failed to hold up to scrutiny [79–81]. By hypothesis, aeons have neither a beginning nor an end and contain only massless particles, photons and gravitons. Penrose’s theory includes the existence of erebons, hypothetical heavy particles with masses of about the Planck mass that are candidate particles for dark matter but which are ultimately unstable since at the end of an aeon there must be an absence of mass to get to the conformal invariance pivotal to CCC.

It is a popular claim that because entropy is an extensive property, the reason violations of the SLT are not seen is due to molar statistics: as systems reduce in size, fluctuations (sic uncertainties) increase so that violations ought to become more probable. Challenges to the SLT and proposals for its replacement abound [8–10, 82–84, for e.g.]. However, without their independent verification including computer simulations that openly demonstrate the positivity* of dynamics [85, 86], the SLT is indomitable regardless of premature reports of its putative demise.

Pioneering work by Hill [87] in the early 1960s showed how thermodynamics could be applied to many small systems – aerosols, colloids, dust, and nanosystems. The thermodynamics of small systems has taken on a new importance due to the development of nanoscience, with thermodynamics as applied to nanoscale particles being now known as nanothermodynamics [88, 89]. The nanothermodynamics community has for some time broadened its enquiries into the single-molecule domain beyond the thermodynamic limit [90–93] without invoking quantum phenomena. Quantum thermodynamics [94, 95] tries to go even further by striving to extend classical thermodynamics and nonequilibrium statistical physics to ensembles of sizes below the thermodynamic limit with the full inclusion of quantum effects, even for nanoscale objects [96] and single trapped quantum systems [97]. It differs from statistical mechanics in its attention to dynamical processes out of equilibrium [98]. Kosloff [99] has provided a perspective on a dynamical view of quantum thermodynamics in which the laws of thermodynamics are true in any quantum circumstance [100, et passim].

Extending thermodynamics beyond its bulk matter limits

*Adjusting what should be a positive solution to zero on first detecting it going negative is an all too-common programming practice.

is increasingly prevalent in the push towards the fabrication of miniaturized systems offering technological advantages. The main benefit of single-molecule investigation is the deconstruction of ensemble averages to provide information about complex systems since in natural systems the average outcome of the group is rarely the same as the outcome of the individual which may be all that is important. Ensemble averages depend on probability distribution functions and a medley of principles and assumptions that are not applicable to a lone system. Even though the time average of an observable of a system is directly related to experiment, empiricism has lost favor lately to computer simulation that replaces averages over time by instantaneous averages over an ensemble. Quantum mechanics governs the dynamics of individual subatomic, atomic, and molecular systems with well-predicted outcomes. Whether a system is small (a molecule) or not (the known Universe) is relative to its context and how that affects it and our attention to it.

Interest in single molecule behavior received a significant boost following Neher and Sakmann's 1991 award of the Nobel Prize in Physiology or Medicine for discoveries revealing the function of single ion channels via their development of the patch clamp technique (*Scientific American*, March 1992) through which biological scientists could inexpensively isolate ion channels of cell membranes that engage in cellular signaling processes. This resulted in a momentous revolution in cell biology – unseen in physics notwithstanding Schrödinger's *What is Life* manifesto proclaiming physics' dominance over biology – leading to greater understanding of disease mechanisms and the discovery of new therapeutic drugs. As recently as the early 1980s, the notion of cell membranes and their information networks of single ion channels were being challenged by the now debunked [101] and obdurate belief [102] that the cell and even life itself is explicable in terms of the “nano-protoplasm” whose function and properties are inextricably tethered to the framework of statistical mechanics. The rapid progress in quantitative single-molecule measurements are well documented [103, 104, et passim] and contrast with the obsolete “new view” [105, et passim] energy landscape ensemble approach to the protein folding problem which relies almost exclusively on computer simulation of the chemical physics modeling [106, 107] of such.

X-ray crystallography and cryo-electron microscopy have traditionally allowed the imaging of biomolecules at the atomic level using samples that have been crystalized at ultracold temperatures. Atomic force microscopy (AFM) of molecules allows them to be probed under more physiologically appropriate conditions. A localization image reconstruction algorithm [108] can process data from multiple scans of single molecules and can even be used retroactively to reveal new details hidden in old AFM data. Instead of observations on hundreds of molecules, the same molecule is observed hundreds of times in calculating a high-resolution map. Such

a map, from the same molecule as it transits from one conformation to the next and not from thousands of molecules in one or the other conformation, mitigates the potentially misleading results that can occur when averaging data from many molecules when only one matters. Advances in single-molecule microscopy have evolved to permit the study of systems ranging from small molecules to living cells with the prospect of revolutionizing the modern biosciences [109–111, for e.g.].

In principle, reliable structural information in conjunction with the use of computational methods should guide structure-based screening to drug discovery and design. Long after Dirac [112, loc. cit., p. 714] advised that it “... becomes desirable that approximate practical methods of applying quantum mechanics should be developed, which can lead to an explanation of the main features of complex atomic systems without too much computation,” such pursuit led to the realization [113, loc. cit., p. 109] of the “central embarrassment of molecular mechanics, namely that energy minimization or molecular dynamics generally leads to a model that is less like the experimental structure,” whether through such excuses as deficiencies in force fields (potentials), limitations in computational power allegedly to be solved with supercomputers of the past but now demanding quantum computers of tomorrow, artifacts in structures [114] that result from collecting crystallographic data under cryogenic conditions to minimize radiation damage, etc.

With its roots in phenomenology, Clausius' inequality defines the change in entropy for a cyclic process (including full-body immersion in its surroundings) and its role as a measure of the dispersal of energy or heat at a specified temperature. If the amount of energy added by heating and the temperature can be measured during the process, Clausius' inequality can be used to determine whether the process is reversible or irreversible by carrying out the integration in the inequality. The following provides an alternative way of distinguishing between the two extremes for systems whose notion of work is no different than that in all of physics even if their dynamics is governed by time-reversible quantum mechanics without resort to any particular entropy functional.

Introduction of the concept of entropy and its permissible changes through Clausius' expression of the SLT predated both Gibbs' notion of the statistical ensemble and Boltzmann's specific entropy functional connecting the macroscopic system with the probabilistic populations of microscopic states amenable to that ensemble. Unlike thermodynamics, Boltzmann-Gibbs statistical mechanics, whatever its successes, has limited domains of applicability as known to its practitioners, including so-called anomalous systems that have strong long-range effects, nonlocal correlations between different subsystems of a system, nonMarkovian behavior, violations of reductionism for such thermodynamic properties as entropy and internal energy, etc. Having found no systematic way to uniquely determine how to describe the en-

trophy of dynamical systems who survey their configuration spaces in ways more complex than prescribed by ergodicity, Tsallis [115] proposed a nonextensive (nonadditive) measure [116] which generalizes Boltzmann-Gibbs extensive (additive) metric to deal with such anomalous systems. The Boltzmann-Gibbs and Tsallis entropies are each time invariant and applicable at best to systems at or near thermal equilibrium. Neither of these entropies are *a priori* applicable to nonequilibrium systems which is why here, in consideration of a single molecule, no appeal to either extensive or nonextensive statistical mechanics is made but rather to classical thermodynamics, electrodynamics, and quantum mechanics as appropriate descriptors in their respective macroscopic and microscopic milieus. Time-dependent entropy changes are given by Clausius' inequality as follows from his formulation of the SLT on the basis of a cyclical thermodynamic process to distinguish an irreversible from a reversible change of a lone system in a thermal field.

Thermodynamic systems under sentient observation are embedded in the known Universe and are never "isolated" [117] or "notional": they are either closed or open, closed if they exchange only heat with their environment and open if they exchange mass with or without the exchange of heat with their surroundings. For all their intrigue, such quasi "isolated" systems as Bose-Einstein [118, 119] and Fermi-Dirac [120] condensates do neither and are of no interest here. According to the SLT, systems of interest generate entropy in a time-asymmetric way in accord with the macroscopic concept of entropy and common experience. That classical and quantum dynamics and electrodynamics suggest otherwise has led to a deluge of researches in recent years that offer explanations for this so-called time-reversal symmetry breaking or claims that the SLT is subject to regular violations. Here, the primary intent is to show that, at the microscopic level, entropy is T-asymmetric and requires neither the intercession of time-reversal symmetry breaking mechanisms nor assent to the belief that the SLT can be controllably broken.

The purpose of this paper is to provide the physical basis for the SLT's T-asymmetry from T-symmetric quantum mechanics and electrodynamics without obliging either of them to relinquish their mutual time-reversal invariance. The route to this is simple if somewhat circuitous relative to that of Stenger [121, loc. cit., 3972]'s, say:

It is hard to see how the breakdown of T-symmetry at the microscale implies time irreversibility at the macroscale, although I am not prepared to rule it out,

an opinion easily brought up to speed as will be shown by beginning in the first instance at the molecular scale before moving on to reveal that the same considerations apply in larger-scale self-gravitating systems.

Materials and structures are the products of the evolution of the Universe. How they appeared and their subsequent

transformations are pivotal to our understanding of the Universe and our place within it. All dissipative structures in the Universe including all forms of life, owe their existence to the fact that the Universe started in a low entropy state and has not yet reached equilibrium [122, et passim]. Deep considerations of such phenomena are beyond the scope of this paper and its specific purpose: to explain why the arrow of time is asymmetric regardless of the time-reversal invariance of quantum mechanics and electrodynamics.

The paper uses the nonrelativistic quantum mechanics of a single molecule to relate its wave function's local phase to forces acting on its nuclei and electrons in the presence of a thermal environment. In the intake of sensible heat from its surroundings, such a molecule's entropy increases with the gain in entropy determined by its molecular structure as connected to the gradient field of its wave function's local phase whose subharmonicity is shown to be a necessary and sufficient condition for it to comply with the SLT. The thermodynamic arrow of time necessitates irreversible over reversible processes as determined by the gradient field of the local phase. Conservative Lorentz-Faraday forces impressing on the nuclei and electrons of the molecule engender irreversible (reversible) change and entropy gain (stasis) in its exchange of heat with its environment under the discernment of the thermodynamic arrow of time and regardless of the time-reversal symmetry [123], [124, cf. Ch. 26] of quantum mechanics or electrodynamics. The implications of the gradient of the local phase on entropy production and Faraday's law of induction are also explored. Additionally, it is shown that in a heat bath a molecule in molar amounts is stable provided its internal electrodynamic potential is subharmonic within its nominal volume V , a fact first anticipated long ago by Earnshaw [125]. This leads into the question of molecular stability as gauged by the virial theorem and by extension to the stability of self-gravitating objects.

A molecule – with its myriad of allowed relative motions determined by its stabilizing potential in analogy with the vibrations of an oscillating string – serves here as a spoiler to its Universe and its equally important if less familiar subsystems. The paper draws a comparison between a single molecule described quantum mechanically in the nonrelativistic limit and its Universe treated in the weak field limit of general relativity, each interrogated under similar thermal circumstances, prior to their respective destinies in anticipation that across such disparate spacetime scales what one learns might surprise in their similarity and simplicity.

1.2 Notation

Rationalized Planck units are used throughout unless otherwise indicated (wayward 4π 's excepted). The gradient ∇ formally operates on vector and scalar fields drawn from a Euclidean space whose fiber bundle is a trivial Cartesian product mapping $R^n = \mathbf{R}^M \times \mathbf{r}^N$ of the molecular structure of an elec-

trically neutral molecule of M nuclei (base, \mathbf{R} with gradient $\partial/\partial\mathbf{R} = \nabla_{\mathbf{R}}$) of known elemental composition (atomic number Z_i , $i = 1, M$) and the coordinate space (fiber, \mathbf{r} with gradient $\partial/\partial\mathbf{r} = \nabla_{\mathbf{r}}$) of its N electrons so that each of the $n = M+N$ elements of \mathbf{x} lies in R^3 . If $m_{k_j} > 0$, $j = 1, 2, 3$; $k = 1, \dots, n$ are the masses of the particles and $[\]$ denotes the integer part, $k_j = 1 + [(j-1)/3]$ in order that all three coordinates of a particle relative to a body-fixed origin in the observer's frame at the center of mass are scaled by the same mass. The kinetic energy, its virial, and related quantities of any system of interest (be it an atom, molecule, ion, the known Universe, etc.) free from the clutter of the masses of nuclei and electrons are expressed here as Lebesgue integrals whose operative measures (for volumes V , positions \mathbf{x} , etc.) use mass-weighted coordinates. The only limit on n is that imposed by Nature [126, et passim] so that neutral (i.e. $\sum_{i=1}^M Z_i = N$) polyatomic molecules (governed by the Coulomb potential) or the known Universe (governed by the Newtonian potential), while their sizes cannot estimate *a priori*, both are $n \geq 4$ -body systems whose dynamics are unknown and perhaps even unknowable. The inner product $\langle \mathbf{x}, \mathbf{y} \rangle$ of $\mathbf{x}, \mathbf{y} \in R^n$ is a scalar as is the Euclidean norm $\|\mathbf{x}\| = \sqrt{\langle \mathbf{x}, \mathbf{x} \rangle}$. An orientable surface ∂V has a unit normal $\hat{\mathbf{n}} = \nabla V / |\nabla V|$ at a regular point where $\nabla = \nabla_{\mathbf{R}} \times \nabla_{\mathbf{r}}$ and is undefined at a critical point where ∇V vanishes. The normal $\hat{\mathbf{n}}$ to V twists and turns from regular point to regular point as the boundary ∂V bends in different directions, behavior captured by the local self-adjoint shape operator $\mathbf{S} = -\nabla \cdot \hat{\mathbf{n}}$ [130, cf. Ch. 5], [131, cf. Ch. 6, Ex. 11, pp. 141–142]. The directional derivative of V at a regular point is $D_{\hat{\mathbf{n}}}V = \nabla V \cdot \hat{\mathbf{n}} = \partial V / \partial \hat{\mathbf{n}}$ which is a maximum of $|\nabla V|$ (minimum of $-|\nabla V|$) when $\hat{\mathbf{n}}$ is in the same (opposite) direction as (to) $\hat{\mathbf{n}}$, respectively. The eigenvectors and eigenvalues of \mathbf{S} provide the principal directions and principal curvatures of V , respectively. The principal directions specify the directions a curve embedded in V must travel to have maximum and minimum curvature, these being given by the principal curvatures. Quantum expectation values are denoted by angular parentheses $\langle \blacksquare \rangle$ and their time averages by an over bar $\langle \blacksquare \rangle$. Without loss of generality, generic functions are smooth with compact support $C^\infty(R^n)$.

1.3 Outline

The article is organized as follows: In the next section, the thermodynamics of a single molecule in contact with a heat bath is considered. This is followed by consideration of the Faradaic induction of a single molecule. In the succeeding section the relation of the two featured topics are discussed in detail. The central finding of the T-asymmetry of entropy is

*Finite binary cross products \times exist only in R^3 and R^7 [127]. Their extension to R^n is through the Hodge dual of the exterior product \wedge of $n-1$ vectors in R^n and their Gramian determinant [128, cf. Ch. 7], [129, cf. Ch. 8]. The use here of vector calculus instead of the exterior calculus of differential forms is that it more clearly serves as the universal lingua franca of general physics for the disparate topics under discussion.

shown to rest on the hypothesis that the thermodynamic arrow of time is set by the local phase of the wave function of the system of interest whose falsifiability is illustrated through a number of demonstrations for self-gravitating systems. The requirement that the phase be subharmonic in a volume under curvature flow is emphasized whatever the size and shape of the system.

It is not the intent here to calculate the entropy in any system, be it a single molecule or any other particle or structure in its known Universe, but rather to point out that, whatever their fate in a thermal field, the T-asymmetry of entropy changes will feature in their evolution until it hardly matters. Both experimental demonstration and computer simulation are outside the scope of this paper. Equally, deliberations of generalized thermodynamics specific to black holes are not part of this paper.

2 Thermodynamics in a thermal field

Recall that quantum theory distinguishes between two types of system states, viz. pure and mixed [132]. A system in a pure state possesses both a well-defined probability amplitude and phase. In contrast, the mixed state describes a system whose phase information is incomplete. Since the density matrix ρ for a system to be in a statistical ensemble of different pure states is a positive semi-definite, self-adjoint operator, it has a spectral decomposition $\rho = \sum_i \lambda_i |\varphi_i\rangle \langle \varphi_i|$ where $|\varphi_i\rangle$ are orthonormal state vectors with $\lambda_i > 0$ and $\sum_i \lambda_i = 1$. ρ evolves via the von Neumann equation $\dot{\rho} = [H, \rho]$ where H is the Hamiltonian operator of the system. The von Neumann entropy of the ensemble of pure states is [133] $S(\rho) = -\sum_i \lambda_i \ln \lambda_i = -\text{Tr}(\rho \ln \rho)$, with the number of states needed to describe the system being the number of eigenvalues λ_i of ρ , each of which provides the weight of its respective state. Thus, $S(\rho) > 0$ for a mixed state and $S(\rho) = 0$ for a pure state (with $\lambda_1 = 1$). As $\rho = |\psi\rangle \langle \psi|$ casually goes from a pure ($\text{Tr}(\rho^2) = 1$; $S(\rho) = 0$) to a mixed ($\text{Tr}(\rho^2) < 1$; $S(\rho) > 0$) state, the entropy gain ΔS increases. For mixed states the entropy measures how far the state is from being pure. Apart from a factor of $k_B \ln(2)$ involving the Boltzmann constant, Gibbs thermodynamic entropy is identical to the von Neuman entropy and is most relevant for systems with a large number of degrees of freedom.

Consider a single molecule in a pure state $\psi(\mathbf{x}, t)$ of charge density $\rho(\mathbf{x}, t) = |\psi(\mathbf{x}, t)|^2$ that is $(-1)^{2s}$ -symmetrized for boson (s , integer spin) and fermion (s , half-integer spin) coordinates [134, et passim]. The molecule is free of spatial confinement other than that provided by the Coulomb potential. Nuclei with integer spins are bosons and those with half-integer spins are fermions as are electrons which are spin 1/2 elementary particles. Both $\psi(\mathbf{x}, t)$ and the operator $O(\mathbf{x}, t)$ are time dependent in the interaction picture of quantum dynamics. A state is pure if the density matrix $\rho = |\psi\rangle \langle \psi|$ for some unit state vector ψ so that $\rho^2 = \rho$ and the expectation value

of a self-adjoint operator O is $\langle O \rangle = \text{Tr}(\rho O) = \langle \psi, O\psi \rangle$. Pure states are relevant if they come from the ground state in which the first excited state has a large energy gap that exceeds $\sim k_B T$ at the absolute temperature T . If O has a complete set of eigenvectors ϕ_j with real eigenvalues o_j , then $\langle \psi, O\psi \rangle = \sum_j o_j \langle \psi | \phi_j \rangle^2$ where the o_j 's are the possible outcomes of the measurement of O and $\langle \psi | \phi_j \rangle^2$ is the transition probability that this outcome occurs. This choice of state is consistent with Bridgman [135]'s operationalism with the inclusion of quantum mechanical considerations by Giles [136, 137] in a rigorous formulation [138] of thermodynamics. By and large the paper adopts the Ithaca [139] interpretation of quantum mechanics.

It is always the case that $\psi(\mathbf{x}, t)$ complies with the Pauli exclusion principle (PEP). Any pair of point particles whose exchange is constrained by the PEP are distinguishable if their separation is large compared to their de Broglie wavelength ($\lambda_{\text{th}} \sim 1/k_B T$ for massless particles [140] such as the photon or the graviton). Thus, while symmetrization is of undoubted importance, it is increasingly less crucial the further away from equilibrium a system is driven to where the very identification of $\psi(\mathbf{x}, t)$ is in doubt. Entropy quantifies the extent to which the exact state of a system of interest is in doubt and reflects deficits in whatever information is at hand to correctly make that specification. For arbitrary t , $\psi(\mathbf{x}, t)$ is given. When the system is perturbed, the state evolves with increasing loss of information or gain in entropy about its current condition. The system of minimum entropy evolves via the time-dependent Schrödinger equation and its probabilistic underpinnings. Subsequent entropy production will be related in what follows to the spontaneous work done on such a system in a heat bath by electrodynamic forces internal to the system and not to a statistical prescription of entropy more appropriate to an ensemble of such systems at or near thermal equilibrium.

In electromagnetic theory charge density is idealized as a smooth scalar function of position to be regarded as a continuous distribution, somewhat like a fluid or field. If the wave vector in its coordinate \mathbf{x} representation is accompanied by an arbitrary local phase factor, nonrelativistic quantum mechanics is invariant under a local gauge transformation whether in an external [141, cf. Sec. 22 and 27] or internal [142, 143] electromagnetic field. In the latter case the evolution of the probability density $\rho = |\psi|^2$ fulfills the continuity equation, a quasilinear first-order conservation law partial differential equation (PDE),

$$\frac{\partial \rho}{\partial t} + \nabla \cdot \mathbf{j} = 0, \tag{1a}$$

within a deformable volume element dV centered at \mathbf{x} in terms of the divergence of the probability current

$$\mathbf{j}(\mathbf{x}, t) = -\frac{i}{2} (\psi^*(\mathbf{x}, t) \nabla \psi(\mathbf{x}, t) - \psi(\mathbf{x}, t) \nabla \psi^*(\mathbf{x}, t)) \tag{1b}$$

to ensure unitarity at all (\mathbf{x}, t) in analogy with the maintenance

of mass, charge, and heat balance in continuum mechanics, electrodynamics, and thermodynamics, respectively. When $\nabla \cdot \mathbf{j} > 0$ so that the number density is decreasing in dV then $\partial \rho / \partial t < 0$ and conversely. If V is large enough to be essentially unbounded, ψ is square integrable and vanishes at infinity where Sommerfeld [144, cf. §28]'s radiation condition ensures that infinity is an absorber (sink) but not an emitter (source) and that once probability current exits the scene it does not reenter (a rigorous requirement for the existence and uniqueness of ψ). For future reference, notice that the current density $\mathbf{j}(\mathbf{x}, t)$ is an even function of time [145], i.e. $\mathbf{j}(\mathbf{x}, t) = \mathbf{j}(\mathbf{x}, -t)$, under Wigner [123], [124, cf. Ch. 26]'s prescription for time reversal in quantum mechanics. Recall [145] also that the probability density ρ is even in t .

For ψ expressed in polar form as $\psi(\mathbf{x}, t) = e^{i\theta(\mathbf{x}, t)} \sqrt{\rho(\mathbf{x}, t)}$, the continuity equation reduces to

$$\frac{\partial \rho}{\partial t} + \nabla \cdot (\rho \nabla \theta) = 0 \tag{2}$$

in terms of the probability density ρ and a finite local phase factor θ which has units of action, i.e. [energy][time] or [momentum][length]. With ψ being single valued so too is ρ . Wherever ψ vanishes so too do ρ and $\mathbf{j} = \rho \nabla \theta$.

If $\nabla \theta$ vanishes so does \mathbf{j} and the system is in a stationary state with normalizable ρ . Here the focus is on the situation where $\nabla \theta$ is finite almost everywhere, a circumstance governed by the Morse-Sard theorem [146, 147] to the effect that critical points at which $\nabla \theta = 0$ are few to none compared to regular points where $\nabla \theta \neq 0$. That said, there are several reasons to support the view that θ is subharmonic ($\nabla^2 \theta > 0$) in V [148, 149], viz.

1. At nodes in ψ , $\theta = \tan^{-1}(\text{Im } \psi / \text{Re } \psi)$ is indeterminate. If the potential energy part of H has no explicit time dependence, Hamilton's principal function $\theta(\mathbf{x}, t)$ (classically, W) is additively separable in \mathbf{x} and t , i.e. $\theta(\mathbf{x}, t) = \phi(\mathbf{x}) - Et$, where $E = \langle \psi | H | \psi \rangle$ is the energy expectation value for normalized ψ , $\phi(\mathbf{x})$ (classically, S) is Hamilton's characteristic function, and $\nabla \theta(\mathbf{x}, t) = \nabla \phi(\mathbf{x})$ is the time-invariant gradient or relative phase*. In the hydrodynamic interpretation [152], [153, et passim] of quantum mechanics, where substituting $\psi = e^{i\theta} |\psi|$ into the Schrödinger equation gives a system of two coupled PDEs, viz. a continuity equation for ρ treated as a classical fluid and a surreal quantum potential modification of the classical Hamilton-Jacobi equation for θ which is of $O(\hbar^2)$ in the rationalized Planck constant \hbar , $\nabla \theta = \nabla \phi$ is taken to represent the momenta of all particles (nuclei and electrons), an interpretation adopted by Schrödinger in formulating wave mechanics following both Hamilton's analogy between geometric optics

* Schrödinger [150] explained how he had come upon the wave equation and identified ϕ as what he termed the "phase angle of the wave function" [150, loc. cit., p. 499; p. 505] it regulates, as inspired by de Broglie [151].

and classical mechanics and de Broglie’s wave-particle hypothesis [151, 154], [155, cf. Ch. VIII], [156], [157, cf. Ch. 2.2.4] in which a wave train is associated with the motion of a material particle, the frequency and wavelength being related to the energy and momentum by the Planck-Einstein relation for radiation quanta.

The optico-mechanical analogy invoked by Schrödinger [158] in arriving at his eponymous wave equation for $\psi(\mathbf{x}, t)$ is well documented [159–162] and does not need to be rehashed here. Suffices to say that in his interpretation and adaption of de Broglie’s “phase wave” ideas, Schrödinger denied any real meaning to ϕ since to do so would imply that one could speak meaningfully of electric charge being in a particular place or following a single path (sic trajectory) in an atom and capitalized *inter alia* on two interrelated observations [163], viz. (i) recognition that the gradients $\nabla\theta(\mathbf{x}, t) = \nabla\phi(\mathbf{x})$ are normal to the wave fronts or level sets of $\theta(\mathbf{x}, t)$, the surfaces of constant action; and, (ii) that since the light rays of optics are normal to those wave fronts, so too are particles whose uncertain loci follow the undulations in $\nabla\phi(\mathbf{x})$ so that the direction of $\mathbf{j} = \rho\nabla\phi$ is locally normal to the level sets of de Broglie waves* of local phase ϕ . Note that $\nabla\phi$ is distinct from the group velocity of its localized wave packet†.

In retracing this optico-mechanical analogy one sees that to $O(\hbar^0)$ the Hamilton-Jacobi equation for the relative phase $\nabla\phi$ is

$$\frac{1}{2}(\nabla\phi)^2 = E - \mathcal{V}, \tag{3a}$$

where \mathcal{V} is the potential energy. Schrödinger recognized that (3a) has the solution $e^{i\nabla\psi}$ whereupon

$$\frac{1}{2}(\nabla\psi)^2 - (E - \mathcal{V})\psi^2 = 0, \tag{3b}$$

and a variational problem [168] on ψ leads to the time-independent wave equation which he applied to the H

*In showing the equivalence of his formulation of wave mechanics to the matrix mechanics approach of Heisenberg et al [164–166], Schrödinger acknowledged [167, loc. cit., p. 735, fn. 2] his indebtedness to de Broglie’s extension of wave-particle duality for photons to matter and Einstein’s advocacy of that extension to him.

†The amplitude $\sqrt{\rho}$ has no unique position or velocity but is smeared over space as a wave packet of phase ϕ . In a double-slit interferometer it is particles that are detected, not delocalized waves as $\sqrt{\rho}$ implies: photons and particles travel as waves but hit the detector as particles. This raises the problem of how $\sqrt{\rho}$ from its source changes from wave to particle. Bohr and Heisenberg (in their Copenhagen interpretation of quantum mechanics) claimed that it was the observer who decides the outcome. ρ is a wave of probability (via Born’s conjecture, according to which one must expect to find the particle where ρ is high) provided $\sqrt{\rho}$ collapses at the screen regardless that it arrived there as a wave travelling through all slits without prejudice while interfering as a wave enroute to the detector. Just how $\sqrt{\rho}$ collapses is an open question whose resolution endures as the so-called “measurement problem” whose most popular if arguable rationalization is the many worlds interpretation of quantum mechanics.

atom and post haste produced its time-dependent equivalent wherewith wave mechanics was born [163, et passim]. At this point ϕ and $\nabla\phi$ appear to have fallen through the cracks to be replaced by all things ψ until de Broglie [151, 154]’s and Madelung [152]’s earlier work was resuscitated by David Bohm in the early 1950s, through his retention of the connection $\nabla\phi = \mathbf{j}/\rho$ as a guidance law governing particle motions pursuant to their deterministic trajectories in what is an active alternative [169–171, et passim] to the Copenhagen interpretation of quantum mechanics with its focus on probabilistic energy and angular momentum eigenvalues, and dubbed de Broglie-Bohm mechanics, pilot-wave theory, causal interpretation, etc. by its practitioners [172, for e.g.]. Hereon while $\mathbf{j} = \rho\nabla\phi$ in terms of the wave-particle velocity $\nabla\phi$ and the charge density $\rho = |\psi|^2$ is acknowledged, Bohmism is otherwise ignored in proceeding.

Invoking de Broglie [151, 154]’s interpretation of Sommerfeld [173]’s (and Wilson [174]’s) quantization rule, a condition which ensures that matter waves make standing waves only at discrete energies, suggests that

$$\oint_{\partial V} da \hat{\mathbf{n}} \cdot \nabla\phi = \int_V d\mathbf{x} \nabla^2\phi = 2\pi k, \tag{4}$$

where $\hat{\mathbf{n}}$ is a unit normal to ∂V on a patch of area da , ϕ is both multivalued and subharmonic in V , and $k \in \mathbb{Z}^+$. At nodes in ρ , \mathbf{j} vanishes but not necessarily $\nabla\phi$ which may jump in discrete amounts and, since by Stoke’s theorem $\int_V d\mathbf{x} \cdot \nabla \times \nabla\phi$ vanishes, there are no accompanying vortices should any such jumps occur. A measurement on a system subject to (4) would result in a jump in its state, a collapse of its wave function ψ following which its phase ϕ and its gradient $\nabla\phi$ would vanish whereupon it would find itself in a reversible state.

2. The flux of the probability current \mathbf{j} has two contributions, viz.

$$\nabla \cdot \mathbf{j} = \rho \nabla^2\phi + \nabla\rho \cdot \nabla\phi, \tag{5}$$

the first of which is positive if ϕ is subharmonic while the second governs whether the amount of charge within a differential volume dV is decreasing (increasing) according as it is of positive (negative) sign.

This allows (1a) to be rewritten as

$$\frac{D\rho}{Dt} + \rho \nabla^2\phi = 0 \tag{6}$$

in terms of the substantial derivative $D/Dt = \partial/\partial t + \nabla\phi \cdot \nabla$. In an Eulerian specification of the flow field of ρ , the total derivative consists of two terms, the first $\partial/\partial t$ of which provides the changes at a fixed position due to unsteadiness in the flow while the second $\nabla\phi \cdot \nabla$

gives the rate at which ρ is convected to that location. Neither contribution vanishes in an unsteady flow. The substantive flow of ρ will be accelerating if ϕ is subharmonic ($\nabla^2\phi > 0$). Physically, pursuit of ρ whether it relates to a single molecule or any other particle or structure in its known Universe from a Lagrangian or an Eulerian perspective is a matter of convenience. For the present purposes the latter is chosen.

3. If \mathbf{j} is decomposed via the Helmholtz-Hodge theorem [175–178] to the sum of longitudinal and transverse parts whereby $\mathbf{j} = \mathbf{j}_{\parallel} + \mathbf{j}_{\perp}$ with \mathbf{j}_{\parallel} and \mathbf{j}_{\perp} being parallel and orthogonal to $\nabla\phi$ and $\nabla \times \mathbf{j}_{\parallel} = 0$ and $\nabla \cdot \mathbf{j}_{\perp} = 0$, respectively, then $\rho \nabla^2\phi = \nabla \cdot \mathbf{j}_{\perp} = 0$ and $\nabla\rho \cdot \nabla\phi = \nabla \cdot \mathbf{j}_{\parallel}$, where for $\mathbf{x}, \mathbf{x}' \in V \subseteq R^n$

$$\mathbf{j}_{\parallel}(\mathbf{x}, t) = - \int_V d\mathbf{x}' \frac{\nabla' \cdot \mathbf{j}(\mathbf{x}', t)}{4\pi|\mathbf{x} - \mathbf{x}'|} + \oint_{\partial V} da' \frac{\hat{\mathbf{n}}' \cdot \mathbf{j}(\mathbf{x}', t)}{4\pi|\mathbf{x} - \mathbf{x}'|} \quad (7a)$$

and

$$\mathbf{j}_{\perp}(\mathbf{x}, t) = \int_V d\mathbf{x}' \frac{\nabla' \times \mathbf{j}(\mathbf{x}', t)}{4\pi|\mathbf{x} - \mathbf{x}'|} - \oint_{\partial V} da' \frac{\hat{\mathbf{n}}' \times \mathbf{j}(\mathbf{x}', t)}{4\pi|\mathbf{x} - \mathbf{x}'|}, \quad (7b)$$

so that $\nabla \cdot \mathbf{j} = \nabla \cdot \mathbf{j}_{\parallel}$. If V recedes to infinity and \mathbf{j} is regular there, the above surface integrals vanish. This decomposition of \mathbf{j} results in ϕ being harmonic which is not pursued for the aforesaid reasons in addition to the following.

4. By the maximum principle [149, 179], if ϕ is subharmonic in V it attains its maximum on ∂V and not in the interior of V .
5. In the finale of this paper, an arguably propitious ending to a moribund and timeless Universe [180, 181, for e.g.] is suggested.

A molecule is a sufficiently stable, electrically neutral group of at least two atoms in all manner of configurations and shapes held together by covalent bonds in the long-range Coulomb field acting between its constituent electrons and nuclei. It may consist of atoms of a single or different elements or of isotopes of the same element. Molecules are of many types and shapes but for each the problem in describing their nuclear motions differ. The arrangement of their atoms allows them to rotate coupling to the vibrations of their nuclei as well as to the orbital and spin angular momenta of their electrons. Condensed phases exhibiting metallic bonding, noncovalent bonds (ionic and hydrogen bonds), glasses (solids in a vitreous state), and materials of several classes (dielectrics, conductors, semiconductors, insulators, etc.) do not strictly present as single molecules, that object whose response to minimal interrogation is consistent with reduction-

ist inquiry. As a single molecule contacts a heat bath of low-to-moderate temperature on ∂V it becomes excited: its nuclei move with the absorption of photons (vibrational energy) or rotons (angular momentum energy) and under the aegis of its Hamiltonian operator the configuration of its electrons and nuclei changes while endeavoring to maintain stability as it restores equilibrium through the redistribution of energy among its low-frequency degrees of freedom. If equilibrium is unattainable or the heat reservoir is at a high enough temperature the molecule will rip apart, dissociating into other smaller molecules or sundry reactive fragments (free radicals, atoms, ions, bare nuclei, free electrons, etc.) which eventually relax to stable entities through collisional deactivation with each other or the spontaneous emission of light. In macromolecules the transduction of the energy available falls within physiologically sustainable thermal limits of biological processes when mediated by specific enzymes with the involvement of ancillary molecular devices (membranes, filaments, channels, templates, etc.) [182].

Thermodynamics [183, for e.g.] is independent of quantum mechanics and its concepts which equate the internal energy U to the sum of the kinetic and potential energies of all elementary particles that comprise the system. Molecular stability does not rest solely with the Hamiltonian operator of the “isolated” molecule. Neither the system’s state ψ nor its expected energy $\langle H \rangle$ is a stationary state or an energy level of the molecule, respectively, whose environment contains both matter and radiation [184], the molecule being amenable to the receipt of sensible heat only from its environment. In addition to the conservative Coulomb interactions included in the potential part of the Hamiltonian operator are Lorentz-Faraday interactions between the electrons and nuclei of the molecule that are affected by the surroundings in which a molecule resides. The internal force $\mathbf{F}_{\text{int}}(\mathbf{x}, t)$ acting within a molecule viewed as a closed conservative system (*vide infra*) is

$$\mathbf{F}_{\text{int}} = \frac{\partial \mathbf{j}}{\partial t} u(T), \quad (8a)$$

where $u(T)$ is the Heaviside step function, it being 1 if $T > 0$ and 0 otherwise (when the system is “isolated”). Hereon $u(T)$ is dropped in \mathbf{F}_{int} , its requisite presence being understood. At finite T , \mathbf{F}_{int} is a conservative Lorentz-Faraday force acting on the nuclei and electrons of the molecule and gives rise to an energy contribution $\nabla \cdot \mathbf{F}_{\text{int}}(\mathbf{x}, t)$ to their kinematic motions; otherwise \mathbf{F}_{int} is zero and inoperative. Like $\mathbf{j}(\mathbf{x}, t)$, $\mathbf{F}_{\text{int}}(\mathbf{x}, t)$ is a self-adjoint operator.

Since $\mathbf{j}(\mathbf{x}, t) = \rho(\mathbf{x}, t) \nabla\phi(\mathbf{x})$ and with the use of (1a), (8a) may be rewritten as

$$\frac{\partial \mathbf{j}}{\partial t} + \nabla\phi \nabla \cdot \mathbf{j} = 0, \quad (8b)$$

a quasilinear first-order PDE for $\mathbf{j}(\mathbf{x}, t)$. In contrast to (1a), (8b) is not a continuity but rather an advection equation. Un-

der time reversal (8b) is

$$\frac{\partial \mathbf{j}}{\partial t} - \nabla \phi \nabla \cdot \mathbf{j} = 0. \tag{8c}$$

If the initial/boundary-value problem PDE in (8b) has the solution $\mathbf{j}(\mathbf{x}, t) = \rho(\mathbf{x}, t) \nabla \phi(\mathbf{x})$, the backward initial/boundary-value problem PDE in (8c) is physically equivalent to the forward time (8b) with the sign of $\nabla \cdot \mathbf{j}$ flipped. If ϕ is subharmonic, $\nabla^2 \phi > 0$ independently of the sign of t .

A thermodynamic process changes the state of a system under the action of a driving force, external or internal. The larger the force, the more the process proceeds, perhaps, subject to kinetic constraints. A reversible process is an idealization that can be reversed at any time by an infinitesimal change in the driving force that reverses its sign; it must occur infinitely slowly so that the system and its surroundings have time to relax through staged equilibria ultimately leading each to reach stasis. There are no truly reversible processes in Nature, only calculations for them that are applied to real processes which are irreversible and whose original state cannot be restored without concomitant changes to the surroundings.

Thermodynamics is concerned only with the effects of heat and work in the interaction between a system and its environment. Its laws not only exert their influence in every field of the natural sciences, but also play a part in all industrial processes in which energy is transferred. It does not inquire into the mechanism of phenomena and so it is unconcerned with what happens on an atomic or subatomic scale even though that perspective can help to give deeper meaning to its laws and concepts. The branch of science concerned with this is statistical mechanics, the mechanics of such a large number of atoms or molecules that specifying the state of each is impossible and one is forced to use statistical methods. Entropy is calculated via Boltzmann-Gibbs statistics applicable to ensemble representations of the system under study which, however, are unavailable here. Single molecule techniques [185, 186] reveal behavior masked in ensemble averages of complex systems.

There are many physical statements of the SLT any one of which can be used to show its equivalence to another and to prove the mathematical statement of the SLT: there exists a state function (entropy, S) whose change ΔS for any spontaneous process satisfies the Clausius inequality [53, 187]

$$\Delta S(t) \geq \oint_{\partial V} \frac{dQ}{T} \geq 0 \tag{9}$$

which encapsulates the increase in entropy principle. The distinction between the system and its surroundings must be unambiguous through the presence of a *bona fide* boundary across which the flux of matter, charge, heat, etc. can freely pass. A constant-temperature (T) heat bath with which the system is in contact through its boundary ∂V serves as the

surroundings. The integral is over the surface ∂V that constitutes the boundary between the molecule of volume V and its environment. The Clausius integral $\oint_{\partial V} dQ/T$ is positive for irreversible processes, is zero for reversible processes, and can never be negative. The inequality implies that the entropy given to the environment is greater than the entropy transferred as heat from the hot reservoir. The operative Carnot cycle here is a fiduciary audit of the net exodus of efflux over the coverage of ∂V contacting the heat bath. It is this audit that undermines all supposed objections to the SLT, just as Planck [7, loc. cit., pp. 103–104] anticipated. If $\oint_{\partial V} dQ/T$ vanishes, $1/T$ is an integrating factor [188, 189] for dQ , an inexact differential.

The two best-known statements of the SLT are: (1) If a system undergoes a Carnot cyclic process it cannot turn heat entering the system into work done on the surroundings with unit fractional efficiency (Kelvin-Planck statement); (2) Heat cannot flow spontaneously from a cooler to a hotter object (Clausius' statement). Historically, the mathematical formulation of the SLT was reached through the empirical study of the limitations of steam-driven heat engines designed to convert one form of energy (sensible heat) into mechanical energy (work) at the start of the industrial revolution. Nowadays engines or motors run the gamut from electrical, pneumatic, hydraulic, molecular, etc. using sundry working media. The exchange of work and the working element between a system and its surroundings is always an irreversible process. An alternative mathematical approach to the foundations of thermodynamics emerged from the study of nonlinear deformations of continuous media [190, for e.g.].

The Clausius inequality provides a means of delimiting the entropy change of any process that begins at equilibrium to which state it returns as if nothing happened with no overall change in the entropy of the system and its surroundings, or begins in an arbitrary state to end with a net production of entropy; it means that no process can decrease the entropy of the Universe and, together with the zeroth law of thermodynamics, implies that a temperature of absolute zero is unreachable. Equipped with a false antecedent, the claim that the concept of entropy is inapplicable to single systems (a molecule and its Universe, for e.g.) but only to ensembles of them is as counterfactual [191] as it is casuistic [192]. The Clausius inequality is based on his statement of the SLT and provides a means of distinguishing reversible from irreversible processes based on the earlier findings of Carnot (without his view that heat is a fluid) and independently of volume number density (sic thermodynamic limit).

The first law of thermodynamics relates the internal energy or enthalpy U to heat Q and work W as

$$dU = dQ + dW, \tag{10a}$$

or

$$-dW \leq -dF, \tag{10b}$$

an expression of the fact that the same change dU in U can be produced either by the sole addition of sensible heat dQ or work dW or by contributions from both. The signs used correspond to the IUPAC* and not the Clausius convention whereby all net energy transfers from the surroundings (system) to the system (surroundings) are positive (negative), respectively. Here, $dQ = TdS$ and relates U to T , S , and the Helmholtz free energy $F = U - TS$, this being the amount of energy free to do work in response to entropy losses. Gradients in F are the driving forces of all biochemical processes and their reliable calculation [193, et passim] is intensively pursued. The internal energy U is the sum of the sensible heat Q accumulated by the system and the work W done by it although physically each differs from the other. Like dQ , dW is an inexact differential and is called the configuration work; it is the amount of work done changing the configuration of a system from one to another and depends on how the work is done, i.e. on the path taken between the initial and final configurations. Energy (kinetic, potential) is an attribute that matter and radiation have or can acquire or lose. Unlike entropy, energy is a conserved quantity but this is difficult to audit especially when it dissipates or thermalizes. Both kinetic and potential energies are interconvertible and their scales are arbitrary. Heat (thermal, radiation) is a process in which a system acquires or loses energy as a consequence of it having a different temperature than its surroundings. Work is a transfer of energy to or from a system by any means other than heat; it can be fully converted into heat as in friction but heat can only be partially converted to work. There is no entropy associated with energy transfer as work. Although the first law places no restriction on the direction of a process, it does not guarantee that the process will occur, that being decided by the SLT in conjunction with physical and chemical kinetics considerations.

The SLT asserts that [133, 194, for e.g.] natural processes are irreversible, i.e. the entropy $S(t)$ always increases as the system strays from equilibrium at an absolute temperature $T(\mathbf{x}, t)$ via an exchange of heat (and its transformation to mechanical work) $dQ = d\mathbf{x} \cdot \mathbf{F}_{\text{int}}(\mathbf{x}, t)$ with its surroundings. The zeroth law of thermodynamics leads to a definition of temperature via the relation $1/T = (\partial S/\partial U)_V$ that forms the empirical basis for the calorific measurement of entropy, with $TdS = dQ$ describing how entropy changes in the amount dS when an inexact differential amount of energy dQ is introduced as heat into the system at a finite temperature $T > 0$ delineated by the zeroth law of thermodynamics.

The Clausius inequality in (9) stipulates that ΔS equals or exceeds the quantity $\oint_{\partial V} dQ/T$. Here dQ is heat or energy or work. There is nothing in science or beyond to prevent the integrand in $\oint_{\partial V} dQ/T$ from being taken to be and applied to an arbitrary system without reference to Boltzmann-Gibbs or Tsallis statistical mechanics. This is precisely what is done

here in accepting dQ for what it is, i.e. the heat (energy) or work (mechanical energy) conversion that occurs between the system of interest and a heat bath (its minimal environment) which it ineluctably contacts.

Regardless of the notion of temperature fluctuations [195–197, et passim] or indeterminacy providing justification for the complementarity relation $\Delta U \Delta(1/T) \geq k_B$ [198–200] in analogy with Heisenberg’s uncertainty principle for position and momentum in quantum mechanics, here T is taken to be a parameter that is characteristic of the heat reservoir and is known *a priori* with thermal noise viewed as [201, loc. cit., p. 191] “the least disturbing for the physicist” unconcerned with emerging technologies. If T is the known temperature of the heat bath, $T(\mathbf{x}, t)$ is the temperature at $\mathbf{x} \in \partial V$. To de Broglie [202, loc. cit., p. 29] in discussing no less than the Boltzmann-Gibbs canonical distribution “... the notion of temperature is meaningful for just one molecule when that molecule is found to be in energetic contact with a thermostat of temperature T that imposes its temperature upon the molecule.” For present purposes the thermostat is not hidden as is de Broglie [202]’s based on Bohm and Vigier [203]’s subquantum hypothesis, but rather $T = T(\mathbf{x}, t) \forall \mathbf{x} \in \partial V$ at any time t [188] as tacitly assumed by Clausius. Consequently

$$\begin{aligned} \Delta S(t) &\geq \oint_{\partial V} \frac{dQ}{T} = \oint_{\partial V} \frac{da}{T} \hat{\mathbf{n}} \cdot \mathbf{F}_{\text{int}} \\ &= \oint_{\partial V} \frac{da}{T} \hat{\mathbf{n}} \cdot \frac{\partial \mathbf{j}}{\partial t}. \end{aligned} \quad (11a)$$

Quantum mechanically $\hat{T}\mathbf{j}(\mathbf{x}, t)\hat{T}^{-1} = \mathbf{j}(\mathbf{x}, -t)$ so that \mathbf{j} is even in t since the Wigner time reversal operator \hat{T} is antiunitary and $\hat{T}i\hat{T}^{-1} = -i$ as was noted earlier. Consequently, $\mathbf{F}_{\text{int}}(\mathbf{x}, t) = \partial \mathbf{j}(\mathbf{x}, t)/\partial t$ is odd in t . Since $\mathbf{F}_{\text{int}}(\mathbf{x}, t)$ is odd because $\mathbf{j}(\mathbf{x}, t)$ is even under time reversal, it follows with reference to (8b) and (8c) that the gain in entropy $\Delta S(t)$ as given in (11a) is asymmetric in time[†], i.e. $\Delta S(t) = \Delta S(-t)$. Traveling backwards in time as is permitted by both quantum mechanics and electrodynamics would cause $\Delta S(t)$ to decrease contrary to the SLT and is consequently forbidden. Whether the process is reversible or irreversible, ΔS treats time $t \geq 0$ as a positive semi-definite parameter. Using (1a), (5), and (11a) it is clear that

$$\langle \Delta S(t) \rangle \geq \oint_{\partial V} \frac{da}{T} \rho (\rho \nabla^2 \phi + \nabla \rho \cdot \nabla \phi) \hat{\mathbf{n}} \cdot \nabla \phi \quad (11b)$$

which is the quantum Clausius inequality for the expectation value of the asymmetric $\langle \Delta S(t) \rangle = \langle \Delta S(-t) \rangle$ entropy change of a molecule in contact with a thermostat at time t . $\langle \Delta S(t) \rangle$ is monotone increasing [122, cf. Fig. 9] provided ϕ is subharmonic.

[†]A real function $f(x)$ of a real variable x is odd (asymmetric via a π reflection through the origin) iff $f(x) = -f(-x)$ or even (symmetric about the $f(x)$ axis) iff $f(x) = f(-x)$ in the domain of f .

*International Union of Pure and Applied Chemistry

If the single molecule under investigation here were one of an ensemble of noninteracting replicas, each similarly prepared in the same state ψ and to which considerations of Bose-Einstein, Fermi-Dirac, or Maxwell-Boltzmann statistics are not required [204, cf. §2.01], one has the same problem treated by von Neumann [205, cf. §5.2] in his appeal to Szilard [206]’s one-molecule heat engine, a scenario criticized by some [207, for e.g.], validated by many [208, cf. Ch. VI], [97, 209–213], and the first to point out the connection between entropy and information. In the absence of demons and pistons*, the thermodynamic limit [214–217], [218, cf. Ch. 14] issue is irrelevant since it does not apply to a lone molecule in a thermal bath whose sole task is to supply heat to maintain that molecule’s fluctuating charge density $\rho(\mathbf{x}, t)$, current density $\mathbf{j}(\mathbf{x}, t)$, and deformable volume V . Nor does a thermodynamic limit apply to the known Universe. Previously, using only the elementary notion of work, $dQ = d\mathbf{x} \cdot \mathbf{F}_{\text{int}}(\mathbf{x}, t)$ was identified as the action over a differential displacement $d\mathbf{x}$ in V of the quantum mechanical Lorentz-Faraday force $\mathbf{F}_{\text{int}}(\mathbf{x}, t)$ given in (8a) in terms of the thermally-driven current density \mathbf{j} of a single molecule.

The integrand of the integral in (11b) is also the integrand in the Clausius inequality given in (9). If it is to be estimated, it is best done using statistical methods where the integrand’s dependencies ($\rho, \phi, T, \mathbf{x}$) at time t are treated as independent and identically distributed random fluctuating variables drawn repeatedly from appropriate probability distributions under the auspices of the law of large numbers. That part of the integrand in parenthesis is the outward flux of \mathbf{j} across ∂V . The two inner products $\nabla\rho \cdot \nabla\phi$ and $\hat{\mathbf{n}} \cdot \nabla\phi$ in the integrand each involve outbound gradients and are positive [219–224] since these gradients make more probable glancing and head-on egress across ∂V than the biased presumption that they be tangent to the boundary ∂V , exclusively or otherwise. The only term that can cause the integral to change from positive to negative in violation of Clausius’ inequality is that involving $\nabla^2\phi$ thus making it necessary and sufficient that ϕ be subharmonic [148, 149] in V so that no such transgression occurs. Whether the Hamiltonian operator of the system of interest is autonomous or not has no bearing†

*Zurek [210, loc. cit., p. 152]’s rebuttal of Jauch and Báron [211]’s primary argument reads “One may argue that the one-molecule engine cannot be analyzed by means of thermodynamics (sic statistical mechanics), because it is nowhere near the thermodynamic limit. This objection is overruled by noting that arbitrarily many “Szilard’s engines” can be linked together to get a “many-cylinder” version of the original design. This will cut down fluctuations and allow one to apply thermodynamic (sic statistical mechanics) concepts without difficulty”. Indeed, the entropy increase in time of an ensemble of entities is determined by their current states as affected by internal conservative potentials (Coulomb, Newtonian, thermal Lorentz-Faraday, etc.), prevailing pair-wise force fields (Lennard-Jones and more-exotic empirical variants), and external nonconservative potentials (catalysts, lasers, particle beams, etc.) that aspire to control them.

†This is consistent with Landau and Lifshitz [225, loc. cit., p. 51]’s observation that “The form of the Hamiltonian for a system of particles which interact with one another cannot be derived from the general principles of

on the T-asymmetry of $\langle\Delta S(t)\rangle$ and likewise does not negate the T-symmetry of either quantum mechanics or electro-dynamics.

Besides distinguishing between two possible types of processes on the basis of changes in entropy as determined by finite $\nabla\phi$, there are several other features of Clausius’ inequality worth recalling: (a) it is a consequence of the SLT; (b) it is not an evolutionary relationship; (c) it does not rely on knowledge of a system’s microstates, just the current state; (d) entropy is the outcome of a process; (e) it is T-asymmetric without obliging the same of any allied dynamical framework including quantum mechanics‡.

The lone molecule ensconced in a heat bath is free to visit the entirety of its configuration space demarcated by V . Since it has been shown that $\langle\Delta S(t)\rangle = \langle\Delta S(-t)\rangle$ and as an alternative to ensemble averaging, its Laplace long-time average $\langle\Delta S_\tau\rangle$ may be taken [235, cf. p. 68] as

$$\begin{aligned}\overline{\langle\Delta S_\tau\rangle} &= \frac{1}{\tau} \int_0^\infty dt e^{-t/\tau} \langle\Delta S(t)\rangle \\ &= \int_0^1 dt e^{-t} \langle\Delta S(\tau t)\rangle,\end{aligned}\tag{11c}$$

where $\tau > 0$ is a phenomenological relaxation time for ubiquitous exponential decay [236] that has both system and environment dependencies. Independently of τ , $\langle\Delta S(t)\rangle$ fluctuates en route to $\langle\Delta S_\tau\rangle$ with a variance $\sigma_\tau^2 = \langle\Delta S_\tau^2\rangle - \langle\Delta S_\tau\rangle^2$. Since (11c) provides a means of time averaging under nonstandard state conditions and with the accommodation of relaxation, it obviates subjective biases related to the unmeasured properties of an ensemble of replica systems. Unlike electromechanical systems where molar statistics is apropos, Avogadro quantities of macromolecules are not always available in biological and nanoscale systems where finite-time measurements come to the fore, ergodic behavior is arguably applicable, and ensembles are moot. The same applies to the known Universe. The provision of $\Delta S(t)$ data is through calorimetry or via Monte Carlo-Markov chain techniques [237, 238]. This Laplace time-averaging is equally applicable to Helmholtz $\Delta F(t)$ and Gibbs $\Delta G(t)$ free energies whose time averages $\langle\Delta F_\tau\rangle$ and $\langle\Delta G_\tau\rangle$ are roughly equal for entropy-driven pro-

quantum mechanics alone.”

‡Bohm, Gadella and coworkers [226, et passim] postulate a time asymmetric quantum theory (TAQT) by associating states and observables to two different Hardy subspaces dense in the same Hilbert space that does not distinguish between the in-states and out-states of scattering theory but which in TAQT would cause the dynamical equations (in the Schrödinger and Heisenberg pictures) to integrate to a semigroup evolution. TAQT is not without its critics [227–230]. Within a cellular automaton interpretation of quantum theory, ’t Hooft [231] makes similar claims. Oliver Penrose (esteemed thermodynamicist and older brother of Roger)’s critical review [232] of Mackey [233]’s book are equally apropos to any proposal that requires quantum mechanics to waive its time reversal invariance, an imposition obviated by the SLT as will be revealed in this paper. Kuzemsky [234, et passim] has surveyed foundational issues of the problem of time and its asymmetry, a consideration outside the scope of this paper.

cesses and identical for an uncompressed single molecule [183].

Entropy generation S_{gen} (what Clausius [239, cf. Eq. 71] called production rate) is the entropy produced during a process as given by

$$S_{\text{gen}}(t) = \Delta S(t) - \oint_{\partial V} \frac{dQ}{T}. \quad (11d)$$

It is zero or positive for a reversible or irreversible process [240, 241], respectively. Irreversibilities degrade the performance of systems and S_{gen} is a measure of their magnitude during a process. It is impossible for $S_{\text{gen}} < 0$ so that it cannot influence the thermodynamic arrow of time any more than can F_{int} . However, whereas F_{int} is inherent to the system and its dynamics, S_{gen} is part of the process. The entropy generation S_{gen} would vanish if the requirement that ϕ be subharmonic were relaxed to it being simply harmonic in V which was previously dismissed: (11b) and (11d) imply that

$$S_{\text{gen}}^{\nabla^2\phi>0}(t) \geq S_{\text{gen}}^{\nabla^2\phi=0}(t) \geq 0, \quad (11e)$$

so that subharmonic ϕ favors entropy generation more than harmonic ϕ .

In thermodynamics, work performed by a system is energy it transfers to its surroundings and the surroundings transfers energy to the system and both transfers incur a price. Even though $\oint_{\partial V} dQ/T$ is finite for natural processes, reflecting the fact that entropy is not conserved, use of the divergence theorem on $\oint_{\partial V} dQ$ gives

$$\oint_{\partial V} dQ = \oint_{\partial V} da \hat{\mathbf{n}} \cdot \mathbf{F}_{\text{int}} = \int_V d\mathbf{x} \nabla \cdot \mathbf{F}_{\text{int}} \quad (12a)$$

as the work done by \mathbf{F}_{int} . The orientable manifold V of configuration space encloses the flux $\nabla \cdot \mathbf{F}_{\text{int}}$ of \mathbf{F}_{int} and the generalized Stokes theorem [242, 243, for e.g.] further provides

$$\oint_{\partial V} dQ = \int_V d\mathbf{x} \nabla \cdot \mathbf{F}_{\text{int}} = \int_V d\mathbf{x} \cdot \nabla \times \mathbf{F}_{\text{int}}. \quad (12b)$$

The divergence and curl of \mathbf{F}_{int} are

$$\nabla \cdot \mathbf{F}_{\text{int}}(\mathbf{x}, t) = \psi^*(\mathbf{x}, t) \nabla^2 \psi(\mathbf{x}, t) - \psi(\mathbf{x}, t) \nabla^2 \psi^*(\mathbf{x}, t), \quad (12c)$$

and

$$\nabla \times \mathbf{F}_{\text{int}}(\mathbf{x}, t) = \nabla \psi^*(\mathbf{x}, t) \times \nabla \psi(\mathbf{x}, t) - \nabla \psi(\mathbf{x}, t) \times \nabla \psi^*(\mathbf{x}, t) \quad (12d)$$

respectively. The curl of \mathbf{F}_{int} vanishes for all $\mathbf{x} \in R^n$. However, the divergence of \mathbf{F}_{int} vanishes locally only when ψ or $\nabla\psi$ does so. Since there is no creation or destruction of charge within V and the Laplacian operator is self-adjoint, $\oint_{\partial V} dQ$ vanishes so that \mathbf{F}_{int} does no work, i.e.

$$\begin{aligned} Q &= \int_{\partial V} d\mathbf{x} dQ = \int_V d\mathbf{x} \nabla \cdot \mathbf{F}_{\text{int}} \\ &= - \int_V d\mathbf{x} \nabla^2 \mathcal{V}_{\text{int}} = 0, \end{aligned} \quad (12e)$$

where $\mathbf{F}_{\text{int}}(\mathbf{x}, t) = -\nabla \mathcal{V}_{\text{int}}(\mathbf{x}, t)$ with $\mathcal{V}_{\text{int}}(\mathbf{x}, t)$ being the potential energy function of $\mathbf{F}_{\text{int}}(\mathbf{x}, t)$. Thus, despite its spatial and time dependence, $\mathbf{F}_{\text{int}}(\mathbf{x}, t)$ is a conservative and not a dissipative force like friction or viscous drag that does negative work in the direction opposite to the displacement of its target which consequently loses energy as heat in the amount removed by such a force. The subharmonicity of ϕ is what makes \mathbf{F}_{int} a conservative force, one that conserves mechanical energy.

3 Faradaic induction in a thermal field

Gauge theories [244] enable a reduction in the number of variables necessary to define a physical state quantum mechanically (configuration space, \mathbf{x}) over that required classically (phase space, \mathbf{x} and \mathbf{p}). Electrodynamics was the first field theory to exploit gauge symmetry by recognizing that any function that can be written as a gradient could be added to the vector potential without affecting the magnetic field. Acting on a suggestion by London [245], Weyl [246, pp. 100-101] replaced the gauge scale factor with a complex quantity and turned the scale transformation into a change of phase. The gauge field of electrodynamics associates an element of the group $U(1)$ of unit complex numbers under multiplication to each path: the phase that a charged particle gets when going through a loop is the magnetic flux through the loop. The physical states of quantized systems are described [141, for e.g.] by vectors ψ of unit norm belonging to a complex Hilbert space \mathcal{H} . Physical observables are associated with self-adjoint operators \mathcal{O} acting on \mathcal{H} whose expectation values are scalar inner products $\langle \psi | \mathcal{O} \psi \rangle$ in \mathcal{H} that are unaffected by unitary transformations which act on both state vectors $\psi \mapsto U\psi$ and operators $\mathcal{O} \mapsto \mathcal{O}U\mathcal{O}^\dagger$, where U is unitary. Thus, the multiplication of state vectors by a phase (a $U(1)$ global group transformation) $\psi \mapsto e^{i\phi}\psi$ leaves operators and physical predictions unchanged provided \mathcal{O} does not differentiate ψ either spatially or temporally. Neither $\mathbf{j}(\mathbf{x}, t)$ nor $\partial\mathbf{j}(\mathbf{x}, t)/\partial t$ are such-like operators so that their inclusion of $U(1) = e^{i\phi}$ cannot be disregarded since the $U(1)$ phase $\phi(\mathbf{x})$ is local. This is reminiscent of earlier speculations by Schrödinger [247] based on Weyl [246]’s spacetime theory in connection with the Wilson-Sommerfeld [173, 174] quantization condition for Bohr’s old quantum theory of the H atom. For this reason, ϕ is referred herein as the unadorned “phase”, rather than Schrödinger [150]’s “phase angle”, de Broglie’s “phase wave”, or Weyl’s “gauge transformation”, all three being essentially one and the same. Failure to notice that the Schrödinger equation is not gauge invariant under a local gauge transformation is due in large to two commonly-held notions, viz. that it takes an external electromagnetic field to do so when in fact it does not [142, 143], and that, in confounding local with global, the phase of the wave function is arbitrary when in fact it is not [248] unless it is global.

The thermal field induces an internal electromagnetic con-

servative force field $\mathbf{F}_{\text{int}}(\mathbf{x}, t)$ of scalar potential Φ and vector potential \mathbf{A} in the system whose Helmholtz-Hodge decomposition [176–178] reads as

$$\mathbf{F}_{\text{int}} = -\nabla\Phi + \nabla \times \mathbf{A} \tag{13a}$$

into the scalar longitudinal (irrotational, curl-free) potential $\Phi(\mathbf{x}, t)$ and the vector transverse (solenoidal, div-free) potential $\mathbf{A}(\mathbf{x}, t)$ which provide, via Maxwell’s equations, for the *internal* microscopic electric

$$\mathbf{E}_{\text{int}} = -\nabla\Phi - \partial\mathbf{A}/\partial t \tag{13b}$$

and the *internal* microscopic magnetic induction

$$\mathbf{B}_{\text{int}} = \nabla \times \mathbf{A} \tag{13c}$$

fields which at every point in space and time obey the microscopic Maxwell equations. There is only one kind of charge and the amount of it anywhere can be positive, negative, or zero subject solely to its conservation regardless of whether it is believed to be associated with a nucleus or an electron. The prominence of electromagnetic potentials in quantum theory is due in large to the work of Aharonov and Bohm [249, 250].

Rhetorically, $\mathbf{A}(\mathbf{x}, t)$ generates $\mathbf{B}_{\text{int}}(\mathbf{x}, t)$ through its circulation and $\mathbf{E}_{\text{int}}(\mathbf{x}, t)$ through its time dependence with $\rho(\mathbf{x}, t)$ and $\mathbf{j}(\mathbf{x}, t)$ playing supporting roles encapsulated in the Lorentz microscopic force density

$$\mathbf{F}_{\text{int}} = \rho\mathbf{E}_{\text{int}} + \mathbf{j} \times \mathbf{B}_{\text{int}}, \tag{13d}$$

where

$$\begin{aligned} F_{\text{tot}}(t) &= \int_V d\mathbf{x} \cdot \mathbf{F}_{\text{int}}(\mathbf{x}, t) \\ &= \oint_{\partial V} da \hat{\mathbf{n}} \cdot \boldsymbol{\sigma}_{\text{int}}(\mathbf{x}, t) - \frac{d}{dt} \int_V d\mathbf{x} \cdot \mathbf{S}_{\text{int}}(\mathbf{x}, t), \end{aligned} \tag{13e}$$

is the total electromagnetic field on the charges in V , $\boldsymbol{\sigma}_{\text{int}}$ is the Maxwell stress tensor, and the Poynting vector \mathbf{S}_{int} is given by

$$\mathbf{S}_{\text{int}} = \mathbf{E}_{\text{int}} \times \mathbf{B}_{\text{int}}, \tag{13f}$$

and

$$\mathbf{F}_{\text{int}} = \nabla \cdot \boldsymbol{\sigma}_{\text{int}} - \dot{\mathbf{S}}_{\text{int}} \tag{13g}$$

pursuant to the conservation of linear momentum. In (13g) the last term on the right is the time derivative of the field’s photon momentum density while the first is the divergence of the stress tensor bearing on the charges in V .

Both $\Phi(\mathbf{x}, t)$ and $\mathbf{A}(\mathbf{x}, t)$ retain their spatial and nonretarded time dependencies without the \mathbf{E}_{int} and \mathbf{B}_{int} fields descending to electrostatics since the Lorenz condition [251–255] has not been invoked. Mathematically, the potentials $\Phi(\mathbf{x}, t)$ and $\mathbf{A}(\mathbf{x}, t)$ are volume integrals of the divergence and curl of $\mathbf{F}_{\text{int}}(\mathbf{x}, t)$ scaled by the Green’s function for the Laplacian

analogously to (7a) and (7b), respectively. It is clear from (1a), (5), and (13a) that the irrotational part of \mathbf{F}_{int} is

$$\nabla\Phi = \rho\nabla^2\phi\nabla\phi \tag{14a}$$

while the solenoidal part is

$$\nabla \times \mathbf{A} = -\nabla\phi \cdot \nabla\rho\nabla\phi, \tag{14b}$$

with both parts being in the same direction as $\nabla\phi$. Neither potential is directly measurable and may be replaced by gauge-equivalent potentials θ and $\mathbf{A} + \nabla\phi$, respectively, to yield the same $\mathbf{E}_{\text{int}}(\mathbf{x}, t)$ and $\mathbf{B}_{\text{int}}(\mathbf{x}, t)$.

Maxwell’s equations are linear dynamical PDEs that have a unique solution for given initial and boundary conditions. From these equations it is straightforward to show that the scalar $\Phi(\mathbf{x}, t)$ and vector $\mathbf{A}(\mathbf{x}, t)$ potentials satisfy

$$\square\Phi = -\frac{\partial}{\partial t} \left(\nabla \cdot \mathbf{A} + \frac{\partial\Phi}{\partial t} \right) - \rho \tag{15a}$$

and

$$\square\mathbf{A} = \nabla \left(\nabla \cdot \mathbf{A} + \frac{\partial\Phi}{\partial t} \right) - \mathbf{j}, \tag{15b}$$

respectively, where $\square = \nabla^2 - \partial^2/\partial t^2$ is the d’Alembertian operator. These promote use of the Lorentz condition in which the term in parenthesis common to both is set to zero, a gauge strategy of historic [244] importance to physics.

Alternatively, use of the curl of the curl identity, Gauss’s law of electricity in the curl of Faraday’s law, and Gauss’s law of magnetism in the curl of Maxwell-Ampère’s law, allows one to arrive at the coupled inhomogeneous wave equations [256] for the $\mathbf{E}_{\text{int}}(\mathbf{x}, t)$ and $\mathbf{B}_{\text{int}}(\mathbf{x}, t)$ fields as

$$\square\mathbf{E}_{\text{int}} = 4\pi \left(\nabla\rho + \frac{\partial\mathbf{j}}{\partial t} \right) \tag{16a}$$

and

$$\square\mathbf{B}_{\text{int}} = -4\pi\nabla \times \mathbf{j}, \tag{16b}$$

respectively. In (16a) and (16b), \square acting on $\mathbf{E}_{\text{int}}(\mathbf{x}, t)$ and $\mathbf{B}_{\text{int}}(\mathbf{x}, t)$ generates inextricably coupled electromagnetic waves given sources in gradients of ρ , time-varying changes in \mathbf{j} , and circulations of \mathbf{j} . The Lorentz-Faraday force $\mathbf{F}_{\text{int}}(\mathbf{x}, t)$ first introduced here in (8a) is none other than one of two source terms for the wave equation of $\mathbf{E}_{\text{int}}(\mathbf{x}, t)$ and leads to the possibility of the oscillation or acceleration of charge which radiates more or less transverse to the direction of propagation. At idealized $T = 0$ where $\mathbf{F}_{\text{int}}(\mathbf{x}, t)$ is absent, the charges in an “isolated” (sic stationary state) molecule oscillate in place without accelerating and their Coulomb radiation field decays as $1/|R'|^2$ where R' is the line of sight distance to a charge [256]. More realistically, $T > 0$ causes charges in the molecule to oscillate and accelerate. This produces self-sustaining electric and magnetic fields propagating as electromagnetic waves at the speed of light which transport energy

and momentum to charged particles at large distances from the source at the expense of the accelerated charge. The electric and magnetic fields are orthogonal to each other. When $T > 0$ such that $F_{\text{int}}(\mathbf{x}, t)$ is operative, the charges oscillate and accelerate and their radiation field decays as $1/|R'|$ to surpass their shorter-ranged Coulomb radiation field [256]. Since $\nabla\rho$ ultimately vanishes* and $\nabla\times\mathbf{j} = \nabla\rho\times\nabla\phi$, the internal $\mathbf{E}_{\text{int}}(\mathbf{x}, t)$ and $\mathbf{B}_{\text{int}}(\mathbf{x}, t)$ fields are pervasive and are the source of photons to be absorbed and emitted within V in the manner first treated by Einstein [257, 258] and later by Dirac [259, 260] in analogy with gravitoelectromagnetic phenomena [261, 262], e.g. Lense-Thirring frame-dragging effects [263, 264], whose internal $\mathbf{E}_{\text{int,g}}$ and $\mathbf{B}_{\text{int,g}}$ fields (or equivalently, $\Phi_{\text{int,g}}$ and $\mathbf{A}_{\text{int,g}}$) are caused by the gravitational interaction of massive celestial objects with neighboring ones.

The $U(1)$ gauge symmetry of electromagnetism represents the group of rotations around a fixed axis. Since the end of the quark era, $U(1)$ has broken the $SU(2) \times U(1)$ gauge symmetry of the electroweak force whose three massive bosons W^\pm and Z^0 are accompanied by a fourth massless one, the photon. Helmholtz-Hodge photons induce electrically neutral currents in a molecule, in analogy with the decay of Z^0 to neutrinos which scatter off electrons in electroweak interactions [265], and mediate scattering between nuclei and electrons that entail the transfer of momentum, spin, and energy via photon exchange but to the exclusion of charge. $U(1)$ symmetry comes from the fact that the absolute phase ϕ of ρ cannot be measured unlike its finite relative change $\nabla\phi$ as first pointed out by Weyl [248] and adopted by Dirac [266]. The importance of $U(1)$ symmetry comes from Emmy Noether's theorem which states that such gauge symmetries lead to the conservation of a related quantity. Two types of $U(1)$ gauge symmetry are salient, viz. global gauge symmetry where the phase change $\nabla\phi$ vanishes at critical points in space and leads to the conservation of charge; and local gauge symmetry where the phase is not the same at all locations and requires the introduction of an additional gauge field to keep it invariant under such finite relative changes. One may view the local gauge field as signaling phase changes from one point to another by radiatively communicating such changes and in doing so leading a molecule to engage in its own intramolecular entanglement frontier[†]. Molecules have many degrees of freedom but only two types of material constituents whose positions are not only correlated with each other – a type of correlation known as entanglement [267, cf. Ch. 16], [268, cf. Ch. 5], [269, cf. Ch. 17] and a key property of quantized systems exploited to effect quantum compu-

* $\nabla\rho$ is the source of charge that is accelerated by $F_{\text{int}} = \partial\mathbf{j}/\partial t$. Its inclusion in Clausius' inequality is unnecessary since $\langle\nabla^2\rho\rangle$ vanishes.

[†]With two entangled particles one knows something about their combined properties but their individual properties are indeterminate until one makes a measurement of the state of one particle at which point one has some, but not all, information about the other. Entanglement is a nonlocal correlation between nonseparable states.

tation [270] in concert with the superposition principle – but also with its internal Helmholtz-Hodge photons whose “wave functions” [271] are inherently part of ψ .

At their prevailing low energies, Helmholtz-Hodge photons serve as the carriers of the nonconservative electromotive force (emf) [272, Sec. 6.1], [273, cf. Ch. 7]

$$\mathcal{E}(t) = \oint_{\partial V} da \hat{\mathbf{n}} \cdot (\mathbf{E}_{\text{int}} + \nabla\phi \times \mathbf{B}_{\text{int}}) = -\frac{d}{dt}\Phi_{\mathbf{B}_{\text{int}}}(t) \quad (17a)$$

of molecules through their in situ photon absorption and emission regardless of Faradaic fixtures (wires, circuits, electrodes, batteries, etc.). Emf produces a charge imbalance that causes the lighter electrons to move from nucleophilic to electrophilic regions, this movement being what is recognized as electric current. Electrons can gain or lose energy due to their interaction with \mathbf{B}_{int} and \mathbf{E}_{int} whereby \mathbf{B}_{int} guides their motion, \mathbf{E}_{int} accelerates them, and Lenz's law prescribes their direction. Of course, being internal fields rooted in the molecule's structure, \mathbf{B}_{int} and \mathbf{E}_{int} are not amenable to manipulation or so-called control. The deformation of V due to the magnetic Lorentz force acting on charges is the motional emf while the remaining part of \mathcal{E} is the transformer emf generated by an electric field induced by a changing magnetic field. Eddy currents induced in the cores of transformers and generators dissipate energy as heat loss giving rise to temperature increases.

The quantity on the far right in (17a) is formally

$$\frac{d}{dt}\Phi_{\mathbf{B}_{\text{int}}}(t) = \oint_{\partial V} da \hat{\mathbf{n}} \cdot \left[\frac{\partial\mathbf{B}_{\text{int}}}{\partial t} - \nabla \times (\nabla\phi \times \mathbf{B}_{\text{int}}) \right], \quad (17b)$$

where $\Phi_{\mathbf{B}_{\text{int}}}(t)$ represents the internal magnetic flux of the molecule and the Maxwell relation $\nabla \cdot \mathbf{B}_{\text{int}} = 0$ holds due to the absence of magnetic charges in Nature. The induced $\mathcal{E}(t)$ and the rate of change in $\Phi_{\mathbf{B}_{\text{int}}}(t)$ have opposite signs so that the cause (induced field) opposes the effect (changing current) in analogy with Newton's third law.

Recall that the binding of electrons to nuclei is modified somewhat by parity-violating Z^0 exchanges that manifest as parity nonconservation in both atoms [274, 275] and molecules [276, 277].

4 Discussion

4.1 Going forward

Obviously

$$\nabla\phi(\mathbf{x}) = \frac{\partial\mathbf{j}(\mathbf{x}, t)}{\partial\rho(\mathbf{x}, t)} \quad (18)$$

thus exposing the elusiveness of the relative phase which clearly changes sign under P because \mathbf{j} does and ρ does not. Neither C nor T changes $\nabla\phi$. The popular assertion that the phase of ψ is arbitrary and has no physical significance is true only if that phase is global. The phase is local, however, and provides an unequivocal link to the Lorentz-Faraday force

$F_{\text{int}}(\mathbf{x}, t)$ whose effects are manifest in the unremitting operation of the SLT in blockading quantum mechanics from providing a portal to the past and without curtailing even massive objects from ultimately reaching stasis in going forward. The Lorentz-Faraday force $F_{\text{int}}(\mathbf{x}, t)$ is intrinsically T-asymmetric regardless of the initial and boundary conditions of this or other universes and without electrodynamics or quantum mechanics having to forfeit their innate time-reversal symmetries.

Weak measurement techniques [278–280] have now been extended beyond the massless photon. As long anticipated by Aharonov et al. [281], Bednorz et al. [282] have shown that weak measurements are time-reversal symmetric classically but not so quantum mechanically. More recently, Jayaseelan et al. [283], in weak measurements of the spin of ultra-cold atoms, provided evidence for absolute irreversibility and a strictly positive average arrow-of-time captured by a fluctuation theorem; they further demonstrated absolute irreversibility for measurements performed on a many-body entangled wave function. These demonstrations are consistent with Borel [284, loc. cit., pp. 2–3]’s quip that “Events with a sufficiently small probability never occur,” following which he goes on to quantify “sufficiently small” for probabilities that are negligible on the human, terrestrial, and cosmic scale as descending in the order 10^{-6} , 10^{-15} , and 10^{-80} , respectively. Recall that in particle physics, the gold standard for a discovery is 5σ , in which there is a one in 3.5 million chance of the result being a fluke. The BaBar Collaboration found [13] a 1 in 10^{43} (14σ) level of certainty for their T-asymmetry measurements and CP violation was also observed at the 16σ level, far more than needed to declare a discovery. These observations of T reversal violations in electroweak interactions are consistent with the SLT being T reversal forbidden, the primary revelation of this paper. It remains to be seen (*vide infra*) if T reversal violations are also observed in strong-force interactions.

Manifestly, $\Delta S(t)$ increases and the process is reversible or irreversible according as the gradient in ϕ vanishes or not on ∂V , respectively. The entropy gain ΔS will be proportional to the area of the boundary ∂V enclosing the nominal volume V of the system interfacing its surroundings, just as with black holes. Unlike black holes, however, molecules lack horizons and their gain of entropy is settled by the gradient field of their local phase ϕ in guaranteeing their participation in natural processes without losses from the universe of itself and its heat reservoir. Since the vorticity $\nabla \times \nabla\phi$ vanishes except [285] at nodes in ρ (and $\nabla\phi$ is singular), the entropy gain by the molecule in contacting a heat bath is sheltered from meteorological losses consistent with the absence of swirl in F_{int} when the heat is withdrawn.

Equations (17a) and (17b) reveal that Faraday’s law of induction holds for a single molecule provided the gradient of its local phase is finite, a condition necessary and sufficient for it not to present with its well-known paradoxes [286–288].

Measurements of the emf $\mathcal{E}(t)$, the Helmholtz-Hodge fields E_{int} and B_{int} , and their ancillary lines of force first envisioned by Faraday [289], for a single molecule using a test charge would be as difficult as it is in quantum electrodynamics [290] but perhaps for different reasons. The long-standing validity of Faraday’s law $\mathcal{E}(t) \sim \pm d\Phi_{B_{\text{int}}}(t)/dt$ in engineering applications now has a quantum basis. Of course Faraday’s law induces potential, not current which is simply the induced voltage divided by the resistance of the loop. With multiple identical loops Faradays law is additive (sic extensive), i.e. $N\mathcal{E}(t)$ where $N \gg 1$ is the number of loops (windings).

4.2 The stability of a molecule

Clausius’ classical virial theorem [291] relating the time averages of the kinetic energy (“vis viva”) of a system of discrete particles and the virial (“ergal” or mechanical work) of the system, that being the work done by the gravitational forces (or equivalently, by $-\nabla\mathcal{V}_C$ for a molecule of Coulomb potential \mathcal{V}_C) has long served [292] cosmology in accounting for the stability of the most virialized objects in the Universe, clusters of stars and galaxies. The latter are filled with the intrastellar (cluster) medium (IS(C)M), an X-ray-emitting hot plasma with a typical temperature $\sim 10^7$ K. The interstellar medium (ISM), consisting of the matter (atomic, ionic, molecular, dust, cosmic rays) and radiation that occupies the space between the star systems in a galaxy, interacts magnetohydrodynamically with the ICM. Clusters are characterized by the virial radius within which the cluster’s mass can be determined under the assumption of the ICM being in hydrostatic equilibrium. Clusters are thought to grow into larger systems through mass accretion flows which are merged into the ICM at a radius of several times the virial radius. Properties such as the temperature or density around the virial radius are not well known because of observational difficulties. The virial theorem holds even for systems that are not in thermal equilibrium. Dark matter’s existence was first hypothesized by Zwicky [293] to account for the mass deficit found when the total sum of the masses of individual members in a galactic cluster falls far short of the virial mass whose use assumes that the cluster is stable, an assumption questioned by Ambastumian [294] who maintained that not only are the clusters unstable but they are also exploding, a controversial hypothesis whose history and impact on cosmology is reviewed by Bland-Hawthorn and Freeman [295, cf. 1.10]. A pivotal discovery in this history was Vera Rubin and Kent Ford’s confirmation [296] that dark matter is required to account for the rotation of stars and spiral galaxies. Other indicators of the presence of dark matter comes from gravitational lensing [297] and from fluctuations in the power spectrum of the CMB [298].

As the Universe expanded and cooled following the Big Bang, energy was converted to subatomic particles which merged to form protons – the nuclei of H atoms, some of

those nuclei fused to form He so that the early Universe consisted almost entirely of hydrogen, helium, and in lesser amounts, lithium, beryllium, and boron. In time, these dense molecular clouds collapsed under gravity to form stars. Nuclear fusion reactions in these stars spawned more elements and stellar explosions forged even more in the process of nucleosynthesis. The most abundant (greater than 90%) element in the Universe is H followed by He all of whose isotopes are stable except for minuscule amounts of tritium (^3H). Molecules account for most of the observable matter in the Universe and are remarkably stable against change. That matter at equilibrium is stable is so self evident that were it otherwise its existential proof would be as redundant as it would be specious. Ordinary matter [299, for e.g.], as comprised of atoms and molecules, has both mass and volume with the former concentrated in its positively charged nuclei and the latter occupied mainly by negatively charged electrons that are of much smaller size than a typical nucleus and are ~ 2000 times lighter than a proton. The mass number A is the sum of the total number of protons (atomic number, Z) and neutrons with differing number of neutrons for the same Z giving different A 's for the isotopes of that element. Bulk matter does not implode or eventually explode and is self-evidently stable across low-energy scales from fluids [300, for e.g.], to solids [301, for e.g.], to engineered structures designed and safety-certified without reference to atomistic considerations [302, for e.g.]. Whereas nuclei have the *Chart of the Nuclides* (~ 3000 in number) and atoms have the *Periodic Table of the Elements* (~ 120 in number), molecules (countless in number) have no such iconic organizational motif. The stability of matter resides in its nuclei, the majority of which are radioactive and undergo decay while the rest are located in the valley of stability between the proton and neutron drip lines as determined by their constitutive proton/neutron ratio and with an island of stability indicative of far longer-lived (but yet to be observed) isotopes of super-heavy elements than the known isotopes of these elements. The nucleons in the nucleus are fermions which obey the PEP and in the case of identical nucleons this results in the small but finite size of nuclei. Nuclides that do not undergo spontaneous decay are stable isotopes. There are about 252 stable isotopes among 80 elements with ^{56}Fe being the most abundant and ^{62}Ni the most stable. The nuclear (or residual strong) force binds nucleons into nuclei through the energy equivalence of their mass defects. This force is relatively short ranged compared to the Coulomb repulsion between protons, being attractive between spin-aligned nucleons until it falls off with distance and repulsive when their separations are small. Additionally, interactions between the spins and angular momenta of nucleons lead to the deformation of nuclei from purely spherical shapes. The nuclear force is known semi-empirically only but is more complicated than the Coulomb force operative between nuclei and electrons in atoms and molecules and its extension beyond the shell model is an active area of research [303, 304, for e.g.].

Supersymmetry (SUSY) is the principle that there is an unknown symmetry between fermions and bosons. SUSY was developed to explain the hierarchical disparity between the strength of the electroweak force and gravity by proffering the existence of superpartners of known particles, each having the same properties as the originals except for spin, so as to curtail the magnitude of the Higgs mass from undermining the very stability of the SM construction. SUSY is the source of hypothetical WIMPs in galactic halos. There is currently no evidence for SUSY at high energies.

When Feynman remarked [305, loc. cit., pp. 3–4]:

It appears to be one of the few places in physics where there is a rule which can be stated very simply, but for which no one has found a simple and easy explanation . . . This probably means that we do not have a complete understanding of the fundamental principle involved,

he was referring to the spin-statistics theorem (SST). Succinctly put, the SST [306] is more easily invoked than its basis and applicability are understood. The SST links the spin (half-integer or integer) property of a physical system comprised of fermions and bosons with the statistics (Fermi-Dirac or Bose-Einstein) it obeys and provides a foundation for the PEP which has long been part of even high school physics and chemistry curricula.

Proof of the SST lies outside the scope of nonrelativistic quantum mechanics: it requires the full arsenal of relativistic quantum field theory, specifically that the fields are invariant under the Poincare group, that there is a vacuum state that is invariant under this group, that all states can be built up from the vacuum by applying field operators, that the Hamiltonian is bounded below, and locality in that the fields either commute or anticommute at spacelike separations. The theorem then says that at spacelike separations boson fields of integer spin commute while fermion fields of half-integer spin anticommute whereupon the PEP emerges. As Feynman was later to recount [307], the CPT theorem illustrates why every subatomic particle must have an antiparticle partner and links to the SST with fermion wave functions changing by a sign under two CPT reflections while bosons do not. Some proofs use CPT invariance to prove the SST while other proofs do the opposite. Nonrelativistic quantum mechanics lacks analogs of both the CPT and SST. After almost a century of use, the PEP continues to lack a theoretical basis [308–311] even though experimental evidence indicates [312] that its violation has yet to be found although the search [313, 314] goes on. The PEP is a scientific principle whose philosophical status continues to be worthy of further scrutiny [315, 316, for e.g.] ever since Margenau [317] first identified it as such. Inspired as it was primarily by the work of Stoner [318] on atomic transitions and Pauli [319]'s own recognition of a binary ambiguity in the response of an electron to a Zeeman field with its intimation of a necessary "spin

quantum number” to be added to those already well known (principal, angular momentum) [154, 173, 174, 320, 321, for e.g.], few possess the deep insight into the PEP [322], particularly in respect to the conditions of its violation and their consequences for quantum gravity, say, regardless of its high-level rationale for the layout of the *Periodic Table* and its provision of degeneracy pressure accounting for the stability of white dwarfs and neutron stars.

The nuclei of many isotopes have a characteristic spin (I). Some nuclei have integral, some have fractional spins, and a few have no spin. Nuclear spin is related to the nucleon composition of a nucleus: odd A -nuclei (i.e. those having an odd number of nucleons) have fractional spins, e.g. $I = 1/2$ (^1H , ^{13}C , ^{19}F), $I = 3/2$ (^{11}B), and $I = 5/2$ (^{17}O); even A -nuclei composed of odd numbers of protons and neutrons have integral spins, e.g. $I = 1$ (^2H , ^{14}N); and even A -nuclei composed of even numbers of protons and neutrons have zero spin, e.g. $I = 0$ (^{12}C , ^{16}O , ^{32}S). Spin-1/2 nuclei have a spherical charge distribution, others have nonspherical (prolate or oblate) charge distributions and are often isomeric (long-lived excited states). Nuclei with finite spins have magnetic moments but the nonspherical nuclei also have an electric quadrupole moment. In an arbitrary molecule, some of its nuclei may be fermions (e.g. ^1H , ^{23}Na , ^{31}P , etc.). The PEP results in the “exclusion” of any state whose wave function does not change sign on exchanging a pair of indistinguishable fermions, whether they be spin 1/2 electrons or half-integer spin nuclei. Just so, with respect to pair interchanges, wave functions are asymmetric on the exchange of identical fermions and are symmetric on the exchange of bosons. The bosons in a molecule are nuclei whose effective charges [323–325] are reduced or shielded by the innermost electrons thus lessening their Coulombic repulsion. For the wave function $\psi(\mathbf{x}, t) = e^{i\theta(\mathbf{x}, t)}|\psi(\mathbf{x}, t)|$ the relative phase $\nabla\phi(\mathbf{x}) = \tan^{-1} \nabla(\text{Im} \psi(\mathbf{x}, t)/\text{Re} \psi(\mathbf{x}, t))$ is constrained by the PEP through its permutation symmetry action on $\psi(\mathbf{x}, t)$ by hypothesis. This is the essence of the PEP as it applies to an orbital-free single molecule.

Atoms and molecules have innumerable states the lowest of which is the ground state. This state persists indefinitely at the global minimum of the potential in joint compliance with the classical theorem of Earnshaw [125] and the nonrelativistic energy-time uncertainty relation [326] of Mandelstam and Tamm for a quantum system in a nonstationary state ψ [327–331]. In the ground state, the system in dynamical equilibrium with its environment resists irreversible change in its structure unless driven beyond its thermodynamic stability, primarily through temperature and pressure changes. Excited states have finite lifetimes but not definite energies: each time they decay, the energy released is slightly different with the average energy of the emitted photon peaking at the nominal energy of the state but distributed with finite width, termed the natural linewidth. The faster they decay the broader their linewidths, and conversely [332, for e.g.]. In a

thermal field, a molecule is not passively inert (sic dead) but is ready to go wherever the SLT takes it.

In engineering parlance, a molecule is a mechanical system whose input, if small, effects temporary changes through internal processes that disappear when the input is withdrawn and the system reverses to its original state with no apparent output, or whose input, if large, effects permanent changes to the system which is indelibly altered. This is like a rubber band or a balloon which when stretched or blown up too far breaks or bursts. If the stretching or blowing are not too great both objects revert reversibly back to their original states. If you repeat the stretching or blowing often enough elasticity diminishes until what a gentle tug or blow used to do no longer holds and ultimately an irreversible change occurs. The ability of a molecule to resist distortion by an outside agent and to return to its original size and shape in accord with Hooke’s law when the perturbing force (optical tweezers, electromagnetic fields, interface surfaces, heat sources, etc.) is removed, qualifies it as elastic in that it undergoes reversible changes that make no distinction between the past and the future in agreement with both time-invariant classical and quantum mechanics. Most molecules are elastic only to small perturbations, beyond which permanent modification occurs with the disintegration of the molecule into sundry fragments. The limits of elasticity does not usually apply to electronic transitions, which, unlike distortions within an harmonic approximation where the energies and intensities of the disturbances are low, involve internal processes of higher excitation energies and larger oscillator strengths resulting in irreversible changes that distinguish the past from the future just as do time-asymmetric entropy increases. Stability, even in elastic systems, demands dynamical analysis [333–335, for e.g.] since static stability alone does not generally imply stability under more inelastic conditions so that just like engineered structures, molecular structures engender their own future depending on their imposed input. On opening, the Millennial Bridge across the Thames in London, forced its pedestrians to walk transversely in stride to keep their balance, unwittingly accentuating its sideways wobble until it could be cleared of people without injuries. The designers went back to the drawing board to correct what, for them, was an unanticipated synchronicity previously exhibited almost two centuries before at the Broughton Suspension Bridge near Manchester, UK, one of the earliest of such span bridge designs, where mechanical resonance induced by a platoon of troops marching in step across the bridge caused it to collapse, resulting in command to direct that in future, troops break stride on crossing bridges. The futuristic Millennial span opened some two years later to worldwide applause after remedial corrections and so far it has not duplicated Tacoma. The moral of this mechanical linear-nonlinear abyss is that caution and due diligence be exercised when dealing with bridges, aircraft, and even the macroscopic effects of molecules: Nature does not provide warranties, just

surprises. A modest Murano piece or an extravagant Koon bubble structure that shatters cannot be restored to its original state by the most skillful of artisans anymore than a denatured protein can regain its primary tertiary structure in the hands of a chemist, a biologist, or a physicist.

There is an important distinction to be made between the stability of bulk matter and the stability of a single molecule. Bulk matter stability requires [214, 215] that for a bounded potential* $E_0 > -\infty$ (stability of the first kind) or $E_0 > -a(M + N)$ (stability of the second kind), where $a > 0$ is constant and E_0 is the ground-state energy, in order that the grand canonical partition function exist in finite volume and that a thermodynamic limit exist. These prerequisites for the stability of bulk matter do not pertain to the stability of a single molecule.

The PEP was found by Dyson and Lenard [337] to be a sufficient requirement in their *pace* treatment of the stability of matter in its state of stationarity, an issue considered earlier by Onsager [338] and later by Fisher and Ruelle [339] among others where the notion of stability is not, as one would reasonably expect, related to the inclination to change because of electromechanical disturbances but rather to ensuring that the classical configuration energy or quantum mechanical ground state of a system be bounded extensively from below because energy is so and in warranting that the thermodynamic limit be shown to exist. A thermodynamic limit does not always exist and for single-molecule and some nanoscale systems in particular it does not, even though stable single molecules do exist [340, for e.g.] and their reaction dynamics are observable [341–345, for e.g.]. Dyson [346] further claimed that the PEP is necessary for the stability of a system whose electrons and nuclei are of equal or of greater mass and charge, neither of which is true in Nature any more than matter fails to implode before exploding because the PEP is operative as necessary to a bewildering explication via a cascade of inequalities [218, et passim].

Echoing Wigner [347], Astumian [348] ascribes the unreasonable effectiveness of equilibrium theory for interpreting single-molecule systems that are far from thermodynamic equilibrium to their closeness to mechanical equilibrium. The primary determinant of structures available to a molecule lies in its Coulomb potential, not in peripheral diversions such as the PEP, whether Pauli repulsions are in the mind of the beholder, etc. How the Coulomb potential responds to deformations is transparently gauged by Earnshaw [125]’s theorem which, as will be shown in the following, indicates that the Coulomb potential is robust against elastic distortions so that the molecule is consequently stable until it transitions to a mixed state under environmental influences whereupon to no great surprise it may destabilize.

Earnshaw’s theorem [125], as recounted by Maxwell

*This is a condition deemed necessary [336] for the Coulomb Hamiltonian operator to be self-adjoint.

[349, cf. 116] and Jeans [350, cf. 192], basically states that harmonic matter is not stable since it has no interior minima in V the least of which could correspond to a configuration where the molecule has an equilibrium point, as first defined by Lagrange [351, cf. Part 1, §3, No. 16, p. 38] for mechanical systems, which computational scientists routinely detect in electronic structure calculations as positive definite second variations [352, for e.g.] of the energy functional $E = \langle \psi, H\psi \rangle / \langle \psi, \psi \rangle \geq E_0$, where E_0 is the true ground-state energy of the self-adjoint Coulomb Hamiltonian operator [336] from which molecular thermodynamic stabilities are assessed.

The Coulomb potential energy function $\mathcal{V}_C(\mathbf{x})$ of a molecule is the sum of its attractive electron-nucleus, repulsive electron-electron, and repulsive nuclei-nuclei potentials of interaction, viz.

$$4\pi\mathcal{V}_C(\mathbf{x}) = - \sum_{i=1}^N \sum_{j=1}^M Z_j / |\mathbf{r}_i - \mathbf{R}_j| + \sum_{1 \leq i < j}^N 1 / |\mathbf{r}_i - \mathbf{r}_j| + \sum_{1 \leq i < j}^M Z_i Z_j / |\mathbf{R}_i - \mathbf{R}_j|, \quad (19a)$$

where $\mathbf{x} \in \mathbf{R}^M \times \mathbf{r}^N$. There are no self-repulsion terms (of nuclei or electrons) in \mathcal{V}_C . Of course, the Coulomb force $\mathbf{F}_C(\mathbf{x}) = -\nabla\mathcal{V}_C(\mathbf{x})$ is conservative. Equally, $\nabla \times \mathbf{F}_C = 0$ as is also required of a conservative force. Formally, the Laplacian of $\mathcal{V}_C(\mathbf{x})$ is

$$4\pi\nabla^2\mathcal{V}_C(\mathbf{x}) = - \sum_{i=1}^M Z_i \delta(\mathbf{x} - \mathbf{R}_i) + \sum_{i=1}^N \delta(\mathbf{x} - \mathbf{r}_i) + \sum_{i=1}^M Z_i^2 \delta(\mathbf{x} - \mathbf{R}_i), \quad (19b)$$

where the first two terms on the right are the net nuclear and electronic charge density, respectively. Thus

$$4\pi \int_V d\mathbf{x} \nabla^2 \mathcal{V}_C(\mathbf{x}) = \sum_{i=1}^M Z_i^2 - z, \quad (19c)$$

where

$$z = \sum_{i=1}^M Z_i - N \quad (19d)$$

is the net charge of a polyatomic ion. Earnshaw’s theorem applies: $\mathcal{V}_C(\mathbf{x})$ is subharmonic ($\nabla^2\mathcal{V}_C > 0$) and sustains interior minima in V corresponding to stable mechanical configurations. Consequently, the Coulomb potential $\mathcal{V}_C(\mathbf{x})$ is stabilizing. The stability of a polyatomic ion is due entirely to the bilateral repulsion between its nuclei. Any reduction in this repulsion through, say, nuclear screening [323] – a phenomenon unavailable to self-gravitating systems[†] – destabi-

[†]Even though the gravitational and Coulomb forces are both inverse square relations, the former is always attractive because of the positive mass theorem [353, 354] while the latter may be attractive or repulsive according as the charges are different or alike.

lizes a neutral molecule or polyatomic ion. The PEP promotes stabilization by boosting nuclear screening through the dispersal of fermions and the assembly of bosons that characterizes its vague role.

The work done on an arbitrary particle (electron or nucleus) of charge q in V is

$$\int_V d\mathbf{x} \nabla \cdot \mathbf{F}_{C,q}(\mathbf{x}) = -q \sum_{i=1}^n q_i \int_V d\mathbf{x} \nabla_{\mathbf{x}_i}^2 \left(\frac{1}{|\mathbf{x} - \mathbf{x}_i|} \right) \quad (20a)$$

$$= -4\pi qz,$$

where

$$\mathbf{F}_{C,q}(\mathbf{x}) = -q \sum_{i=1}^n q_i \nabla_{\mathbf{x}_i} \left(\frac{1}{|\mathbf{x} - \mathbf{x}_i|} \right), \quad (20b)$$

with q_i and $\mathbf{x}_i \in \mathbf{R}^M \times \mathbf{r}^N$ as the charge and location, respectively, of any of the molecule's $n = M + N$ particles (including the one under consideration), which vanishes if $z = 0$, is exothermic if $z < 0$ as in anion formation, and endothermic if $z > 0$ as in cation formation and consistent with our previous finding that nuclear screening increases with stabilizing anion formation, and conversely. The propensity of an atomic or polyatomic species to form ions is a measure of its stability and consequent reactivity in context [355, 356, for e.g.]. The findings of Lieb and Loss [357] (whose assumptions on the separability or disentanglement of all nuclei – regardless if they in bulk supply have fractional integer spins as to follow Fermi-Dirac statistics – from the fermionic pool, we avoid) are in accord with our revelation of the preference for anion formation as observed empirically.

The Lorentz-Faraday conservative force $\mathbf{F}_{\text{int}} = -\nabla \mathcal{V}_{\text{int}}$ in (13a) is the sum of the negative gradient of the scalar potential Φ as given in (14a) and the curl of the vector potential \mathbf{A} as given in (14b). Since the div curl vanishes, it is clear that $\nabla^2 \mathcal{V}_{\text{int}}(\mathbf{x}, t) = \nabla^2 \Phi(\mathbf{x}, t)$ so that the Lorentz-Faraday force \mathbf{F}_{int} is stabilising just like the Coulomb force \mathbf{F}_C provided ϕ is subharmonic at $\mathbf{x} \in V$.

Earnshaw's theorem reveals the propensities of a fixed aggregation of nuclei and electrons acting collectively under the Coulomb potential to form mechanically stable species (molecules or polyatomic ions), isomers with identical chemical formulas but different arrangements of nuclei giving rise to structural isomerism in which chemical bonds between nuclei differ, or stereoisomerism in which the bonds are the same but the relative positions of the nuclei differ. Such isomers generally have different physical and chemical properties. Thus, the paradigmatic classical molecular structures [358–360] of chemistry are evidentially a consequence of the subharmonic nature of the Coulomb potential and not a self-styled conundrum [361] whose long-crusading resolution [362, et passim] would have it devolve to a foundational defect of quantum theory.

This proof of the mechanical stability of matter based on Earnshaw's theorem is within the grasp of anyone with high

school “calculus and vectors” preparation. Additionally, the proof makes no distinction between the stability of a single molecule over that of molar amounts of them within the scope of the extensivity-intensivity [363, 364] divide. Mechanical stability of molecules as gauged by Earnshaw's criterion is of paramount importance regardless of quantum mechanics. Shell and orbital models are used to describe the arrangements of protons and neutrons in atomic nuclei and electrons in atoms and molecules, respectively. The shells or orbitals are filled with fermions in order of increasing energies except when the binding energy of the next addition is less than the last and in post hoc compliance with the PEP and Hund's rule of maximum multiplicity. The motion of the electrons in a molecule constrains the nuclei to a particular geometric configuration, one that minimizes their energy functional.

The widespread belief that the PEP is necessary and sufficient for the stability of molecules would appear to have entrenched itself in the lore of chemistry and physics when Niels Bohr proclaimed it to be so in his *Faraday Lecture* to the Chemical Society [198]. This should not come as a surprise given that the forces responsible for molecule formation in the most reductionist way from their constituent nuclei and electrons are entirely classical in origin. Since the Coulomb potential was shown to be subharmonic, Earnshaw's theorem lends credence to the fact that aggregates of nuclei and electrons can be mechanically stable independently of both the PEP and the overarching assumption that even the heaviest of nuclei cannot be fermions regardless of their spin. The Lorentz-Faraday potential is purely quantum mechanical in origin, it is operative under thermal conditions, and it is subharmonic and stabilizing.

As Chandrasekhar [365, 366] demonstrated in revealing the limiting mass above which electron degeneracy pressure in a star's core is insufficient to balance the star's own gravitational self-attraction, the PEP cannot be naively invoked independently of the Heisenberg uncertainty principle, although most chemists and high school science teachers routinely do so.

Slater [367] was first to point out the relevance of the quantum mechanical counterpart of Clausius' classical virial theorem for stationary state molecular systems [368, for e.g.]. The quantum mechanical virial theorem has been proved for polyatomics [369] and reads as

$$2\overline{\langle KE \rangle} + \overline{\langle \mathcal{V}_C \rangle} = 0, \quad (21)$$

where $\overline{\langle KE \rangle}$ and $\overline{\langle \mathcal{V}_C \rangle}$ are the time-averaged expectation values of the kinetic KE and potential \mathcal{V}_C energies, respectively, without drawing any distinction between the masses of nuclei relative to electrons, the sole difference being in relation to their spins. Since $E = \overline{\langle KE \rangle} + \overline{\langle \mathcal{V}_C \rangle} = 1/2\overline{\langle \mathcal{V}_C \rangle}$, clearly the virial theorem is closely related to the conservation of energy principle.

Clausius' derivation of the classical virial theorem used Jacobi [370]'s extension of Lagrange's treatment of the 3-

body problem to many-body systems which, in conjunction with the first law of thermodynamics, permitted him to investigate the stability of self-gravitating systems. Jacobi's approach applies equally to a molecule whether in a stationary state under Coulomb control or in a dynamic state under Lorentz-Faraday control. In this regard, the equivalence of the stability criteria of Jacobi and Earnshaw is clear: they both maintain that an harmonic molecule is unstable regardless of the PEP which of course was unknown to them. Whether molar quantities of harmonic molecules are stable or not depends on how they interact and in so doing could make each other anharmonic and potentially less stable or even unstable. Thus, water condenses to liquid and further solidifies under sundry conditions but with differences in their underlying stabilities determined by their hydrogen-bonding networks without necessarily invoking the PEP.

The virial theorem states that if any system whose conservative forces come from a potential energy function which is a power law of the distance between its constituents – such as a self-gravitating body (\mathcal{V}_g) or a Coulomb molecule (\mathcal{V}_C) – settles into equilibrium then its total energy will be balanced between the kinetic energy of those constituents and the potential energy stored due to their mutual interaction. As previously remarked, the virial theorem presupposes the applicability of the first law of thermodynamics for a stationary system. In a thermal field where the SLT reigns, the first law takes an hiatus and the steady-state virial theorem given in (21) is supervened upon by its dynamical counterpart as will now be explained. Before doing so, however, it is appropriate to note that Pollard [371] gave a derivation of the classical virial theorem which eliminates its unnecessary assumption that the system is bounded in the sense that distances between particles and the velocities of the particles remain bounded as was Ambartsumian [294]'s objection to Zwicky [293]'s use of the virial theorem, and replaced it by the condition that for the theorem to hold it is both necessary and sufficient that for $\mathbf{x}_i \in \mathbf{x}$, $\max_{i < j \leq n} |\mathbf{x}_i - \mathbf{x}_j| = o(t)$ as $t \rightarrow \infty$.

In an “isolated” molecule $\mathbf{F}_{\text{int}}(\mathbf{x}, t)$ is dormant but the Coulomb molecule is stable and undergoes reversible ($\Delta S = 0$) processes without the involvement of the phase. The Coulomb potential is classical with a basis in field theory [3, for e.g.] that sees it as involving the exchange of “virtual” photons created only for the duration of the exchange process. Such an exchange force may be either attractive or repulsive and whose range is set by the energy-time uncertainty principle so that a particle of mass m and rest energy $E = mc^2$ has a range of no more than $1/2mc$ which is infinite for a massless photon whose finite momentum can exert a force known as radiation pressure. However, if it were to be driven out of equilibrium by the stabilizing $\mathbf{F}_{\text{int}}(\mathbf{x}, t)$ at $T > 0$ the local phase would regulate irreversible ($\Delta S(t) > 0$) changes in the molecule. Unlike the Coulomb force, the Lorentz-Faraday force is quantum mechanical which, when operative at fi-

nite T , produces real Helmholtz-Hodge photons of unlimited range but of finite lifetime. Since photons are bosons of unit spin, transitions involving their absorption and emission must result in unit change in the angular momentum of the system for a net-zero change consistent with the absence of internal vortices in a heated molecule as was previously noted*.

The probability density $\rho(\mathbf{x}, t) = |\psi(\mathbf{x}, t)|^2$, written identically as

$$\rho(\mathbf{x}, t) = \int_V d\mathbf{x}' \psi^*(\mathbf{x}', t) \delta(\mathbf{x} - \mathbf{x}') \psi(\mathbf{x}', t), \quad (22a)$$

where the configurational kernel is formally

$$\delta(\mathbf{x} - \mathbf{x}') = \sum_{i=1}^M \delta(\mathbf{x} - \mathbf{R}_i) + \sum_{j=1}^N \delta(\mathbf{x} - \mathbf{r}_j) \quad (22b)$$

with $\mathbf{x}, \mathbf{x}' \in V \subseteq R^n = \mathbf{R}^M \times \mathbf{r}^N$ and $n = M + N$ is a normalization constant so that

$$\int_V d\mathbf{x} \rho(\mathbf{x}, t) = n, \quad (22c)$$

to give the expectation value of the kinetic energy of motion of the molecule's constituents as

$$\begin{aligned} \langle KE(t) \rangle &= \frac{1}{2} \int_V d\mathbf{x} \rho(\mathbf{x}, t) |\nabla \phi(\mathbf{x})|^2 \\ &= \frac{1}{2} \int_V d\mathbf{x} \left(\sum_{i=1}^M |\nabla_{\mathbf{R}_i} \phi(\mathbf{x})|^2 + \sum_{j=1}^N |\nabla_{\mathbf{r}_j} \phi(\mathbf{x})|^2 \right). \end{aligned} \quad (22d)$$

The virial of $\mathbf{F}_{\text{int}}(\mathbf{x}, t)$ being $\oint_{\partial V} da \hat{\mathbf{n}} \cdot \mathbf{F}_{\text{int}}$, within V its expectation value is

$$\begin{aligned} \langle \nabla \cdot \mathbf{F}_{\text{int}}(t) \rangle &= \int_V d\mathbf{x} \rho(\mathbf{x}, t) \nabla \cdot \mathbf{F}_{\text{int}}(\mathbf{x}, t) \\ &= \int_V d\mathbf{x} \left(\sum_{i=1}^M \phi(\mathbf{x}) \nabla_{\mathbf{R}_i}^2 \phi(\mathbf{x}) + \sum_{j=1}^N \phi(\mathbf{x}) \nabla_{\mathbf{r}_j}^2 \phi(\mathbf{x}) \right) \end{aligned} \quad (22e)$$

which is the work done $Q(t)$ by \mathbf{F}_{int} that the change in entropy exceeds at $T > 0$ as given by the quantized Clausius inequality in (11a) or (11b).

The sum of $2\langle KE(t) \rangle$ and $\langle \nabla \cdot \mathbf{F}_{\text{int}}(t) \rangle$ vanishes[†]

$$2\langle KE(t) \rangle + \langle \nabla \cdot \mathbf{F}_{\text{int}}(t) \rangle = 0. \quad (22f)$$

*The Coulomb force acting between two charges is generally not parallel to the vector separating them and so exerts a torque on each which means that the angular momentum of any charge changes all the time with the two charges merely “exchanging angular momentum” whose total is conserved. A similar but more complex exchange process [372, for e.g.] undoubtedly takes place between the charged constituents of a molecule and its internal Helmholtz-Hodge electromagnetic field.

[†]Wigner has pointed out [373, loc. cit., p. viii] that “It is a well known fact . . .” (pausing until resuming his unswerving accuracy) “It is well known to some people that every operator can be made self-adjoint.” For $f \in L^2$, $\langle f, \nabla^2 f \rangle + \langle \nabla f, \nabla f \rangle = 0$, a fact acknowledged by Slater [367].

This extension of the virial theorem to nonstationary dynamics involving internal Lorentz-Faraday forces is consistent with Milne [374]’s demonstration that the virial theorem continues to hold true if the particles are acted on by external frictional forces proportional to their velocities and Collins’ [375, loc. cit., p. 97] remark:

To date the virial theorem has been applied to systems in or near equilibrium. It is worth remembering that perhaps the most important aspect of the theorem is that it is a global theorem. Thus systems in a state of rapid dynamic change are still subject to its time dependent form.

The relation of KE to Q often presents as an unwitting pitfall. Recall that heat and temperature are not the same: heat is the total kinetic energy while temperature is the average kinetic energy with the difference depending on the number of degrees of freedom of the system and the dispersal or spread of energy at that temperature as quantified by entropy [376, et passim]. Nor are work and heat synonymous. As remarked before, work is the transfer of energy by any means other than heat except if associated with a nonconservative force like friction, but heat can only be partly converted to work.

The Morse-Sard theorem [146, 147] precludes the sum $2KE + \nabla \cdot \mathbf{F}_{\text{int}}$ from vanishing locally except at the critical points of ϕ , a set of measure zero. This means that $2KE + \nabla \cdot \mathbf{F}_{\text{int}}$ does not vanish over subregions or fragments of the molecule (or a self-gravitating body) as to provide virialized building blocks transferable in noumena to other molecules (or self-gravitating bodies) in violation of the no-cloning theorem [377–379] of quantum mechanics.

Just as with entropy changes $\overline{\langle \Delta S_\tau \rangle}$ given by (11c) for arbitrary relaxation times ($1/\text{rates}$) under nonstandard state conditions, the Laplace long-time averages

$$\overline{\langle KE_\tau \rangle} = \int_0^1 ds e^{-s} \langle KE(\tau s) \rangle \quad (22g)$$

and

$$\overline{\langle \nabla \cdot \mathbf{F}_{\text{int}\tau} \rangle} = \int_0^1 ds e^{-s} \langle \nabla \cdot \mathbf{F}_{\text{int}}(\tau s) \rangle \quad (22h)$$

and their fluctuations are to be ascertained empirically. The time average of (22f) is $2\overline{\langle KE_\tau \rangle} + \overline{\langle \nabla \cdot \mathbf{F}_{\text{int}\tau} \rangle}$ and vanishes.

All objects at finite T emit thermal radiation as quantified by their emissivity [380], a dimensionless number $0 < \epsilon < 1$ covering the range from perfect reflector to perfect emitter and defined as the ratio of the energy radiated to that radiated by a blackbody at the same temperature and wavelength and under the same viewing conditions. An exception to this are black holes: classically, they are black body absorbers that do not emit anything but with the inclusion of quantum processes they can emit radiation and particles. Molecules emit energy that departs from a Planck distribution so the infrared light emitted by vibrating molecules can be used to identify their presence.

The energy density carried by an electromagnetic wave whose source lies in the internal fields of the molecule is given by their Poynting vector [381, 382, for e.g.] and the resultant radiation pressure is

$$\mathbf{p}_{\text{rad}}(\mathbf{x}, t) = \mathbf{E}_{\text{int}}(\mathbf{x}, t) \times \mathbf{B}_{\text{int}}(\mathbf{x}, t). \quad (23a)$$

Ideally, the photons constitute a black-body photon gas of low but finite intensity due to their relativistic speed. Consequently,

$$W = \oint_{\partial V} dW = \oint_{\partial V} da \hat{\mathbf{n}} \cdot \mathbf{p}_{\text{rad}}(\mathbf{x}, t) = \epsilon \sigma_{\text{SB}} T^4 V, \quad (23b)$$

where $\sigma_{\text{SB}} = \pi^2/60$ is the Stefan-Boltzmann constant. This, together with (12e), ensures that U is in compliance with the first law of thermodynamics and with d’Alembert’s principle from which the conservation of energy follows as a consequence [155, cf. Ch. IV]. In the absence of a thermal context, the molecule is a stationary system with the conservative internal force \mathbf{F}_{int} inoperative and with the Coulomb force \mathbf{F}_C providing for its stability. The wave function’s local phase has no bearing on the first law and features only when the system is open to exchanges of heat with its surroundings at finite $T > 0$. Even in the absence of a cyclotron, a heated atomic-ionic-molecular system would be expected to exhibit cyclotron-like radiation emissions [383] contributing to W as its electrons and ions accelerate in the magnetic part of its internal Helmholtz-Hodge radiation field. If an atom at rest in the vicinity of a black hole can undergo spontaneous emission [384] there is nothing to prevent a molecule in a heat bath from doing likewise.

The Higgs potential determines whether the Universe is in a true (stable) or a false (metastable) vacuum state. The SM indicates [385] that the known Universe is in a metastable state that could spontaneously collapse through tunneling decay although not anytime soon since the lifetime of a metastable universe is predicted to be much longer than the current age (~ 13.8 Gyr) of the known Universe [386].

4.3 The absence of magnetic monopoles

Dirac [266] introduced magnetic monopoles to explain the quantization of electric charge [387] and to promote reciprocity between electricity and magnetism. He showed that the magnetic charge g_D and the electric charge e are related by $2g_D e = k$, where $k \in \mathbb{Z}$ thus uncovering the quantization of electric charge, so that when $k = 1$, say $g_D = e/2\alpha \approx 68.5e$, where $\alpha (\approx 1/137)$ is the Sommerfeld fine-structure constant. Assuming that the classical radius of an electron and the “radius” of a Dirac monopole are equal, one finds that their masses m_e and m_m are related by $m_m \approx 4700m_e$, making the magnetic (and gravitational forces) between two monopoles many times stronger than those between two electrons, on which basis searches have been conducted at every new accelerator.

If magnetic charges ρ_m and magnetic currents \mathbf{j}_m were to exist, Faraday's law resulting from taking the curl of \mathbf{E}_{int} as given in (13b) while recalling that curl grad vanishes and then replacing the curl in \mathbf{A} by \mathbf{B}_{int} as given in (13c), would read as

$$-\nabla \times \mathbf{E}_{\text{int}} = \alpha \left(4\pi \mathbf{j}_m + \frac{\partial \mathbf{B}_{\text{int}}}{\partial t} \right) \quad (24a)$$

and the Ampère-Maxwell law would read as

$$\nabla \times \mathbf{B}_{\text{int}} = \alpha \left(4\pi \mathbf{j} + \frac{\partial \mathbf{E}_{\text{int}}}{\partial t} \right), \quad (24b)$$

and the two would look more alike. The curl of \mathbf{E}_{int} suggests that its solenoidal part would be generated by the time-varying \mathbf{B}_{int} and moving magnetic charges \mathbf{j}_m while the curl of \mathbf{B}_{int} would imply that its solenoidal part would be generated by the time-varying \mathbf{E}_{int} and moving electric charges \mathbf{j} . In both cases it is the movement of charge, whether magnetic or electric, that causes current flow while the time-varying fields are mutually generative. Additionally, the analogs of (1a) and (13d) are

$$\frac{\partial \rho_m}{\partial t} + \nabla \cdot \mathbf{j}_m = 0, \quad (25a)$$

and

$$\mathbf{F}_m = \rho_m \mathbf{B}_{\text{int}} - \mathbf{j}_m \times \mathbf{E}_{\text{int}}, \quad (25b)$$

respectively, while the coupled wave equations in (16a) and (16b) have the electric and magnetic fields and their sources interchanged to give

$$\square \mathbf{B}_{\text{int}} = -4\pi \left(\nabla \rho_m + \frac{\partial \mathbf{j}_m}{\partial t} \right) \quad (25c)$$

and

$$\square \mathbf{E}_{\text{int}} = -4\pi \nabla \times \mathbf{j}_m, \quad (25d)$$

respectively.

Dirac [266]'s seminal paper makes specific reference to Weyl [388]'s gauge phase $U(1)$ and thereafter [266, 387] alludes to the vector potential of an external electromagnetic field without recourse to the adiabatic theorem [389]. The addition of the action $4\pi q_D k$ to the local phase ϕ makes no difference to its relative phase $\nabla \phi$ so that as a gauge fix this inclusion of the Dirac magnetic monopole does not ensure its detection.

However, in contrast to the polar vector \mathbf{j} which is T even, the axial vector \mathbf{j}_m is T odd so that the magnetic monopole's analog $\partial \mathbf{j}_m / \partial t$ of the Lorentz-Faraday force given in (8a) is even in time, a circumstance that would not only cause it to decelerate magnetic charge via (25c) but more importantly cause $\Delta S(t)$ to be symmetric in time at finite T in violation of the SLT as was argued earlier. This violation, perhaps, is why Nature has found no recent use for the elusive magnetic monopole [390–394], there being only a couple of reports [395, 396] of its detection neither of which were ever

replicated. Were one to exist, a magnetic monopole would rank as a new elementary particle for which $\nabla \cdot \mathbf{B}_{\text{int}} = 4\pi \rho_m$ is finite and would exhibit a PT violation so as to change sign under C [397, cf. Sec. 8]. Driven by $T > 0$, the integrability of $\theta = \phi - Et$ conveyed in (4) does not require the presence of a nodal line emanating from a magnetic monopole to cause ϕ to jump in value upon each complete cycle it makes around ∂V . Currently there is no explanation for the quantization of electric charge and it is taken to be an empirical fact.

Dirac's synthesis [266] implies that magnetic monopoles may exist. Their dismissal here applies equally to alternative proposals for their production. Grand unification theories [398–400, for e.g.] (GUTs) predict that shortly after the Big Bang magnetic monopoles were created whose conservation of magnetic charge stabilized them against decay as relics of the past. Indeed, the original impetus for inflationary theories [401, 402, for e.g.] of the Universe [403–407] was the so-called "monopole problem". If the early Universe underwent a phase transition because the symmetry of GUT accruing from the supposed coupling of electromagnetic interactions with the electroweak and strong forces into a single force was broken then, in principle, magnetic monopoles should have been produced in abundance. As yet, there is no empirical evidence for any such primordial monopoles. Inflation supposedly diluted their density in the Universe so that it is unlikely in Borel's sense that one will ever be detected. An alternative to the dilution explanation is simply that there are none. Forty years after his provocative paper, Dirac is quoted [408, loc. cit., p. vii] in a letter written to Abdus Salam at Trieste that "I am inclined now to believe that monopoles do not exist. Too many years have gone without any encouragement from the experimental side." Thermodynamics requires that electric charge be a scalar and magnetic charge be a pseudoscalar under T reversal. Since both charges are alike and cannot independently flip signs only one of them exists and it is not the magnetic monopole. This has not led to any curb in the enthusiastic pursuit of monopoles wherever they hide. However, the MoEDAL Collaboration at the LHC* failed [409, et passim] to detect magnetic monopoles with $g_D = 1, 2, 3$ and masses up to $75 \text{ GeV}/c^2$ at the 95 % confidence level via the magnetic dual of the Sauter-Schwinger [410, 411] proposal[†].

4.4 The scarcity of antimatter

The known Universe is primarily filled with matter, not antimatter [30, cf. Ch. 7]. There are no natural forms of antiparticles on Earth. Yet, antiprotons and positrons, the antiparticles of protons and electrons, respectively, can be produced in particle accelerators to serve vital roles in medical

*Large Hadron Collider

[†]This proposal of a mechanism for pair production is not a demonstrable "effect" in the ranks of the photoelectron, Zeeman, Stark, etc., each of which has been experimentally confirmed while to date the Sauter-Schwinger proposal has not.

physics [412]. The production of light antinuclei (\bar{d} , ${}^3\bar{\text{He}}$, and ${}^4\bar{\text{He}}$, for e.g.) composed of antiprotons and antineutrons in high-energy cosmic-ray collisions with the ISM or from their annihilation of unknown dark-matter particles are under scrutiny within the AMS Collaboration on the ISS [413] and the ALICE Collaboration at CERN [414]. It has been intimated [415,416] that the observation of antihelium is the existence of antimatter-dominated regions containing anticlouds or antistars, it being estimated that there are ~ 2.5 ppb antistars within several hundred light years from our Sun.

If the C symmetry of the Lorentz-Faraday force $F_{\text{int}} = \partial \mathbf{j} / \partial t$ were possible it would amount to its T reversal (equivalently, a CP-violation) which is prohibited by the SLT. The baryon number is conserved in all interactions of the SM with the exception of chiral anomalies involving sphalerons – saddle points of the electroweak potential – for which there is no experimental evidence. Both GUT and SUSY allow violations of the conservation of baryon and lepton numbers through proton decay, but this too has never been observed.

The oppositely-charged proton and electron are the primary representatives of the baryonic and leptonic particles and their antiproton and positron particles are of opposite sign. In their electromagnetic interactions, C symmetry on the proton would result in a T reversal since the Lorentz-Faraday force will go from being odd to even in t . For the electron, however, no such T reversal occurs since the Lorentz-Faraday force remains odd in t for the positron. In short, the SLT rules out the copious presence of antiprotons in the Universe for the same reason as the nonobservance there of magnetic monopoles: they are both in violation of the SLT. In contrast, the production of positrons in the Universe is in compliance with the SLT.

Neutrinos have many sources: supernovae, the Sun, the Earth and its atmosphere, nuclear reactors, particle accelerators, etc.; they have no charge; they interact via the electroweak force and, perhaps, gravity; they are observed indirectly via the particles that emerge when a neutrino hits a detector; they have left-handed helicities (spin antiparallel to momentum). Nobody knows if neutrinos (ν_e, ν_μ, ν_τ) are their own antiparticles ($\bar{\nu}_e, \bar{\nu}_\mu, \bar{\nu}_\tau$) but all six leptons are regarded as distinct elementary particles in the SM. Neutrinos are the most abundant matter particles in the Universe and are candidates for dark matter. Hypothetical sterile neutrinos (which are believed to be right-handed and to interact only by gravity) have not been found in either the MicroBooNE [417] or the STEREO [418] experiments. The primary international experiments for neutrino science are NOvA, T2K, and DUNE. Due in large to their small but finite masses [419], neutrinos change flavor (e, μ, τ) in flight, a transformation known as neutrino oscillation [420, 421], behavior that lies beyond the purview of the SM. If the oscillations of neutrinos are different from that of their antineutrinos – a result which is currently not known within the 5σ standard of the SM – CP is broken with which neutrinos violate T-symmetry. This

would relegate neutrinos to the same league of CP violators as quarks [422, cf. Sec. 13]. Cosmic leptogenesis [423, 424, for e.g.] and baryogenesis [425, 426, for e.g.] are related if for no other arguable reason than that they both occur under the same conditions of thermal disequilibrium to which statistical mechanics is inapplicable.

If B and L are the baryon and lepton numbers, at thermal equilibrium both $\langle B \rangle_T$ and $\langle L \rangle_T$ vanish so there is no net generation of either number. This justifies our prior application of Clausius' inequality for the time-dependent change in the entropy to show that baryons are in violation of the T-asymmetry of the SLT. This equally applies to leptons (neutrino oscillations, regardless) and is consistent with Sakharov [427, 428]'s departure from thermal equilibrium criterion for particle asymmetry, be it a baryon or a lepton.

Leptons and baryons are in violation of the SLT through their disregard for the T-asymmetry of entropy that accrues from the subharmonicity of the local phase ϕ whose gradient $\nabla\phi$ is the velocity of the wave packet of the lepton or baryon resulting in their mutual observed asymmetry. In short, the SLT is the reason why the cosmos is free of antimatter whether it be leptonic or baryonic.

4.5 The strong CP problem

Probe images [429] of the light outside the Milky Way (the cosmic optical background, COB) have implicated axions, hypothetical finite mass, neutral, spin zero, long-lived bosons, as candidate sources [430, 431] of dark matter to explain why through their decay into photons the light seen in the COB is brighter than expected. The original reason [432, 433] for proposing the existence of axions was to explain why CP violations present in weak interactions are absent in strong interactions [14, 15, et passim] as evidenced by the nonobservance [434] of an EDM of a neutron. Prompted by Peccei-Quinn axion theory [432, 433] for the strong CP problem, Wilczek and coworkers [435, 436] were among the first to identify axions as possible progenitors of wave-like dark matter. Because low-mass axions are thought to emanate from the interiors of hot stars as possible cold Bose-Einstein condensates [437] and to couple to two photons in a magnetic field, the CAST Collaboration at CERN [438] directs a strong magnetic field at our Sun to detect the X-ray photons from axions but has yet to report any findings. The search continues [439–441] but has so far failed to report their presence. Regardless, elusive axions could serve a purpose different from being suggestive of an equally elusive dark matter.

Wilczek [442] showed that the electrodynamics of axions can be described if one adds a term of the form $a\mathbf{B}_{\text{int}} \cdot \mathbf{E}_{\text{int}}$ to the Maxwell Lagrangian for an electromagnetic field ($\mathbf{E}_{\text{int}}, \mathbf{B}_{\text{int}}$), where a describes the strength of the axion field. This adds further charge density $-\nabla a \cdot \mathbf{B}_{\text{int}}$ to Gauss' law and current density $\nabla a \times \mathbf{E}_{\text{int}} + \dot{a}\mathbf{B}_{\text{int}}$ to Maxwell-Ampere's law, reflecting the fact that $a(\mathbf{x}, t)$ is both P and T odd. Recall-

ing [145] that under T reversal, \mathbf{E}_{int} is even while \mathbf{B}_{int} is odd, the inclusion of axions as sources of $(\mathbf{E}_{\text{int}}, \mathbf{B}_{\text{int}})$ in (16a,16b) does not reverse the arrow of time in violation of the SLT so that CPT invariance holds for axion-mediated strong interactions. This contrasts to both magnetic monopoles and antimatter discussed previously where the opposite is true and neither are observed in accord with the reality of the SLT.

A recent study [443] of a single gravitationally-lensed quasar found its Einstein rings [444] to exhibit anomalies suggesting the presence of wave-like behavior consistent with ultralight axions as a more viable dark matter candidate than WIMPs.

SM predicted EDMs are many orders of magnitude below current experimental limits. The aforesaid SLT restoration of CPT invariance for strong CP interactions via axions does not bode well for measurement of the EDMs of subatomic particles which have never been found [445–447, for e.g.] below what is effectively naught for a bona fide dipole moment regardless of significant instrumental and Bayesian data processing advances. Neither the SM nor the SMC provides an explanation for leptonic or baryonic asymmetry.

4.6 Heaviside dark energy and the expansion of the Universe

Imagine replacing the nuclei and electrons of a molecule with uncharged point particles of arbitrary masses such that their Coulomb potential is replaced by the gravitational potential and ρ , ϕ , \mathbf{j} , and \mathbf{F}_{int} go over into ρ_g , ϕ_g , \mathbf{j}_g , and $\mathbf{F}_{\text{int},g}$, respectively, as the electromagnetic molecule analogizes to a self-gravitating body, which will proxy here as the Universe. Unlike the molecule in a heat bath catered to by the zeroth law of thermodynamics at finite temperature T , the Universe is alone in a CMB mean temperature [448] of ~ 2.725 K.

Gravitoelectromagnetism (GEM) connects the mass density ρ_g and the mass current density $\mathbf{j}_g = \rho_g \nabla \phi_g$ in a gravitational field as Maxwell-like equations, an analogy (with $\epsilon_0 \rightarrow -1/4\pi G$) first pointed out by the late-nineteenth century physicist and electrical engineer Oliver Heaviside [449, 450]. As a linear approximation to GTR [451, 452] in the weak-field limit without being Lorentz invariant, GEM is the field theory for the hypothesized graviton, a neutral and massless boson thought to propagate transversely on the null geodesics of the metric tensor at the speed of light, just as photons do in geometric optics.

On 11 February 2016 the Laser Interferometer Gravitational Wave Observatory (LIGO) announced [453] it had detected gravitational waves produced by the merger of two black holes more than a billion light years from Earth. The Universe is filled with massive objects which undergo rapid accelerations that generate detectable gravitational waves of four LIGO-defined categories, viz. Continuous, Compact Binary Inspiral, Stochastic, and Burst. Through their specific interactions these massive objects cause $\partial \mathbf{j}_g / \partial t$ to accelerate

a test particle of velocity $\nabla \phi_g$ with attendant gravitational waves: just like \mathbf{F}_{int} , this source $\mathbf{F}_{\text{int},g}$ is odd in time and is fueled by the gradient in ρ_g . Gravitational waves do not travel backwards despite the indifference of electrodynamics and quantum mechanics to the direction of time. Consequently, within the range of validity of GEM, the Universe is T-asymmetric in compliance with the SLT and harbors neither gravitomagnetic monopoles nor antimatter contrary to the earlier findings of Sakharov [427, 428] who restored CPT invariance by invoking an anti-Universe that proceeded in reverse time since the Big Bang and where antimatter dominates. Paradoxically, Sakharov's anti-Universe was rediscovered recently by Turok and coworkers [454, 455] in a new cosmological model that *inter alia* includes a sterile neutrino-based dark matter hypothesis. Like Sakharov's, it too violates the T-asymmetry of the SLT as does their mutual anti-Universe.

Recall that the Maxwell stress tensor $\sigma_{\text{int},g}$ has units of negative pressure*, with the diagonal elements providing the tension and the off-diagonal elements the shear, and represents the contribution of electromagnetism to the source of the gravitational field (curvature of spacetime) in GTR. The Poynting vector $\mathbf{S}_{\text{int},g} = \mathbf{E}_{\text{int},g} \times \mathbf{B}_{\text{int},g}$ provides the energy density of the gravitational waves emanating from the self-gravitating object as it expands at a rate that is accelerating just like the known Universe [457, et passim] due to the repulsive effect of $\mathbf{F}_{\text{int},g}$ on the gravitational field. Dark energy is the work done by the Heaviside analog $\mathbf{F}_{\text{int},g} = \nabla \cdot \sigma_{\text{int},g} - \dot{\mathbf{S}}_{\text{int},g}$ of the Lorentz-Faraday force in causing this accelerating expansion, such energy being dark because gravitons are likely undetectable [458, 459].

The recently launched European Euclid telescope plans to investigate dark energy and dark matter in a Universe wherein $\sim 95\%$ of its inventory is unknown. Dark energy is quantified by an equation of state parameter [460, for e.g.] w , the ratio of pressure to density. All indications are that w is close to -1 suggesting that the pressure is both outward (sic negative) and constant.

Alternatively,

$$w(t) \propto \mathbf{F}_{\text{int},g} / \rho_g = \nabla \phi_g \ln \dot{\rho}_g. \quad (26)$$

For the known Universe, $w(t)$ affects both its geometry, via $\nabla \phi_g$, and the growth rate of its structures, via $\ln \dot{\rho}_g$, so that $w(t) \leq 0$. The dark energy induced expansion is irreversible provided $\nabla \phi_g$ is finite in conjunction with $\ln \dot{\rho}_g$ serving as a time-varying sensitivity measure for $w(t)$; otherwise the Universe is in steady-state or is imploding, neither of which is believed to be true.

No one knows how the world will end but Katie Mack provides a guide [181] to some of the possibilities. Since

*Botanists [456, for e.g.] use the negative pressure $\rho h g$ of sap to explain how in the absence of an internal pump, ρ -density water ascends a height h through the xylem and phloem tissue against the acceleration due to gravity g for the tallest of trees.

the guide first appeared, several other speculative hypotheses have come along. For example, new early dark energy [461] with the potential to resolve the tension between recent local measurements of the expansion rate of the Universe using supernovae data and the expansion rate inferred from the early Universe via the CMB; dark matter particles with an extra force [462] proportional to the velocity squared mimics the temporal evolution of the effect of a cosmological constant; a mechanism [463] by which a dynamical form (quintessence) of dark energy could cause the acceleration of the Universe to cease and then transition from expansion to a phase of slow contraction of yet-another cyclic universe.

In contrast to such prevailing dogma, the preceding identification via (26) herein of dark energy as the work done by the Heaviside analog of the Lorentz-Faraday force in causing this accelerating expansion makes no reference to a cosmological constant Λ [464, 465] and its relation to the accelerating expansion of the cosmos [466]. There is no known experiment that can distinguish between Λ and a vacuum energy density. This ambiguity results in dark energy [467] and vacuum energy [468] being pursued as the leading candidates of finite Λ . Unruh and coworkers [469] tackled this beguiling problem in favor of the gravitational property of the quantum vacuum (assuming it gravitates in compliance with the equivalence principle of GTR) to suggest that there is no necessity for a finite Λ to explain the observed slowly accelerating expansion of the Universe as opposed to its catastrophic explosion*. Were T to approach zero, the self-gravitating object would no longer expand but could conceivably fragment or implode before dying as it ceases to emit further gravitons in assuring that its enthalpy U vanishes in compliance with the first law of thermodynamics†. If the Universe is stable, dark energy can maintain its current value, the laws of physics prevail into the future, and its fate will be an eventual heat death. However, if as is popularly believed, it is unstable or metastable because the mass of the Higgs boson is appreciably less than that of the top quark [471], the quantum vacuum may spontaneously decay to a lower-energy state whereupon black holes consume galaxies and each other before eventually evaporating via Hawking radiation [472] emissions. At that point, all that remains in the Universe are photons and gravitons and wayward masses so remote from each other that they do not interact with anything, gravitationally or otherwise. Frautschi [473, loc. cit. p. 599] failed to identify a scheme for the immortality of life: his hope that radiant energy produc-

*After a brief ($\ll 1$ s) period of inflationary expansion (sic stretching), the Universe ostensibly contracted for ~ 9 billion years before it started to expand again at an accelerating rate fueled by dark energy or, equivalently, an energy density homogeneously distributed in the vacuum that is many orders of magnitude larger than the value Einstein thought it ought to have.

†If ever $0 < T \ll 1$, Q and W vanish via (12e) and (23b), respectively, so that $U = 0$ and $F = 0$ whereat nothing further happens since no more work can be done at which time ΔS vanishes, a view first proposed by Thomson (sic Kelvin) [470] and commonly known as the Heat Death (aka Big Freeze) of the Universe.

tion would continue without limit so that life capable of using it forever can be created is not likely to transpire.

As the only survivors of that *fin de cosmos*, photon and graviton fields resort interminably to Gertsenshtein [474] exchange in which one field produces the other under the aegis of their respective $\mathbf{B}_{\text{int.g}}$. The process is irreversible in accord with the quantum Clausius inequality given in (11b) provided the respective ϕ_g for the photon and graviton field is subharmonic. At this juncture time stops and is superfluous since in the absence of mass it lacks measure.

With possibly one provocative exception [475–477], all indications [478] are that the known Universe is flat or, if it has any curvature, it is small. Since the boundary ∂V is embedded in $V(t)$, the Willmore functional [479] of $V(t)$ given by

$$\mathcal{W}(V(t)) = \oint_{\partial V} da \hat{\mathbf{n}} \cdot (H(\mathbf{x})^2 - K(\mathbf{x})) \geq 0, \quad (27)$$

serves as a measure of how much $V(t)$ deviates from a hypersphere on which $H^2 = K$ everywhere, where H is the local mean curvature (average trace of \mathbf{S} , the shape operator) and K is the local Gaussian curvature (determinant of \mathbf{S}) of $V(t)$. Finite $\mathcal{W}(V(t))$ provides a route to monitor local changes under Willmore flow [480] and provides an alternative to the pursuit of a cosmological constant based on the Weyl curvature of the Maxwell stress tensor $\sigma_{\text{int.g}}$ [74, 481].

Once the Willmore flow of $V(t)$ is established, the phase $\phi_{\text{int.g}}$ is provided via the Perron-Wiener-Brelot solutions to a Dirichlet problem [482, cf. Ch. 4] on the boundary ∂V whereon it is maximized and within which it is subharmonic. The phase is furthermore relatable to its hyperspherical harmonic expansions [483, 484] available in principle for many-body systems beyond banal one- and two-particle approaches. With $\mathcal{W}(V(t))$ and $\phi_{\text{int.g}}$ so determined, the de Broglie-Sommerfeld condition in (4) comes into its own in providing the distribution of mass $\rho_{\text{int.g}}$ in the system as a function of energy and its sidekick, entropy.

4.7 Recirculation

Under extreme mechanical loading or shearing conditions, materials are driven so far from equilibrium that they and their molecules change shape irreversibly. Cell membranes tend to position themselves so as to minimize their Willmore energy [485], a finding consistent with the long-standing importance for both biologic [486, cf. Ch. 9], [487], [488] and nonbiologic [489] specificity disregarded in the fog of one upmanship [490].

A neutral atom of atomic number Z has a boundary $\partial V \subseteq R^N$ with $N = Z$. A lone atom in V at $T > 0$ is orientationally spherical and its V is of finite mean curvature $1/r_Z$ and Gaussian curvature $1/r_Z^2$, where r_Z is the atomic radius. For a molecule at $T > 0$ within $\partial V \subseteq R^n$ with $n = M + N$, the stabilizing Lorentz-Faraday $\mathcal{V}_{\text{int}}(\mathbf{x})$ and Coulomb $\mathcal{V}_C(\mathbf{x})$ potentials are noncentral and V is unlikely to be spherical. There is

no *a priori* reason why any but the simplest of molecules cannot take on knotted configurations in their chemical graphs. The volume of a molecule is not necessarily a simply connected surface whose boundary is free of holes. Pursuit of the protean development of V for a molecule under Willmore flow might provide an algorithmic basis for those notions of molecular volume and shape in use since pioneered by Einstein and Perrin but found wanting by some [362, et passim].

5 Conclusion

By simplifying the system of interest to that of a single entity – a molecule or any other particle or structure in its known Universe – whose only descriptor is its wave function from which the Lorentz-Faraday force emerges without appeal to the equipartition theorem [491, for e.g.] but rather from the gradient of its phase when the system connects to a thermal field, whence it relays both the direction of time and entropy increases to the observable macroscopic world of thermodynamics from the microscopic worlds of quantum mechanics and electrodynamics.

Both the SLT and Faraday's law of electrodynamics are of similar vintage and status. Surprisingly, they share a hitherto unrecognized connection at the microscopic level. Whereas the former receives unrelenting challenges and suggested modifications, the latter presents just a few conceptual difficulties and paradoxes for some but without offers to replace it for any technological benefit over that which it has long wielded. Here it was shown that both laws are easily understood by standard quantum mechanics that does not dismiss the local phase of a system's state as being as physically unimportant as is widely promulgated.

The relationship between the thermodynamic arrow of time and time-reversal symmetry in nonrelativistic quantum mechanics was shown to lie in the continuity equation for the probability density and its connection to the probability current through the local phase of the charge amplitude. The change in the entropy of an autonomous molecule in contact with a heat bath was shown to be asymmetric in time and increases (irreversible process) or remains unchanged (reversible process) according as the relative change in its wave function's local phase is finite or vanishes, respectively. Thermal equilibrium is attained though weak neutral currents caused by internal electric and magnetic fields originating with the conservative Lorentz-Faraday forces acting on the nuclei and electrons of a molecule as affected by its hotter environment.

The evolution of \mathbf{j} as identified in (8b) is driven by the feedback $\nabla \cdot \mathbf{j}$ as modulated by the finite time-independent gradient of ϕ , the phase of the wave function ψ . This feedback is integral to a system in a thermal field and however it determines the dynamics of the system, in no way does it control that dynamics. If the feedback is negative it tends to produce stability as evidenced by the fulfillment of the virial theorem.

The SLT determines that the feedback loop evolution is negative, consistent with Sommerfeld [144, cf. §28]'s radiation condition on ψ as was previously noted (*vide supra*). If, however, the feedback is positive as identified in (8c), it gives rise to instabilities as manifested by violations of the virial theorem, exemplified by dark energy acceleration of the Universe in the weak field limit, for instance.

Processes between the system and its surroundings driven by nonthermal gradients are similarly accompanied by an increase in the total entropy whose T-asymmetry prevails through its ongoing relation to the rate of change in the probability current, an operator that is even in time. While the wave function's local phase was shown not to influence the system's necessary fulfillment of the first law of thermodynamics, its subharmonicity was shown to be a necessary and sufficient condition for it to comply with the SLT as first formulated by Clausius. The time asymmetry of $\Delta S(t)$ additionally implies that the detection of permanent EDMs of subatomic particles (electron, proton, neutron, muon) – a consequence of CP violations and T-asymmetry in particle physics, with or without the assumptions of CPT symmetry [28, 29] – may never succeed. Indeed, the latest high-precision measurement [492] of the EDM of an electron drew a blank. The spectroscopic technique used by Roussy et al. [492] has an estimated mass reach of 40 TeV, an order of magnitude higher than at the LHC.

It is worth noting that the Hamiltonian operator of the system has played no explicit role in this exposition other than through the ubiquitous self-adjointness of the Laplacian, confined or free. Entropy production is greater when the local phase is subharmonic on the boundary rather than within the molecular volume. Faraday's law of induction was shown to hold for a single molecule provided the gradient of its local phase is finite, a necessary and sufficient condition for it not to present with its well-known paradoxes.

The primary contribution of this paper is the identification of internal conservative Lorentz-Faraday forces acting on the nuclei and electrons of a molecule in a thermal field and their decomposition into coupled internal electric and magnetic fields. This highlights the role of the dynamic probability current in causing entropy changes to be T-asymmetric contrary to the received word [98, 493–495, for e.g.] that the direction of the arrow of time in macroscopic systems ought to originate from dominant (sic fundamental) time-reversal symmetric classical and microscopic dynamics or quantum fluctuation relations when in reality the opposite applies due to fact that the world is observed macroscopically even if perceived microscopically. Additionally, it brings out the role of the local phase of the state in distinguishing reversible from irreversible thermodynamic processes in accord with Clausius' formulation of the SLT and in providing a microscopic basis for Faraday's law of induction through the presence of electrically neutral currents mediated by photon exchange in all intramolecular interactions involving the nuclei and elec-

trons of the molecule and so revealing the greater importance of electrodynamics over electrostatics as long ago asserted by Earnshaw in accounting for the stability of molecules.

Due to its failure to fully live up to its marquee standing, the SMC has spurred many explorations beyond its domain for “new physics” but without first addressing what is its most fundamental oversight: its failure to comply with the SLT and its corollary, that entropy increases in irreversible processes to punctuate the evolution of the known Universe.

By going back to Clausius’ inequality and interpreting it quantum mechanically, what has been done here is to refute the claim that time is reversible in showing that the entropy gain is T-asymmetric for a molecule – or any other particle or structure in its Universe – from their initial appearance in a thermal field to their final destiny. This paper makes only one prediction: travel to the past is impossible either quantum mechanically or electromagnetically, not because it is as highly improbable as it is found to be, but because it would cause entropy changes to decrease contrary to the SLT. The GTR has played no role in this finding*.

The asymmetry in entropy invalidates several falsifiable predictions of the SMC attributable to its disregard for the SLT – including, the cosmic facts that magnetic monopoles do not exist, that antimatter is scarce to none, that hypothetical axions explain the strong CP paradox without necessarily accounting for dark matter, and that dark energy is the basis for the accelerated expansion of the known Universe.

In the practice of reductionism, macroscopic physics supervenes upon the microscopic, the SLT being the most conspicuous exception to that superfluous tenet. The supersedence of classical thermodynamics over quantum mechanics and electrodynamics across spatio-temporal scales ranging from an individual quantized system to its known Universe has been shown herein. Additionally, in showing that reversible (irreversibility) processes are affiliated with the particle $\nabla\phi = 0$ (wave $\nabla\phi > 0$) behavior of matter, attention has been drawn to a heretofore overlooked connection between the different roles of classical thermodynamics and time-invariant quantum mechanics and electrodynamics in respect to arrow-of-time asymmetry and wave-particle duality.

Acknowledgements

To Katyg Behesnilian (1950-2022) my long-time partner and muse, shine on bubrig until the end of time.

Received on August 16, 2023

*Solutions to the GTR field equations exist that purport to provide for time travel via closed time-like curves [496, et passim]. These speculative universes accommodate an Orwellian endless present where history pauses, just as in the case of reversible processes where $\Delta S(t) = 0$ and distinguishing later from earlier (and vice versa) events does not matter. With irreversible processes, however, $\Delta S(t) > 0$ and discerning current from past events counts as it does in the known Universe in harmony with the SLT; attempting to know past from present events implies that $\Delta S(t) < 0$ whereby evolution reverses, a physical impossibility that historians and allied scholars adroitly avoid.

References

1. G. Lüders. Proof of the TCP Theorem. *Ann. Phys.*, 1957, v. 2, 1–15.
2. C.P. Burgess and G.D. Moore. *The Standard Model: A Primer*. Cambridge University Press, New York, 2007.
3. M.D. Schwartz. *Quantum Field Theory and the Standard Model*. Cambridge University Press, New York, 2014.
4. R.G. Sachs. *The Physics of Time Reversal*. University of Chicago Press, Chicago and London, 1987.
5. T.D. Lee and C.N. Yang. Question of Parity Conservation in Weak Interactions. *Phys. Rev.*, 1956, v. 104, 254–258.
6. Chien-Shiung Wu, E. Ambler, R.W. Hayward *et al.* Experimental Test of Parity Conservation in Beta Decay. *Phys. Rev.*, 1957, v. 105, 1413–1415.
7. M. Planck. *Treatise on Thermodynamics*. Longmans, Green & Co., London, New York, & Bombay, 1903.
8. V. Čápek and D.P. Sheehan. *Challenges to the Second Law of Thermodynamics*. Springer, Dordrecht, Netherlands, 2005.
9. F. Brandao, M. Horodecki, N. Ng *et al.* The second laws of quantum thermodynamics. *Proc. Natl. Acad. Sci. USA*, 2015, v. 112, 3275–3279.
10. G.E. Crooks and S. Still. Marginal and conditional second laws of thermodynamics. *EPL*, 2019, v. 125, 40005.
11. J.H. Christenson, J.W. Cronin, V.L. Fitch *et al.* Evidence for the 2π Decay of the K_m^0 Meson. *Phys. Rev. Lett.*, 1964, v. 13, 138–140.
12. A. Alavi-Harati *et al.* [The KTeV Collaboration]. Observation of Direct CP Violation in $K_{S,L} \rightarrow \pi\pi$ Decays. *Phys. Rev. Lett.*, 1999, v. 83, 23–27.
13. J.P. Lees *et al.* [The BABAR Collaboration]. Observation of Time-Reversal Violation in the B^0 Meson System. *Phys. Rev. Lett.*, 2012, v. 109, 211801.
14. K.R. Schubert. T violation and CPT tests in neutral-meson systems. *Prog. Part. Nucl. Phys.*, 2015, v. 81, 1–38.
15. J. Bernabéu and F. Martínez-Vidal. Time-Reversal Violation. *Annu. Rev. Nucl. Part. Sci.*, 2015, v. 65, 403–427.
16. T.E. Chupp, P. Fierlinger, M.J. Ramsey-Musolf *et al.* Electric dipole moments of atoms, molecules, nuclei, and particles. *Rev. Mod. Phys.*, 2019, v. 91, 015001.
17. I.B. Khriplovich and S.K. Lamoreaux. *CP Violation Without Strangeness*. Springer-Verlag, Berlin and Heidelberg, 1997.
18. E.A. Hinds. Testing Time Reversal Symmetry Using Molecules. *Phys. Scr.*, 1997, v. T70, 34–41.
19. E.D. Commins. Electric Dipole Moments of Leptons. *Adv. At. Mol. Opt. Phys.*, 1999, v. 40, 1–55.
20. J. Engel, M.J. Ramsey-Musolf, and U. van Kolck. Electric dipole moments of nucleons, nuclei, and atoms: The Standard Model and beyond. *Prog. Part. Nucl. Phys.*, 2013, v. 71, 21–74.
21. T. Chupp and M. Ramsey-Musolf. Electric dipole moments: a global analysis. *Phys. Rev. C*, 2014, v. 91, 035502.
22. W.B. Cairncross and J. Ye. Atoms and molecules in the search for time-reversal symmetry violation. *Nat. Rev. Phys.*, 2019, v. 1, 510–521.
23. P. Mohanmurthy and J.A. Winger. Estimation of CP violating EDMs from known mechanisms in the SM. *PoS*, 2021, v. ICHEP2020, 265–276.
24. C. Patrignani *et al.* (Particle Data Group). Review of Particle Physics. *Chin. Phys. C*, 2016, v. 40, 100001.
25. S. Okubo. Decay of the Σ^+ Hyperon and its Antiparticle. *Phys. Rev.*, 1958, v. 109, 984–985.
26. R. Aaij *et al.* [The LHCb Collaboration]. Measurement of matter-antimatter differences in beauty baryon decays. *Nat. Phys.*, 2017, v. 13, 391–396.

27. M. Ablikim *et al.* [The BESIII Collaboration]. Probing CP symmetry and weak phases with entangled double-strange baryons. *Nature*, 2022, v. 606, 64–69.
28. D. Babusci *et al.* [The KLOE-2 Collaboration]. Precision tests of quantum mechanics and *CPT* symmetry with entangled neutral kaons at KLOE. *J. High Energ. Phys.*, 2022, v. 59.
29. P. Moskal, A. Gajos, M. Mohammed *et al.* Testing CPT symmetry in ortho-positronium decays with positronium annihilation tomography. *Nat. Commun.*, 2021, v. 12, 5658.
30. C. Bambi and A. D. Dolgov. Introduction to Particle Cosmology. Springer-Verlag, Berlin and Heidelberg, 2016.
31. A. G. Riess *et al.* [High-Z Supernova Search Team]. Observational evidence from supernovae for an accelerating universe and a cosmological constant. *Astron. J.*, 1998, v. 116, 1009–1038.
32. S. Perlmutter *et al.* [Supernova Cosmology Project]. Measurements of Ω and Λ from 42 high-redshift supernovae. *Ap. J.*, 1999, v. 517, 565–586.
33. B. Carr, F. Kühnel, and M. Sandstad. Primordial black holes as dark matter. *Phys. Rev. D*, 2016, v. 94, 083504.
34. P. W. Graham, I. G. Irastorza, S. K. Lamoreaux *et al.* Experimental Searches for the Axion and Axion-Like Particles. *Ann. Rev. Nucl. Part. Sci.*, 2015, v. 65, 485–514.
35. A. Boyarsky, M. Drewes, T. Lasserre *et al.* Sterile Neutrino Dark Matter. *Prog. Part. Nucl. Phys.*, 2019, v. 104, 1–45.
36. D. Buttazzo, P. Panci, N. Rossi *et al.* Annual modulations from secular variations: relaxing DAMA? *J. High Energ. Phys.*, 2020, v. 137.
37. R. Penrose. The Big Bang and its Dark-Matter Content: Whence, Whither, and Wherefore. *Found. Phys.*, 2018, v. 48, 1177–1190.
38. S. van den Bergh. A Short History of the Missing Mass and Dark Energy Paradigms. In: V. J. Martínez, V. Trimble, and M. J. Pons-Bordería, eds. Historical Development of Modern Cosmology, Volume 252. ASP Conference Proceedings, San Francisco, 2001, pp. 75–83.
39. E. Oks. Brief review of recent advances in understanding dark matter and dark energy. *New Astron. Rev.*, 2021, v. 93, 101632.
40. J. Liu, X. Chen, and X. Ji. Current status of direct dark matter detection experiments. *Nat. Phys.*, 2017, v. 13, 212–216.
41. S. Vagnozzi, L. Visinelli, P. Brax *et al.* Direct detection of dark energy: The XENON1T excess and future prospects. *Phys. Rev. D*, 2021, v. 104, 063023.
42. L. Perivolaropoulos and F. Skara. Challenges for Λ CDM: An update. *New Astron. Rev.*, 2022, v. 95, 101659.
43. M. A. Green, J. W. Moffat, and V. T. Toth. Modified gravity (MOG), the speed of gravitational radiation and the event GW170817/GRB170817A. *Phys. Lett. B*, 2018, v. 780, 300–302.
44. C. Skordis and T. Zlošnik. New Relativistic Theory for Modified Newtonian Dynamics. *Phys. Rev. Lett.*, 2021, v. 127, 161302.
45. P. D. Mannheim. Alternatives to dark matter and dark energy. *Prog. Part. Nuc. Phys.*, 2006, v. 56, 340–445.
46. S. Dodelson. The Real Problem with MOND. *Int. J. Mod. Phys. D*, 2011, v. 20, 2749–2753.
47. G. D. Starkman. Modifying gravity: you cannot always get what you want. *Phil. Trans. R. Soc. A*, 2011, v. 369, 5018–5041.
48. E. Abdalla, G. F. Abellán, A. Aboubrahim *et al.* Cosmology intertwined: A review of the particle physics, astrophysics, and cosmology associated with the cosmological tensions and anomalies. *J. High Energ. Ap*, 2022, v. 34, 49–211.
49. N. Menci, M. Castellano, P. Santini *et al.* High-redshift Galaxies from Early JWST Observations: Constraints on Dark Energy Models. *Astrophys. J.*, 2022, v. 938, L5.
50. M. Boylan-Kolchin. Stress testing Λ CDM with high-redshift galaxy candidates. *Nat. Astron.*, 2023.
51. I. Labbé, P. van Dokkum, E. Nelson *et al.* A population of red candidate massive galaxies ~ 600 Myr after the Big Bang. *Nature*, 2023, v. 616, 266–269.
52. R. H. Thurston, ed. Reflections on the Motive Power of Heat. John Wiley & Sons, New York, 1897.
53. R. Clausius and W. R. Browne, transl. The Mechanical Theory of Heat. McMillan, London, 1879.
54. E. B. Starikov. Many Faces of Entropy or Bayesian Statistical Mechanics. *ChemPhysChem*, 2010, v. 11, 3387–3394.
55. G. A. Linhart. The Relation Between Entropy and Probability. The Integration of the Entropy Equation. *J. Am. Chem. Soc.*, 1922, v. 44, 140–142.
56. G. A. Linhart. Correlation of Entropy and Probability. *J. Am. Chem. Soc.*, 1922, v. 44, 1881–1886.
57. G. A. Linhart. Correlation of Heat Capacity, Absolute Temperature and Entropy. *J. Chem. Phys.*, 1933, v. 1, 795–797.
58. A. S. Eddington. The Nature of the Physical World. McMillan, London, 1928.
59. A. Vilenkin. Boundary conditions in quantum cosmology. *Phys. Rev. D*, 1986, v. 33, 3560–3569.
60. D. S. Goldwirth and T. Piran. Entropy, Inflation and the Arrow of Time. *Class. Quant. Grav.*, 1991, v. 8, L155–L160.
61. S. W. Hawking, R. Laflamme, and G. W. Lyons. Origin of time asymmetry. *Phys. Rev. D*, 1997, v. 47, 5342–5356.
62. S. M. Carroll and J. Chen. Spontaneous Inflation and the Origin of the Arrow of Time. Technical Report EFI-2004-33, Enrico Fermi Institute, Department of Physics, and Kavli Institute for Cosmological Physics, University of Chicago, Chicago, 2004.
63. C. Kiefer. Quantum Cosmology and the Arrow of Time. *Braz. J. Phys.*, 2005, v. 35, 296–299.
64. R. M. Wald. The Arrow of Time and the Initial Conditions of the Universe. *Stud. Hist. Phil. Mod. Phys.*, 2006, v. 37, 394–398.
65. L. M. Krauss and R. J. Scherrer. The return of a static universe and the end of cosmology. *Gen. Rel. Grav.*, 2007, v. 39, 1545–1550.
66. J. J. Halliwell, J. Perez-Mercader, and W. H. Zurek, eds. Physical Origins of Time Asymmetry. Cambridge University Press, New York, 1993.
67. H. Price. Time’s Arrow & Archimedes’ Point. Oxford University Press, New York, 1996.
68. H. D. Zeh. The Physical Basis of the Direction of Time. Springer, Berlin, Heidelberg, and New York, 5 edition, 2007.
69. S. Carroll. From Eternity to Here: The Quest for the Ultimate Theory of Time. Dutton, New York, 2010.
70. L. Mersini-Houghton and R. Vaas, eds. The Arrows of Time: A Debate in Cosmology. Springer-Verlag, Berlin and Heidelberg, 2012.
71. V. K. Narayanan and R. A. Croft. Recovering the primordial density fluctuations: a comparison of methods. *Astrophys. J.*, 1999, v. 515, 471–486.
72. U. Frisch, S. Matarrese, R. Mohayaee *et al.* A reconstruction of the initial conditions of the Universe by optimal mass transportation. *Nature*, 2002, v. 417, 260–262.
73. R. Feynman. The Character of Physical Law. MIT Press, Cambridge, MA, 1967.
74. R. Penrose. Singularities and time-asymmetry. In: S. W. Hawking and W. Israel, eds. General Relativity: An Einstein Centenary Survey. Cambridge University Press, Cambridge, UK, 1979, pp. 581–638.
75. R. Penrose. Causality, quantum theory and cosmology. In: S. Majid, ed. On Space and Time. Cambridge University Press, New York, 2008, pp 150–200.

76. R. Penrose. *Cycles of Time: An Extraordinary New View of the Universe*. The Bodley Head, London, 2010.
77. M. López, P. Bonizzi, K. Driessens *et al.* Searching for ring-like structures in the cosmic microwave background. *Mon. Not. R. Astron. Soc.*, 2023, v. 519, 922–930.
78. D. An, K. A. Meissner, P. Nurowski *et al.* Apparent evidence for Hawking points in the CMB Sky. *Mon. Not. R. Astron. Soc.*, 2020, v. 495, 3403–3408.
79. D. L. Jow and D. Scott. Re-evaluating evidence for Hawking points in the CMB. *J. Cosmol. Astropart. Phys.*, 2020, v. 2020, 021–031.
80. R. Fernández-Cobos, A. Marcos-Caballero, and E. Martínez-González. Radial derivatives as a test of pre-Big-Bang events on the Planck data. *Mon. Not. R. Astron. Soc.*, 2020, v. 499, 1300–1311.
81. E. Bodnia, V. Isenbaev, K. Colburn *et al.* Conformal Cyclic Cosmology Signatures and Anomalies of the CMB Sky. *J. Cosmol. Astropart. Phys.*, 2023, v. 2023, 0xx21–0xx31.
82. G. M. Wang, E. M. Sevick, R. Mittag *et al.* Experimental Demonstration of Violations of the Second Law of Thermodynamics for Small Systems and Short Time Scales. *Phys. Rev. Lett.*, 2002, v. 89, 050601.
83. D. M. Carberry, J. C. Reid, G. M. Wang *et al.* Fluctuations and Irreversibility: An Experimental Demonstration of a Second-Law-Like Theorem Using a Colloidal Particle Held in an Optical Trap. *Phys. Rev. Lett.*, 2004, v. 101, 140601.
84. S. Deffner and E. Lutz. Generalized Clausius Inequality for Nonequilibrium Quantum Processes. *Phys. Rev. Lett.*, 2010, v. 105, 170402.
85. G. Argenterieri, F. Benatti, R. Floreanini *et al.* Violations of the second law of thermodynamics by a non-completely positive dynamics. *EPL*, 2014, v. 107, 5007.
86. G. Argenterieri, F. Benatti, R. Floreanini *et al.* Complete Positivity and Thermodynamics in a Driven Open Quantum System. *J. Stat. Phys.*, 2015, v. 159, 1127–1153.
87. T. L. Hill. Thermodynamics of Small Systems. *J. Chem. Phys.*, 1962, v. 36, 3182–3197.
88. T. L. Hill. A Different Approach to Nanothermodynamics. *Nano Lett.*, 2001, v. 1, 273–275.
89. D. Bedeaux, S. Kjelstrup, and S. K. Schnell. *Nanothermodynamics: General Theory*. PoreLab, Trondheim, Norway, 2020.
90. D. Keller, D. Swigon, and C. Bustamante. Relating Single-Molecule Measurements to Thermodynamics. *Biophys. J.*, 2003, v. 84, 733–738.
91. C. Bustamante, J. Liphardt, and F. Ritort. The Nonequilibrium Thermodynamics of Small Systems. *Physics Today*, 2005, v. 87, 43–48.
92. J. M. Rubi, D. Bedeaux, and S. Kjelstrup. Thermodynamics for Single-Molecule Stretching Experiments. *J. Phys. Chem. B*, 2006, v. 110, 12733–12737.
93. E. Bering, S. Kjelstrup, D. Bedeaux *et al.* Entropy Production beyond the Thermodynamic Limit from Single-Molecule Stretching Simulations. *J. Phys. Chem. B*, 2020, v. 124, 8909–8917.
94. J. Gemmer, M. Michel, and G. Mahler. *Quantum Thermodynamics: Emergence of Thermodynamic Behavior Within Composite Quantum Systems*. Springer, Berlin and Heidelberg, 2 edition, 2009.
95. F. Binder, L. A. Correa, C. Gogolin, J. Anders, and G. Adesso, eds. *Thermodynamics in the Quantum Regime*. Springer Nature, Switzerland, 2018.
96. R. S. Whitney, R. Sánchez, and J. Splettstoesser. Quantum Thermodynamics of Nanoscale Thermoelectrics and Electronic Devices. In: F. Binder, L. A. Correa, C. Gogolin, J. Anders, and G. Adesso, eds. *Thermodynamics in the Quantum Regime*. Springer Nature, Switzerland, 2018, pp. 175–206.
97. S. T. Dawkins, O. Abah, K. Singer *et al.* Single Atom Heat Engine in a Tapered Ion Trap. In: F. Binder, L. A. Correa, C. Gogolin, J. Anders, and G. Adesso, eds. *Thermodynamics in the Quantum Regime*. Springer Nature, Switzerland, 2018, pp. 887–896.
98. K. Funo, M. Ueda, and T. Sagawa. Quantum Fluctuation Theorems. In: F. Binder, L. A. Correa, C. Gogolin, J. Anders, and G. Adesso, eds. *Thermodynamics in the Quantum Regime*. Springer Nature, Switzerland, 2018, pp. 249–274.
99. R. Kosloff. *Quantum Thermodynamics: A Dynamical Viewpoint*. *Entropy*, 2013, v. 15, 2100–2128.
100. R. Alicki and R. Kosloff. Introduction to Quantum Thermodynamics: History and Prospects. In: F. Binder, L. A. Correa, C. Gogolin, J. Anders, and G. Adesso, eds. *Thermodynamics in the Quantum Regime*. Springer Nature, Switzerland, 2018, pp. 1–36.
101. L. G. Palmer and J. Gulati. Potassium Accumulation in Muscle: A Test of the Binding Hypothesis. *Science*, 1976, v. 194, 521–523.
102. G. Ling. Nano-protoplasm: the Ultimate Unit of Life. *Physiol. Chem. Phys. & Med. NMR*, 2007, v. 39, 111–234.
103. A. A. Deniz, S. Mukhopadhyay, and A. Lemke. Single-molecule biophysics: at the interface of biology, physics and chemistry. *J. R. Soc. Interface*, 2008, v. 5, 15–45.
104. S. A. Claridge, J. J. Schwartz, and P. S. Weiss. Electrons, Photons, and Force: Quantitative Single-Molecule Measurements from Physics to Biology. *ACS Nano*, 2011, v. 5, 693–729.
105. R. L. Baldwin. The nature of protein folding pathways: The classical versus the new view. *J. Biomol. NMR*, 1995, v. 5, 103–109.
106. C. L. Brooks III, M. Gruebele, J. N. Onuchic *et al.* Chemical physics of protein folding. *Proc. Natl. Acad. Sci. USA*, 1998, v. 95, 11037–11038.
107. P. G. Wolynes, W. A. Eaton, and A. R. Fersht. Chemical physics of protein folding. *Proc. Natl. Acad. Sci. USA*, 2012, v. 109, 17770–17771.
108. G. R. Heath, E. Kots, J. L. Robertson *et al.* Localization atomic force microscopy. *Nature*, 2021, v. 594, 385–390.
109. N. G. Walter, C.-Y. Huang, A. J. Manzo *et al.* Do-it-yourself guide: how to use the modern single-molecule toolkit. *Nat. Meth.*, 2008, v. 5, 475–489.
110. M. C. Leake. *Single-Molecule Cellular Biophysics*. Cambridge University Press, Cambridge, UK, 2013.
111. M. C. Leake. The physics of life: one molecule at a time. *Phil. Trans. R. Soc. B*, 2013, v. 368, 20120248.
112. P. A. M. Dirac. Quantum Mechanics of Many-Electron Systems. *Proc. R. Soc. Lond. A*, 1929, v. 123, 714–733.
113. P. Koehl and M. Levitt. A brighter future for protein structure prediction. *Nat. Struct. Biol.*, 1999, v. 6, 108–111.
114. S. Y. C. Bradford, L. E. Khoury, Y. Ge *et al.* Temperature artifacts in protein structures bias ligand-binding predictions. *Chem. Sci.*, 2021, v. 12, 11275–11293.
115. C. Tsallis. Nonextensive Statistical Mechanics: Construction and Physical Interpretation. In: M. Gell-Mann and C. Tsallis, eds. *Nonextensive Entropy: Interdisciplinary Applications*. Oxford University Press, New York, 2004, pp. 1–53.
116. C. Tsallis. *Introduction to Nonextensive Statistical Mechanics*. Springer, New York, 2009.
117. C. Caratheodory. Untersuchungen über die Grundlagen der Thermodynamik. *Math. Ann.*, 1909, v. 67, 355–386.
118. M. H. Anderson, J. R. Ensher, M. R. Matthews *et al.* Observation of Bose-Einstein Condensation in a Dilute Atomic Vapor. *Science*, 1995, v. 269, 192–201.
119. K. B. Davis, M. O. Mewes, M. R. Andrews *et al.* Bose-Einstein Condensation in a Gas of Sodium Atoms. *Phys. Rev. Lett.*, 1995, v. 75, 3969–3973.
120. C. A. Regal, M. Greiner, and D. S. Jin. Observation of Resonance Condensation of Fermionic Atom Pairs. *Phys. Rev. Lett.*, 2004, v. 92, 040403.
121. V. J. Stenger. *Timeless Reality*. Prometheus Books, Amherst, NY, kindle edition, 2000.

122. C. H. Lineweaver and C. A. Egan. Life, gravity and the second law of thermodynamics. *Phys. Life Revs.*, 2008, v. 5, 225–242.
123. E. P. Wigner. Über die Operation der Zeitumkehr in der Quantenmechanik. *Göttinger Nachrichten, Math-Phys.*, 1932, 546–559.
124. E. P. Wigner. Group Theory. Academic Press, New York, 1959.
125. S. Earnshaw. On the Nature of the Molecular Forces which regulate the Constitution of the Luminiferous Ether. *Trans. Camb. Phil. Soc.*, 1842, v. 7, 97–114.
126. B. Zhang *et al.* The Largest Synthetic Structure with Molecular Precision: Towards a Molecular Object. *Angew. Chem. Int. Ed. Engl.*, 2011, v. 50, 737–740.
127. Z. K. Silagadze. Multi-dimensional vector product. *J. Phys. A*, 2002, v. 35, 4949–4953.
128. P. Lounesto. Clifford Algebras and Spinors. Cambridge University Press, Cambridge, UK, 2 edition, 2001.
129. J. Gallier. Geometric Methods and Applications. Springer, New York, Dordrecht, Heidelberg, and London, 2 edition, 2011.
130. B. O'Neill. Elementary Differential Geometry. Academic Press, Boston, 2 edition, 2006.
131. M. P. do Carmo. Riemannian Geometry. Birkhäuser, Boston, 1992.
132. U. Fano. Description of states in quantum mechanics by density matrix and operator techniques. *Rev. Mod. Phys.*, 1957, v. 29, 74–93.
133. F. Reif. *Fundamentals of Statistical and Thermal Physics*. McGraw-Hill, New York, 1965.
134. A. Jabs. Connecting Spin and Statistics in Quantum Mechanics. *Found. Phys.*, 2010, v. 40, 776–792.
135. P. W. Bridgman. The Thermodynamics of Plastic Deformation and Generalized Entropy. *Rev. Mod. Phys.*, 1950, v. 22, 56–63.
136. R. Giles. Mathematical Foundations of Thermodynamics. Pergamon Press, New York, 1964.
137. R. Giles. An Elementary Introduction to Entropy via Irreversibility. *Pure & Appl. Chem.*, 1970, v. 22, 503–509.
138. W. K. Burton. Constructive Thermodynamics. In: L. Beklemishev, ed. Contributions to Mathematical Logic, Volume 50. North Holland, Amsterdam, 1968, pp. 75–89.
139. N. D. Mermin. The Ithaca interpretation of quantum mechanics. *Pramana – J. Phys.*, 1998, v. 51, 549–565.
140. Z. Yan. General thermal wavelength and its applications. *Eur. J. Phys.*, 2000, v. 21, 625–631.
141. P. A. M. Dirac. The Principles of Quantum Mechanics. Oxford University Press, London, 4 edition, 1967.
142. T. K. R. Dastidar and K. R. Dastidar. Gauge Invariance in Non-Relativistic Quantum Mechanics. *Nuov. Cim. B*, 1994, v. 109, 1115–1118.
143. T. K. R. Dastidar and K. R. Dastidar. Local Gauge Invariance of Relativistic Quantum Mechanics and Classical Relativistic Fields. *Mod. Phys. Lett. A*, 1995, v. 10, 1843–1846.
144. A. Sommerfeld. Partial Differential Equations of Physics. Academic Press, New York, 1949.
145. E. H. Wichmann. Symmetries and the Connection Between Spin and Statistics in Rigorous Quantum Field Theory. *AIP Conf. Proc.*, 2001, v. 596, 201–231.
146. A. P. Morse. The behaviour of a function on its critical set. *Ann. Math.*, 1939, v. 40, 62–70.
147. A. Sard. The measure of the critical values of differentiable maps. *Bull. Amer. Math. Soc.*, 1942, v. 48, 883–890.
148. W. K. Hayman and P. B. Kennedy. Subharmonic Functions, Vol. 1. Academic Press, London, New York, and San Francisco, 1976.
149. W. K. Hayman. Subharmonic Functions, Vol. 2. Academic Press, San Diego, CA, 1989.
150. E. Schrödinger. Quantisierung als Eigenwertproblem. *Ann. Phys.*, 1926, v. 384, 489–527.
151. L. de Broglie. Recherches sur la théorie des Quanta. *Ann. Phys. (Paris)*, 1925, v. 10, 22–128.
152. E. Madelung. Quantentheorie in hydrodynamischer Form. *Z. Phys.*, 1926, v. 40, 322–326.
153. W. P. Schleich, D. M. Greenberger, D. H. Kobe *et al.* Schrödinger equation revisited. *Proc. Natl. Acad. Sci. USA*, 2013, v. 110, 5374–5379.
154. L. de Broglie. A tentative theory of light quanta. *Phil. Mag.*, 1924, v. 47, 446–458.
155. C. Lanczos. The Variational Principles of Mechanics. University of Toronto Press, Toronto, 1949.
156. J. Masoliver and A. Ros. From classical to quantum mechanics through optics. *Eur. J. Phys.*, 2010, v. 31, 171–192.
157. J. J. Sakurai and J. Napolitano. Modern Quantum Mechanics. Cambridge University Press, Cambridge, UK, 3 edition, 2021.
158. E. Schrödinger. Collected Papers on Wave Mechanics. Chelsea Publishing Company, New York, 3 edition, 1982.
159. L. Wessels. Schrödinger's Route to Wave Mechanics. *Stud. Hist. Phil. Sci.*, 1979, v. 10, 311–340.
160. H. Kragh. Erwin Schrödinger and the Wave Equation: The Crucial Phase. *Cemauu*, 1982, v. 26, 154–197.
161. J. Mehra and H. Rechenberg. The Historical Development of Quantum Theory, Volume 5, Erwin Schrödinger and the Rise of Wave Mechanics, Part 1: Schrödinger in Vienna and Zurich 1887–1925. Springer-Verlag, New York, 1987.
162. J. Mehra and H. Rechenberg. The Historical Development of Quantum Theory, Volume 5, Erwin Schrödinger and the Rise of Wave Mechanics, Part 2: The Creation of Wave Mechanics; Early Response and Applications 1925–1926. Springer-Verlag, New York, 1987.
163. E. Schrödinger. An Undulatory Theory of the Mechanics of Atoms and Molecules. *Phys. Rev.*, 1926, v. 28, 1049–1070.
164. W. Heisenberg. Über quantentheoretische Umdeutung kinematischer und mechanischer Beziehungen. *Z. Phys.*, 1925, v. 33, 879–893.
165. M. Born and P. Jordan. Zur Quantenmechanik. *Z. Phys.*, 1925, v. 34, 858–888.
166. M. Born, W. Heisenberg, and P. Jordan. Zur Quantenmechanik II. *Z. Phys.*, 1926, v. 35, 557–615.
167. E. Schrödinger. Über das Verhältnis der Heisenberg-Born-Jordanschen Quantenmechanik zu der meinen. *Ann. Phys.*, 1926, v. 384, 734–756.
168. E. Schrödinger. Quantisierung als Eigenwertproblem. *Ann. Phys.*, 1926, v. 384, 361–376.
169. X. Oriols and J. Mompart, eds. Applied Bohmian Mechanics: From Nanoscale Systems to Cosmology. Jenny Stanford Publishing Pte. Ltd., Singapore, 2 edition, 2019.
170. Á S. Sanz and S. Miret-Artés. A Trajectory Description of Quantum Processes. I. Fundamentals. Springer-Verlag, Berlin and Heidelberg, 2012.
171. Á S. Sanz and S. Miret-Artés. A Trajectory Description of Quantum Processes. II. Applications. Springer-Verlag, Berlin and Heidelberg, 2014.
172. A. Drezet. Forewords for the Special Issue 'Pilot-wave and Beyond: Louis de Broglie and David Bohm's Quest for a Quantum Ontology'. *Found. Phys.*, 2023, v. 53, 62.
173. A. Sommerfeld. Zur Quantentheorie der Spectrallinien. *Ann. Phys.*, 1916, v. 356, 1–94.
174. W. Wilson. The Quantum-Theory of Radiation and Line Spectra. *Phil. Mag.*, 1915, v. 29, 795–802.
175. D. H. Kobe. Helmholtz's theorem revisited. *Am. J. Phys.*, 1986, v. 54, 552–554.

176. J. Cantarella, D. DeTurck, and H. Gluck. Vector calculus and the topology of domains in 3-space. *Am. Math. Monthly*, 2002, v. 109, 409–442.
177. H. Bhatia, G. Norgard, V. Pascucci *et al.* The Helmholtz-Hodge Decomposition – A Survey. *IEEE Trans. Vis. Comput. Graph.*, 2013, v. 10, 1386–1404.
178. H. Bhatia, V. Pascucci, and P-T. Bremer. The Natural Helmholtz-Hodge Decomposition for Open-Boundary Flow Analysis. *IEEE Trans. Vis. Comput. Graph.*, 2013, v. 20, 1566–1578.
179. L. E. Fraenkel. An Introduction to Maximum Principles and Symmetry in Elliptic Problems. Cambridge University Press, Cambridge, UK, 2000.
180. F. C. Adams and G. Laughlin. The Five Ages of the Universe. TOUCHSTONE, New York, 1999.
181. K. Mack. The End of Everything: Astrophysically Speaking. Scribner, New York, 2020.
182. D. E. Green and H. D. Zande. Universal energy principle of biological systems and the unity of bioenergetics. *Proc. Natl. Acad. Sci. USA*, 1981, v. 78, 5344–5347.
183. R. Haase. Survey of Fundamental Laws. In: W. Jost, ed. Physical Chemistry: An Advanced Treatise. Volume I, Thermodynamics. Academic Press, Inc., New York, 1971, pp. 1–239.
184. H. C. Longuet-Higgins. The quantum mechanical theory of environmental effects. *Proc. R. Soc. Lond. A*, 1960, v. 255, 63–68.
185. R. Rigler, M. Orrit, and T. Basché, eds. Single Molecule Spectroscopy. Springer, New York, 2001.
186. A. Gräslund, R. Rigler, and J. Widengren, eds. Single Molecule Spectroscopy in Chemistry, Physics and Biology. Springer, New York, 2010.
187. W. H. Cropper. Rudolf Clausius and the road to entropy. *Am. J. Phys.*, 1986, v. 54, 1068–1074.
188. R. C. Tolman and P. C. Fine. On the Irreversible Production of Entropy. *Rev. Mod. Phys.*, 1948, v. 20, 51–77.
189. V. C. Weiss. The uniqueness of Clausius’s integrating factor. *Am. J. Phys.*, 2006, v. 74, 699–705.
190. D. R. Owen. A First Course in the Mathematical Foundations of Thermodynamics. Springer-Verlag, New York, 1984.
191. D. Lewis. Counterfactual Dependence and Time’s Arrow. *Noûs*, 1979, v. 13, 455–476.
192. J. Dunn. Fried Eggs, Thermodynamics, and the Special Sciences. *Brit. J. Phil. Sci.*, 2011, v. 62, 71–98.
193. Ch. Chipot and A. Pohorille, eds. Free Energy Calculations. Springer, Berlin, Heidelberg, and New York, 2007.
194. D. Kondepudi and I. Prigogine. Modern Thermodynamics. John Wiley & Sons, Chichester, UK, 2 edition, 2015.
195. U. Seifert. Stochastic thermodynamics, fluctuation theorems and molecular machines. *Rep. Prog. Phys.*, 2012, v. 75, 126001.
196. A. Puglisi, A. Sarracino, and A. Vulpiani. Temperature in and out of equilibrium: A review of concepts, tools and attempts. *Physics Reports*, 2017, v. 709–710, 1–60.
197. D. Zhang, X. Zheng, and M. Di Ventra. Local temperatures out of equilibrium. *Physics Reports*, 2019, v. 830, 1–66.
198. N. Bohr. Chemistry and Quantum Theory of Atomic Constitution. *J. Chem. Soc.*, 1932, v. 1, 349–384.
199. H. J. D. Miller and J. Anders. Energy-temperature uncertainty relation in quantum thermodynamics. *Nat. Commun.*, 2018, v. 9, 2203.
200. Z. Roupas. Thermodynamic origin of quantum time-energy uncertainty relation. *J. Stat. Mech.*, 2021, v. 2021, 093207.
201. B. Mandelbrot. An Outline of a Purely Phenomenological Theory of Statistical Thermodynamics: I. Canonical Ensembles. *IRE Trans. Inform. Theory*, 1956, v. IT-2, 190–203.
202. L. de Broglie. The Thermodynamics of the isolated particle (or the hidden thermodynamics of particles. Gauthier-Villars Editor, Paris, 1964.
203. D. Bohm and J. P. Vigier. Model of the Causal Interpretation of Quantum Theory in Terms of a Fluid with Irregular Fluctuations. *Phys. Rev.*, 1954, v. 96, 208–216..
204. E. A. Guggenheim. Thermodynamics. Elsevier, New York, 7 edition, 1985.
205. J. von Neumann, R. T. Beyer, transl., and N. A. Wheeler, ed. Mathematical Foundations of Quantum Mechanics. Princeton University Press, Princeton, NJ, New edition, 2018.
206. L. Szilard. Über die Entropieerminderung in einem thermodynamischen System bei Eingriffen intelligenter Wesen. *Z. Phys.*, 1929, v. 53, 840–856.
207. J. M. Jauch and J. G. Báron. Entropy, Information, and Szilard’s Paradox. *Helv. Phys. Acta*, 1972, v. 45, 220–232.
208. O. Penrose. Foundations of Statistical Mechanics. Pergamon Press, New York, 1970.
209. C. de Beaugregard and M. Tribus. Information and Thermodynamics. *Helv. Phys. Acta*, 1972, v. 47, 238–247.
210. W. H. Zurek. Maxwell’s Demon, Szilard’s Engine and Quantum Measurements. In: G. T. Moore and M. O. Scully, eds. Frontiers of Nonequilibrium Statistical Physics. Plenum Press, New York, 1984, pp. 151–161.
211. E. Lubkin. Keeping the Entropy of Measurement: Szilard Revisited. *Int. J. Theor. Phys.*, 1987, v. 26, 523–535.
212. L. C. Biedenharn and J. C. Solem. A Quantum-Mechanical Treatment of Szilard’s Engine: Implications for the Entropy of Information. *Found. Phys.*, 1995, v. 25, 1221–1229.
213. J. V. Koski, V. F. Maisi, J. P. Pekola *et al.* Experimental realization of a Szilard engine with a single electron. *Proc. Natl. Acad. Sci. USA*, 2014, v. 111, 13786–13789.
214. J. L. Lebowitz and E. H. Lieb. Existence of Thermodynamics for Real Matter with Coulomb Forces. *Phys. Rev. Lett.*, 1969, v. 22, 631–634.
215. E. H. Lieb and J. L. Lebowitz. The Constitution of Matter: Existence of Thermodynamics for Systems Composed of Electrons and Nuclei. *Adv. Math.*, 1972, v. 9, 316–398.
216. C. Hainzl, M. Lewin, and J. P. Solovej. The thermodynamic limit of quantum Coulomb systems. Part I. General theory. *Adv. Math.*, 2009, v. 221, 454–487.
217. C. Hainzl, M. Lewin, and J. P. Solovej. The thermodynamic limit of quantum Coulomb systems. Part II. Applications. *Adv. Math.*, 2009, v. 221, 488–546.
218. E. H. Lieb and R. Seiringer. The Stability of Matter in Quantum Mechanics. Cambridge University Press, Cambridge, UK, 2009.
219. R. C. Geary. The Frequency Distribution of the Quotient of Two Normal Variables. *J. R. Stat. Soc.*, 1930, v. 93, 442–446.
220. E. V. Huntington. Frequency Distributions of Products and Quotients. *Ann. Math. Stat.*, 1939, v. 10, 195–198.
221. C. C. Craig. On the Frequency Function of XY. *Ann. Math. Stat.*, 1936, v. 7, 1–15.
222. C. C. Craig. On the Frequency Distributions of the Quotient and of the Product of Two Statistical Variables. *Am. Math. Mon.*, 1942, v. 49, 26–32.
223. L. A. Aroian. Some Methods of Evaluation of a Sum. *J. Am. Stat. Assoc.*, 1944, v. 39, 511–515.
224. L. A. Aroian. The Probability Function of the Product of Two Normally Distributed Random Variables. *Ann. Math. Stat.*, 1947, v. 18, 265–271.
225. L. B. Landau and E. M. Lifshitz. Quantum Mechanics: Non-relativistic Theory. Pergamon Press, Oxford, 2 edition.
226. A. R. Bohm, M. Gadella, and P. Kielanowski. Time Asymmetric Quantum Mechanics. *SIGMA*, 2011, v. 7, 086.

227. R. de la Madrid. On the inconsistency of the Bohm-Gadella theory with quantum mechanics. *J. Phys. A*, 2006, v. 39, 9255–9268.
228. M. Gadella and S. Wickramasekara. Comment on 'On the inconsistency of the Bohm-Gadella theory with quantum mechanics'. *J. Phys. A*, 2007, v. 40, 4665–4669.
229. R. de la Madrid. Reply to "Comment on 'On the inconsistency of the Bohm-Gadella theory with quantum mechanics'". *J. Phys. A*, 2007, v. 40, 4671–4681.
230. H. Baumgärtel. Time asymmetry in quantum mechanics: a pure mathematical point of view. *J. Phys. A*, 2008, v. 41, 304017.
231. G. 't Hooft. *The Cellular Automaton Interpretation of Quantum Mechanics*. Springer, Cham, Heidelberg, New York, Dordrecht, and London, 2016.
232. O. Penrose. Time warp. *Nature*, 1993, v. 362, 510.
233. M. C. Mackey. *Time's Arrow: The Origins of Thermodynamic Behavior*. Springer-Verlag, New York, 1992.
234. A. L. Kuzemsky. In Search of Time Lost: Asymmetry of Time and Irreversibility in Natural Processes. *Found. Sci.*, 2020, v. 25, 597–645.
235. S. Golden. *Quantum Statistical Foundation of Chemical Kinetics*. Clarendon Press, Oxford, 1969.
236. L. Fonda, G. C. Ghirardi, A. Rimini *et al.* On the Quantum Foundations of the Exponential Decay Law. *Nuov. Cim. A*, 1973, v. 15, 689–704.
237. N. Metropolis, A. W. Rosenbluth, M. N. Rosenbluth *et al.* Equation of State Calculations by Fast Computing Machines. *J. Chem. Phys.*, 1953, v. 23, 1087–1092.
238. W. K. Hastings. Monte Carlo sampling methods using Markov chains and their applications. *Biometrika*, 1970, v. 57, 97–109.
239. R. Clausius. Ueber verschiedene für die Anwendung bequeme Formen der Hauptgleichungen der mechanischen Wärmetheorie. *Ann. Phys. Chem.*, 1865, v. 201, 353–400.
240. S. I. Sandler. *Chemical, Biochemical, and Engineering Thermodynamics*. John Wiley & Sons, Hoboken, NJ, 5 edition, 2016.
241. Y. Demirel and V. Gerbaud. *Nonequilibrium Thermodynamics*. Elsevier, Amsterdam and New York, 4 edition, 2019.
242. C. Nash and S. Sen. *Topology and Geometry for Physicists*. Academic Press, Orlando, FL, 1983.
243. H. Whitney. *Geometric Integration Theory*. Princeton University Press, Princeton, NJ, 1957.
244. L. O'Raiifeartaigh. *The Dawning of Gauge Theory*. Princeton University Press, Princeton, NJ, 1997.
245. F. London. Quantenmechanische Deutung der Theorie von Weyl. *Z. Phys.*, 1927, v. 42, 375–389.
246. H. Weyl. *The Theory of Groups and Quantum Mechanics*. Dover Publications, Inc., New York, 1950. P. H. Robinson, transl. Gruppentheorie und Quantenmechanik, 2nd rev. ed., 1930.
247. E. Schrödinger. Über eine bemerkenswerte Eigenschaft der Quantenbahnen eines einzelnen Elektrons. *Z. Phys.*, 1923, v. 12, 13–23.
248. H. Weyl. Gravitation and the Electron. *Proc. Natl. Acad. Sci. USA*, 1929, v. 15, 323–334.
249. Y. Aharonov and D. Bohm. Significance of electromagnetic potentials in the quantum theory. *Phys. Rev.*, 1959, v. 115, 485–491.
250. Y. Aharonov and D. Bohm. Further considerations on electromagnetic potentials in the quantum theory. *Phys. Rev.*, 1961, v. 123, 1511–1524.
251. W. K. H. Panofsky and M. Phillips. *Classical Electricity and Magnetism*. Addison Wesley, New York, 2 edition, 1962.
252. A. O'Rahilly. *Electromagnetic Theory: A Critical Examination of Fundamentals*. Dover Publications, Inc., Mineola, NY, 1965.
253. J. D. Jackson. *Classical Electrodynamics*. John Wiley & Sons, Hoboken, NJ, 3 edition, 1999.
254. A. Zangwill. *Modern Electrodynamics*. Cambridge University Press, New York, 2012.
255. D. J. Griffiths. *Introduction to Electrodynamics*. Pearson, Upper Saddle River, NJ, 4 edition, 2013.
256. J. Schwinger, L. L. DeRaad Jr., K. A. Milton and W. y. Tsai. *Classical Electrodynamics*. CRC Press, Boca Raton, FL, 2018.
257. A. Einstein. Strahlungs-Emission und -Absorption nach der Quantentheorie. *Verhandl. D. Deutch. Phys. Ges.*, 1916, v. 18, 318–323.
258. A. Einstein. Zur Quantentheorie der Strahlung. *Phys. Zeit.*, 1917, v. 18, 121–128.
259. P. A. M. Dirac. The Quantum Theory of the Emission and Absorption of Radiation. *Proc. R. Soc. Lond. A*, 1927, v. 114, 243–265.
260. P. A. M. Dirac. The Quantum Theory of Dispersion. *Proc. R. Soc. Lond. A*, 1927, v. 114, 710–728.
261. B. Mashhoon. Gravitoelectromagnetism: A Brief Review. In: L. Iorio, ed. *The Measurement of Gravitomagnetism: A Challenging Enterprise*. NOVA Science Publishers, Inc., Hauppauge, NY, 2007, pp. 29–40.
262. C. W. F. Everitt *et al.* Gravity Probe B: Final Results of a Space Experiment to Test General Relativity. *Phys. Rev. Lett.*, 2011, v. 106, 221101.
263. W. de Sitter. On Einstein's theory of gravitation, and its astronomical consequences. *Mon. Not. R. Astron. Soc.*, 1916, v. 77, 155–184.
264. B. Mashhoon, F. W. Hehl, and D. S. Theiss. On the gravitational effects of rotating masses: The Thirring-Lense papers. *Gen. Rel. Grav.*, 1984, v. 16, 711–750.
265. P. D. B. Collins, A. D. Martin, and E. J. Squires. *Particle Physics and Cosmology*. Wiley-Interscience, New York, 1989.
266. P. A. M. Dirac. Quantised Singularities in the Electromagnetic Field. *Proc. R. Soc. Lond. A*, 1931, v. 133, 60–72.
267. G. Auletta, M. Fortunato, and G. Parisi. *Quantum Mechanics*. Cambridge University Press, New York, 2009.
268. G. Grynberg, A. Aspect, and C. Fabre. *Introduction to Quantum Optics*. Cambridge University Press, New York, 2010.
269. T. Engel and P. Reid. *Physical Chemistry*. Pearson Education, Inc., New York, 3 edition, 2012.
270. T. D. Ladd, F. Jelezko, R. Laflamme *et al.* Quantum Computers. *Nature*, 2010, v. 464, 45–53.
271. J. E. Sipe. Photon wave functions. *Phys. Rev. A*, 1995, v. 52, 1875–1893.
272. D. M. Cook. *The Theory of the Electromagnetic Field*. Dover Publications, Inc., New York, 2002.
273. D. K. Cheng. *Field and Wave Electromagnetics*. Addison Wesley, Reading, MA, 2 edition, 1989.
274. C. S. Wood, S. C. Bennett, D. Cho *et al.* Measurement of Parity Non-conservation and an Anapole Moment in Cesium. *Science*, 1997, v. 275, 1759–1763.
275. M.-A. Bouchiat. Atomic parity violation: Early days, present results, prospects. *Nuov. Cim. C*, 2012, v. 35, 78–84.
276. M. S. Safronova, D. Budker, D. DeMille *et al.* Search for new physics with atoms and molecules. *Rev. Mod. Phys.*, 2018, v. 90, 025008.
277. J. W. Blanchard, J. P. King, T. F. Sjolander *et al.* Molecular parity non-conservation in nuclear spin couplings. *Phys. Rev. Research*, 2020, v. 2, 023258.
278. Y. Aharonov, D. Z. Albert, and L. Vaidman. How the result of a measurement of a component of the spin of a spin- $\frac{1}{2}$ particle can turn out to be 100. *Phys. Rev. Lett.*, 1988, v. 60, 1351–1354.
279. J. Dressel, M. Malik, F. M. Miatto *et al.* Understanding quantum weak values: Basics and applications. *Rev. Mod. Phys.*, 2014, v. 86, 307–316.
280. L. Vaidman. Weak value controversy. *Phil. Trans. R. Soc. A*, 2017, v. 375, 20160395.

281. Y. Aharonov, P.G. Bergmann, and J.L. Lebowitz. Time Symmetry in the Quantum Process of Measurement. *Phys. Rev.*, 1964, v. 134, 1410–1416.
282. A. Bednorz, K. Franke, and W. Belzi. Noninvasiveness and time symmetry of weak measurements. *New J. Phys.*, 2013, v. 15, 023043.
283. M. Jayaseelan, S.K. Manikandan, A.N. Jordan *et al.* Quantum measurement arrow of time and fluctuation relations for measuring spin of ultracold atoms. *Nature Communications*, 2021, v. 12 (1), 1847.
284. É. Borel. Probabilities and Life. Dover Publications, Inc., New York, 1962.
285. J.O. Hirschfelder. The angular momentum, creation, and significance of quantized vortices. *J. Chem. Phys.*, 1977, v. 67, 5477–5483.
286. A. Nussbaum. Faraday's law paradoxes. *Phys. Educ.*, 1972, v. 7, 231–232.
287. A. López-Ramos, J.R. Menéndez, and C. Piqué. Conditions for the validity of Faraday's law of induction and their experimental confirmation. *Eur. J. Phys.*, 2008, v. 29, 1069–1076.
288. P. Kinsler. Faraday's Law and Magnetic Induction: Cause and Effect, Experiment and Theory. *Physics*, 2020, v. 2, 150–163.
289. M. Faraday. Thoughts on Ray-vibrations. *Phil. Mag. S. 3.*, 1846, v. 28, 345–350.
290. N. Bohr and L. Rosenfeld. Field and Charge Measurements in Quantum Electrodynamics. *Phys. Rev.*, 1950, v. 78, 794–798.
291. R. Clausius. On a Mechanical Theorem Applicable to Heat. *Phil. Mag.*, 1870, v. 40, 122–127.
292. A. S. Eddington. The Kinetic Energy of a Star Cluster. *Mon. Not. R. Astron. Soc.*, 1916, v. 76, 525–548.
293. F. Zwicky. On the Masses of Nebulae and of Clusters of Nebulae. *Ap. J.*, 1937, v. 86, 217–246.
294. V.A. Ambartsumian. On the Evolution of Galaxies. In: R. Stoops, ed. *La Structure et révolution de l'univers*. 13th Solvay Conference, Brussels, 1958, pp. 241–279.
295. J. Bland-Hawthorn and K. Freeman. Near Field Cosmology – The Origin of the Galaxy and the Local Group. In: B. Moore, ed. *The Origin of the Galaxy and Local Group*. Springer, Berlin and Heidelberg, 2014, pp. 3–156.
296. V.C. Rubin and W.K. Ford Jr. Rotation of the Andromeda Nebula from a Spectroscopic Survey of Emission Regions. *Ap. J.*, 1970, v. 159.
297. D. Walsh, R.F. Carswell, and R.J. Weymann. 0957 + 561 A, B: twin quasistellar objects or gravitational lens? *Nature*, 1979, v. 279, 381–384.
298. D.N. Spergel, R. Bean, O. Doré *et al.* Three-Year Wilkinson Microwave Anisotropy Probe (WMAP) Observations: Implications for Cosmology. *Astrophys. J. Suppl.*, 2007, v. 170, 377–408.
299. J.J. Brehm and W.J. Mullin. Introduction to the Structure of Matter. John Wiley & Sons, New York, 1989.
300. J.O. Hirschfelder, C.F. Curtiss, and R.B. Bird. Molecular Theory of Gases and Liquids. John Wiley & Sons, New York, 1954.
301. M. Born and K. Huang. Dynamical Theory of Crystal Lattices. Oxford University Press, London, 1962.
302. K.S. Surana. Advanced Mechanics of Continua. CRC Press, Boca Raton, FL, 2015.
303. D.J. Dean. Beyond the nuclear shell model. *Phys. Today*, 2007, v. 60, 48–53.
304. N. Schunck, ed. Energy Density Functional Methods for Atomic Nuclei. Institute of Physics, Bristol and Philadelphia, 2019.
305. R.P. Feynman, R.B. Leighton, and M. Sands. The Feynman Lectures on Physics, v. 3, Quantum Mechanics. Addison-Wesley, Reading, MA, 1965.
306. R.F. Streater and A.S. Wightman. PCT, Spin and Statistics, and All That. Addison Wesley, Reading, MA, 1989.
307. R.P. Feynman. The Reason for Antiparticles. In: Elementary Particles and the Laws of Physics: The 1986 Dirac Memorial Lectures. Cambridge University Press, New York, 1987, pp. 1–59.
308. M. Altunbulak and A. Klyachko. The Pauli Principle Revisited. *Commun. Math. Phys.*, 2008, v. 282, 287–322.
309. I.G. Kaplan. The Pauli Exclusion Principle. Can It Be Proved? *Found. Phys.*, 2013, v. 43, 1233–1251.
310. I.G. Kaplan. The Pauli Exclusion Principle. John Wiley & Sons, New York, 2017.
311. I.G. Kaplan. Modern State of the Pauli Exclusion Principle and the Problems of Its Theoretical Foundation. *Symmetry*, 2021, v. 13, 21–37.
312. I.G. Kaplan. The Pauli Exclusion Principle and the Problems of Its Experimental Verification. *Symmetry*, 2020, v. 12, 320–334.
313. S.R. Elliott, B.H. LaRoque, V.M. Gehman *et al.* An Improved Limit on Pauli-Exclusion-Principle Forbidden Atomic Transitions. *Fortschr. Phys.*, 2012, v. 42, 1015–1030.
314. J. Marton, C. Berucci, M. Cargnelli *et al.* Underground Test of Quantum Mechanics: The VIP2 Experiment. In: A. Khrennikov and B. Toni, eds. *Quantum Foundations, Probability and Information*. Springer International Publishing AG, Cham, Germany, 2018.
315. M. Massimi. Pauli's Exclusion Principle. Cambridge University Press, New York, 2006.
316. J. Bain. CPT Invariance and the Spin-Statistics Connection. Oxford University Press, Oxford, 2016.
317. H. Margenau. The Exclusion Principle and Its Philosophical Importance. *Phil. Sci.*, 1944, v. 11, 187–208.
318. E.C. Stoner. The Distribution of Electrons amongst Atomic Levels. *Phil. Mag.*, 1924, v. 48, 719–736.
319. W. Pauli. Über den Einfluß der Geschwindigkeitsabhängigkeit der Elektronenmasse auf den Zeemaneffekt. *Z. Phys.*, 1925, v. 31, 373–385.
320. L. de Broglie. Waves and Quanta. *Nature*, 1923, v. 112, 540.
321. N. Bohr and D. Coster. Röntgenspektren und periodisches System der Elemente. *Z. Phys.*, 1923, v. 12, 342–374.
322. W. Pauli. Über den Zusammenhang des Abschlusses der Elektronengruppen im Atom mit der Komplexstruktur der Spektren (On the Connection between the Completion of Electron Groups in an Atom with the Complex Structure of Spectra). *Z. Phys.*, 1925, v. 31, 765–783.
323. J.C. Slater. Atomic Shielding Constants. *Phys. Rev.*, 1930, v. 36, 57–64.
324. E. Clementi and D.L. Raimondi. Atomic Screening Constants from SCF Functions. *J. Chem. Phys.*, 1963, v. 38, 2686–2689.
325. E. Clementi, D.L. Raimondi, and W.P. Reinhardt. Atomic Screening Constants from SCF Functions. II. Atoms with 37 to 86 Electrons. *J. Chem. Phys.*, 1967, v. 47, 1300–1307.
326. L. Mandelstam and I. Tamm. The Uncertainty Relation Between Energy and Time in Non-relativistic Quantum Mechanics. *J. Phys. USSR*, 1945, v. 9, 249–254.
327. E.P. Wigner. On the Time-Energy Uncertainty Relation. In: A. Salam and E.P. Wigner, eds. *Aspects of Quantum Theory*. Cambridge University Press, Cambridge, UK, 1972, pp. 237–247.
328. P. Busch. On the Energy-Time Uncertainty Relation. Part I: Dynamical Time and Time Indeterminacy. *Found. Phys.*, 1990, v. 20, 1–32.
329. P. Busch. On the Energy-Time Uncertainty Relation. Part II: Pragmatic Time Versus Energy Indeterminacy. *Found. Phys.*, 1990, v. 20, 33–43.
330. J. Hilgevoord. The uncertainty principle for energy and time. *Am. J. Phys.*, 1996, v. 64, 1451–1456.
331. J. Hilgevoord. The uncertainty principle for energy and time. II. *Am. J. Phys.*, 1998, v. 66, 396–402.
332. W.R. Hindmarsh. Atomic Spectra. Pergamon Press, Oxford and New York, 1967.

333. V. V. Bolotin. The Dynamic Stability of Elastic Systems. Holden-Day, San Francisco, CA, 1964.
334. R. W. Clough and J. Penzien. Dynamics of Structures. Computers & Structures, Inc., Berkeley, CA, 3 edition, 2003.
335. Z. P. Bazant and L. Cedolin. Stability of Structures. World Scientific Publishing, Singapore, 2010.
336. T. Kato. Fundamental properties of Hamiltonian operators of Schrödinger type. *Trans. Am. Math. Soc.*, 1951, v. 70, 195–211.
337. F. J. Dyson and A. Lenard. Stability of Matter I. *J. Math. Phys.*, 1967, v. 8, 423–434.
338. L. Onsager. Electrostatic interaction of molecules. *J. Phys. Chem.*, 1939, v. 43, 189–196.
339. M. E. Fisher and D. Ruelle. The Stability of Many-Particle Systems. *J. Math. Phys.*, 1966, v. 7, 260–270.
340. X. He, K. Wang, J. Zhuang *et al.* Coherently forming a single molecule in an optical trap. *Science*, 2020, v. 370, 331–335.
341. S. W. Hla, L. Bartels, G. Meyer *et al.* Inducing All Steps of a Chemical Reaction with the Scanning Tunneling Microscope Tip: Towards Single Molecule Engineering. *Phys. Rev. Lett.*, 2000, v. 85, 2777–2780.
342. D. G. de Oteyza, P. Gorman, Y.-C. Chen *et al.* Direct Imaging of Covalent Bond Structure in Single-Molecule Chemical Reactions. *Science*, 2013, v. 340, 1434–1437.
343. A. Riss, A. P. Paz, S. Wickenburg *et al.* Imaging single-molecule reaction intermediates stabilized by surface dissipation and entropy. *Nat. Chem.*, 2016, v. 8, 678–683.
344. T. W. Chamberlain, J. Biskupek, S. T. Skowro *et al.* Stop-Frame Filming and Discovery of Reactions at the Single-Molecule Level by Transmission Electron Microscopy. *ACS Nano*, 2017, v. 11, 2509–2520.
345. Y. Liu, M.-G. Hu, M. A. Nichols *et al.* Precision test of statistical dynamics with state-to-state ultracold chemistry. *Nature*, 2021, v. 593, 379–384.
346. F. J. Dyson. Ground-State Energy of a Finite System of Charged Particles. *J. Math. Phys.*, 1967, v. 8, 1538–1545.
347. E. P. Wigner. The Unreasonable Effectiveness of Mathematics in the Natural Sciences. *Commun. Pure App. Math.*, 1960, v. 13, 1–14.
348. R. D. Astumian. The unreasonable effectiveness of equilibrium theory for interpreting nonequilibrium experiments. *Am. J. Phys.*, 2006, v. 74, 683–688.
349. J. C. Maxwell. Treatise on Electricity and Magnetism, Vol. 1. Oxford University Press, Oxford, 1873.
350. J. H. Jeans. The Mathematical Theory of Electricity and Magnetism. Cambridge University Press, Cambridge, UK, 5 edition, 1927.
351. J. L. Lagrange. Mécanique Analytique. La Veuve Desaint, Paris, 1788.
352. J. Cizek and J. Paldus. Stability Conditions for the Solutions of the Hartree-Fock Equations for Atomic and Molecular Systems. Application to the Pi-Electron Model of Cyclic Polyenes. *J. Chem. Phys.*, 1967, v. 47, 3976–3985.
353. R. Schoen and S.-T. Yau. The Energy and the Linear Momentum of Space-Times in General Relativity. *Commun. Math. Phys.*, 1981, v. 79, 47–51.
354. E. Witten. A New Proof of the Positive Energy Theorem. *Commun. Math. Phys.*, 1981, v. 80, 381–402.
355. Y. Marcus. A simple empirical model describing the thermodynamics of hydration of ions of widely varying charges, sizes, and shapes. *Biophys. Chem.*, 1994, v. 51, 111–127.
356. J. D. Gillaspay. Highly charged ions. *J. Phys. B*, 2001, v. 34, 93–130.
357. E. H. Lieb and M. Loss. Existence of Atoms and Molecules in Non-Relativistic Quantum Electrodynamics. *Adv. Theor. Math. Phys.*, 2003, v. 7, 667–710.
358. L. Pauling and S. B. Hendricks. The Prediction of the Relative Stabilities of Isoelectric Isomeric Ions and Molecules. *J. Am. Chem. Soc.*, 1926, v. 48, 641–651.
359. L. Pauling. The Nature of the Chemical Bond. Cornell University Press, Ithaca, NY, 3 edition, 1960.
360. L. Pauling. The Architecture of Molecules. *Proc. Natl. Acad. Sci. USA*, 1964, v. 51, 977–984.
361. S. J. Weininger. The Molecular Structure Conundrum: Can Classical Chemistry be Reduced to Quantum Chemistry? *J. Chem. Ed.*, 1984, v. 61, 939–944.
362. R. G. Woolley. The Molecular Structure Conundrum. *J. Chem. Ed.*, 1985, v. 62, 1082–1084.
363. R. C. Tolman. The Measurable Quantities of Physics. *Phys. Rev.*, 1917, v. 9, 237–253.
364. O. Redlich. Intensive and Extensive Properties. *J. Chem. Ed.*, 1970, v. 47, 154–156.
365. S. Chandrasekhar. On stars, their evolution and their stability. *Rev. Mod. Phys.*, 1984, v. 56, 137–147.
366. S. Chandrasekhar. The Highly Collapsed Configurations of a Stellar Mass. (Second Paper.). *Mon. Not. R. Astron. Soc.*, 1935, v. 95, 207–225.
367. J. C. Slater. The Virial and Molecular Structure. *J. Chem. Phys.*, 1933, v. 1, 687–691.
368. G. Marc and W. G. McMillan. The Virial Theorem. *Adv. Chem. Phys.*, 1985, v. 58, 209–361.
369. M. A. Ranade. Virial Theorem for a Molecule. Master's thesis, North Texas State University, Denton, TX, 1972.
370. A. Clebsch, ed. Jacobi's Lectures on Dynamics. Hindustan Book Agency, New Delhi, 2 edition, 2009.
371. H. Pollard. A Sharp Form of the Virial Theorem. *Bull. Amer. Math. Soc.*, 1964, v. 70, 703–705.
372. K. Y. Bliokh, J. Dressel, and F. Nori. Conservation of the spin and orbital angular momenta in electromagnetism. *New J. Phys.*, 2014, v. 16, 093037.
373. J. Lewins and M. Becker, eds. Advances in Nuclear Science and Technology: Volume 19. Festschrift in Honor of Eugene P. Wigner. Plenum Press, New York, 1987.
374. A. E. Milne. An Extension of the Theorem of the Virial. *Phil. Mag.*, 1925, v. 50, 409–414.
375. G. W. Collins II. The Virial Theorem in Stellar Astrophysics. Pachart Pub. House, Tucson, AZ, 1978.
376. H. S. Leff. Entropy, Its Language, and Interpretation. *Found. Phys.*, 2007, v. 37, 1744–1766.
377. J. L. Park. The Concept of Transition in Quantum Mechanics. *Found. Phys.*, 1970, v. 1, 23–33.
378. W. K. Wootters and W. H. Zurek. A single quantum cannot be cloned. *Nature*, 1982, v. 299, 802–803.
379. V. Buzek and M. Hillery. Quantum copying: Beyond the no-cloning theorem. *Phys. Rev. A*, 1996, v. 54, 1844–1852.
380. S. Msindo, G. G. Nyambuya, and C. Nyamhere. Plausible Fundamental Origins of Emissivity (I). *Prog. Phys.*, 2021, v. 17, 10–13.
381. M. Dalarsson N. Dalarsson and L. Golubović. Introductory Statistical Thermodynamics. Academic Press, Burlington, MA, 2011.
382. F. Schwabl. Statistical Mechanics. Springer-Verlag, Berlin, Heidelberg, and New York, 2 edition, 2010.
383. O. Heaviside. The Radiation from an Electron describing a Circular Orbit. *Nature*, 1904, v. 69, 293–294.
384. H. Yu and W. Zhou. Do static atoms outside a Schwarzschild black hole spontaneously excite? *Phys. Rev. D*, 2007, v. 76, 044023.

385. G. Degrossi, S. Di Vita, J. Elias-Miró *et al.* Higgs mass and vacuum stability in the Standard Model at NNLO. *J. High Energ. Phys.*, 2012, v. 98.
386. [Planck Collaboration]. Planck 2018 results. VI. Cosmological parameters. *Astron. Astrophys.*, 2020, v. 641, A6.
387. P. A. M. Dirac. The Theory of Magnetic Poles. *Phys. Rev.*, 1948, v. 74, 817–830.
388. H. Weyl. Gravitation and electricity. *Sitzungsber. Königl. Preuss. Akad. Wiss.*, 1918, v. 26, 465–480.
389. M. Born and V. Fock. Beweis des Adiabatsatzes. *Z. Phys.*, 1928, v. 51, 165–180.
390. E. Amaldi. On the Dirac Magnetic Poles. In: G. Putti, ed. *Old and New Problems in Elementary Particles*. Addison Wesley, New York and London, 1968, pp. 1–61.
391. E. Amaldi and N. Cabibbo. On the Dirac Magnetic Poles. In: A. Salam and E. P. Wigner, eds. *Aspects of Quantum Theory*. Cambridge University Press, Cambridge, UK, 1972, pp. 185–212.
392. A. S. Goldhaber and W. P. Trower. Resource letter MM1: magnetic monopoles. *Am. J. Phys.*, 1990, v. 58, 429–439.
393. K. A. Milton. Theoretical and experimental status of magnetic monopoles. 2006, v. 69, 1637–1711.
394. L. Patrizii and M. Spurio. Status of Searches for Magnetic Monopoles. *Annu. Rev. Nucl. Part. Sci.*, 2015, v. 65, 279–302.
395. P. B. Price, E. K. Shirk, W. Z. Osborne *et al.* Evidence for Detection of a Moving Magnetic Monopole. *Phys. Rev. Lett.*, 1975, v. 35, 487–490.
396. B. Cabrera. First Results from a Superconductive Detector for Moving Magnetic Monopoles. *Phys. Rev. Lett.*, 1982, v. 48, 1378–1381.
397. P. G. H. Sandars. Magnetic Charge. *Contemp. Phys.*, 1966, v. 7, 419–429.
398. G. 't Hooft. Magnetic monopoles in unified gauge theories. *Nucl. Phys. B*, 1974, v. 79, 276–284.
399. A. M. Polyakov. Particle spectrum in the quantum field theory. *JETP Lett.*, 1974, v. 20, 194–195.
400. T. W. B. Kibble. Some Implications of a Cosmological Phase Transition. *Phys. Rev.*, 1980, v. 67, 183–199.
401. J. A. Gonzalo. *Inflationary Cosmology Revisited*. World Scientific Publishing, Singapore, 2005.
402. M. Lemoine, J. Martin, and P. Peter, eds. *Inflationary Cosmology*. Springer-Verlag, Berlin and Heidelberg, 2010.
403. A. A. Starobinsky. A New Type of Isotropic Cosmological Models Without Singularity. *Phys. Lett. B*, 1980, v. 91, 99–102.
404. A. H. Guth. Inflationary universe: A possible solution to the horizon and flatness problems. *Phys. Rev. D*, 1981, v. 23, 347–356.
405. M. B. Einhorn and K. Sato. Monopole Production in the Very Early Universe in a First-Order Phase Transition. *Nucl. Phys. B*, 1981, v. 180, 385–404.
406. A. D. Linde. A New Inflationary Universe Scenario: A Possible Solution of the Horizon, Flatness, Homogeneity, Isotropy and Primordial Monopole Problems. *Phys. Lett. B*, 1982, v. 108, 389–393.
407. A. Albrecht and P. J. Steinhardt. Cosmology for Grand Unified Theories with Radiatively Induced Symmetry Breaking. *Phys. Rev. Lett.*, 1982, v. 48, 1220–1223.
408. N. Craigie, P. Goddard, and W. Nahm, eds. *Monopoles in Quantum Field Theory: Proceedings of the Monopole Meeting, Trieste, Italy, December, 1981*. World Scientific Publishing, Singapore, 1982.
409. B. Acharya *et al.* [The MoEDAL Collaboration]. Search for magnetic monopoles produced via the Schwinger mechanism. *Nature*, 2022, v. 602, 63–67.
410. F. Sauter. Über das Verhalten eines Elektrons im homogenen elektrischen Feld nach der relativistischen Theorie Diracs. *Z. Phys.*, 1931, v. 69, 742–764.
411. J. Schwinger. On Gauge Invariance and Vacuum Polarization. *Phys. Rev.*, 1951, v. 82, 664–679.
412. R. A. Lewis, G. A. Smith, and S. D. Howe. Antiproton portable traps and medical applications. *Hyperfine Inter.*, 1997, v. 109, 155–164.
413. M. Aguilar *et al.* [The AMS Collaboration]. Antiproton Flux, Antiproton-to-Proton Flux Ratio, and Properties of Elementary Particle Fluxes in Primary Cosmic Rays Measured with the Alpha Magnetic Spectrometer on the International Space Station. *Phys. Rev. Lett.*, 2016, v. 117, 091103.
414. S. Acharya *et al.* [The ALICE Collaboration]. Measurement of anti-³He nuclei absorption in matter and impact on their propagation in the Galaxy. *Nat. Phys.*, 2023, v. 19, 61–71.
415. V. Poulin, P. Salati, I. Cholis *et al.* Where do the AMS-02 antihelium events come from? *Phys. Rev. D*, 2019, v. 99, 023016.
416. S. Dupourqué, L. Tibaldo, and P. von Ballmoos. Constraints on the antistar fraction in the Solar System neighborhood from the 10-year Fermi Large Area Telescope gamma-ray source catalog. *Phys. Rev. D*, 2021, v. 103, 083016.
417. P. Abratenko *et al.* [The MicroBooNE Collaboration]. Search for Neutrino-Induced Neutral-Current Δ Radiative Decay in MicroBooNE and a First Test of the MiniBooNE Low Energy Excess under a Single-Photon Hypothesis. *Phys. Rev. Lett.*, 2022, v. 128, 111801–111809.
418. H. Almazán *et al.* [The STEREO Collaboration]. Interpreting Reactor Antineutrino Anomalies with STEREO data. *Nature*, 2023, v. 613, 257–261.
419. H. Murayama. The origin of neutrino mass. *Phys. World*, 2002, v. 15, 35–39.
420. Y. Fukuda *et al.* [The Super-Kamiokande Collaboration]. Evidence for Oscillation of Atmospheric Neutrinos. *Phys. Rev. Lett.*, 1998, v. 81, 1562–1567.
421. Q. R. Ahmad *et al.* [The SNO Collaboration]. Direct Evidence for Neutrino Flavor Transformation from Neutral-Current Interactions in the Sudbury Neutrino Observatory. *Phys. Rev. Lett.*, 2002, v. 89, 011301.
422. M. Tanabashi *et al.* [Particle Data Group]. Review of Particle Physics. *Phys. Rev. D*, 2018, v. 98, 030001.
423. S. Davidson, E. Nardi, and Y. Nir. Leptogenesis. *Phys. Rev.*, 2008, v. 466, 105–177.
424. C. S. Fong, E. Nardi, and A. Riotto. Leptogenesis in the Universe. *Adv. High Energy Phys.*, 2012, v. 2012, 158303.
425. A. Riotto and M. Trodden. Recent Progress in Baryogenesis. *Ann. Rev. Nucl. Part. Sci.*, 1999, v. 49, 35–75.
426. P. Fileviez Pérez, C. Murgui, and A. D. Plascencia. Baryogenesis via leptogenesis: Spontaneous B and L violation. *Phys. Rev. D*, 2021, v. 104, 055007.
427. A. D. Sakharov. Violation of CP Invariance, C Asymmetry, and Baryon Asymmetry of the Universe. *Sov. Phys. JETPL*, 1967, v. 5, 24–27.
428. A. D. Sakharov. Cosmological models of the Universe with reversal of time's arrow. *Sov. Phys. JETP*, 1980, v. 52, 349–351.
429. J. L. Bernal, G. Sato-Polito, and M. Kamionkowski. Cosmic Optical Background Excess, Dark Matter, and Line-Intensity Mapping. *Phys. Rev. Lett.*, 2022, v. 129, 231301.
430. P. Sikivie. Dark Matter Axions. *Int. J. Mod. Phys. A*, 2010, v. 25, 554–563.
431. D. J. E. Marsh. Axion cosmology. *Phys. Reports*, 2016, v. 643, 1–79.
432. R. D. Peccei and H. R. Quinn. CP Conservation in the Presence of Pseudoparticles. *Phys. Rev. Lett.*, 1977, v. 38, 1440–1443.
433. R. D. Peccei and H. R. Quinn. Constraints imposed by CP conservation in the presence of pseudoparticles. *Phys. Rev. D*, 1977, v. 16, 1791–1797.
434. C. Abel *et al.* Measurement of the Permanent Electric Dipole Moment of the Neutron. *Phys. Rev. Lett.*, 2020, v. 124, 081803.

435. F. Wilczek. Problem of strong P and T invariance in the presence of instantons. *Phys. Rev. Lett.*, 1978, v. 40, 279–282.
436. J. Preskill, M. B. Wise, and F. Wilczek. Cosmology of the Invisible Axion. *Phys. Lett. B*, 1983, v. 120, 127–132.
437. P. Sikivie and Q. Yang. Bose-Einstein Condensation of Dark Matter Axions. *Phys. Rev. Lett.*, 2009, v. 103, 111301.
438. V. Anastassopoulos *et al.* [The CAST Collaboration]. New CAST limit on the axion-photon interaction. *Nat. Phys.*, 2017, v. 13, 584–590.
439. T. Braine *et al.* [The ADMX Collaboration]. Extended Search for the Invisible Axion with the Axion Dark Matter Experiment. *Phys. Rev. A*, 2020, v. 124, 101303.
440. F. Chadha-Day, J. Ellis, and D. J. E. Marsh. Axion dark matter: What is it and why now? *Science*, 2022, v. 8, 3618.
441. Y. K. Semertzidis and S. Youn. Axion dark matter: How to see it? *Sci. Adv.*, 2022, v. 8, 9928.
442. F. Wilczek. Two Applications of Axion Electrodynamics. *Phys. Rev. Lett.*, 1987, v. 58, 1799–1802.
443. A. Amruth, T. Broadhurst, J. Lim, *et al.* Einstein rings modulated by wavelike dark matter from anomalies in gravitationally lensed images. *Nat. Astron.*, 2023.
444. A. Einstein. Lens-Like Action of a Star by the Deviation of Light in the Gravitational Field. *Science*, 1936, v. 84, 506–507.
445. J. J. Hudson, D. M. Kara, I. J. Smallman *et al.* Improved measurement of the shape of the electron. *Nature*, 2011, v. 473, 493–497.
446. J. Baron *et al.* [The ACME Collaboration]. Order of Magnitude Smaller Limit on the Electric Dipole Moment of the Electron. *Science*, 2014, v. 343, 269–272.
447. V. Andreev *et al.* [The ACME Collaboration]. Improved limit on the electric dipole moment of the electron. *Nature*, 2018, v. 562, 355–360.
448. D. J. Fixsen. The Temperature of the Cosmic Microwave Background. *Astrophys. J.*, 2009, v. 707, 916–920.
449. O. Heaviside. A Gravitational and Electromagnetic Analogy. *The Electrician*, 1893, v. 31, 281–282.
450. O. Heaviside. A Gravitational and Electromagnetic Analogy. *The Electrician*, 1893, v. 31, 359.
451. R. M. Wald. *General Relativity*. The University of Chicago Press, Chicago, IL, 1984.
452. M. Maggiore. *Gravitational Waves, Volume 1: Theory and Experiment*. Oxford University Press, New York, 2008.
453. B. P. Abbott *et al.* [The LIGO Scientific Collaboration and Virgo Collaboration]. Observation of Gravitational Waves from a Binary Black Hole Merger. *Phys. Rev. Lett.*, 2016, v. 116, 061102.
454. L. Boyle, K. Finn, and N. Turok. CPT-Symmetric Universe. *Phys. Rev. Lett.*, 2018, v. 121, 251301.
455. L. Boyle, K. Finn, and N. Turok. The Big Bang, CPT, and Neutrino Dark Matter. *Ann. Phys.*, 2020, v. 438, 168767.
456. M. T. Tyree and M. H. Zimmermann. *Xylem Structure and the Ascent of Sap*. Springer-Verlag, Berlin, Heidelberg, and New York, 2 edition, 2002.
457. P. J. E. Peebles and B. Ratra. The cosmological constant and dark energy. *Rev. Mod. Phys.*, 2003, v. 75, 559–606.
458. T. Rothman and S. Boughn. Can Gravitons be Detected? *Found. Phys.*, 2006, v. 36, 1801–1825.
459. F. Dyson. Is a Graviton Detectable? *Int. J. Mod. Phys. A*, 2013, v. 28, 1330041.
460. M. Kunz. The phenomenological approach to modeling the dark energy. *C. R. Phys.*, 2012, v. 13, 539–565.
461. F. Niedermann and M. S. Sloth. Resolving the Hubble tension with new early dark energy. *Phys. Rev. D*, 2020, v. 102, 063527.
462. K. Loeve, K. S. Nielsen, and S. H. Hansen. Consistency Analysis of a Dark Matter Velocity-dependent Force as an Alternative to the Cosmological Constant. *Astrophys. J.*, 2021, v. 910, 98–101.
463. C. Andrei, A. Ijjas, and P. J. Steinhardt. Rapidly descending dark energy and the end of cosmic expansion. *Proc. Natl. Acad. Sci. USA*, 2022, v. 119, e2200539119.
464. S. Weinberg. The cosmological constant. *Rev. Mod. Phys.*, 1989, v. 61, 1–23.
465. J. Martin. Everything you always wanted to know about the cosmological constant problem (but were afraid to ask). *C. R. Phys.*, 2012, v. 13, 566–665.
466. P. Astier and R. Pain. Observational evidence of the accelerated expansion of the universe. *C. R. Phys.*, 2012, v. 13, 521–538.
467. R. Durrer. What do we really know about dark energy? *Phil. Trans. R. Soc. A*, 2011, v. 369, 5102–5114.
468. J. Solà. Cosmological constant and vacuum energy: old and new ideas. *J. Phys.: Conf. Ser.*, 2013, v. 453, 012015.
469. Q. Wang, Z. Zhu, and W. G. Unruh. How the huge energy of quantum vacuum gravitates to drive the slow accelerating expansion of the Universe. *Phys. Rev. D*, 2017, v. 95, 103504.
470. W. Thomson. On a Universal Tendency in Nature to the Dissipation of Mechanical Energy. *Proc. R. Soc. Edin.*, 1857, v. 3, 139–142.
471. T. Markkanen, A. Rajantie, and S. Stopyra. Cosmological Aspects of Higgs Vacuum Metastability. *Front. Astron. Space Sci.*, 2018, v. 5, 40.
472. S. W. Hawking. Particle Creation by Black Holes. *Commun. Math. Phys.*, 1975, v. 43, 199–220.
473. S. Frautschi. Entropy in an Expanding Universe. *Science*, 1982, v. 217, 593–599.
474. M. E. Gertsenshtein. Wave resonance of light and gravitational waves. *Sov. Phys. JETP*, 1961, v. 41, 113–114.
475. E. Di Valentino, A. Melchiorri, and J. Silk. Planck evidence for a closed Universe and a possible crisis for cosmology. *Nat. Astron.*, 2020, v. 4, 196–203.
476. E. Di Valentino, O. Mena, S. Pan *et al.* In the realm of the Hubble tension – a review of solutions. *Class. Quantum Grav.*, 2021, v. 38, 153001.
477. E. Di Valentino. Challenges of the Standard Cosmological Model. *Universe*, 2022, v. 8, 399.
478. N. Aghanim *et al.* [The Planck Collaboration]. Planck 2018 results VI. Cosmological parameters. *A&A*, 2020, v. 641, A6.
479. T. Willmore. *Riemannian Geometry*. Clarendon Press, Oxford, 1993.
480. M. Droske and M. Rumpf. A level set formulation for Willmore flow. *Interfaces Free Bound.*, 2004, v. 6, 361–378.
481. R. Penrose. Difficulties with Inflationary Cosmology. *Ann. NY Acad. Sci.*, 1989, v. 571, 249–264.
482. D. Medková. *The Laplace Equation*. Springer International Publishing AG, Cham, Germany, 2018.
483. T. K. Das. *Hyperspherical Harmonics Expansion Techniques*. Springer India, New Delhi, 2016.
484. J. E. Avery and J. S. Avery. *Hyperspherical Harmonics and Their Physical Applications*. World Scientific Publishing, Singapore, 2018.
485. S. Müller and M. Röger. Confined Structures of Least Bending Energy. *J. Diff. Geom.*, 2014, v. 97, 109–139.
486. M. V. Vol'kenshtein. *Molecules and Life*. Plenum Press, New York, 1970.
487. L. E. Kay. Molecular Biology and Pauling's Immunochemistry: A Neglected Dimension. *Hist. Phil. Life Sci.*, 1989, v. 11, 211–219.
488. L. Pauling. Molecular basis of biological specificity. *Nature*, 1974, v. 248, 769–771.

489. L. Pauling. Analogies between Antibodies and Simpler Chemical Substances. *Chem. & Eng. News*, 1946, v. 24, 1064–1065.
490. D. Chandler and P.G. Wolynes. Exploiting the isomorphism between quantum theory and classical statistical mechanics of polyatomic fluids. *J. Chem. Phys.*, 1981, v. 74, 4078–4095.
491. P.L. Taylor and J. Tabachnik. Entropic forces – making the connection between mechanics and thermodynamics in an exactly soluble model. *Eur. J. Phys.*, 2013, v. 34, 729–736.
492. T. S. Roussy, L. Caldwell, T. Wright *et al.* An improved bound on the electron's electric dipole moment. *Science*, 2023, v. 381, 46–50.
493. E. M. Sevick, R. Prabhakar, S.R. Williams *et al.* Fluctuation Theorems. *Annu. Rev. Phys. Chem.*, 2008, v. 59, 603–633.
494. M. Campisi and P. Hänggi. Fluctuation, Dissipation and the Arrow of Time. *Entropy*, 2011, v. 13, 2024–2035.
495. C. Jarzynski. Equalities and Inequalities: Irreversibility and the Second Law of Thermodynamics at the Nanoscale. *Annu. Rev. Condens. Matter Phys.*, 2011, v. 2, 329–351.
496. P. Marquet. The Exact Gödel Metric. *Prog. Phys.*, 2021, v. 17, 133–138.
-

Fractal Quantization of Speed in Physics of Numerical Relations

Hartmut Müller

Rome, Italy

E-mail: hm@interscalar.com

The paper proposes a numeric-relational approach to the stability of real systems of coupled periodical processes and shows that it leads to fractal quantization of frequencies, wavelengths, and speeds caused by fractal scalar fields of transcendental numerical attractors. Applied to the stability of planetary systems, the approach predicts fractal quantization of orbits, orbital and rotational periods, and orbital speeds. On examples, the paper shows that the mean orbital speeds of planets, planetoids and large moons of the solar system are consistent with the prediction.

Introduction

Towards the end of the 19th century, many physicists were convinced that the theoretical basics were complete and that there was nothing fundamentally new to discover. History proved them wrong. They didn't yet know quantum physics.

First it was the periodicity of the chemical properties of the elements, then there were regularities in the atomic spectra that pointed to a new physics.

Today, many physicists are convinced that the only thing that matters is to unite quantum theory with general relativity. But again, unexpected regularities appear on the empirical horizon, which are still dismissed as coincidences. This time we are dealing with regularities in the dynamics of planetary systems that cannot be derived from Kepler's laws or Einstein's theory of gravity. These are regularities in the distribution of orbital and rotational periods as well as gravitational parameters. Some of these regularities are highlighted in my papers [1, 2].

In the present article, we deal with regularities in the distribution of orbital speeds. For example, why is Jupiter's orbital speed identical to that of its moon Europa? Why is Saturn's orbital speed identical to that of its moon Dione? By the way, both moons are the fourth largest in their systems. Why is the orbital speed of Uranus identical to that of its moon Miranda? Why is the orbital speed of Jupiter's moon Io identical to that of the planetoid Ceres?

From the perspective of celestial mechanics, these regularities are not more than coincidences. From the perspective of our numeric-relational approach, these regularities are expected effects of a new relational physics.

Theoretical Approach

In a series of papers [1–6] and a book [7] I have introduced a numeric-relational approach to physics and demonstrated its application in particle physics, astrophysics, geophysics, engineering, and biophysics.

In particular, this approach leads to the conclusion that coupled periodical processes can avoid destabilizing mutual parametric resonance, if their frequency ratios approximate

transcendental numbers. Among all transcendental numbers, Euler's number $e = 2.71828\dots$ and Archimedes' number $\pi = 3.14159\dots$ are unique. Indeed, the real power function of Euler's number is the only one that coincides with its own derivatives. In the consequence, Euler's number allows avoiding mutual parametric resonance between any coupled periodic processes including their derivatives [8]. In this way, Euler's number acts as primeval source of stability in systems of coupled periodic processes.

Archimedes' number determines the length of the circumference. The transcendence of the circumference avoids interruptions and makes impossible to define the start or endpoint of circular or elliptical motion. Hence, Archimedes' number makes possible eternal orbital motion, rotation, and oscillation. Perhaps that is why it is impossible to *completely* stop oscillations, for example, the thermal oscillations of atoms. In this way, Archimedes' number acts as primeval source of motion and kinetic energy.

Integer and rational powers of $e = 2.71828\dots$ and $\pi = 3.14159\dots$ form two complementary fractal scalar fields of transcendental attractors – the *Euler field* and the *Archimedes field*, as I have shown in [6]:

$$\mathcal{E} = e^{\mathcal{F}} \quad \mathcal{A} = \pi^{\mathcal{F}}$$

Both fields are k -dimensional projections of the fundamental fractal \mathcal{F} that is given by finite canonical continued fractions of integer attractors $n_0, n_1, n_2, \dots, n_k$:

$$\mathcal{F} = \langle n_0; n_1, n_2, \dots, n_k \rangle = n_0 + \frac{1}{n_1 + \frac{1}{n_2 + \dots + \frac{1}{n_k}}}$$

In astronomical scales, the orbital periods and distances of the planets, planetoids and large moons in the solar system obey both the Euler field and the Archimedes field. Also their rotational periods obey the Euler field, as shown in [9]. In subatomic scales, the mass-ratios of elementary particles obey the Euler field [10].

Compared to the majority of known particles, electron and proton are exceptionally stable. Their life-spans top everything that is measurable, exceeding 10^{29} years [11]. This is why normal matter is formed by nucleons and electrons. According to our numeric-relational approach, electron and proton are stable, because the ratio of their eigenfrequencies approximates an integer power of Euler's number and its square root, which makes impossible proton-electron parametric resonance in their ground states.

The eigenfrequencies and harmonics of the proton and the electron are natural frequencies of any type of matter, also of the accreted matter of a planet. Given the enormous number of protons and electrons that form a planet, eigenresonance must be avoided in the long term. This affects any periodical process including orbital and rotational motion. This is why the planets in the solar system and in hundreds of exoplanetary systems have orbital periods that approximate integer and rational powers of Euler's number relative to the natural oscillation periods of the proton and the electron, as shown in my paper [1]. The perihelion and aphelion of a planetary orbit, if expressed in units of the Compton wavelength of the electron, give the lower and upper approximations of integer powers of Euler's number, as I have shown in [2]. As a consequence, the gravitational parameters of the Sun and its planets, if expressed in electron units, approximate integer powers of Euler's number. These findings allow us to interpret the approximation of integer powers of Euler's number and its roots as a general evolutionary trend of numerical relations in real systems of many coupled periodical processes. This evolutionary trend drastically reduces the diversity of preferred orbital periods, distances, and speeds, increasing the likelihood of matches in different planetary or lunar systems.

Exemplary Applications

Since the orbital period of a planet approximates an integer power of Euler's number multiplied by the oscillation period of the electron, and its perihelion and aphelion approximate an integer power of Euler's number multiplied by the Compton wavelength of the electron, the orbital speed of the planet approximates the speed of light, divided by an integer power of Euler's number. For instance, Jupiter's distance from Sun approximates the 56^{th} power of Euler's number multiplied by the Compton wavelength of the electron $\lambda_e = 3.86159 \cdot 10^{-13}$ m. The aphelion 5.45492 AU = $8.160444 \cdot 10^{11}$ m delivers the upper approximation:

$$\ln\left(\frac{A(\text{Jupiter})}{\lambda_e}\right) = \ln\left(\frac{8.160444 \cdot 10^{11} \text{ m}}{3.86159 \cdot 10^{-13} \text{ m}}\right) = 56.01$$

The perihelion 4.95029 AU = $7.405528 \cdot 10^{11}$ m delivers the lower approximation:

$$\ln\left(\frac{P(\text{Jupiter})}{\lambda_e}\right) = \ln\left(\frac{7.405528 \cdot 10^{11} \text{ m}}{3.86159 \cdot 10^{-13} \text{ m}}\right) = 55.91$$

Jupiter's orbital period 4332.59 days equals the 66^{th} power of Euler's number multiplied by the oscillation period of the electron ($\tau_e = \lambda_e/c = 1.28809 \cdot 10^{-21}$ s is the angular oscillation period of the electron):

$$\ln\left(\frac{T(\text{Jupiter})}{2\pi \cdot \tau_e}\right) = \ln\left(\frac{4332.59 \cdot 86400 \text{ s}}{2\pi \cdot 1.28809 \cdot 10^{-21} \text{ s}}\right) = 66.00$$

Consequently, Jupiter's orbital speed approximates the speed of light, divided by the 10^{th} power of Euler's number, because $66 - 56 = 10$. Indeed, Jupiter's average orbital speed equals 13.07 km/s:

$$\ln\left(\frac{V(\text{Jupiter})}{c}\right) = \ln\left(\frac{13.07 \text{ km/s}}{c}\right) = -10.04$$

The orbital speed of Jupiter's fourth largest moon Europa approximates the same attractor $\mathcal{E}(-10)$ of the Euler field. The average orbital speed of Europa equals 13.74 km/s:

$$\ln\left(\frac{V(\text{Europa})}{c}\right) = \ln\left(\frac{13.74 \text{ km/s}}{c}\right) = -9.99$$

The orbital speeds of the other 3 Galilean moons of Jupiter approximate subattractors of the Euler field that correspond to reciprocal integer powers of Euler's number: The orbital speed of the moon Io approximates $\mathcal{E}(-10; +4)$, the orbital speed of Ganymede approximates $\mathcal{E}(-10; -4)$, and the orbital speed of Callisto approximates $\mathcal{E}(-10; -2)$.

Venus' distance from Sun approximates the 54^{th} power of Euler's number multiplied by the Compton wavelength of the electron λ_e . The aphelion 0.728213 AU = $1.08939 \cdot 10^{11}$ m delivers the upper approximation:

$$\ln\left(\frac{A(\text{Venus})}{\lambda_e}\right) = \ln\left(\frac{1.08939 \cdot 10^{11} \text{ m}}{3.86159 \cdot 10^{-13} \text{ m}}\right) = 54.00$$

The perihelion 0.718440 AU = $1.07477 \cdot 10^{11}$ m delivers the lower approximation:

$$\ln\left(\frac{P(\text{Venus})}{\lambda_e}\right) = \ln\left(\frac{1.07477 \cdot 10^{11} \text{ m}}{3.86159 \cdot 10^{-13} \text{ m}}\right) = 53.98$$

The orbital period 224.701 days of Venus approximates the 63^{th} power of Euler's number multiplied by the oscillation period of the electron:

$$\ln\left(\frac{T(\text{Venus})}{2\pi \cdot \tau_e}\right) = \ln\left(\frac{224.701 \cdot 86400 \text{ s}}{2\pi \cdot 1.28809 \cdot 10^{-21} \text{ s}}\right) = 63.04$$

Consequently, the orbital speed of Venus approximates the speed of light, divided by the 9^{th} power of Euler's number, because $63 - 54 = 9$. In fact, the average orbital speed of Venus equals 35.02 km/s:

$$\ln\left(\frac{V(\text{Venus})}{c}\right) = \ln\left(\frac{35.02 \text{ km/s}}{c}\right) = -9.05$$

Since e and π are transcendental, there are no rational powers of these numbers that can produce identical results. Therefore, attractors of the Archimedes field are different from attractors of the Euler field. For instance, the mean orbital speed 9.68 km/s of Saturn does not approximate a main attractor of the Euler field, but approximates the main attractor $\mathcal{A}(-9)$ of the Archimedes field:

$$\text{lp}\left(\frac{V(\text{Saturn})}{c}\right) = \text{lp}\left(\frac{9.68 \text{ km/s}}{c}\right) = -9.03$$

We use the symbol “lp” for the logarithm to the base π :

$$\text{lp}(x) = \frac{\ln(x)}{\ln(\pi)}$$

This circumstance suggests that transcendental relations not only stabilize orbits preventing them from mutual parametric resonance, but also assign orbits to the numerical field to which they belong.

For instance, the mean orbital speed 4.743 km/s of Pluto approximates the main attractor $\mathcal{E}(-11)$ of the Euler field:

$$\ln\left(\frac{V(\text{Pluto})}{c}\right) = \ln\left(\frac{4.743 \text{ km/s}}{c}\right) = -11.05$$

while the mean orbital speed 3.434 km/s of Eris approximates the main attractor $\mathcal{A}(-10)$ of the Archimedes field:

$$\text{lp}\left(\frac{V(\text{Eris})}{c}\right) = \text{lp}\left(\frac{3.434 \text{ km/s}}{c}\right) = -9.94$$

Also the mean orbital speed 29.7827 km/s of the Earth does not approximate a main attractor of the Euler field, but approximates the main attractor $\mathcal{A}(-8)$ of the Archimedes field:

$$\text{lp}\left(\frac{V(\text{Earth})}{c}\right) = \text{lp}\left(\frac{29.7827 \text{ km/s}}{c}\right) = -8.05$$

Possibly this indicates a transcendental duality of Euler- and Archimedes-orbits in the solar system. The orbital speeds $V_E(\mathcal{F})$ belong to the Euler field while the $V_A(\mathcal{F})$ belong to the Archimedes field:

$$V_E(\mathcal{F}) = \frac{c}{e^{\mathcal{F}}} \quad V_A(\mathcal{F}) = \frac{c}{\pi^{\mathcal{F}}}$$

Orbital speeds that correspond to the base layer of the fundamental fractal \mathcal{F} approximate the speed of light divided by integer powers of e and π .

Conclusion

In [6] I have shown that the proposed here numeric-relational approach to the stability of real systems of coupled periodical processes predicts a fractal quantization of frequencies and wavelengths caused by fractal scalar fields of transcendental numerical attractors – the Euler field and the Archimedes

field. In the case of planetary systems, for example the solar system, the Euler field and the Archimedes field cause a fractal quantization of orbits and orbital periods.

The current article shows that stable orbital speeds derive from the speed of light divided by integer and reciprocal integer powers of e or π . This circumstance drastically reduces the diversity of preferred orbits, orbital periods, and speeds, increasing the likelihood of matches in different planetary or lunar systems. This is why in the solar system, the orbital speeds of some moons coincide with the orbital speeds of some planets and planetoids. Considering the described here fractal quantization of orbits as general evolutionary trend, orbital speeds corresponding to integer powers of e or π should be widespread in the galaxy.

The duality of Euler- and Archimedes-orbits in the solar system suggests that the orbits differ in their function. Based on my previous research [6], I hypothesize that Euler-orbits act as stabilizers of the system, while Archimedes-orbits act as energizers.

Acknowledgements

The author is grateful to Alexandr Beliaev, Rainer Viehweger, Erwin Müller and Leili Khosravi for valuable discussions.

Submitted on September 24, 2023

References

1. Müller H. Physics of Transcendental Numbers meets Gravitation. *Progress in Physics*, 2021, v. 17, 83–92.
2. Müller H. Physics of Transcendental Numbers as Forming Factor of the Solar System. *Progress in Physics*, 2022, v. 18, 56–61.
3. Müller H. The Physics of Transcendental Numbers. *Progress in Physics*, 2019, v. 15, 148–155.
4. Müller H. Physics of Transcendental Numbers Determines Star Distribution. *Progress in Physics*, 2021, v. 17, 164–167.
5. Müller H. Physics of Transcendental Numbers on the Origin of Astrogeophysical Cycles. *Progress in Physics*, 2021, v. 17, 225–228.
6. Müller H. Physics of Irrational Numbers. *Progress in Physics*, 2022, v. 18, 103–109.
7. Müller H. Global Scaling. The Fundamentals of Interscalar Cosmology. *New Heritage Publishers*, Brooklyn, New York, USA, ISBN 978-0-9981894-0-6, (2018).
8. Müller H. On the Cosmological Significance of Euler’s Number. *Progress in Physics*, 2019, v. 15, 17–21.
9. Müller H. Natural Metrology in Physics of Numerical Relations. *Progress in Physics*, 2023, v. 19, 102–105.
10. Müller H. Fractal Scaling Models of Natural Oscillations in Chain Systems and the Mass Distribution of Particles. *Progress in Physics*, 2010, v. 6, 61–66.
11. Workman R. L. et al. (Particle Data Group), *Prog. Theor. Exp. Phys.*, 083C01 (2022), www.pdg.lbl.gov

From Particle Physics to Cosmology, on the Gravitational Sub-structure of Everything

Jacques Consiglio

52 Chemin de Labarthe, 31600 Labastidette, France.
E-mail: Jacques.Consiglio@gmail.com

We show, through resonance formulas, that the free parameters of the standard models of particle physics and cosmology fit a single resonant system – from the mass of elementary particles to gravitation and cosmology, and couplings mirroring resonances; and finally that all is encoded in the Planck mass resonance. Instead of extending the theory or its degrees of freedom to obtain predictions, we consider the reverse problem; paying interest to the free parameters structure we find formulas which consistency implies physical constraints hitherto unknown.

1 Introduction

Here we take a hypothesis that extends and generalizes Louis de Broglie's original idea of a wave and its resonance:

A single resonant phenomenon defines the physical world in its entirety where pulsations, wave numbers, and rotations refer to the same quantum and compare as lengths.

It leads to the direct calculation of the Sommerfeld constant with all the precision available [5]. This calculation implies a composite wave, so that the electron has a wave substructure, governed by mechanisms, of which electrodynamics is one effect – and then the same must be said of all particles. It is an intermediate result of a wider exploration published in part [5,6,8] which initially ranges from the mass of the electron to that of the Planck particle, via the associated couplings. This text presents more advanced results through a sequence of formulas consistent with each other and available data, with minimal concepts, and now extends to cosmology (following [7] in particular).

From the beginning of physics, the first aim is not to build a theory, but to explore virgin territory, analyze data and discover its internal logic and structure; mathematical theories always come after. Hence we present the results of an exploration of free parameters; first those obtained at the level of masses, second the associated couplings, third an approach to the origin, fourth the resulting natural cosmology, and last a few logical extensions. The method is straightforward: Find a general structure to a data set, insist on precision, understand the minimum and move on to the next set based on what is understood. Most importantly, precision will allow understanding some unexpected links between different data sets. Again, the aim is not to build a theory, but to poke holes in a supposed invisible wall of ignorance, a few bricks of which can be seen in the above-mentioned calculation.

This exploration is easily justified by the fact that theories beyond the Standard Model (SM) have nothing new to model and are therefore motivated by some kind of faith that something is missing. The various interpretations of quantum

mechanics strongly suggest that something is missing at the bottom, and there is definitely a problem with our understanding of the nature of reality, a psycho-philosophical issue; so we shall discuss some formulas about its structure.

2 The mass spectrum

The Standard Model divides massive particles into four distinct groups of interaction symmetries. These symmetries necessarily reflect the internal mechanisms we assume. We must therefore rely on these groups to analyze masses and extract invariant quantities and universal mechanisms. The exception is the three massive bosons whose masses come from the same potential. The analysis is therefore reduced to three groups, with the three bosons forming one.

Particles are studied as resonances, which can be modeled as a cyclic phenomena. Suppose that the electron matter wave is made up of two waves crossing each other in a resonator of unit size. In one dimension, the harmonic N in a length l gives a frequency N^2 at which the anti-nodes of the two waves cross; N^2 is a wave number and $1/N^2$ a length. Then we add a coupling also modeled as a length, we get $K D$, with D the coupling-length and K an integer used to quantize. Now in one dimension we have a mass formula

$$m = \frac{1}{\left(\frac{1}{N^2} + K D\right)}, \quad (1)$$

which is roughly equivalent to the inverse relation between a mass and its Compton wavelength, and can be extended to more components; we may have composite resonances or couplings. In essence it addresses a harmonic system deformed by quantized couplings where mass is a harmonic mean – but this is only the 1-dimension case. In three dimensions, the resonance can be radial like in (1), circular or mixed, and are identified with three groups of particles. The radial case will correspond to the three electrons, bosons to the circular case, and the mixed case to quarks.

2.1 Electrons

The first mass formula applies to electrons and quarks:

$$m = \frac{X}{\left(\frac{1}{NP} + KD\right)^3} + \mu, \tag{2}$$

where

- X is a mass constant, the choice of a unit.
- (1) is raised to the cube since the wave occupies a three-dimensional volume. This formula is now thermodynamics' $PV = K_B T$, with a constant volume V where the oscillator defines $P \equiv T$.
- NP are two integers for two waves components; either face to face (so $N = P$), or mixed with P radial and N circular (so $N \neq P$ and $2NP\pi \approx \text{integer}$).
- And μ in units of mass represents a bridge between two complementary cuts of the resonance responding to each other, which is necessary to fit the electron masses, and justified by $U(1)_Y \times SU(2)_L \rightarrow U(1)_{EM}$.

So this formula must admit two solutions for each of the three electrons, with two sets of constants and resonances. The first one corresponds to a radial resonance and therefore $N = P$, which we call the primary field since the same constants will be used for all other particles. But the magnetic moment suggests a rotation, and in 3 dimensions a rotation implies an axis and one set of parallel planes is conserved; then $P = K$ imposes two synchronous axis combining the resonance and the effect of the rotation in the product NP , rotation to which N is orthogonal. We call this cut the secondary field.

An adjustment of the parameters to find the known masses with $N = P$ and a choice of minimal harmonics N, P, K lead to the primary field constants below (index e) and the harmonics and masses calculated in Table 1.

$$X_e = 8.14512139242128 \text{ KeV}/c^2. \tag{3}$$

$$\mu_e = 0.24167661872330 \text{ KeV}/c^2. \tag{4}$$

$$D_e = 8.53221893719202 \times 10^{-4}. \tag{5}$$

Table 1: Primary resonances; electron, muon, tau (KeV/c²).

-	P=N	K	Calculated	Reference
e	2	2	510.99895000	510.99895000 (15)
μ	7-2	3	105,658.3760	105,658.3755 (23)
τ	7+2	5	1 776,840	1 776,861 (118)

For the secondary field we start with $N = P = K = 2$ for the electron as the three phases are synchronous in Table 1; imposing $P = K$ for the other two particles gives the constants

below (index α) and Table 2, where the calculated masses are identical to those in Table 1 only for the decimals shown,

$$X_\alpha = 8.021608017449 \text{ KeV}/c^2, \tag{6}$$

$$D_\alpha = 2.255984540570 \times 10^{-4}, \tag{7}$$

and μ_α in (8) linked to μ_e (4) by an empirical relation of obvious interest as we find three length ratios between rotations (giving π in the numerators) and twice the main term of the Sommerfeld constant calculation (137 in the denominators):

$$\frac{\mu_\alpha}{\mu_e} = \frac{\pi}{2} + \frac{\pi}{137} + \left(\frac{2\pi}{137}\right)^2 \tag{8}$$

$$\rightarrow \mu_\alpha = 0.3856750508181 \text{ KeV}/c^2. \tag{9}$$

Table 2: Secondary resonances; electrons, muon, tau (KeV/c²).

-	P=K	N	Calculated	Reference
e	2	2 ¹	510.99895000	510.99895000 (15)
μ	3	2 ³	105,658.3760	105,658.3755 (23)
τ	4	2 ⁴	1 776,840	1 776,861 (118)

Note 1) that the harmonics $P = K$ are minimal, and the powers of 2 for N ; 2) that $KD > 0$ in Tables 1 and 2 is reminiscent of the Poincaré stress; and 3) that in the reduction $N = P = 7 \pm 2$ Table 1, which can be seen artificial in this table, 7 will be recurring for the other particles.

2.2 Quarks

For quarks, the formula (2) is used with $N \neq P$ for a mixed resonance where P is radial and N circular, and $\mu = 0$. The parameter X_e is that of the primary field (3), the coupling is composite, and combines D_e and Sommerfeld's constant α :

$$D_q = D_e (1 + \alpha). \tag{10}$$

Table 3 shows the harmonics and calculated masses where the reference masses are in the natural scheme taken from Wikipedia (not found elsewhere in this scheme), and for the top quark a direct measurement average (PDG 2023).

Table 3: Quark resonances (MeV/c²).

-	P	N	K	Calculated	Reference
u	3	14/7	-8	2.00	2.01 ± 0.14
d	3	19/7	-4	4.79	4.79 ± 0.16
s	3	7	-6	106	105 ± 25
c	3	14	-6	1,255	1250 ± 100
b	3	19	-6	4,286	4350 ± 150
t	3	38	-6	172,380	172, 690 ± 300

Several points in this table are remarkable:

- $P = 3$ is constant and appears consistent with fractional charges since $N = P = 2$ for the electron, and 2 ± 7 for the muon and tauon; meaning that 2 comes from the electric charge and 7 from something else.
- $K = -6$ for the four heavy quarks, the sum of the Ks is -12 for any generation.
- All N depend on 2, 7, and 19.
- In all three generations, there is a factor 2 in one resonance (N , or K), fitting the ratio of electric charge; consistent with α part of the coupling.
- The resonances of the u and d can actually be seen as a double mixture of the four others since $14/7 = 38/19$ and $19/7 = 38/14$.
- A mixed resonance imposes $2\pi NP \approx$ integer, which is well verified for all.

The coupling is composite and the parameter K is negative, indicating a second attractive force reminiscent of the strong force, and the new coupling term $\sim \alpha D_e$ tells us that it is about 137 times stronger than the coupling D_e of the electron masses. The reference allows a value in a range $D_e/(137 \pm 10)$, so αD_e is tentative.

2.3 Massive bosons

A double circular resonance gives $N = P$, and since the Higgs potential is unique, NP is independent of the particle. This circular resonance creates a radial wave, so the mass must be reduced by a factor π to extract the radial equivalent (just as with $2\pi NP \approx$ integer for the mixed resonance we have NP in the mass formula); a mixed resonance imposes a phase constraint between its two components; so we need a correction to ensure the internal coherence of the phases of these particles. At a single potential, they cannot admit a mass μ , which must therefore be integrated into the formula to reason at constant X_e , which gives

$$m = \frac{m_e}{m_e - \mu_e} \times \frac{X_e}{k \pi \left(\frac{1}{N^2} + K D_b \right)^3}, \quad (11)$$

where m_e is the electron mass and D_b a boson-dependent coupling; and where the small k in the denominator represents the correction quoted above. After a first estimate of the couplings, and assuming charge transport, by the simple but relatively long reasoning detailed in [8] we deduce two couplings composites of α and D_e , identical for Z^0 and W^\pm

$$D_{WZ} = \frac{\alpha^2}{1 + \alpha^2} + \frac{\alpha D_e}{2(1 + \alpha^2)} - \frac{D_e^2}{6(1 - \alpha^2)}, \quad (12)$$

and very close but different for the H^0

$$D_H = \frac{\alpha^2}{1 + \alpha^2} + \frac{\alpha D_e}{2(1 + \alpha^2)} - \frac{D_e^2}{1 - \alpha^2}, \quad (13)$$

where α^2 represents a free field and the denominators are given by infinite interaction loops. We also showed (see also section 8.1) that the small k of (11) must be computed from

$$k^3 \frac{\pi}{144} = 266 D_b \left(\frac{\pi}{k} \right)^{1/3}, \quad (14)$$

where D_b is the related boson coupling and the resonances (144 and 266). On this basis, Table 4 shows the harmonics and calculated masses (reference PDG 2023*).

Table 4: Massive bosons resonances (MeV/c²).

-	P=N	K	Calculated	Reference
W^\pm	12	-2	80,384.9	80,385 (15)
Z^0	12	-7	91,187.3	91,187.6 (2.1)
H^0	12	-19	125,206	125,250 (170)

We also checked in [8] the phase loop between the circular path, $N^2 = 12^2$, and the radial path in 266 with the three values of $K \in \{-2, -7, -19\}$. Phase coherence with -7 and -19 is trivial since $12 = 19 - 7$. The W^\pm loop is also synchronous with $K = -2$, since $266 - 2$ is a multiple of 12, of which 2 is a sub-multiple. Internal phase coherence therefore allows all three resonances to exist. On the other hand, reasoning in the same way and on the same model, the other divisors of 266, $K \in \{-133, -38, -14\}$ do not check.

It is important to see that it is “really” the fine-structure constant in the expressions of D_{WZ} and D_H , and not a close value; because if we replace this value by $1/137$, the mass of the Z^0 becomes $91.2097 \text{ GeV}/c^2$, a factor of 10 outside the experimental uncertainty. Similarly, the specificity of D_H is necessary; without it we would get $M_H = 126.5 \text{ GeV}/c^2$.

2.4 Boson widths

With (11), a resonance formula we calculate pole masses; we should therefore be able to calculate their total widths from the resonance geometry. There is no way of varying N , P , which are integers, nor D , which depends on charges; widths should therefore be given by a displacement of charges giving $K \rightarrow K + \Delta K \rightarrow \Delta m$ needed for the resonance to blow.

These three particles carry multiple charges organized in a minimal way; at the ends of a simple line for the W^\pm and Z^0 , and at the vertices of a tetrahedron for the H^0 (giving the difference between D_{WZ} and D_H). Then for the first two, $\pm 1/2$ on the radial axis and half of $1/12$ from the circular path gives

$$W^\pm \rightarrow \Delta K = \left(1 + \frac{1}{24} \right) \rightarrow \Gamma_W = 2.0857 \text{ GeV}/c^2, \quad (15)$$

in great agreement with the reference $2.085 \pm 0.042 \text{ GeV}/c^2$.

$$Z^0 \rightarrow \Delta K = \left(1 + \frac{1}{24} \right) \rightarrow \Gamma_Z = 2.4684 \text{ GeV}/c^2, \quad (16)$$

*Particle Data Group

1% less than the reference (2.4952 ± 0.0023 GeV). And for the H^0 , the tetrahedron is stable in K but the six line of forces can stand a displacement of $\pm 1/144/2$, so

$$H^0 \rightarrow \Delta K = \frac{1}{144 \times 6} \rightarrow \Gamma_H = 4.11 \text{ MeV}/c^2, \quad (17)$$

also to 1% of the theoretical reference. So at first order, the widths are in good agreement with experiment and theory. A small difference remains for the Z^0 , which calls for a complement that can only depend on the charges it transports, assuming $2 \times \pm e/3$ and/or $2 \times \pm 2e/3$, gives the fit:

$$\Delta K = \left(1 + \frac{1}{24} + \frac{1.5}{137}\right) \rightarrow \Gamma_Z = 2.4946 \text{ GeV}/c^2. \quad (18)$$

The H^0 width will be re-discussed in section 5.6.

2.5 Neutrinos

The masses of neutrinos are much lesser than the constants X_e and X_α , so we cannot fit the formula parameters in the same way as for other particles. We suppose an inversion and fit the mass formula parameters from constraints that then seem logical:

- There is a progression of α and D_e powers in the couplings, up to D_e^2 and α^2 for the bosons. So no new coupling (use D_e and/or α), and we are looking for a negative power of α or D_e .
- Similarly there is a progression of resonances N, P ; a unitary resonance is all that is left, we impose $NP = 1$ and only K varies.
- Use the lepton mass equation (3) with $\mu = 0$ and the primary field constant X_e (7).
- Assume a resonance conservation law (in-line with section 8.3), and use resonances inherited from the corresponding electron; thus an echo of the related electron N and K constitutes a neutrino K .

The coupling is

$$D_\nu = \frac{2}{\alpha} \approx 274, \quad (19)$$

and corresponds to the inverse of the Dirac monopole, and the constraints above lead to Table 5 where the echo of the

Table 5: Neutrinos resonances (eV/c²).

-	P = N	K	Calculated mass
ν_e	1	1/2	0.00310
ν_μ	1	1/(3 - 1/9)	0.00924
ν_τ	1	1/(5 + 1/9)	0.04998

related electron resonances is obvious:

- $K \rightarrow 1/K$, and

- $N = P = 7 \pm 2 \rightarrow 1/(K \pm 1/9)$, with the sign of ± 2 .

Table 6 compares the results with the corresponding limits (reference Δm^2_{ij} 1 σ NO, NuFIT 5.2-2022 – where $\Delta m^2_{31} = \Delta m^2_{32}$).

Table 6: Comparison to reference data.

Quantity	Calculated	Reference	Unit
Δm^2_{21}	0.0000759	0.0000741 $\begin{pmatrix} +21 \\ -20 \end{pmatrix}$	(eV/c ²) ²
Δm^2_{31}	0.002488	0.002511 $\begin{pmatrix} +28 \\ -27 \end{pmatrix}$	(eV/c ²) ²
Δm^2_{32}	0.002412	0.002511 $\begin{pmatrix} +28 \\ -27 \end{pmatrix}$	(eV/c ²) ²
$\max\{m_i\}$	0.0500	≥ 0.0501 $\begin{pmatrix} +28 \\ -27 \end{pmatrix}$	eV/c ²
m_{tot}	0.062	$0.06 < m_{tot} < 0.12$	eV/c ²

2.6 The μ_e mass

The μ_e mass can be seen as an artifice since it is needed only for electrons and all particles are supposedly elementary, but its existence is now easy to justify.

Firstly, the calculation of the Sommerfeld constant in [5] requires four dimensions and two rotations. A rotation in four dimensions implies two planes conserved. A cut of a four-dimensional resonance to the three space dimensions (x, y, z) will give a rotation axis, i.e. the magnetic moment axis, say z , then in Table 1 $N = P$ for x and y . But we can make a second cut on (x, z, t) and impose $P = K$ on z, t ; if the two rotations are synchronous we get Table 2 (or $P = nK$ or $P = K/n$ with n integer which would only affect D_α – but is eventually not needed). From this we need a couple of masses μ_e and μ_α linked by a constant factor because in this process we eliminate one of the two rotations in Table 1, and take the ratio of both in Table 2. It is still possible to make any other cut that will mix space and time differently, but hard to believe that the mass μ can be set to zero or close enough without using large integers for the resonances.

Secondly, we can see it in all non unitary resonances, but in three different ways:

- Like a simple addition for electrons (Table 1).
- With the coupling D_q of quarks (Table 3).
- And integrated into the resonance mass coefficient (11) in the case of bosons (Table 4).

The second form is indirect because here it appears from the ratio μ_α/μ_e when we look at (8) and (10) $D_q = D_e(1 + \alpha)$ means that a scaling in α or 2α is omnipresent; but when we discuss resonance length ratios it becomes 137 or 68.5.

Now the μ_e mass is part of the primary field and we need to find its resonance. It is understood as one side of the invariant bridge to the secondary field; hence its resonances in the two fields should be synchronous with those of the three electrons. So in order to estimate it we impose:

- A composite resonance compatible with those of all three electrons in both fields, Tables 1 and 2 simultaneously.
- Use of the primary field constant X_e (3).
- No new coupling (D_e and/or α).

As a result, the coupling (best fit) is composite and uses Sommerfeld’s constant

$$D_{\mu_e} = (\exp(1) + 1) \alpha - \ln(1 + \alpha). \quad (20)$$

The logarithm and its base in this expression are typical signatures of cumulative phenomena. The expression below gives the mass in (4), and includes two resonance

$$\mu_e = X_e \left(\frac{7}{2} - \frac{1}{4} - D_\mu \right)^{-3}. \quad (21)$$

The fractions are equivalent to two resonances – $NP = 2/7$ and $NP = 4$ – and take the numbers of the primary resonances of the three electrons ($N = P \in \{2, 7 - 2, 7 + 2\}$), and 4 is also the electron resonance of Table 2, compatible with the others as it is a submultiple of the three products NP of this Table.

Finally the coupling of the μ_e mass depends solely on α and mathematically natural constants or functions, meaning that the couple it forms with μ_α “is” an electric charge on one side and looks like a magnetic current on the other.

2.7 Comments

Tables 1 and 2 use four degrees of freedom each, for two mass ratios, hence of no value if considered alone. Tables 3 and 4, on the other hand, use only one variable integer (or two for the u and d), and combine known couplings (α , D_e). With variations using only 2, 7 and 19 in these two tables for 9 particles, we must suppose that there is no freedom here; and neutrinos and electron resonances also fit the same numbers. Last, the μ_e resonance is synchronous of all electrons. Hence a global scheme is present.

Note that for the calculated masses, excluding neutrinos and μ_e , we have

$$|NPKD| < 1, \quad (22)$$

which, since we start with a unit-size resonator, should express a geometric constraint limiting the particle spectrum. If we imagine a fourth generation of electrons as a continuation of Tables 1 the next resonance is $N = P = 19 - 2$ (starting from $\{2, 7, 19\}$), and $K = 7$ at the very least (following the progression of Table 1), and this inequality is not verified. The same result applies to quarks since the next product of two numbers from the same set is $N = 7 \times 19 = 133$, and P and K are constant Table 3 for the heavy quarks. The impossibility of bosons with masses other than those in Table 4, and using the same resonance model, is verified with the resonance paths coherence in $N = P$ and K (essentially $N = P = 12 = 19 - 7$ and $266 - 2$ is multiple of 12).

3 Couplings

3.1 Analysis

Table 2 shows two components of the Sommerfeld constant calculation [5, Eq. (4)], as a reminder:

$$\alpha^{-2} = 137^2 + \pi^2 - \frac{1}{137.5} \left(\frac{1}{2} + \frac{1}{8} \pm \frac{1}{137.5} \left(\frac{1}{2} \pm \frac{1}{8} \right) \right), \quad (23)$$

namely $N = 2^1$ for the electron and $N = 2^3$ for the muon, the inverses of $1/2$ and $1/8$ identified in this calculation as identical resonances in 1 and 3 dimensions; the third resonance, that of the tau $N = 16$ is their product, therefore 3+1 dimensions.

The relation (8) between μ_e and μ_α uses twice the number 137, which implies an underlying origin, as it is one of the two common aspects of the three electrons. Now one way or another all particles discussed so far couple in α , meaning it constrains their resonances; then we calculate the sum of all the *integral and distinct* resonances in N and P (omitting fractions: μ_e , neutrinos, and quarks u and d):

$$\Sigma_{NP} = 2+3+4+5+7+8+9+12+14+16+19+38 = 137. \quad (24)$$

It is from this sum that we can first imagine to calculate Sommerfeld’s constant using the Bohm-de Broglie model, as it simply suggests that resonance and couplings act in mirror in a finite harmonic system; and again that the full mass spectrum is known. We must then look at the other axis K , and take into account the boson mass calculation which uses submultiples of 266 on this axis. So, again excluding μ_e , neutrinos and the quarks u and d , taking all the distinct K and replacing those of the bosons by +266, the sum

$$\Sigma_K = (2 \times 7 \times 19) + 2 + 3 + 4 + 5 - 6 = 274, \quad (25)$$

is also compatible with a harmonic system between couplings and resonances, where the factor 2 with $\Sigma_{NP} = 137$ would constitute a second level of harmony.

3.2 D_e and D_α

According to this logic, the three couplings used, intervening at the same level in the mass formulas, should proceed from a unique mechanism and obey the same constraints; their geometrical structures should therefore be similar and their formulation obey the same pattern that we know from Sommerfeld’s constant (23), i.e.

$$D^{-2} = a^2 + b\pi^2 + \frac{c}{d}, \quad (26)$$

with geometric and action constraints between their components, which dictate that

1. a is the integer whose square is closest to D^{-2} ,
2. b is the integer such that $a^2 + b\pi^2 - D^{-2}$ is minimal in absolute value,

3. d is a rotation term where π^2 is suppressed,
4. $|b| > |c/d|$,
5. one of the terms is negative, and
6. all terms are numbers known through resonances.

Then a constrained division of the empirical value gives

$$D_e^{-2} = ((7-3) \times (274+19))^2 + 7\pi^2 - \frac{19\pi}{19-1}, \quad (27)$$

$$D_\alpha^{-2} = ((19-3) \times (274+3))^2 + 2 \times (274+19+1)\pi^2 - \frac{19}{4\pi}. \quad (28)$$

After reducing a to prime numbers, we make 274, 7 and 19 appear from which 3 is subtracted. We find in the b term of D_α the electron wave signature present in α with $275\pi^2$, but augmented of 19 like 274 in the a term of D_e . There is a neat numerical recurrence between the couplings, a form of similarity between D_e and D_α , and a double connection with α (and two more if we also count $274 = 2 \times 137$). As expected, it agrees with a one to one mirror effect between couplings and resonances.

3.3 Ghost coupling

The three couplings appear to take the same resonances as particles, with 274 twice and $274 + 1$; they include two isolated rotations $1\pi^2$ and $7\pi^2$, the expected third $19\pi^2$ is absent; it is found in the resonance of two quarks t and b , $K = -19$ to calculate the mass of the H^0 , and twice added to 274. We find 274 twice in the a terms and 137 only once. So we are missing a coupling that will include 137 like Sommerfeld's constant and $-19\pi^2$, the latter negative to fit subtraction at the denominator of the term d of D_e where the $1p^2$ and $19\pi^2$ subtract. The missing elements give a and b and a spin 2 gives c :

$$D_p^{-2} = 137^2 - 19\pi^2 + \frac{4\pi}{19}, \quad (29)$$

each term of which and/or its inverse is present in the other couplings formulas, therefore adds no new resonance, and which force has no coupling effect on the calculus of masses (so can we guess at this stage).

3.4 Comments

We note that all the conditions listed in section 3.2 are verified for three couplings, i.e. less than one chance in 10^5 for a random draw of three values. For D_p the point 1 is violated; this is imposed by $+137$ positive and $-19\pi^2$ negative, without which there would be no consistency either with α or with the terms in 19 of D_e and D_α .

The geometrical form and connections of the couplings extend the underlying unity found in masses, and imply the non-separability of the forces.

4 The Planck mass

4.1 Notations

From now on, we shall use the Planck mass and length in their original formulations:

$$m_p = \sqrt{\frac{\hbar c}{G}}; \quad l_p = \sqrt{\frac{\hbar G}{c^3}}, \quad (30)$$

denoted in lower case. We shall be using SI units. The values of the constants used are

$$G = 6.67430(15) \times 10^{-11} \text{ N m}^2 \text{ kg}^{-2}. \quad (31)$$

and by definition

$$h = 6.62607015 \times 10^{-34} \text{ J s}; \quad c = 299792458 \text{ m s}^{-1}. \quad (32)$$

We shall also use the Planck mass integrating the constant of quantum theories \hbar and the Einstein constant $8\pi G$:

$$M_p = \frac{m_p}{4\pi} = \sqrt{\frac{\hbar c}{8\pi G}} = 4.341358(47) \times 10^{-9} \text{ kg}, \quad (33)$$

denoted capitalized. The value of the constant X_e (3) is in SI:

$$X_e = 1.451999775331 \times 10^{-32} \text{ kg}. \quad (34)$$

To avoid confusion, the subscript p will be used for quantities calculated with the classical formulas, and with the subscript ω when calculated from the harmonic system.

4.2 Unity and GR-QM reverse symmetry

The denominator of mass formulas relates a resonance expressed as a length ($1/NP$) within a resonator of length 1 – equivalent to stress or pressure – to a force expressed as a coupling (KD). In terms of Einstein's field equations, this is the fundamental unity of force, stress and energy: here, mass is stress, and therefore, by a natural extension, all forms of energy. There is a trivial geometric and quantitative symmetry between GR and QM, which is *a priori* compatible with the preceding results, since the three following relations must be compatible with the harmonic system:

- Newton's force in its natural quantum form, as each mass ratio must be physically homogeneous:

$$F = -\frac{G m_1 m_2}{r^2} = -\frac{2\pi \hbar c}{r^2} \frac{m_1}{m_p} \frac{m_2}{m_p}. \quad (35)$$

- The relation for a given mass between a Schwarzschild radius and a Compton wavelength:

$$R_S \lambda = 2l_p^2. \quad (36)$$

- Or, in the form of three unitless ratios,

$$\frac{m}{m_p} = \frac{l_p}{\lambda} = \frac{R_S}{2l_p}. \quad (37)$$

The volume at the denominator of the mass formula then represents two inverse quantities, depending on whether we see $1/NP$ in the denominator or its inverse in the numerator. By writing it in the following form

$$m = X \left(\frac{NP}{1 + NPKD} \right)^{+3}, \tag{38}$$

the couplings appear as a mirror effect characterized by the product $NPKD$ which, according to (36) in particular, must be centered on a resonance corresponding to the Planck particle. Its mass should therefore be calculable with

1. a mass formula,
2. what is missing, 266 and D_p ,
3. and what is universal, X_e and D_e ,
4. taking into account a dispersion in 4π ,

because then X_e cancels in the ratio m/m_p of (35) and it expresses only stress ratios in a unique harmony. We find

$$M_\omega = X_e \left(\frac{D_e}{266^2} + D_p^4 \right)^{-3} = 4.341421 \times 10^{-9} \text{ kg}, \tag{39}$$

which is the Planck mass M_p (33).

4.3 Comments

Now the harmony, its formulas and its two universal parameters cover the twenty-one orders of magnitude separating the mass of the Planck particle from that of the electron – or thirty with neutrinos. It shows once again the underlying unity, and that the form given to the couplings is correct as well as their assumed connections.

5 Toward the origin

While the origin of the resonances is not understood there is all the material needed in the mass M_ω (39) with two couplings D_e and D_p based respectively on $\Sigma_{N,P} = 137$ and $\Sigma_K = 274$, a term in 266, and the constant X_e . It suggests that we are close to the end and that the next step is to find an origin of the particle resonances; for this we need to find the constraints that apply. Since the Planck mass defines gravity we need to find-out how it defines space-time locally and globally and why it oscillates.

5.1 Classical anomaly

The calculation of M_ω (39) uses two couplings $D_e/266^2$ and D_p^4 ; two orthogonal forces and lengths, respectively the sine and cosine of an angle

$$\Omega = \arctan \left(\frac{D_e}{266^2} \times \frac{1}{D_p^4} \right) = 1.33509\dots \approx \frac{4}{3} \text{ rad}. \tag{40}$$

Now assume a spherical object with radius R greater than its Schwarzschild radius R_S ; in the Newtonian gravity case, for a test particle at $D < R$ which wave function is $\psi = e^{i\phi}$, the

phase shift $\Delta\phi$ in R for the momentum $\hat{p}\psi$ along \vec{r} would only depend on mass and obey:

$$\int_0^R 4\pi r^2 \rho(r) dr = \Lambda \int_D^R d\phi, \tag{41}$$

where the right-hand side is just the phase shift between D and R , $\rho(r)$ the energy density in r , and Λ a constant independent of R and R_S . Above all, this equation represents the effect of one phase variance, that of the massive object, say S , on another, that of the particle momentum. Now, the constitutive stress of this object is locally $\rho(r) = S/\pi$ because, firstly, there is here identity between stress, energy and phase variance, and secondly, the point of no return is π ; so (41) can be written in unitless form where ϕ , S and Λ are three angles:

$$\int_0^R 4\pi \left(\frac{S}{\pi} \right)^2 d \left(\frac{S}{\pi} \right) = \Lambda \int_D^R d\phi. \tag{42}$$

So if R tends to R_S , the integral of the left-hand side tends to $4\pi/3$ (S tends to π) and that of the right-hand side to π , hence $\Lambda = 4/3$. Now we compare two forces in (40) to their effects in (42) – where there is identity, then in the Newtonian gravity case we should find $\Omega = 4/3$. It is easy to see that the difference is not due to the precision of G , hence neither D_e nor D_p . It only expresses the incompleteness of our knowledge of the forces structure – and therefore of their effects. Then, since all energies gravitate we assume a complement also coming from the harmonic system representing all possible interactions through D_e and the powers of D_p , which should cover all the oscillator forms, known or not; thus a quantized series $h_i D_p^i$ such that:

$$\sum_{i=0}^n \frac{h_i D_p^i}{D_p^4} \times \frac{D_e}{266^2} = \tan \left(\frac{4}{3} \right), \tag{43}$$

where $h_0 = 1$ for the Planck mass, and n any, possibly infinite.

5.2 Method

The series in (43) will be used as a probe; for this we need to estimate its terms one by one (h_1 , then h_2 , etc...). But we do not yet know what to search as there is *a priori* no experimental data to rely on. Still, each step must bridge part of the gap and reflect the unity that has so far been expressed through couplings and resonances; geometric shapes, a topology covering all forms of the oscillator as each of the products $D_e D_p^i$ corresponds to an increasingly large coupling, and the whole to a nested topology. So

- From the couplings at its origin, the sequence should talk of Sommerfeld's constant and particle resonances. These aspects should make its terms identifiable, hence logic imposes to recognize what we find.
- There is no turning back, then each term should reduce the residual by roughly 2 orders of magnitude – or maybe more.

- The precision of each term is infinite; the very structure of the sequence as a quantized oscillator implies that approximation is illusory.

These constraints severely limit the field of exploration; we use them with the following method:

1. At step n consider the residue, and divide by D_p^n .
2. Recognize what it is, round up or down to significant number(s) in line with $n - 1$ and compute the residue.
3. If the residue is small enough go to step 1 for $n + 1$, and continue with the next quantity of similar kind.
4. If not it may be a border then if h_n describes a known shape go to step 1 for $n + 1$; or h_n is wrong, then go back to step 2 and make a better guess.

Two high precision online calculators [15] and [16] are used to calculate and check.

5.3 Sector one, particle resonances

M_ω corresponds to

$$h_0 = 1 \quad [+1.9 \times 10^{-3}], \quad (44)$$

with the residue with respect to $\tan(4/3)$ in square brackets.

$$h_1 = -1 \quad [+8.4 \times 10^{-5}], \quad (45)$$

a unit resonance represents a massless particle that can be identified with either a photon or neutrino(s).

$$h_2 = -3 - 4 \quad [-2.2 \times 10^{-6}], \quad (46)$$

is a little more complex, -4 is identified to the resonances of the electron (NP = 4 Table 1), and -3 with the P of quarks (Table 3) – two radial components linked to the electric field, the latter to fractional charges. In addition $-4 - 3 = -7$, twice the first part of the μ_e resonance $7/2$, and 4 is the inverse of $1/4$, the second part.

$$h_3 = +25 \quad [+5.1 \times 10^{-8}], \quad (47)$$

the muon resonance (NP = 25 Table 1, and NP = 24 Table 2 is close to optimum).

$$h_4 = -81 \quad [-2.7 \times 10^{-9}], \quad (48)$$

the tau resonance (NP = 81 Table 1, and NP = 64 Table 2 is also in the optimum range).

$$h_5 = 2\pi \left(7 + 14 + 19 + 38 + \frac{38}{19} + \frac{14}{7} + \frac{38}{14} + \frac{19}{7} \right) \quad [2 \times 10^{-11}], \quad (49)$$

the sum of quarks' N (Table 3) by 2π for circular paths.

$$h_6 = -556 = -8 \times 69.5 \quad [5.7 \times 10^{-14}], \quad (50)$$

which, by its position must correspond to the gluons eight degrees of freedom; without mass it would be either 1 or 8×1 , this a point to understand. The last harmonic of this sector is

$$h_7 = -217 = -144 \times \frac{3}{2} - 1 \quad [3.9 \times 10^{-17}]. \quad (51)$$

The first term -144 identifies the resonances of the three massive bosons (Table 4) with a factor of $3/2$; and the second either the photon or the neutrino(s) with -1 .

The resonances N , P of all particle of the Standard Model are entirely covered by this sector and simple to identify – including massless particles or supposed so. Note 1) that all h_i give directly comparable quantities, irrespective of the power associated with D_p ; 2) that within a single harmonic all terms have the same sign, otherwise the result would be meaningless; 3) that the presence of 2π for quarks is consistent with the inferred geometry, as is its absence for electrons and massive bosons; 4) that the assumed logic of generating the Sommerfeld constant is verified for particles of known mass; 5) the μ_e mass resonance may also be here in h_2 (the part $7/2$); and 6) the unitary resonance of h_1 or h_7 justifies the neutrino mass calculation in section 2.5.

5.4 Sector two, spheres

The second sector starts with spherical coefficients of dimensions 4 to 7, with phase variances according to the template of the M_ω anomaly, then similar but inverted coefficients.

$$h_8 = -2\pi^2 - \frac{1}{\pi} \quad [7.2 \times 10^{-20}], \quad (52)$$

the four-dimensional sphere surface coefficient ($2\pi^2$) and a phase variance ($1/\pi$).

$$h_9 = -\frac{8\pi^2}{15} + \frac{1}{2\pi} \quad [1.2 \times 10^{-22}], \quad (53)$$

the five-dimensional sphere volume coefficient ($8\pi^2/15$) and a phase variance ($1/2\pi$).

$$h_{10} = -\frac{\pi^2}{6} + \frac{3}{2\pi} \quad [-5.7 \times 10^{-24}], \quad (54)$$

both a) the six-dimensional sphere volume coefficient ($\pi^3/6$) divided by π , b) its surface coefficient divided by 6π , and c) curiously, the Riemann function, $\zeta(2) = \pi^2/6$, and a phase variance ($+3/2\pi$).

$$h_{11} = +\frac{3}{2} \times \frac{16\pi^3}{105} + \frac{1}{\pi} \quad [1.7 \times 10^{-27}], \quad (55)$$

the seven-dimensional sphere volume coefficient ($16\pi^3/105$) times $3/2$, i.e. $16\pi^3/70$, and a phase variance ($+1/\pi$). The same factor $3/2$ is also present in h_7 .

$$h_{12} = -\frac{1}{\pi} \quad [-6.3 \times 10^{-29}], \quad (56)$$

a simple phase variance, which defines a boundary.

$$h_{13} = +\frac{2}{5\pi^2} - \frac{\pi}{2} [3.3 \times 10^{-32}], \quad (57)$$

an inversion of h_9 , with $\pi \rightarrow \pi^{-1}$ by multiplying the first term by 3/4, the inverse of the original tangent.

$$h_{14} = -\frac{1}{4\pi} - \frac{1}{\pi^3} [-5.6 \times 10^{-34}], \quad (58)$$

the inverse of the surface coefficient of a three-dimensional sphere (4π), and that of a six-dimensional sphere (π^3).

This sector, like the others, identifies stress coefficients and therefore forces and shapes. Finding spherical coefficients and phase variance terms can be identified with forces in at least 7-dimensional space. The signs of the components in (and between) harmonics are not always the same, possibly indicating opposite effects.

5.5 Sector three, wave and coupling

Convergence in this sector is extreme.

$$h_{15} = +\frac{1}{2^2} + \frac{1}{133\pi + \frac{\pi}{6}} [2.5 \times 10^{-40}], \quad (59)$$

two phase variances (or inverted resonances).

$$h_{16} = \frac{-1}{266^2 - 69.5^2 - 137 - \frac{3}{2} \times \left(1 + \frac{1}{69.5} - \frac{\pi}{8 \times 69.5 + 3}\right)} [3.8 \times 10^{-51}], \quad (60)$$

corresponds, by its shape, to the difference of the squares of two couplings ($A^2 - B^2$), separating for instance the three terms in 69.5 from the others.

5.6 Sector four

The fourth sector is separated from the third by seven null harmonics (h_{17} to h_{23} inclusive) and begins with two identically shaped resonances that seem to complement each other.

$$h_{24} = -3^3 - \frac{2\pi^3}{3^4 \left(1 - \frac{1}{2 \times 7}\right)} [-5.2 \times 10^{-56}], \quad (61)$$

a resonance term associated with a coefficient in π^3 that must be associated with a dimension. Then $h_{25} = 0$, and

$$h_{26} = +2^2 + \frac{3\pi^3}{2^4 \left(2 - \left(\frac{3}{2}\right)^3 \times \frac{1}{2 \times 19}\right)} [5.7 \times 10^{-60}], \quad (62)$$

whose form is an almost exact copy of the previous one, reversing 3 and 2, and 7 and 19. Then $h_{27} = 0$ and finally

$$h_{28} = -\frac{144}{\pi^2} + \frac{1}{24} + \frac{1}{(144+1) \times 6\pi} [3.0 \times 10^{-68}]. \quad (63)$$

This harmonic corresponds to the three bosons resonance (i.e. $NP = 144$) and their resonance widths ($1/24$ and $1/144/6$) seen in the radial direction. The last term being different from the expected one, we recalculate the H^0 width:

$$H^0 \rightarrow \Delta K = 1/((144+1) \times 6) \rightarrow \Gamma_H = 4.079 \text{ MeV}/c^2, \quad (64)$$

which, if compared to (17), is closer to the theoretical value at $125.206 \text{ GeV}/c^2$.

6 Coherence

The sequence can only be proven based on a detailed knowledge of the geometry it defines; we are not there, we do not know how it works or whether it ends or not. We can, firstly, find internal correspondences and, secondly, relate it to known quantities. This is the purpose of this section, whose aim is to get a first estimate of coherence with the harmonic system, in particular the mass spectrum.

6.1 First points

We recognize many structuring points; a non-exhaustive list:

- First sector: All resonance numbers (N, P or NP) of massive particles are present with two well-defined orders, 1) that of total resonance lengths, and 2) that of the internal couplings progression in the primary field, and therefore groupings either in the same zone or in the same harmonic, the resonances of particles with similar properties.
- First sector: Similarly we find first all radial resonances (from h_2 to h_4), and then rotations (with h_5 and h_7); mixed quark resonances are split in two between h_2 for the radial part P , and h_5 for rotations N .
- First sector: So, having assumed that at this level the forces and their effects are one, which leads to equation (43), we have complemented the structure of the forces with the known structure of their effects, the resonances.
- Second sector: Contains four spherical coefficients, h_8 to h_{11} , in order from 4 to 7 dimensions. Then what identifies with interactions between these structures in h_{13} and h_{14} , and a single phase variance h_{12} in the middle that looks either like the interaction center between these spaces, or a pure absorber in 8 dimensions.
- h_{15} : We find $133 + 4 = 137 = \Sigma_{NP}$, inverting the two main terms and removing π and $\pi/6$.
- h_{15} : The numbers 4, and $133\pi = 7 \times 19 \times \pi$ correspond respectively to the resonances of electrons and quarks. So this harmonic is linked to the fermionic wave.
- h_{15} : the term $\pi/6$ is a phase advance for 133π ; if it corresponds to an inverted length $\pi/6\pi^2$ we get $133 + 6 = 139$, the full resonance spectrum ($\Sigma_{NP} = 137$ plus the two unit resonances) – excluding $h_6 = 8 \times 69.5$, but $139 = 2 \times 69.5$, the same ratio as between Σ_K and Σ_{NP} .

- h_{15} : 133π is a harmonic of quark resonances 7 and 19 (plus a factor of 2 for charges $2/3$), and $\pi/6$ a phase advance giving a negative length; so $K = -6$ Table 3.
- h_{24} and h_{26} : The two phase advances in the denominator multiply to give 133 and 266, depending on how the factors 2 is considered.
- h_{24} and h_{26} : Taking into account the factor 2 in the denominator of the second, as well as the ratio $3^3/2^3$ we obtain 27 and 8, their difference is 19. There are also 7 and 19, the two rotations of D_e and D_p respectively.
- h_{28} : The bosons resonance and widths. This harmonic therefore represents the Higgs field potential – unique as assumed – and h_{28} is complete and in agreement with the calculation of boson masses and lifetimes.

Such structure means an extremely entangled system where each element has a specific role – a global equilibrium working as a whole, coherent and inseparable.

6.2 The electrons, h_6 and h_{16}

We find 8×69.5 in h_6 , which is rather strange as we expect gluons supposedly massless. Conversely, meson spectroscopy has been suggesting a monopole (e.g. [1]) for several decades without finding it, and we could also write $h_6 = 8 \times 1 + 8 \times 68.5$. But we also find 69.5 three times in h_{16} , twice in the denominators and 69.5^2 , which makes it unbreakable; but suggests considering

$$69.5^2 = 68.5^2 + 137 + 1^2, \tag{65}$$

by the similarity of this expression with the ratio between the two mass constants μ_e and μ_α given by the empirical relation (8), except for the last term for which we would expect 2 instead of 1. In Table 1, the resonances N and P are 2, 7–2 and 7+2, while in Table 2 we have 2^1 , 2^3 and 2^4 for N . These two tables represent the primary and secondary fields. So the 1^2 divides to give resonances 2, with Table 2 rotations in π for P and radial terms for N ; and Table 1 only radial components for 2 (mixed with 7 if it is circular). Then divide 69.5 by π , invert each term of (65) replace 1 by 2π , and the sum of the inverses gives a ratio of resonance, therefore of masses:

$$\left(\frac{69.5}{\pi}\right)^2 \rightarrow \frac{\pi}{2} + \frac{\pi}{137} + \left(\frac{2\pi}{137}\right)^2, \tag{66}$$

is the ratio μ_α/μ_e (8). This expression also corresponds term to term to that of Sommerfeld’s constant (23) and to the logic to its calculus, but in an inverse manner:

- $(2\pi/137)^2$ for 137^2 , the electron pulsation.
- $\pi/137$ for π^2 , the electron spin,
- and $\pi/2$ for $1/137.5 \times (1/2\dots)$, the wave.

Consequently, this relation must be reflected in the difference between X_e and X_α as well as in the composite coupling D_{μ_e}

(20); considering those as two pressure fields, each being a dynamic transformation of the other, and inverting the relation (8) by taking into account the common share of the resonances of the three electrons leads to the following semi-empirical formula:

$$\frac{X_e(1 - \exp(1)\alpha^2) + X_\alpha(1 + \exp(1)\alpha^2)}{X_e(1 - \alpha) - X_\alpha(1 + \alpha)} = \frac{137^2}{2\pi} \times \left(1 - \frac{\pi}{137}\right), \tag{67}$$

whose relative accuracy is 1.4×10^{-8} , and then relative errors of 4.8×10^{-12} on X_e and X_α in opposite directions, better than the uncertainty range on lepton masses (3×10^{-10} for the electron). The formula used here for α is expression (6) of [5].

The left hand side contains α , which is also found in the D_{μ_e} coupling (20), as well as the basis of the natural logarithm. The main term, $137/2\pi$ of the right hand side is modified by $(137 - \pi)$, which includes a phase advance; we find again the logic of the calculation of the constant α [5] with $137^2/2\pi$ for an electron pulsation and a phase delay $\pi/137$ per pulsation corresponding to the spin, and we obtain a resonance length $\sqrt{137^2 + \pi^2}$ where the fractional wave terms of α , which are related to the electron movement, are naturally absent. Both expressions (8) and (67) therefore speak of a dynamical shift between the primary and secondary fields, which corresponds to electrodynamics and its coupling.

6.3 The Planck length

The Planck length is identified to the maximum resolution and is expressed in units of length. But here it may be inscribed in the denominator of the mass M_ω , which is a pure number. We will therefore calculate the Planck length as an angular resolution independent of the system of units – even though the ice becomes thin as it questions units systems.

In h_{15} we recognize the fermion wave, which is obvious, and h_{16} as the universal coupling forming particles on the surface of a 4D sphere defined by h_8 dominating the first sector, for we can write it $h_{16} = A^2 - B^2 \sim m^2 c^4 = E^2 - p^2 c^2$. They must then define the Planck length or Planck time, which we must be able to calculate with very good accuracy since this sector covers 17 orders of magnitude. Starting with h_{15} , we consider 4 and 133π as resonances and $\pi/6$ as a phase advance, and calculate an uncertainty from distinct paths; each path corresponds to a synchronicity S :

- 4 is the electron resonance, also present in the muon and tauon, and defines a 2π cycle. The first length is therefore a quarter of 2π .

$$S_1 = \frac{\pi}{2}. \tag{68}$$

- 133π , is directly a length so

$$S_2 = 133\pi. \tag{69}$$

- The phase advance $\pi/6$ desynchronizes the two resonances. Combine it with $1/4$, the length to consider is:

$$S_3 = \frac{\pi}{6} \times \frac{1}{4} = +\frac{\pi}{24}. \quad (70)$$

- It remains to combine the three terms; $\pi/6$ represents a phase advance for 133 and shortens its length; the harmonic h_5 is a multiple of 2π so since 133 is multiplied by π and 6 divides it, for a full turn this makes a length $2\pi \times (133 - 1/3)$, which applies to the denominator of $1/4$. A simple phase advance gives a negative quantity, hence a minus sign:

$$S_4 = -\pi \left(2^3 \left(133 - \frac{1}{3} \right) \right)^{-1}. \quad (71)$$

To obtain a quantity relating to order zero of the sequence, i.e. relative to one unit, we take into account the coupling D_p^{15} corresponding to h_{15} , which gives:

$$L_0 = \frac{D_p^{15}}{S_1 + S_2 + S_3 + S_4} = 2.2856968.. \times 10^{-35} \text{ rad}. \quad (72)$$

Then h_{16} is a coupling that modifies L_0 , also a length and no degrees of freedom, but we have to unfold rotations to obtain a full length.

$$\frac{\pi}{8 \times (69.5 + 3/8)} \rightarrow 8\pi^2 \times (69.5 - 3/8), \quad (73)$$

where the sign of the phase advance (3/8) is inverted to obtain the corresponding length, and for the other term

$$\frac{1}{69.5} \rightarrow 69.5\pi. \quad (74)$$

Those allow us to calculate a quantity h_{16}^* by making the above replacements in the expression of h_{16} . We need to add a geometric factor to h_{16} , since it is also this coupling that compresses the surface of the 4D sphere h_8 . Then, as h_{16} depends on D_p^{16} , we multiply by D_p to obtain a value relative to L_0 , which gives a correction that may seem marginal

$$\frac{h_{16}^* D_p}{2\pi^2} = -5.0462626214390 \times 10^{-9}. \quad (75)$$

Then by posing

$$L_\omega = \frac{D_p^{15} \sqrt{\pi}}{S_1 + S_2 + S_3 + S_4} \times \left(1 + \frac{h_{16}^* D_p}{2\pi^2} \right), \quad (76)$$

we obtain the unreduced Planck length

$$L_\omega = 4.051292235148901 \times 10^{-35} \text{ rad}, \quad (77)$$

Using M_ω to cancel the uncertainty on G , we get Planck's constant, $h = m_p l_p c$ with a relative precision of 6×10^{-13} :

$$4\pi M_\omega L_\omega c = 6.626070150004 \times 10^{-34} \text{ J s}. \quad (78)$$

The fact that the Planck length is calculated in this way makes it independent of the system of units. We calculate an angular correction and speak of the GR-QM symmetry given by the relation

$$\frac{R_S \lambda}{2} = l_p^2 = L_\omega^2, \quad (79)$$

which is then read in steradian (or radian²), where $R_S \lambda/2\pi$ is the product of the two half-axes of an ellipse of invariant surface (independent of the particle) inscribed on a sphere of unit radius seen from its center; in other words, the angular resolution in a three-dimensional space – the surface of an ellipse is πab , in agreement with the square root of π in the expression (76). The term on the right is therefore a solid angle and $L_\omega/\sqrt{\pi}$ the angle of the cone that defines it, both of which are independent of the system of units (see also section 7.1). Now we can calculate Newton's constant with the precision of the constant X_e , equivalent in principle to that of the electron mass; using $G = L_\omega c^2/4\pi M_\omega$ we get:

$$G = 6.67410788487 (180) \times 10^{-11} \text{ m}^3 \text{ kg}^{-1} \text{ s}^{-2}. \quad (80)$$

The above decimals are the same if we calculate $G = L_\omega^2 c^3/h$ (which is not guaranteed at all as (80) depends on M_ω), the next differs in accordance with the residual error on h (78). The Bohr radius a_0 is then also a pure number:

$$a_0 = \frac{\hbar}{\alpha m_e c} = \frac{2 M_\omega}{m_e} \times \frac{L_\omega}{\alpha}, \quad (81)$$

because in this expression the mass ratio is a harmonic ratio. Consequently, the interpretation of L_ω holds because α is calculated as the inverse of a resonance length, like L_ω .

6.4 Space-time and couplings

The first sector of the h_i gives the particle resonances, NP , as a product or separately, meaning that the resonances are part of the structure of space-time; but nothing about their couplings and K , which play at the same level in the mass formulas. Resonances are given in a specific order; for massive particles whose resonances are not unitary, the couplings increase with the i index and mix D_e and α . Hence couplings and K should also be inscribed in the space-time structure in the same order.

When calculating Ω the angle $4\pi/3$ is in 3D space as well as the phase reversal of π . So there is nothing here about space-time and $3 + 1D$, which would seem to be mandatory. A resonance in space-time means a period, the time needed for a resonance to loop which is a space-time interval; we can then use the standard invariant

$$c^2 t^2 - r^2 = c^2 \tau^2, \quad (82)$$

where τ is a particle period and defines, for this particle, a hyperboloid – and is reminiscent of de Sitter space. Then we pose R and u in hyperbolic coordinates

$$r = R \cosh(u) ; \quad ct = R \sinh(u). \quad (83)$$

The ratio between space and time is

$$\frac{r}{ct} = \coth(u), \quad (84)$$

which is independent of R . Then for the angle Ω (40) notice

$$\coth(\Omega^{-1}) \approx \frac{\pi}{2}, \quad (85)$$

close but not equal, and $\cot(\pi/2) = 0$; the meaning of which is that the ratio of forces in M_ω does not fit flat space-time, so let us check what is missing. With the h_i we get the NPs which response in the mass formulas are the KDs , and all this is perfectly ordered since we cannot mix the resonances and couplings at random. Then, in order to find the KDs ' origin we should complement a second series as follows:

$$A = \arctan\left(\sum_{i=0}^n c_i \times \frac{D_e}{266^2 D_p^4}\right), \quad (86)$$

with n any, where the c_i should complement the mass formulas; so that

$$\coth(A^{-1}) = \frac{\pi}{2}, \quad (87)$$

and eventually relates to forces meaning that space-time is flat, because then

$$\cos(\coth(A^{-1})) = 0 ; \quad \sin(\coth(A^{-1})) = 1. \quad (88)$$

The resolution logic for this series is basically the same as for the h_i ; but we know a little more of what to search. The first sequence gives the particle resonances in order of mass and of increasing gravitational couplings D_p^i ; we should logically expect a similar order with the couplings α and D_e . Then since $D_e \approx 16\alpha^2$, the gain at each step may be rather chaotic but show the same progression as for the h_i , with a *known* coupling responding to $D_e D_p^i$. The two couplings giving a minima the progression α , D_e , αD_e , and D_e^2 ; respectively that of μ_e , electrons, quarks, and bosons; we should not use α^2 as it represents infinite loops in the boson mass couplings D_{WZ} and D_H . On this basis the empirically fit sequence is

$$c_0 = +1 \quad [3.2 \times 10^{-3}]. \quad (89)$$

for the Planck particle.

$$c_1 = -\alpha \times \frac{7}{2} = -\alpha \times \left(4 - \frac{1}{2}\right) \quad [1.6 \times 10^{-4}]. \quad (90)$$

This is $h_2 = 7$ divided by 2, and the coupling and primary resonance of μ_e , which indirectly responds to h_2 , h_3 and h_4 . It also decomposes in $4 - 1/2$, where 4 is the electron resonance Table 1 and sub-multiple of all NP of Table 2; and a resonance $1/2$.

$$c_2 = -D_e \times \left(\frac{1}{2} + \frac{1}{25} + \frac{1}{81}\right) \quad [6.8 \times 10^{-5}]. \quad (91)$$

The primary coupling and the inverse of the resonances N or NP of the three electrons Table 1, though for the electron we would expect $1/4$ instead of $1/2$; we consider it responds to h_2 , h_3 and h_4 with D_e .

$$c_3 = -\alpha D_e \times \frac{h_5}{4\pi} \quad [1.4 \times 10^{-5}]. \quad (92)$$

The primary field coupling appearing with quarks (αD_e), and the associated quark resonances N Table 3. So it responds to h_5 (49) but only for the coupling appearing with quarks.

$$c_4 = -D_e^2 \times \left(144 \times \frac{2}{3} + 2 - \frac{1}{7} - \frac{1}{19}\right) \quad [3.6 \times 10^{-9}]. \quad (93)$$

The primary coupling specific to bosons (D_e^2) and associated resonances, though multiplied by $2/3$ instead of $3/2$ in h_7 for 144, and the other numbers fit the boson's K . Again it responds to the coupling appearing with bosons except α^2 . We have all what we know of, but let us continue.

$$c_5 = -\alpha D_e^2 \times \left(\frac{7}{2}\right) \quad [7.8 \times 10^{-11}]. \quad (94)$$

Now $c_5 = c_1 D_e^2$.

$$c_6 = +D_e^3 \times \left(\frac{1}{2} + \frac{1}{25} + \frac{1}{81}\right) \quad [9.8 \times 10^{-12}]. \quad (95)$$

And now $c_6 = -c_2 D_e^2$. We stop here because we do not have enough precision on α to continue (even c_6 is doubtful).

Overall, we have a progression of the primary couplings together with the resonances they apply to – plus maybe a bit more that repeats the same resonances. We notice:

1. That the rotations of quarks appear radially to the associated piece of coupling.
2. That the factor $3/2$ of h_7 is inverted.
3. That the electrons N or NP appear as inverses.
4. That nothing comes out for gluons h_6 , neutrinos h_1 , photons in h_8 .

6.5 Connection $h_i - c_i$

Connecting this sequence to the h_i is not difficult as it obeys the following rules:

1. For a given particle group, the resonances N , P and the strongest part of the associated coupling can be taken from a single element of this suite.
2. Any integer is a resonance NP or K , to be taken as is.
3. Any fraction is an inverted NP or K , whose sign must be reversed.

With the following consequences:

- The NP resonances of electrons is the inverse number of c_2 , except for the electron where we get $N = P = K = 2$ for Tables 1 and 2.

- A circular resonance N of a quark is taken in c_3 as radial effect of the same number in h_5 .
- The resonances NP , K of the massive bosons are in c_4 , with $3/2$ and two of the K s inverted.

Overall, we get the N , P , D_{max} , where D_{max} is the strongest part of a particle coupling, and the boson's K . But we can complement the couplings for each particle group with a simple addition of D_{n-1} to D_n :

- The K of the bosons being known from c_4 we use the same number from c_3 to get the part in $\alpha D_e/2$; the factor $1/2$ comes from the interaction of two charges.
- For quarks, we get $D_q = D_e + \alpha D_e$ taking D_e from c_1 .
- For electrons, the coupling is complete from c_2 ; and we get the electrodynamics coupling α from c_1 – which is also valid for quarks.
- Massive bosons are composites, then α^2 is taken as the square of α from c_1 ; in agreement with a free field giving the denominators of D_{WZ} and D_H by infinite interaction loops.

We miss the electrons and quarks K , which origin is still unknown. And by the way, the bosons resonance $NP = 144 = \left(\left(\frac{3}{2} \times 144\right) \times \left(\frac{2}{3} \times 144\right)\right)^{1/2}$ is the geometric mean of two components from h_7 and c_4 .

6.6 Comments

The two sequences h_i and c_i appear to be working together with respect to the particle resonances. We first showed that the angle Ω must be complemented to $4/3$ to get the harmonics N , P , and then that the hyperbolic cotangent of its inverse must be complemented to $\pi/2$ to get a mix of coupling and resonances – both sequences in the same “right” order. Now we have

$$\coth(\Omega^{-1}) > \frac{\pi}{2} > \coth\left(\frac{3}{4}\right), \quad (96)$$

so M_ω , a black hole, does not reach $\pi/2$, and $4/3$ exceeds it. So the particle spectrum is needed to get to $\pi/2$, and this is done by the coupling α . Consequently, D_p (gravitation) and α (electromagnetism) are complementary to each other for the existence of space-time. Electromagnetism is born from gravitation, which cannot survive without it.

We now have several points justifying the limits of the particle spectrum:

- The first sector of the h_i defines resonances, there are no others.
- It defines the NP products of the primary field as a set of elementary oscillators occupying the Planck length. Hence the limitation $|NPKD| < 1$ suggested by the resonances of the primary field makes sense because otherwise the resonance of a particle would overflow

the Planck length. The resonator of unit length imagined to get the mass formula is simply a Planck particle defining a unitary box.

- The wave h_{15} and the coupling h_{16} only use numbers known through the mass spectrum and h_6 .
- The Higgs field as it appears at h_{28} requires no other particles.
- The second sector involves interactions directed by dimensions and there then by symmetries; this is more than enough to encompass the symmetries of the standard model but also imply a form of selection by the fact that all the second sector must work together – a form of filtering.

We understand that space-time, particle resonances, and couplings are of gravitational and electromagnetic origin and that there is no freedom in the structure of the particle spectrum. The resulting laws and parameters form a coherent, compact, inseparable, and non-adjustable block.

7 Wave-coherent cosmology

An expanding universe where the laws of physics are everywhere identical and whose parameters are consistent with the preceding sections is necessarily a single resonance with a localized origin; if considered homogeneous its macroscopic quantities cannot have any degree of freedom. All must therefore be calculated from its geometry; hence from its age alone or from its horizon.

7.1 Black holes

The calculation of the Planck mass from an oscillator made of pure numbers poses a real problem, because the oscillator alone must define space-time; hence the metric by which it scales the particle resonances; therefore the Planck length varies in space and time. Consequently for a Schwarzschild black hole of mass M , the radius

$$R_S = \frac{2GM}{c^2}, \quad (97)$$

can only be a wave number. We naturally think of

$$R_S = n l_p \pm l_p, \quad (98)$$

with n an integer and $\pm l_p$ an uncertainty. But its characteristics are entirely defined by a real factor E defined by $M = E M_\omega$ and verify:

$$R_S \equiv M = E M_\omega = E X_e \left(\frac{D_e}{266^2} + D_p^4 \right)^{-3}, \quad (99)$$

and its average mass density ρ_S reported inside the sphere of radius R_S verifies:

$$R_S \equiv M = \frac{4\pi}{3} \rho_S R_S^3 \rightarrow \rho_S \sim R_S^{-2}. \quad (100)$$

Then we identify the squares and the cubes in this relation

$$M = EM_\omega = \rho_S R_S^3 = \frac{E^3}{E^2} M_\omega$$

$$\rightarrow \rho_s \equiv \frac{X_e}{E^2}; \quad R_S \equiv E \left(\frac{D_e}{266^2} + D_p^4 \right)^{-1}. \quad (101)$$

This expression shows the gravitational nature and structure of the mass formulas, and that the Schwarzschild radius of the Planck mass, say R_ω , can be considered as a unit wavelength because in natural units

$$R_\omega = 4\pi l_p \equiv 4\pi \left(\frac{D_e}{266^2} + D_p^4 \right)^{-1}. \quad (102)$$

We then recognize the Hawking temperature which, even if in principle external, can only be the effect of the harmonic system:

$$K_B T_H = \frac{\hbar c^3}{8\pi G M} = M_\omega c^2 \frac{M_\omega}{M} = \frac{M_\omega c^2}{E}, \quad (103)$$

where we recover the scale factor E of the expression (99). And M_ω is a resonance; this relation identifies this temperature to its wavelength; giving a GR – MQ symmetry where l_p , λ and R_S evolve together in the gravitational field for a particle at rest seen by a distant observer, and not the other way round for the last two. Likewise it comes

$$K_B T_H = \frac{\hbar c^3}{8\pi G M} = \frac{h\nu_\omega}{E}, \quad (104)$$

where $\nu_\omega = M_\omega c^2/h$ is a frequency, and ν_ω/E is that of the black hole. The wavelength of a black hole then varies like its mass and its radius, and its frequency conversely. Now the similarity with the equation of an ideal gas $PV = K_B T$ already discussed after the formula (2) is obvious. In the case of a black hole, P represents a surface pressure, but in the case of an ideal gas the internal pressure is constant, which perfectly fits the scale factor E . However, according to (101) we can identify a wave internal to the black hole whose dispersion at $r > R_S$ defines the metric. This wave is then the effective Planck length at the place considered, the maximum resolution decreases near the black hole down to R_S at its surface; we note the absence of singularity.

With the connections between the couplings and the two sums Σ_{NP} and Σ_K , we have linked gravity (as a force) to resonances and couplings through relative variations of the Planck length, therefore of the relative resolution. Consequently, the harmonic h_8 expressing a constraint in the form of a four-dimensional sphere surface coefficient ($2\pi^2$) associated with a phase variance ($1/\pi$) and dominating the spectrum of resonances, the universe is studied as the surface of a resonant 4-sphere which expands into a four-dimensional exterior. We consider a homogeneous universe where the celerity c is constant and where, due to homogeneity, the effective Planck

length l_p varies only in time and defines a homogeneous metric in 3-space at any time. Obviously we forbid ourselves to add particles or fields, but suppose a single field or space undergoing a transformation. In this way the past is static, the future dynamic, and the present a phase transition.

7.2 Universe mini-model

Expanding into an exterior, the universe is modeled by a solid expanding 4-sphere centered on its origin of which 3D space (the present) is the surface. We therefore assume that the particles are growing strings, and that the interior of the sphere is fixed in the sense of the events – not in the sense of the phases of the resonances, but in the sense of the derivatives of the phase variations of the wave at any point.

In a perfectly homogeneous universe the cosmic time T is the meaningful physical quantity; in wave number $n = T/t_p$ is the number of “Planck sheets” or layers constituting the past. Taking the original event at $n = 1$, its resonance length L_1 , then for $n \gg 1$ the sum of the inverses of the resonance lengths is

$$\frac{1}{L(n)} = \frac{1}{L_1} \sum_{i=1}^n \frac{1}{i} = \frac{1}{L_1} (\ln(n) + \gamma), \quad (105)$$

with γ the Euler-Mascheroni constant. This formulation corresponds to the fact that in an expanding universe the surface of the layer n depends on n^3 , which complies with the mass formulas; this expression means that the present “feeds” the past and that a source energy is consumed (actually of unit $Jm \sim hc$). The sphere is divided into layers, the weight of each is its layer number, and we sum the inverses according to the rule. The energy of the layer n then evolves like

$$E(n) = E(1) (\ln(n) + \gamma) = E(1) \ln(kn). \quad (106)$$

Massive particles are harmonics of the Planck mass; it is then necessary to count in Planck time to obtain a universal clock, since it is the natural one and the logarithm implies that the numerical results depend on the clock we choose. In the absence of creation of matter, the Compton wavelength of a particle is therefore

$$\lambda(n) = \frac{\lambda(1)}{\ln(kn)}. \quad (107)$$

This mechanism and this formula apply to any particle and therefore to the Planck length. This relation amounts to writing $\Delta E \Delta t = 1$ for any string between any two layers with a naturally oriented time; that is one quantum of action exchanges between any two layers of any string; actually not action h but hc , which in 4D is to energy what energy is to power in 3D.

Now if masses add up, charges multiply; then from the same logic as for the evolution of wavelengths, we obtain a charge formula for a given epoch

$$C = \sum_{i=1}^n \frac{1}{n!} = \exp(1). \quad (108)$$

For the observable universe $n > 10^{55}$, we can therefore write an equality. The base of the natural logarithm also intervenes in the coupling D_{μ_e} (20) with Sommerfeld's constant in the form $\exp(1) \times \alpha$; a logarithm is also present in the same formula; these component denote temporal resonances.

The expression (107) defining the wavelengths evolution is all we need to discuss cosmology. The rest of this section contains only solutions to outstanding tensions and mysteries which, as far as we know, cosmological models do not relate to each other; all derived from the geometry of this mini-model and this expression.

7.3 The Hubble parameter

The immediate application concerns the Hubble parameter which is a function of time $H(n)$. We have on the one hand the expansion of the 4D sphere, therefore of 3D space at its surface, which depends only on proper time. The associated scale factor is therefore for a homogeneous spherical universe, still using the Planck time and lengths as units

$$a_e(n) = n. \tag{109}$$

The expansion implies a second scale factor coming from the contraction of wavelengths (107),

$$a_m(n) = \ln(kn), \tag{110}$$

which corresponds to a contraction of rulers. Their product gives the transformation of measurable space-time intervals

$$a_{it}(n) = a_e(n) a_m(n) = n \ln(kn). \tag{111}$$

In the laboratory the space intervals defining the measurement rods evolve over time

$$a_l(n) = \frac{1}{a_m(n)} = \frac{1}{\ln(kn)}. \tag{112}$$

The cosmic microwave background by which the Hubble parameter H_{cmb} is measured was emitted at

$$T_{cmb} = 380\,000 \text{ years} \rightarrow p = \frac{T_{cmb}}{t_p} = 8.87 \times 10^{55},$$

a unitless wave number; and we now are at

$$T = 13.801 \text{ Gy} \rightarrow n = \frac{T}{t_p} = 3.22 \times 10^{60},$$

and according to (112) the contraction of ruler between these two epochs is

$$\frac{\ln(p)}{\ln(n)} \approx \frac{1}{1.082}. \tag{113}$$

The photon is a string like any other, its wavelength evolves exactly like that of massive particles. So the Hubble parameter H_{cmb} measured through the frequency shift of the fossil radiation depends only on a_e , the scale factor due to recession.

At the opposite, the local Hubble parameter H_{loc} is measured from supernovae luminosity, so 1) as a time interval, since this signal has a duration, and 2) as a solid angle which depends on the telescope and the expansion. Nothing new on the principle, but the measurement of the signal duration depends on a_{it} , and its instantaneous power of the solid angle of capture of the signal, that is $a_l^2/a_e^2 = a_{it}^{-2}$ because space has expanded between emission and reception, and simultaneously the lengths defining the telescope have contracted. The instantaneous luminosity therefore depends on a_{it}^{-3} and the total luminosity measured on a_{it}^{-2} ; the measured recession is therefore a_{it} . In the end, therefore, we have the following dependence between the two methods of measurement

$$H_{loc} = H_{cmb} \frac{\ln(n)}{\ln(p)} = H_{cmb} \times 1.082. \tag{114}$$

Estimates using standard candles methods [14] concentrate around $H_{loc} = 73 \text{ km/s/Mpc}$, and the Planck mission indicates [13] $H_{cmb} = 67.66 (42) \text{ km/s/Mpc}$. The relation (114) gives

$$67.66 (42) \times 1.082 = 73.17 (45).$$

Here the associated tensions are natural and explained. The precision may seem very good, but this is not so because the logarithm attenuates the errors on n ; if we multiply n by 2 we obtain 1.083, by 10 we get 1.10, not much but we clearly see this ratio increasing over time. Consequently, the universe is permanently building resolution.

The Λ CDM model interprets these measurements as an accelerated expansion because a cosmological constant is the natural solution in GR. Then, deriving (110) to (112) and using the cosmological radius $R_U = cT$, it comes

$$\ddot{a}_m = (\dot{a}_m)^2 = \frac{1}{a_e^2} = \frac{1}{n^2} \rightarrow \frac{1}{R_U^2} \approx 0.6 \times 10^{-52} \text{ m}^{-2}, \tag{115}$$

which is close to the estimated value of the cosmological constant (to within a factor of the order of 2).

Let us now return to the Planck clock and the rulers contraction between two epochs. With another clock such that $n \rightarrow n/q$ and $q > 1$, it comes

$$\frac{\ln(n)}{\ln(p)} \rightarrow \frac{\ln(n) - \ln(q)}{\ln(p) - \ln(q)} = \frac{\log_q(n) - 1}{\log_q(p) - 1}, \tag{116}$$

which amounts to changing the constant of integration. It is only when the constant is zero that the universe has unit size at the origin. We can also see there a change of base of the logarithm and the introduction of a negative constant of integration showing that the length of the ruler is in excess, then irrelevant, and that the beginning physically compares only to the Planck time. We can also write

$$\frac{a_m(n)}{a_m(q)} = \frac{\ln(n)}{\ln(q)} = \log_q(n) = \log_q\left(\frac{n}{q}\right) + 1, \tag{117}$$

which clearly indicates the choice of time unit and allows us to change it, on the condition of knowing the absolute date.

7.4 Dark energies and energy

The object of this section is to study the correspondence with the Λ CDM model through the respective proportions of its four main parameters, namely the proportions of ordinary matter, dark matter, dark energy, and the total density. We do not yet look for absolute quantities, only to understand how these parameters relate to each other in relative terms.

Consider a uniform positive pressure P in the surface of nonzero thickness of a four-dimensional Euclidean sphere of radius R . The condensation of a new layer corresponds to an absorption producing the growth of the strings and a pressure deficit which, seen by an observer in the surface of the sphere using GR to model cosmology, will guess a constant negative pressure. This negative pressure is understood here as a condensation density simultaneously generating the particles' energy and gravity. The source energy M_S invested in the condensation must then be separated into three parts, namely 1) the visible energy, 2) a remainder of force without visible source (dark mass) because the wavelengths vary from one time to another, and 3) a dark energy of negative pressure causing the expansion of the sphere. Condensation can be modeled in 3+1D as a kinetic energy $M_S = pc$; but here it is the transformation $X_e \leftrightarrow X_a$ which is equivalent to a bounce and implies $M_S = 2pc$. The dark energy of the standard model therefore represents 2/3 of all (2 for the source energy and 1 for the masses). Quantitatively, the condensation occurs with h_8 which implies proportions 1 for ordinary matter and $2\pi^2$ for source energy (1 is the time axis, $2\pi^2$ the surface of the sphere); so for convenience let us define

$$\phi = \frac{1}{2\pi^2}. \quad (118)$$

The Λ CDM model considers ordinary matter separated from the dark side, its proportion of mass is therefore given by

$$\frac{M_V}{\phi} = \frac{M_S}{1 + \frac{2\phi}{3}} \rightarrow \frac{M_V}{M_S} = 4.90\%. \quad (119)$$

The mass of matter will be one-third the source energy, but is separated into ordinary and dark matter; the proportion of the latter is therefore

$$\frac{M_D}{M_S} = \frac{1}{3 \times (1 + \phi)} - \frac{M_V}{M_S} = 26.83\%, \quad (120)$$

and dark energy is the remainder

$$M_{DE} = M_S - M_D - M_V \rightarrow \frac{M_{DE}}{M_S} = 68.27\%. \quad (121)$$

Finally:

1. These proportions are invariant over time.
2. They agree perfectly with the Planck mission results [13]: $M_B = 4.9\%$, $M_D = 26.8\%$, and $M_{DE} = 68.3\%$.

3. The absorption density is the saturation point known from the mass M_ω , imposed by the mechanism: The entire source energy intervenes there through the division by ϕ giving a surface density on the 4-sphere.

On this basis we can complement the calculation of the cosmological constant. Using \ddot{a}_m (115), the expansion factor of space is that of a 3-sphere in GR, $4\pi/3$, and there is the factor 1/2 from $M_S = 2pc$ to take into account. Then using the Hubble factor

$$\Lambda = \frac{2\pi H_{cmb}^2}{3c^2} = 1.121 \times 10^{-52} \text{ m}^{-2}, \quad (122)$$

in good agreement with the Planck mission results (to 1.3%).

$$\Lambda_{Planck} = 1.106 \times 10^{-52} \text{ m}^{-2}. \quad (123)$$

The current value, using $H_{loc} = 73.17 \text{ km/s/Mpc}$ gives

$$\Lambda_{loc} = \frac{2\pi H_{loc}^2}{3c^2} = 1.31 \times 10^{-52} \text{ m}^{-2}. \quad (124)$$

Last, using the cosmological radius $R_U = cT$, which is the legitimate way in this mini-model

$$\Lambda_{R_U} = \frac{2\pi}{3R_U^2} = 1.23 \times 10^{-52} \text{ m}^{-2}, \quad (125)$$

logically a median value.

7.5 The cosmological constant

The method used here to model the impact of $a_e a_m$ is to reverse their roles; we model an increase of masses, insert it into the Schwarzschild solution, and modify it *à la* de Sitter; with a little more because the masses are not constant. By setting the total universe energy to $M_T = M_S$, the previous section states

$$2G = \frac{R_U c^2}{M_T}, \quad (126)$$

where $R_U = cT$ is the cosmological radius at date T and M_T the total energy of the Λ CDM at T , which symmetries the Schwarzschild solution

$$\frac{R_s}{r} = \frac{R_U M}{M_T r}. \quad (127)$$

This equation simply indicates that Newton's constant conforms to a condensation whose saturation point is the density of a mass $E M_\omega$ on the observable scale. It is legitimate with R_U (and the following calculations can only work) because the proportions of matter and dark energy are constant over time, and the resonance is temporal. We therefore perform the calculations as if the universe was a plane, of size R_U , and of constant densities. To continue, it is necessary to add variable terms that depend on r/R_U , which requires two parameters α, β ,

$$\frac{R_s}{r} = \frac{R_U M}{M_T r} \rightarrow \frac{R_U M}{M_T r} \times \frac{R_U - \alpha r}{R_U + \beta r}. \quad (128)$$

The term in α in the numerator corresponds to the expansion of the source energy like R_U , and the term in β in the denominator to the derivative of the masses expansion. The two terms are obtained by adding lengths because we are talking about the inverse of the gradient of L_p in space and the inverse of its derivative in time, which also inverts the signs. A series expansion to the second order gives

$$\frac{R_U M}{M_T r} \rightarrow \frac{R_U M}{M_T r} - (\alpha + \beta) \frac{M}{M_T} + \beta (\alpha + \beta) \frac{M r}{M_T R_U}. \quad (129)$$

Let us examine this expression:

- The first term is nominal and defines static space, fields, and masses; the others can then be considered as addition of a variable gravity field.
- The middle term is independent of r and therefore involves the total mass of the universe; M must then be integrated to M_V , and the total must give -1 the flat metric. Then we have $\alpha + \beta = 2\pi^2 + 1$.
- So the term on the right must also be integrated into M_V to give M_T (and becomes r/R_U); therefore $\beta = 1$ the visible masses and $\alpha = 2\pi^2$ the source energy.

Note that with a series expansion in r we cannot integrate to R_U , but we can do it to M_V as the central term requires. In the end, after replacements and integration to M_V we find

$$\frac{R_s}{r} = \frac{R_U M}{M_T r} \rightarrow \frac{2GM}{rc^2} - 1 + \frac{r}{R_U}. \quad (130)$$

The Schwarzschild-de Sitter solution has a similar formulation

$$-\frac{R_s}{r} \rightarrow -\frac{R_s}{r} - \frac{\Lambda r^2}{3}. \quad (131)$$

Adding a variable term then gives

$$-\frac{R_s}{r} - \Lambda r^2 \rightarrow -\frac{R_s}{r} - \Lambda r^2 - \delta\Lambda r^2, \quad (132)$$

which is identified term to term with (130), and where the factor $1/3$ of (131) is removed because it comes by integration to give $\Lambda r^2/3$, and here it is $\delta\Lambda r^2$ which must be integrated. The introduction of a geometrical constant k allows to solve the equation as it must give (130):

$$-k\Lambda r^2 - \delta\Lambda r^2 \rightarrow -1 + \frac{r}{R_U}. \quad (133)$$

Since Λ is now constant, integration to R_U is possible and gives the flat metric identified in the unit term of (130); hence:

$$-k\Lambda \int_0^{R_U} r^2 dr = -1 \rightarrow k\Lambda = -\frac{3}{R_U^3}. \quad (134)$$

Now we need to derive $k\Lambda$, but here masses increase and Λ constant, and $\delta\Lambda$ represents the inverse of the masses derivative; so we need to derive the inverse to get $\delta\Lambda$; for all r we set $R_U \rightarrow r$, and since k is a geometrical factor we remove it

$$\delta(\Lambda(r)) = \left(\frac{d}{dr} \left(\frac{r^3}{3} \right) dr \right)^{-1} \rightarrow -\delta(\Lambda(r)) = -\frac{1}{r^2}, \quad (135)$$

and put it back to cancel the integration factor over the solid angle; then multiply by $1/2$ and identify with $-r/R_U$ we get

$$\frac{4\pi k}{2} \int -\delta(\Lambda(r)) r^2 dr = \int -2\pi k dr = -\frac{r}{R_U}. \quad (136)$$

Therefore

$$k = \frac{1}{2\pi R_U}. \quad (137)$$

Last, report in (134)

$$\Lambda = \frac{2\pi}{3R_U^2}, \quad (138)$$

as expected we get (125). The Schwarzschild and de Sitter solutions as modified here amount to differential equations that we integrate; it corresponds to the mini-model but contradict GR, but recall Einstein designed this theory with a static universe in mind – proof is his famous mistake to stabilize it. This is why in this mini-model space and time are not on strict equal grounds. Moreover, because of integration to M_V made after (129) the results are independent of the creation of particles at any time.

7.6 Anomalous accelerations, MOND

The standard model of cosmology evaluates the parameters necessary for its operation; but here the absence of dark matter particles makes it incompatible with the phenomenology of gravitation. However, in the absence of dark matter particles we can use the mini-model to recover MOND [11], [12].

The radius of the universe 4-sphere being n its circumference is $2\pi n$; and from (110) an observer will see the expansion accelerating. The instantaneous acceleration A of the expansion will depend on

$$\dot{a}_m = \frac{1}{n} \rightarrow A = \frac{1}{2\pi R_U} \text{ m}^{-1}, \quad (139)$$

which, as we expect, is the k factor in (137). A remote object recession will be seen accelerating:

$$\frac{d^2 r}{dt^2} = A c^2 \rightarrow a = \frac{c^2}{2\pi R_U} = 1.185 \times 10^{-10} \text{ m s}^{-2}, \quad (140)$$

which, according to Milgrom is MOND limit acceleration $1.20(\pm 0.2) \times 10^{-10} \text{ m s}^{-2}$ [11] [12]. Another direct way to this result is to understand the effect of the evolution of the electron Compton wavelength on the Bohr radius; it shrinks when the wavelength decreases

$$a_0 = \frac{\lambda_{dB}}{2\pi} = \frac{\lambda}{2\pi\alpha}, \quad (141)$$

where the factor 2π is consistent with (140) and implies that, unlike energy, angular momentum is absolute and conserved; in agreement with QM and with the interpretation of $\Delta E \Delta t$ in (106). Now we can discuss the central mass problem in

which the expansion of the central mass adds a term to the classical potential, making it increase in time. Therefore a simple sum of a and the Newtonian acceleration A_N giving $A_N + a$ is unacceptable, as the so-called anomalous accelerations are free fall in an evolving gravity pit. We therefore return to the weak equivalence principle, according to which an acceleration is indistinguishable from gravity; the opposite case makes it possible to reason by symmetry on the acceleration formula. A force f on an object of mass m in free fall with a Newtonian acceleration A_N giving an effective acceleration A_{eff} is felt as $A_r > 0$:

$$A_N \left(1 + \frac{A_r}{A_N} \right) = A_{eff} \rightarrow A_r = \frac{f}{m}, \quad (142)$$

here the acceleration felt, $A_r = f/m$, is the effect of inertia and we are looking for the effect of an increase in gravity. So to link the effective acceleration A_{eff} and the two quantities A_N and a in a classical form we need to write the transformation inverse to (142); an inversion of the roles which amounts to calculating A_N . Firstly we rewrite (142):

$$A_N = A_{eff} \left(1 + \frac{A_r}{A_N} \right)^{-1} \rightarrow A_r = \frac{f}{m},$$

Secondly, we use the fact that Newton's acceleration A_N have no physical reality; on the right-hand side we replace it with the real one, and the acceleration felt by the unfelt:

$$A_{eff} \left(1 + \frac{a}{A_{eff}} \right)^{-1} = A_N \rightarrow A_r = 0. \quad (143)$$

This expression is MOND simple interpolation function, one of three possible [12]. We can also derive the same formula from the harmonic system in a direct and elegant manner that treat space and time on natural non-equal grounds: A_{eff} depends on the gradient of the effective Planck length, which has two components, 1) its instantaneous gradient in space, and 2) its variation in time. The former gives the classical acceleration A_N , which can be approximated by subtracting the effect of the latter from the total. Then by adding the inverses, we subtract from the effective gradient of resonance length (total gradient with A_{eff}) its variation over time in proportion of the gradient (a/A_{eff}) at the considered location to get A_N , i.e.

$$\frac{1}{A_N} = \frac{1}{A_{eff}} \left(1 + \frac{a}{A_{eff}} \right) \rightarrow A_r = 0, \quad (144)$$

which is identical to (143). We use again the same formula for length addition, now applied to the variations of resolution in space and in time. The evolution of a is immediate as it depends on $1/T$ and decreases with time; this acceleration is therefore a lot stronger in the early universe than at present time, up to $a \rightarrow \infty$ when $T \rightarrow 0$.

7.7 Comments

To begin this section, we applied the length addition formula used for masses to the entire universe, simply our initial hypothesis, to obtain a temporal resonance formula (106) based on a logarithm which complies with the mass formulas. Then, by extending the logic to charges, we found an exponential (107); both are in the calculation of the μ_e mass (21) and in the relation (67) between X_e and X_a , and only there, showing a scaling effect.

On this basis we deduced the Hubble factor correction, the four densities, the cosmological constant, the limit acceleration and interpolation formula of MOND; we obtained eight coherent quantities from the age of the universe alone, which is not possible with the models and theories that use them.

We remark that the expansion of space a_e (109) and energies a_m (110) can be inverted, resulting in a logarithmic expansion of space and a linear expansion of energy (as we did in section 7.5); the resulting model gives the same results provided that the unitary resonances of neutrinos and photons have specific properties. We discussed the simplest scheme where the dimension that we call time expands linearly in 4-space.

8 Questions and extensions

8.1 Dimensions and resonances

The whole sequence h_i seems to include a triple cycle, 4 to 4, 7 to 7, and 8 to 8. The dimensional coefficients from h_8 to h_{11} rise from 4 to 7; the objects present for h_{13} are the 3D and 5D sphere volumes, and for h_{14} two sphere surfaces in 6D and 3D. Then we apparently have a limit with 8D. Since the super-coupling h_{16} can be decomposed into two, we also assume that it is in $4+4=8D$. Consequently, D_p and D_e are dimensional couplings and the first sector range from 1 to 7 dimensions. Since particle resonances are radial or rotations, a single 4D space is sufficient for resonances to build a 7 or 8D structure: We assume for the discussion that a 4D space is native and, from the sequences h_i and c_i , that space-time is built by the interplay of resonances. The first sector and the particle resonances K are then explained by Table 7; the particle spectrum is defined by the dimension of each resonance.

- Sign = the resonance has an echo of same dimension.
- Sign + the dimensions add.
- Sign \neq distinct resonances in the two spaces.

We find the following concordances

- The larger the resonance dimension, the larger the mass and the stronger the coupling strongest component.
- Tables 1 and 2 use the same K for the electron and muon, simply the dimension of their resonances.

Table 7: Resonances and dimensions.

-	Particle	Dim	4D	↔	3+1D	Tbl
h_0	M_ω	0/8	0/4	=	0/3+1	(43)
h_1	ν	1	1	=	1	6
h_2	e	2	1	+	1	1, 2
h_2	$q(P)$	2	1	+	1	3
h_3	μ	3	3	=	3	1, 2
h_4	τ	4	4	≠	3+1	1, 2
h_5	$q(N)$	5	4	+	1	3
h_6	g	6	3	+	3	-
h_7	W, Z, H, γ	7	3	+	3+1	5

- The tauon is exceptional in that it admits two unequal solutions, two distinct ways of oscillating in 3+1 and 4 dimensions.
- The rotational part N of quarks mix, this is clear for the u and d , and not P the radial part, but $P = 3$ constant pose no problem to mixing.
- We understand that the left-hand side of the relation (14) giving the small k of the boson resonance, which seems a bit strange in 3 dimensions, corresponds to 3+(3+1) dimensions with a resonance of a 6-sphere as seen in 3; by introducing a factor $k\pi$ in the denominator of the mass formula (11) the volume of the 6-sphere becomes

$$\pi^3 r^6 \rightarrow \pi^3 (kr)^6 \rightarrow \pi^2 (kr)^6, \tag{145}$$

then taking the square root to return to 3 dimensions we obtain the term on the left of (14)

$$\pi^2 (kr)^6 \rightarrow \pi (kr)^3, \tag{146}$$

with $r = 1$ and $\pi \rightarrow \pi/144$, since this part is circular. And on the right-hand side, we calculate a radial impact as the compression of a 1 dimension line by stress or forces in 3 dimensions, i.e. with an inverse effect between forces and lengths:

$$\frac{\pi r^3}{k} \rightarrow \left(\frac{\pi}{k}\right)^{1/3} r, \tag{147}$$

now with $r = 266 D_b$. Since r is a wave number or its inverse, we introduce it as the two sides of the resonance and obtain (14).

Resonances organize well by counting only 1, 3 or 4 dimensions, and all bosons use at least 3+3 dimensions. Logically, the photon is in h_7 and neutrinos in h_1 ; leptonic resonances from h_1 to h_4 , and bosonic resonances from h_5 to h_7 . Quarks are supposed to mix; they take one component of each side with $P = 3$ in h_2 and one of the rotations of h_5 for N .

The electrons and quarks K are given here by the dimension, provided that time counts for 2D in space-time:

- The electron resonance in h_2 is in 2 dimensions of time.
- The muon h_3 , 3 dimensions of space.
- The tau h_4 , 4 dimensions in native space and $K = 4$ Table 2, and 3+1 in space-time where time counts double then $K = 3 + 2 = 5$ Table 1.
- Heavy quarks ring in 2 dimensions h_2 , and 5 dimensions h_5 , but time must be accounted for only once then subtract 5D from 2D to get $K = 2 \times (2 - 5) = -6$.
- Light quarks ring in 2 dimensions h_2 , but N uses two rotations and time may be accounted for differently, then possibly:
 - d remove one, 4D and $K = 2 \times (2 + (1 - 5)) = -4$;
 - u multiply by 2 for charge 2/3 versus 1/3 for the d .

8.2 Super-minimal super-strings?

In the universe mini-model the present feeds the past, which means that downtime currents feed the strings, providing the necessary “power” for both downtime and uptime currents. There should be a dissymmetry in strength between up-time and down-time in a ratio 1 to 2. Downtime currents twice as strong as the uptime will give double charges; i.e. 2/3 and 1/3 and impact the resonance by a factor of 2 like in Table 3, the electron charge being the fusion of the two. The explanation for the existence of 3 elementary electric charges is very basic and can correspond to a quantitative law of transformation. In the two series h_i and c_i resonances and couplings appear separately, like in the mass formulas, and the couplings do mirror resonances. Overall, three different manners to observe the same mirror where $1/NP > KD$ for all resonances where $NP > 1$ which can mean a form of super-strings – except for M_ω where the resonance can be seen inverted since $D_p^4 < D_e/266^2$. Then we associate the apparent electric charge of a particle with the direction of a current independently of the resonance. On this basis we need four rules to complete the elementary particles’ charges contents which we denote with arrow and sign:

1. The signs correspond by convention to the current, the measurable electric charge reverses for downtime currents (like electricity going backward in time).
2. Two currents of opposite charge can combine to form a single string, or a (sub)string within a string.
3. Two currents of the same charge cannot.
4. Currents can make massive particles, then vertical arrows propagating in time like a massive particle; or mass-less, then propagating on the light cone, oblique arrows (neutrinos and photons).

Table 8 shows all particle types regardless of their resonance. The parentheses represent sub-strings association, and brackets a particle contents.

The mass μ_e is the proper mass of [$+$ \uparrow , $-$ \downarrow], which can fall into the three electron resonances (h_2, h_3, h_4), as can

Table 8: Minimal scheme for currents symmetry.

Charge	Particle	Spin	Currents
0	ν	1/2	$[(-\swarrow + \searrow)(-\nearrow + \nwarrow)]$
+1	μ_e/μ_α	1/2	$[(+\uparrow - \downarrow)]$
-2/3	u, c, t	1/2	$[(+\downarrow)]$
+1/3	d, s, b	1/2	$[(+\uparrow)]$
+1	W^+	1	$[(+\uparrow)(-\downarrow)]$
0	Z^0	1	$[(-\downarrow + \downarrow)(-\uparrow + \uparrow)]$
0	H^0	0 or 2	$[(-\uparrow)(+\downarrow)(+\uparrow)(-\downarrow)]$
0	γ	1	$[(-\swarrow + \searrow)(-\nwarrow + \nearrow)]$

quarks with $[\pm \uparrow]$ and $[\pm \downarrow]$ and h_5 , and the four bosons with h_{28} . The distinctions between W^\pm , H^0 and Z^0 are consistent with the calculation of their masses and widths. The spins agree with 1/2 for any inner string (the most inner parenthesis for each scheme). In the end, there is only one type of current, oriented only in charge and with respect to time; all assemblies are symmetrical except for quarks, which are confined. We're missing the gluons, which should correspond to eight separate horizontal arrows, with the ubiquitous quality of also manifesting like a monopole. Now let us draw a few examples of transmutations, to begin with $d^+ \rightarrow u^- + W^+$

$$[(+\uparrow)] \rightarrow [(+\downarrow)] + [(-\downarrow)(+\uparrow)]. \tag{148}$$

The d^+ current is conserved and passes into the W^+ , what remains (i.e. the $(+\downarrow)$ and $(-\downarrow)$ not underlined) does not exist as a particle; if this is a systematic rule it prohibits FCNC because in the following case the remainder is also a Z^0 which is an existing particle, $s^+ \rightarrow d^+ + Z^0$

$$[(+\uparrow)] \rightarrow [(+\uparrow)] + [(-\downarrow + \downarrow)(-\uparrow + \uparrow)]. \tag{149}$$

The muon case, $\mu^- \rightarrow W^- + \nu_\mu$:

$$[(-\uparrow + \downarrow)] \rightarrow [(-\uparrow)(+\downarrow)] + [(-\swarrow + \searrow)(-\nearrow + \nwarrow)], \tag{150}$$

next is its symmetric, $W^- + \bar{\nu}_e \rightarrow e^-$:

$$[(-\uparrow)(+\downarrow)] + [(-\swarrow + \searrow)(-\nearrow + \nwarrow)] \rightarrow [(-\uparrow + \downarrow)]. \tag{151}$$

This is because neutrino and anti-neutrino are identical. Two up-time or down-time arrows for neutrinos and Z^0 can also be removed for the same results; the choice made here is that every up-time current is associated with a downtime current, and conversely – except for quarks, where currents have the same sign and the association of particles/strings is made by confinement.

The γ and Z^0 cases are the simplest, as we obtain (for example) the following two reversible cases. For $e^+ + e^- \rightarrow Z^0$:

$$[(+\uparrow - \downarrow)] + [(-\uparrow + \downarrow)] \rightarrow [(-\downarrow + \downarrow)(-\uparrow + \uparrow)] \tag{152}$$

and for a photon, $e^+ + e^- \rightarrow \gamma$:

$$[(+\uparrow - \downarrow)] + [(-\uparrow + \downarrow)] \rightarrow [(-\swarrow + \searrow)(-\nwarrow + \nearrow)]. \tag{153}$$

A minimal form of (super) symmetry is evident, where each lepton charge (μ_e mass or neutrino) is associated with a boson of same charge. Since we find 8 resonances for quarks in h_5 (49) and c_3 (92), including twice two indistinguishable masses for u and d , we're all set with 8 gluons in h_6 . It is the μ_e mass and h_6 , together with the separation of resonances and couplings in the sequences h_i and c_i that makes this minimal scheme possible as the resonances (N, P) do not define charges and spin, the couplings and inner currents do.

8.3 Transmutation and resonance

At the general level, the $N = P = 19 - 7$ of bosons includes all circular resonances (7 and 19), enabling transmutations of N or P of electrons and quarks; the product of their $K = 266$ includes all primary field resonances. In transmutations, this allows exchanges of resonances by sums and products:

- by product, with the $K = -2$ of the W^\pm for the N of quarks within the second or third generation.
- for u and d quarks, by product with the $K = -2$ of the W^\pm for the K , and cross exchanges of 14 and 19 for N .
- by sum $\pm 12 = 19 - 7$ associated with a product exchange by the $K = -2$ of the W^\pm between the second and third generation of quarks.
- by mixed exchanges of the previous ones when the first and another generation is involved.
- FCNC would imply a product exchange in N which is not the K of a neutral boson.
- by sum or subtraction of the $K = -7$ of the Z^0 for the N and P of the electrons.
- The resonances of neutrinos (K) are an inverted echo of the resonances N, P of the corresponding electron, there is a form of conservation in these transmutations to which the Z^0 and the W^\pm are neutral.
- All particles couple in N, P , sometimes separated, with D_p^i through its 137 and $-19\pi^2$, which is the $K = -19$ of the H^0 , coupling in mass in the Standard Model.

Recall also that the total resonance widths of the three bosons were calculated in section 2.4. Hence the resonances speak directly of transmutations; the form of which obeys, and then implements, some conservation of the resonances geometry.

8.4 And the strong force coupling?

According to Table 8, quarks should be the expression of the most fundamental components of massive particles, and then also the quark mass coupling D_q , which we compare to that of electrons to get a ratio of lengths:

$$\frac{D_q}{D_e} = 1 + \alpha, \tag{154}$$

and specifically for the full coupling $K D$ of the electron itself compared to that of a heavy quark

$$\frac{-6 D_q}{2 D_e} = -3 - 3 \alpha . \quad (155)$$

Now recall that in Table 3 the charge ratio of $1/3$ to $2/3$ corresponds to a resonance ratio ($N \rightarrow 2N$ for the second and third generation, and $K \rightarrow 2K$ for the d and u), hence we find again the signature of a monopole with α , including the ratio of charge 1 to $1/3$. But according to h_6 (50) and h_{16} (60), it is the gluon that rings in 69.5 and it does “make” the coupling α for the mass μ_e , and the ratio μ_α/μ_e . So, consider D_e the most fundamental mass coupling and compare

$$\frac{D_e}{\alpha} = 0.1169 \quad (156)$$

and, since $139 = \Sigma_{N,P} + 2$ includes the photon and neutrino unitary resonances corresponds to the entire particles field:

$$139 D_e = 0.1186 , \quad (157)$$

to the range of values of $\alpha_S(M_Z^2)$ reported in the literature

$$0.117 \leq \alpha_S(M_Z^2) \leq 0.119 . \quad (158)$$

8.5 Do photons have mass?

The current limit of the photon mass is $m_\gamma < 10^{-18}$ eV (PDG 2023). Now, from the calculation of neutrinos masses and the identification of the photon resonance in h_7 , we can ask whether the photon has mass. If so, we should be able to estimate its resonance; for this we apply an inversion similar to neutrinos, which was $D_e \rightarrow 1/\alpha$, this time from the components of D_{WZ} and D_H the coupling should be as a minimum

$$D_\gamma = \frac{-1}{D_e^2} . \quad (159)$$

The choice of K is not immediate; since $NP = 1$ for this resonance and not 144 we cannot make use of any phase coherence constraint. The best we can provide is a possible lower limit with $K = \pm 266$, since 266 is part of Σ_K and not used in any other particle resonance. We obtain

$$m_\gamma \geq \frac{m_e}{m_e - \mu_e} \times \frac{X_e}{\pi(1 \pm 266 D_\gamma)^3} \approx 5.3 \times 10^{-23} \text{ eV}/c^2 . \quad (160)$$

Using $K = -19$ gives $\approx 1.5 \times 10^{-19}$ eV/ c^2 a likely maximum since using $K = -7$ the calculated mass exceeds the limit by a factor of 3 . In this logic the last candidate would be $K = -133$ giving $\approx 4.3 \times 10^{-22}$ eV/ c^2 .

8.6 SM symmetries and resonances?

The standard model of particle physics is based on $U(1) \times SU(2) \times SU(3)$ with $U(1)_Y \times SU(2)_L \rightarrow U(1)_{EM}$. With respect to the three rotations in the primary field couplings formulas of α , D_e and D_p which are respectively $+1\pi^2$, $+7\pi^2$, $-19\pi^2$, we naively notice:

$$7 = 2^3 - 1^3 , \quad (161)$$

and

$$19 = 3^3 - 2^3 . \quad (162)$$

Simultaneously, except for the mass μ_e all resonances N , P of the primary field use $1, 2, 3, 7, 19$, and $12 = 19-7$; and the mass μ_e includes $2/7$. Here we find a bijective correspondence between the symmetries of the SM and the resonances which states that 1 is an instance of $U(1)$, 2 of $SU(2)$ and 3 of $SU(3)$. This is straightforward and needs no comment; but what could it mean?

The mass formulas are based on a cube and represents stress in the form $PV = K_B T$ where only P and T can vary (except maybe for gravitation, which is of no importance here as we only discuss particles). So, except for the electron the resonance N , P systematically include a cube difference in a cube! For the three bosons we get $m \sim 144^3 = ((19-7)^2)^3$ which is a power six of the difference of two cube differences. It means a general mechanism by which symmetries resonate individually and with each other. For electrons and quarks:

- A symmetry of order N will give N^3 as say a number of “resonance points” per unit volume.
- The symmetries of order $N-1$ will remove $(N-1)^3$ from the order N resonance.
- And $SU(3)$ includes instances of $SU(2)$ which includes instances of $U(1)$.

It means that each and every “resonance point” is a unitary resonance with unitary impact on the mass calculation.

- For the three electrons we only have 2 and 7 in the resonances meaning that $SU(3)$ is absent at this level, and may intervene only through the coupling of the mass μ_e .
- for quarks, $SU(3)$ is present giving 19 and 38 ; $SU(3)$ includes instances of $SU(2)$, then 7 and 14 , the u and d include the four possible fractions using these numbers where from Table 3 $N = a/b > 1$.
- For the three (massive) bosons we find the same structure, this time not with respect to the symmetries but to the fermion field elementary resonances $2, 7$, and 19 , giving $12 = 19 - 7$ and $266 = 2 \times 7 \times 19$.

Now for $U(1)$ we should have 1 instead of 2 ; but with the three electrons we have two symmetries in resonance with each other. And we get the product $NP = 1$ for the photon and the neutrinos; hence, all along, it looks like we only counted all combinations of possible unitary resonances given by the SM symmetries; a logic that extends to transmutations.

9 Conclusion

Based on a single hypothesis used to study the parameters of the standard models of particle physics and cosmology, we found a suite of formulas, coherent with each other, showing how it holds from the mass of neutrinos to the energy parameters of cosmology – down to the last known decimal places; and some ideas, new or otherwise, about the internal structure of the system under study: *A unique resonance where each and every quantity we addressed is a dynamical substructure.*

Each one of those appear to be part of a single physical object, which expression is found in the Planck mass oscillator, and where each formula speaks directly of the others in various manners. Therefore, we have most probably discussed the shapes of an unknown or poorly understood level of physical reality – some information hidden in the structures of space-time and fundamental particles.

Hence, in conclusion, highlight that the expressions (106) and (108), together with the suite h_i and c_i , seem to reveal the nature of quantum mechanics as they fit the de Broglie-Bohm [3] [2] and Cramer [9] interpretations – where 4-space, space-time, and strings, are ringing as a whole, permanently communicating between any two epochs down to the origin in one Planck time. Of course energy cannot be transferred instantly between any two points in space and time – of course; but now energy, what is it made of?

Received on September 23, 2023

References

1. Akers D. Further evidence for magnetic charge from meson spectroscopy. *Int J Theor Phys*, 1987, v. 26, 1169–1173.
2. Bohm D. A Suggested Interpretation of the Quantum Theory in Terms of “Hidden Variables”. *Physical Review*, 1952, v. 85, 166–179.
3. De Broglie L. Recherches sur la théorie des quanta. *Annales de Physique*, Janvier-Février 1925, 10e série, Tome III.
4. De Broglie L. Théorie de la double solution. *Journal de Physique*, Mai 1927.
5. Consiglio J. L'Onde et la Constante de Sommerfeld. *Annales de la Fondation Louis de Broglie*, 2022, v. 47 (2), 267–272.
6. Consiglio J. Toward the Fields Origin. *Progress in Physics*, 2019, v. 15 (1), 9–16.
7. Consiglio J. Are Energy and Space-time Expanding Together? *Progress in Physics*, 2017, v. 13 (3), 156–160.
8. Consiglio J. On Quantization and the Resonance Paths. *Progress in Physics*, 2016, v. 12 (3), 259–275.
9. Cramer J. The transactional interpretation of quantum mechanics. *Rev. Mod. Phys.*, 1986, v. 58 (3).
10. Dirac P. A. M. Quantized singularities in the Electromagnetic Field. *Proc. Roy. Soc. A*, 1931, v. 133, 60.
11. Milgrom M. A modification of the Newtonian dynamics as a possible alternative to the hidden mass hypothesis. *Astrophysical Journal*, 1983, v. 270, 365–370.
12. Milgrom M. MOND theory. arXiv: astro-ph/1404.7661v2.
13. The Planck Collaboration. Planck 2018 results. VI. [//www.cosmos.esa.int/web/planck/publications#Planck2018](http://www.cosmos.esa.int/web/planck/publications#Planck2018).
14. [//fr.wikipedia.org/wiki/Constante_de_Hubble](https://fr.wikipedia.org/wiki/Constante_de_Hubble), Dec. 2022.
15. [//keisan.casio.com/has10/Free.cgi](http://keisan.casio.com/has10/Free.cgi) (site closed since 09/20/2023)
16. [//www.mathsisfun.com/calculator-precision.html](http://www.mathsisfun.com/calculator-precision.html)

Gamow Theory for Diproton Decays of Proton-Rich Heavy Nuclei ^{45}Fe and ^{67}Kr

Tianxi Zhang and Cornelius Salonis

Department of Physics, Chemistry, and Mathematics, Alabama A&M University, Normal, Alabama 35762, USA.
E-mail: tianxi.zhang@aamu.edu

A diproton is an unusual particle, made of only two protons, which are believed to be unbound. In the core of a main sequence star such as the Sun, protons first combine to form diprotons in order for the proton-proton chain nuclear fusion reactions to occur. Exploring properties and activities of diprotons plays an important role in understanding the physics of stellar energy generation by nuclear fusion. In laboratories, it has been shown experimentally that some proton-rich radioactive heavy nuclei such as ^{45}Fe and ^{67}Kr can decay with emissions of diprotons and longer lifetimes in comparison with lighter nuclei. In this study, we investigate diproton decays of proton-rich or neutron-rare radioactive heavy nuclei. We first quantum-mechanically analyze to formulate the expressions for the transmission probability and lifetime of the diproton decays. Then, we numerically calculate the transmission probabilities and lifetimes of the diproton decays. The numerical results obtained for the diproton decays of the two typical proton-rich radioactive heavy nuclei ^{45}Fe and ^{67}Kr are plotted as functions of the energy of the emitted diproton and further compared with the measurements. It is shown that the transmission probabilities rapidly increase with the energy of the emitted diprotons, while the lifetimes for the diproton decays decrease with the energy of the emitted diproton and can be consistent with the laboratory measurements.

1 Introduction

A diproton is the nucleus of a rare isotope of helium, ^2He , and consists of only two protons. It is extremely unstable and believed to be in an unbound state with a negative binding energy due to the spins of the two protons to be anti-aligned according to the Pauli exclusive principle [1, 2]. A diproton does not stably exist in nature but can be formed temporarily in two ways (see Fig. 1): (1) combination of two separate protons and (2) decay of proton-rich radioactive heavy nuclei. Two separate protons, when they collide with enough energy to tunnel through the Coulomb barrier between them, form a diproton, $^1\text{H} + ^1\text{H} + \text{Energy} \rightarrow ^2\text{He}$. This frequently occurs in the core of the Sun or any star in the main sequence. Approximately, there are about 10^{63} diprotons formed every second in the core of the Sun. Most of them quickly separate back to protons, $^2\text{He} \rightarrow ^1\text{H} + ^1\text{H}$, and only a very small part rarely get fused into deuterons via positron decays with emissions of neutrinos, $^2\text{He} \rightarrow ^2\text{H} + e^+ + \nu_e$. The fusion rate of the Sun should be about 10^{39} protons per second according to its luminosity, which is about 10^{24} times lower than the rate of diproton formation. In addition to the rareness of positron decays and difficultness of Coulomb barrier penetrations or quantum tunneling, plasma waves or oscillations may also play a significant role in the reduction of the rate of fusion in the core of the Sun [3, 4].

In laboratories, on the other hand, scientists have experimentally discovered that some proton-rich (or neutron-rare) heavy nuclei can emit diprotons [5, 6]. For instance, the proton-rich radioactive nuclei ^{15}Ne , ^{45}Fe and ^{67}Kr can decay into

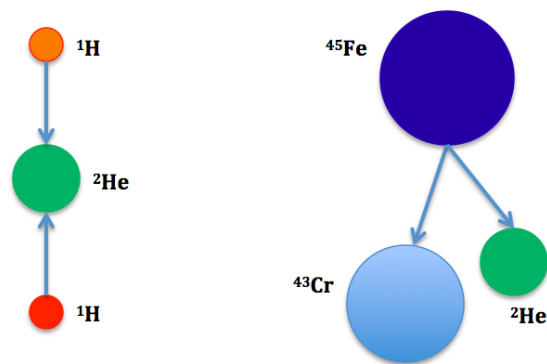


Fig. 1: Two ways of diproton formation: either formed from combination of two separate protons or emitted from decay of proton-rich radioactive heavy nuclei such as ^{15}Ne , ^{45}Fe , ^{67}Kr , and so on. The right panel shows a schematic diagram for a ^{45}Fe nucleus to decay into ^{43}Cr after it emits a diproton ^2He .

^{13}O , ^{43}Cr , and ^{65}Se , respectively, after emitting a diproton [7–9]. The emission of a diproton from a proton-rich heavy nucleus is usually called diproton decay. The diproton decay is a rare decay mode found in a few nuclei beyond the proton drip line [10]. It is found, on the basis of the shell-model mass extrapolation, that ^{45}Fe nuclei are unbound and emit diprotons in the decay. The half-life of ^{45}Fe calculated using an R-matrix formula for the contribution due to the diproton decay agrees with the experimental values [8]. The diproton tunneling half-life decreases with the decay energy. First

observations of diproton decays from ^{45}Fe showed the half-life to be about 3.8 ms and the energy about 1.15 MeV [5, 6]. Fig. 2 shows the observations of diproton decay of ^{45}Fe and its half-life [6, 11]. Observations also show that the unbound proton-rich nucleus ^{15}Ne directly decays to ^{13}O with a simultaneous diproton emission [7]. The diproton decay of ^{67}Kr is measured to be unexpectedly fast [9].

Recently, the first author of this paper has theoretically modeled and numerically studied the transmission and proton decay of unbound diprotons, transmission and positron decay of protons, and transmission and diproton decay of unbound proton-rich heavy nucleus ^{15}Ne in accordance with the Gamow theory for the quantum tunneling and radioactive decays [14]. It was shown that an unbound diproton is extremely unstable and quickly decays through two types of decay modes with lifetime to be extremely short down to about 10^{-21} seconds. A diproton mostly undergoes a proton decay to be two separate protons with a transmission probability higher than 99.99%, and rarely undergoes a β^+ decay to form a deuteron with a transmission probability lower than 0.01%. The transmission probability for the diproton decay of ^{15}Ne increases with the energy.

In this paper, we quantum-mechanically study the transmission probability and lifetime for the diproton decays of proton-rich radioactive nuclei according to the Gamow theory that describes and models the quantum tunneling of the Coulomb barrier between the emitted diproton and the leftover nucleus. We obtain that the transmission probability and lifetime of unbound proton-rich heavy nuclei depend on the energy of the emitted or decayed diprotons. In general, the probability increases with the energy, while the lifetime decreases with the energy. With a certain probability, the heavier the nucleus is, the greater the energy of the emitted diproton is. For ^{45}Fe nuclei, the lifetime of the diproton decay with energy about 1.1-1.2 MeV, obtained from this study, is about some milliseconds, which is consistent with the measurements [8].

2 Quantum theory for diproton decay of heavy nuclei

In 1928, on the basis of quantum mechanics, George Gamow proposed a theory for the α -decay of radioactive heavy nuclei [15]. In this study, we apply the Gamow theory to describe and explain the diproton decay of proton-rich radioactive heavy nuclei. An α particle is a helium nucleus, ^4He , while a diproton is an isotope of helium, ^2He . Both are electrically charged by $2e$, where e is the electric charge of proton. The Gamow theory that was developed for the α -decay of radioactive nuclei should be applicable to the diproton decay of radioactive nuclei. During the diproton decay of a proton-rich radioactive heavy nucleus, a diproton is electrically repelled by and further escapes from the leftover nucleus. In the Gamow theory, the potential energy function is approximately modeled by a finite potential square well to represent

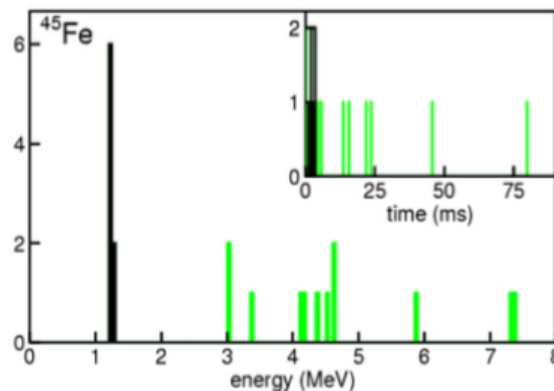


Fig. 2: The energy and time distribution of decay events from ^{45}Fe , measured in experiments by GANIL [12] and GSI [13]. The events represented by black lines corresponding to the diproton decays, while other high frequency events represented by green lines represented the β -decays.

the attractive nuclear force and joined with a Coulomb repulsive potential tail [14, 16],

$$V(r) = \begin{cases} -V_0, & \text{if } 0 < r < r_1 \\ \frac{1}{4\pi\epsilon_0} \frac{Z_1 Z_2 e^2}{r}, & \text{if } r_1 \leq r < \infty \end{cases} \quad (1)$$

Here Z_1 and Z_2 are atomic numbers or charge states of the emitted particle and leftover nucleus; ϵ_0 is the electric permittivity constant in free space; and V_0 is the depth of the potential square well. Fig. 3 is a schematic diagram for the potential energy $V(r)$ given by (1) as a function of the radial distance r in all the classical and quantum regions. The width of the potential square well, denoted by r_1 , can be determined as the radius of the nucleus, given by a constant times the cubic root of the mass number of the nucleus as

$$r_1 = r_0 A^{1/3} \quad (2)$$

where A is the mass number of the nucleus and the constant is $r_0 = 1.2 \times 10^{-15}$ m. The depth of the potential square well, V_0 , is much greater than the maximum height of the Coulomb barrier, U_c , given by

$$U_c = \frac{Z_1 Z_2 e^2}{4\pi\epsilon_0 r_1} \ll V_0. \quad (3)$$

The outer turning point (i.e. at $r = r_2$) can be determined, in terms of the energy E of the emitted α particle to be equal to the potential energy at r_2 , by

$$r_2 = \frac{Z_1 Z_2 e^2}{4\pi\epsilon_0 E}. \quad (4)$$

In this central force problem with potential $V(r)$ given by (1) or shown in Fig. 3, the radial Schrödinger equation of the

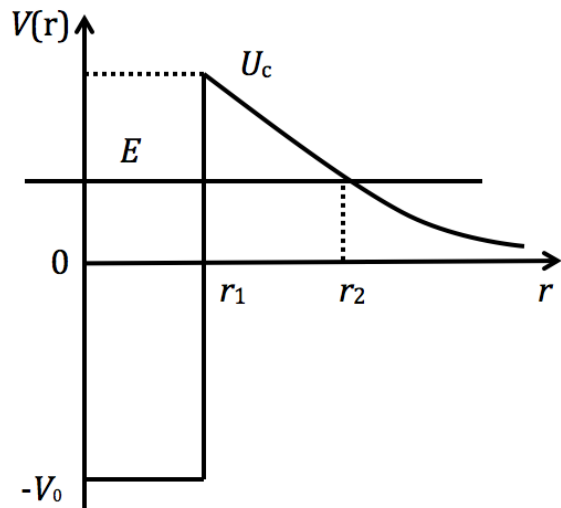


Fig. 3: The Gamow model for the potential energy of an electrically charged particle to be emitted from a radioactive nucleus. It consists of the potential energy square well for the attractive nuclear force and the Coulomb potential energy tail for the repulsive electric force between the emitted particle and the leftover nucleus of the decay.

particle wave is [14, 16],

$$\frac{d^2u(r)}{dr^2} = \frac{2\mu}{\hbar^2}[V(r) - E]u(r) + \frac{l(l+1)}{r^2}u(r), \quad (5)$$

where $u(r)$ is the radial wave function, $\mu = m_1m_2/(m_1 + m_2)$ is the reduced mass with m_1 the mass of the emitted particle and m_2 the mass of the leftover nucleus. The integer l is the quantum number for the magnitude of angular momentum and $h = 2\pi\hbar$ is the Planck constant. A two-body system with a central force or potential can be generally described as a system of one body with the reduced mass.

According to the WKB approximation of quantum mechanics, we can approximately solve the radial Schrödinger equation and find the radial wave functions to be

$$u(r) = \frac{C}{\sqrt{|p(r)|}} \exp\left[\pm \frac{1}{\hbar} \int |p(r')| dr'\right], \quad (6)$$

where the parameter $p(r)$ is defined by

$$p(r) = \sqrt{2\mu[V(r) - E]}. \quad (7)$$

Here, it should be pointed out that the general solution of the radial Schrödinger equation should be the combination of these two corresponding to the plus sign and minus sign. We have also neglected the effect of angular motion and considered the case of $l = 0$.

Then, from the solved wave function, the transmission (or tunneling) probability for the electrically charged particle to tunnel through the Coulomb barrier is obtained as [14, 16]

$$T = e^{-2\gamma}, \quad (8)$$

where the parameter γ is determined by

$$\begin{aligned} \gamma &= \frac{1}{\hbar} \int_{r_1}^{r_2} dr \sqrt{2\mu[V(r) - E]} \\ &= \frac{\sqrt{2\mu E}}{\hbar} \left[r_2 \left(\frac{\pi}{2} - \arcsin \sqrt{\frac{r_1}{r_2}} \right) - \sqrt{r_1(r_2 - r_1)} \right]. \end{aligned} \quad (9)$$

And the lifetime of the parent nucleus or decay is given by

$$\tau = \frac{2r_1}{v} e^{2\gamma}, \quad (10)$$

where $v = \sqrt{2E/m_1}$ is simply chosen to be the speed of the emitted (or α) particle. It should be noted that, although being proposed for explaining the α -decay of radioactive nuclei, the Gamow model is applicable in general for the decay or emission of any type of charged particles from a radioactive nucleus such as the β^+ decay from a proton, and emission of a proton or a diproton from a proton-rich radioactive heavy nucleus (e.g. diproton decays of ^{15}Ne , ^{45}Fe , ^{67}Kr , and so on).

3 Probability and lifetime of diproton decay

A heavy nucleus with the elemental formula A_ZX , if it is proton-rich (or $A < 2Z$), may be radioactive and decay. If the emitted particle of the decay is a diproton, we call the diproton decay. Here X is the elemental symbol of the nucleus, usually called the parent nucleus, Z is the atomic number of the parent nucleus, and A is the mass number of the parent nucleus. In this diproton decay, we have $Z_1 = 2$, $Z_2 = Z - 2$, $m_1 = 2m_p$, $m_2 = (A - 2)m_p$, and $\mu = (m_1 \times m_2)/(m_1 + m_2)$, where $m_p = 1.67 \times 10^{-27}$ kg is the proton mass. We have approximately considered both proton and neutron having about the same mass. The width of the potential square well or the radius of the parent nucleus, r_1 , can be estimated from (2) and the outer turning point, r_2 , can be calculated from (4). With the values of these parameters and given a nucleus' Z and A , we can calculate, from (8) to (10), the transmission probability and lifetime of the diproton decay. For the typical proton-rich radioactive heavy nuclei ^{45}Fe and ^{67}Kr , we have plotted the results obtained from calculations of the transmission probability and lifetimes of the diproton decay.

For the diproton decay of ^{45}Fe , the leftover nucleus is ^{43}Cr . In this case, we have $Z = 26$, $A = 45$, $Z_1 = 2$, $Z_2 = 24$, $m_1 = 2m_p$, $m_2 = 43m_p$, $\mu = 1.91m_p$. The width of the potential square well or the radius of ^{45}Fe nucleus can be obtained from (2) as $r_1 \approx 4.27 \times 10^{-15}$ m. With the values of these parameters and (8) to (10), we can plot, in Fig. 4, the transmission probability for the diproton decay from a radioactive nucleus ^{45}Fe (red line) and the lifetime of the nucleus ^{45}Fe via this diproton decay mode (blue line) as a function of the energy of the diproton. It is seen that the transmission probability increases with the energy. In the energy range from 1 MeV to 5 MeV, the transmission probability of the diproton

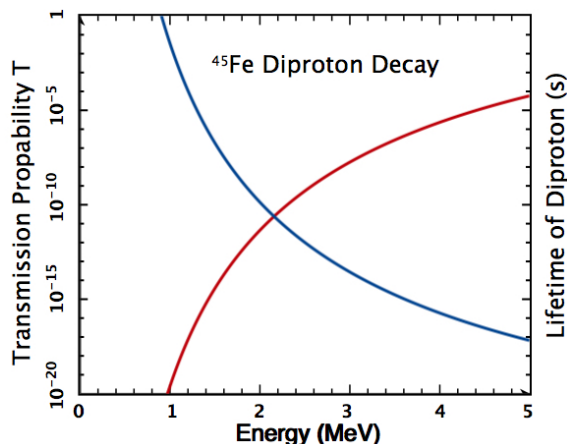


Fig. 4: Diproton decay transmission probability and lifetime of ^{45}Fe nucleus. The red line plots the transmission probability of emitting a diproton from the radioactive nucleus ^{45}Fe in the potential energy well to tunnel through the Coulomb barrier as a function of the energy of the diproton. The blue line plots the lifetime of diproton decay.

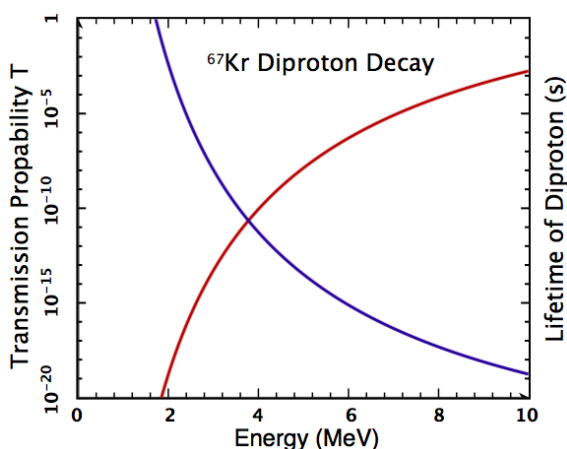


Fig. 5: Diproton decay transmission probability and lifetime of ^{67}Kr nucleus. The red line plots the transmission probability of emitting a diproton from the radioactive nucleus ^{67}Kr in the potential energy well to tunnel through the Coulomb barrier as a function of the energy of the diproton. The blue line plots the lifetime of diproton decay.

decay increases from 10^{-20} to 10^{-4} , while the lifetime decreases from 10^{-3} s to 10^{-17} s. It is consistent with the measurement at energy 1.15 MeV with the lifetime of diproton decay from ^{45}Fe to be of order 10^{-3} s [8].

For the diproton decay of ^{67}Kr , the leftover nucleus is ^{65}Se . In this case, we have $Z = 36$, $A = 67$, $Z_1 = 2$, $Z_2 = 34$, $m_1 = 2m_p$, $m_2 = 65m_p$, $\mu = 1.94m_p$. The width of the potential square well or the radius of ^{67}Kr nucleus can be obtained from (2) as $r_1 \approx 4.87 \times 10^{-15}$ m. With the values of these

parameters and (8) to (10), we can plot, in Fig. 5, the transmission probability for the diproton decay from a radioactive nucleus ^{67}Kr (red line) and the lifetime of the nucleus ^{67}Kr via this diproton decay mode (blue line) as a function of the energy of the diproton. It is seen that the transmission probability increases with the energy. In the energy range from 2 MeV to 10 MeV, the transmission probability of the diproton decay increases from 10^{-20} to 10^{-3} , while the lifetime decreases from 10^{-4} s to 10^{-19} s.

4 Discussions and conclusions

The fact or observations that diprotons are emitted from the decays of proton-rich radioactive nuclei implies that diprotons might have bound states with a positive binding energy. Even if a diproton is only weakly bound with an extremely small but positive binding energy, e.g. 0.384 MeV [17], a star such as the Sun would fuse its protons to deuterons at a rate many orders faster (i.e. $\gg 10^{39}$ protons/s) so that the star becomes much brighter in luminosity (i.e. $\gg 10^{26}$ W). This will result in a universe to fail the life support [18, 19]. This diproton disaster can be overcome by plasma oscillations or waves, which have been shown recently by the first author of this paper to be extremely efficient in inhibiting the nuclear reaction [3, 4], to have the observed luminosity without need to adjust the stars' central temperature, density, and initial number of deuterons. We will study in more details the transmission probability of bound diprotons for the fusion reaction in future.

As a consequence of this study, we have investigated diproton decays of two typical proton-rich (or neutron-rare) radioactive heavy nuclei ^{45}Fe and ^{67}Kr . First, we have applied the Gamow theory for the α -decay of radioactive heavy nuclei to quantum-mechanically model the diproton decay of proton-rich radioactive heavy nuclei. We have derived expressions for the transmission probability and lifetime of diproton decay. Then, for the two typical proton-rich radioactive nuclei, we have numerically calculated the transmission probabilities and lifetimes of the diproton decays. We have found that the transmission probabilities rapidly increase with the energy of the emitted diprotons, and the lifetimes for the diproton decay decrease with the energy of the emitted particle. And finally, we have compared our obtained results with laboratory measurements. At the energy of 1.15 MeV, the lifetime for the diproton decay of ^{45}Fe is observed to be about the order of milliseconds, which is consistent with the results of Gamow modeling obtained from this study.

Acknowledgements

This work was partially supported by the NSF HBCU-UP program and IBM-HBCU Quantum Center via the awarded projects.

Received on November 10, 2023

References

1. Pauli W. Exclusion Principle and Quantum Mechanics. *Writings on Physics and Philosophy*, 1946, 165–198.
2. Bertulani C. A. Nuclear Physics in a Nutshell. Princeton University Press, 2007, ISBN 978-0-691-12505-3.
3. Zhang T. X. The Role of Plasma Oscillation Played in Solar Nuclear Fusion. *Bulletin of American Astronomical Society*, 2020, v. 52, 106.05.
4. Zhang T. X. The Role of Plasma Oscillation in Solar Nuclear Fusion. *Progress in Physics*, 2021, v. 17, 67–71.
5. Blank B. *et al.* First Observation of Two-Proton Decay from Radioactivity Nucleus. *Comptes Rendus Physique*, 2003, v. 4, 521–527.
6. Blank B., Ploszajczak M. Two-Proton Radioactivity. *Reports on Progress in Physics*, 2008, v. 71, 046301.
7. Wamers F. *et al.* First Observation of the Unbound Nucleus ^{15}Ne . *Physical Review Letters*, 2014, v. 112, 132502.
8. Brown B. A. and Barker F. C. Diproton Decay of ^{45}Fe . *Phys. Rev. C*, 2003, v. 67, 041304.
9. Wang S. M. Puzzling Two Proton Decay of ^{67}Kr . *Phys. Rev. Lett.*, 2008, v. 120, 212502.
10. Brown B. A. Diproton Decay of Nuclei on the Drip Line. *Phys. Rev. C*, 1991, v. 43, R1513.
11. Giovinazzo J. *et al.* Two-proton radioactivity: 10 years of experimental progresses. *Journal of Physics: Conference Series*, 2013, v. 436, 012057.
12. Giovinazzo J. *et al.* Two-proton radioactivity of ^{45}Fe . *Phys. Rev. Lett.*, 2002, v. 89, 102501.
13. Pfützner M. *et al.* First Evidence for the two-proton decay of ^{45}Fe . *The European Physical Journal A*, 2002, v. 14, 279–285.
14. Zhang T. X. Gamow Theory for Transmission Probability and Decay of Unbound Diprotons. *Progress in Physics*, 2021, v. 17, 185–188.
15. Gamow G. Zur Quantentheorie des Atomkernes. *Z. Physik*, 1928, v. 51, 204–212.
16. Griffiths D. J. Introduction to Quantum Mechanics, 2nd Edition. Person Prentice Hall, 2005.
17. Kadenko I. M. *et al.* Bound Diproton: An “Illusive” Particle or Exotic Nucleus? *Acta Physica Polonica A*, 2022, v. 142, 337–341.
18. Bradford R. A. W. The Effect of Hypothetical Diproton Stability on the Universe. *J. of Astrophys. Astron.*, 2009, v. 30, 119–131.
19. Barnes L. A. Binding the Diproton in Stars: Anthropic Limits on the Strength of Gravity. *JCAP*, 2015, No. 12, 050.

Surprising Results from Experiments of a Longitudinally Separated Slit

Xianming Meng

Research School of Physics, Australian National University, Canberra, ACT 2601. E-mail: xianming.meng@anu.edu.au

For the first time, the paper reports the experimental results of a longitudinal separated single slit. The asymmetric diffraction pattern in the experiments cannot be explained by either the wave theory of light or quantum electrodynamics, and thus calls for a theoretical breakthrough. The paper also upgrades the slit diffraction formula to include the longitudinal separation distance and the formula fits the experimental data well. However, the absolute value of the fitted parameter differs for the left and right fringe patterns and for different experimental setting, suggesting potential role of factors other than slit width, light frequency, and longitudinal separation.

1 Introduction

The studies on light diffraction and interference have a long history and have dramatic impact on our understanding of the nature of light. The effect of light diffraction were carefully observed by Francesco Grimaldi before 1660 [1]. Christiaan Huygens studied diffraction phenomenon in great details and established his wave theory of light [2] which, however, was suppressed by Newton’s corpuscles theory of light [3]. The famous double-slit experiment of Thomas Young [4] reinvigorated Huygens’ theory and Fresnel [5, 6] did further experimental studies and landed support for the wave theory of light. Later, the wave theory was again challenged by Einstein [7], who showed the particle nature of light. Eventually, Bohr [8] and de Broglie [9] suggested the wave-particle duality for light and for mass particles. With the ascendance of quantum mechanics, Feynman [10] invented the path integral method which was applied to study the quantum nature of light diffraction and interference. Now the quantum theory is used to explain not only the diffraction and interference of light but also of massive particles such as electrons, photoelectrons, neutrons, atoms and molecules [11–22].

It seems that the experiments of light diffraction from slits have examined all possible factors such as slit widths, light frequencies, slit shapes, and the number of slits, but all experiments so far have adhered strictly to the traditional definition of a slit: the closely placed barriers to restrict the passage of light or particles. This paper reports on an innovative single slit experiment that breaks the definition of slit. In the experiment, the barriers of a traditional slit are broken into two to form two half slits which can be placed at different positions along the light propagation direction.

2 Predictions from existing theories

Before we proceed to the experiments, we briefly discuss the expected experimental results based on the currently main theories related to light diffraction: the wave theory of light and the quantum electrodynamics. The diffraction patterns predicted by the wave theory of light is illustrated in Fig. 1.

When a laser beam hits the half-slit A, the wave theory

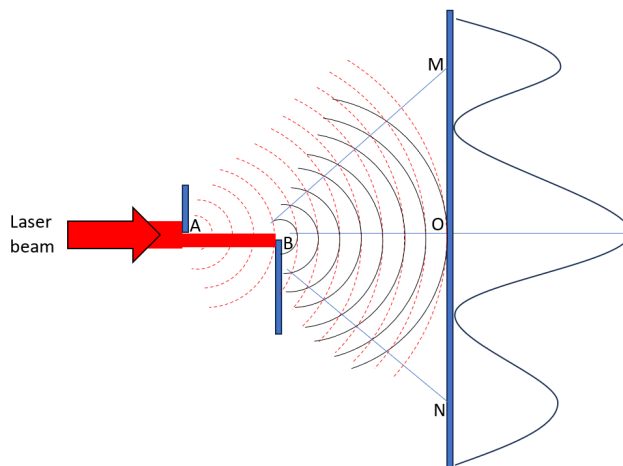


Fig. 1: Wave explanation of light diffraction from a longitudinally separated slit.

suggests that the diffraction occurs because the light at A acts as a point source of light waves illustrated by the spherical red dashed curves (the diffraction angle is exaggerated for clearer illustration). Similarly, the light at half slit B acts as a point source of light waves shown as the solid black curves. Since the light waves from both A and B interfere with each other, the interference pattern will form at the observer plane MN. Due to the nature of spherical wave propagation, the interference pattern on the observing plane should be symmetric, i.e. $OM=ON$, a result similar to the normal single slit interference pattern.

In the above discussion considering only two wave sources at point A and B, it may be argued that this is an oversimplification because Huygens’ principle indicates that light at any point between A and B can act as a source of light waves. With the aid of Fig. 2, we can show that using n wave sources give the same result.

In a traditional way we use the n coherent oscillators to indicate n wave sources. In a traditional slit A_0B , n oscillators are evenly positioned on the dashed line between A_0 and B .

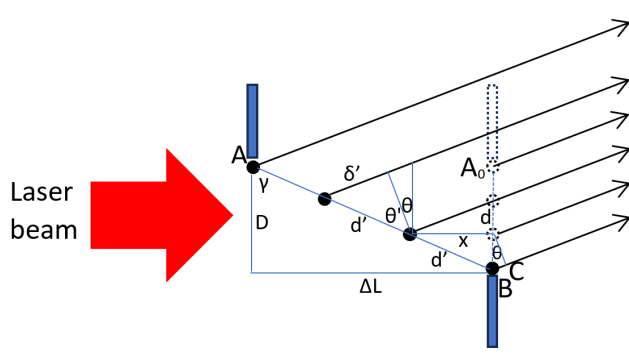


Fig. 2: Wavelets explanation of light diffraction from a longitudinally separated slit.

A textbook derivation (e.g. [23]) gives the following intensity of the diffraction pattern at the observer plane:

$$I = I_0 \frac{\sin^2(N\delta/2)}{\sin^2(\delta/2)} \quad (1)$$

where I and I_0 are light intensity at the observer plane and at the source respectively; $\delta = kd \sin \theta$ is the phase difference of neighbouring coherent oscillators, k the wave vector, and θ the diffraction angle; $d \sin \theta$ is the length difference of neighbouring propagation paths, as shown as BC in Fig. 2. The principal maxima of the fringes occur at $\delta = kd \sin \theta = 2m\pi$, where $m = 0, \pm 1, \pm 2, \dots$. This gives the diffraction formula:

$$d \sin \theta = m\lambda. \quad (2)$$

In the case of longitudinally separated slit AB, the n wave sources should be equally positioned between A and B. As shown in Fig. 2, the phase difference of neighbouring coherent oscillators δ should be calculated as $\delta' = kd' \sin \theta'$, with $d' = \sqrt{x^2 + d^2}$. We can also add a fixed initial phase difference ϕ between neighbouring oscillators and upgrade δ' to $\delta' = kd' \sin \theta' + \phi$. One may worry about applying to the current case the wave amplitude approximation used in the traditional derivation. As the longitudinal separation between A and B is much smaller than their distance to the observer plane, the longitudinal separation hardly affects the light intensity at the observer plane and the approximation condition for deriving the diffraction pattern holds.

For the setting shown in Fig. 2, half-slit A is at the left of half-slit B, we have $\Delta L < 0, \gamma < 0$, and $\theta' < 0$, so we can relate the diffraction angle θ to θ' by:

$$\theta = -(\gamma - \theta') = \arctan(\Delta L/D) + \theta'. \quad (3)$$

As such, the traditional derivation should give the same formula as (1). The only difference is that we need replace δ with δ' . Consequently, the diffraction formula for the longitudinal separated slit should be: $kd' \sin \theta' + \phi = 2m\pi$, or

$d' \sin \theta' = (m - \phi/2\pi)\lambda$. Solving for θ' and substituting into (3), we have:

$$\theta = -(\gamma - \theta') = \arctan(\Delta L/D) + \arcsin[(m - \phi/2\pi)\lambda/d']. \quad (4)$$

From this formula, it is apparent that the width of fringes indicated by θ is different from that in (2), but the fringe width should be almost equally spaced just as in the case of normal single slit.

The wave-theory explanation of knife-edge diffraction is also relevant here but it is unable to predict the pattern diffraction from a longitudinally separated slit. Based on Fresnel's integrals and Kirchoff's scalar diffraction theory, Sommerfeld [24, 25] provided a rigorous solution to knife edge diffraction pattern, which explained the fringe pattern of diffraction on the unrestricted side of a knife edge and the decay of the diffracted light intensity (with no fringe) in the shadow area. While the energy losses in the shadow areas due to single and multiple knife-edge diffraction are intensively studied and modelled, so far there is no study on the diffraction pattern from knife edges that are placed on opposite sides. An apparent reason is that the diffraction pattern in Summerfeld's solution is hard to be generalized to oppositely placed knife edges.

The explanation from quantum electrodynamics (QED) also gives rise to a symmetric diffraction pattern for longitudinally separated slits. In the view of QED, the single-slit diffraction pattern results from the momentum distribution of the diffracted particles, and the probability of the momentum distribution can be calculated by the square of amplitudes of momentum-space wavefunction [26–29]. When a photon passes through a slit, the real-space wavefunction of the photon is constrained by the slit width. A Fourier transformation of the constrained real-space wavefunction into the momentum-space wavefunction gives the probability amplitude and thus the diffraction pattern.

The real-space wave function can be expressed as [28]:

$$\Psi(y, w) = \begin{cases} 1/\sqrt{w}, & \text{for } -w/2 \leq y \leq w/2 \\ 0, & \text{otherwise} \end{cases}$$

where w is the transverse width of the slit, y the transverse distance from the centre of the slit.

A Fourier transform of this wave function into the momentum space gives the following momentum wave function:

$$\begin{aligned} \Phi(p_y, w) &= \int_{-w/2}^{w/2} \frac{1}{\sqrt{2\pi\hbar}} \exp\left(-\frac{ip_y y}{\hbar}\right) \frac{1}{\sqrt{w}} dy \\ &= \sqrt{\frac{2\hbar}{\pi w}} \frac{\sin \frac{p_y w}{2\hbar}}{p_y}. \end{aligned}$$

The diffraction pattern is given by the square of the amplitude of the momentum wave function $|\Phi(p_y, w)|^2$. Apparently, the fringe minimals occur at $\frac{p_y w}{2\hbar} = \pm n\pi$. This gives a symmetric pattern for both sides of the central maximum. It has

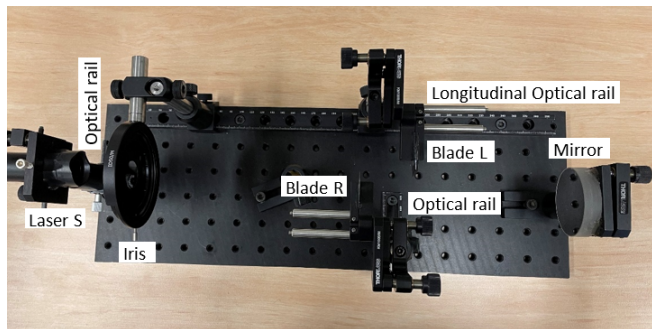


Fig. 3: Experimental setup.

been showed that Feynman’s path integral method also gives the same results [26, 30, 31].

Since our longitudinally separated slit maintains the same transverse slit width w , the constraint on the real-space wavefunction (as well as on Feynman path integral) is unchanged, so the wave function in both real and momentum space should be the same as those for a traditional single slit. Consequently, a QED explanation should also give a symmetric diffraction pattern as in the case of normal single slit experiments.

3 Experimental setup and results

To test the prediction from both the wave theory of light and QED, an experiment of a longitudinal movable slit is designed. The simple experimental setup is shown in Fig. 3.

The laser source S is a common red laser pointer of wavelength of 532 ± 10 nm. The razor blade R is movable transversely so as to change slit width while the blade L can move along the longitudinal optical rail to change longitudinal separation. Since the transverse width of the slit (i.e. the transverse distance between two blades) is small and crucial to the interference pattern, it is important that this width has minimum variation when the blade L is moving along the rail. As such, it is important to align the laser beam to be parallel to the longitudinal optical rail. This is achieved by centering the laser beam on the centre of the adjustable iris when moving it along the rail. To be sure that the laser beam is parallel to the longitudinal when the laser source moves along a transversely placed optical rail, a reflection mirror is employed to confirm the overlapping of the retro-reflected light with incident light. The mirror is removed during the fringe pattern measurement. By putting the two blades in the same plane to form a normal single slit and measuring the total length of two blades, the transverse width of the slit is measured indirectly by subtracting the length of each blade from the length of two blades at the normal single slit position.

The typical experimental results are shown in Table 1. Scenario 3 shows the case of zero longitudinal separation, i.e. the normal single slit case. The fringe pattern is, as expected, symmetric. However, the fringe patterns in other sce-

Scenario	Position of Blade L (mm)	Position of Blade R (mm)	Longitude Separation (mm)	Fringe patterns
1	160	200	-40	
2	190	200	-10	
3	200	200	0	
4	213	200	13	
5	220	200	20	
6	N/A	200	N/A	

Table 1: Selected experiment measurement.

narios are not expected. In scenarios 1 and 2 where the blade L on the left side is closer to the light source (and thus farther away from the observer plane), the left side of fringe patterns have smaller width while the right side of the fringe patterns have much larger width. The larger longitude separation is, the greater difference in fringe widths of both sides are. In scenarios 4 and 5, where the blade L on the left side is closer to the observing plane, it is the opposite story – the left-hand side of fringes have larger widths. Qualitatively, this experimental result is not consistent with the Huygens-Fresnel principle or the prediction of QED.

One may argue that the pattern may be related to the Fresnel diffraction of the single blade or due to possible changes in the transverse width of the slit as it moves along the rail. Regarding the first argument, we display a diffraction pattern caused by the edge of one blade in the last row of Table 1. The diffraction from one blade does agree with knife-edge diffraction theory – there is no fringes in the shadow area but fringes appear on the other side. However, the fringe width is very small and can be observed directly, but cannot be observed from the photo due to resolution limitation. As explained earlier, how this fringe pattern affects the fringes after the second blade is still a mystery. For the second argument, we admit that there is a nonzero possibility of a change in transverse width of the slit, but this would affect equally the fringe width of both sides, and thus its impact should also be symmetric. As a result, these factors can be ruled out as the cause of asymmetric fringe pattern.

Asymmetric diffraction patterns are not rare phenomena, but all asymmetric patterns must have contributing factors and mechanisms. The light diffraction patterns in our daily life are often asymmetric or even have weird shapes, e.g. the diffraction pattern from a spider web, skin hairs, spilt oil surface. These kinds of uncontrolled natural experiments have many contributing factors which are hard to disentangle. The asymmetry in the diffraction pattern of a grating can rise due to periodic errors [32]. The Bragg diffraction on thick grating

involves multi-wave interference [33]. Asymmetric diffraction in a periodic potential can be generated by phase gradients and randomness [34,35]. In the present paper, the asymmetric pattern is clearly caused by longitudinal separation, but how the longitudinal distance affects the fringe pattern is still a mystery.

In order to examine the relationship between the longitudinal distance and the fringe pattern, the left and right fringe widths are measured for a given longitudinal position of blade L. The measurement of fringe width is limited by the 1 mm accuracy of the ruler. However, this accuracy can be improved by further measuring the width of the magnified images. For the case of multiple fringe spots on one side, the measurement accuracy can be improved by measuring the average width of many spots. The measurement of longitudinal distance is also limited by the 1 mm accuracy of the optical rail, but this limit can be offset partially by the large distance between the observer plane and the fixed half-slit. This distance is $L=1600$ mm in our experiment. The measured transverse width of the slit is $D=0.26$ mm for the above results, which is consistent with the calibration based on the diffraction formula together with the measured fringe width and known wavelength. To reduce the chance of possible change in transverse width of slit when longitudinal distance changes, the laser beam is aligned carefully and the position of the left half-slit is locked properly after each movement.

4 An empirical formula explaining experimental results

Our target is to develop an empirical formula for fringe width for the longitudinally separated slit. Since the experiments show that both longitudinal distance and transverse width affect fringe width, we assume that longitudinal separation ΔL has a similar role to the transverse width D , so we can modify the formula for normal slits slightly for our longitudinally-separated slit:

$$\sin \theta = \frac{\lambda}{D + A \Delta L} \tag{5}$$

where $\sin \theta$ indicates fringe width, λ the wavelength of light, D the transverse width of the slit, ΔL the longitudinal separation. A is the parameter to be calibrated.

Because $D \gg \lambda$ in our experiments, the diffraction angle θ is very small, so we can use an approximation $\sin \theta \approx \Delta y/L$ for the above diffraction formula, where L is the distance between the observer plane and the fixed half-slit, and Δy the fringe width. A brief inspection reveals that the formula can produce results that qualitatively agree with experiment results. Namely, when $\Delta L < 0$, i.e. the left half-slit is farther away from the observer plane, the formula with a positive parameter A will produce a larger width for the right fringe. Conversely, when $\Delta L > 0$, the left half-slit is closer to the observer plane, the formula with a positive parameter A produces a smaller width for the right fringe. For left fringes, the formula should also work well if parameter A takes a negative value.

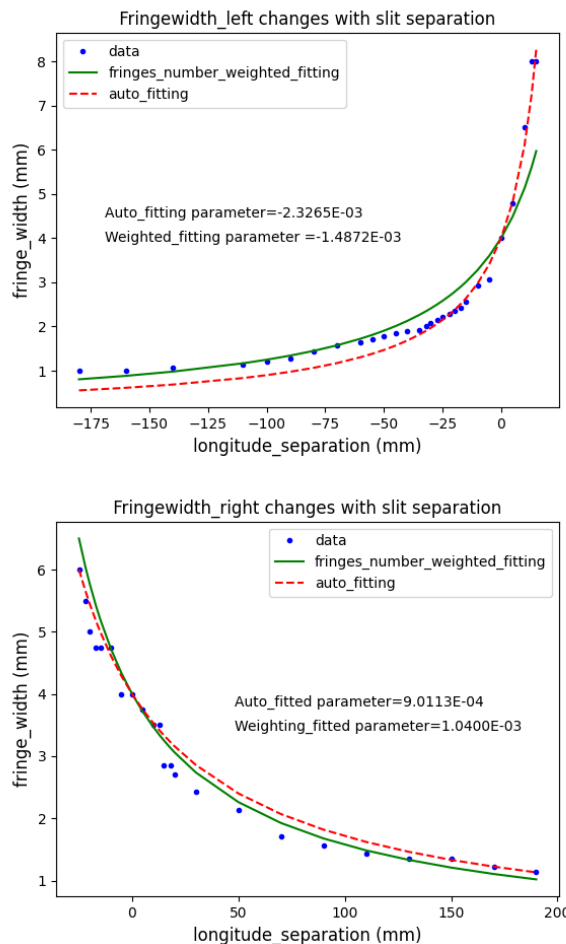


Fig. 4: Fitting of experimental data with the proposed formula.

However, experimenting with different transverse width of slit shows that the impact of ΔL on Δy is very sensitive to this width. A smaller transverse width D' (with λ and L unchanged) corresponds to a significantly larger $\Delta y'$ and dramatically smaller $\Delta L'$, suggesting that the impact of ΔL on Δy is inversely constrained by width D . Considering this as well as the approximation for a small θ , we upgrade the formula to:

$$\Delta y = \frac{L\lambda}{D + A \Delta L/D} \tag{6}$$

Next, we confront this formula with data. With experimental measurements of D , L , ΔL and Δy , as well as known λ , we can fit the data with the above formula. The fitting results are shown in Fig. 4.

The red dash curves are the automatic fitting based on the least squares method. Overall, this fitting is pretty good, and the fitted parameter A has the expected sign: negative value for the left fringes and positive value for right fringes. However, the absolute values of the two fitted parameters differ

considerably by about 2.5 times.

The automatic fitting fits the data especially well for the parts of high fringe width. However, the measurement for high fringe width is relatively less reliable for two reasons. One is that only one or very few fringes are visible so the method of reducing measurement error by averaging a number of fringe widths is not applicable. The other reason is that the sizes of the first and the last fringes differ considerably in some cases (see rows 4 and 5 in Table 1). Considering these factors, we can improve the fitting by giving more weights to smaller fringe widths, which are obtained by averaging a number of fringes at a given longitudinal separation. The weighted fittings are shown in green solid curves, which fit much better the data at small widths.

The parameter values of weighed fitting for the left and right fringes are closer compared with the auto fitted values. Although the absolute parameter values for left and right fringes data are of the same magnitude, they still differ by 50 percent. Since the fitting for both left and right fringes is based on the same value of L , D , ΔL , λ , the significant difference in fitted parameter values for both sides suggest that some other factors may also affect fringe width.

5 Conclusion

Performing the same experiments with slits of different transverse widths and with light of different wavelengths, we find that the experiment data fit well with the proposed formula. However, the fitted parameter values are quite different, suggesting other factors may play a significant role. Future experiments may find missing variables and fit a constant parameter for experiments of all settings.

Received on December 11, 2023

References

- Brewster D. A Treatise on Optics.. London: Longman, Rees, Orme, Brown & Green and John Taylor, 1831.
- Huygens C. Traité de la Lumière. Leyden: Van der Aa, 1690.
- Newton I. Opticks: or, a treatise of the reflexions, refractions, inflexions and colours of light. London, 1704.
- Young T. The Bakerian Lecture: experiments and calculations relative to physical optics. *Philosophical Transactions of the Royal Society of London*, 1804, v. 94, 1–16.
- Fresnel A. Mémoire sur la diffraction de la lumière (Memoir on the diffraction of light). *Annales de Chimie et de Physique*, 1816, v. 1, 239–281.
- Fresnel A. Mémoire sur la diffraction de la lumière (Memoir on the diffraction of light). 1818, in Mémoires de l'Académie Royale des Sciences de l'Institut de France, vol. V (for 1821 & 1822, printed 1826)
- Einstein A. On a heuristic point of view concerning the production and transformation of light. *Annalen der Physik*, 1905, v. 17, 132–148.
- Bohr N. The Quantum postulate and the recent development of atomic theory. *Nature*, 1928, v. 121, 580–590.
- de Broglie L. Waves and quanta. *Nature*, 1923, v. 112, 540.
- Feynman R.P. Space-time approach to non-relativistic quantum mechanics. *Review of Modern Physics*, 1948, v. 20, 367–387.
- Davison C., Germer L. The scattering of electrons by a single crystal of nickle. *Nature*, 1927, v. 119 558–560.
- Estermann I.E., Stern O. Beugung von Molekularstrahlen. *Zeitschrift für Physik*, 1930, v. 61, 95–125.
- Gahler R., Zeilinger A. Wave-optical experiments with very cold neutrons. *American Journal of Physics*, 1991, v. 59, 316–324.
- Jonsson C. Electron diffraction at multiple slits. *American Journal of Physics*, 1974, v. 42, 4–11.
- Zeilinger A., Gahler R., Shull C.G., Treimer W., Mampe, W. Single and double-slit diffraction of neutrons. *Review of Modern Physics*, 1988, v. 60, 1067–1073.
- Carnal O., Mlynek J. Young's double-slit experiment with atoms: a simple atom interferometer. *Physical Review Letters*, 1991, v. 66, 2689–2692.
- Schollkopf W., Toennies J. Nondestructive mass selection of small van der Waals clusters. *Science*, 1996, v. 266, 1345–1348.
- Borde C., Courtier N., Burck F.D. Goncharov A., Gorlicki, M. Molecular interferometry experiments. *Physics Letters A*, 1994, v. 188, 187–197.
- Arndt M., Nairz O., Vos-Andreae J., Keller C., van der Zouw G., Zeilinger A. Wave-particle duality of C(60) molecules. *Nature*, 1999, v. 401, 680.
- Eibenberger S., Gerlich S., Arndt M., Mayor M., Tuxen J. Matter-wave interference of particles selected from a molecular library with masses exceeding 10 000 amu. *Physical Chemistry Chemical Physics*, 2013, v. 15, 14696.
- Pursehouse J., Murray A.J., Watzel J., Berakdar J. Dynamic double-slit experiment in a single atom. *Physical Review Letters*, 2019, v. 122, 053204.
- Zhou H., Perreault W., Mukherjee N., Zare R.N. Quantum mechanical double slit for molecular scattering. *Science*, 2021, v. 274, 960–964.
- Hecht E. Optics, 5th ed. Pearson Education Limited. 2017.
- Sommerfeld A. Mathematische Theorie der diffraction. *Mathematische Annalen*, 1896, v. 47, 317–374.
- Sommerfeld A. Optics: Lectures on Theoretical Physics. Academic Press, New York, 1954.
- Marcella T.V. Quantum interference with slits. *European Journal of Physics*, 2002, v. 23, 615–621.
- Muino P.L. Introducing the uncertainty principle using diffraction of light waves. *Journal of Chemistry Education*, 2000, v. 77, 1025–1027.
- Rioux F. Calculating diffraction patterns. *European Journal of Physics*, 2003, v. 24, N1–N3.
- Wu X., Zhang B., Yang J., Chi L., Liu X., Wu Y., Wang Q., Wang Y., Li J., Guo Y. Quantum theory of light diffraction. *Journal of Modern Optics*, 2010, v. 57 (20), 2082–2091.
- Stöhr J. Diffraction without waves: emergence of the quantum substructure of light. arXiv: quant-ph/2003.14217.
- Stöhr J. Overcoming the diffraction limit by multi-photon interference: a tutorial. *Advances in Optics and Photonics*, 2019, opg.optica.org/aop/fulltext.cfm?uri=aop-11-1-215&id=407746.
- Preston R.C. Asymmetry in the diffraction pattern of a grating due to periodic errors. *Optica Acta*, 1970, v. 17 (11), 857–867.
- Cronin A.D., Schmiedmayer J., Oritchard D.E. Optics and interferometry with atoms and molecules. *Review of Modern Physics*, 1957, v. 81 (3), 1051.
- Zhou S., Groswasser D., Keil M., Japha Y., Folman R. Robust spatial coherence 5 um from a room-temperature atom chip. *Physical Review A*, 2016, v. 93, 063615.
- Liu Y., Xiang Y., Mohammed A. A. Asymmetric diffraction grating via optical vortex light in a tunneling quantum dot molecule. *Laser Physics letters*, 2022, v. 19, 095205.

Scalar Field Effects on the Space-Time Continuum and the Appearance of the Rest-Mass

Haidar Raief

Institute of Physical Research and Technology Peoples' Friendship University of Russia (RUDN), 117198, Moscow, St.Miklukho-Maclay.
E-mail: raief.haidar@gmail.com

The failure to fulfill Lorentz's condition leads to the emergence of a new scalar field, which in turn should have the meaning of a new physical field. In this study, we prove that the appearance of the scalar field in the theory of the Elastodynamics of the Space-Time Continuum can more clearly explain the emergence of rest-mass and the expression of elementary particles through symmetric and anti-symmetric electromagnetic tensors. The use of the scalar field in the previous theory requires a redefinition of both the Lorentz force and the electrodynamic power, and then a rewrite of the electromagnetic stress tensor.

1 Introduction

In modern physics, we can ask the question *what is the origin of mass?* Einstein's famous equation $E = mc^2$ of special relativity theory can be written in an alternative form as $m = E/c^2$. When expressed in this form, it suggests the possibility of explaining mass in terms of energy. Einstein was aware of this possibility from the beginning. Indeed, his original 1905 paper was titled, "Does the Inertia of a Body Depend on Its Energy Content?". Anyway, when a collision between a high-energy electron and a high-energy positron occurs, we often observe that many particles emerge from this event. The total mass of these particles can be thousands of times the mass of the original electron and positron. Thus, mass has been physically created from energy. So energy and mass are equivalent, but the question remains: how is energy transformed into rest-mass?

Using the theory of the Elastodynamics of the Spacetime Continuum [9, 16] (which is a result of applying mechanical continuum laws (elastic continuum) to the space-time continuum), it can be shown that rest-mass energy density arises from the volume dilatation deformation of the space-time continuum, while distortion deformations correspond to massless shear transverse waves. Applying the previous theory to the electromagnetic waves, we find that there is no volume dilatation, which means that the rest-mass density of the photon is equal to zero. But with the existence of the scalar field Ψ (which requires a generalization of the Maxwell-Heaviside equations), it can be proven that rest-mass is no longer equal to zero.

2 Materials and methods

2.1 Generalize the Lorentz force and the electrodynamic power

The basic laws of classical electrodynamics can be summarized in differential form (Maxwell/Heaviside equations) by

these four equations [1, see pp. 24]:

$$\vec{\nabla} \cdot \vec{E} = \frac{\rho_e}{\epsilon_0} \quad (1)$$

$$\vec{\nabla} \times \vec{B} - \epsilon_0 \mu_0 \frac{\partial \vec{E}}{\partial t} = \mu_0 \vec{J} \quad (2)$$

$$\vec{\nabla} \times \vec{E} + \frac{\partial \vec{B}}{\partial t} = \vec{0} \quad (3)$$

$$\vec{\nabla} \cdot \vec{B} = 0. \quad (4)$$

Let \vec{A} and φ be, respectively, the vector and scalar potentials of the classical electromagnetic field; they can be connected via different relations, called gauges or gauge conditions/relations, since they contain some arbitrariness. An important example of this is the Lorentz gauge [2]:

$$\epsilon_0 \mu_0 \frac{\partial \varphi}{\partial t} + \vec{\nabla} \cdot \vec{A} = 0. \quad (5)$$

We will now assume that equality in (5) is not satisfied; that is, in addition to the presence of the electric and magnetic fields, there is a scalar field Ψ [3]:

$$\epsilon_0 \mu_0 \frac{\partial \varphi}{\partial t} + \vec{\nabla} \cdot \vec{A} = 0$$

$$\vec{B} = \vec{\nabla} \times \vec{A}$$

$$\Psi = \epsilon_0 \mu_0 \frac{\partial \varphi}{\partial t} + \vec{\nabla} \cdot \vec{A}. \quad (6)$$

In order to introduce the scalar field into electromagnetic theory, Either new terms must be introduced into the Lagrangian of the electromagnetic field [4], which guarantees the expression of longitudinal waves in the equations of field motion. Or by introducing the invariant scalar field (our case) into Maxwell's equations, which provide a description of the longitudinal waves [5]. By adding derivatives of the field Ψ to Maxwell/Heaviside equations, we get the following [4–7]:

$$\frac{\partial \vec{B}}{\partial t} + \vec{\nabla} \times \vec{E} = 0$$

$$\begin{aligned} \vec{\nabla} \times \vec{B} - \epsilon_0 \mu_0 \frac{\partial \vec{E}}{\partial t} - \vec{\nabla} \cdot \Psi &= \mu_0 \vec{J} \\ \vec{\nabla} \cdot \vec{B} &= 0 \\ \vec{\nabla} \cdot \vec{E} + \frac{\partial \Psi}{\partial t} &= \frac{\rho_e}{\epsilon_0}. \end{aligned} \tag{7}$$

Using (6)–(7), we can obtain the inhomogeneous potential wave equations (automatically) for both scalar and vector potentials without an extra gauge condition:

$$\epsilon_0 \mu_0 \frac{\partial^2 \varphi}{\partial t^2} - \nabla^2 \varphi = \frac{\rho_e}{\epsilon_0}. \tag{8}$$

$$\epsilon_0 \mu_0 \frac{\partial^2 \vec{A}}{\partial t^2} - \nabla^2 \vec{A} = \mu_0 \vec{J}. \tag{9}$$

From (7), we can make sure that the electric field, the magnetic field, and the scalar field all satisfy the following inhomogeneous field wave equations:

$$\epsilon_0 \mu_0 \frac{\partial^2 \vec{E}}{\partial t^2} - \nabla^2 \vec{E} = \mu_0 \left(-\nabla \frac{\rho_e}{\epsilon_0} - \frac{\partial \vec{J}}{\partial t} \right) \tag{10}$$

$$\epsilon_0 \mu_0 \frac{\partial^2 \vec{B}}{\partial t^2} - \nabla^2 \vec{B} = \mu_0 \vec{\nabla} \times \vec{J} \tag{11}$$

$$\epsilon_0 \mu_0 \frac{\partial^2 \Psi}{\partial t^2} - \nabla^2 \Psi = \mu_0 \left(\vec{\nabla} \cdot \vec{J} + \frac{\partial \rho_e}{\partial t} \right). \tag{12}$$

The existence of the longitudinal expansion/contraction waves (12), implies the existence of an elastic continuum (which has volume dilatation) [6–9]. Maxwell’s theory does not accept the existence of this type of wave, because Maxwell’s theory is described by an antisymmetric tensor

$$F_{\mu\theta} = \partial_\mu A_\theta - \partial_\theta A_\mu$$

the trace of which equals zero, where A_μ is the four-dimensional electromagnetic potential. This tensor $F_{\mu\theta}$ can only describe transverse waves, which means that the vacuum used in electromagnetism cannot be compressed. Therefore, there was a need to introduce an elastic continuum by analogy with a continuous elastic medium (mechanical continuum) like the Foka-Podolsky Lagrangian [6]. In order to obtain both the generalized power and the generalized Lorentz force, a source transformation must be defined [7]:

$$\rho'_e = \rho_e - \epsilon_0 \frac{\partial \Psi}{\partial t}, \quad \vec{J}' = \vec{J} + \frac{1}{\mu_0} \vec{\nabla} \cdot \Psi. \tag{13}$$

The scalar field \mathbf{S} used in [7], is associated with Ψ by $\Psi = -\mathbf{S}$. The electrodynamics power theorem is given by:

$$\mu_0 (\vec{J} \cdot \vec{E}) = -\frac{1}{2} \frac{\partial}{\partial t} (\epsilon_0 \mu_0 \vec{E}^2 + \vec{B}^2) - \vec{\nabla} \cdot (\vec{E} \times \vec{B}). \tag{14}$$

Using (13–14), the electrodynamics power is transformed in the following way:

$$\begin{aligned} \vec{J} \cdot \vec{E} - \Psi \frac{\rho_e}{\mu_0 \epsilon_0} &= -\frac{1}{2} \frac{\partial}{\partial t} \left(\epsilon_0 \vec{E}^2 + \frac{\vec{B}^2}{\mu_0} + \frac{\Psi^2}{\mu_0} \right) \\ &\quad - \frac{1}{\mu_0} \vec{\nabla} \cdot (\vec{E} \times \vec{B} + \vec{E} \cdot \Psi) \end{aligned} \tag{15}$$

where $\vec{J} \cdot \vec{E} - \Psi \frac{\rho_e}{\mu_0 \epsilon_0}$ represents the volume creation rate of electromagnetic energy (joules per cubic meter per second) or alternatively represents the rate of change of mechanical energy per unit volume, i.e. the rate at which the field does work on the charges per unit volume. The Lorentz force is given by:

$$\begin{aligned} \mu_0 (\rho_e \vec{E} + \vec{J} \times \vec{B}) &= \epsilon_0 \mu_0 ((\vec{\nabla} \cdot \vec{E}) \cdot \vec{E} + (\vec{\nabla} \times \vec{E}) \times \vec{E}) + \\ &\quad + (\vec{\nabla} \times \vec{B}) \times \vec{B} - \epsilon_0 \mu_0 \frac{\partial}{\partial t} (\vec{E} \times \vec{B}). \end{aligned} \tag{16}$$

Using (13), the generalized Lorentz force is transformed into the following form:

$$\begin{aligned} \rho_e \cdot \vec{E} + \vec{J} \times \vec{B} - \Psi \vec{J} &= \epsilon_0 ((\vec{\nabla} \cdot \vec{E}) \cdot \vec{E} + (\vec{\nabla} \times \vec{E}) \times \vec{E}) + \\ &\quad + \frac{1}{\mu_0} ((\vec{\nabla} \times \vec{B}) \times \vec{B} - \epsilon_0 \frac{\partial}{\partial t} (\vec{E} \times \vec{B} - \Psi \cdot \vec{E})) + \\ &\quad + \frac{1}{2\mu_0} \vec{\nabla} \Psi^2 - \frac{1}{\mu_0} \vec{\nabla} \times (\Psi \cdot \vec{B}) \end{aligned} \tag{17}$$

where $(\rho_e \cdot \vec{E} + \vec{J} \times \vec{B} - \Psi \vec{J})$ represents the rate of change of mechanical momentum per unit volume and time. Note that the scalar field and the electric vector field have different signs indicating that the scalar field decelerates the charge, and that the deceleration is proportional to the current density, which in turn is proportional to the velocity of the charge. Thus, the electric vector field accelerates the charge while the scalar field decelerates it.

3 Elastodynamics of the Space-Time Continuum

Einstein’s general theory of relativity is based on the geometry of continuous spacetime, which can be described by the following field equation [8, see pp. 875]:

$$R_{\mu\theta} - \frac{1}{2} g_{\mu\theta} R + g_{\mu\theta} L = \frac{8\pi G}{c} T_{\mu\theta} \tag{18}$$

where

$R_{\mu\theta}$: Ricci curvature tensor,

$g_{\mu\theta}$: metric tensor,

R : curvature scalar,

L : the cosmological constant, which can be neglected for small distances,

$T_{\mu\theta}$: the stress energy-momentum tensor.

In (18), everything on the left-hand side refers to the curvature of spacetime, and everything on the right-hand side refers to mass and energy.

According to the theory of the Elastodynamics of the Space-Time Continuum [9, 16], energy propagates in the Space-Time Continuum, which causes deformation of the Space-Time Continuum with longitudinal waves corresponding to mass and transverse waves corresponding to massless field energy. This leads implicitly to the proposition that the space-time continuum must be a deformable continuum. This deformation, which has a physical nature [9], can be expressed through strain that results from stress, so the stress energy-momentum tensor results in strains in the space-time continuum (strained space-time). The presence of strain in the space-time continuum leads to a deformation in the geometry of this space-time continuum. We can say it in the following way: the energy-momentum stress tensor produces a strain in the spacetime continuum, and that strain changes the geometry of the space-time continuum, and leads to the deformations with the longitudinal component being mass. The stress-strain relation for an isotropic and homogeneous space-time continuum can be written as the following [10]:

$$2\Upsilon_0 \varepsilon^{\mu\theta} + \lambda_0 g^{\mu\theta} \varepsilon = T^{\mu\theta} . \tag{19}$$

Eq. (19) gives the stress in term of strain for a homogeneous and isotropic space-time continuum, both Υ_0 and λ_0 are Lamé constants, and they are linked together through K_0 the bulk modulus:

$$\frac{1}{2} \Upsilon_0 = K_0 - \lambda_0 . \tag{20}$$

Here Y_0 is the shear modulus, which corresponds to the resistance of the space-time continuum to distortions, K_0 represents the resistance of the space-time continuum to dilatation, where distortions describe a change of shape of the space-time continuum without a change in volume, and dilatation describes a change of volume without a change of shape of the space-time continuum [9-10], $T^{\mu\theta}$ is the energy-momentum stress tensor, the tensor $\varepsilon^{\mu\theta}$ is the strain tensor, the volume dilatation $\varepsilon = \varepsilon^\alpha_\alpha$ is the trace $\varepsilon^{\mu\theta}$. If we compare (19) and (18) we find an interesting similarity [9] (if we neglect the cosmological constant). The trace T^α_α of (19) takes the following relation:

$$2(\Upsilon_0 + 2\lambda_0) \varepsilon = T^\alpha_\alpha . \tag{21}$$

The total rest-mass energy density of the system is related to the trace T^α_α , by the following [11-12]:

$$T^\alpha_\alpha (x^k) = \rho c^2 . \tag{22}$$

Using the last formula in (21), we get the relation between the invariant volume dilatation and the invariant rest-mass:

$$2(\Upsilon_0 + 2\lambda_0) \varepsilon = \rho c^2 . \tag{23}$$

By using (20), (23) takes the following expression:

$$4K_0 \varepsilon = \rho c^2 . \tag{24}$$

Eq. (24) shows that the rest-mass is the result of the dilatation of the spacetime continuum; the volume dilatation is an invariant, as is the rest-mass energy density. The strain energy density of the space-time continuum is a scalar given by [9]:

$$\mathcal{E} = \frac{1}{2} T^{\mu\theta} \varepsilon_{\mu\theta} . \tag{25}$$

In order to get the dilatation energy density and distortion energy density, we first need to write the tensor decomposition of $\varepsilon^{\mu\theta}$ as a sum of a strain deviator (distortion) tensor $e^{\mu\theta}$ and a scalar (dilatation) tensor e_s [9]:

$$\varepsilon^{\mu\theta} = e^{\mu\theta} + e_s g^{\mu\theta} \tag{26}$$

where:

$$e^\mu_\theta = \varepsilon^\mu_\theta - e_s \delta^\mu_\theta ,$$

$$e_s = \frac{1}{4} e^\alpha_\alpha = \frac{1}{4} \varepsilon . \tag{27}$$

In the same way, the energy-momentum stress tensor is decomposed into a stress deviator tensor $t^{\mu\theta}$ and a scalar t_s [9]:

$$T^{\mu\theta} = t^{\mu\theta} + t_s g^{\mu\theta} \tag{28}$$

where:

$$t^\mu_\theta = T^\mu_\theta - t_s \delta^\mu_\theta ,$$

$$t_s = \frac{1}{4} T^\alpha_\alpha . \tag{29}$$

Using (26–29), one can get the following expression for the scalar \mathcal{E} [13]:

$$\mathcal{E} = \frac{1}{2} K_0 \varepsilon^2 + \Upsilon_0 e^{\mu\theta} e_{\mu\theta} = \mathcal{E}_\parallel + \mathcal{E}_\perp \tag{30}$$

where:

$$\mathcal{E}_\parallel = \frac{1}{32K_0} (\rho c^2)^2 = \frac{1}{2} K_0 \varepsilon^2 , \quad \mathcal{E}_\perp = \Upsilon_0 e^{\mu\theta} e_{\mu\theta} . \tag{31}$$

The strain energy density of the space-time continuum can also be written in the following way [13]:

$$\mathcal{E} = \frac{1}{2K_0} t_s^2 + \frac{1}{4\Upsilon_0} t^{\mu\theta} t_{\mu\theta} . \tag{32}$$

From (30) or (32), we can see that the strain energy density is separated into two terms: the first term corresponds to the rest-mass longitudinal density (the dilatation energy density), while the second is the massless transverse term (the distortion energy density). Now we need to calculate the strain energy density in two cases:

$$\tilde{\sigma}^{\mu\theta} = \begin{pmatrix} \frac{1}{2} \left(\epsilon_0 \vec{E}^2 + \frac{1}{\mu_0} \vec{B}^2 + \frac{1}{\mu_0} \Psi^2 \right) & S_x/c - \sqrt{\frac{\epsilon_0}{\mu_0}} E_x \Psi & S_y/c - \sqrt{\frac{\epsilon_0}{\mu_0}} E_y \Psi & S_z/c - \sqrt{\frac{\epsilon_0}{\mu_0}} E_z \Psi \\ S_x/c + \sqrt{\frac{\epsilon_0}{\mu_0}} E_x \Psi & -T_{xx} - \frac{1}{2\mu_0} \Psi^2 & -T_{xy} - \frac{1}{\mu_0} \Psi B_z & -T_{xz} + \frac{1}{\mu_0} \Psi B_y \\ S_y/c + \sqrt{\frac{\epsilon_0}{\mu_0}} E_y \Psi & -T_{yx} + \frac{1}{\mu_0} \Psi B_z & -T_{yy} - \frac{1}{2\mu_0} \Psi^2 & -T_{yz} - \frac{1}{\mu_0} \Psi B_x \\ S_z/c + \sqrt{\frac{\epsilon_0}{\mu_0}} E_z \Psi & -T_{zx} - \frac{1}{\mu_0} \Psi B_y & -T_{zy} + \frac{1}{\mu_0} \Psi B_x & -T_{zz} - \frac{1}{2\mu_0} \Psi^2 \end{pmatrix}$$

3.1 Case number (1)

Electromagnetic stress tensor $\sigma^{\mu\theta}$ as strain energy density (in case $\Psi = 0$). Using $\sigma_{\alpha\beta} = \eta_{\alpha\mu} \eta_{\beta\theta} \sigma^{\mu\theta}$, we obtain the following [9]:

$$\sigma_{\alpha\beta} = \begin{pmatrix} \frac{\epsilon_0}{2} \vec{E}^2 + \frac{1}{2\mu_0} \vec{B}^2 & -S_x/c & -S_y/c & -S_z/c \\ -S_x/c & -T_{xx} & -T_{xy} & -T_{xz} \\ -S_y/c & -T_{yx} & -T_{yy} & -T_{yz} \\ -S_z/c & -T_{zx} & -T_{zy} & -T_{zz} \end{pmatrix} \quad (33)$$

where $T_{ij} = \epsilon_0 (E_i E_j - \frac{1}{2} \delta_{ij} E^2) + \frac{1}{\mu_0} (B_i B_j - \frac{1}{2} \delta_{ij} B^2)$ is the Maxwell stress tensor. The dilatation energy density (the ‘‘mass’’ longitudinal term) is given by [9]:

$$\mathcal{E}_{||} = \frac{1}{2} K_0 \epsilon^2 = \frac{1}{2K_0} t_s^2 = \frac{1}{32K_0} (\sigma^\alpha_\alpha)^2 \quad (34)$$

where:

$$\sigma^\alpha_\alpha = \eta_{00} \sigma^{00} + \eta_{11} \sigma^{11} + \eta_{22} \sigma^{22} + \eta_{33} \sigma^{33} \quad (35)$$

with the metric $\eta^{\theta\mu}$ of signature $(+1, -1, -1, -1)$.

The tensor σ^α_α can be calculated [9,13]:

$$\sigma^\alpha_\alpha = \frac{1}{2} \left(\epsilon_0 \vec{E}^2 + \frac{1}{\mu_0} \vec{B}^2 \right) + T_{xx} + T_{yy} + T_{zz} = 0 \quad (36)$$

giving $\sigma^\alpha_\alpha = 0$, which means the longitudinal term (the rest-mass term) is equal to zero:

$$\mathcal{E}_{||} = \frac{1}{32K_0} (\rho c^2)^2 = \frac{1}{32K_0} (\sigma^\alpha_\alpha)^2 = 0. \quad (37)$$

In another sense, the rest-mass of the photon is zero. The term \mathcal{E}_\perp is given by (31) and takes the final expression [9,13]:

$$\mathcal{E}_\perp = \frac{1}{4\Upsilon_0} \sigma^{\mu\theta} \sigma_{\mu\theta} = \frac{1}{\Upsilon_0} \left(U_{em}^2 - \frac{1}{c^2} S^2 \right) \quad (38)$$

where: $U_{em} = \frac{1}{2} \epsilon_0 (\vec{E}^2 + c^2 \vec{B}^2)$ is the electromagnetic field energy density.

3.2 Case Number (2)

Electromagnetic stress tensor as strain energy density (in case $\Psi \neq 0$). We found that when $\Psi = 0$, the rest mass density is

zero. Now, we need to repeat the previous procedure of Case (1) with the existence of the scalar field ($\Psi \neq 0$). To achieve this we should calculate the tensor $\sigma_{\alpha\beta}$ with the existence of the scalar field Ψ : when $\Psi \neq 0$, the tensor $\sigma^{\mu\theta}$ changes to the tensor $\tilde{\sigma}^{\mu\theta}$ and this new tensor must fulfill the relations (15-17):

$$\partial_\mu \tilde{\sigma}^{\mu\theta} = \begin{pmatrix} -\frac{1}{c} \left(\vec{J} \cdot \vec{E} - \Psi \frac{\rho_e}{\mu_0 \epsilon_0} \right) \\ -(\rho_e \cdot \vec{E} + \vec{J} \times \vec{B} - \Psi \vec{J}) \end{pmatrix}. \quad (39)$$

The tensor $\tilde{\sigma}^{\mu\theta}$ that achieves the relation (39) is written in the following Eq. (40) shown at the top of the page.

Shown at the top of the page. (40)

Note that when $\Psi \rightarrow 0$, then $\tilde{\sigma}^{\mu\theta} \rightarrow \sigma^{\mu\theta}$, and quantity $\sqrt{\frac{\epsilon_0}{\mu_0}}$ is the inverse of the impedance of free space z_0^{-1} . The next step is to calculate the longitudinal mass term:

$$\begin{aligned} \tilde{\sigma}^\alpha_\alpha &= \eta_{00} \tilde{\sigma}^{00} + \eta_{11} \tilde{\sigma}^{11} + \eta_{22} \tilde{\sigma}^{22} + \eta_{33} \tilde{\sigma}^{33} = \\ &= \frac{1}{2} \left(\epsilon_0 \vec{E}^2 + \frac{1}{\mu_0} \vec{B}^2 + \frac{1}{\mu_0} \Psi^2 \right) + T_{xx} + \frac{1}{2\mu_0} \Psi^2 + \\ &+ T_{yy} + \frac{1}{2\mu_0} \Psi^2 + T_{zz} + \frac{1}{2\mu_0} \Psi^2. \end{aligned} \quad (41)$$

Taking into account the properties of tensor T_{ij} and (35–37), we find the following:

$$\tilde{\sigma}^\alpha_\alpha = \frac{2}{\mu_0} \Psi^2. \quad (42)$$

Thus, the mass term is no longer equal to zero:

$$\tilde{\mathcal{E}}_{||} = \frac{1}{32K_0} (\rho c^2)^2 = \frac{1}{32K_0} (\tilde{\sigma}^\alpha_\alpha)^2 = \frac{1}{32K_0} \frac{4}{\mu_0^2} \Psi^4. \quad (43)$$

The rest-mass term takes the following expression:

$$\rho = \pm 2\epsilon_0 |\Psi|^2. \quad (44)$$

The massless transverse terms (the distortion energy density) can be calculated as follows:

$$\tilde{\mathcal{E}}_\perp = \frac{1}{4\Upsilon_0} \tilde{\mu}^{\mu\theta} \tilde{t}_{\mu\theta}, \quad \text{where } \tilde{\mu}^{\mu\theta} = \tilde{\sigma}^{\mu\theta} \text{ and } \tilde{t}_{\mu\theta} = \tilde{\sigma}_{\mu\theta}.$$

$$\tilde{\sigma}_{\alpha\beta} = \begin{pmatrix} \frac{1}{2} \left(\epsilon_0 \vec{E}^2 + \frac{1}{\mu_0} \vec{B}^2 + \frac{1}{\mu_0} \Psi^2 \right) & -S_x/c + \sqrt{\frac{\epsilon_0}{\mu_0}} E_x \Psi & -S_y/c + \sqrt{\frac{\epsilon_0}{\mu_0}} E_y \Psi & -S_z/c + \sqrt{\frac{\epsilon_0}{\mu_0}} E_z \Psi \\ -S_x/c - \sqrt{\frac{\epsilon_0}{\mu_0}} E_x \Psi & -T_{xx} - \frac{1}{2\mu_0} \Psi^2 & -T_{xy} - \frac{1}{\mu_0} \Psi B_z & -T_{xz} + \frac{1}{\mu_0} \Psi B_y \\ -S_y/c - \sqrt{\frac{\epsilon_0}{\mu_0}} E_y \Psi & -T_{yx} + \frac{1}{\mu_0} \Psi B_z & -T_{yy} - \frac{1}{2\mu_0} \Psi^2 & -T_{yz} - \frac{1}{\mu_0} \Psi B_x \\ -S_z/c - \sqrt{\frac{\epsilon_0}{\mu_0}} E_z \Psi & -T_{zx} - \frac{1}{\mu_0} \Psi B_y & -T_{zy} + \frac{1}{\mu_0} \Psi B_x & -T_{zz} - \frac{1}{2\mu_0} \Psi^2 \end{pmatrix}. \tag{45}$$

By using $\tilde{\sigma}_{\alpha\beta} = \eta_{\alpha\mu}\eta_{\beta\theta}\tilde{\sigma}^{\mu\theta}$, the tensor $\tilde{\sigma}_{\mu\theta}$ can be written as in (45) above at the top of the page. The term $\tilde{\sigma}^{\mu\theta}\tilde{\sigma}_{\mu\theta}$ can now be calculated as in (46) below. The formula in (46) is simplified as in (47) below.

$$\begin{aligned} \tilde{\sigma}^{\mu\theta}\tilde{\sigma}_{\mu\theta} &= \frac{1}{4} \left(\epsilon_0 \vec{E}^2 + \frac{1}{\mu_0} \vec{B}^2 + \frac{1}{\mu_0} \Psi^2 \right)^2 + T_{xx}^2 + \\ &+ \frac{1}{\mu_0} T_{xx} \Psi^2 + \frac{1}{4\mu_0^2} \Psi^4 + T_{yy}^2 + \frac{1}{\mu_0} T_{yy} \Psi^2 + \\ &+ \frac{1}{4\mu_0^2} \Psi^4 + T_{zz}^2 + \frac{1}{\mu_0} T_{zz} \Psi^2 + \frac{1}{4\mu_0^2} \Psi^4 - \\ &- 2 \left(\frac{S_x}{c} \right)^2 - 2 \left(\sqrt{\frac{\epsilon_0}{\mu_0}} E_x \Psi \right)^2 - 2 \left(\frac{S_y}{c} \right)^2 - \\ &- 2 \left(\sqrt{\frac{\epsilon_0}{\mu_0}} E_y \Psi \right)^2 - 2 \left(\frac{S_z}{c} \right)^2 - 2 \left(\sqrt{\frac{\epsilon_0}{\mu_0}} E_z \Psi \right)^2 + \\ &+ 2 (T_{xy})^2 + 2 \left(\frac{1}{\mu_0} \Psi B_x \right)^2 + 2 (T_{xz})^2 + \\ &+ 2 \left(\frac{1}{\mu_0} \Psi B_y \right)^2 + 2 (T_{zy})^2 + 2 \left(\frac{1}{\mu_0} \Psi B_z \right)^2. \end{aligned} \tag{46}$$

$$\begin{aligned} \tilde{\sigma}^{\mu\theta}\tilde{\sigma}_{\mu\theta} &= \left\{ \frac{1}{4} \left(\epsilon_0 \vec{E}^2 + \frac{1}{\mu_0} \vec{B}^2 \right)^2 + T_{xx}^2 + T_{yy}^2 + \right. \\ &+ T_{zz}^2 - 2 \left(\frac{S_x}{c} \right)^2 - 2 \left(\frac{S_y}{c} \right)^2 - 2 \left(\frac{S_z}{c} \right)^2 \\ &+ 2 (T_{xy})^2 + 2 (T_{xz})^2 + 2 (T_{zy})^2 \left. \right\} + \\ &+ \left\{ \frac{1}{2} \left(\epsilon_0 \vec{E}^2 + \frac{1}{\mu_0} \vec{B}^2 \right) + T_{xx} + T_{yy} + T_{zz} \right\} \cdot \frac{1}{\mu_0} \Psi^2 + \\ &+ \frac{2}{\mu_0} \Psi^2 \left\{ \frac{\vec{B}^2}{\mu_0} - \epsilon_0 \vec{E}^2 \right\} + \frac{1}{\mu_0^2} \Psi^4. \end{aligned} \tag{47}$$

By making use of (36–38), we find the following [9]:

$$\begin{aligned} &\frac{1}{4} \left(\epsilon_0 \vec{E}^2 + \frac{1}{\mu_0} \vec{B}^2 \right)^2 + T_{xx}^2 + T_{yy}^2 + T_{zz}^2 - \\ &- 2 \left(\frac{S_x}{c} \right)^2 - 2 \left(\frac{S_y}{c} \right)^2 - 2 \left(\frac{S_z}{c} \right)^2 + \\ &+ 2 (T_{xy})^2 + 2 (T_{xz})^2 + 2 (T_{zy})^2 = \\ &= \epsilon_0^2 \left(\vec{E}^2 + c^2 \vec{B}^2 \right)^2 - \frac{4}{c^2} (S_x^2 + S_y^2 + S_z^2) = \sigma^{\mu\theta} \sigma_{\mu\theta} \end{aligned} \tag{48}$$

$$\frac{1}{2} \left(\epsilon_0 \vec{E}^2 + \frac{1}{\mu_0} \vec{B}^2 \right) + T_{xx} + T_{yy} + T_{zz} = \sigma^\alpha{}_\alpha = 0. \tag{49}$$

Finally:

$$\tilde{\sigma}^{\mu\theta}\tilde{\sigma}_{\mu\theta} = \sigma^{\mu\theta}\sigma_{\mu\theta} + \frac{2}{\mu_0} \Psi^2 \left\{ \frac{\vec{B}^2}{\mu_0} - \epsilon_0 \vec{E}^2 \right\} + \frac{1}{\mu_0^2} \Psi^4 \tag{50}$$

which means that the massless transverse terms (the distortion energy density) take the following expression:

$$\tilde{\mathcal{E}}_\perp = \mathcal{E}_\perp + \frac{1}{2\Upsilon_0\mu_0} \Psi^2 \left\{ \frac{\vec{B}^2}{\mu_0} - \epsilon_0 \vec{E}^2 \right\} + \frac{1}{4\Upsilon_0\mu_0^2} \Psi^4. \tag{51}$$

4 Results and discussions

Because of the continuity equation (when $\vec{\nabla} \cdot \vec{J} + \frac{\partial \rho_e}{\partial t} = 0$), the discovery of the scalar field Ψ is not as easy as the discovery of the electromagnetic fields. This means that the left-hand side of (12) can be zero for a scalar field that is not equal to zero. Then (12) can be written in the form of two equations:

$$\epsilon_0\mu_0 \frac{\partial^2 \Psi}{\partial t^2} - \nabla^2 \Psi = 0, \quad \vec{\nabla} \cdot \vec{J} + \frac{\partial \rho_e}{\partial t} = 0.$$

From the last two equations, we can note that the wave equation $\epsilon_0\mu_0 \frac{\partial^2 \Psi}{\partial t^2} - \nabla^2 \Psi = 0$, is as fundamental an equation as the continuity equation $\vec{\nabla} \cdot \vec{J} + \frac{\partial \rho_e}{\partial t} = 0$ [6]. Because the existence of the scalar field is linked to the appearance of the rest mass in the electromagnetic field, the motion of charges in accordance with the equation $\vec{\nabla} \cdot \vec{J} + \frac{\partial \rho_e}{\partial t} = 0$, always conjugates the longitudinal waves and happens with volume dilatation. We can write Maxwell's equations (1–4) through the electromagnetic tensor $F_{\mu\theta}$:

$$\partial^\mu [F_{\mu\theta}] = J_\theta. \tag{52}$$

The previous tensor is an antisymmetric tensor, which can be written in the following formula:

$$[F_{\mu\theta}] = \frac{1}{2} \left([a_{\mu\theta}] - [a_{\theta\mu}] \right) \tag{53}$$

where $a_{\mu\theta}$ is an asymmetric tensor, which takes the following

$$[S_{\mu\theta}] = \frac{1}{2} \begin{pmatrix} \frac{2}{c^2} \frac{\partial\varphi}{\partial t} & -\frac{\partial A^x}{\partial t} + \frac{1}{c} \frac{\partial\varphi}{\partial x} & -\frac{\partial A^y}{\partial t} + \frac{1}{c} \frac{\partial\varphi}{\partial y} & -\frac{\partial A^z}{\partial t} + \frac{1}{c} \frac{\partial\varphi}{\partial z} \\ -\frac{\partial A^x}{\partial t} + \frac{1}{c} \frac{\partial\varphi}{\partial x} & -2\frac{\partial A^x}{\partial x} & -\frac{\partial A^y}{\partial y} - \frac{\partial A^x}{\partial x} & -\frac{\partial A^z}{\partial z} - \frac{\partial A^x}{\partial x} \\ -\frac{\partial A^y}{\partial t} + \frac{1}{c} \frac{\partial\varphi}{\partial y} & \frac{\partial A^y}{\partial x} - \frac{\partial A^x}{\partial y} & -2\frac{\partial A^y}{\partial y} & -\frac{\partial A^z}{\partial z} - \frac{\partial A^y}{\partial y} \\ -\frac{\partial A^z}{\partial t} + \frac{1}{c} \frac{\partial\varphi}{\partial z} & \frac{\partial A^z}{\partial x} - \frac{\partial A^x}{\partial z} & \frac{\partial A^z}{\partial y} - \frac{\partial A^y}{\partial z} & -2\frac{\partial A^z}{\partial z} \end{pmatrix}$$

expression:

$$[a_{\mu\theta}] = \begin{pmatrix} \frac{1}{c^2} \frac{\partial\varphi}{\partial t} & \frac{\partial A^x}{\partial t} & \frac{\partial A^y}{\partial t} & \frac{\partial A^z}{\partial t} \\ \frac{1}{c} \frac{\partial\varphi}{\partial x} & \frac{\partial A^x}{\partial x} & \frac{\partial A^y}{\partial x} & \frac{\partial A^z}{\partial x} \\ \frac{1}{c} \frac{\partial\varphi}{\partial y} & \frac{\partial A^x}{\partial y} & \frac{\partial A^y}{\partial y} & \frac{\partial A^z}{\partial y} \\ \frac{1}{c} \frac{\partial\varphi}{\partial z} & \frac{\partial A^x}{\partial z} & \frac{\partial A^y}{\partial z} & \frac{\partial A^z}{\partial z} \end{pmatrix}. \tag{54}$$

We can write another tensor, which is a symmetric tensor $S_{\mu\theta}$:

$$[S_{\mu\theta}] = \frac{1}{2} ([a_{\mu\theta}] + [a_{\theta\mu}]), \tag{55}$$

which is given explicitly at the top of this page.

Using the formula $S^\alpha_\alpha = \eta^{\alpha\beta} S_{\alpha\beta}$, we can get the diagonal components of this tensor to describe the electromagnetic potential $\partial^\theta A_\theta$:

$$S^\alpha_\alpha = \Psi = \epsilon_0 \mu_0 \frac{\partial\varphi}{\partial t} + \vec{\nabla} \cdot \vec{A}. \tag{56}$$

Therefore, the Lorentz condition is a cancellation of four-dimensional volume dilatation from the space-time continuum. According to [14-15], the pair $(S_{\mu\theta}, F_{\mu\theta})$ of tensors can explain the matter-field duality, $F_{\mu\theta}$ describes the field properties ($F_{\mu\theta}$ as the field tensor.) and $S_{\mu\theta}$ contains matter waves (matter tensor with $S^\alpha_\alpha \neq 0$), which corresponds to (44), and also to (17), which confirms that the scalar field hinders the movement and therefore plays a role similar to inertia. Both tensors $(S_{\mu\theta}, F_{\mu\theta})$ can display fundamental properties such as energies or electric charge or rest-mass. Tensor $a_{\mu\theta}$ is equivalent to the formula $\{a_{\mu\theta} \sim \partial_\mu A_\theta\}$, and the tensor $F_{\mu\theta}$ is equivalent to formula $\{\partial_\mu A_\theta - \partial_\theta A_\mu\}$, finally the tensor $S_{\mu\theta}$ is $\{\partial_\mu A_\theta + \partial_\theta A_\mu\}$.

According to the theory of the Elastodynamics of the Space-Time Continuum, the antisymmetric rotation tensor $\omega^{\mu\theta}$ can be written in the following [9-11]:

$$\omega^{\mu\theta} = \frac{1}{2} (u^{\mu;\theta} - u^{\theta;\mu}) \tag{57}$$

where u^μ is the displacement of an infinitesimal element of the spacetime continuum from its unstrained position x_μ . The tensor in (57) corresponds to tensor $F^{\mu\theta}$ [9, 16, see pp. 64]:

$$F^{\mu\theta} = \varphi_0 \omega^{\mu\theta}. \tag{58}$$

In order to fulfill Lorentz's condition, the electromagnetic potential four-vector A^μ satisfies the following relationship [9, 16]:

$$A^\mu = -\frac{1}{2} \varphi_0 u^\mu_\perp \tag{59}$$

where the constant φ_0 is referred to as the "space-time continuum electromagnetic shearing potential constant" [9, 16, see pp. 64] and u^μ_\perp indicates that the relation holds for a transverse displacement. From the last equation, we get the Lorentz condition directly $\partial_\mu A^\mu = 0$. The previous case corresponds to antisymmetric tensor $F^{\mu\theta}$. However, in our case, Lorentz's condition is not satisfied, and therefore we need to generalize the previous relationship (59) to include symmetric tensor $S_{\mu\theta}$. According to the theory of the Elastodynamics of the Space-Time Continuum, the symmetric strain tensor $\varepsilon^{\mu\theta}$, which is equivalent to a tensor $S^{\mu\theta}$, can be written as the following [9, 16, see pp. 53]:

$$\varepsilon^{\mu\theta} = \frac{1}{2} (u^{\mu;\theta} + u^{\theta;\mu}). \tag{60}$$

The displacements in expressions derived from (60) are written as $u_{||}$, which means that symmetric displacements are along the direction of motion (longitudinal). We can now write (59) in the following general form:

$$A^\mu = f(u^\mu). \tag{61}$$

From (57), we can write the following:

$$\partial_\theta A^\mu = \partial_\theta f(u^\mu) = \frac{\partial f(u^\mu)}{\partial u^\mu} \frac{\partial u^\mu}{\partial x_\theta} = \frac{\partial f(u^\mu)}{\partial u^\mu} \{\varepsilon^\mu_\theta + \omega^\mu_\theta\}. \tag{62}$$

Eq. (62) also comes automatically from [9, 16], therefore, we can consider the field A^μ as a real physical vacuum in which both electromagnetic waves and elementary particles can propagate and arise due to the dynamic distortion and dilatation of this medium. The mass that appeared in (44) is real rest-mass density, but there are two options: positive rest-mass

density and negative rest-mass density ($\rho \sim \pm|\Psi|^2$). By multiplying (32) by (32 K_0) and taking into account (31) and the scalar function, we get the following [9, 16]:

$$32K_0\varepsilon = (\rho c^2)^2 + \frac{8K_0}{\Upsilon_0} \tilde{\gamma}^{\mu\theta} \tilde{\gamma}_{\mu\theta}. \quad (63)$$

The last expression is similar to the energy relation of Special Relativity, which can be written after taking the square root as follows:

$$E = \pm\hbar\omega = \pm c \sqrt{(\rho c)^2 + \frac{8K_0}{c^2\Upsilon_0} \tilde{\gamma}^{\mu\theta} \tilde{\gamma}_{\mu\theta}} \quad (64)$$

where E is the total energy density, noting that $\tilde{\gamma}^{\mu\theta} \tilde{\gamma}_{\mu\theta}$ is quadratic in structure [13], and equivalent to the momentum density. As we see in (64), the energy equation accepts negative solutions. Generally, (63) is the Klein-Gordon equation. Eq. (44) is reminiscent of the wave function in quantum mechanics, which means the volume density of the particles; thus, we can say that the wave function in quantum mechanics describes the propagation of longitudinal waves in the spacetime continuum [9]. Finally, note that the tensor $\sigma^{\mu\theta}$ is symmetric, but the tensor $\tilde{\sigma}^{\mu\theta}$ is not; the symmetry was broken after the mass appeared. We can confirm that the equations that describe the behavior of elementary particles become fundamentally simpler and more symmetric when the mass of the particles is zero.

5 Conclusion

We found that the addition of the scalar field to the Maxwell-Heaviside equations requires a generalization of both the Lorentz force and power. Using the Elastodynamics of the Spacetime Continuum theorem, and after calculating the electromagnetic stress tensor which includes the previous generalizations, the positive rest-mass and the negative rest-mass appear, meaning that the photon acquires mass, which in turn corresponds to the volume dilatation of the space-time continuum.

Received on October 22, 2023

References

1. Weng C. C. Lectures on Electromagnetic Field Theory. Purdue University, 2019.
2. Bozhidar Z. I. The "Lorenz gauge" is named in honour of Ludwig Valentin Lorenz! Bulgarian Academy of Sciences, arXiv: physics.hist-ph/0803.0047.
3. van Vlaenderen K. J. and Waser A. Electrodynamics with the scalar field. *Hadronic Journal*, 2001
4. van Vlaenderen K. J. and Waser A. Generalisation of classical electrodynamics to admit a scalar field and longitudinal waves. *Hadronic Journal*, 2001, v. 24, 609–628.
5. Podgajny D. V., Zaimidoroga O. A. Relativistic Dynamics of a Charged Particle in an Electroscalar Field. arXiv: math-ph/1203.2490.

6. Spirichev Y. A. About Longitudinal Waves of an Electromagnetic Field. The State Atomic Energy Corporation ROSATOM, Research and Design Institute of Radio-Electronic Engineering, Zarechny, Penza region, Russia, 2017.
7. van Vlaenderen K. J. A generalisation of classical electrodynamics for the prediction of scalar field effects. Institute for Basic Research, arXiv: physics/0305098.
8. Matthias B. Lecture Notes on General Relativity. Albert Einstein Center for Fundamental Physics, Bern University, Switzerland, 2023.
9. Millette P. A. Elastodynamics of the Spacetime Continuum. *The Abraham Zelmanov Journal*, 2012, v. 5, 221–277.
10. Millette P. A. On the Decomposition of the Spacetime Metric Tensor and of Tensor Fields in Strained Spacetime. *Progress in Physics*, 2012, v. 8 (4), 5–8.
11. Millette P. A. The Elastodynamics of the Spacetime Continuum as a Framework for Strained Spacetime. *Progress in Physics*, 2013, v. 9 (1), 55–59.
12. Padmanabhan T. Gravitation, Foundations and Frontiers. Cambridge University Press, Cambridge, 2010.
13. Millette P. A. Strain Energy Density in the Elastodynamics of the Spacetime Continuum and the Electromagnetic Field. *Progress in Physics*, 2013, v. 9 (2), 82–86.
14. Stephan G. M. Electromagnetic Particles. *Fund. J. Modern Phys.*, 2017, v. 10, 87–133. hal-01446417.
15. Stephan G. M. Electromagnetic Particles. *Fund. J. Modern Phys.*, 2022. hal-03593153.
16. Millette P. A. Elastodynamics of the Spacetime Continuum, Second Expanded Edition. American Research Press, Rehoboth, NM, 2019.

Progress in Physics is an American scientific journal on advanced studies in physics, registered with the Library of Congress (DC, USA): ISSN 1555-5534 (print version) and ISSN 1555-5615 (online version). The journal is peer reviewed.

Progress in Physics is an open-access journal, which is published and distributed in accordance with the Budapest Open Initiative. This means that the electronic copies of both full-size version of the journal and the individual papers published therein will always be accessed for reading, download, and copying for any user free of charge.

Electronic version of this journal: <http://www.ptep-online.com>

Editorial Board:
Pierre Millette
Andreas Ries
Florentin Smarandache
Ebenezer Chifu

Postal address:
Department of Mathematics and Science, University of New Mexico,
705 Gurley Avenue, Gallup, NM 87301, USA

